

TECHNISCHE UNIVERSITÄT MÜNCHEN

Lehrstuhl für Entwicklungsgenetik

Specification, maintenance and fate determination of neural
progenitor pools in the zebrafish central nervous system

Christian Stigloher

Vollständiger Abdruck der von der Fakultät Wissenschaftszentrum Weihenstephan für Ernährung, Landwirtschaft und Umwelt der Technischen Universität München zur Erlangung des akademischen Grades eines

Doktors der Naturwissenschaften

genehmigten Dissertation.

Vorsitzender: Univ.-Prof. Dr. E. Grill

Prüfer der Dissertation: 1. Univ.-Prof. Dr. W. Wurst

2. Univ.-Prof. Dr. K. H. Schneitz

3. Univ.-Prof. Dr. A. Gierl

Die Dissertation wurde am 28.5.2008 bei der Technischen Universität München eingereicht und durch die Fakultät Wissenschaftszentrum Weihenstephan für Ernährung, Landwirtschaft und Umwelt am 15.9.2008 angenommen.

Specification, maintenance and fate determination of neural progenitor pools in the zebrafish central nervous system

Kumulative Arbeit

Christian Stigloher

Abstract

The development of a vertebrate brain relies on neural progenitor pools that provide a source of undifferentiated and proliferating cells for a prolonged period of time. Some of these progenitor pools allocate even life-long sources for brain growth, plasticity and regeneration. Thus, a better insight into the processes that control neural progenitor pools is of prime importance for a solid understanding of nervous system development and function and for potential therapeutic approaches. The main aim of my PhD project is to contribute to the understanding of the processes of specification and maintenance of progenitor pools and the mechanisms of fate determination in the vertebrate central nervous system using zebrafish as neurogenetic model organism.

First, to set the basis for a further dissection of the molecular processes that specify and maintain neural progenitor pools, I contributed to a comprehensive review summarizing current knowledge on the role of 'Enhancer of Split' (E(Spl)) factors for progenitors in the embryonic and adult brain in vertebrates. Special focus was placed on the midbrain-hindbrain boundary (MHB) progenitor pool in the zebrafish and mouse model. E(Spl) factors were first described in *Drosophila* and are crucially involved in the control of neural progenitors. In zebrafish the homologs of E(Spl) factors are called 'Hairy and E(Spl) related' (Her) factors and the mouse homologs are called 'Hairy and E(Spl)' (Hes). A subset of zebrafish Her factors, namely Her3, Her5, Her9 and Her11, mark specifically progenitor pools in the neural plate and show a non-canonical regulation by Notch-signalling. Hes1 is the functional representative of this special subgroup in the mouse brain.

In order to discover molecular mechanisms that are crucial for specification and maintenance of progenitor pools, I participated in a morphology-based recessive mutagenesis screen. Looking for specific deficiencies in progenitor pools, I analyzed a mutant line displaying a loss of the eye field progenitor pool. Molecular analysis revealed a single nucleotide exchange in the *retinal homeobox gene 3 (rx3)* as the causative mutation. Marker analysis and direct lineage tracing revealed a fate transformation from eye field progenitor pool to telencephalic fate in this mutant line. With transplantation experiments I could show that *rx3* works cell-autonomously to specify the eye field progenitor pool. Together, my cellular and molecular analyses of the *rx3* mutant line unravelled an important part of the process that separates the eye field progenitor pool from the telencephalic primordium during early stages of neural plate development.

Further on, I concentrated on the E(Spl) activity at the MHB progenitor pool. I contributed with data that helps us understand the processes that account for the variation of E(Spl) activity along the mediolateral axis. We identified "Glioma associated oncogene homolog" (Gli1) as a factor crucially involved in this process. Importantly, Gli1 is not regulated by the Hedgehog pathway in this process. Furthermore, I contributed to the understanding of the late processes that maintain the MHB progenitor pool. A combination of loss-of-function and gain-of-function approaches revealed the crucial role of a microRNA, miR-9, in the control of E(Spl) activity in the late MHB progenitor pool.

In order to dissect the cellular role of the progenitor pool-specific Her factors Her3/5/9/11, I compared several cellular characteristics between the MHB progenitor pool and neighboring proliferating precursor populations. Using a time-lapse imaging approach I could show that the MHB progenitor pool and neighboring proliferating

precursor populations differ in their cell division properties. I further addressed whether Her-based mechanisms could be at play to maintain progenitors in the adult brain. I showed that *her3* and *her9* are both expressed in adult neural progenitor pools, opening towards a further dissection of the role of non-canonical *her* genes in adult neurogenesis. Along the same lines, my contribution to the detailed expression analysis of 'Fibroblast growth factor' (Fgf)-signalling components in adult brains is a basis for future work on adult neurogenesis in the zebrafish. Interestingly, this analysis clearly revealed that the *fgf8* synexpression group that has been described for embryonic stages is widely diverging in the adult brain.

Finally, I analyzed how the midbrain-hindbrain (MH) neurons originating from the MHB progenitor pool acquire their specific identities. I established a map of basal MH neuronal identities, including the analysis of new markers such as an early marker of hindbrain serotonergic neurons. I used this neuronal identity map to test for the contribution of a timer mechanism to the determination of neuronal identities in the MH domain.

Taken together, my PhD project provides a deeper understanding of the processes that control specification and maintenance of neural progenitor pools in the zebrafish CNS. Furthermore, it sheds light on the mechanisms that are involved in fate determination in the MH domain.

Zusammenfassung

Die Entwicklung des Wirbeltiergehirns basiert auf neuronalen Vorläuferzell-Populationen („Progenitor Pools“), die eine lang anhaltende Quelle für undifferenzierte und proliferierende Zellen darstellen. Einige dieser Vorläuferzell-Populationen sind sogar zeitlebens ein Reservoir für Wachstum, Plastizität und Regeneration des Gehirns. Deshalb ist eine bessere Einsicht in die Prozesse, die Vorläuferzell-Populationen kontrollieren, von besonderer Bedeutung für ein tiefgreifenderes Verständnis der Entwicklung des Nervensystems und dessen Funktionsweise. Auch für potentielle therapeutische Heilungsmethoden ist dies von großer Bedeutung. Das Hauptziel meiner Doktorarbeit ist es, zum besseren Verständnis der Prozesse der Spezifizierung und des Erhalts von neuronalen Vorläuferzell-Populationen und der Mechanismen der Festlegung des Zell-Schicksals im Zentralnervensystem beizutragen. Dafür verwendete ich Zebrafische als neurogenetische Modell-Organismen.

Um eine solide Basis für die detaillierte Analyse der Vorläuferzell-Populationen zu schaffen, trug ich zur Erstellung eines Übersichtsartikels bei. Dieser Artikel ist eine Zusammenfassung des derzeitigen Wissens über die Rolle der „Enhancer of Split“ (E(Spl)) Faktoren für Vorläuferzellen im embryonalen und erwachsenen Wirbeltiergehirn. Das besondere Augenmerk liegt dabei auf der Vorläuferzell-Population der Mittelhirn-Hinterhirn-Grenze (MHG) im Zebrafisch- und Mausmodell. E(Spl) Faktoren wurden ursprünglich bei *Drosophila* beschrieben und sind entscheidend beteiligt an der Kontrolle der neuronalen Vorläuferzellen. Die Zebrafisch-Homologe der E(Spl) Faktoren werden „Hairy and E(Spl) related“ (Her) und die Maus-Homologe „Hairy and E(Spl)“ (Hes) genannt. Die Zebrafisch Her Faktoren Her3, Her5, Her9 und Her11 bilden eine eigene Unterfamilie, die spezifisch Vorläuferzell-Populationen in der Neuralplatte markiert und sich durch eine untypische Regulation durch Notch auszeichnet. Hes1 ist ein vergleichbarer Vertreter dieser Unterfamilie in der Maus.

Um die molekularen Mechanismen zu entschlüsseln, die entscheidend für die Spezifizierung und den Erhalt der Vorläuferzell-Populationen sind, beteiligte ich mich an einem rezessiven Mutagenese-Screen, der auf morphologischen Kriterien basierte. Ich konzentrierte mich dabei auf spezifische Defekte in Vorläuferzell-Populationen. Darauf aufbauend, untersuchte ich eine Mutante, die einen Verlust der Vorläuferzell-Population der frühen Augenanlage zeigt. Die molekulare Analyse dieser Mutante offenbarte eine Basenaustauschmutation im „Retinalen Homeobox Gen 3“ (*rx3*) als Ursache des Phänotyps. Markeranalysen und Zellmarkierungsexperimente zeigten den Verlust der Augenvorläuferzell-Population und eine Veränderung hin zu telencephalem Schicksal. Mit Transplantationsexperimenten konnte ich nachweisen, dass *rx3* bei der Spezifizierung der Augenanlage zellautonom wirkt. Insgesamt haben meine Analysen mit der *rx3* Mutante auf der zellulären und molekularen Ebene einen wichtigen Teil des Prozesses beschrieben, der die Augenvorläuferzell-Population von der telencephalen Anlage während früher Entwicklungsstadien trennt.

Weiterhin konzentrierte ich mich auf die Regulation der E(Spl)-Aktivität in der Vorläuferzell-Population an der MHG. Ich trug zum Verständnis der Prozesse bei, die E(Spl)-Aktivitäten zwischen medialen und lateralen Bereichen der MHG Vorläuferzell-Population variieren lassen. Dabei identifizierten wir das „Glioma assoziierte Onkogen Homolog“ (Gli1) als für diesen Prozess entscheidenden Faktor. Hierbei ist es wichtig zu erwähnen, dass Gli1 in diesem Zusammenhang nicht über den

„Hedgehog“ vermittelten Signalweg reguliert ist. Weiterhin, trug ich zum Verständnis der Prozesse bei, die Vorläuferzell-Population an der MHG in der späteren Entwicklung kontrollieren. Eine Kombination aus Überaktivierungs- und Funktionsverluststudien zeigten, dass die MikroRNA „miR-9“ in späteren Entwicklungsstadien entscheidend bei der Kontrolle der E(Spl)-Aktivität der Vorläuferzell-Population an der MHG beteiligt ist.

Um die zellulären Funktionen der für die Vorläuferzell-Population spezifischen Her Faktoren *Her3/5/9/11* zu entschlüsseln, verglich ich zelluläre Eigenschaften zwischen Vorläuferzellen an der MHG und proliferierenden Vorläuferzellen aus benachbarten Regionen. Dafür benutzte ich Zeitraffer-Aufnahmen früher neuraler Entwicklungsprozesse und konnte damit zeigen, dass sich Vorläuferzellen an der MHG und proliferierende Vorläuferzellen aus benachbarten Regionen in ihren Zellteilungseigenschaften unterscheiden. Weiterhin untersuchte ich, inwiefern ein auf *her* Genen basierender Prozess auch im erwachsenen Gehirn Vorläuferzell-Populationen kontrolliert. Ich konnte zeigen, dass *her3* und *her9* in adulten Vorläuferzell-Populationen exprimiert sind. Diese Erkenntnis eröffnet die Möglichkeit, diese *her* Gene im adulten Gehirn weiter auf ihre Rolle in der Neurogenese zu untersuchen. In dieselbe Richtung zielte auch mein Beitrag zu detaillierten Expressionsstudien von „Fibroblasten-Wachstums-Faktoren“ (*Fgf*) im adulten Gehirn des Zebrafisches. Interessanterweise haben diese Studien gezeigt, dass die *fgf8* Synexpressions-Gruppe, die für embryonale Stadien beschrieben wurde, im adulten Gehirn aufgespalten ist.

Schließlich untersuchte ich, auf welche Weise Neuronen in der Mittelhirn-Hinterhirn Region, die von der MHG abstammen, ihre spezifischen neuronalen Identitäten erwerben. Hierfür etablierte ich eine Karte mit neuronalen Identitäten der basalen Mittelhirn-Hinterhirn Region. Dabei analysierte ich auch bisher im Zebrafisch unbekannte Marker, so zum Beispiel ein Gen, das früh in serotonergen Neuronen im Hinterhirn exprimiert ist. Diese Karte benutzte ich, um die Rolle von zeitabhängigen Mechanismen für die Bestimmung dieser neuronaler Identitäten in der Mittelhirn-Hinterhirn Region zu untersuchen.

Insgesamt vermittelt meine Doktorarbeit ein tiefgehendes Verständnis der Prozesse der Spezifizierung und des Erhalts von neuronalen Vorläuferzell-Populationen und der Mechanismen der Festlegung der neuronalen Identitäten im Zentralnervensystem des Zebrafisches.

Index

Abstract	I
Zusammenfassung	III
Index.....	V
1. Introduction	1
1.1. Morphogenesis of the zebrafish early embryonic neural tube	2
1.2. Neural induction and early patterning	5
1.2.1. Neural Induction.....	6
1.2.2. Early anterior/posterior patterning of the anterior nervous system	8
1.2.2.1. Early forebrain patterning.....	8
1.2.2.2. Patterning of the midbrain-hindbrain domain	10
1.3. Neurogenesis control.....	17
1.3.1. bHLH transcription factors involved in neurogenesis: basic knowledge from <i>Drosophila</i>	19
1.3.2. The basic helix-loop-helix transcription factors	20
1.3.3. <i>Hairy</i> and <i>E(Spl)</i> genes in vertebrates	21
1.3.4. Delta/Notch signalling and lateral Inhibition in vertebrates	24
1.3.5. Non-canonical <i>her</i> genes in zebrafish and <i>Hes</i> genes in mouse.....	26
1.3.5.1. Zebrafish <i>her</i> genes	26
1.3.5.2. <i>Hes</i> genes in the mouse	26
1.3.6. Initiation of the neuronal differentiation program	29
1.3.7. Role of miRNAs in neurogenesis control	30
1.3.7.1. Biogenesis of miRNAs	30
1.3.7.2. Known roles of miRNAs in neurogenesis control.....	32
1.3.7.3. Open questions of the roles of miRNAs in neurogenesis control.....	32
1.3.8. Neurogenesis and E(Spl) factors in the adult brain	32
1.4. Determination of neuronal identities	34
1.4.1. Morphogen gradients as determinants for neuronal identities	34
1.4.2. Timer mechanisms as determinants for neuronal identities.....	37
1.4.2.1. Differentiation timing in <i>Drosophila</i> neuroblasts.....	37
1.4.2.2. Differentiation timing in the vertebrate neocortex	38
1.4.2.3. Differentiation timing in the vertebrate retina	40
1.4.3. Neuronal identity specification in the basal MH domain	41
1.5. Neuronal differentiation	43
2. Aims and achievements.....	45
3. Results.....	47
3.1. Specification and maintenance of progenitor pools in the embryonic and adult CNS	47
3.1.1. Non canonical E(spl) factors define neural progenitor pools	47
3.1.2. Specification of the eye field progenitor pool during early forebrain development	50
3.1.3. Interactors and cooperators of E(Spl) factors in specification and maintenance of the MHB neural progenitor pool.....	53
3.1.4. Identification of factors limiting the activity of E(Spl) factors at the MHB	55

3.1.5.	Transition between progenitor subtype is accompanied not only by a change in E(spl) factor expression but also by a change of specific cellular properties	58
3.1.6.	Correlation of mechanisms defining neural progenitor pools between the embryonic and adult brain	66
3.2.	Neuronal identity specification in the embryonic midbrain-hindbrain domain	69
3.2.1.	Serotonergic neurons of the anterior Raphe nucleus are defined by expression of the transcription factor Pet1 and originate from the MHB progenitor pool	69
3.2.2.	Screen for mutations affecting serotonergic raphe neurons	71
3.2.3.	The role of a timer in neuronal identity definition in the midbrain-hindbrain domain.....	71
4.	<i>Discussion and perspectives</i>	87
5.	<i>Bibliography</i>	95
6.	<i>Abbreviations</i>	113
7.	<i>Index of definitions</i>	119
8.	<i>Appendices</i>	121

1. Introduction

The main aim of my PhD thesis project is to contribute to the understanding of the molecular and cellular processes that specify and maintain neural progenitor pools within the vertebrate central nervous system (CNS), and of the processes that determine their cellular fate. These processes are the basis for the development of the highly complex vertebrate brains, such as our own, where the mature neocortex alone has an estimated number of 50-65 billion cells, including neurons and glia [1], not to mention the much higher level of complexity at the level of neuronal connectivity [2].

To contribute to the understanding of processes that are at the very basis of this complexity, i.e. neurogenesis control and fate determination, I used zebrafish (*Danio rerio*) as model organism. This small tropical freshwater teleost is a highly suitable vertebrate model to study developmental neurogenetics [3]. It was first recognized and established as a vertebrate genetic model organism by George Streisinger [4]. Large scale forward genetic screens have both proven the genetic tractability and provide a solid basis for functional studies [3,5-7]. Furthermore, a large range of experimental approaches is available for the zebrafish model, ranging from classical embryological transplantation and fate tracing experiments to very powerful live imaging approaches. Importantly, in the last years the genetic toolkit freely available for the zebrafish research community^a expanded considerably, nowadays providing relatively easy and quick methods for transgenesis [8], enhancer trapping [9], gene trapping [10] and the versatile binary Gal4/UAS^b system [11], just to name a few important examples. In addition, zebrafish is not only a perfect model to study early stages of neurogenesis but it is also a highly interesting model to study adult neurogenesis, as in adult stages neurogenesis is widespread and experimentally tractable [12-14].

I will start the introduction to development of the early zebrafish brain with references to other vertebrate model organisms, in particular the mouse. In addition, I will also refer to one invertebrate model, the fruit fly *Drosophila melanogaster*^c, as it was this model that contributed significantly from the very beginning of experimental neurogenetics to the molecular understanding of neurogenesis and often provided the groundwork to understand certain aspects of vertebrate neurogenesis [15,16]. A special focus will always be neural progenitor pools.

In this introduction, I will first describe embryonic brain patterning and morphogenesis in the zebrafish, as these processes are the basis for the development of a complex brain. Secondly, in relation to the first part of my PhD project, I will summarize current knowledge on neurogenesis, spanning from neural induction to the final steps of differentiation. Thereby I will put a special focus on those regions that undergo delayed neurogenesis and are the source for later neurogenesis events: neural progenitor pools. These are of crucial importance for proper brain development not only during embryonic stages but also during adulthood. Furthermore, neural progenitor pools are not only crucially important for brain growth but also for patterning. In particular boundary regions are often both progenitor pools and crucial organizing centers. I will focus on one specific boundary region that is a prime example for a boundary region with progenitor pool and organizer properties, the

^a Zebrafish Information Network (ZFIN): www.zfin.org

^b GAL4 is a DNA-binding transcription factor from yeast that is required for the activation of the galactose metabolism (GAL) genes mediating a response to galactose and binds specifically to 'Upstream activating sequences' (UAS)

^c Furtheron just named *Drosophila*

midbrain-hindbrain boundary (MHB), which harbors the Isthmic Organizer (IsO). Then I will proceed with the important topic of how neural identities are defined, in the CNS in general and in the Midbrain-Hindbrain (MH) domain in particular. This issue has been the main focus of the second part of my thesis project.

On these topics, the remaining open questions that my work directly addressed are:

1. What are common features between embryonic and adult progenitor pools in zebrafish and mouse? (see 3.1.1 and 3.1.6)
2. How is the eye field progenitor pool specified? (see 3.1.2)
3. Which factors control neurogenesis at the MHB? (see 3.1.3 and 3.1.4)
4. Which cellular characteristics differentiate the MHB progenitor pool from neighboring proliferating precursor populations? (see 3.1.5)
5. How are neuronal identities specified in the MH domain? (see 3.2)

1.1. Morphogenesis of the zebrafish early embryonic neural tube

The zebrafish egg and early zebrafish embryo divides in a meroblastic fashion, and displays axial symmetry until the onset of gastrulation (“shield” stage) [17-20], which is the first stage at which a fate map could be established. At this stage, in particular, a clear regional fate mapping of the neural plate anlage has been produced, showing that the dorsal part (i.e. located on the same side as the shield) of the blastoderm is the origin of the later neuroectoderm [19,21] (see Figure 2). Starting with the beginning of gastrulation, the cells of the future neural plate converge towards the midline and concomitantly expand along the anterior-posterior axis, driven by convergence-extension movements [22] and active migration [23]. The first morphologically visible processes of neurulation start at early somitogenesis stages after gastrulation is completed. First, the neural plate can be distinguished from neighbouring ectodermal tissue by a characteristic thickening due to the transition of cells from a cuboidal to a more columnar shape [24]. Two lateral thickenings become visible (see Figure 1). Subsequently, at the 6- to 10-somite stage, the neural plate condenses and the two lateral thickenings move towards the midline in an infolding movement. The solid structure that results from these rearrangements is called ‘neural keel’ [25,26]. These morphological movements follow a spatial order in a way that lateral cells end up more dorsal in the keel, while cells that were medial dive to deeper ventral positions [27] (see Figure 1). The keel rounds up and forms a cylindrical structure called ‘neural rod’ that detaches from the adjacent skin ectoderm. Beginning at the 17-somite stage, a neural lumen forms in a secondary cavitation process [24,26]. A peculiarity of the early stages of zebrafish neurulation is the fact that, until lumen formation, ‘mirror symmetric’ cell divisions (also called ‘C-divisions’) give rise to bilaterally positioned offspring cells [27,28].

Already shortly before the central cavity appears, constrictions are formed that subdivide the neural structures in anterior/posterior (A/P) positioned segments, called ‘neuromeres’ [18]. One very prominent example of these constrictions, the isthmus or isthmus constriction, at the MHB, harbors one of the two progenitor pools that I focused on in my thesis project (see 3.1 and 3.2). The isthmus constriction becomes morphologically visible at around 10-15 somites. At the 18-somite stage, 10 neuromeres are visible, whereof the rostral three are the primordia of the telencephalon, diencephalon and mesencephalon. The caudal seven neuromeres, located in the rhombencephalon, are called rhombomeres [24]. While most

neuromeres remain in their anterior-posterior position, the forebrain neuromeres show two peculiar morphological movements that are highly important for the development of eye field progenitor pool^a (see Figure 3), the second of the two progenitor pools that I focused on in my thesis project (see 3.1.2). The medially positioned hypothalamic primordium moves rostrally and thereby divides the eye field progenitor pool into two halves [23] that evaginate from the neural keel starting at the 4 somite-stage [18]. The eye primordium is the first morphologically visible structure of the anterior CNS [18]. During segmentation stages the morphological subdivisions of the brain appear progressively. At 24hpf (hours post fertilization), all major morphological subdivisions of the brain are visible.

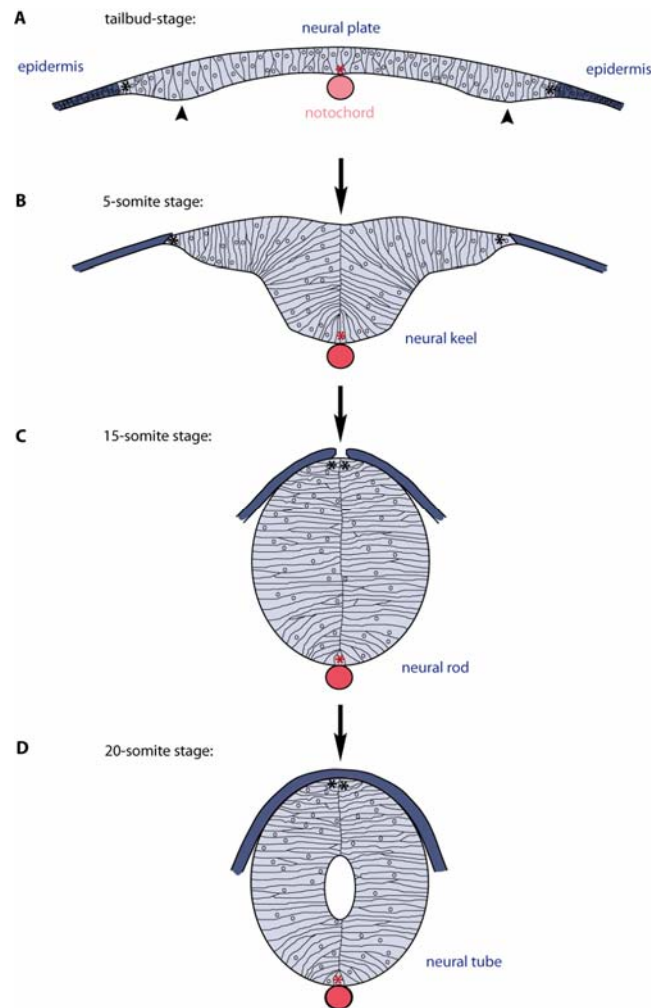


Figure 1: Morphogenetic processes during neurulation in zebrafish. Depicted are schematized optical cross sections through the early zebrafish embryo. Dorsal is up. (A) At the tailbud stage the neural plate is a pseudostratified epithelium that shows two lateral bulges (indicated by black arrowheads) and the epidermis is adjacent to them. Cell membranes are shown as black lines and nuclei as small circles. The notochord is positioned medially and depicted in red. (B) At the 5-somite stage convergent movements towards the ventral midline have formed a ventrally expanded solid neural keel. Note that the lateral bulges have moved towards the midline. (C) At the 15-somite stage convergence movements have seized and an oval shaped solid neural rod has formed. The epidermis closes above the neural rod. (D) At the 20-somite stage a neural lumen has formed by a secondary cavitation process and the epidermis fully covers the neural tube. Note that originally lateral positions at the tailbud stage in (A) end up as dorsal positions at the 20-somite stage in (D) (indicated by black asterisks). In contrast to that, originally medial positions end up as ventral most (indicated by red asterisks). Modified from [24-27].

^a 'eye field' and 'eye field progenitor pool' are used synonymously

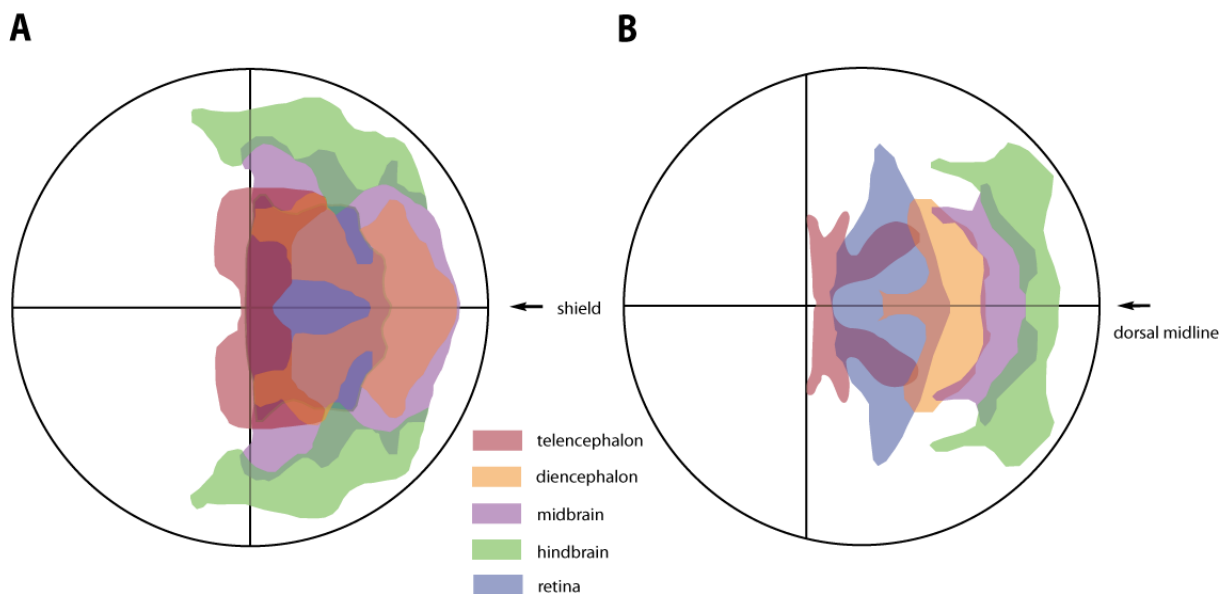


Figure 2: Summary of the early neural fate map of the zebrafish CNS. (A) Fate map of the 6hpf embryo is summarized in one comprehensive figure representing a view onto the animal pole. Black circle denotes the circumference of the embryo. Fate mapped future brain subdivisions are color coded. Note the large degree of overlap of fate mapped regions. Position of the shield is indicated by black arrow. Anterior is to the left. (B) Dorsal view on the the summary of the fate map at 10hpf shows less overlap of color coded future brain regions. Note that the fate map has expanded in anterior/posterior extent. Animal pole is indicated by intersection of the two black lines. Position of the dorsal midline is indicated by black arrow. Adapted from [21].

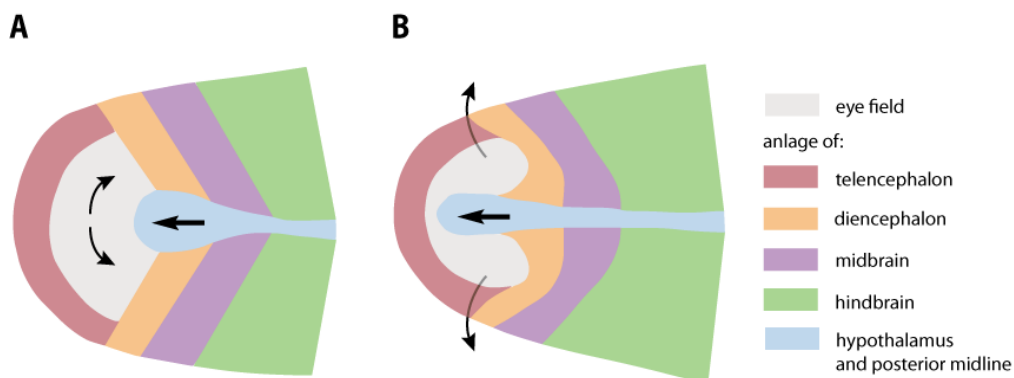


Figure 3: Regional organization of the rostral neural tube. Schemes represent dorsal views onto the rostral neural plate with color coded prospective fate. Anterior is to the left. (A) At the end of gastrulation the eye field is still a single structure broadly spanning the midline of the embryo but starts to separate laterally (indicated by bent black arrows). The hypothalamic primordium is medial and protrudes anteriorly (indicated by single straight black arrow). (B) At a slightly later stage during early somitogenesis the hypothalamic primordium has protruded anteriorly and divided the eye field into two halves that will subsequently leave the brain proper (indicated by bent black arrows). Adapted from [29].

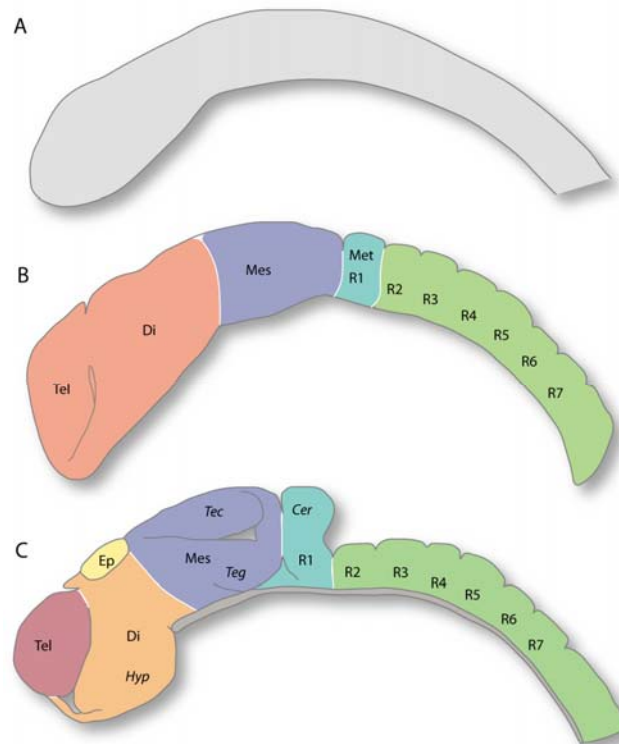


Figure 4: Early partitioning of the zebrafish brain into neuromeres. (A) At 12hpf the brain has no major morphological subdivisions. (B) At 18hpf the developing brain is subdivided into 10 morphological visible neuromeres. The forebrain (prosencephalon, orange) contains the telencephalic and the diencephalic primordium. The MH domain consists of the mesencephalic primordium (dark blue) and rhombomere 1 (metencephalon, turquoise). Note that the rhombomere 1 is also the anteriormost part of the rhombencephalon^a (R1 in turquoise and R2 to R7 in green). (C) At 24hpf brain morphogenesis is advanced and manifold morphological substructures have become visible. All schemes represent sagittal views and anterior is to the left. The eye primordium is not included in these schemes. Modified from [24]. Abbreviations: Cer: Cerebellum, Di: Diencephalon, Ep: Epiphysis, Hyp: Hypothalamus, Mes: Mesencephalon, Met: Metencephalon, R1 – R7: Rhombomeres 1 to 7, Tec: Tectum, Teg: Tegmentum, Tel: Telencephalon.

1.2. Neural induction and early patterning

Vertebrate nervous systems are highly complex structures that are built from a relatively simply organized precursor cell population during the multi-step process of neurogenesis. Neurogenesis, in its broadest definition, comprises the steps spanning from neural induction to the terminal differentiation of neurons and glia [30][26]. Thereby cells progress from a precursor state (= precursor cell, progenitor cell or neuroblast) through a postmitotic, committed state (= early differentiating neuron or early postmitotic neuron) to the differentiated state [26]. It is important to mention that not all cells in the developing nervous system progress through these steps in parallel: while some neurons differentiate early on, giving rise to the primary neuronal scaffold (see Figure 12 and Figure 13), some cells are kept undifferentiated in so called 'progenitor pools' several of which persist into adulthood. The cells in the progenitor pool successively give rise to new neurons and glia at later stages.

^a The metencephalon/rhombomere 1 is sometimes also called 'rhombomere 0'

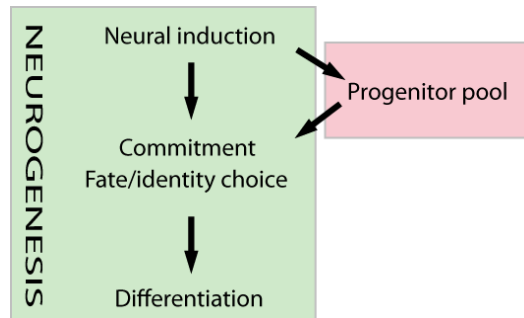


Figure 5: Overview on the phases of neurogenesis. After neural induction neural progenitors can follow a direct pathway leading to differentiation (as depicted in green box). Besides the direct way progenitors can also contribute to a progenitor pool (shown in red box) and later join the differentiation pathway.

1.2.1. Neural Induction

The first step in the neurogenesis cascade that specifies the neural plate is neural induction [31]. This process specifies embryonic ectodermal cells towards the more restricted fate of neuroectodermal cells, i.e. neural stem or precursor cells. This transition is induced by the interplay of several secreted signalling components. The ‘default model’ of neural induction was mainly derived from experiments with the frog gastrula, where it was found that ectodermal cells have the innate tendency to differentiate into neural tissue if they are not inhibited by ‘Bone Morphogenetic Proteins’ (BMP) [31,32]. The BMP inhibitors Noggin, Chordin and Follistatin mediate this protection from non-neural fates. These factors are secreted from cells of the primary organizer^a during gastrulation [33]. In line with this, zebrafish mutations in the *chordin* ortholog *chordino* [34] or in *bozozok*, required for *chordino* expression [35], lead to embryos with a reduced neural plate [33]. In contrast to this, *bmp2b/swirl* [36], *bmp7/snailhouse* [37] and *smad5^b/somitabun* [38] mutations lead to an expanded neural plate.

More recently, evidence for an additional positive active, rather than inhibitory, process in neural induction accumulated [31,39]. In particular Fgfs [40-44] and ‘Insulin-like growth factors’ (Igf) [45,46] have been proposed as neural inducing signals that act even before onset of gastrulation [33] and therefore before BMP inhibition by the primary organizer (see Figure 6A). The integration of these different signals converges at Smad1. Phosphorylation of Smad1 through BMP signalling is activating, while phosphorylation in the Smad1 linker region through Fgf/Igf signalling is repressive [47,48](see Figure 6B). In fitting with this, a new Fgf/BMP neural induction model recently emerged for zebrafish. This new model spatially separates the influence of BMP and Fgf signalling. According to this model, inhibition of BMP signalling is needed to induce more anterior parts of the CNS, while Fgf signalling is responsible for neural induction in more posterior parts with an intermediate region where both are acting [31,43,49-51] (see Figure 6C). Fgf acts as a neural inducing factor via Smad1 inhibitory phosphorylation by the MAPK/Erk^c cascade, but most likely also via a BMP-signalling-independent positive influence on neural gene expression [39,51](see Figure 6B).

^a Primary organizer = Spemann-Mangold organizer; in zebrafish: ‘shield’

^b Small Mothers Against Decapentaplegic (SMAD) in ZFIN nomenclature: *MAD homolog (Drosophila)*

^c Mitogen-Activated Protein Kinase (MAPK); Extracellular-signal Regulated Kinase (ERK)

All these processes modulating neural induction happen before and during gastrulation stages and, in sum, lead to a broad upregulation of the neural plate markers *sox2/3^a* (pre-neural genes/neural induction markers) [26,31]. At the end of gastrulation the responsiveness to neural induction ceases and cells that have been previously induced are now committed to neural differentiation [33] or to the neural progenitor state.

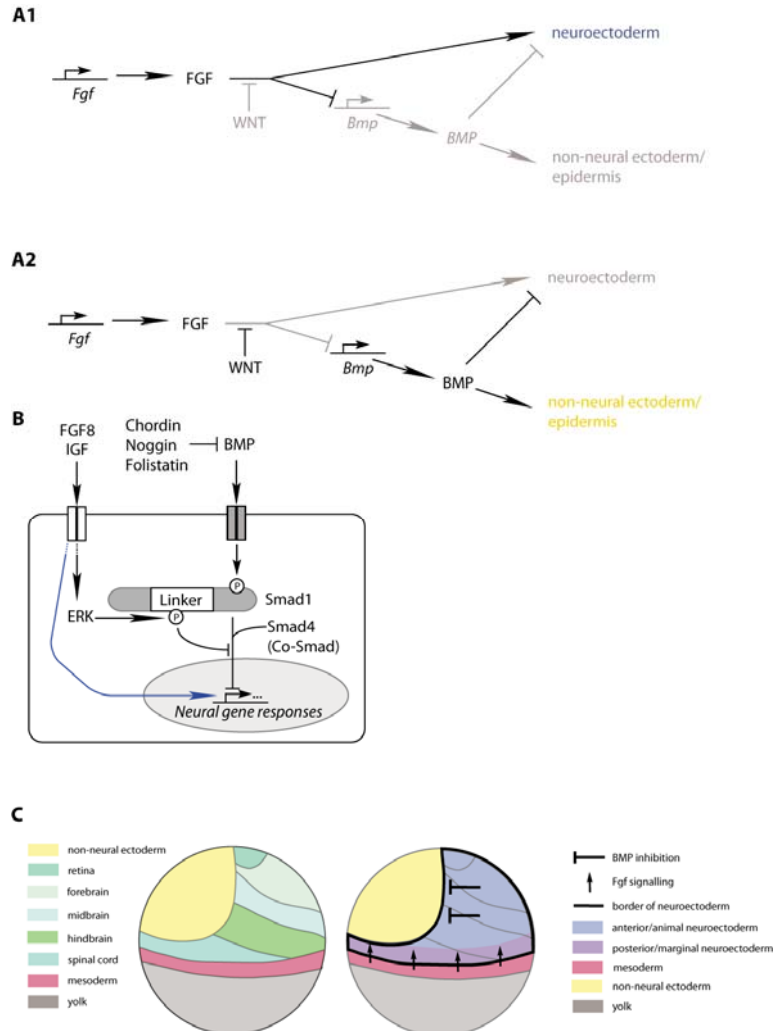


Figure 6: The process of neural induction. (A1) Schematic representation of neural induction pathway as inferred from experiments in chicken [33]. At blastula stages chick medial epiblast cells are a source of FGFs but not Wnts (represented in upper panel). This leads to the induction of neuroectoderm by repression of BMPs and a direct induction of neural tissue (active pathway components in black, inactive components in gray). (A2) In contrast to the medial epiblast cells, lateral cells express both, FGFs and Wnts. The Wnt signal inhibits the influence of FGFs, which leads to a disinhibition of BMPs that induce epidermal fate and block neural induction. Note that in this situation BMP inhibitors are still able to induce neural fate. Adapted from [33]. (B) Extended model of convergence of neuronal induction control on the level of Smad1 phosphorylation. While BMP signalling leads to Smad1 activation and therefore neural gene repression, FGF and IGF signalling blocks the BMP signalling axis by an inhibitory phosphorylation of the Smad1 linker domain. Independently of that FGF and IGF signalling can also directly activate neural gene expression (indicated by blue arrow). Note that inhibition BMP signalling on the extracellular level can also promote proneural gene expression by blocking the BMP signalling axis (classical view of neural induction by BMP inhibition). Adapted from [47][48]. (C) Left panel shows approximate fate map of the early gastrulating zebrafish embryo (color coded). Right panel represents an overlay of this fate map and the two separate neuralizing influences arising from dorsal ectoderm (BMP inhibition; blue zone) and mesoderm (Fgf signalling; violet). Adapted from [51].

^a *SRY-box containing gene (sox)* (ZFIN); *Sex-determining Region of Y* (chromosome) (SRY)

1.2.2. Early anterior/posterior patterning of the anterior nervous system

Following and partially concomitant to neural induction is the establishment of neural plate/tube patterning, and the following section will focus on this process along the A/P axis. It is important to mention that both processes, neural induction and A/P patterning of the early neural plate, are neither clearly separated in time and space nor by the factors that are at play. They are rather happening in concert with each other. One important function of early A/P patterning is the establishment of secondary organizers such as the anterior border of the neural plate (ANB)^a, the zona limitans intrathalamica (ZLI), a Wnt8b^b source in the diencephalon, and the IsO at the MHB. These secondary or local organizers then confer a further refined regional patterning. Importantly, these organizers are in general also progenitor pools.

As this thesis is focused on the eye field and midbrain-hindbrain boundary (MHB) progenitor pools that are both located in the anterior aspects of the CNS I will discuss here only the patterning of the anterior CNS. I will start with the description of forebrain patterning and then consider the patterning processes that set up the MHB progenitor pool and the IsO.

1.2.2.1. Early forebrain patterning

In order to obtain rostral fates, anteriorly located neural progenitors have to be protected from posteriorizing influences [29]. This is accomplished in three ways. Firstly, caudalizing factors are expressed only locally and in posterior positions. Secondly, morphogenetic movements keep anterior parts out of the influence of caudalizing factors. Thirdly, secreted inhibitors of the caudalizing factors are produced in the anterior neural plate. One prominent early caudalizing mechanism is Wnt-signalling. Zebrafish *masterblind* (*mb1*) mutants, which have a mutation in the canonical Wnt pathway component *axin1*, show a striking caudalized phenotype due to over-activated Wnt signalling: diencephalic fates are expanded anteriorly at the expense of telencephalon and eye structures [52,53]. The responsible caudalizing Wnt ligand is most likely Wnt8b that is secreted from the prospective diencephalon at gastrulation stages [54] but other Wnts might contribute as well [29]. Furthermore, loss of function of the negative Wnt regulators *tcf3*^c and *six3*^d leads to similar caudalized phenotypes than observed in *mb1* mutants [55-57]. In zebrafish, anterior neural plate cells are protected from this caudalizing influence by the Wnt inhibitor Tlc^e that is secreted by cells of the ANB, the anteriormost local organizer of the CNS [58]. Tlc is a member of the family of secreted Frizzled Related Proteins (sFRP) [59]. At early stages of gastrulation Tlc is expressed in a broad domain [59] encompassing the common anlage for telencephalon and eye. Taken together, a relatively simple model for initial forebrain patterning can be hypothesized, whereby a caudal high to rostral low Wnt gradient is established [29] and antagonized by a rostral high and caudal low gradient of Wnt inhibitor Tlc. The anlage for telencephalon and eye develops under low (or no) Wnt activity, whereas the diencephalic anlage forms in an area of high Wnt activity (see Figure 7).

^a Also known as anterior neural ridge (ANR)

^b Wingless-type MMTV integration site (Wnt) ; Mouse Mammary Tumor Virus (MMTV)

^c transcription factor 3 (*tcf3*) (ZFIN)

^d *Sine oculis homeobox homolog* (ZFIN)

^e Renamed by ZFIN: *secreted frizzled related protein* (*sfrp*)

Despite intensive work on early forebrain patterning in the last decade, the mechanisms and factors leading to the separation of the initially common eye and telencephalic fields into distinct anlagen remain unknown. This process is of particular interest as it defines the progenitor pool of the eye field as a separate developmental entity. A prime candidate to be involved in this process in zebrafish is the early eye field marker *retinal homeobox gene 3 (rx3)* that arises already at the end of gastrulation [60,61]. Zebrafish *rx3* mutants show a dramatic ‘loss of eye’ phenotype and have therefore been named *chokh (chk)*, which is the Bangla word for ‘eye’. Similar defects have been observed in the *rx3/eyeless* mutant in Medaka [62]. The phenotype has been explained as a failure of eye vesicle evagination [62-64]. Interestingly, the onset of expression of *rx3* precedes the first morphological events of eye vesicle formation of about two to three hours in zebrafish [61]. The crucial question if Rx3 plays an earlier role at the level of forebrain patterning, and in particular in the separation of eye field and telencephalon, remained unresolved in previous studies. This question gets even more interesting in the light of the fact that the early onset of *retinal homeobox gene* expression at gastrulation stages is highly conserved in vertebrate evolution [61,65-67]. Additionally, experiments done in *Xenopus laevis*^a hint towards a crucial importance of Rx genes in the control of early eye field development (see Figure 8). With my analysis of zebrafish mutants that lose the eye field progenitor pool, I could directly address this critical question in forebrain patterning (see 3.1.2).

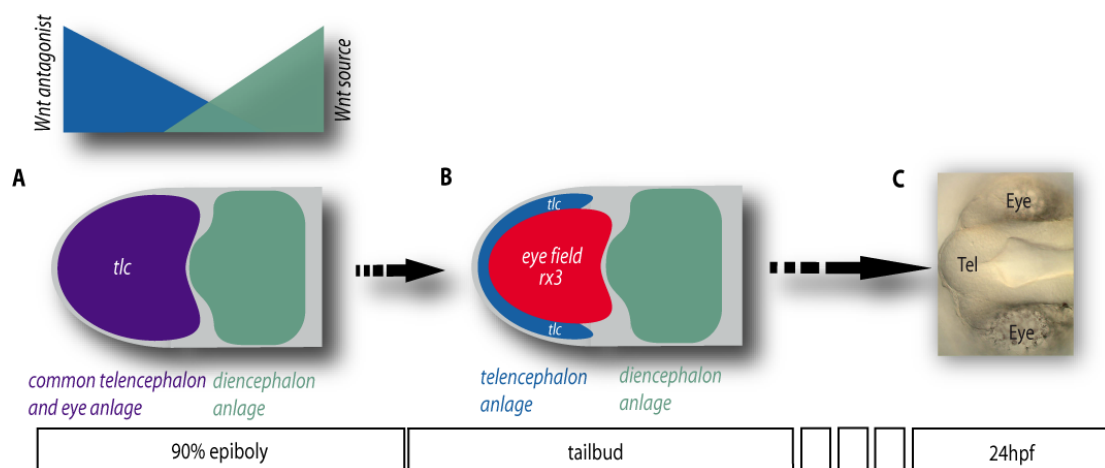


Figure 7: Early forebrain patterning in zebrafish. All panels represent dorsal views and anterior is to the left. (A) At the end of gastrulation the future eye field progenitor pool and the telencephalic primordium are still a common anlage that is marked by *tlc* expression (in violet) and constitutes an area of high Wnt repression (in blue) against a caudalizing Wnt source originating from the diencephalon (in green) as indicated with gradients above the forebrain scheme. (B) Shortly later, at tailbud stage, the sickle shaped telencephalon anlage is still marked by *tlc* expression (in blue) but is separated now from the eye field progenitor pool that has upregulated *rx3* expression. (C) These early patterning processes separating telencephalon anlage from the eye field progenitor pool constitute the basis for an appropriate development of its derivatives, the telencephalon (Tel) and the eyes respectively, shown here at 24hpf.

^a *Xenopus laevis* furtheron in the text called *Xenopus*; note that recently also *Xenopus tropicalis* is used as model organism (very recent data may refer to this species rather than the first)

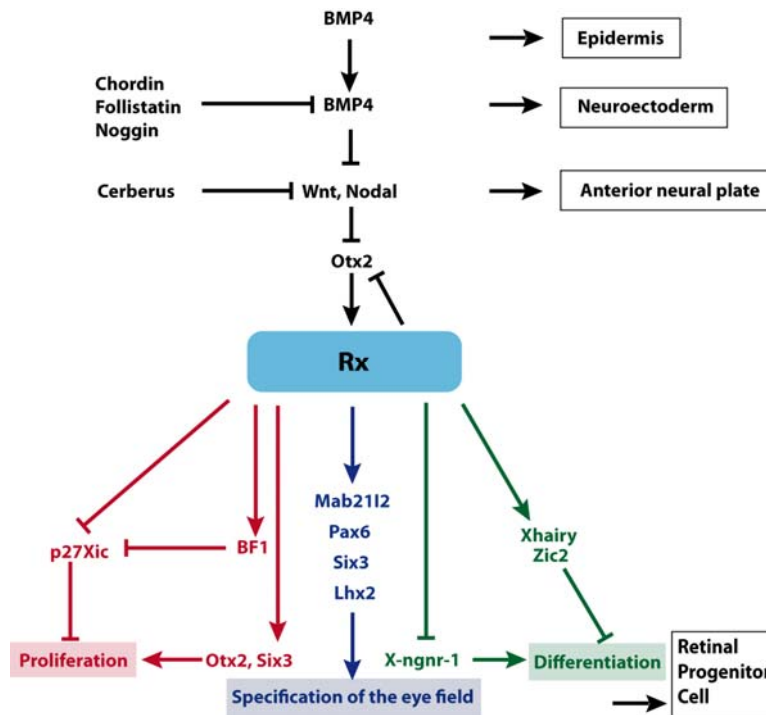


Figure 8: Comprehensive view of the previously described roles of Rx genes in retinal progenitor cell specification in *Xenopus*. Upper part of the panel represents early steps of the classical view of neural induction by BMP inhibition and subsequent steps of early anterior neural plate patterning leading to the induction of Rx expression in the eye field (in black). Note that Rx represents its inducer Otx2. Rx promotes retinal progenitor fate on three main axes. Firstly, it induces proliferation (in red), secondly, it inhibits differentiation (in green) and, thirdly, it promotes specification of eye field fate (in blue). For gene and protein abbreviations please see chapter 6. Adapted from [68].

1.2.2.2. Patterning of the midbrain-hindbrain domain

The progenitor pool at the MHB is of crucial importance for the development of the whole MH domain, i.e. the midbrain and the anterior hindbrain [69]. It does not only give rise to the whole MH domain over time [70] but it also harbours the IsO [71] that plays a central role for patterning the MH domain, giving rise to many important neural structures such as alar parts of the midbrain (inferior and superior colliculi or tectum), the ventral midbrain nuclei, anterior hindbrain nuclei and the cerebellum [72,73].

Quail/chick grafting experiments have clearly demonstrated that posterior mesencephalic structures, when ectopically transplanted within the neural tube, maintain their own fate and, in addition, are capable of inducing ectopic mesencephalic structures and gene expression in competent tissues even as far anterior as the prosencephalon [74-78]. In the converse experiment, where prosencephalic tissue was grafted into the isthmic region, the grafted tissue acquired the MH fate [79]. Furthermore, ablation of the IsO and immediately surrounding tissue leads to a loss of the entire MH domain [80]. Remarkably, in addition to its inductive role, the IsO also has patterning activity. After inversion of a rostral mesencephalic region, excluding the IsO, the tissue polarity is adjusted according to the new environmental cues [81,82]. Therefore, the IsO fulfils all requirements of a classical organizer [83].

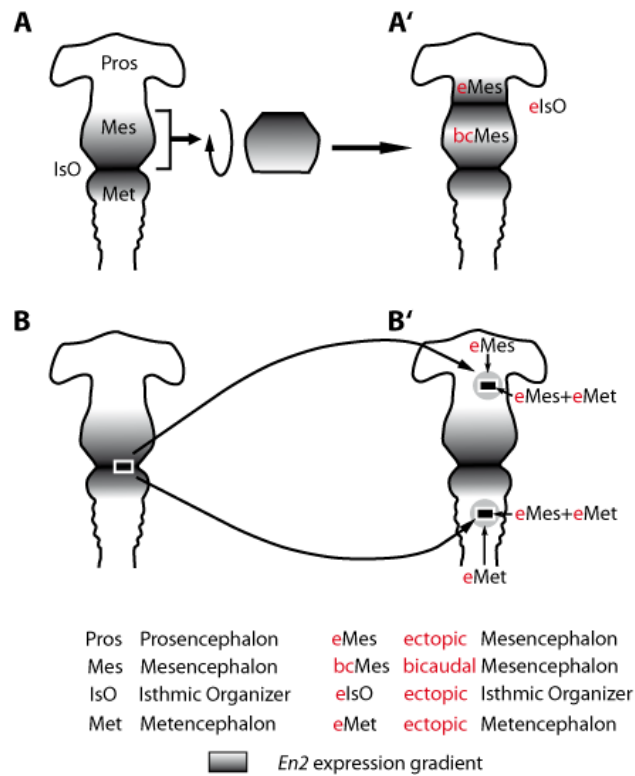


Figure 9: Transplantation experiments in chicken showing the organizer function of the isthmic region. (A) The inversion of the whole mesencephalon primordium at Hamburger-Hamilton (HH) stage 10 leads to a bicaudal midbrain and a transformation of the adjacent caudal forebrain to an ectopic midbrain (see A'). (B) Also the transplantation of a small piece of IsO tissue into competent neighboring non-MH tissues leads to induction of MH characteristic genes (see B'). (All panels are dorsal and anterior is up. Adapted from [82].

These classical transplantation experiments have been the foundation for a precise molecular analysis that has pinpointed several crucial factors involved in IsO positioning, activity and maintenance. Overall, the development of the IsO can be separated into three phases: (i) firstly, an early induction, establishment and specification phase during gastrulation stages, where IsO genes are mainly expressed independently of each other, and, starting at mid-somitogenesis in zebrafish, (ii) secondly, a maintenance phase, where the expression of IsO factors becomes dependent of each other and builds up a 'maintenance loop' [69,84] and thirdly, a late maintenance phase.

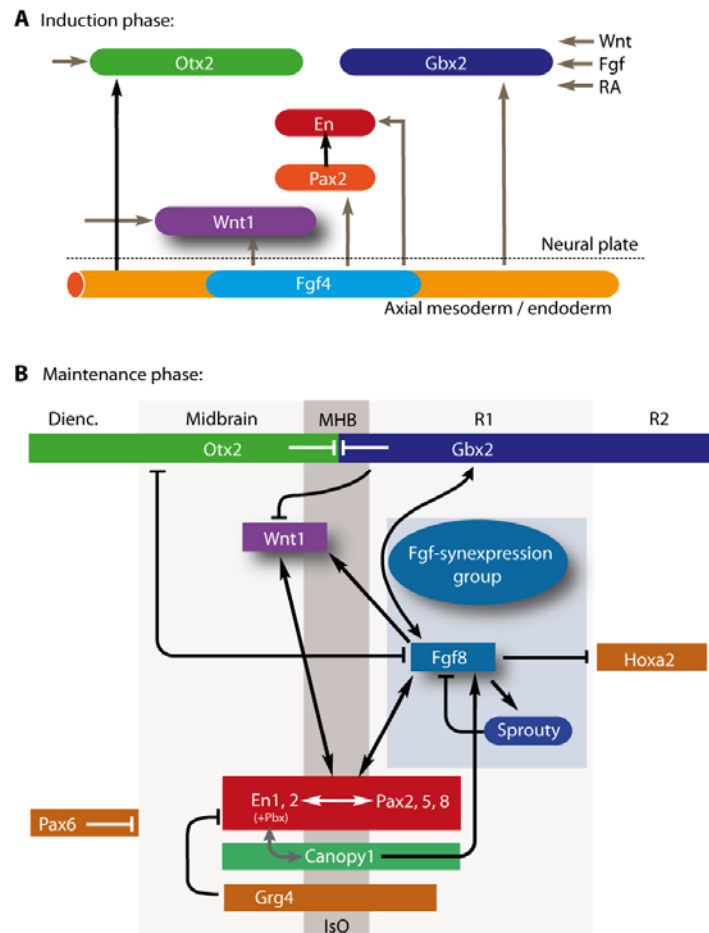


Figure 10: Gene expression and regulation at the MH domain during induction and maintenance phase. Anterior is left in both schemes. Black arrows depict genetic interactions that do not have to be necessarily direct. Gray arrows depict hypothetical interactions. Nomenclature is following the mouse homologs. (A) At neural plate stages initial MH gene expressions are set up within the neural plate. In addition to that inductive signals are also arising from the underlying axial mesoderm and endoderm as indicated below hatched line. (B) During somitogenesis the gene expressions at the MH domain get interdependent and more diverse. A positive regulatory loop is built up ('maintenance loop') that is necessary for MH identity. The *Fgf8* synexpression group is indicated by blue box. For clarity reasons only *Fgf8* itself and one prominent feedback factor (*Sprouty*) are schematized (for details see text). Note that *En1* and *Canopy1* might be coregulated [85] (indicated by gray bent double arrow). For gene and protein abbreviations please see chapter 6. Modified from [69].

Induction phase

Sequence of expression of classical MHB markers

After neural induction at the end of gastrulation, the two homeobox genes *Otx2* and *Gbx2* (*gbx1* in zebrafish) are expressed in a mostly non-overlapping manner in the anterior and posterior neural plate, respectively [69,86-92]. In concordance with the boundary model for secondary embryonic fields [93] a signalling center is induced at the junction of *Otx2* and *Gbx2* expression [69,94]. To which extent the juxtaposition of *Otx2* and *Gbx2* expression itself induces the IsO is still debated. A strong argument against this hypothesis is the fact that *Fgf8* and *Pax2* are expressed even in the absence of both *Gbx2* and *Otx2*. *Gbx2* and *Otx2* might be rather necessary for the spatial refinement of the IsO than for its initial induction [83,95]. The first MH domain-specific gene that starts to be expressed in the tissue at and around the *Otx2/Gbx2*

boundary is *Pax2*, shortly before the start of somitogenesis in mouse [96,97], and within its domain soon follows the expression of the transcription factors Engrailed 1 (En1), Engrailed 2 (En2) and the secreted glycoprotein Wnt1[98-100]. A comparable early phase of MH gene expression has been observed in zebrafish, where *pax2a* starts to be expressed in the MH-primordium at the end of gastrulation [97,101-103], concomitant with or slightly later followed by *eng1a* and the co-expressed gene pair *wnt1/wnt10b* [69,104]. Zebrafish *no isthmus (noi)* mutants have mutation in the *pax2a* locus that leads to a strong impairment of *eng2* expression and a total loss of *eng3* while *wnt1* and *fgf8* appear normal, speaking in favor of an initial independent induction of *pax2a*, *wnt1* and *fgf8* at the MHB [105,106]. In the mouse, a bit later in development, *Pax5* [107] and *En2* start to be expressed in the presumptive MH domain [69,92]. Similarly, in zebrafish *pax5* and *eng2* [108] are next to become expressed in the MH domain. Interestingly, vertebrate *pax*, *en* and *wnt* genes are orthologues of the *Drosophila* genes *paired*, *engrailed* and *wingless*, respectively, that are involved in the definition of posterior compartment boundaries in larval segmentation [109] suggesting an evolutionary conservation of the genes used to define compartment boundaries between *Drosophila* and vertebrates. The secreted factor Fgf8 starts to be expressed in the anterior metencephalon at about the same time as Pax5 and En2 (3-5 somite stage in mouse), but already at the end of gastrulation in zebrafish [84].

Mechanisms and factors known to influence IsO induction

A factor necessary for IsO induction in zebrafish is the POU-domain transcription factor Pou5f1^a that is encoded by the *spiel ohne grenzen (spg)* locus [110,111]. It shows high homology to mouse Oct3/Oct4 and has been reported to be necessary both for the establishment and early maintenance of MHB gene expression [111-113]. Furthermore, an important upstream regulator of IsO induction has been identified in zebrafish by a homology approach. *Bts1* is the homolog of the *Drosophila buttonhead (btd)* gene that specifies the head/thorax junction of the *Drosophila* embryo. The zebrafish *buttonhead/Sp5* gene codes for a Zinc-Finger type transcription factor of the Sp family that is expressed from 70% epiboly onwards within the presumptive MH domain [114]. *Bts1* is both necessary and sufficient for proper *pax2a* induction at the MH domain, but not for the expression of *her5*, *wnt1* or *fgf8*. These findings are in line with the notion that there are several independent cascades inducing the first IsO characteristic gene expressions [114]. In addition, there are influences from non-neural tissues on IsO induction. In chicken it has been shown that Fgf4, secreted transiently from the anterior notochord underlying the future IsO, potentially participates in induction of *En1* in the neural tube at gastrulation stages [115].

Maintenance loop

After initial induction of IsO genes, expression domains get further refined and they start to become interdependent in a complex regulatory network – the so called MHB or IsO ‘maintenance loop’. One important mechanism mediating this genetic loop is the synexpression group of the Fgf signalling components at the MHB, in short ‘*fgf8* synexpression group’ [116-118]. A synexpression group is a group of genes that ‘share a complex spatial expression pattern’ [119]. In terms of signalling pathways, synexpression groups often consist of several positive and negative feedbacks of a

^a POU domain, class 5, transcription factor 1 (ZFIN) previous names: *oct4*, *pou2*

given pathway, which integrate in a synergistic manner to form a stable and concise signalling unit, as is the case for the BMP, Delta and Fgf8 synexpression groups [118]. Because of its central importance for the IsO and therefore for several crucial aspects of my thesis project I will describe the known components of the Fgf8 synexpression group here in more detail (see also Figure 10):

The main ligands of the Fgf8 synexpression group at the MHB are Fgf8a, Fgf8b, Fgf17 and Fgf18 [120-124]. They all belong to the Fgf8 subfamily [125] but have crucial differences in their organizer activities [124] and their onset of expression [123,126,127]. FGF17 and FGF18 are expressed slightly after FGF8 [73]. The central role of Fgf8 in IsO activity has been shown earlier by bead implantation experiments in chicken where beads soaked with Fgf8 were implanted in diencephalic or rhombencephalic tissue leading to the ectopic expression of markers of the MH domain such as *En1*, *En2*, *Wnt1* and *Fgf8* itself [128-130]. Further evidence for the central role of Fgf8 for IsO activity and maintenance comes from Fgf8 overexpression and knockout mice that show a hyperplasia or a gradual loss of the MH tissue, respectively [131,132].

Interestingly, two different splice forms of FGF8, FGF8a and FGF8b, have crucially different patterning activities at the MHB. Significantly, the signalling activity of FGF8b has been quantified as being 100 times stronger than that of Fgf8a [124,133]. A very detailed structural analysis in combination with developmental assays has shown that alternative splicing between FGF8a and FGF8b isoforms leads to one additional contact in the FGF8b ligand/receptor interaction and that mutation of a single amino acid functionally converts FGF8b to FGF8a in chick embryos and mouse midbrain explants. This study showed clearly that binding affinities directly correlate with the patterning activities of the different FGF ligands [124].

Interestingly, zebrafish has not only different *fgf8* splice forms but possesses two *fgf8* paralogs, *fgf8a* and *fgf8b^a* [134-136]. Among the zebrafish *fgf8* family members, *fgf8a* has the more pivotal role in IsO activity. This has been clearly demonstrated by the in depth analysis of the *acerebellar* (*ace*) mutant zebrafish that carry the causative mutation at the *fgf8a* locus. Homozygous *fgf8a* (*ace*) mutants show a complete loss of the cerebellum and of the characteristic MHB fold. MHB marker analysis revealed that *fgf8a* is necessary for the maintenance but not the initiation of the IsO [84].

The crucial mediators of Fgf-signalling that transfer the signal from the extra- to the intracellular space across the cell membrane are the Fgf-receptors (Fgfr). Of the four mammalian Fgfrs, three are expressed within the MH domain [73]. Whereas *Fgfr1* is expressed across the whole extent of the MH domain, *Fgfr2* and *Fgfr3* avoid the MHB [73,122,137-140]. Of these three Fgfrs, *Fgfr1* plays the most central role within the MH domain [140,141]. While experimental inactivation of *Fgfr1* leads to severe defects in MH domain development, *Fgfr2* and *Fgfr3* on their own are not required for proper MH-development in the mouse [142]. Similarly, *Fgfr1* has been reported to be the central receptor for Fgf signalling at the zebrafish MH domain [138]. Furthermore, FGFs associate with cell surface heparan sulphate proteoglycans that might be necessary for Fgf signal transduction and might at the same time prevent long-range signalling [143-146]. Successful binding of Fgf ligands to Fgfr induces Fgfr dimerization and transphosphorylation [73] that leads to activation of Fgf downstream signalling cascades, including the MAPK, phosphatidylinositol-3-kinase (PI-3-K) and phospholipase C-gamma (PLC γ) pathways [147]. Notably, the ligand receptor complex can be internalized and form a so called 'signalling endosome' [148]. The relative roles of these downstream cascades for MH domain development are not yet resolved [73]. Known downstream nuclear effectors of Fgf signalling in the MH

^a Formerly: *fgf17* or *fgf17a*

domain are Erm^a and Pea3^b that are expressed in a gradient like fashion around the MHB [149-151].

Besides the direct signalling axis, several factors have been recently identified that modulate Fgf-signalling positively or negatively and help to fine-tune the signalling system [118] and thereby also guarantee correct IsO activity. Among the attenuators of Fgf signalling are the Sprouty proteins (Spry)^c that are intracellular negative feedback modulators [152-155]. Their expression is induced by Fgf signalling and they act repressively by blocking intracellular Fgf signal transduction [156-158]. Further attenuators of Fgf signalling are the transmembrane protein 'Similar expression to fgf genes' (Sef)^d, that acts repressive on the Ras/Raf/MAPK^e downstream axis of Fgf signalling [116-118,159] and the 'Dual specificity phosphatase 6' (Dusp6)^f that binds and dephosphorylates activated MAPK proteins [160]. All these players work tightly together to build up a stable and refined Fgf signalling center that mediates an important part of IsO activity. This has been described in great detail for embryonic stages in the vertebrate model organisms mouse, zebrafish, *Xenopus* and chicken, but whether this synexpression group also exists at adult stages remains an open question. Together with colleagues in the laboratory, I contributed to address this issue (see 3.1.6).

Canopy – positive feedback for Fgf-signalling

Interestingly, recent studies reported a previously undescribed regulatory input to IsO Fgf signalling. The factor involved is the Saposin-related protein Canopy1 (Cnpy1), a putative positive feedback regulator of Fgf-signalling. Cnpy1 is expressed at the MHB^g both in zebrafish and mouse [85,161], and its expression is induced by Fgf8, as revealed by Fgf8 bead implantations and the loss of Cnpy1 expression in *ace* mutants [161]. Intriguingly, because of its specific MHB restriction^h, Cnpy1 is not part of the Fgf8 synexpression group. Downregulation of Cnpy1 by Morpholino mediated knock down leads to cell death in the MH domain and a loss of the isthmus constriction. MHB marker analysis showed that Cnpy1 plays a pivotal role in the maintenance phase rather than in the induction phase of the IsO. It is an Endoplasmic Reticulum (ER) resident protein that physically interacts with the extracellular partⁱ of Fgfr1 [161], and it acts cell-autonomously on Fgf signalling at the MHB. It has been proposed that Cnpy1 enhances Fgf signalling by maturing and/or modifying Fgfr1 in the ER and/or associated compartments.

Intriguingly, the mouse *Cnpy1* gene is genetically closely linked to the *En2* gene, which could indicate shared genomic regulatory elements [85]. This conspicuous genomic linkage is also conserved in zebrafish where *engrailed 2b* (*eng2b*) is closely linked to *cnpy1*^j. A highly interesting question remains to be solved: as *cnpy1* is obviously not directly part of the Fgf8 synexpression group, how is it integrated in the regulation network of the IsO? Furthermore, no negative regulatory input on *cnpy1* has been identified yet, although it is to be expected that such regulation must exist

^a ETS related molecule (Erm); Erythroblast Transformation Specific (ETS)

^b Polyomavirus enhancer activator (Pea)

^c ZFIN gene name: *sprouty* (*Drosophila*) homolog (*spry*)

^d renamed by ZFIN: interleukin 17 receptor D (*il17rd*)

^e Rat sarcoma (Ras); Rapidly growing fibrosarcoma (Raf); Mitogen-activated protein kinase kinase (MAPK)

^f also known as MAP Kinase Phosphatase 3 (MKP3)

^g there is also transient expression in the polster and weak expression in the tail bud mesenchymal cells of the caudal fin primordial at 26hpf reported [161]

^h there is also transient expression in the polster and weak expression in the tail bud mesenchymal cells of the caudal fin primordial at 26hpf reported [161]

ⁱ corresponds to intravesicular part in the signalling endosome

^j Ensemble Genome Browser (Release 49, Zv7): <http://www.ensembl.org/>

to keep the loop under control. As a starting point to answer these questions, I have contributed to the understanding of this regulatory integration of *cnpy1* into the late IsO regulation with the analysis of miR-9 (see 3.1.4).

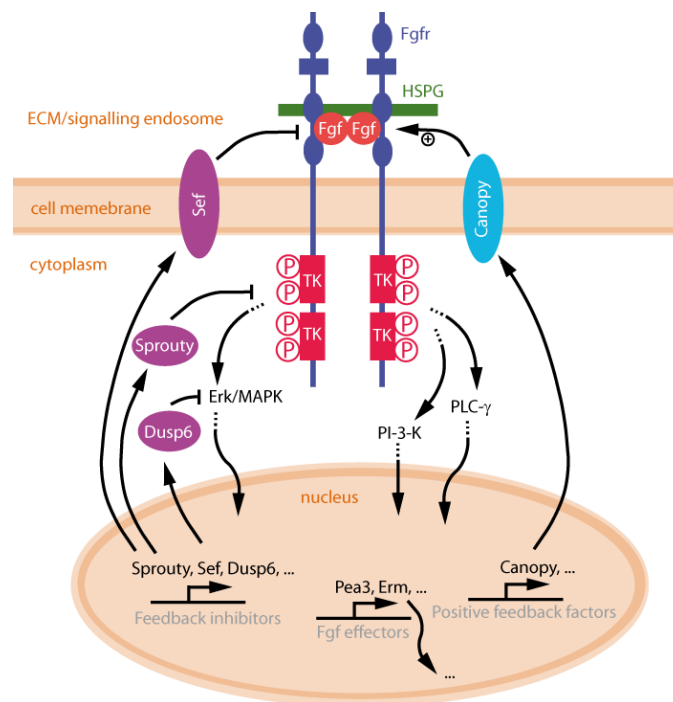


Figure 11: Overview on Fibroblast growth factor signalling components at the MHB. Cellular structures are schematized and named in orange. The Fgf ligands (red) are binding to dimerizing Fgfrs (blue) which are transmembrane receptor tyrosine kinases that get activated upon ligand binding. Note that heparan sulphate proteoglycans (HSPG; green) are co-factors for this activation. The tyrosine kinase moieties (TK; red) of the activated receptor complex start the Fgf downstream signalling cascades by phosphorylating key upstream pathway components. There are several parallel downstream signalling pathways such as the MAPK/ERK, PI-3-K and PLC γ pathways. These cascades ultimately lead to changes in nuclear transcriptional control regulating the expression levels of Fgf effectors (such as Pea3 and Erm), feedback inhibitors (such as Sprouty, Sef and Dusp6) and positive feedback factors (such as Canopy). Note that the active Fgfr signalling complex can be both at the cellular membrane or internalized by a so called ‘signalling endosome’. Modified from [125].

Further players in MHB maintenance

In addition, homeobox transcription factors of the Pbx^a family, the vertebrate homologues of *Drosophila* Extradenticle (Exd), have been shown recently in zebrafish to be involved in MHB loop maintenance as necessary co-factors for Engrailed proteins [162]. A concomitant loss of Pbx2 and Pbx4 function allows normal IsO gene induction but leads to a progressive loss of *eng2a*, *pax2a*, *fgf8*, *gbx2* and *wnt1* expression [162].

Furthermore, the two LIM homeobox transcription factor orthologues *lmx1b.1* and *lmx1b.2* are implicated in MHB maintenance in zebrafish. A concomitant knockdown of these two genes leads to a loss of *wnt1*, *wnt3a*, *wnt10b*, *pax8* and *fgf8* expression at the MHB and it has been proposed that *lmx1b.1* and *lmx1b.2* function is necessary for maintenance of cell survival at the MH domain [163].

^a Pre-B-cell leukemia homeobox transcription factor (Pbx)

Late maintenance phase

Fate tracing analysis in mouse indicates that a lineage restriction boundary is established at the MHB between embryonic day (E) 8.5 and E9.5 [72]. Similarly, in zebrafish starting at late gastrulation a lineage restriction boundary is established at the MHB [164]. Interestingly, in clear contrast to the full *Wnt1* knockout [165], embryos homozygous for the hypomorphic *Wnt1* allele *swaying* (*Wnt1^{sw/sw}*) [166] maintain most of the MH domain but show an intriguing intermixing of midbrain and hindbrain fates around the MHB [167]. This suggests that *Wnt1* is initially required for the specification of midbrain fates and later for separation of midbrain from anterior hindbrain fates and therefore boundary maintenance [69,167].

This speaks strongly for the existence of a separate late MHB maintenance phase whereby the maintenance of the lineage restriction boundary seems to be an important feature. Nevertheless, the molecular mechanisms that control this late phase are still elusive. With the analysis of the role of miR-9 in MHB maintenance, I identified a novel mechanism orchestrating late IsO activity and MHB progenitor pool control (see 3.1.4).

1.3. Neurogenesis control

The IsO has not only an important role in patterning the MH domain but also in sustaining the progenitor pool at the MHB. Although during neural induction the whole neural plate adopts a generic neural fate, the neural plate and its derivatives do not differentiate homogeneously later in development [168-170]. Rather, specific 'proneural clusters' with actively ongoing neurogenesis are separated from 'progenitor pools' where cells stay in an undifferentiated state [26] (Figure 12).

Interestingly, early zebrafish neurogenesis appears in two waves, referred to as primary and secondary neurogenesis. The first wave starts at around 8hpf and builds up a primary neuronal scaffold that enables the early fish larva to conduct first behaviours such as escape reflexes [171]. The early primary neuronal scaffold gets, at least partly, replaced or refined by the secondary scaffold that starts to be built up at around 48hpf. Furthermore, new and more complex circuits are added. Although some processes of neurogenesis control may be different [172] molecular data strongly supports that mostly the same processes are used in the early steps of primary and secondary neurogenesis [26,173-175]. Therefore I focus in the following on the processes of primary neurogenesis.

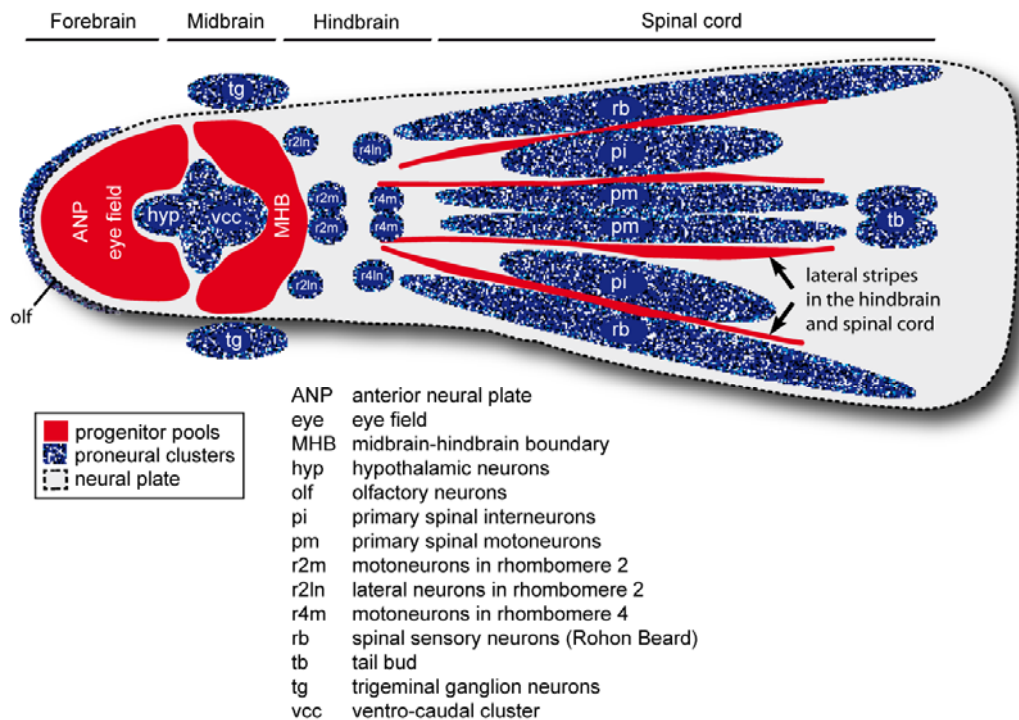


Figure 12: Distribution of proneural clusters and progenitor pools in the zebrafish neural plate. Schematized is a dorsal view onto the neural plate at the 3-somite stage. Proneural clusters are depicted in a blue/white speckle pattern indicating the salt and pepper distribution of progenitors and differentiating neurons. Intermingling zones are progenitor pools (in red). Anterior is left. Note that only a subset of neural plate progenitor pools is depicted. Modified from [176].

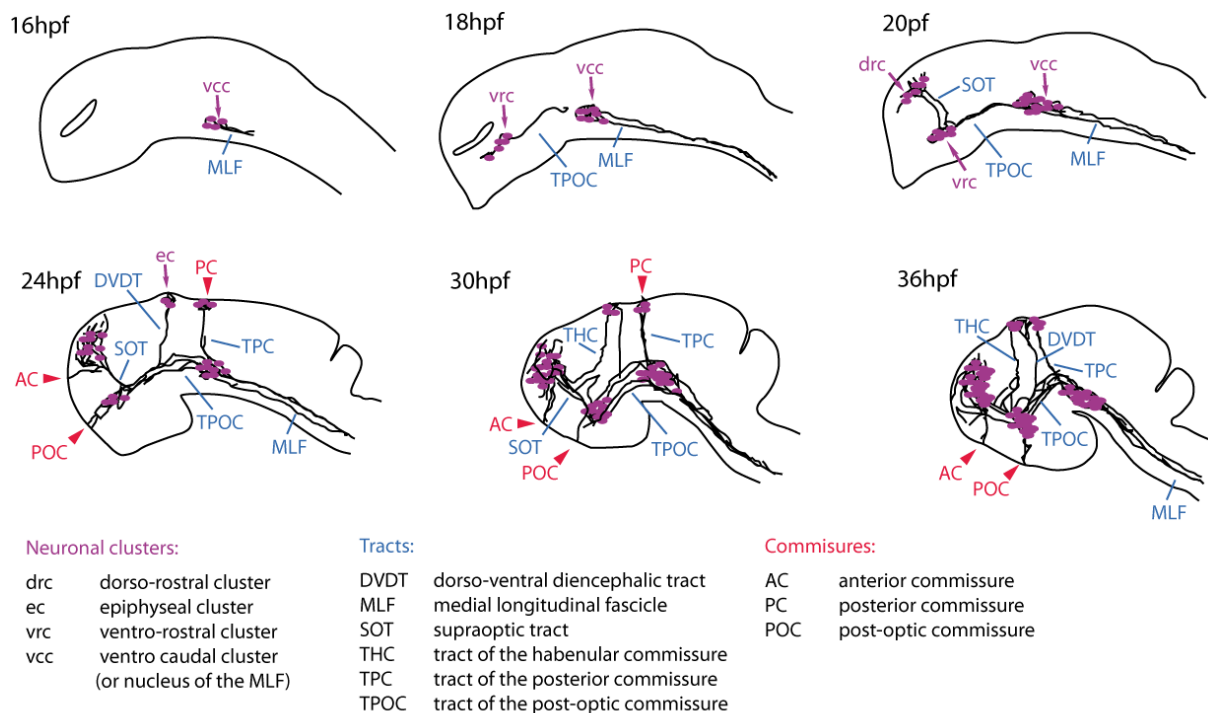


Figure 13: Development of initial tracts and neuronal clusters in the early rostral zebrafish brain. All schemes are sagittal views and dorsal is to the left. The age is indicated on the upper left of the corresponding scheme. Modified from [26,177].

Neurogenesis prepatterning processes

The processes that define the position of proneural clusters versus progenitor pools are grouped under the term ‘prepatterning’ [26]. The expression of prepatterning genes itself is dependent on broader patterning events initiated at earlier stages of development, such as Wnt- and BMP-signalling (see 1.2.1). The prepatterning process links early patterning to localized neurogenesis induction [26]. Prepatterning factors that promote neural differentiation are mainly represented by members of the Sox, Gli, Zic, POU and Iroquois protein families and Geminin [39]. They are first broadly expressed across the neural plate [39]. One crucial and intensively described group of prepatterning genes is the Iroquois homeobox gene family. The *iroquois* (*iro*) genes have been originally described in *Drosophila* as homeobox transcription factors that are prepatterning sensory bristle fields and induce proneural gene activity (see also below) [178]. Iroquois genes have similar roles in vertebrates as described for *Xenopus Xiro1*, *Xiro2* and *Xiro3* that control the expression of proneural genes, such as *Xash-3^a*, *X-ngnr-1^b* and *Xath-3^c* [179,180]. Similarly, in zebrafish the *iroquois* homeobox genes are involved upstream in the regulation of neurogenesis. *irx1b^d*, *irx7^e* are expressed in the early MH domain downstream of Wnt signalling mediated patterning and are required for *neurogenin 1* (*neurog1*) induction [181]. Notably, the downregulation of these two genes leads to a loss of the expression of *eng2*, *pax2.1*, *fgf8* and *wnt1* in the MH domain and further genetic analysis puts them far upstream in the IsO induction process [181]. Moreover, the *Drosophila* bHLH transcription factor coding gene *hairy* has been identified as a prepatterning gene that represses neurogenesis in broad domains [182]. In zebrafish, this repressive prepatterning role is represented by the ‘*hairy and E(Spl) related*’ (*her*) genes *her3* [183], *her5* [170,184], *her9* [185] and *her11* [186]. All these genes are broadly expressed in a partly overlapping manner in progenitor pools, such as the eye field, the MHB, the lateral stripes of the hindbrain and spinal cord (see Figure 12). Similarly, in mouse the ‘*Hairy and E(Spl)*’ (*Hes*) genes *Hes1* and *Hes3* take over this repressive prepatterning role. It is important to note that these genes are not all direct homologs of *Drosophila hairy* but some are rather closely related to the *Enhancer of Split* factors (for details see next paragraphs) [187].

1.3.1. bHLH transcription factors involved in neurogenesis: basic knowledge from *Drosophila*

The original description of proneural clusters and crucial genes involved in neurogenesis comes from research done in *Drosophila*, especially in the peripheral nervous system (PNS) [182]. Interestingly, the basic Helix-Loop-Helix (bHLH) type transcription factors are highly over-represented in the control of neurogenesis in the *Drosophila* PNS [15]. These bHLH factors can be separated into two classes, the repressor type genes on the one hand and the activator type or “proneural” genes on the other hand. Repressor genes contain seven *Enhancer of split Complex* (*E(Spl)*) members and *deadpan*, all being transcriptional repressors and, because of their structural and functional parallels to *hairy*, also called *hairy-related* genes. The

^a *Xenopus achaete-scute homolog-3*

^b *Xenopus neurogenin related-1*

^c *Xenopus atonal homolog-3*

^d *Iroquois homeobox protein 1, b* (ZFIN)

^e *Iroquois homeobox protein 7* (ZFIN)

common feature of *hairy*-related genes is the four amino-acid motif WRPW at the very C-terminus that binds the repressor protein Groucho [188]. Activator genes foster a sensor-hair or neuronal fate including *daughterless* and four *achaete-scute* complex (AS-C) members (*achaete*, *scute*, *lethal of scute* and *asense*) and *atonal* [182].

Furthermore, the selection of cells that undergo neurogenesis in *Drosophila* is mediated by the process of lateral inhibition via the Delta/Notch pathway. When the Notch receptor gets bound by the Delta ligand, the intracellular domain of Notch (NICD) is cleaved off and translocates to the nucleus where it activates Suppressor of Hairless (Su(H)). This upregulates the expression of Notch downstream effectors, such as the members of the *E(Spl)* family that subsequently repress proneural activity, such as genes of the AS-C and *atonal* [26,189]. In contrast to this, cells that are highly expressing Delta ligands keep a high level of proneural factors and Delta expression. Stochastic processes are thought to produce initial small differences in this system that get amplified by lateral inhibition and finally result in a salt and pepper pattern of cells undergoing neurogenesis and cells kept back in a progenitor state [26].

1.3.2. The basic helix-loop-helix transcription factors

The common feature of most proneural genes is that they share a highly conserved bHLH domain [16,190,191]. Proneural bHLH proteins build heterodimeric complexes with ubiquitously available bHLH interaction partners of the Daughterless (*Da*)/E-Protein^a family to specifically bind DNA recognition sites [16]. The protein/protein interaction is mediated via the helices of the bHLH domain, resulting in a four helix bundle [192]. Many bHLH transcription factors are activators of transcription but there are subclasses of bHLH factors that mainly act as repressors, such as the Hairy and E(Spl) factors.

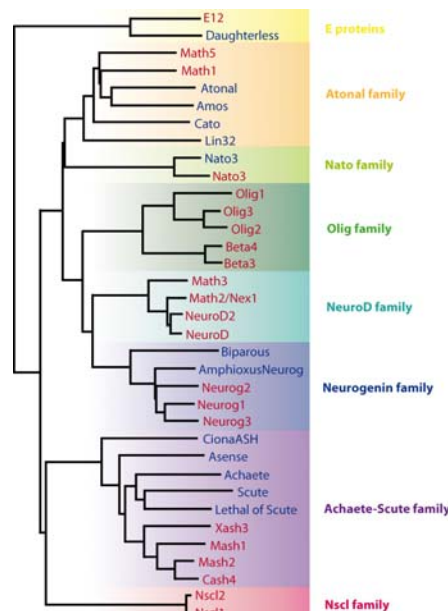


Figure 14: Families of neural bHLH transcription factors. Proteins are grouped according to their bHLH domain sequence similarities. Protein families are color coded. Invertebrate proteins are written in blue and vertebrate proteins in red. Adapted from [16].

^a Mammalian homologues of *Drosophila Da* are: E12, E47, HEB and E2-2 [16]

Proneural genes

Proneural genes code for transcription factors that promote a neural fate. Interestingly, a large majority of these factors belong to the bHLH transcription factors. These can be grouped into two large subfamilies according to their sequence relationship and the origin of their description in *Drosophila*: the *atonal* (*ato*)^a and the AS-C family^b. The vertebrate homologues of these *Drosophila* genes have very similar proneural activity, for example the mouse homologues *Mash1*, *Neurog1*, *Neurog2* [193] and most likely also *Math1* and *Math5* [16]. Similarly, the zebrafish corresponding homologues *neurog1*^c [194,195], *neurog3*^d [196], *ascl1a*^e [197], *ascl1b*^f [197], *atoh1a*^g [195,198], *atoh1b*^h [199], *bhlhb5*ⁱ [199] and *neurod4*^j [200] are expressed in proneural domains or differentiating neurons. In addition, the non-basic HLH factor *coe2*^k is expressed in these domains [201]. Proneural activity has been shown experimentally in zebrafish for *neurog1* [194,195]. Proneural proteins specifically bind to DNA sequences that contain an E-Box with the core hexanucleotide motif CANNTG [187].

1.3.3. *Hairy* and *E(Spl)* genes in vertebrates

In *Drosophila* the pre patterning factor *Hairy* (and *Deadpan*) is clearly separated from the lateral inhibition mediating *E(Spl)* factors in terms of sequence relationship. This is not the case for the vertebrate homologs. In mammals they are grouped together under the name ‘*Hairy and E(Spl)*’ (*Hes*) factors and in zebrafish under ‘*Hairy and E(Spl)* related’ (*Her*) factors [187]. Therefore it is important to note that in zebrafish, for example, pre patterning factors, such as *Her5* and *Her3*, cannot be separated from lateral inhibition mediating factors, such as *Her4*^l, just based on their sequence relationships (see Figure 15).

^a first described to be necessary for the specification of internal proprioceptors (chordotonal organs) in *Drosophila* [16]

^b first described to be necessary for the patterning of external sense organs (*chaete/hair*) in *Drosophila* [16]

^c *neurogenin 1* (ZFIN)

^d *neurogenin 3* (ZFIN)

^e *achaete-scute complex-like 1a* (*Drosophila*); formerly: *ash1a* (ZFIN)

^f *achaete-scute complex-like 1b* (*Drosophila*); formerly: *ash1b* (ZFIN)

^g *atonal homolog 1a* (ZFIN)

^h *atonal homolog 1b* (ZFIN)

ⁱ *basic helix-loop-helix domain containing, class B, 5* (ZFIN); formerly known as: *beta3.1*

^j *neurogenic differentiation 4* (ZFIN); formerly known as *zath3*

^k *Collier/Olf-1/EBF*; formerly known as *zcoe2* (ZFIN)

^l *her4* has recently been renamed *her4.1* to account for the identified paralog which has been named *her4.2* (ZFIN)

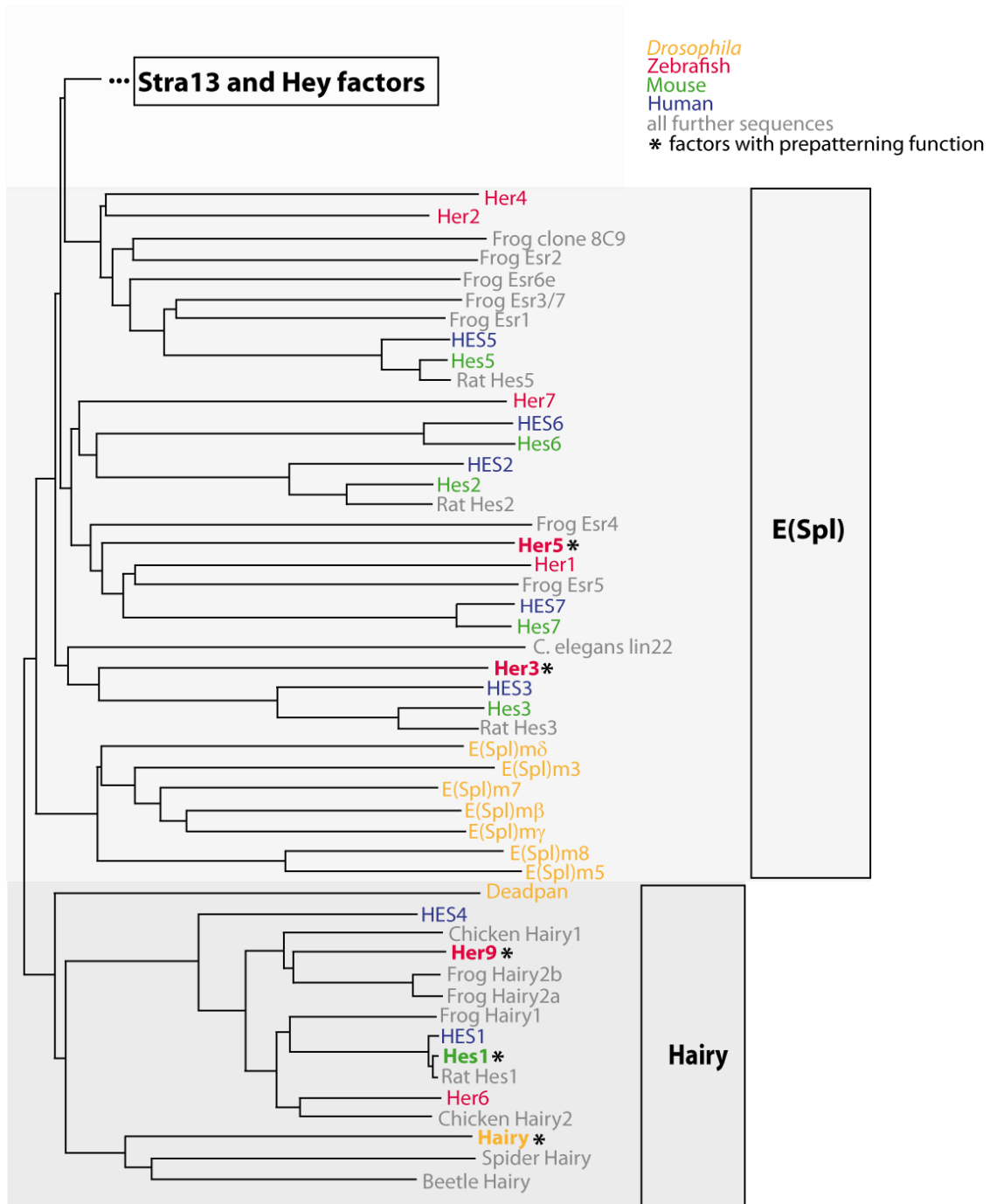


Figure 15: Protein sequence relationships of bHLH-O factors. Animal from which the sequence originates are color coded. Zebrafish factors with pre patterning function are indicated by asterisk. Note that zebrafish pre patterning factors Her3 and Her9 are part of the E(Spl) family and not the Hairy family. Modified from [187].

All these factors share as a common sequence feature the tandem arrangement of a bHLH domain and an 'Orange' domain. The Orange domain serves as protein binding platform and can mediate repressive functions [202]. Because of these shared feature the Hairy and E(Spl) factors are as also named 'bHLH-Orange' (bHLH-O) factors [187]. A further feature of bHLH-O proteins is their carboxy-terminal WRPW^a domain that can bind the co-repressor Groucho [202] (see Figure 16).

^a 'WRPW' stands for the four C-terminal amino acids (Tryptophan-Arginine-Proline-Tryptophan)

^c Vertebrate orthologues of *Drosophila* Groucho are the 'Transducin-Like Enhancer of Split homolog, *Drosophila*' (TLE1 – 4) in mammals and Groucho 1 and Groucho 2 in zebrafish

bHLH-O factors can bind to both E-boxes (see above) and/or N-boxes that have the common core sequence CACNAG [187]. bHLH-O factors can mediate their repressive function in several different ways (see Figure 17). The most common mechanism is the recruitment of Groucho^c/TLE co-repressor proteins in order to build a quaternary repressor complex that directly binds to the DNA of regulated loci [187,202] (see Figure 17A). In addition, the Groucho/TLE bHLH-O complex can also bind and repress DNA-bound transcriptional activators [202] (see Figure 17B). Furthermore, hetero-dimerization of proneural factors with repressor bHLH-O partners can block proneural transcriptional activity by forming heterodimers that lack DNA-binding capabilities [16] (see Figure 17C). bHLH-O factors can also repress transcription without binding to DNA sites themselves but by protein-protein interactions with transcriptional activators that thereby get repressed or even inhibited from binding to DNA [187,202] (see Figure 17D). Finally, bHLH-O dimers can also repress proneural factors by competitively binding to shared DNA binding sites [187] (see Figure 17E) or sequestering the activator complex without Groucho/TLE (see Figure 17F).

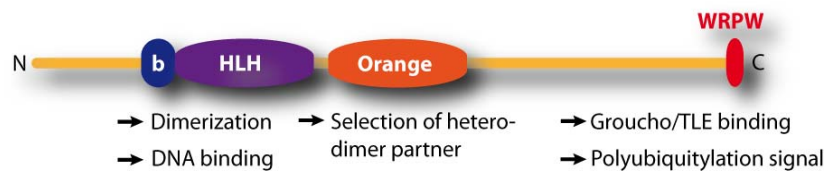


Figure 16: Domain structure of E(Spl)/bHLH-O factors. The corresponding functions of the domains are given below the domain. Note the tandem arrangement of the bHLH and Orange domain. Adapted from [203].

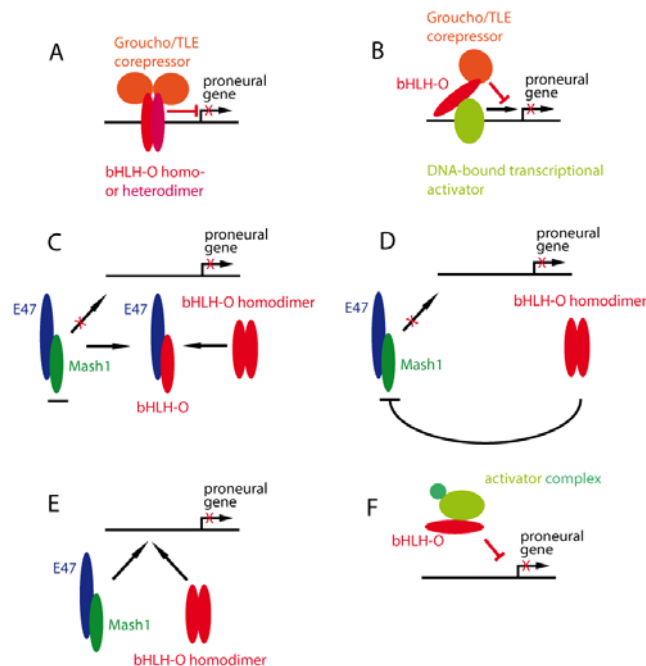


Figure 17: Models of transcriptional repression of bHLH-O proteins. bHLH-O factors are shown in red. (A) The bHLH-O homodimer or heterodimer can bind Groucho/TLE co-repressors and thereby block proneural gene transcription. (B) bHLH-O factors in conjunction with Groucho/TLE co-repressors can also inhibit DNA-bound transcriptional activators. (C) A competitive binding and sequestration of E47 can block proneural factor activity. (D) bHLH-O homodimers can either directly block proneural factor/E47 heterodimers from binding their targets or competitively bind to their targets (E). (F) A single bHLH-O factor can also sequester activator complexes. Adapted from [187,202].

1.3.4. Delta/Notch signalling and lateral Inhibition in vertebrates

The process of lateral inhibition is important to select single progenitors to undergo neurogenesis, while neighbouring progenitors are repressed from a neural fate and remain in their progenitor state. Above I already briefly described the Delta/Notch-mediated lateral inhibition mechanism as it has been originally discovered in *Drosophila*. Here I want to focus on the Delta/Notch pathway and lateral inhibition in vertebrates.

Notch is a single-pass transmembrane receptor that gets activated by being bound by the Delta/Delta-like/Jagged/Serrate ligands, which are themselves single-pass transmembrane proteins present at the surface of neighbouring cells. The ligand/receptor interaction is followed by two events of Notch cleavage, mediated firstly, by the ADAM10/TACE^a (S2-cleavage), and secondly, by the γ -secretase enzymes (S3-cleavage) [204]. The 'Notch intracellular domain' (NICD) is then free to translocate to the nucleus where it interacts with the DNA-binding factor RBPJ κ /CBF1, the vertebrate counterparts to 'Suppressor of Hairless' (Su(H)) in *Drosophila*. Before NICD binding, RBPJ κ /CBF1 is normally associated with co-repressors, such as CtBP. Binding of NICD expels the co-repressors and mediates further binding of co-activators, such as Mastermind/MAML and p300/CBP, to the protein/DNA complex that now is capable of inducing transcription of target genes (see Figure 18). Notably, crosstalks between Delta/Notch and other pathways, such as BMP/TGF- β , JAK-STAT and Ras pathways, that enhance E(Spl) gene transcription, have been reported. Furthermore, Notch can also signal via non-RBPJ κ /CBF1/Su(H) mediated pathways, such as interaction with the Wnt-pathway via the Wnt-repressor Dishevelled [205] or during asymmetric cell division via the RNA-binding protein Musashi [202,206-208]. The protein activity, but not the transcription, of the RNA binding protein Musashi is regulated by Notch. This has originally been described in *Drosophila*. Musashi itself binds to the mRNA of the Zinc-finger transcriptional repressor Tramtrack69 and thereby regulates the translation of its target and thereby the neuronal versus non-neuronal lineages choice via asymmetric division control [206,209]. How far these processes are also used in vertebrates is still elusive.

Similar to *Drosophila*, in zebrafish, several neurogenic mutants that map to members of the lateral inhibition cascade have been described: *deltaA* (*dla*) [210], *after eight* (*aei*) mutants have mutations in the *deltaD* (*dld*) gene [211] and *deadly seven* (*des*) mutants have the causative mutation in *notch homolog 1 a* (*notch1a*) [212]. They all show a moderate increase in their number of neurons, a mild phenotype most likely due to redundancy of Notch and Delta paralogs [26]. On the contrary, *mind bomb* (*mib*)^b mutants, which carry a mutation in a RING ubiquitin ligase mediating Notch cleavage, show a much stronger neurogenic phenotype [213]. Again, similar to *Drosophila*, loss of function mutations in neurogenic genes such as *neurog1* [184,214,215] lead to a reduction in the number of neurons in zebrafish. On the other hand, experimentally increased Delta activity leads to exaggerated high level of *neurog1* transcription in proneural clusters [216-219]. Furthermore, blocking γ -secretase activity with the specific chemical blocker DAPT^c [220] leads to a loss of functional Notch signalling and a strong neurogenic phenotype due to abolished lateral inhibition [221]. Altogether, lateral inhibition is necessary to select only a

^a A Disintegrin And Metalloproteinase (ADAM); Tumor necrosis factor-Alpha-Converting Enzyme (TACE)

^b Formerly known as *white tail* (*wit*) (ZFIN)

^c N-[N-(3,5-difluorophenacetyl)-l-alanyl]-S-phenylglycine t-butyl ester

subset of progenitors to undergo neuronal differentiation, a mechanism that has been highly conserved between *Drosophila* and vertebrates.

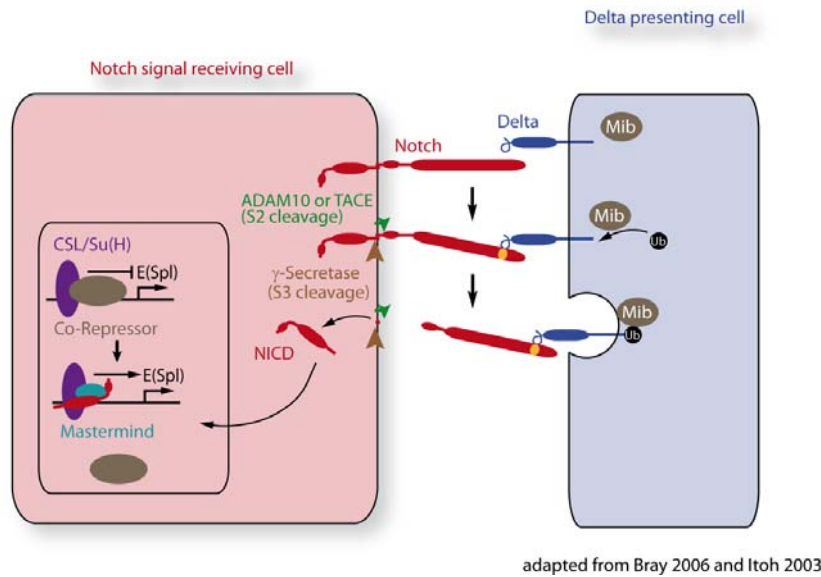


Figure 18: The core of the Delta/Notch signalling pathway. Binding of Delta on one cell to Notch of a neighboring cells leads to the induction of sequential S2 and S3 proteolytic cleavage events that free the Notch Intracellular Domain (NICD). NICD is now free to translocate into the nucleus where it binds CSL/Su(H) and replaces co-repressors. Therefore previously repressed E(Spl) gene loci are now actively transcribing. Note that 'Mind bomb' (Mib) supports the cleavage process by mediating the internalization of the remaining Delta/Notch protein complex into the Delta presenting cell by a process called transendocytosis. Modified from [204,213].

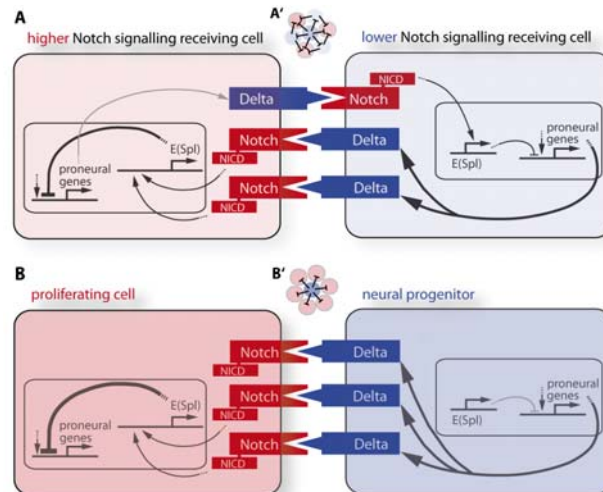


Figure 19: Lateral inhibition in neuronal differentiation. (A') Initially cells show only small differences in Delta and Notch levels. By the process of lateral inhibition one cell in a cluster gets singled out and expresses increasingly high levels of Delta and thereby more and more represses neighboring cells from doing so (B'). (A) Activation of Notch by Delta leads to internalization of NICD and subsequently to the expression of E(Spl) factors that repress proneural gene transcription (see also Figure 18). This leads to lower levels of Delta expression in the higher Notch signalling receiving cells (red; represented by left cell). In the lower Notch signal receiving cells (blue; represented by right cell) E(Spl) factors are less active and therefore proneural genes are more active leading to higher Delta levels. (B) This leads to a positive feedback that results in highly Notch presenting cells (represented by left cell) that stay proliferative and highly Delta presenting cells that undergo neuronal differentiation (represented by right cell).

1.3.5. Non-canonical *her* genes in zebrafish and *Hes* genes in mouse

1.3.5.1. Zebrafish *her* genes

In zebrafish, the classical pathway of *her* gene induction occurs via lateral inhibition, where NICD translocated to the nucleus induces expression of canonical *her* genes, such as *her4*, which subsequently leads to repression of *neurog1* transcription and prevents the expressing cells from undergoing neuronal differentiation [222].

Interestingly, there are also several ‘non-canonically’ induced *her* genes in zebrafish. These genes repress neurogenesis but do not need Notch signalling for their induction [170,183-186]. On the contrary, upon ectopic activation of Notch signaling, these genes rather become repressed. These non-canonical *her* genes are prominently expressed in progenitor pools, i.e. zones with delayed neurogenesis and free of Notch/Delta signalling.

Up to now four non-canonical *her* genes have been described: *her3*, *her5*, *her9* and *her11* [170,183-186]. All four of them are expressed in an overlapping manner within the MHB progenitor pool (for details see Figure 32). At early somitogenesis *her3* is expressed in two longitudinal stripes parallel to the midline in the hindbrain and spinal cord and reaches into the medio-lateral region of the MHB-progenitor pool [183]. Similarly, at early somitogenesis *her9* is expressed in longitudinal domains, i.e. the lateral and intermediate stripes, constituting inter-proneural domains. It is also expressed along the midline in the hindbrain and spinal cord, as well as in additional domains such as the midbrain, placodal fields and the eye field progenitor pool [223]. I found out that *her9* expression covers the anterior part of the MHB progenitor pool (see Figure 32 and Figure 37). The CNS expression of *her5* is limited to the MHB progenitor pool, where it is necessary for inhibition of neurogenesis [170,184,224]. In a similar way, the genetically closely linked gene *her11*^a is expressed across the MHB progenitor pool and is also necessary for repression of neurogenesis. In isolation, each of the latter two genes is necessary for maintaining neuronal inhibition across the medial aspect^b of the MHB progenitor pool. However, when both genes are invalidated, ectopic neurogenesis spreads into the entire MHB pool. Hence, *her5* and *her11* have redundant functions to repress neurogenesis across the MHB progenitor pool [186]. How the activity of Her5 and Her11 is sensed differently by medial and lateral cells of the progenitor pool (i.e. the threshold of inhibition being higher in medial than in lateral cells to maintain the pool) is a question that is addressed in this thesis (see 3.1.3).

1.3.5.2. *Hes* genes in the mouse

Expression domains

In the mouse model, the expression and function of E(Spl) genes in the nervous system have been intensively studied. There are seven *Hes* genes known in mouse, but only *Hes1*, *Hes3* and *Hes5* (*Hes1/3/5*) are expressed in neural progenitors [203]. *Hes1* and *Hes3* but not *Hes5* are already expressed at the neural plate stage [225].

^a also known as *her5 image (him)* (ZFIN) [186]

^b also referred to as Medial Intervening Zone (MIZ), while the lateral aspect is called Lateral Intervening Zone (LIZ)

^d MicroRNA nomenclature is still controversial;

in the following used if appropriate: miRBase nomenclature (<http://microrna.sanger.ac.uk/>)

During the transition from neuroepithelial progenitors to radial glial progenitors at around E8.5, *Hes3* expression decreases and *Hes5* expression starts. *Hes3* gets more and more restricted to the IsO during the neural tube stage. At the same time *Hes5* expression increases [203]. This leads to a complementary expression of *Hes1* and *Hes5* [225]. At E10.5 nearly the whole CNS shows *Hes1* and/or *Hes5* expression [203]. Finally, *Hes1* and *Hes5* expression get localized only to the ventricular zone where the radial glial cell bodies are situated [226,227].

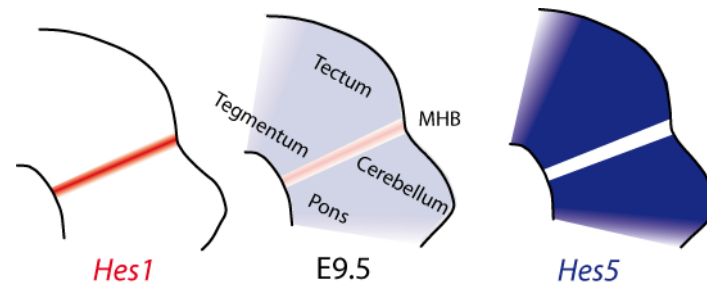


Figure 20: *Hes1* and *Hes5* expression domains in the MH of the E9.5 mouse brain are mutually exclusive. Gene expression domains are color coded. Note that *Hes1* is highly expressed at the MHB where *Hes5* has a clear gap of expression. Rostral is left. Modified from [225].

Roles in neurogenesis

Experimental depletion of these genes first leads to increased levels of proneural gene activity, followed by loss of neural progenitors and premature differentiation [228]. These genes are at least partially redundant, as they can complement each other in single and double knockouts [229]. *Hes1/3/5* compound knockouts show a strong penetrant premature differentiation phenotype [225]. Interestingly, the neuroepithelial cells are first properly formed, but are not maintained in these triple knockouts. This indicates that *Hes1/3/5* are necessary for maintenance but not for induction of neuroepithelial cells [225]. Interestingly, a loss of *Hes1* and *Hes3* leads to premature differentiation and finally loss of IsO gene expression such as *Fgf8*, *Wnt1* and *Pax2/5*, indicating that *Hes1* and *Hes3* prevent premature neurogenesis and are necessary for the maintenance of IsO activity [230]. Gain of function experiments with these *Hes* genes inhibit neurogenesis and lead to a prolonged maintenance of the neural stem cell pool [231,232].

Roles at boundaries

An interesting observation is that the above mentioned *Hes* genes are crucially involved in the maintenance of boundary populations, such as the progenitor pool at the MHB [203,233]. Initial upregulation of *Hes1* and *Hes3* in neuroepithelial cells happens in the absence of Notch signalling, indicating that these two genes can follow a Notch-independent mode of regulation. They become however later dependent on Notch signalling, speaking for an yet unidentified switch in regulation of gene expression within the E(Spl) family. In contrast to that, *Hes5* is upregulated together with Notch signalling components, indicating that *Hes5* is dependent on Notch signalling from the onset of its expression [203]. Significantly, NICD is unable to inhibit neurogenesis in the absence of *Hes1* and *Hes5* [229].

Cyclic regulation of expression

In particular *Hes1* shows an additional regulation phenomenon. It is both expressed at neural tube boundaries (such as the MHB, or interrhombomeric boundaries) and at neighbouring 'compartments', i.e. regions that undergo neurogenesis but also contain a cycling progenitor population similar to proneural clusters in zebrafish. While *Hes1* is persistently highly expressed in boundary regions, it is expressed at periodically changing lower levels in compartmental progenitors [203]. The periodicity of its expression is at least partly controlled by a self-regulatory feedback loop and the high instability of the transcript and protein. As the *Hes1* promoter has N-box-type binding sites for *Hes1* itself [234], initial *Hes1* upregulation next represses its own transcription. This leads to an autonomously induced cycling with a periodicity of about two hours [235]. Notably, this periodic expression pattern was found in fibroblasts in cell culture, in cells of the presomitic mesoderm (PSM) as well as neural stem cells [235-238]. The cycling characteristics of *Hes1* expression is functionally relevant, as enforced high expression of *Hes1* in compartment cells inhibits neuronal differentiation and at the same time lengthens the G1 phase of the cell cycle [233,239]. Interestingly, *Neurog2* and *Delta-like1* (*Dll1*) were also found to show a periodic cycling [238].

Similarly to the situation for *her3/5/9/11* in zebrafish, the factors that regulate the initial, Notch-independent expression of *Hes1* and *Hes3* in the mouse remain enigmatic [203]. Furthermore, how the function of the four non-canonical *her* genes in zebrafish relates to that of *E(Spl)* genes in mouse and other vertebrate model organisms remains an open question. I have addressed this point in my thesis by reviewing and comparing current knowledge about *E(Spl)* genes in neural progenitor populations in zebrafish and mouse (see 3.1.1).

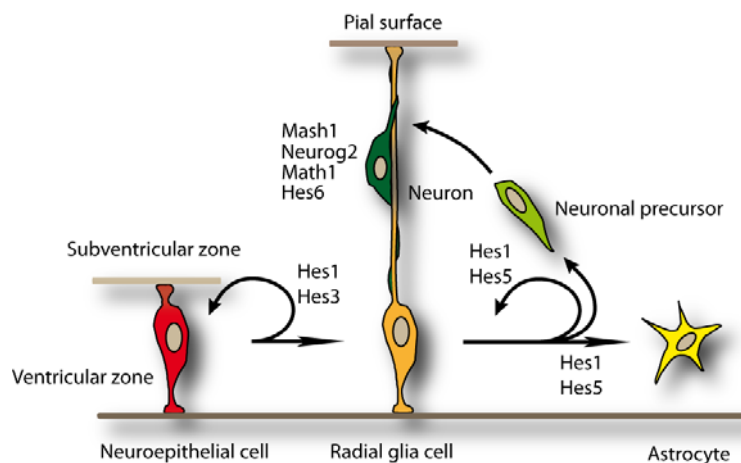


Figure 21: Overview on the role of mouse Hes factors in neurogenesis. Highly proliferative neuroepithelial cells (red) express the repressor type bHLH genes *Hes1* and *Hes3*. Later in development progenitors show radial glia character (orange) that express *Hes1* and *Hes5* and produce neurons (green) by asymmetrical cells division. *Mash1*, *Neurog2*, *Math1* and *Hes6* promote neurogenesis, the latter by specifically antagonizing *Hes1*. Later in development radial glia cells disappear and their progenitor role is taken over by a subset of astrocytes in a process promoted by *Hes1* and *Hes5* function. Adapted from [203].

1.3.6. Initiation of the neuronal differentiation program

After cells have been selected for neuronal differentiation by an initial upregulation of proneural genes induced by lateral inhibition, this differentiation status becomes fixed by progression through the differentiation cascade. This process is reinforced by positive feedback loops. In other words, neural progenitors progress from a reversible selection coupled to the transient expression of proneural genes to an irreversible commitment phase [16]. Key players in this fixation process are transcription factors that are induced by initial proneural gene activity, such as the Zinc-finger protein Senseless [240] in *Drosophila*, as well as the non- basic HLH protein Coe2 [241] and the E(Spl) factor Hes6 [242] in vertebrates [16]. Interestingly, Hes6 represses Hes1 and therefore alleviates neurogenesis blockage [242]. Differentiating neurons subsequently pass through a further level of bHLH transcription factor expression. The corresponding genes at this level are the so called 'differentiation genes' [16]. Ectopic expression of these factors, such as Neurogenic Differentiation (NeuroD), leads to ectopic induction of the neurogenesis program [243] similar to overexpression of proneural factors [194]. Their downstream position in the cascade has been shown by gain of function experiments in *Xenopus* [244] and loss of function studies in mouse [245,246].

The progression through the neuronal differentiation cascade is also coupled to the terminal withdrawal from the cell cycle [39]. This is crucially connected to induction of Cyclin-dependent kinase (Cdk) inhibitors, such as p16, p21, p27 and p57. These factors are highly expressed in differentiating neurons. In *Xenopus*, loss of $p27^{Xic1}$ function inhibits the differentiation of neurons while ectopic overexpression induces ectopic neuronal differentiation [247]. Furthermore, NeuroD is able to activate p21 expression [248]. In zebrafish the p57 homolog *cyclin-dependent kinase inhibitor 1c* (*cdk1c*) is necessary for a correct withdrawal from the cell cycle and neuronal differentiation [249]. The pathways that lead towards neuronal differentiation are summarized in Figure 22.

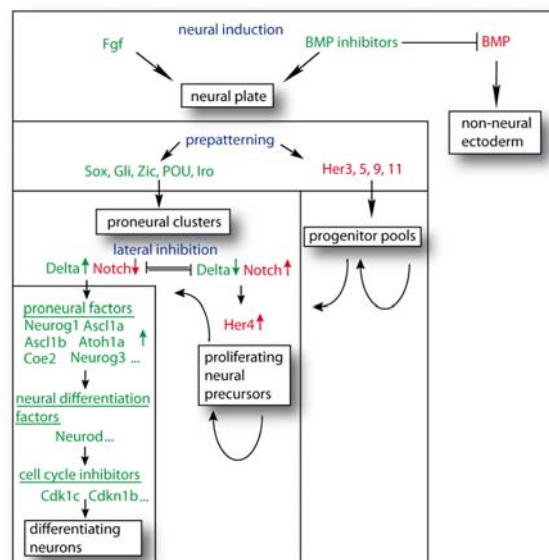


Figure 22: Pathways towards neuronal differentiation. Factors promoting neuronal differentiation are written in green, factors inhibiting neuronal differentiation in red and the selection processes in blue.

1.3.7. Role of miRNAs in neurogenesis control

MicroRNAs (miRNA) are a relatively recently discovered group of small non-coding RNAs that add a new level of transcript regulation to the regulatory networks by post-transcriptional modulation [250-253]. The average size of processed miRNAs is 22 nucleotides [254] hence their name 'micro'-RNAs [255]. Intense work is currently conducted to decipher the pathways of miRNA function and their role in the regulative networks of the cell and the whole organism. miRNAs have been shown to either be directly connected to the transcription of another gene, if they are located in an intron, or can be regulated by their own enhancers similar to those of developmentally regulated genes, as experimentally shown for *miR-9^d* [134]. miRNAs play important roles in many developmental processes [253], a phenomenon also reflected by the fact that the majority of developmentally regulated genes have a higher number of miRNA target sites accumulated during evolution compared to housekeeping genes [253]. A hallmark of miRNA gene organization is that one final miRNA product can be produced from several linked or genetically independent loci [252,254], leading to a functional redundancy of these separate loci [252,256]. For example, zebrafish miR-9 is transcribed from at least five genomic loci^a, each producing the same mature miR-9 sequence.

1.3.7.1. Biogenesis of miRNAs

The pathway of miRNA processing and regulation contains several steps (for an overview see Figure 23) [253]. It begins with the transcription of the pri-miRNA from the genomic locus, which is mostly mediated by RNA Polymerase II. The primary transcriptional product is base pairing with itself to produce a primary miRNA (pri-miRNA) with a characteristic stemloop structure. The exception to this are miRNA loci lying within Alu-elements^b that are transcribed by RNA Polymerase III [257]. Next, the nascent transcript is 5'-capped and obtains a polyA-tail similar to most RNA Polymerase II transcripts and can be spliced in some instances [258]. A multiprotein complex called 'Microprocessor' that contains, as main functional components, the RNase III enzyme Drosha and the double-stranded RNA-binding domain protein Pasha^c, further processes the pri-miRNA [259]. It cleaves the stem-loop resulting in precursor miRNA (pre-miRNA) of approximately 70 nucleotides in length [260]. This primary product is a stem-loop structure that contains a 3' overhang of two nucleotides that is recognized and bound by Exportin-5 [261]. The Exportin-5/pre-miRNA complex is subsequently actively exported from the nucleus into the cytosol [261]. Next, the RNase III enzyme Dicer cleaves the pre-miRNA which leads to the final approximately 22 nucleotide double-stranded miRNA-duplex (miRNA:miRNA*) [262] which is loaded into the 'RNA-induced silencing complex' (RISC). In most cases specifically the strand with a lower base-pairing stability at the 5' region is taken up by RISC while the complementary strand (miRNA*) gets degraded [263,264]. The loaded miRNA serves as template for RISC to target complementary sequences in 3' untranslated regions (UTR) of mRNAs that are currently present in the cytosol. If the miRNA and targeted 3' UTR are completely or nearly completely complementary, the targeted mRNA is cleaved while in cases of only partial complementarity RISC mediates translational repression [265]. While the first situation is very rare, the latter

^a Ensembl (Zv7): www.ensembl.org

^b Short Interspersed Nuclear Element (SINE) that is characterized by *Alu* endonuclease restriction sites

^c Partner of Drosha

mechanism is prevalent to mediate miRNA repression in animals [253]. Most animal miRNAs have a high complementarity only at the very 5' nucleotides 2 to 7 of the miRNA, the so called 'seed' region [266,267].

Interestingly, miRNAs are in many cases expressed together with their targets, in cells transcribing the target mRNAs at a low level [253,268]. Often these regions of miRNA expression and low transcription of the miRNA target(s) are neighbored by regions with high transcription of the miRNA target(s) without expression of the miRNA itself [253]. It has been proposed that the post-transcriptional level of regulation achieved via miRNAs constitutes a safety mechanism to down-regulate leaking expression, and that it allows fast down-regulation of gene expression during developmental transitions, rendering transcriptional regulation more flexible [268]. Therefore, miRNAs add a level of robustness and accuracy to gene regulatory networks during development [253].

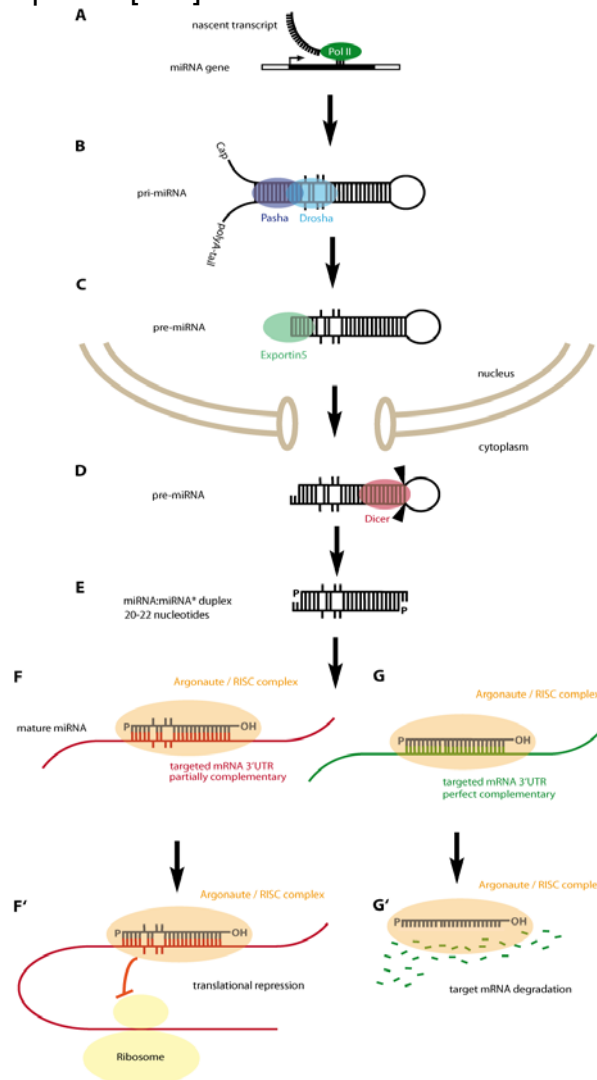


Figure 23: Overview on the different steps of miRNA processing. (A) In most cases miRNA genes are transcribed by RNA Polymerase II (Pol II). The nascent transcript gets capped and polyadenylated similar to most mRNAs and folds back on itself in a characteristic stem loop structure. (B) The resulting 'pri-miRNA' is bound by Drosha and Pasha and further processed (for details see text). (C) Subsequently the 'pre-miRNA' gets bound by Exportin5 that mediates the export from the nucleus. (D) In the cytoplasm the Dicer complex binds to the pre-miRNA to further process it to a 20 to 22 nucleotide miRNA:miRNA* duplex (E). This mature miRNA gets now loaded into the Argonaute/RISC complex where it mediates either translational repression (F and F') or target degradation (G and G') depending on the degree of complementarity to target 3'UTRs. Note that only either the miRNA or the miRNA* gets loaded into the Argonaute/RISC complex (for details see text). Modified from [253,269].

1.3.7.2. Known roles of miRNAs in neurogenesis control

It has been estimated that more than one third of human gene transcripts are directly regulated by miRNAs [266]. Approximately 70% of all miRNAs experimentally detectable up to date are expressed in the brain. Moreover, half of the miRNAs with a tissue specific expression pattern are brain-specific [270]. Therefore, it is likely that miRNA-mediated gene regulation has crucial implications during nervous system development and function. However, we are only at the beginning of understanding this process [270]. Knowledge is especially scarce regarding the implication of miRNAs in neurogenesis regulation [252], although many miRNAs have been described to be expressed in developing vertebrate brains [271,272]. *miR-124* has been implicated in brain-specific alternative splicing [273] and in repression of REST^a in the chicken neural tube and cell culture [274]. The miR-200 family plays a crucial role in olfactory neurogenesis as shown in the mouse and zebrafish model [275]. A particularly interesting candidate for both neurogenesis and IsO control is miR-9 [272,276]. It is expressed in the late embryonic zebrafish brain in a pattern that selectively spares the MHB progenitor pool. Furthermore, several components of the Fgf-signalling pathway that play crucial roles at the IsO as well as E(Spl) factors are predicted targets of miR-9. Also in the mouse miR-9 was found to be highly enriched in particular in the cortex, cerebellum and midbrain [277] and in P19 cells undergoing neuronal differentiation [278]. Interestingly, the regulatory regions of miR-9 and miR-9* in the mouse are enriched in RE1^b-sites [279], suggesting a crucial function of miR-9 in neuronal gene activity. Conversely, miR-9, as well as miR-9*, potentially regulate REST-complex activity in humans [280], therefore providing further support for being crucially involved in neuronal gene control. In addition, the miR-9 homolog in *Drosophila* has been implicated in neurogenesis [281,282].

1.3.7.3. Open questions of the roles of miRNAs in neurogenesis control

Up to now, no miRNA could be directly connected to the regulation of the neural progenitor pool at the MHB. With the dissection of miR-9 function I could demonstrate a new role of miRNAs in nervous system developmental control and in particular in defining the limits of the MHB progenitor pool during later stages of development. The late regulation of progenitor pools was enigmatic but can now be explained, at least to some extent, by the role of the single miRNA miR-9 [283](see chapter 3.1.4 and Appendix 4).

1.3.8. Neurogenesis and E(Spl) factors in the adult brain

It is still a crucial open question to which extent the processes of neurogenesis during embryogenesis are reused during adult neurogenesis. In mammals only two very restricted zones in the brain show de novo neurogenesis, i.e. the subgranular zone (SGZ) of the dentate gyrus in the hippocampal formation and the subependymal zone of the lateral ventricle (SEZ) giving rise to the rostral migratory stream (RMS) [284-287]. In sharp contrast to that, many zones of the adult brain of zebrafish still incorporate the S-Phase marker 5-Bromo-2'-deoxyuridine (BrdU). Long term BrdU

^a Repressor Element 1 Silencing Transcription Factor

^b Repressor Element 1

tracing together with the labelling of neuronal markers indicates widespread neurogenesis in the adult zebrafish brain [13,14,288-290] which is in line with the life long growth of zebrafish. Neurogenic zones are not evenly distributed across the adult brain but are focally concentrated and very often associated with ventricular regions [12]. Interestingly, in many proliferation zones there is expression of proneural genes, such as *ascl1a* and *neurog1*, lateral inhibition components such as the *delta* ligand genes and the *E(Spl)* factor and Notch effector *her4* [13,14]. Similarly, strong expression of Notch1, Jagged1 and Hes5 has been shown in proliferative regions in the adult mouse brain [291]. To which extent the embryonic neuronal selection and differentiation machinery is comparable to the one in adult neurogenesis is still a crucial open question. A first analysis of the cis-regulatory regions driving expression of *neurog1* already hint to a critical difference in proneural gene regulation between embryo and adult, but further analysis is needed to resolve this issue [14]. Furthermore, a particularly interesting open question is whether non-canonical *her* genes also define progenitor pools in the adult. One member of this gene family has been already precisely analyzed: *her5* is expressed at the ‘isthmus proliferation zone’ (IPZ), a progenitor pool at the dorso/ventral (D/V) junction of the tectum and tegmentum and the the A/P junction of the valvula cerebelli and the torus longitudinalis [13]. *her5*-positive cells at this adult progenitor pool proliferate slowly, self-renew and are multipotent. This was shown with the help of a transgenic line driving Enhanced green fluorescent protein (EGFP) under the regulatory elements of *her5* (*Tg(her5PAC:EGFP)*) [70] that marks *her5*-positive cells until adulthood [13]. Interestingly, in a similar transgenic approach in mouse a strong GFP signal driven by *Hes1* regulatory elements was apparent in adult neurogenic zones [292]. The challenge is now to test whether other members of the group of non-canonical *her* genes (*her3/9/11*) also mark progenitor pools in the adult zebrafish brain. In order to unravel this, I have focussed on the IPZ and tested for expression of *her3* and *her9* in this adult progenitor pool (see 3.1.6).

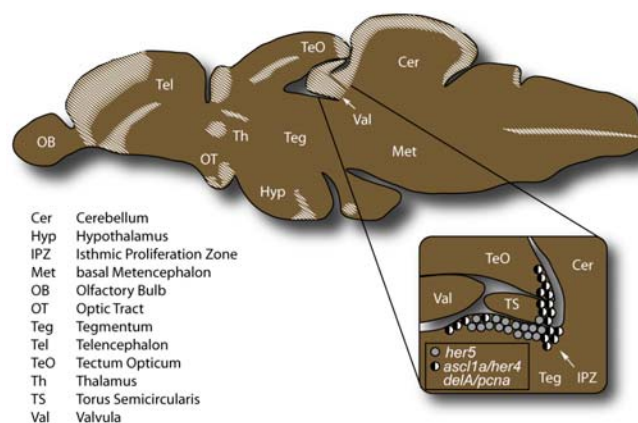


Figure 24: Neurogenic zones in the adult zebrafish brain. Neurogenic zones are shaded in white in this slightly parasagittal schematic view of the adult zebrafish brain. The region around the isthmus proliferation zone (IPZ) is magnified in the inset on the lower right. Note that slowly proliferating *her5*-positive cells are adjacent to *ascl1a/her4/delta/pcna*^a positive cells. Anterior is left and dorsal up. Adapted from [176][293].

^a *proliferating cell nuclear antigen (pcna)* (ZFIN)

1.4. Determination of neuronal identities

A highly important step in the development of a neuron, as well as for the whole nervous system, is the determination of its specific identities. The highly diverse, but precisely defined neuronal identities form the basis of a functionally interconnected and complex vertebrate brain. The type of neuronal identity ranges from characteristics such as neurotransmitter phenotype to projection patterns and decisions for specific synaptic targets. Interestingly, in most parts of the vertebrate CNS neurons are born first and only later glia cells follow [294]. In the following I will concentrate on neuronal rather than glial identities as neuronal fate determination in the MH domain is one of the key questions that I address in my thesis (see 3.2).

The two most crucial processes influencing the choice of a specific neuronal identity are positional information and differentiation timing. In most cases neuronal identities are defined by an interplay of these two mechanisms, but temporal identity can be seen as a separate 'axis of information' that is either generated intrinsically or extrinsically and that can be used by a progenitor to define neuronal fate [295]. Although interwoven in the organism, I will explain these two mechanisms separately in the following sections for reason of clarity.

Both, positional information and/or timing cues are read out as fate determinants during a specific commitment status. This often correlates with a relatively short time window, which is in most cases the period of cell cycle exit, also called the neurons 'birth date', or the last cell divisions just prior to that [26].

1.4.1. Morphogen gradients as determinants for neuronal identities

Morphogens are soluble molecules that normally build up gradients that span many cell diameters. Different levels of these morphogen gradients are often used by cells as positional information to control cell fate specification, a concept that was first recognized by Thomas Hunt Morgan more than a century ago [296]. This mechanism has since then been described in patterning processes in many different tissues throughout development [297][298]. One of the best understood systems where such morphogen gradients orchestrate the specification of neuronal identities is D/V patterning of spinal motoneurons in the vertebrate ventral spinal cord [299]. Sonic hedgehog (Shh) was identified as key ventrally secreted morphogen [300-303]. At least five different classes of ventral spinal cord neurons and floor plate cells are specified by the Shh gradient [304]. In concordance with a gradient model, increasingly ventral cell types have increasing sensitivity thresholds for Shh (see Figure 25). Using clonal expression of a mutated form of the Shh receptor Patched ($Ptc^{\Delta loop2}$), it was shown that Shh is not working via a relay mechanism but is indeed a bona fide long range signal as overexpression of $Ptc^{\Delta loop2}$ in a patch of cells in the ventral neural tube leads to a cell-autonomous reduction of Shh signaling [305] (see Figure 25). It is important to note that $Ptc^{\Delta loop2}$ expressing cells seem to be unable to restrict diffusion of secreted Shh leading to an aberrant dorsal spread of Shh. This is similar to the situation in *Drosophila* [305]. The source of the Shh morphogen gradient is the floorplate, itself previously induced by Shh secreted from the notochord. In the zebrafish hindbrain, D/V patterning defects that fit this model have

been described in *shh* pathway mutants such as *sonic you (syu)*^a or *detour (det)*^b as well as by overexpression of *shh* [306-308]. Interestingly, also dorsal fates in the vertebrate spinal cord are specified by a morphogen gradient. Similar to the situation in the ventral spinal cord, a signalling center gets induced in the roof plate from the neighboring epidermis. The dorsal spinal cord morphogens are BMP4 and BMP7 [309]. Hence, neuronal identities in the spinal cord are specified by reading out positional informations from combined ventral Shh and dorsal BMP morphogen gradients. Notably, positional information can also be given by a cell as close as the direct neighboring cell^c.

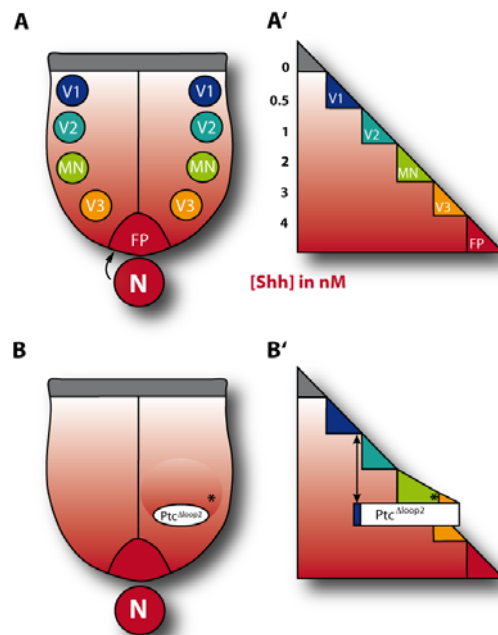


Figure 25: Positional information and neuronal identity specification in the ventral spinal cord. (A) Motoneurons (MN) and ventral interneurons (V1 to V3) in the ventral spinal cord are derived from progenitor populations that are specified by a graded Shh signal (indicated by red gradient). The sources of Shh are in the floor plate (FP) and the notochord (N). Note that the floor plate got previously induced by the notochord (indicated by black arrow). (A') Distinct neuronal populations are specified in between certain Shh concentration ([Shh]) threshold levels. (B) Clonal misexpression of a mutated form of the Shh receptor Patched ($Ptc^{\Delta loop2}$, white ellipse) leads to a cell-autonomous ventral to dorsal shift of neuronal fates (B'; indicated by black double headed arrow), strongly suggesting a gradient mechanism [305]. Note that directly dorsal to the $Ptc^{\Delta loop2}$ expressing clone a separate Shh gradient is built up (indicated by black asterisk; for details, see text). Dorsal is up. Modified from [299][305].

The readout of positional information

Experimental data has shown up to seven different cell types that are specified by a single gradient in *Drosophila* [298,310] and for the Shh gradient in the neural tube [298,304,311,312]. This diversity produced by a gradient raises the question how the individual cells can read out the positional information from the extracellular gradient. The primary extracellular signal, mostly a concentration of a soluble ligand in the extracellular space is first read out by receptors that transfer the signal via a cytoplasmatic cascade to the nucleus. Here the transcriptional regulation machinery

^a *sonic you* mutations map to the *sonic hedgehog a (shha)* locus (ZFIN); zebrafish has the two *shh* paralogs: *shha* (formerly *shh*) and *shhb* (formerly *tiggy-winkle hedgehog (twhh)*); for a more complete D/V patterning related motoneuron loss both paralogs have to be downregulated[306]

^b *detour* mutations map to the *GLI-Krüppel family member 1 (gli1)* locus (ZFIN)

^c 'direct induction'

transfers the signal into a modified output of target gene transcription. This complex cascade implies that there are several crucial steps whereby the ligand concentration thresholds can be modified. First, the receptor level has been clearly shown to be crucial for the threshold of the readout. Furthermore, the following downstream cascade is also critically involved in setting the threshold levels. This has been clearly shown for D/V neural tube patterning in vertebrates. Here different concentrations of the Shh pathway member Smoothed have been identified as necessary and sufficient to set the threshold to induce the different neuronal identities in the ventral neural tube [298,313,314]. The final computing step of the gradient readout happens at the level of transcription regulation of target genes. Here, several different regulatory mechanisms can be at work (see Figure 26). Note that these mechanisms are often used in combinations. Fate specification in the ventral vertebrate nervous system, for example, uses at least the combination of two of them, namely the cross repression and reciprocal repression mechanisms [298,312,315,316]. To conclude, the readout of the positional information by an individual cell has to be seen as combination of mechanisms at several regulation levels, starting at the receptor level and finally compiled at the transcriptional regulation level.

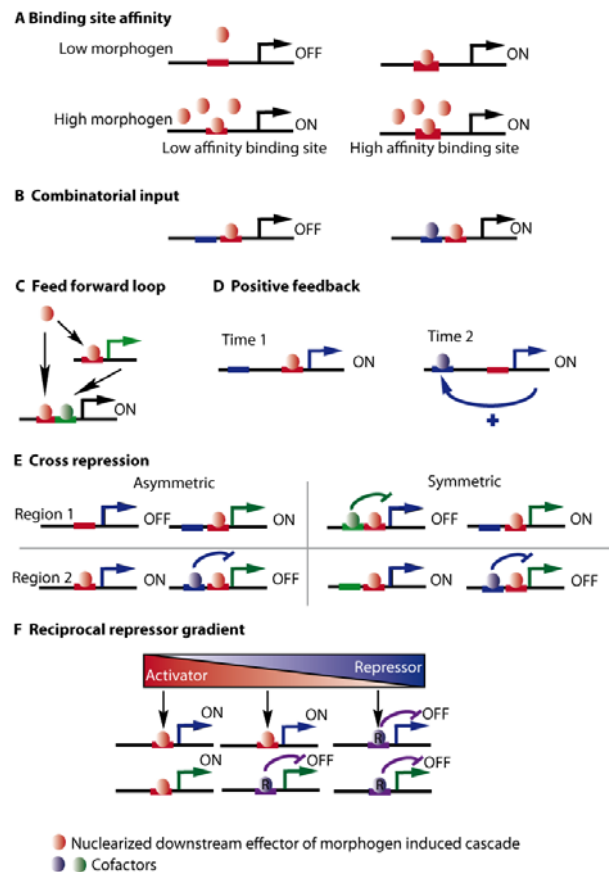


Figure 26: Mechanisms used to readout of positional information at the level of transcriptional control. (A) Threshold responses to gradient level are defined by number and affinity of transcription factor binding sites. (B) Threshold responses are specified by integration of additional positive and/or negative inputs (blue). (C) The gradient readout is relayed via the expression of a second regulator. (D) Morphogen induced gene feeds back positively onto its own expression. (E) Cross repressive interaction between two loci leads to regional differences in gene expression. This mechanism can be symmetric or asymmetric. (F) An inverse transcriptional repressor gradient is set up by the transcriptional effector of the morphogen. The threshold response is then defined by the repressor (R) to activator ratio. This is dependent on the presence of enhancer binding sites. Adapted from [298].

1.4.2. Timer mechanisms as determinants for neuronal identities

Traditionally, positional mechanisms got more attention from scientists while differentiation timing was often neglected [317]. Nevertheless, there are a number of very well described neuronal differentiation timers, such as the intracellular timer of oligodendrocyte progenitors in the optic nerve [317] and the differentiation timers in the vertebrate retina, hindbrain, spinal cord and the mammalian cerebral cortex. I will shortly introduce differentiation timing in the *Drosophila* embryonic CNS and the mammalian cerebral cortex in order to elucidate the diversity of neuronal differentiation timer mechanisms. Subsequently, I will put the main focus on the retinal differentiation timer, not only as these processes follow eye field patterning as described before (see 1.2.2) but also as they have been intensively studied, to some extent also in zebrafish.

In principle two different types of differentiation timers can be found. Again, I show here only the two extremes and therefore it is important to keep in mind that a given progenitor might use both of these mechanisms to a different extent. One type of differentiation timer relies on the variation of intrinsic cues. This is, to a large extent, the case for the *Drosophila* neuroblast timer and the vertebrate retinal timer (see Figure 27). In the second type, extrinsic cues are changing over time. This type prevails in the progenitors of the vertebrate cortex, hindbrain and spinal cord.

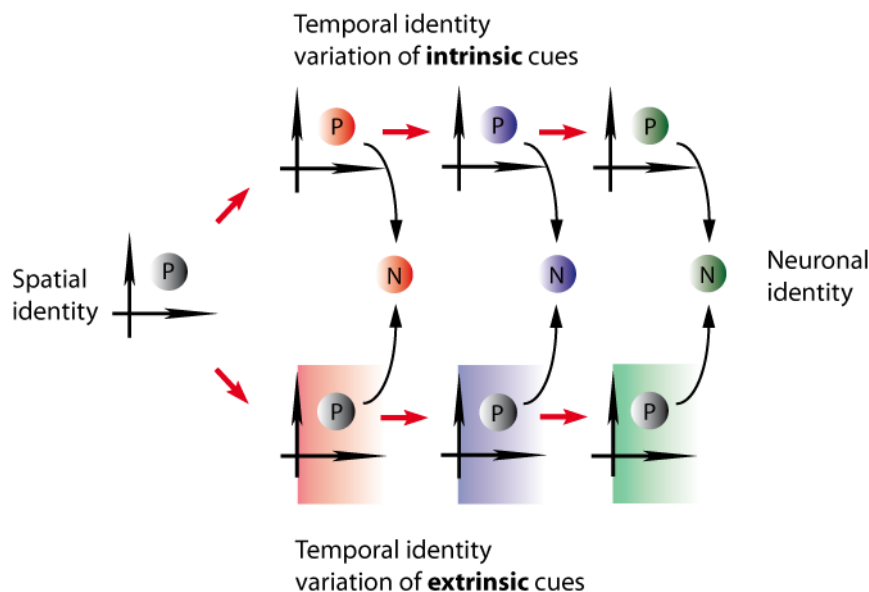


Figure 27: Extrinsic versus intrinsic differentiation timing. Time axis is from left to right. Spatial cues are symbolized by Cartesian coordinates (black arrows). Progenitors (P) produce neuronal progeny (N) with different fates over time (color coded). The timing cue can either be intrinsically (upper row) or extrinsically encoded (lower row). Adapted from [295].

1.4.2.1. Differentiation timing in *Drosophila* neuroblasts

The CNS of the *Drosophila* embryo is derived from progenitor cells called neuroblasts. The neuroblasts form at precisely defined positions and time points. They originate from the ventral neuroectoderm and delaminate into the inside of the embryo. They express a specific combination of molecular markers. Neuroblasts divide asymmetrically and thereby give rise to one further proliferative neuroblast and

a ganglion mother cell (GMC) that only divides once more and thereby produces two postmitotic neurons or glia cells [295]. Cell culture of isolated neuroblasts has shown that they divide asymmetrically to make GMCs and finally clones of neurons of the correct number and cell type in these in vitro conditions as well. This speaks in favour of an intrinsic mechanism [318,295]. Interestingly, many *Drosophila* neuroblasts show a precise temporal expression sequence of Hunchback (Hb), Krüppel (Kr), POU domain protein (Pdm) and Castor (Cas). During each of these expression periods, in average one GMC is born that maintains expression of the factor expressed at its birth date and gives it on to its neuronal progeny while the neuroblast switches to the next factor after division [319] (see Figure 28). This intriguing gene expression pattern is not only marking temporal transitions, but the factors involved can be also instructive themselves. This has been shown for example for Hb that is both necessary and sufficient in the specification of early temporal identity. Loss of Hb function leads to a specific loss of early identities while Hb overexpression leads to supernumerous early identities [319] (see Figure 29). It is important to note that these temporal transitions do not happen in parallel in the whole embryo because of divergent starting timepoints of different neuroblast lineages. This fact makes an extrinsic mechanism unlikely and therefore supports the intrinsic timer hypothesis, as do the in vitro cultures [295]. Nevertheless, the timer mechanism itself is still elusive. Several of the *Drosophila* proteins involved here have vertebrate homologs, such as Ikaros that is the vertebrate homolog of Hb [295]. An involvement of these factors in vertebrate differentiation timers remains to be analyzed.

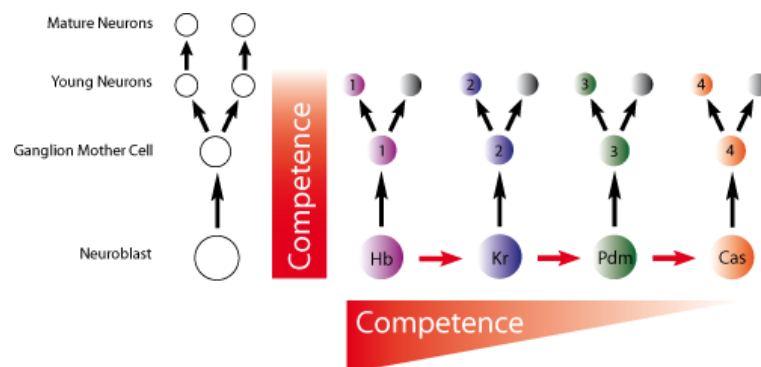


Figure 28: Differentiation timing in the *Drosophila* neuroblast lineages. Neuroblasts give rise to further neuroblasts and ganglion mother cells (GMC) in asymmetric divisions. Note that GMCs keep the temporal identity of the neuroblast prior to division while the neuroblast changes to the next temporal identity after the division event. A GMC divides once more to give rise to two differentiating neurons that again keep the identity that was present before the division event (color coded). Different neuronal identities are numbered. Change in competence over time is indicated by red gradient. Time axis is from left to right. Modified from [295].

1.4.2.2. Differentiation timing in the vertebrate neocortex

The mammalian cerebral neocortex, furtheron referred to as 'cortex', has been an area of intense study in order to describe a differentiation timing process. The cortex develops out of a pseudostartified epithelium with telencephalic fate. Dividing progenitors are situated in the ventricular zone and give rise, over time, to the layers of the cortex in an inside-out sequence whereby the first formed layer 6, followed by layers 5, 4 and finally layer 2/3 are successively arranged in progressively deeper

positions [320-323]. The exception is layer 1 that forms first but remains the most superficial layer [295]. Again, glia cells are formed as the last population [324]. Each of these layers exhibits different projection patterns, which reflect distinct neuronal identities. Heterochronic transplantation experiments have shown a progressive restriction of the fate potential of progenitors [321,324,325]. Furthermore, the critical time point for fate decision could be narrowed down to the last G2-M transition of the cell cycle [295].

In contrast to the situation in *Drosophila* embryonic neuroblasts (see above), during mammalian corticogenesis the identities appear in separate waves. This makes it possible that global, extrinsic fate cues are involved in defining these identities. The winged-helix type repressor of transcription 'Forkhead box G1' (Foxg1) has been identified as bona fide temporal identity factor. Foxg1 is upregulated after layer 1 formation and stays on during the generation of later born neurons. It acts as an active repressor of early fates [326] (see also Figure 29). There are more potential candidates conferring fate determining cues, such as Otx1 and Octamer-6 (Oct6), but the analysis of these factors is only beginning [295]. To conclude, cell layer fates in the mammalian cortex are arising in a time ordered sequence, but again, the nature of the timer itself remains elusive [295,324].

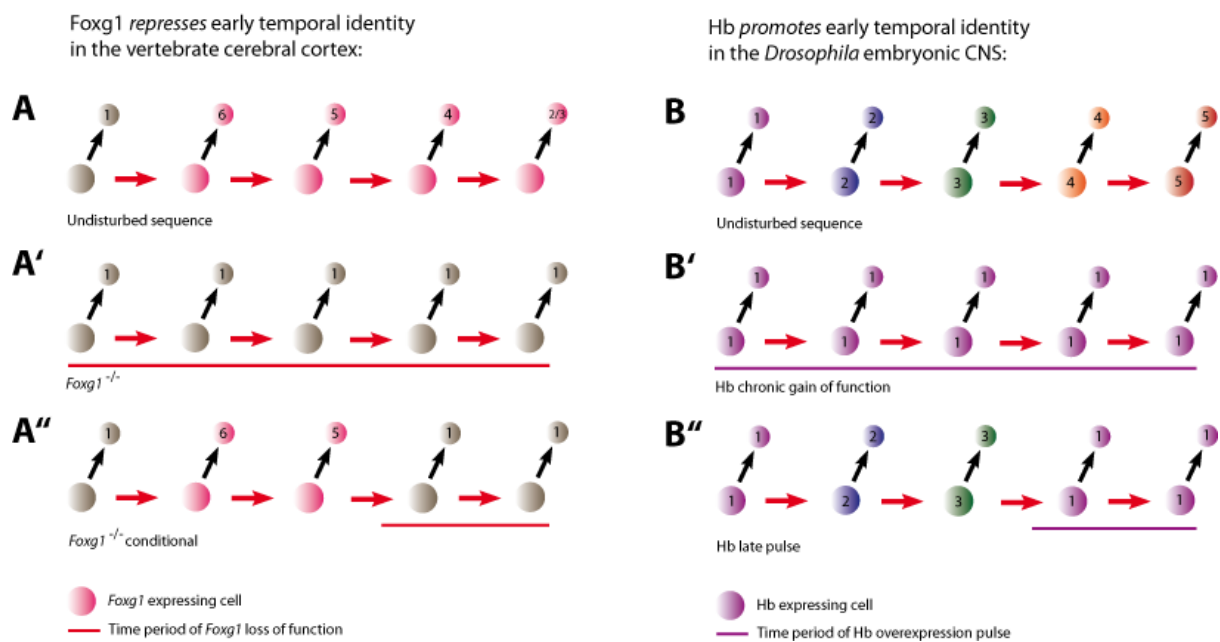


Figure 29: Comparison of factors that confer temporal identity in the vertebrate neocortex and *Drosophila* neuroblasts. Different temporal neuronal identities are color coded and/or indicated by numbers. Progenitors are depicted bigger than neurons. (A) Foxg1 is not present in early cortical progenitors but gets upregulated and stays highly expressed (pink) and represses early fates. Numbers represent the layer identity in the cortex. (A') In *Foxg1* knock out mice (*Foxg1*^{-/-}) early fates ('1'; in grey) cannot be repressed. (A'') In conditional *Foxg1*^{-/-} mice initially later fates can appear but after conditional *Foxg1* activation later fates are repressed. (B) Normal neuroblast differentiation timing gives rise to different neuronal identities over time (see also Figure 28). (B') In a chronic Hunchback expressing cell only early neuronal identities arise. (B'') During a Hunchback overexpression pulse early identities are enforced. Time axis is from left to right. Modified from [295].

1.4.2.3. Differentiation timing in the vertebrate retina

The vertebrate neural retina is a highly organized stratified tissue that lines the inside of the optic cup and consists of seven major cell types. These are born during early development in stereotypic waves starting with ganglion cells, followed by horizontal cells, bipolar cells, amacrine cells, cone photoreceptors, rod photoreceptors and, again last, glia cells, that have radial glia characteristics and are named Müller glia [327-330]. It is important to note that these waves are highly overlapping in time in contrast to the separated waves during corticogenesis (as discussed in the previous paragraph). Similar to the cortex, the retina is a layered structure, consisting of the mainly rod and cone photoreceptor containing outer nuclear layer (ONL), the horizontal, bipolar, amacrine cell containing inner nuclear layer (INL) and the ganglion cell layer (GCL). Müller glia cells span all neuronal layers of the retina with their long cellular projections but their cell bodies lay mostly in the inner nuclear layer (see Figure 30).

Lineage tracing studies showed the multipotency of retinal progenitors, the restriction of this multipotency over time and differences in the fate of sibling cells [331-335]. These experiments speak strongly in favor of a common progenitor pool for all fates and against separate pools for different fates. Moreover, because of the overlap of time windows in which different fates are specified and arise, an intrinsic timer component is very likely, although an extrinsic timing component might be cooperating with it to refine fate definition as has been shown in heterochronic transplantation and co-culture experiments [295,328,336,337]. These extrinsic signals are, at least partly, mediated by the Ciliary neurotrophic factor / Leukemia inhibitory factor (CNTF/LIF) cytokine pathway and act as repressive signals for rod photoreceptor fate [337,338]. Furthermore, the secreted ligand Shh is expressed in a wave in the ganglion cell layer during the early retina neurogenesis, similar to the situation in *Drosophila* where a wave of Hedgehog plays a crucial role in eye differentiation [339]. Interestingly, Shh induces cell cycle exit by activation of the 'cyclin-dependent kinase inhibitor 1c' (*cdkn1c*) [340]. Furthermore, a second Shh wave spreads in the INL and overlaps partly with the first one, giving rise to a subpopulation of amacrine cells that express *shh* [341]. Besides roles in neurogenesis and proliferation control, Shh mediates a feedback mechanism whereby mature ganglion cells inhibit the specification of a further production of ganglion cells [342,343].

To conclude, a combination of an intrinsic timer and extrinsic cues that change over time are at work to define fates in the vertebrate neural retina. The molecular basis of the intrinsic timer mechanism is still a conundrum. Recent work in *Xenopus* points towards a regulation at the translational level [344]. The photoreceptor markers *Xotx5b* and the bipolar cell markers *Xvsx1* and *Xotx2* are initially transcribed but furtheron blocked from translation in early progenitors. This blockade is mediated by the 3' UTRs of these transcripts. Cell cycle progression is necessary to relieve this block and initiate translation of these homeobox factors in the right cell type [344]. Once again, the nature of the factors that mediate this specific translational blockade is still not known, while miRNAs and RNA-binding proteins are interesting candidates [344].

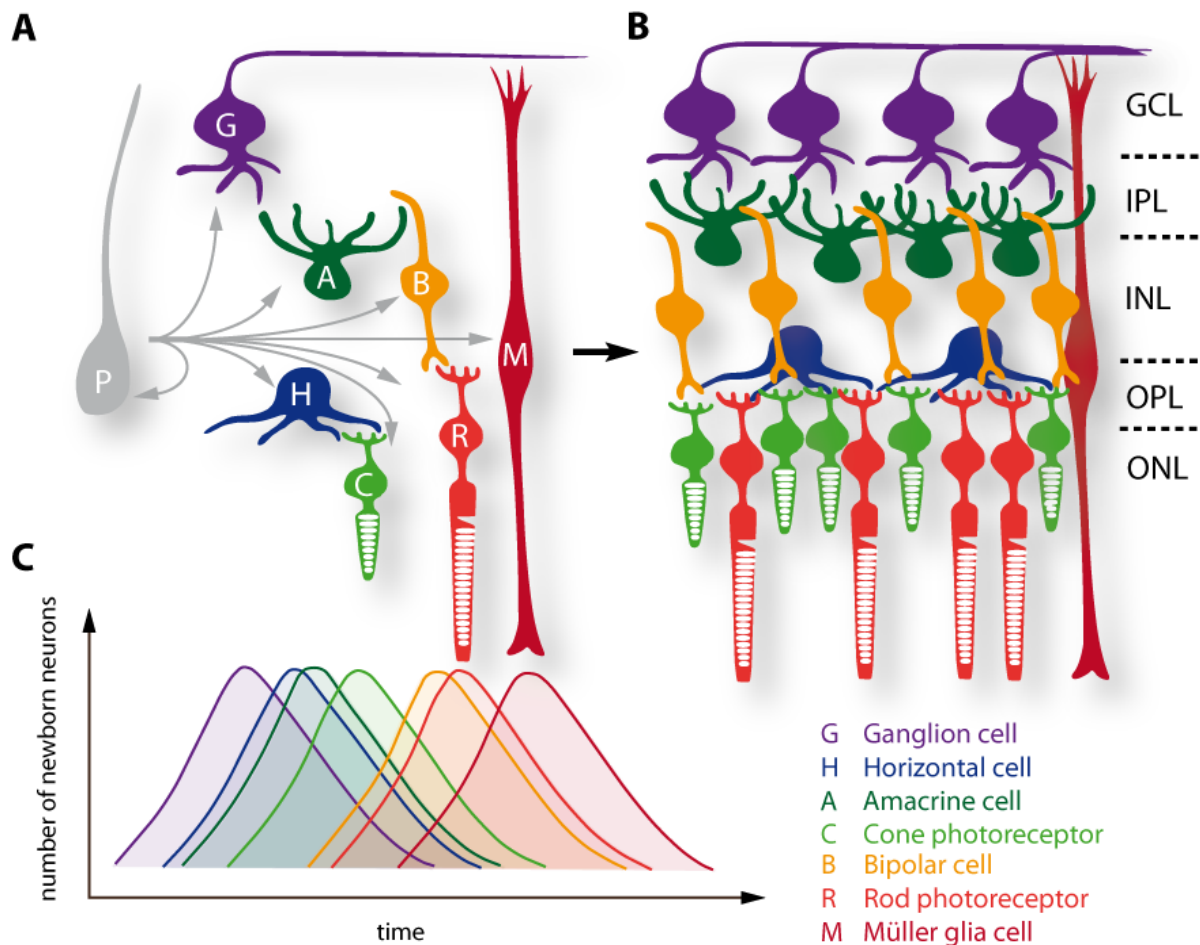


Figure 30: Differentiation timing in the vertebrate retina. Different retinal cell type identities are color coded. Time axis is from left to right. (A) Retinal progenitors ('P') give rise to different retinal cell type identities over time. Müller glia cells are the last cells produced. (C) The relative frequencies of neuronal identities born during retinogenesis are shown in the graph. Note that the distributions are overlapping but peaks are mostly separated. This process leads to the highly organized layered structure of the neural retina (B). Abbreviations: GCL: ganglion cell layer; INL: inner nuclear layer; IPL: inner plexiform layer; ONL: outer nuclear layer; OPL: outer plexiform layer. Adapted from [345].

1.4.3. Neuronal identity specification in the basal MH domain

The MH domain consists of several different neuronal populations, most of them having their own specific neuronal identity in terms of transmitter phenotype, projection pattern, the neuronal input they receive and the physiological functions they control. The basal MH domain has a highly complex structure and I concentrate here only on some crucial landmarks in this brain area. The ventral midbrain consists of several nuclei and some more diffuse neural structures, together building the tegmentum. In mammals there are the dopaminergic populations of the ventral tegmental area (VTA) and the substantia nigra. These dopaminergic structures are not present in the zebrafish ventral midbrain. Lateral to the median floorplate is the motoneuron population of the 'oculomotor nucleus'^a. Ventral to the oculomotor

^a Nucleus of the 3rd cranial nerve (cranial nerve III); this nucleus is here referred to in singular, but it is represented, like many other nuclei, by mirror symmetrically paired structures in the brain

nucleus is another motor nucleus called the ‘red nucleus’^a. Separated from the midbrain by the IsO are again motor structures. The anteriormost of these hindbrain structures is the ‘trochlear nucleus’^b. Further caudal follow the serotonergic ‘raphe nuclei’ that provide widespread serotonergic innervation in the CNS. How these ventral MH domain structures obtain their unique and highly stereotypic neuronal identities is still a subject of intensive research (see 3.2.1, 3.2.2., Appendix 6 and Appendix 7).

The MH domain contains, besides the IsO (as described in detail above), a second signalling center: the notochord along with the floorplate in a ventral longitudinal domain. The combinations of signals from these two signalling centers, Shh and Fgf8 respectively, has been shown to be necessary for proper specification of MH neuronal identities in vitro [347]. Several studies focussing in particular on the role of Shh in ventral MH patterning have shown the crucial function of this morphogen in defining neuronal identities. Furthermore, with in vivo electroporation studies in the chicken neural tube it could be shown that Shh can pattern the ventral midbrain in a concentration dependent manner [348]. In addition, Wnt signals in the midbrain confer positional information [349] (see Figure 31).

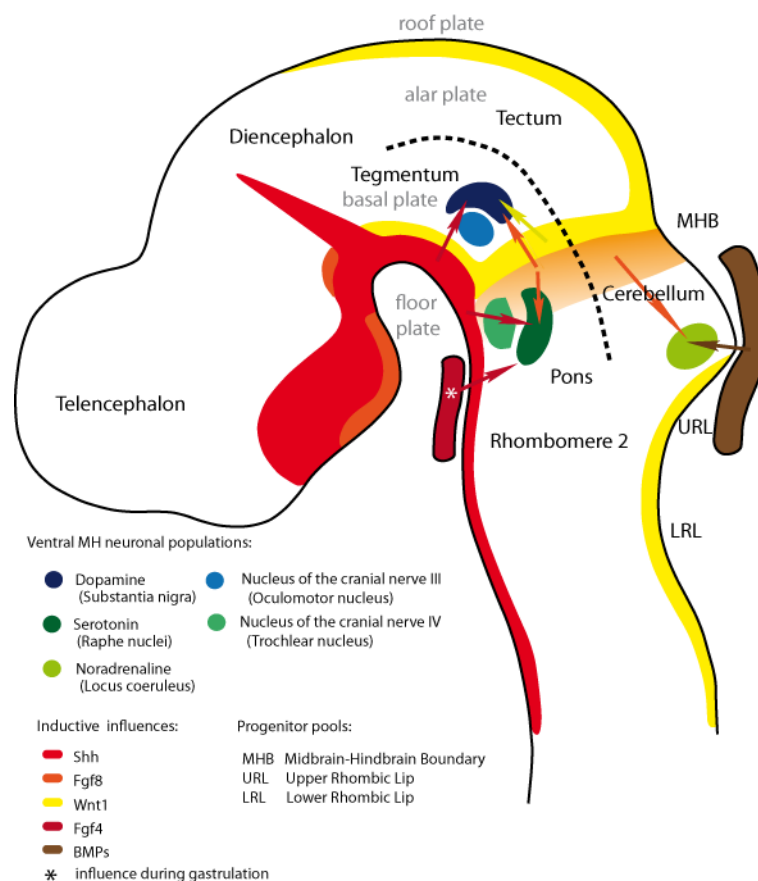


Figure 31: The basal MH domain in the context of morphogen sources and neighboring neuronal populations. Nuclei and inductive influences by morphogens are color coded. Arrows indicate inductive influence by morphogen on particular population. Sagittal view of mouse brain at E11. Rostral is left. Modified from [69].

^a Note that the anteriormost part of the red nucleus is in the caudal diencephalon and therefore a not a basal midbrain structure [346]

^b Nucleus of the 4th cranial nerve (cranial nerve IV); this nucleus is here referred to in singular, but it is represented, like many other nuclei, by mirror symmetrically paired structures in the brain

Remaining open question: Does a differentiation timer contribute to the determination of basal MH-neuronal identities?

Although there seems to be a contribution of midline and IsO derived positional information in setting up midbrain fates, it is still not resolved if positional mechanisms account for the whole complexity of MH identities or if a differentiation timer also contributes crucially to this process. Interestingly, the populations of the oculomotor nucleus are not significantly influenced by increased Shh activity if applied at later stages (E9.5) which has been most likely already determined by then [346]. This suggests that an additional timing axis is important in neuronal identity determination in the MH domain. Furthermore, the serotonergic populations of the anterior Raphe nucleus also appear in a time window after the generation of ventral hindbrain motoneurons. Interestingly, both populations are derived from the same progenitor pool [350]. This again suggests a crucial time component in fate definition in the MH domain. Furthermore, transitions in temporal identity have been also described for the ‘upper rhombic lip’ (URL), a progenitor pool that is part of the dorsal MH domain neighboring the MHB and contributes first to hindbrain precerebellar nuclei and later to the cerebellar granular cells [351].

Interestingly, in zebrafish it has been clearly shown that the MHB progenitor pool is restricting over time [70]. This notion makes a timing processes an even more interesting and plausible candidate to be involved in patterning of neuronal identities in the MH domain, and zebrafish is a very suitable model to study this putative timing processes. In spite of this, a comprehensive time resolved map of basal MH neuronal identities, which constitutes a solid basis for differentiation timing studies, has not been published. In order to unravel the question whether a differentiation timer contributes crucially to MH neuronal identity determination, I therefore established a time resolved map of basal MH neuronal identities. I used this map as basis for experiments, where I disrupted the normal sequence of neurogenesis, and therefore induced premature or delayed differentiation. Subsequently, I assessed changes in the MH neuronal identity map to assess the contribution of a timer (see 3.2.3).

1.5. Neuronal differentiation

After the specification of a particular neuronal identity a maturing neuron goes through further important developmental steps, including migration, molecular and morphological differentiation, setting up of the characteristic cellular contacts and control of survival [26]. As these processes are beyond the scope of this thesis I will discuss them not further here.

To conclude, after more than 25 years of research since George Streisinger's seminal paper in 1981 which constituted the beginning of systematic genetic research using zebrafish as a model organism [4], many aspects of nervous system development have been dissected from the organismal down to the molecular genetic detail using zebrafish. Yet, many important molecular, cellular and systemic aspects of vertebrate nervous system development and function remain to be uncovered and for many of these questions zebrafish constitutes a perfect model organism.

2. Aims and achievements

The overall aim of my PhD project was to analyze the specification and maintenance of progenitor pools and the mechanisms controlling fate determination of newborn neurons in the zebrafish central nervous system.

To set-up the bases for the dissection of the molecular processes specifying and maintaining neural progenitor pools, which involve E(Spl) factors, I first reviewed current knowledge on the role of E(Spl) factors in the embryonic and adult brain, with special focus on the zebrafish and mouse models. In particular this review concentrated on a subset of zebrafish Her factors, namely Her3, Her5, Her9 and Her11, which are specifically expressed in progenitor pools in the neural plate and show a non-canonical regulation of expression by Notch. This review is presented in chapter 3.1.1 and Appendix 1.

For the purpose of unravelling new molecular players in the specification of progenitor pools, I took part in a small scale forward genetic screen run in our lab and focused on the loss of progenitor pools. I specifically analyzed, in cellular and molecular detail, one mutant recovered in this screen and that showed a very clear and striking loss of the eye field progenitor pool. I could identify the causative mutation as a single nucleotide exchange in the retinal homeobox gene *rx3*. My detailed analysis of this new zebrafish mutant demonstrated that Rx3 is a crucial component of the process that separates the eye field progenitor pool from the telencephalic primordium during early neural plate development. This work is described in chapter 3.1.2 and Appendix 2.

Despite the fact that many factors are expressed uniformly across neural progenitor pools, such as *rx3* in the eye field and *her5* and *her11* at the MHB, there are crucial differences in several characteristics across these pools. One such characteristic is the propensity to undergo neurogenesis between the medial and lateral aspects of the MHB. In order to shed light on these differences, I contributed to a collaborative study where we uncovered Gli1 as crucial pro-neurogenic factor that accounts for this mediolateral difference. The background of this analysis and my participation in this project are described in chapter 3.1.3 and Appendix 3.

Still along the line of progenitor maintenance, I directly contributed to the identification of a new level of control of neurogenesis inhibition at the MHB. This mechanism is orchestrated by microRNA miR-9. miR-9 restricts neurogenesis inhibition, as well as Fgf-signalling, a crucial component of organizing activity of the MHB, thereby contributing to the anterior-posterior restriction of the MHB progenitor pool. The discovery of this bipartite effect of miR-9 in the zebrafish MH domain is presented in chapter 3.1.4 and Appendix 4.

To dissect the cellular role of the progenitor pool-specific Her factors, I compared several cellular characteristics between the MHB progenitor pool and neighboring proliferating precursor populations. With the help of a time-lapse imaging approach I could pinpoint cell division characteristics as a cellular parameter that differs between the MHB progenitor pool and neighboring proliferating precursor populations. Results from this analysis are described in chapter 3.1.5.

To broaden our perspective on the processes that control progenitor pool specification and maintenance, I conducted analyzes in the adult brain of zebrafish. First, I concentrated on the factors Her3 and Her9 that have been previously not described in adult progenitor pools. I could show that both of them are expressed within an adult progenitor pool at the MH junction, and thereby draw an interesting parallel between embryonic and adult progenitor pools. Furthermore, I participated in a comprehensive analysis of Fgf signalling in the adult brain which suggests that Fgf signalling is an important component of adult neurogenesis in the zebrafish. These adult brain projects are summarized in chapter 3.1.6 and Appendix 5.

Finally, I focused on the role of progenitor pools in neuronal identity determination in the embryonic MH domain. First, I contributed to describing expression of the ETS-type transcription factor Pet1, a specific and early marker for hindbrain serotonergic neurons located in the raphe nuclei. My contribution and the framework of this project are described in chapter 3.2.1 and Appendix 6. Second, I took part in both a small scale and a large scale forward genetic screen focused on mutants that show alterations in hindbrain serotonergic identities. These efforts and their outcome are summarized in chapter 3.2.2 and Appendix 7. Third, I analyzed the role of a timer mechanism in setting up neuronal identities in the MH domain, i.e. tested whether the moment when progenitors exit the MHB progenitor pool controls their identity. This project is described in chapter 3.2.3.

3. Results

3.1. Specification and maintenance of progenitor pools in the embryonic and adult CNS

Neural progenitor pools in the early CNS are long lasting populations of undifferentiated cells that subsequently give rise to differentiating neurons and glial cells [26,70]. Progenitor pools are of crucial importance for the development and maturation of vertebrate brains. Defects in neural progenitor pools lead to severe aberrations in development [230,352,353], as undifferentiated cells held back in progenitor pools are the basis for brain growth, diversification and perhaps plasticity, regeneration and adaption. In contrast to mammals where adult neurogenesis is restricted, most neural progenitor pools in the zebrafish CNS keep proliferating even in adult stages [12-14,288,289,293,354]. Despite the importance of neural progenitor pools for vertebrate brain development, the molecular processes of their specification and maintenance are only scarcely understood up to date. The first part of my PhD was devoted to addressing this important question.

3.1.1. Non canonical E(spl) factors define neural progenitor pools

Appendix 1 (published article) [176]

In order to get a solid fundament for further detailed analysis and interpretation of the molecular processes orchestrating specification and maintenance of neural progenitor pools, we summarized current knowledge about neural progenitor pools in vertebrates in a review [176]. We put a special focus on E(Spl) factors in the zebrafish embryonic and adult brain and we drew comparisons with the situation in the mouse embryonic brain.

A non-canonical subgroup of E(Spl) factors outlines neural progenitor pools in zebrafish

Characteristic subsets of transcription factors, such as Zic, BF-1(FoxG1), Anf (Hesx1) and Rx proteins, are expressed in neural progenitor pools [26,39]. Recent publications, as well as my observations (see in detail below in chapter 3.1.5) hint towards a specific subset of bHLH transcription factors of the E(Spl) family as specifically marking progenitor pools in the neural plate. These comprise the Her factors Her3, Her5, Her9 and Her11/Him [170,183-186], the expression of which, in various combinations, delineates most neural progenitor pools of the neural plate (for an overview see Figure 32). This subset of *her* genes shows a non-canonical regulation by Notch signalling, I will therefore further on refer to them as 'non-canonical E(Spl) factors'. During normal development, they do not require Notch signaling for their expression. Further, in conditions where Notch signalling is experimentally ectopically activated, they are not induced but, on the contrary, they are repressed by Notch signalling. This is in contrast to neurogenic areas of the neural plate, where shorter-lived progenitors (called 'proliferating neural precursors') are maintained via expression of classical *her* genes (e.g. *her4*, *hes5/her15*, *her2*

and *her12*) that mediate Notch activity [185,222]. Hence, we propose that the neural plate is subdivided into at least two separate zones (for an overview see Figure 32):

- (1) neurogenic zones where proliferating precursors are receiving Notch signalling via lateral inhibition and express genes of the canonical *her* family (*her4*, *hes5/her15*, *her2* and *her12*) and
- (2) progenitor pools that express the non-canonical *her* genes (*her3*, *her5*, *her9* and *her11/him*) and need to be protected from Notch signalling.

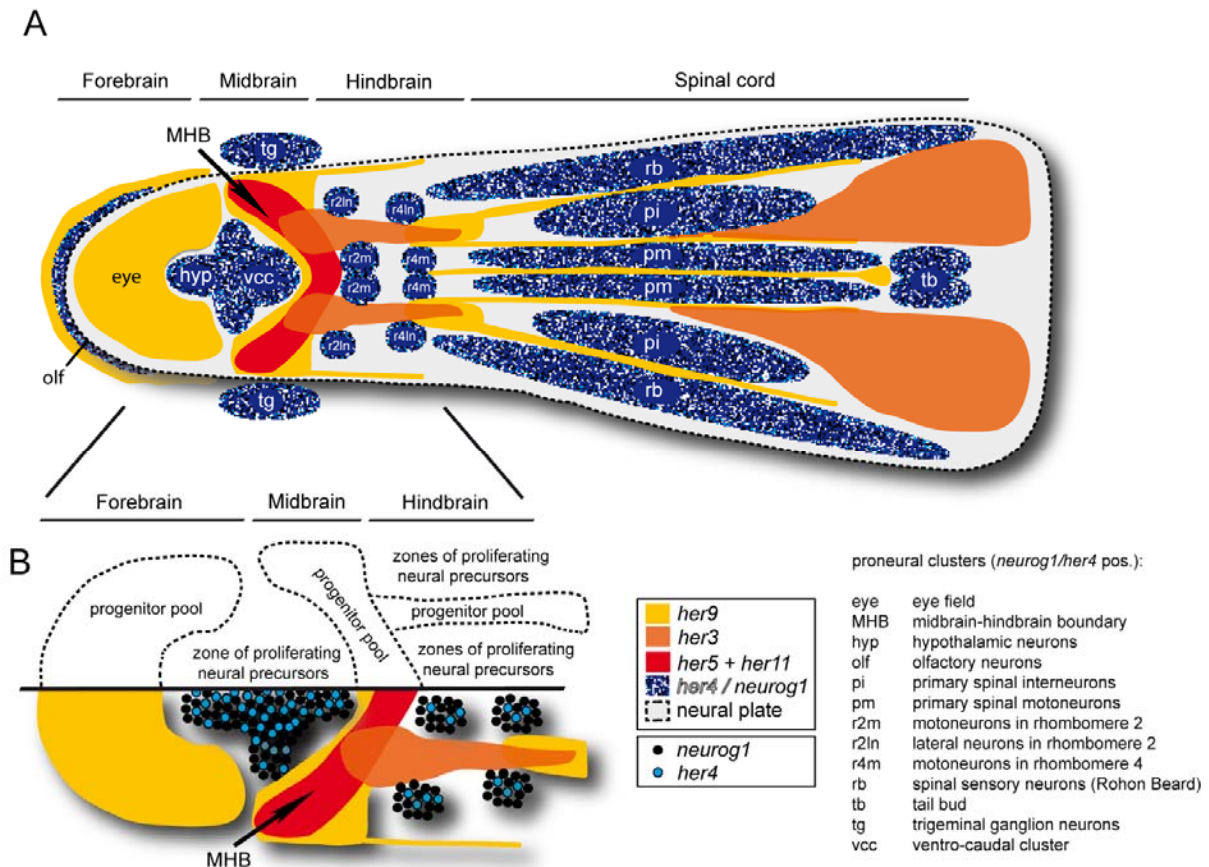


Figure 32: Overview on E(Spl) activity, progenitor pools and proneural clusters in the zebrafish neural plate. (A) Scheme represents a flat-mounted embryo at the 3-somite stage from a dorsal viewpoint. Anterior is to the left. *her* gene expression domains are color-coded. The MHB is highlighted by a black arrow. (B) represents a higher magnification of the midbrain-hindbrain domain. Note that *her4* is expressed in a salt-and-pepper pattern, intermingled by cells positive for *neurog1* while the non-canonical *her* genes are expressed uniformly in the progenitor pools.

The role of E(Spl) factors in neural progenitor pools in the mouse

To assess if the above-mentioned observations have been conserved in vertebrate nervous systems during evolution, we compared the situation in zebrafish with the embryonic situation in mouse. From the set of seven *E(Spl)* genes in mouse, *Hes1*, *Hes3* and *Hes5* are expressed at high levels in the developing nervous system and are required to prevent premature neuronal differentiation [225,230,231], similarly to *her* genes in zebrafish. However, in contrast to *her3/5/9/11* in zebrafish, the expression of *Hes1/3/5* is generally activated by Notch signalling. Interestingly, recent reports state however that the expression of *Hes1* and *Hes3* is preceding Notch

expression in the neural plate [355] and is not lost at the MHB in a *Notch1* knockout background [356]. This makes it possible that a Notch-independent mode of regulation also exists, in some locations and in particular at boundaries, for mouse *Hes* genes. These findings, together with the fact that *Hes1* is expressed at low levels and in a salt-and-pepper pattern in neurogenic zones while it is highly expressed in all cells at boundary zones [233], lead us to a model where distinct progenitor types correspond to the expression of distinct *E(Spl)* genes (or to a different mode of regulation of these genes). This model is schematized below in Figure 33.

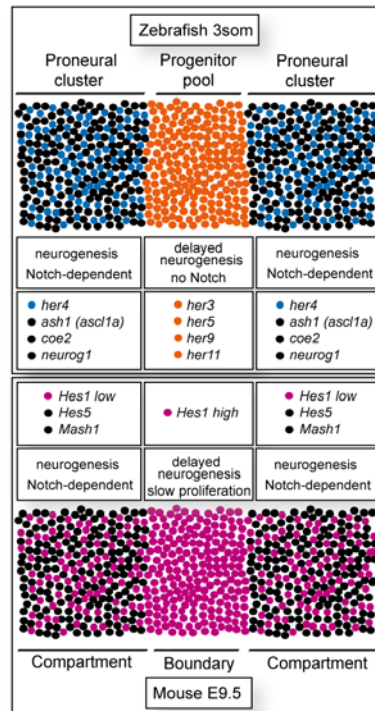


Figure 33: Comparison of *E(Spl)* gene expression in the embryonic MH domain of zebrafish versus mouse. The non-canonical *her* factors *her3/5/9/11* are expressed in the zebrafish MHB progenitor pool and mediate a delay in neurogenesis as depicted in the middle of the upper panel. They do not require Notch for activation. The progenitor pool is flanked on either side by proneural clusters that show a salt-and-pepper pattern of cells either expressing *her4* (proliferating neural precursors) or *neurog1* (cells undergoing neurogenesis). *her4* is a canonical *her* gene that is induced by Notch signalling. The corresponding situation in the early mouse MH domain is depicted in the lower panel. The mouse MHB progenitor pool is characterized by a slow mode of proliferation, delayed neurogenesis and high levels of *Hes1* expression, while the flanking neurogenic domains, also called 'compartments', express *Hes1* in a lower level in a salt-and-pepper pattern [233]. What is accomplished by different sets of *her* genes in zebrafish might be controlled by only one single differentially regulated *Hes* gene in mouse.

Conclusion and perspectives

Our model has to be consolidated by a more extensive lineage analysis coupled to a detailed description of cellular properties of the different progenitor types, in addition to their known molecular differences (for both points see chapter 3.1.5). Furthermore, it will be highly interesting to analyze whether the non-canonical *E(Spl)* genes also highlight a specific subtype of progenitors in the zebrafish adult brain. For instance, their expression might correlate with adult neural stem cells. This point has recently been shown for *her5* at the adult isthmic proliferation zone (IPZ), which is a neural

stem cell population [13]. As a first step towards expanding our knowledge on non-canonical *E(Spl)* genes in the adult zebrafish brain, I have analyzed the adult expression of *her3* and *her9* (for details see 3.1.6). Finally, it will be highly interesting to challenge our model in other systems than the zebrafish. Along these lines, Hes1 has recently been shown to be expressed in adult neural stem cell zones in the mouse [292]. Its role in these cells remains to be tested.

3.1.2. Specification of the eye field progenitor pool during early forebrain development

Appendix 2 (published article) [357]

In order to unravel molecular processes that specify neural progenitor pools, I participated in a recessive ENU (N-ethyl-N-nitrosourea) mutagenesis screen run in our lab and focused on the loss of progenitor pools (see also chapter 3.2.2) [358]. Among several interesting phenotypes I decided to analyze *ne2611*, a mutant line that showed a very clear and striking loss of most eye structures, most likely reflecting defects in specifying or maintaining the eye field neural progenitor pool.

As the eye field neural progenitor pool^a and its derivatives, for their relatively simple structure, are a particularly suitable model system to explore the molecular mechanisms of development of the nervous system [359], I decided to analyse this mutant in morphological and molecular detail.

A point mutation in *rx3* leads to the loss of most eye structures and a concomitant expansion of the telencephalic anlage in *ne2611*

Through a detailed analysis of the morphological phenotype of *ne2611* mutants at 36hpf, I could show that the eye loss phenotype is accompanied by an expansion of telencephalic structures. These defects are highly specific as neighbouring neural structures such as the nasal placodes and the epiphysis are undisturbed, at least at the morphological level.

I could corroborate telencephalic expansion at the molecular level by using the expression of *emx2*, *emx3*, *dlx2* and *tbr1* as early markers of the developing telencephalon^b. Further molecular markers, analyzed at the 15-somite stage, demonstrated that defects in *ne2611* were restricted to the forebrain anlage. I used *lhx5* and *arx* as markers for prethalamus and posterior thalamus respectively, *her5* as marker for the MHB and *krox20*^c as marker for the anterior hindbrain. Only forebrain domains rostral to the *arx* domain were significantly changed in *ne2611* homozygous mutants^d.

Using complementation tests I could show that the *chokh/rx3* (retinal homeobox gene 3) [60,63] locus carries the causative mutation leading to the observed phenotype in *ne2611* (therefore further on called *chk*^{*ne2611*}). Sequencing revealed a T to C transition that leads to a Serine to Proline substitution in a highly conserved region of the paired-like homeodomain of Rx3. I could substantiate this finding by a rescue of the mutant phenotype after injecting a bacterial artificial chromosome (BAC) containing the genomic *rx3* locus and flanking sequences. By over-expressing

^a Furtheron just called eye field

^b Figure 1 and Supplementary Figure1 in Appendix 2

^c renamed to: *early growth response 2b (egr2b)* (ZFIN)

^d Figure 1 in Appendix 2

wildtype and mutant forms of *rx3* I could further show that *chk*^{ne2611} is a full null mutation^a.

Rx3 controls an eye field versus telencephalic identity choice in early forebrain patterning

As the telencephalic expansion phenotype had not been mentioned in previous publications of zebrafish *chokh/rx3* alleles [63,360,361], I reanalyzed the first published *chk*^{s399} null allele [63] in morphological and molecular detail and found comparable telencephalic aberrations leading me to argue that this effect is a true consequence of Rx3 loss of function.

In order to dissect the molecular processes that lead to the morphological defects I pinpointed the first patterning differences in *chk*^{ne2611} mutants. Using the early telencephalic marker *tlc* [59] I could observe forebrain patterning defects already at late gastrulation stages when the eye field is first specified. *tlc*, which is first broadly expressed in the forebrain domain and normally gets downregulated in the forming wildtype eye field, fails to get downregulated in the *chk*^{ne2611} mutant context^b. This speaks strongly for an early onset fate transformation from eye field to telencephalon as a consequence of the *chk*^{ne2611} mutation. The same marker analysis confirmed this phenotype in the *chk*^{s399} allele. Analysis of further early telencephalic markers (*foxg1*, *emx3*) showed a similar ectopic expansion into the eye field of *chk*^{ne2611} mutants^c. Moreover, I could prove the eye field to telencephalic fate transformation with fate tracing experiments. Early prospective eye field cells, traced with the help of activated (uncaged) fluorescein, contributed consistently to the expanded telencephalon in *chk*^{ne2611} mutants^d. Analysis of cell proliferation and cell death showed that these processes do not contribute significantly to the observed phenotype^e.

Rx3 acts in a cell autonomous way

It has been shown by transplantation experiments in Medaka that Rx3 acts in a cell autonomous manner to instruct the process of eye vesicle evagination [62]. Following the outcome of my analysis presented above I wanted to test if the zebrafish Rx3 ortholog also acts in a cell-autonomous manner in the earlier steps of forebrain patterning. In order to assess the cellular identity of the transplanted cells I made use of the *rx3* enhancer trap line CLGY469 that we had established together with our collaborators at the SARS Centre in Bergen, Norway (see also [134,362]). I transplanted rhodamine labelled cells from the *rx3* enhancer trap line homotopically and isochronically into non-transgenic *chk*^{ne2611} mutants. Small patches of transplanted wild-type cells turned on the transgene in a mutant surrounding in a high proportion^f, clearly showing that maintenance of the eye field identity and repression of telencephalic fate is encoded in a cell autonomous way by Rx3.

^a Figure 3 in Appendix 2

^b Figure 4 in Appendix 2

^c Figure 4 in Appendix 2

^d Figure 6 in Appendix 2

^e Figure 5 in Appendix 2

^f Figure 7 in Appendix 2

Conclusion: Model of early forebrain patterning

The forebrain is patterned during gastrulation stages by Wnt signalling whereby the posterior diencephalic Wnt source is counterbalanced by an anterior Wnt antagonist [29] (blue in Figure 34). The resulting gradient defines different identities. High Wnt concentrations instruct presumptive diencephalon (green in Figure 34) while low Wnt concentrations define an anterior domain that is the common anlage for telencephalon and eyes [29] (violet in Figure 34). Soon after, at around tailbud stages at the beginning of neurulation, this anterior domain becomes subdivided into separate telencephalic (blue in Figure 34 upper panels) and eye field (red in Figure 34 upper panels). Summarizing the data obtained from the *rx3* mutant analysis, we propose that Rx3 is crucially involved in this latter subdivision process by actively down-regulating telencephalic fate in the future eye field. In complete absence of functional Rx3, such as in homozygous *chk^{ne2611}* mutants, this downregulation of telencephalic fate in the future eye field does not happen, resulting in a loss of eye structures and an expansion of the telencephalon (lower panels in Figure 34).

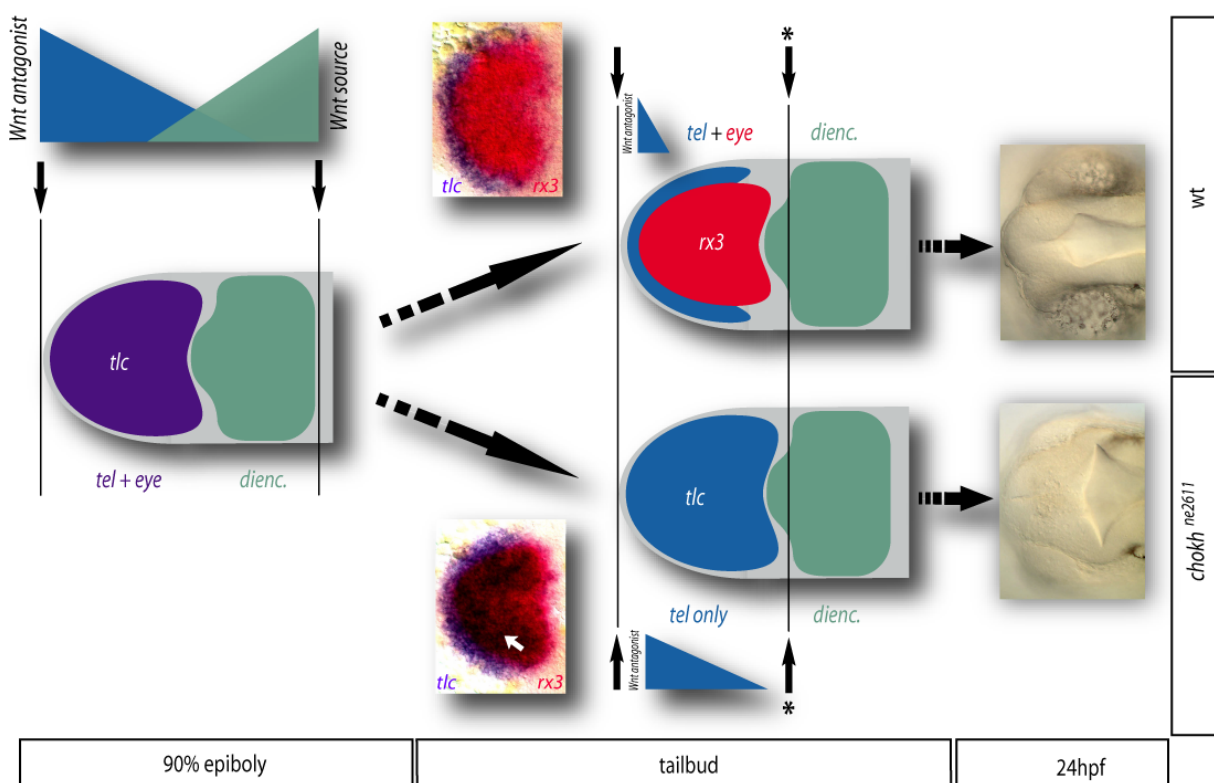


Figure 34: Model of early forebrain patterning with a focus on the role of Rx3 in wt and its loss of function in *chk^{ne2611}*. During gastrulation stages (left side of panel) the forebrain is believed to be patterned as a whole by posterior Wnt activity, favoring diencephalic fates, and anterior Wnt-repression, favoring anterior fates (patterning boundaries are indicated by black lines) [29]. Note that telencephalon and eye field form still a common anlage, revealed by the broad expression of the Wnt-antagonist *tlc*. Shortly afterwards, at tailbud-stage (middle panels) a new posterior patterning boundary is defined in the anteriormost diencephalon (marked by asterisk) isolating anterior from posterior forebrain. In this restricted anterior forebrain domain commencing Rx3 activity downregulates *tlc* expression and mediates eye field fate in the wildtype, leading to a proper development of the eye field progenitor pool and eye structures in the later embryo (upper right part of panel). In *chk^{ne2611}* mutants Rx3 is not functional and therefore *tlc* is not properly downregulated leading to an aberrant eye field specification and results in a loss of retinal structures (lower right part of panel). Examples for flat-mounted preparations of whole-mount in situ hybridization with *tlc* (blue) and *rx3* (red) at tailbud-stage are given in the small insets in the middle of the panel. Note the double expression in the eye field of mutants (white arrowhead). All schemes and images represent dorsal views and anterior is left.

3.1.3. Interactors and cooperators of E(Spl) factors in specification and maintenance of the MHB neural progenitor pool

Appendix 3 (manuscript in revision)

Despite the fact that many determinants are expressed uniformly across neural progenitor pools, as it is the case for example for *rx3* in the early eye field [357] and for *her5* and *her11* at the early MHB [170,176,186], neural progenitor pools are in many respects not of a complete uniform character. A very prominent case for such a difference is the early MHB progenitor pool, also known as 'Intervening Zone' (IZ), that has a higher propensity to undergo neurogenesis medially (medial intervening zone (MIZ)) than laterally (lateral intervening zone (LIZ)) upon experimental downregulation of E(Spl) activity [186]. This difference is later in development reflected by a basal to alar difference in the onset of neuronal maturation [171]. Up to now the molecular mechanisms responsible for this difference in neurogenesis propensity within the early MHB progenitor pool are not known. In order to shed light onto these mechanisms, I joined a project initiated by Jovica Ninkovic where we tested several candidate signalling cascades for their potential implication in this process.

GSK3 β is a crucial factor required for formation and maintenance of the MIZ

Pilot experiments showed that MIZ cells undergo premature neurogenesis after treatment with the Wnt signalling activator LiCl [363,364], at a discrete developmental time window (80% epiboly)^a. Interestingly, epistasis experiments using a conditional heatshock-inducible transgenic line [365] expressing a downstream repressor of canonical Wnt-signalling showed that the observed influence of LiCl treatments on MIZ neurogenesis was not mediated by canonical Wnt signalling^b. This effect, however, involves downregulation of GSK3 β activity, since it could be mimicked using the specific GSK3 β blocker OTDZT^c. Therefore we could pinpoint GSK3 β as a crucial player in formation and early maintenance of the MIZ.

PKA acts in concert with GSK3 β and E(Spl) factors to permit IZ formation

As GSK3 β is implicated in several different signalling pathways by phosphorylating the cAMP-dependent protein kinase A (PKA) [366-368] we tested if manipulation of PKA function had an influence on IZ neurogenesis. Overexpression of a constitutively active form of PKA (PKA*) [369] did not influence neurogenesis by itself but could rescue ectopic MIZ neurogenesis induced by either LiCl treatment or downregulation of E(Spl) activity^d. To clarify if PKA itself is required for IZ formation we blocked PKA signalling with a dominant negative form of the regulatory subunit of PKA (dnReg) [370]. This led to ectopic neurogenesis at the MIZ^e. In addition, after downregulating E(Spl) function by blocking *her5* translation also the LIZ showed ectopic neurogenesis, showing that PKA inhibition increases the tendency of the whole IZ to undergo neurogenesis. Taken together, these analyses indicated that PKA is

^a Figure 2 in Appendix 3

^b Figure 2 in Appendix 3

^c 2,4-Dibenzyl-5-oxothiazolidine-3-thione

^d Figure 3 in Appendix 3

^e Figure 4 in Appendix 3

crucially involved in MIZ neurogenesis inhibition in vivo. Furthermore, a combined inhibition of PKA and GSK3 β led to ectopic neurogenesis at the MIZ as well as at the LIZ^a hinting towards a dose dependent mechanism co-regulated by PKA and GSK3 β . Finally, a dose dependence epistasis test with increased levels of E(Spl) activity did not rescue the ectopic MIZ neurogenesis effect resulting from PKA blockade^b, speaking in favour of a model where GSK3 β /PKA acts downstream of E(Spl) factors. To sum up, we could show that GSK3 β /PKA is a component of neurogenesis inhibition at the IZ that is, similarly to E(Spl) activity, sensed in a different manner by MIZ and LIZ.

The difference between MIZ and LIZ is most likely cell-autonomously encoded and independent of proliferation

In order to clarify if the difference between MIZ and LIZ is cell-autonomously or non-cell-autonomously encoded I traced the lineage of MIZ cells from the onset to the end of gastrulation using caged-fluorescein (for description of method see also [357]). I could show that presumptive MIZ cells, labelled at the beginning of gastrulation, are also found at medial positions at the end of gastrulation, arguing that MIZ and LIZ precursors do not mix during gastrulation^c. This spatial separation makes it possible that MIZ and LIZ cells inherit different determinants.

As cell cycle speed in neural progenitor cells has been shown to be crucially linked to the propensity to undergo neurogenesis [371], we looked for alterations in cell cycle speed between MIZ and LIZ cells. We could not detect any significant difference^d, arguing that the determinants above probably do not act on the cell cycle.

Gli1 acts as pro-neurogenic factor accounting for the difference between MIZ and LIZ

Looking for potential candidates mediating the difference between MIZ and LIZ we identified Gli1 as cellular commitment factor [372] that displays a clear difference in expression level between MIZ and LIZ at stages relevant for our analysis^e. Previous studies also implicated Gli1 in the GSK3 β /PKA pathway as target regulated by PKA [373-375]. We blocked Gli1 function, and our results show that Gli1 exerts a pro-neurogenic function opposing GSK3 β /PKA. Finally we could show that Gli1 antagonizes E(Spl)-mediated neurogenesis repression.

Conclusion: Gli1 is responsible for medial to lateral differences of neurogenesis propensity at the MHB neural progenitor pool

Our study has, for the first time, described a factor that accounts for the intrinsic difference between MIZ and LIZ in their propensity to undergo neurogenesis (Figure 35). An obviously interesting task is now to identify the upstream signalling pathway positioning *gli1* expression at these early stages. By testing several potential signalling pathway candidates, including Fgf-, Shh- and Nodal-signalling, we could, up to now, not successfully identify its upstream regulators.

^a Figure 4 in Appendix 3

^b Figure 4 in Appendix 3

^c Figure 5 in Appendix 3

^d Figure 5 in Appendix 3

^e Figure 5 in Appendix 3

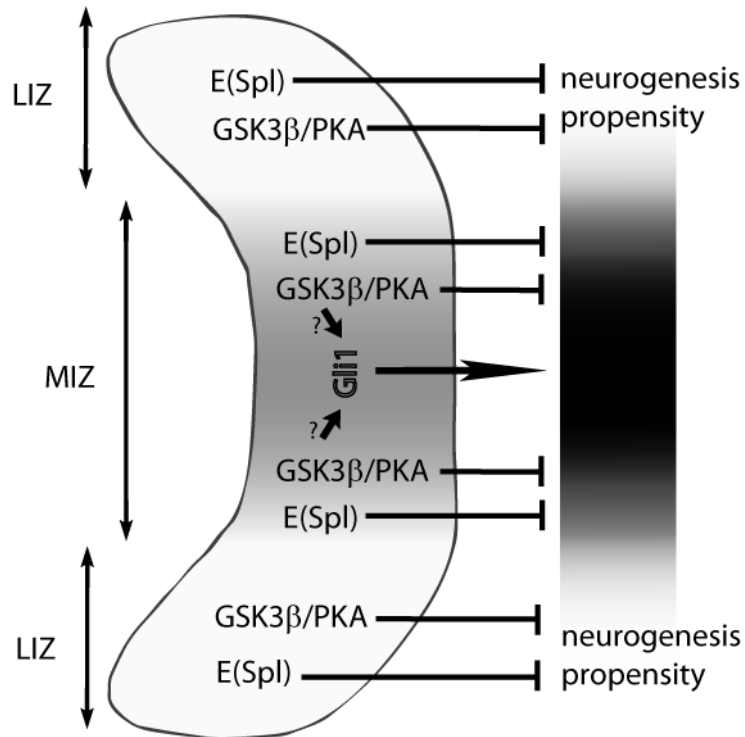


Figure 35: Roles of Gli1 and GSK3 β /PKA in neurogenesis inhibition at the MHB progenitor pool. Schematized dorsal view of the MHB (anterior is left). Medio to lateral gradient of propensity to undergo neurogenesis is denoted by gradient on the right. E(Spl) (Her5/Her11) and GSK3 β /PKA activity cooperatively block neurogenesis across the whole MHB progenitor pool (outlined). Gli1 counteracts this neurogenesis repression leading to a higher neurogenesis propensity in the MIZ compared to the LIZ.

3.1.4. Identification of factors limiting the activity of E(Spl) factors at the MHB

Appendix 4 (published article) [283]

Neural progenitor pools do not only have to be precisely induced but they also have to be restricted in time and space to maintain progenitors and sustain a coordinated development of the nervous system. Up to date we only have a poor understanding of these crucial restriction processes. At the MHB, a striking feature is the spatial coincidence between the progenitor pool and the MHB organizing center, the IsO. The latter, via Fgf signalling, controls patterning of the entire MH domain. These observations suggest that a mechanism involved in positioning or limiting the MHB progenitor pool might be its association with the MHB signalling center. Following this idea together with Christoph Leucht, a former postdoctoral fellow in the laboratory, I embarked on finding and dissecting new molecular processes mediating the spatial association of the organizer and neural progenitor pool at the zebrafish MHB.

MicroRNAs (miR) are good candidates for such a higher order repressive mechanism. They convey repression via specific binding to 3'UTRs. Therefore it was obvious to focus on the 3'UTRs of a battery of prominent MHB genes. miR target site prediction algorithms revealed high probability binding sites for miR-9 in important MHB effectors and Fgf-signalling components such as *fgf8*, *fgfr1* and *canopy* as well as the MHB neurogenesis inhibitors *her5* and *her9*.

miR-9 interacts in vivo with MHB Fgf-signalling components as well as MHB neurogenesis inhibitors

The correctness of the computer predictions could be tested in vivo by sensor assays and quantified by Western-blot. A strong miR-9-mediated repression could be shown on the 3'UTR elements of *her5*, *her9*, *fgf8*, *fgfr1* and *canopy*. By specifically mutating the predicted miR-9 target sites in the *her5* and *fgfr1* 3'UTRs I could further prove the accuracy of the miR-9 target prediction^a. Moreover, I could show that overexpressing miR-9 results in a specific MHB loss, visible at the morphological level and with molecular markers^b.

miR-9 downregulates Fgf-signalling

In order to dissect the effects of miR-9 at the MHB, a first focus was placed on Fgf-signalling. Overexpression of miR-9 reduced the expression of the Fgf downstream effector *dusp6* and abolished *pea3* expression, a further Fgf downstream effector^c. In addition miR-9 overexpression phenocopied the hindbrain-to-midbrain fate transformation of the *fgf8* mutant *ace*. Furthermore, I could rescue the MHB defects by co-injecting, together with miR-9, target protector antisense oligonucleotides ('Morpholinos') that specifically protect the effective miR-9 target site on the 3'UTR of *fgfr1*^d. This indicates that inhibition of *fgfr1* by miR-9 in our overexpression experiments is instrumental in causing MHB loss.

miR-9 promotes neurogenesis

The loss of Fgf-signalling cannot fully explain the observed miR-9 overexpression phenotype, however, in particular not the early onset of MHB marker gene loss. Therefore I analyzed the second group of potential MHB gene targets – the neurogenesis inhibitor genes *her5* and *her9*. Indeed, I found that miR-9 overexpression phenocopies the ectopic MHB neurogenesis effect of a concomitant down-regulation of *her5* and *her9* (via gripNA antisense oligonucleotides)^e. This ectopic neurogenesis could be also documented at later stages of development, a phenotype that is not observable in the *fgf8* mutant *ace*, therefore validating an action of miR-9 on the MHB neurogenesis inhibition pathway independently of its control of Fgf signalling. Again, using the target protection assay, I could show that the MHB loss can be rescued by protecting *her5* from being targeted by miR-9^f.

miR-9 mediates the anterior-posterior restriction of the MHB

Endogenous miR-9 expression commences at 24hpf at the telencephalon and later spreads throughout the CNS, specifically and precisely sparing the MHB^g. This is in line with the overexpression data presented above and underscores a specific role of miR-9 in restricting the MHB in space and time. The notion that miR-9 mediates its MHB regulation both via repressing Fgf-signalling and anti-neurogenic genes, could be further proven by miR-9 loss of function using an anti-miR-9 Morpholino. This

^a Figure 2 in Appendix 4

^b Figure 1 in Appendix 4

^c Figure 3 in Appendix 4

^d Figure 3 and Supplementary Table 1 in Appendix 4

^e Figure 4 in Appendix 4

^f Figure 4 in Appendix 4

^g Figure 5 in Appendix 4

treatment leads to an extensive expansion of *dusp6* expression showing again the direct effect of miR-9 on Fgf-signalling^a. Additionally, I could rescue the anti-neurogenic effect of miR-9 loss-of-function by inhibition of *her9* and could therefore further underscore the specific effect of miR-9 on the neurogenesis inhibition pathway mediated by *her* genes^b.

Conclusion: miR-9 has a bipartite effect on MHB positional control and maintenance

With the description of the roles of miR-9 in orchestrating both MHB organizer function and neurogenesis inhibition (see Figure 36), I could contribute significantly to the understanding of the positional control and late maintenance of the MHB neural progenitor pool. Moreover, my dissection of miR-9 function at the zebrafish MHB suggests a previously unsuspected role of microRNAs, namely the spatial coordination of late neural tube organizers (see Figure 36). Regulating two separate processes, each via several sub-components, with one single microRNA most likely constitutes a metabolically cheap and at the same time robust mechanism to control complex processes such as MHB maintenance.

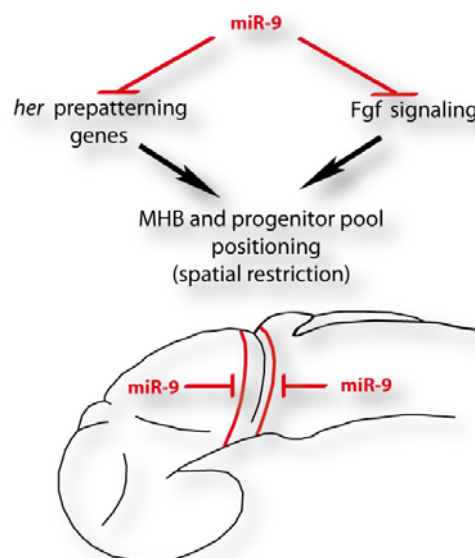


Figure 36: Bipartite function of miR-9 in restricting the MHB organizer and progenitor pool. miR-9 represses independently *her* pre patterning genes and Fgf signalling (upper half of panel). The expression domains of miR-9 in the late embryonic neural tube enclose the MHB progenitor pool.

^a Figure 6 in Appendix 4

^b Figure 7 in Appendix 4

3.1.5. Transition between progenitor subtype is accompanied not only by a change in E(spl) factor expression but also by a change of specific cellular properties

As already discussed in chapter 3.1.1, there is a specific molecular difference between the MHB progenitor pool and neighbouring proliferating precursors, namely the expression of non-canonical *her* genes (*her3*, *her5*, *her9* and *her11*) in the progenitor pool (see Figure 37C and D) [170,183,184,186] versus the expression of the canonical *her* gene *her4* in neighbouring proliferating neural precursors [222]. Interestingly, I observed that the MHB neural progenitor pool can switch towards a proneural cluster state (compare Figure 37A versus B, white arrow) when the function of non-canonical E(Spl) genes is downregulated. This was obtained by injecting into one-celled embryos antisense oligonucleotides targeting specifically *her3*, *her5*, *her9* and *her11* (4xGRIP). This observation extends previous findings showing that the MIZ transforms in a proneural cluster in the absence of Her5 activity [184][186]. Hence, a loss of non-canonical E(Spl) gene activity likely transforms progenitor pool cells into proliferative neural precursors. This highly interesting finding led me to ask whether distinct cellular properties accompany the differential expression of *her* genes. Therefore I tested these two populations for differences in cell division speed, radial glia characteristics and type of cell division. I also assessed whether they are normally related in lineage.

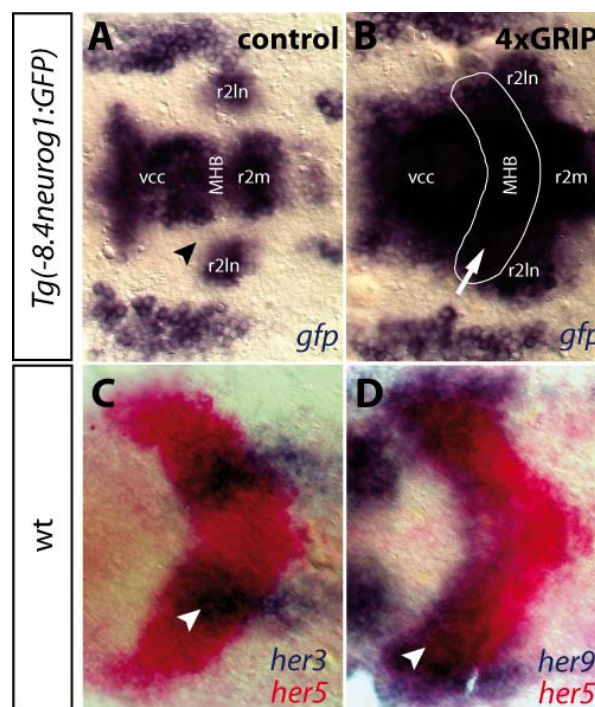


Figure 37: Downregulation of non-canonical E(Spl) activity induces a switch from the progenitor pool to a proneural cluster-like state. (A,B) *Tg(-8.4neurog1:GFP)* embryos [376] probed for *gfp* show that MHB progenitor pool cells switch from a *neurog1:gfp*-negative in control (A, black arrowhead) to a *neurog1:gfp*-positive state in embryos injected with gripNAs targeting *her3*, *her5*, *her9* and *her11* (4xGRIP) at 0,4mM each (the position of the MHB pool is outlined in white in B and indicated by a white arrow). (C) *her3* expression overlaps the junction between MIZ and LIZ (indicated by white arrowhead) speaking for a role in MHB neurogenesis repression [183]. (D) *her9* is expressed in anterior and lateral aspects of the MHB (indicated by white arrowhead). All images are dorsal views oriented anterior to the left and represent flat-mounted embryos at the 3-somite stage after single (A, B) or double (C, D) whole-mount RNA in situ hybridization (probes are given in the lower right of each panel; color coded). MHB: midbrain-hindbrain boundary; r2ln: lateral neurons in rhombomere 2; r2m: motoneurons in rhombomere 2; vcc: ventro-caudal cluster.

MHB progenitor pool and neighbouring proliferating precursors do not differ in expression of the radial glia marker GFAP

The intermediate filament ‘glial fibrillary acidic protein’ (GFAP) is a well characterized radial glia marker in the embryonic and adult zebrafish brain [12-14,377-380]. GFAP-positive cells in zebrafish have a proliferation potential [12,381] and might mark a specific subset of more differentiated progenitors in the embryonic zebrafish brain as it has been shown in the mammalian brain for radial glia cells [382]. Intriguingly, in mouse a difference in *Hes* gene expression and Notch dependency has been postulated to underlie the transition from neuroepithelial to radial glial progenitors, whereby *Hes* dependency precedes Notch dependency in an intermediate progenitor state [225,354]. If an evolutionary parallel in progenitor type progression exists, and because progenitor pool cells do not require Notch while proliferating neural precursors do, I would expect progenitor pool cells to be GFAP-negative with neuroepithelial cell-like characteristics, while the proliferating precursor population would contain more differentiated and fate-restricted radial glia-like GFAP-positive progenitors. To test this hypothesis, I probed zebrafish embryos between tailbud-stage and 25hpf with *gfap* in whole-mount RNA in situ hybridizations (Figure 38A to F). Surprisingly, I could not observe a difference in GFAP expression between MHB cells and neighbouring proliferating precursors. This result was confirmed by immunohistochemistry at the 20-somite stage: GFAP-positive endfeet were spread across the entire MH domain (Figure 38G to G’'). Similar observations have been made by Marcus and Easter [377] at slightly later stages. Therefore, GFAP expression does not distinguish the MHB neural progenitor pool from surrounding proliferating neural precursor populations.

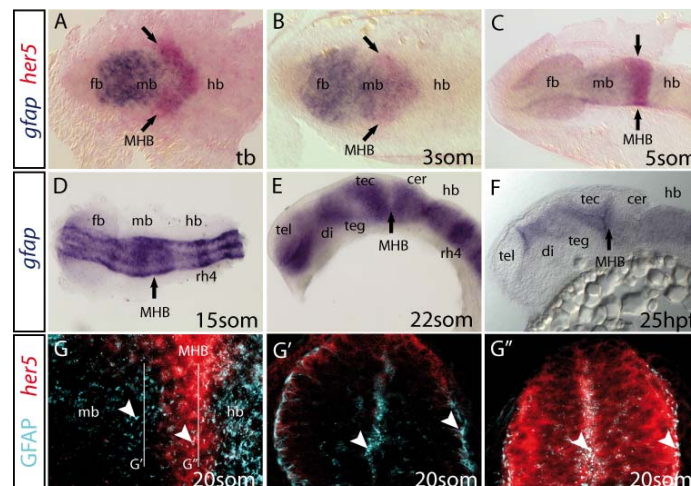


Figure 38: Progenitor pool and proliferating precursor populations do not differ in their expression of GFAP. (A-F) Time series of whole-mount in situ hybridizations with the *gfap* probe between tailbud stage (tb) and 25hpf show *gfap* expression at the MHB (indicated by black arrows) as well as in the neighbouring midbrain at all stages. (G-G’’) confocal projections of combined fluorescent whole-mount RNA in situ hybridization with *her5* as MHB marker and immunohistochemistry detecting GFAP (secondary antibody Cy5-labelled) at the 20-somite stage show no difference in GFAP signal between the MHB progenitor pool and neighboring midbrain and hindbrain regions containing proliferating precursor populations. G is a sagittal section, with focus on the MH domain. G’ and G’’ are cross sections at the A/P levels indicated by white lines in G. Dorsal is up. White arrowheads indicate positions of strongly GFAP-positive endfeet. No difference is visible in GFAP expression when comparing midbrain (G’) and MHB (G’’). (A-G) embryos are oriented anterior to the left. Abbreviations: cer: cerebellum; di: diencephalon; fb: forebrain; hb: hindbrain; hpf: hours post fertilization; mb: midbrain; MHB midbrain-hindbrain boundary; rh4: rhombomere 4; som: somite stage; tb: tailbud-stage; tec: tectum; teg: tegmentum.

Cell proliferation rate does not significantly differ between the MHB progenitor pool and midbrain proliferating precursors at early developmental stages

In mouse, it has been recently shown that cells at boundary zones, and in particular those close to the MHB, are characterized by a lower cell division rate [140,233]. Furthermore, high levels of Hes1 activity, the best candidate functional homolog of non-canonical *her* genes (see 3.1.1) [176], forces cells into a slower proliferation mode when it is expressed at high levels, and this in several systems [233,383]. Finally, the transition from neuroepithelial to radial glia progenitors, and concomitant changes of proliferative to neurogenic divisions, are accompanied by increasing cell cycle length in mouse [382,384]. Therefore I wanted to clarify if differences in proliferation rate are correlated with the two progenitor types in the zebrafish neural tube. To this aim, I conducted a proliferation analysis between the 15-somite stage and 48hpf. Comparing the number of cells in division using an antibody detecting the metaphase maker phosphorylated histone H3 (pH3) [385] in the transgenic line *Tg(her5PAC:EGFP)* shows that there is no significant difference in the proportion of cells in M phase between the *her5* RNA-positive MHB and its *her5PAC:EGFP*-positive derivatives in the midbrain [70] between the 15-somite stage and 27hpf (see Figure 39). In contrast to that, at 36hpf and 48hpf I could observe highly significant differences between the two populations (see Figure 39). To verify that these changes in the proportion of cells in M phase indeed reflect changes in cell cycle speed, I analyzed proliferation as a whole using a marker of all cell cycle phases, *minichromosome maintenance deficient 5 (mcm5)* [386](see Figure 39A'). Double in-situ hybridization for *her5* and *mcm5* demonstrated that all *her5*-positive cells divide throughout the stages studied. Hence, the proportion of cells in M phase reflects the labelling index and we conclude that *her5* RNA-positive cells, i.e. the proliferation pool at the MHB, acquires a slow proliferation mode between 27hpf and 36hpf. Slower cell proliferation is a property of the late MHB progenitor pool (after 27 hpf), but not of the early progenitor pool. Therefore, at least at early stages, cell proliferation rate in the MH domain is not a cellular property under differential control of non-canonical versus canonical *her* genes.

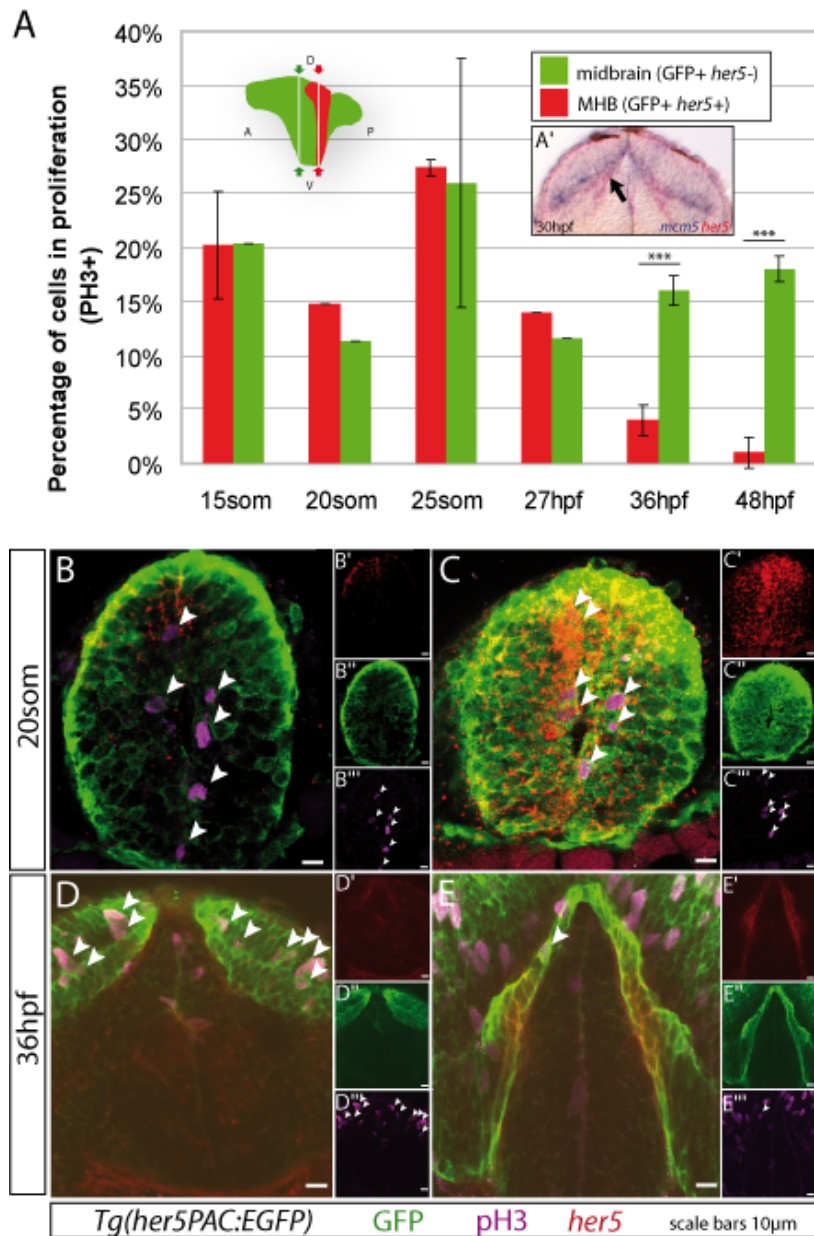


Figure 39: Cell proliferation rate does not differ between MHB progenitor pool and midbrain proliferating precursors before 27hpf. (A) The number of cells in M phase (phosphorylated histone H3-positive, pH3+) [385] at midbrain levels (GFP+ and *her5*-, green in inset scheme and bars) was compared to pH3+ cells at the MHB (GFP+ and *her5*+, red in inset scheme and bars). The number of pH3+ cells was divided by the overall number of ventricular cells (potentially proliferating cells) to obtain the values on the Y axis in A. Note that between 15som and 27hpf there is no significant difference between midbrain and MHB in the percentage of cells in M phase (15som: p-value=0.965 (two-sample t-test; number of cells analyzed n=197; 2 individuals); 20som: p-value=0.7822 (Fisher's exact test; n=114; 1 individual); 25som: p-value=0.8857 (two-sample t-test; n=166; 2 individuals); 27hpf: p-value=0.7941 (Fisher's exact test; n=154; 1 individual)). At later stages there is a highly significant difference - indicated by three stars above bars (36hpf: p-values=0.0000753 (two-sample t-test; n=451; 6 individuals); 48hpf: p-value=0.0000242 (two-sample t-test; n=320; 5 individuals)). Note that, across these stages, all *her5*-positive cells are still proliferating as they are co-labelled with *mcm5* at 30hpf by double whole-mount RNA in situ hybridization (black arrow in A'; 25µm cryo-section; cross section at MHB level). (B-E) Examples of confocal scans of cryo-cross sections used for cell proliferation analysis at 20som (no significant difference, see also A) and 36hpf (highly significant difference, see also A). (B-E) are overlays of the three channels as indicated in the color code. Arrowheads point to representative examples of pH3+ cells in regions relevant for the analysis. Note the strong reduction of dividing cells in the *her5*+ domain in E. Small insets on the right of each overlay show corresponding single channel images. Error bars in A show standard error of the mean. *Tg(her5PAC:EGFP)* embryos were used for all analyses. A: anterior; D: dorsal; P: posterior; V: ventral.

Cells of the MHB progenitor pool give rise to spatially ordered lineages in the MH domain

A further important cellular property of progenitors is their lineage [354]. Therefore I wanted to clarify if cells that express non-canonical *E(Spl)* genes at the MHB have specific cell lineage properties. To first get a global overview, I focused on labelling large cell populations. Later on, I refined the analysis to single cell tracing as described in the next paragraph. The lineage of lateral MHB cells has been previously described in our laboratory by direct lineage tracing of this population using uncaging into the GFP-positive domain of *Tg(her5PAC:EGFP)* transgenic embryos [70]. This study showed that the anterior-posterior order of cells located within the lateral MHB domain at 95% epiboly prefigures the later anteroposterior order of their derivatives in the MH domain. However, the lineage of the medial MHB progenitor pool cells remained elusive. In order to obtain a complete lineage map of the early MHB, I conducted a similar analysis for the medial MHB. My experimental data show that the lineage of medial and lateral MHB progenitor pool cells is very similar. Therefore the notion that the early spatial organization of the MHB prefigures the later spatial relation of its derivatives is also true for the medial MHB progenitor pool (see Figure 40). To conclude, the region of non-canonical E(Spl) activity at the MHB, i.e. the progenitor pool, produces progeny cells that keep their relative spatial arrangement while leaving the MHB. Furthermore, I could substantiate and complement previous findings [70] on the global lineage of the MHB progenitor pool, i.e. the anterior and posterior aspects of the MHB give rise to anterior and posterior domains of the MH domain, respectively. Interestingly, these MHB derivatives contain the proliferating neural precursors, making it highly plausible that progenitors of the MHB proliferation pool directly give rise to MH proliferating precursors. But a final conclusion on how far these two progenitor populations are lineage related needs a more refined lineage tracing as presented in the next section.

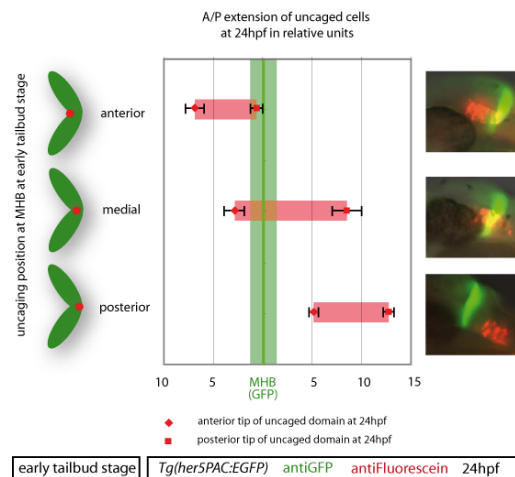


Figure 40: The antero-posterior order of the medial MHB at early tailbud stage prefigures the spatial order of its derivatives at 24hpf. A small population of cells was marked at the early tailbud stage by uncaging of caged-fluorescein injected at the one cell stage into *Tg(her5PAC:EGFP)* embryos. The uncaging spot was positioned at midline regions of the MHB using the EGFP signal as landmark (red dot marks uncaging spot in small schemes on the left; dorsal view on the embryo). At 24hpf, the embryos were fixed and processed for double immunohistochemistry. One representative example for each uncaging position is given in sagittal views on the right (antiGFP shown in green; antiFluorescein shown in red). Red bars show measurements of the anterior-posterior extension of uncaged cells relative to the MHB (indicated in green; relative units). Note the complete spatial separation of anterior from posterior uncaging positions and the only partial overlap with medial positions. Anterior is to the left.

Time-lapse tracing analysis reveals mixed division types for MHB progenitor pool cells but uniformly neurogenic divisions for proliferative precursors

To test whether MH progenitors located at the MHB or in adjacent proneural clusters differ in their mode of cell division, I further traced individual cells from both territories. To be sure to focus on progenitor cells, I specifically traced cells starting from a division event. In order to make single cell tracking feasible, I labelled a mosaic of cells with the red fluorescent membrane tracer *2xlck:mRFP* [387] in *Tg(-8.4neurog1:GFP)* embryos [376] (see Figure 41). With the help of the neurog1:GFP signal I was able to detect, at the end of the tracing, whether the cells of interest had committed to enter the neurogenic pathway. To obtain a comprehensive overview on cellular movements and division events I recorded multiple z-stacks of both the RFP and GFP channels during an extended time period spanning from early neurogenesis stages to late somitogenesis using laser scanning confocal microscopy. The neurog1:GFP signal was also used to localize the MHB, as the GFP-negative domain separating the GFP-positive ventro-caudal cluster (vcc) and rhombomere 2 (r2) domains.

The tracing of proliferating precursors in the vcc as well as r2 motoneurons and lateral neurons areas revealed only symmetric divisions that produced in all cases two neurog1:GFP-positive cells (see Figure 42). This held true whatever the commitment state of the precursor that was traced, i.e. whether it had or had not already upregulated neurog1:GFP expression at the time of division. In clear contrast, cells that divided while located within the the MHB progenitor pool had a more complex outcome. In 83% of cases I observed a symmetric division. In 80% of these, both daughter cells remained neurog1:GFP-negative and therefore likely remained progenitors; such divisions were considered proliferative. In most cases, such progeny cells remained at the MHB after division. In one case however (corresponding to 4% of all traced cases), the progeny cells populated the vcc, directly demonstrating the generation of proliferating neural precursors from precursors of the MHB progenitor pool. The remaining 20% of the symmetric divisions were considered neurogenic, as both daughter cells upregulated neurog1:GFP after the division event. In two cases (17% of the total number of cells traced from the MHB), I could document asymmetric divisions from MHB progenitor pool cells, where one daughter cell turned on the neurog1:GFP signal while the other one stayed neurog1:GFP negative. In one of these two cases the former daughter was located within proneural clusters adjacent to the MHB, while the latter remained at the MHB. To conclude, MHB pool cells, expressing non-canonical E(Spl) gene activity, display diverse cell division characteristics, including a large proportion of symmetric proliferative divisions and a smaller proportion of symmetric neurogenic and asymmetric divisions. This strikingly differs from proliferating precursors, which divide only in a symmetric neurogenic mode. Furthermore, 6 of overall 24 tracing analyses showed a cell displacement from the MHB into the region where proliferating precursors reside, but never the other way around, speaking clearly in favour of a unidirectional lineage relation between these two regions.

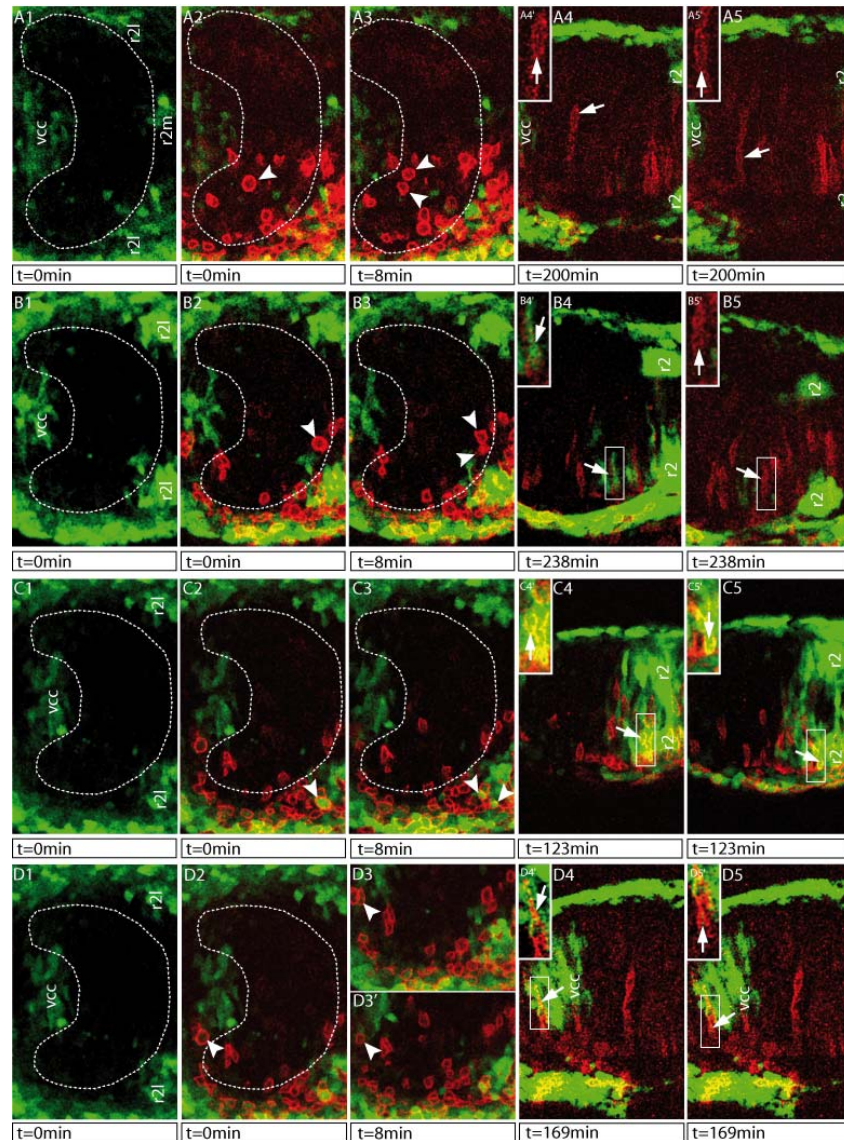


Figure 41: Time-lapse tracing analysis shows that MHB progenitor pool cells undergo mostly symmetric and in few cases asymmetric cell divisions while midbrain proliferating precursors divide symmetrically. Dorsal views of the MH region in *Tg(-8.4neurog1:GFP)* embryos [376] (GFP signal shown in green) injected with 6ng/ μ l *2xIck:mRFP* capped mRNA into 1 of 16 cells at the 16 cell stage leading to a mosaic expression of membrane targeted RFP [387] (RFP signal shown in red). Images represent single optical sections taken from different z- and t-positions of one multiple z-stack time-lapse recorded at a confocal laser scanning microscope [388]. A1, B1 C1 and D1 show the GFP channel only to reveal the extent of the MHB pool (outlined in white). A2, B2, C2 and D2 show the traced cell shortly before (marked by single white arrowhead) and A3, B3, C3 and D3 shortly after the cell division event (both offspring cells marked by white arrowheads). A4, B4, C4 and D4 represent the endpoints of tracing of one offspring, A5, B5, C5 and D5 of the second offspring cell (all marked by white arrow). Small insets show the traced cells in higher magnification, as indicated by the white box in main panel. A1 to A5 represent one example of tracing of a symmetric division at the MHB. Note that both traced offspring cells remain at the MHB and stay GFP-negative. B1 to B5 show one example of a tracing of an asymmetric division at the MHB. One traced offspring cell turns on GFP expression (B4') while the other stays GFP-negative (B5'). One example of a symmetric neurogenic division of a proliferative neural precursor that had already switched on GFP is shown in C1 to C5. Both offspring cells remain GFP-positive (C4' and C5'). D1 to D5 shows one example of a tracing of a symmetric division from a GFP-negative proliferating precursor located within the vcc proneural cluster. Note that both offspring cells turn on GFP (D4' and D5'). GFP+ proneural clusters: r2: rhombomere 2; r2l: lateral neurons in rhombomere 2; r2m: motoneurons in rhombomere 2; vcc: ventro-caudal cluster.

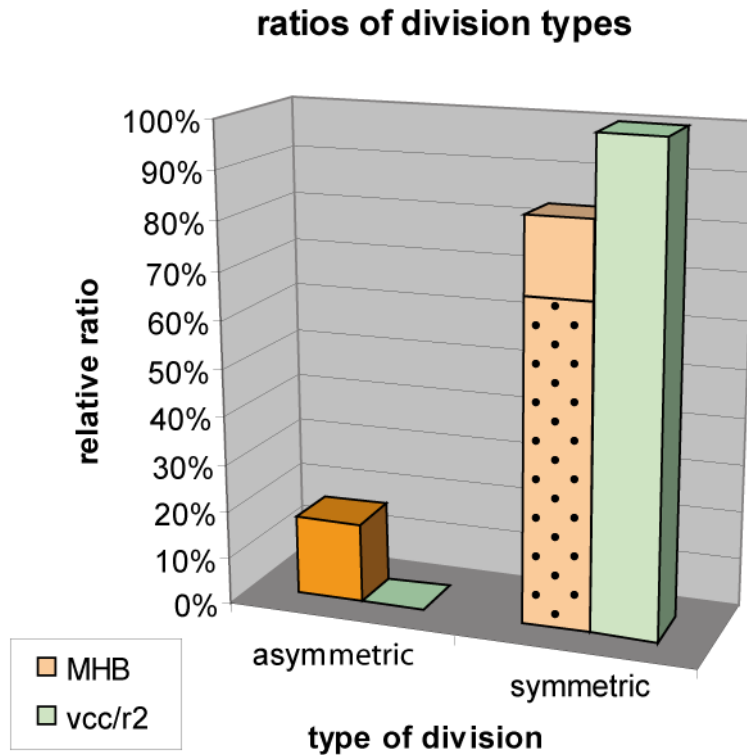


Figure 42: Summary of tracing analysis. Proliferating progenitors traced from the ventro-caudal cluster (vcc) or rhombomere 2 (r2) all divided symmetrically and always gave rise to two GFP+ cells (100%; n=12 traced division events; light green bar). Cells traced from the MHB progenitor pool divided in a high proportion also symmetrically (80%; n=10 traced division events; light orange bar) giving rise to two progenitors (66,4%; GFP-negative; 8 division events; dotted) or two GFP-positive cells (16,6%; GFP-positive; 2 division events; not dotted upper part of light orange bar). In two division events traced from the MHB progenitor pool, an asymmetric cell fate choice was observed (strong orange bar). Three independently recorded movies were analyzed and pooled.

Conclusion: Transition between MH progenitor subtype has an impact on cell lineage and division type properties

With this analysis of progenitor properties at early stages at the MH domain I could show that there are not only molecular differences, namely non-canonical versus canonical *her* gene expression, but also specific differences in cellular attributes between progenitor pool cells and proliferating precursors:

1. MHB progenitors and midbrain-hindbrain proliferating precursors have a unidirectional lineage relation whereby the former progenitor type gives rise to the latter
2. Midbrain-hindbrain proliferating precursors only divide following a symmetric neurogenic mode, while MHB progenitors display a complex mixture of division types (mainly symmetric proliferative divisions and a smaller ratio of symmetric neurogenic and asymmetric divisions)

It would be crucial to determine now to which extent these differences result from the expression of different categories of *E(Spl)* genes.

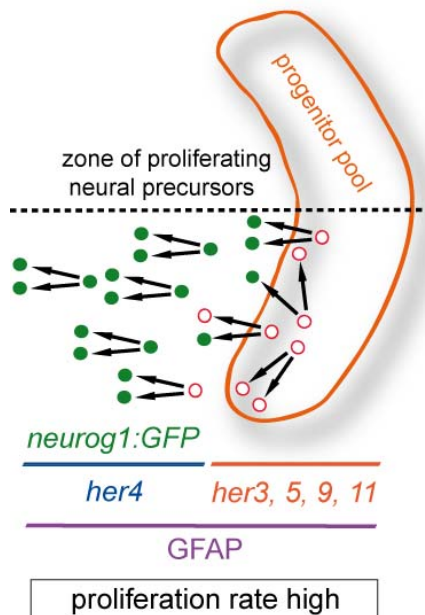


Figure 43: Concluding scheme: Lineage relation and cellular characteristics of zebrafish neural progenitors at early stages. Cells at the MHB progenitor pool (outlined in orange) can be distinguished from proliferating neural precursors by their expression of non-canonical *her* genes *her3*, *her5*, *her9* and *her11*, but not by GFAP expression. At early stages there is no difference in cell proliferation rate. While proliferating neural precursors seem to only divide following a symmetric and neurogenic mode, progenitors at the MHB progenitor pool divide either in a symmetric proliferative symmetric neurogenic or even (in a few cases) asymmetric fashion.

3.1.6. Correlation of mechanisms defining neural progenitor pools between the embryonic and adult brain

As already described conceptually in chapter 3.1.1 [176], it is highly interesting to draw a comparison between the characteristics of progenitor pools in the embryonic and the adult nervous system. This kind of comparative analysis provides insight into how universal the observed mechanisms are.

Non canonical E(Spl) genes mark proliferation zones

To gain understanding of the relation between the embryonic and adult situation, I focussed on the non-canonical E(Spl) genes *her3* and *her9* and studied their expression patterns in the adult brain. In the embryo, *her3* is first broadly expressed in two longitudinal stripes (see Figure 32 and [183]) but soon gets restricted to discrete small domains during later embryonic and larval development. I could also find small and discrete domains of *her3* expression in the adult brain. Interestingly, one *her3* expression domain resides at the IPZ, in a region neighboring the expression domain of *her5* [13] (see Figure 44B). Double-labelling with the proliferation marker MCM5 showed that a subset of *her3* positive cells is still proliferating (see Figure 44B). *her5* expression has already been described in depth by Prisca Chapouton in our lab [13]. Therefore a further analysis of its expression pattern was not necessary and I could take *her5* expression as useful tool to position *her3* expression (see Figure 44B).

Next, I analysed *her9* expression in the adult brain. I realized that, already during neurulation stages, *her9* expression undergoes a dramatic change: it switches from a

rather broad expression pattern covering several progenitor pools to an expression pattern mostly restricted to ventricular zones. A ventricular expression of *her9* turned out to be also the case for the adult brain. This can be clearly seen at the IPZ, for instance, where *her9* is present in nearly all ventricular cells (Figure 44C). *her11* is only expressed at early embryonic stages, and is down-regulated soon afterwards [186]. *her11* is also not detectable at adult stages. To sum up, the non-canonical E(spl)/*her*-gene group members *her3*, *her5* and *her9* are expressed at proliferation zones in the adult brain. How far *her3* and *her9* also overlap with adult neural stem cells will be an interesting question to be addressed in the future.

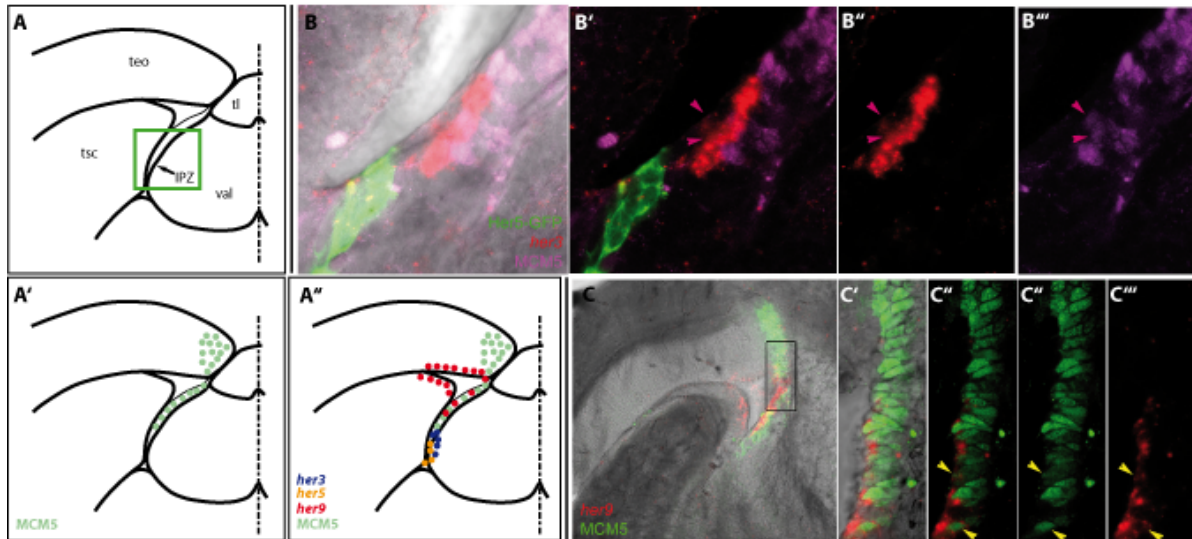


Figure 44: Expression of non-canonical *her* genes *her3*, *her5* and *her9* at the IPZ. Cross sections at IPZ level of adult brains and corresponding schemes are shown all dorsal up. (A) Schematic overview of the part of the midbrain/hindbrain junction that contains the IPZ. (A',A'') Color coded schemes summarizing the expression data shown in (B) and (C). (B to B''') Triple labelling of *her3* (RNA in-situ hybridization), MCM5 immunohistochemistry and GFP immunohistochemistry in *Tg(her5PAC:EGFP)* fish [70][13] show relative position of *her3*, Her5-GFP expression and MCM5+ proliferation zones. Position of panel (B) is indicated with green box in (A). Note proliferating *her3*+ cells (indicated by arrowheads). (C to C''') Double labelling of *her9* (RNA in-situ hybridization) and MCM5 immunohistochemistry shows relative position of *her9* and MCM5+ proliferation zones. (C' to C''') Higher magnifications of zone shown in C (indicated by black box). Note proliferating *her9*+ cells (indicated by arrowheads). Abbreviations: IPZ: isthmus proliferation zone; teo: tectum opticum; tl: torus longitudinalis; tsc: torus semicircularis; val: valvula cerebelli.

Fgf-signalling correlates with the ventricular radial glia state and the embryonic *fgf8* synexpression group diverges in the adult brain

Appendix 5 (manuscript in press)

Fgf-signalling is a crucial component of embryonic organizing centers and neural progenitor pools, as discussed for the MHB in chapter 3.1.4. A highly interesting issue is to clarify to which extent the spatial correlation between Fgf-signalling and progenitor pools is maintained in the adult zebrafish brain. To solve this question I participated in a collaborative project in our lab, where I helped in initial experiments using enhancer trap lines and with the cloning of Fgf pathway genes. Expression analyses experiments were subsequently mainly conducted by Stefanie Topp. Surprisingly, we could show that members of the *fgf8* synexpression group, which are tightly co-expressed in space and time in progenitor pools at multiple organizing centers in the embryo [158], diverge widely in expression in the adult brain (see Figure 45). Interestingly, *dusp6*, P-ERK, *fgfr1-3* and *fgf3* have overlapping expression patterns and are specifically associated with neurogenic zones. These are mostly located at ventricles, overlapping with radial glia cells. However, we noted that the cells receiving Fgf-signalling in these locations are in general not undergoing active proliferation. This finding implies that Fgf signalling in the adult brain governs functions other than neural progenitor proliferation control. To sum up, our data suggests that Fgf signalling, and in particular *fgfr1-3*, P-ERK and *dusp6*, are important components of adult neurogenesis in zebrafish. This study provides for the first time an extensive analysis of Fgf-activity in the zebrafish adult brain. It constitutes a fundament for future functional studies as well as for further comparative efforts.

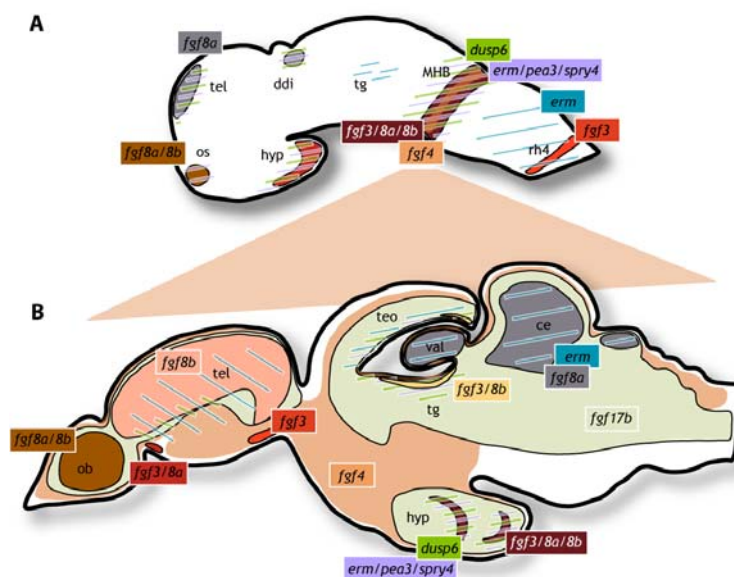


Figure 45: Schematic overview comparing embryonic and adult brain expression domains of genes of the *fgf8* synexpression group. Anterior is to the left. Shown are schematic representations of approximately midsagittal sections. Expression domains are color coded. (A) Expression patterns in the embryonic brain at approximately 24hpf are mostly focally restricted. (B) Several expression domains are spread out in the adult brain (indicated for *fgf4* by trapezoid area connecting embryonic (A) and adult expression (B)). Note that some *fgf8* synexpression group members, such as *fgf3*, stay focally restricted in the adult brain. Abbreviations: ce: corpus cerebellaris; ddi: dorsal diencephalon; hyp: hypothalamus; MHB: midbrain-hindbrain boundary; ob: olfactory bulb; os: optic stalk; rh4: rhombomere 4; tel: telencephalon; tg: tegmentum; teo: tectum opticum; val: valvula cerebelli.

3.2. Neuronal identity specification in the embryonic midbrain-hindbrain domain

Neuronal progenitor pools do not only have a role in keeping back progenitors for future developmental events. They often also overlap with organizing centers and therefore instruct cell fate in adjacent territories of the embryo. The MHB is a clear-cut case for a progenitor pool that is at the same time an organizing center [176]. From the MHB progenitor pool arise a number of different neuronal types that will populate the mid- and hindbrain. Which neurons are exactly formed from the MHB pool has not been analyzed in detail. Next, how these neurons acquire their different identities is not understood. It is possible, in particular, that the moment at which they exit the MHB pool (i.e. their birthdate) controls their identity. Alternatively, their identity might be dependent on their final localization and their distance from the MHB organizing activity. The second focus of my PhD aimed to address these questions.

3.2.1. Serotonergic neurons of the anterior Raphe nucleus are defined by expression of the transcription factor Pet1 and originate from the MHB progenitor pool

Appendix 6 (published article) [389]

To dissect the molecular mechanisms specifying neuronal identity in cells deriving from the MHB, I contributed to molecular and phylogenetic analyses aiming to define the origin and molecular control of raphe serotonergic neurons (project conducted by Christina Lillesaar).

***pet1* is an early specific marker for serotonergic raphe neurons**

To describe the origin and induction of a specific neural population it is crucial to have a specific and early marker. For the serotonergic system in zebrafish, the tryptophan hydroxylase-encoding genes *tph1a*^a, *tph1b*^b [390] and *tph2*^c [391] have been established as specific markers for serotonergic neurons. They are coding for three isoforms of the enzyme tryptophan hydroxylase in zebrafish, and are therefore precise markers for serotonergic neurons. However, as their expression starts rather late during the maturation of the neuron, they are not well suited for early studies of neuronal identity definition. A good putative candidate for early zebrafish raphe serotonergic neurons is the Ets-domain transcription factor Pet1^d (= Fev^e), as its mammalian homolog Pet-1 has been described as an early and specific marker transcribed in immediately postmitotic 5HT neurons [392-394]. Therefore, we cloned the putative zebrafish *pet1* gene and verified it being the true homologue of mouse *Pet-1* by phylogenetic analysis with a set of vertebrate orthologs and nearly related Ets-factors^f. In-situ expression analysis showed that *pet1* is specifically expressed in

^a *tryptophan hydroxylase 1a*; formerly: *tphD1* (ZFIN)

^b *tryptophan hydroxylase 1b*; formerly: *tph1*; *tphD2* (ZFIN)

^c *tryptophan hydroxylase 2*; formerly: *tphR* (ZFIN)

^d Pheochromocytoma 12 ETS (E26 transformation-specific)

^e Fifth ewing sarcoma variant; *pet1* has been recently renamed *fev* after the human homolog (ZFIN)

^f Figure 1 in Appendix 6

serotonergic neurons of the raphe nucleus, preceding expression of *tph2*^a. This finding could be substantiated by double stainings with a newly raised antibody detecting Tph2 at adult stages^b (in collaboration with Dr. Kremmer). Additionally there is an early transient expression in the interrenal organ^c and blood precursors^d. In the adult brain *pet1* is expressed in the anterior raphe nucleus and in scattered posterior cells that most likely are part of the posterior raphe nucleus^e.

Direct tracing shows that *pet1*-positive cells of rhombomere 1 and 2 derive from the MHB neural progenitor pool

With the help of the caged-fluorescein uncaging technology and the transgenic line *Tg(her5PAC:EGFP)* we could show that serotonergic precursors located in rhombomeres 1 and 2 derive from the MHB progenitor pool, unlike those residing in more posterior rhombomeres, which come from more caudal origins (see Figure 46).

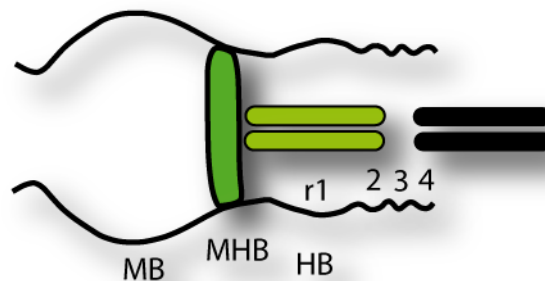


Figure 46: The MHB is the origin of anterior raphe serotonergic neurons. Schematic dorsal representation of the zebrafish midbrain and hindbrain at approximately 36hpf. Anterior is to the left. Horizontal stripes represent the anterior (left; green) and posterior (right; black) serotonergic neurons of the raphe nuclei. Note that the anterior raphe serotonergic neurons are derived from the MHB while the posterior derive from posterior regions of the hindbrain. Abbreviations: HB: hindbrain; MB: midbrain; MHB midbrain-hindbrain boundary; r1: rhombomere 1; 2: rhombomere 2; 3: rhombomere 3; 4: rhombomere 4.

Conclusion: *pet1* is an early marker for maturing serotonergic neurons

In this study we characterized the zebrafish gene *pet1*. We could show that *pet1* is a specific marker for serotonergic neurons of the raphe nucleus, and that the anteriormost component of these neurons derives from the MHB progenitor pool. This study served as the fundament for a first detailed description of raphe serotonergic projections in zebrafish. There, we described in detail the raphe projection network with the help of a newly constructed *Tg(-3.2pet1:EGFP)* transgenic line, where *pet1* cis-regulatory elements drive GFP reporter expression. Although I contributed to this work during my PhD project, I will not discuss it within the frame of this thesis manuscript, as it is too far reaching from the central topic of progenitor pool specification, maintenance and fate determination.

^a Figure 2 in Appendix 6

^b Figure 3 in Appendix 6

^c functional equivalent of adrenal gland in zebrafish

^d Figure 2 in Appendix 6

^e Figure 3 in Appendix 6

3.2.2. Screen for mutations affecting serotonergic raphe neurons

As a starting point for future detailed analysis of the molecular processes specifying MHB derived serotonergic neurons I participated in two recessive screens. The screening procedure that was common for both screens is schematized in Appendix 7.

The first screen was conducted in our laboratory. At 34hpf to 36hpf I conducted a morphological screening focused on loss of progenitor pools (see chapter 3.1.2) [358]. I used this morphological screening step also to exclude batches that have unspecific defects such as broad necrosis and oedemas. For the serotonergic assay I fixed embryos at 48hpf and used the probe for *tph2* (see also 3.2.1) as marker in RNA in situ hybridizations. I focused on changes or loss of the expression patterns of *tph2*. In this screen *ne2611* (see chapter 3.1.2) was recovered. In addition, we could recover one mutant line with a strong reduction of serotonergic neurons. The detailed molecular analysis was conducted by Christina Lillesaar. She mapped the mutant locus to the DNA polymerase *polB*. Further analysis on this mutant line is currently under way.

Furthermore, this screen was used as a pilot screen to participate in the European ZF-Models Consortium Screen conducted at the group of Prof. Dr. Christiane Nüsslein-Volhard at the Max-Planck Institute for Developmental Biology in Tübingen, Germany. I set up my own screening assay there, building on the experience that I got during the pilot screen in our lab. I used again *tph2* as marker for serotonergic neurons but switched to 56hpf for fixation to incorporate also probes for a hypothalamus and pituitary specific screen in collaboration with Dr. Hammerschmidt's laboratory. The thereby found serotonergic mutants are shown in Appendix 7. We decided to focus on the clearest phenotype NI034. Mapping crosses were prepared by Christina Lillesaar and mapping is currently underway at the laboratory of our collaboration partner Dr. Geißler at the Max-Planck Institute for Developmental Biology in Tübingen.

3.2.3. The role of a timer in neuronal identity definition in the midbrain-hindbrain domain

The MHB is of crucial importance for the proper development of several distinct neuronal populations of the midbrain and anterior hindbrain, such as the serotonergic neurons of the anterior raphe nucleus and the motor neurons of the cranial nerve nuclei III and IV to just name a few [69]. Despite the importance of the MHB for brain development and therefore later brain function, the mechanisms defining MHB-derived neuronal identities are still elusive. Several signalling factors, such as Wnt1 and Fgf8, are expressed at the MHB [69]. These ligands produce diffusible morphogen gradients that could define MH neuronal identities. Alternatively, a timing mechanism could define neuronal identities in the MH domain. Timing mechanisms have been shown to play important roles in defining neuronal identities in several other parts of the vertebrate nervous system, such as the retina and the cortex but as well in other nervous systems such as the *Drosophila* embryonic CNS [295] (for details see 1.4.2). Interestingly, the MHB progenitor pool gets restricted over time and therefore cells exit the MHB progenitor pool in a temporal order that also reflects their final distance from the MHB [70] (see also Figure 40). In order to clarify whether a timing mechanism is implicated in setting up MH neuronal identities I established a

spatio-temporal map of basal MH neuronal identities and tested different methods to disrupt the timing of neurogenesis, to determine whether MH neuronal identities are time-dependent.

The basal MH domain consists of distinct neuronal identities

With tracing experiments described in chapter 3.1.5 (see Figure 40) I demonstrated that the basal MH is, at least to a large extent, derived from medial parts of the early MHB in an ordered manner along the A/P axis. I built upon that knowledge and selected as a basis for the neurogenesis timing disruption experiments eight representative basal MH neuronal identity markers (Figure 47 and Figure 48; in collaboration with Andrea Geling, a previous PhD student in the laboratory):

1. The midbrain domain of *six3^a* (*six3a*) marks the nucleus of the medial longitudinal fascicle (nMLF) [395], a homologous structure to the interstitial nucleus of Cajal (INC) [396]. In addition, *six3* expression extends into the diencephalon to label the nucleus of the posterior commissure at the forebrain/midbrain boundary [395].
2. *sax2^b* marks a specific posterior subpopulation of the nMLF next to the tract of the posterior commissure (TOPC) [397], i.e. the descendants of the ventrocaudal cluster (vcc) [396].
3. The midbrain expression domain of *hoxa1a* marks a posterior subpopulation of the nMLF [398,399].
4. *emx2* marks the red nucleus (nucleus ruber) in chicken[396,400], and a possibly equivalent anterior midbrain population in zebrafish^c.
5. *phox2a* marks ventrally the progenitors and neurons of the oculomotor and trochlear motor nucleus (nucleus of the cranial nerves III and IV, respectively) [402]; *phox2b* is also expressed ventrally in the oculomotor and trochlear motor nucleus, but only in postmitotic cells[230,403,404].
6. *gata3* domains in the ventral hindbrain comprise the serotonergic populations of the raphe nuclei, but *gata3* is expressed in broader domain than the following two more specific serotonergic markers [405].
7. *pet1* expression in the hindbrain is an early and highly specific marker for serotonergic neurons of the raphe nucleus [389] (see also 3.2.1).
8. *tph2* expression in the hindbrain is a marker for differentiated serotonergic neurons [389,391] (see also 3.2.1).

^a *six3* is also known as *six3a* (ZFIN)

^b *sax2* is also known as *nkx1.2lb* (ZFIN)

^c The red nucleus has been described in the zebrafish adult brain [401] but has not been mapped at embryonic stages yet

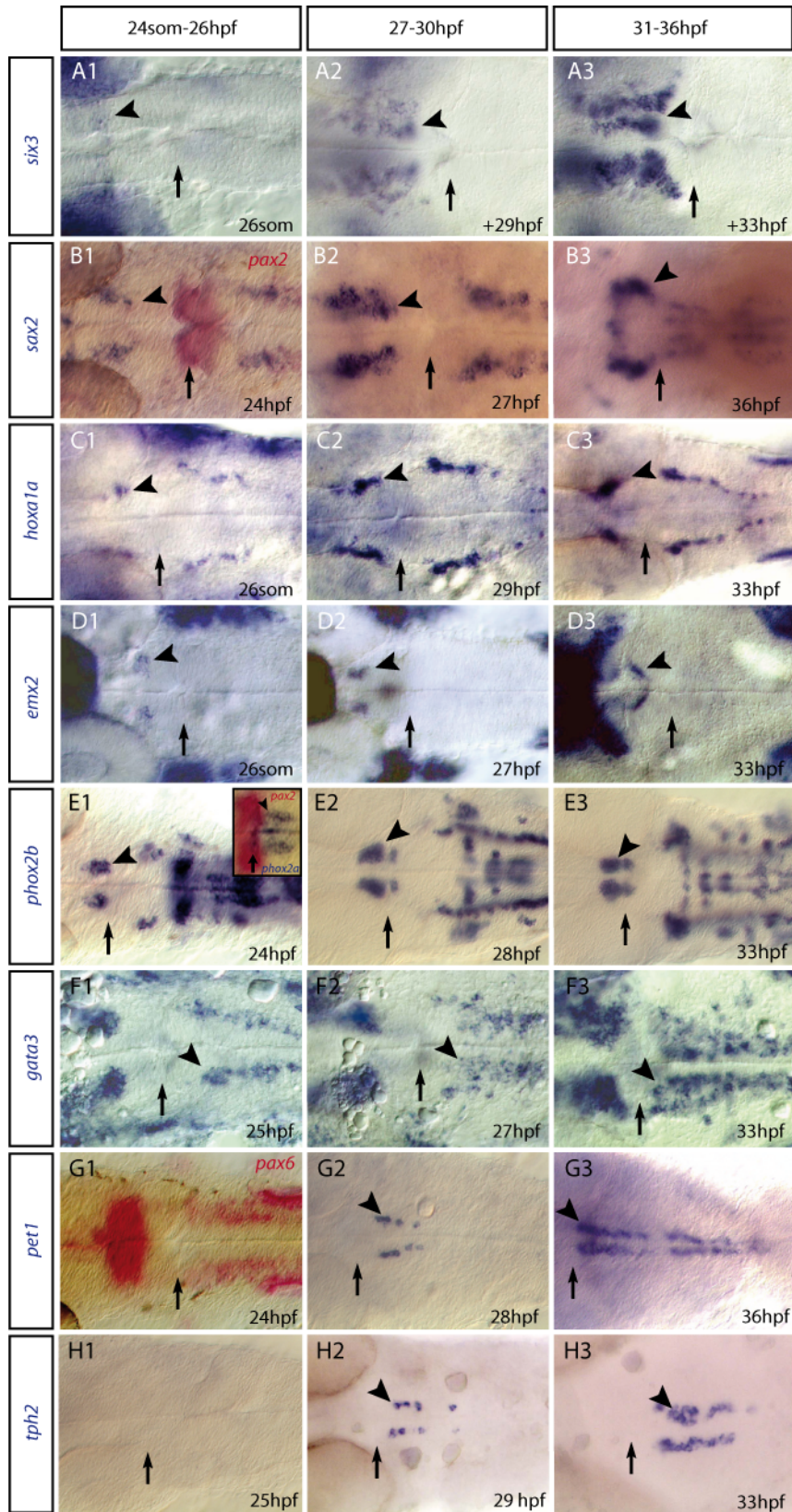


Figure 47: Early basal neuronal identities in the MH domain. Dorsal views of whole-mount RNA in situ hybridizations of representative neuronal identity markers (indicated on the left) of the MH region are given at three different time intervals (indicated above panels). Black arrowheads point to characteristic MH expression domains. Anterior is left. Black arrows indicate the position of the MHB.

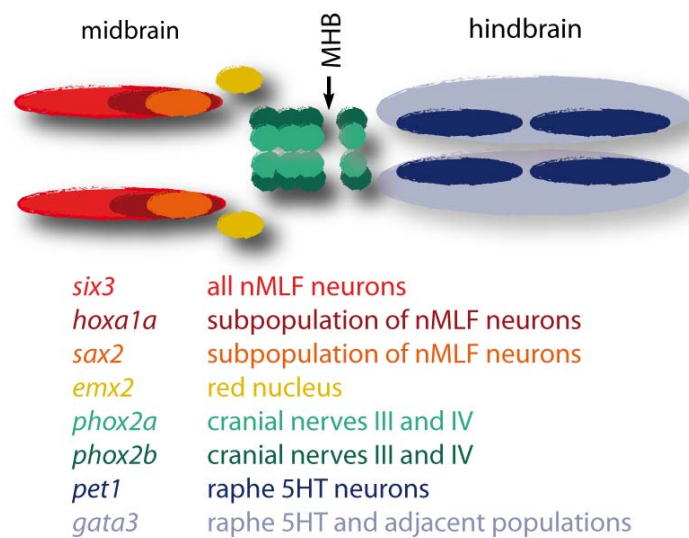


Figure 48: Overview of early neuronal identities in the basal MH domain. Schematic dorsal view of the MH neuronal identity marker domains shown in Figure 47. Representative expression domains in basal MH and corresponding genes are color-coded. Anterior is left.

Most midbrain-hindbrain neuronal identity markers are post-mitotic

In order to clarify if the MH populations expressing the markers shown in Figure 47 and Figure 48 are pre- or postmitotic, I conducted double labelling analyses of these marker genes with the M-phase marker pH3 [385] (see also 3.1.6 and Figure 39). *hoxa1a*, *emx2* and *pet1* appeared postmitotic at the stages analyzed, since I could never find marker-expressing cells positive for pH3 (see Figure 49A). In contrast to that, the midline aspect of the *phox2a* positive domain encompassing cranial nuclei III and IV contained pH3+ cells at all stages analyzed (Figure 49A and B). This is in line with the fact that *hoxa1a*, *emx2* and *pet1* expression domains are separated from the ventricle while *phox2a* expression spans ventricular regions. As the other markers of the neuronal identity map are also not ventricular (see Figure 47 and Figure 48) these are most likely also post-mitotic markers. A crucial determinant for timer-mediated cell fate definition is the birth date of a neuron, i.e. the time point of the final division. As most of the neuronal identity markers are post mitotic, only the analysis with a permanent tracer of the cells' proliferating status, such as BrdU, would provide an accurate picture of the sequence of neuronal birth dates for the different neuronal identities. Unfortunately, up to now, I could not successfully conduct BrdU birth dating at the stages of interest. The labelling difficulties are most likely due to insufficient BrdU penetration through the forming skin of the embryo after the tailbud stage.

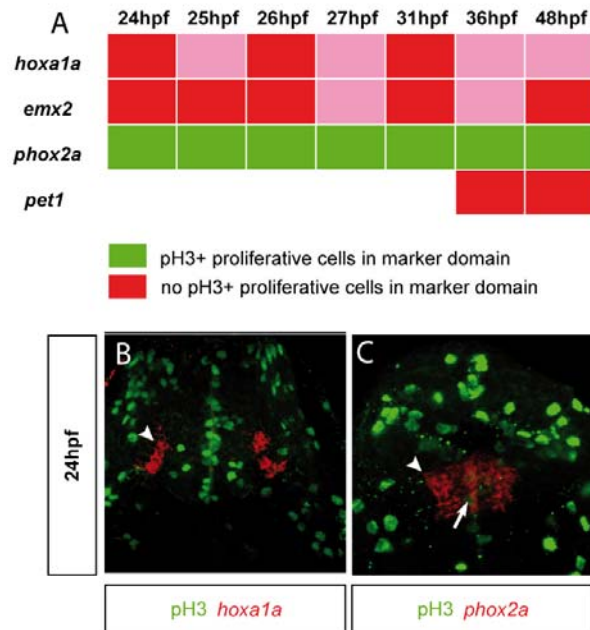


Figure 49: Proliferation analysis of MH identity markers. (A) Summary of data obtained by double labelling with fluorescent RNA in-situ hybridization of MH-markers and anti-pH3 immunohistochemistry (color-coded; light red boxes represent time points where no analysis was conducted, but where the non-proliferating status was inferred from data obtained at neighboring time points). Examples of analyzed cross-sections show a post-mitotic marker at 24hpf in (B) and a mitotic marker in (C) (white arrow points to double positive cell). White arrowhead indicates MH-marker domain.

Downregulation of non-canonical E(Spl) gene activity leads to a progressive loss of the MH domain

In order to disrupt the timing of neurogenesis at the MH domain, I downregulated non-canonical E(Spl)-activity at the MHB using gripNA modified antisense oligonucleotides mediating a concomitant knockdown of *her3*, *her5*, *her9* and *her11* (4xGRIP; as described in 3.1.5.). This leads to ectopic *neurog1* expression in medial and lateral aspects of the MHB at the 3-somite stage (see Figure 37). To test if this manipulation induced changes of neuronal identities, I analyzed the markers *hoxa1a* and *phox2b*. Interestingly, I could observe a reduction of the distance between the midbrain and hindbrain domains of *hoxa1a* expression (indicated by arrows in Figure 50A and B) and a reduction in the intensity of expression of *phox2b* in the domains of the cranial nerve nuclei III and IV (depicted by arrowheads in Figure 50C and D). In order to clarify if these phenotypes resulted from changed neuronal identities or were caused by a loss of tissue of the MH domain, I used *fgfr3* as a negative marker for the MH [406], together with the MHB marker *fgf8*. Up to the 20-somite stage I could not observe obvious changes for these markers in 4xGRIP-injected embryos, but at the 25-somite stage the *fgfr3*-negative MH domain as well as the *fgf8* signal appeared dramatically reduced. This effect got even more obvious at 48hpf (depicted in Figure 50E to L) and with a clear morphological phenotype at 3dpf (see Figure 50 W and X). These observations are in line with findings in the mouse CNS where a concomitant knockout of *Hes1* and *Hes3* has been shown to result in a loss of expression of the MHB marker genes *Fgf8*, *Wnt1*, and *Pax2/5* and a loss of MH tissue [230]. As the combined knockout of *Hes1* and *Hes3* does not lead to increased cell death rates [230], I tested if this is also the case in 4xGRIP injected embryos. To answer that, I conducted a cell death analysis using the Acridine Orange

incorporation assay [70, 405, 407]. I could not detect increased rates of cell death in 4xGRIP-injected embryos (see Figure 50M to V). Therefore, comparable processes seem to happen in the mouse *Hes1/Hes3* double-knockouts and the 4xGRIP-injected zebrafish. Besides being by itself an interesting finding, this effect renders the 4xGRIP approach unsuitable to analyze the role of a timer mechanism in defining neuronal identities in the MH domain.

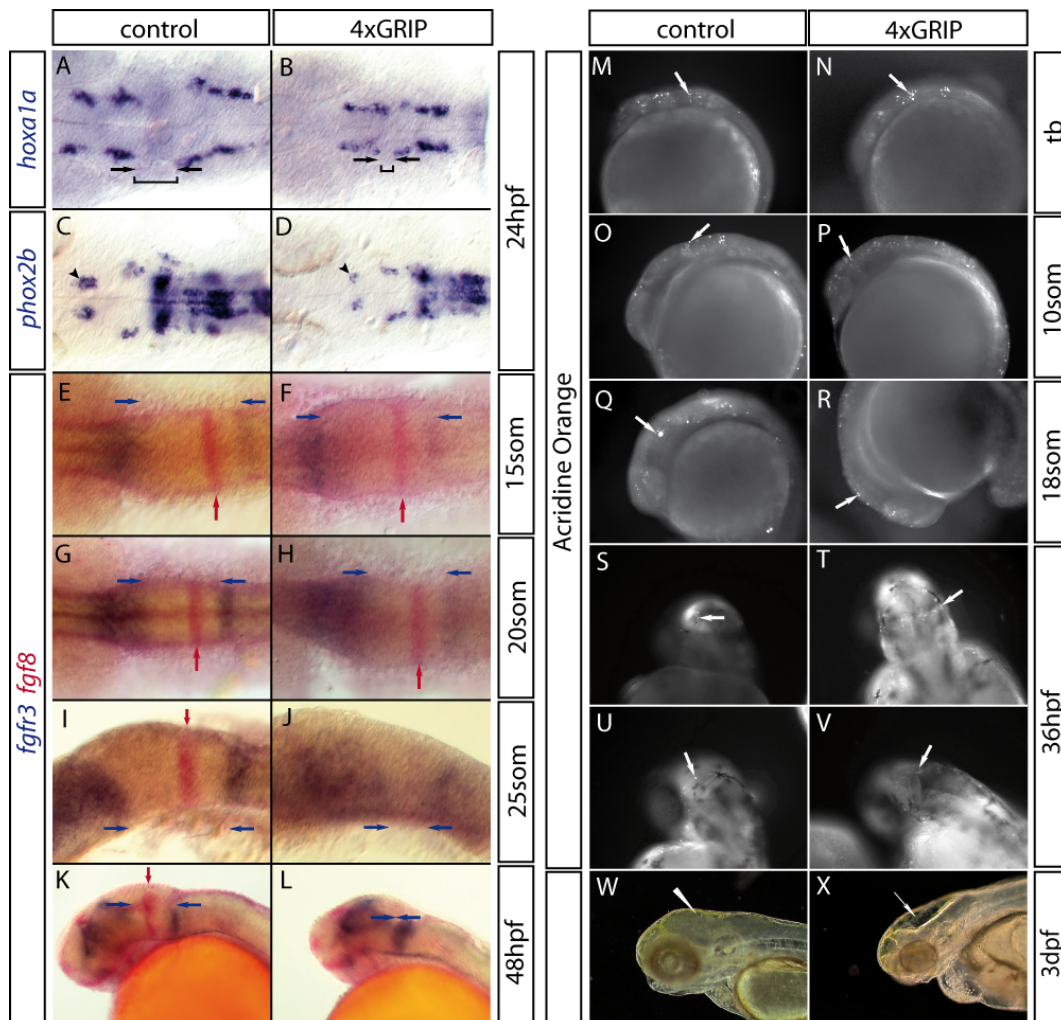


Figure 50: Downregulation of non-canonical E(Spl) activity at the MHB leads to a loss of the MH domain. Effect of down-regulation of non-canonical E(Spl)-activity ('4xGRIP' stand as short code for combination of *her3*, *her5*, *her9* and *her11* gripNAs injected at 0,4mM each at the 1-cell stage) is compared to non-injected controls as indicated above the panels (the markers used are indicated on the left; color-coded; the age of the embryos is indicated on the right). (A-D) Effect of down-regulation of non-canonical E(Spl) activity on selected MH neuronal identity markers. (A, B) 4xGRIP treatment leads to a reduction in the distance between the midbrain and hindbrain expression domains of *hoxa1a* (compare distance between black arrows). (C, D) 4xGRIP injection reduces the size of *phox2b* domains (midbrain domain indicated by arrowhead). (E-L) 4xGRIP injection leads to a loss of the MH domain over time (MH domain spans region in between *fgfr3* expression domains [406]) (indicated by blue arrows; position of MHB is indicated by red arrow). Note the loss of MHB marker expression at the 25-somite stage (J) and the juxtaposition of *fgfr3*-domains at 48hpf (L) in 4xGRIP-injected embryos. (M-V) The loss of MH domain in 4xGRIP injected embryos does not correlate with a higher rate of cell death, as revealed by the cell death indicator Acridine Orange [70, 407] (white arrows point to examples of Acridine Orange-positive cells in the MH domain). (W-X) 4xGRIP injection leads to the dramatic absence of dorsal midbrain tissues (X; indicated by white arrow) compared to control (W; indicated by arrowhead) at 3dpf.

Early burst of ectopic *neurog1* expression after downregulation of non-canonical E(Spl) gene activity is not followed by neuronal differentiation

In order to test if the ectopic induction of neurogenesis at the MHB proliferation pool that follows 4xGRIP injection results in ectopic neuronal differentiation or is only a transient effect, I conducted a time course analysis using *neurog1*, *coe2* and *deltaB* (*dlb*) as markers representing different stages in the neurogenesis cascade [170]. Surprisingly, the initial burst of *neurog1* expression, clearly visible at the 3-somite stage (see Figure 37), is already strongly reduced at the 5-somite stage (see Figure 51A to D) and is further reduced at the 7-somite stage. As *neurog1* is a very early marker of neurogenesis[194,408,409], I looked at the later neurogenesis markers *coe2*^a [201] and *dlb* [218] in order to test if the ectopic *neurog1*-positive cells proceed properly through the neurogenesis cascade. I observed that only a small group of ectopic cells at the MHB proceed further through neurogenesis by expressing *coe2* and *dlb* at later somitogenesis stages (see Figure 51I to P). Taken together, the initial burst of *neurog1* expression at the 3-somite stage in embryos with downregulated non-canonical E(Spl) gene activity, i.e. 4xGRIP-injected, is soon afterwards downregulated, with the exception of a small lateral subpopulation of cells. Because of this inefficient induction of neurogenesis, this approach does not allow me to assess if a timing mechanism has a crucial role in setting up MH neuronal identities.

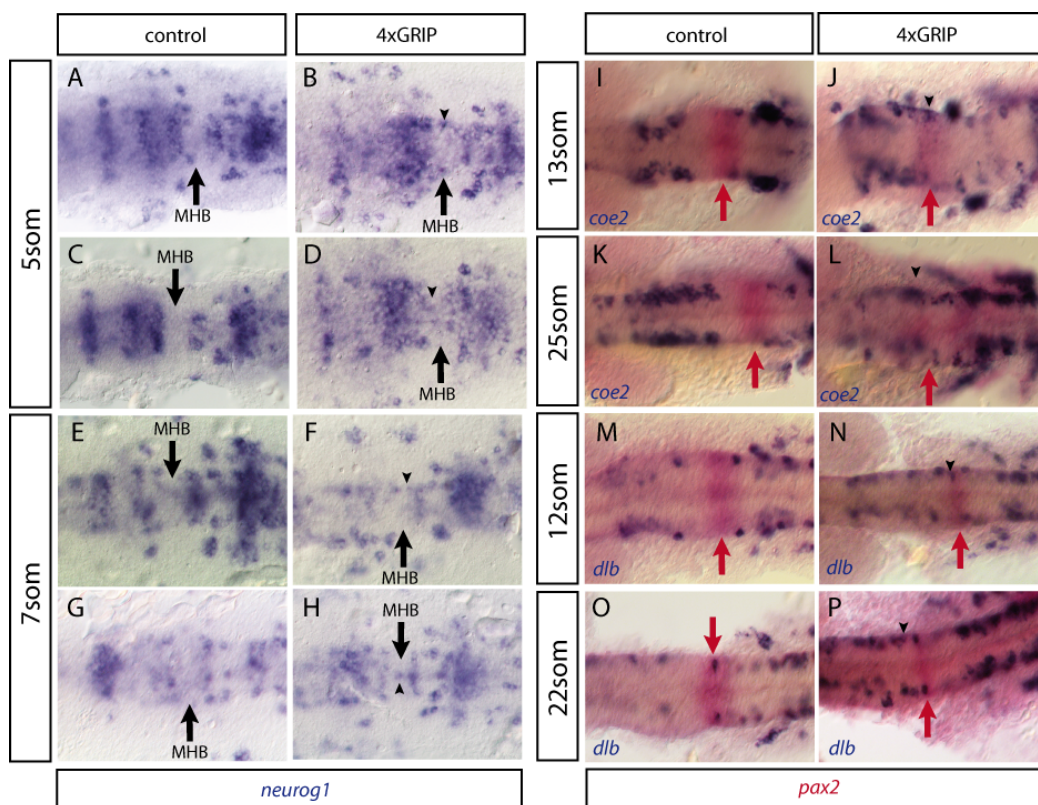


Figure 51: Downregulation of non-canonical E(Spl) activity leads to a mostly transient induction of neurogenesis. Dorsal views of flat mount preparations of RNA in-situ hybridizations (anterior is to the left). Arrows indicate the position of the MHB. Arrowheads point to ectopic cells in the MH domain in 4xGRIP injected embryos. Note that ectopic *neurog1* expression at the MHB in 4xGRIP injected embryos is only transient (A-H; see also Figure 37) while ectopic *coe2* and *dlb* staining persists in a small cell subpopulation (I-P; arrowheads).

^a *coe2* also has a very early phase of expression before the tailbud stage, preceding *neurog1*

Broad domains of ectopic neurons can not be induced in the midbrain by reverting non-canonical E(Spl) activity or directly overexpressing *neurog1* itself

To test whether more drastic changes in E(Spl) activity could more efficiently induce neurogenesis at the MHB, I overexpressed the *her5VP16* construct in a mosaic manner. In *her5VP16* the WRPW Groucho repressor binding site of Her5 is replaced by two copies of the minimal activation domain of VP16. Therefore, this construct not only induces a loss of Her5 function but activates genes that would be normally repressed by Her5 [410]. Overexpression of *her5VP16* has been described to induce ectopic *neurog1* expression [184]. I observed that *her5VP16* overexpression did not lead to ectopic expression of the early neuronal marker HuC [411] (see Figure 52A to H). Therefore, reverting the function of non-canonical *her* genes is not sufficient to produce ectopic neurons.

As a final attempt to generate stable premature neurogenesis across the MHB, I overexpressed a *myc*-tagged *neurog1* construct (*neurog1-myc*) [194] and looked for ectopically induced HuC-positive differentiating neurons [411]. I observed that ectopic neurons were induced at a high rate at the margin of the *neurog1-myc*-positive clones, but that induction largely failed within the clones themselves (see Figure 52I to L). Therefore, it seems that *neurog1*-positive cells within the clone are inhibited from successfully proceeding through neurogenesis. A plausible explanation for this finding is that cells within the *neurog1* over-expressing clones inhibit each other via lateral inhibition because of their artificially high levels of the Notch signalling activator Delta, itself induced by *neurog1*. This prompted me to test if I can induce a broader neurogenic effect by 4xGRIP injection when concomitantly blocking lateral inhibition by prolonged DAPT treatment [221]. Notably, this did not lead to large increase in ectopic differentiating neurons at the MHB (see Figure 52M to P). It is possible that an additional cue, such as a concomitant inhibition of cell cycle progression, is needed to instruct the complete MHB progenitor pool to successfully undergo neurogenesis.

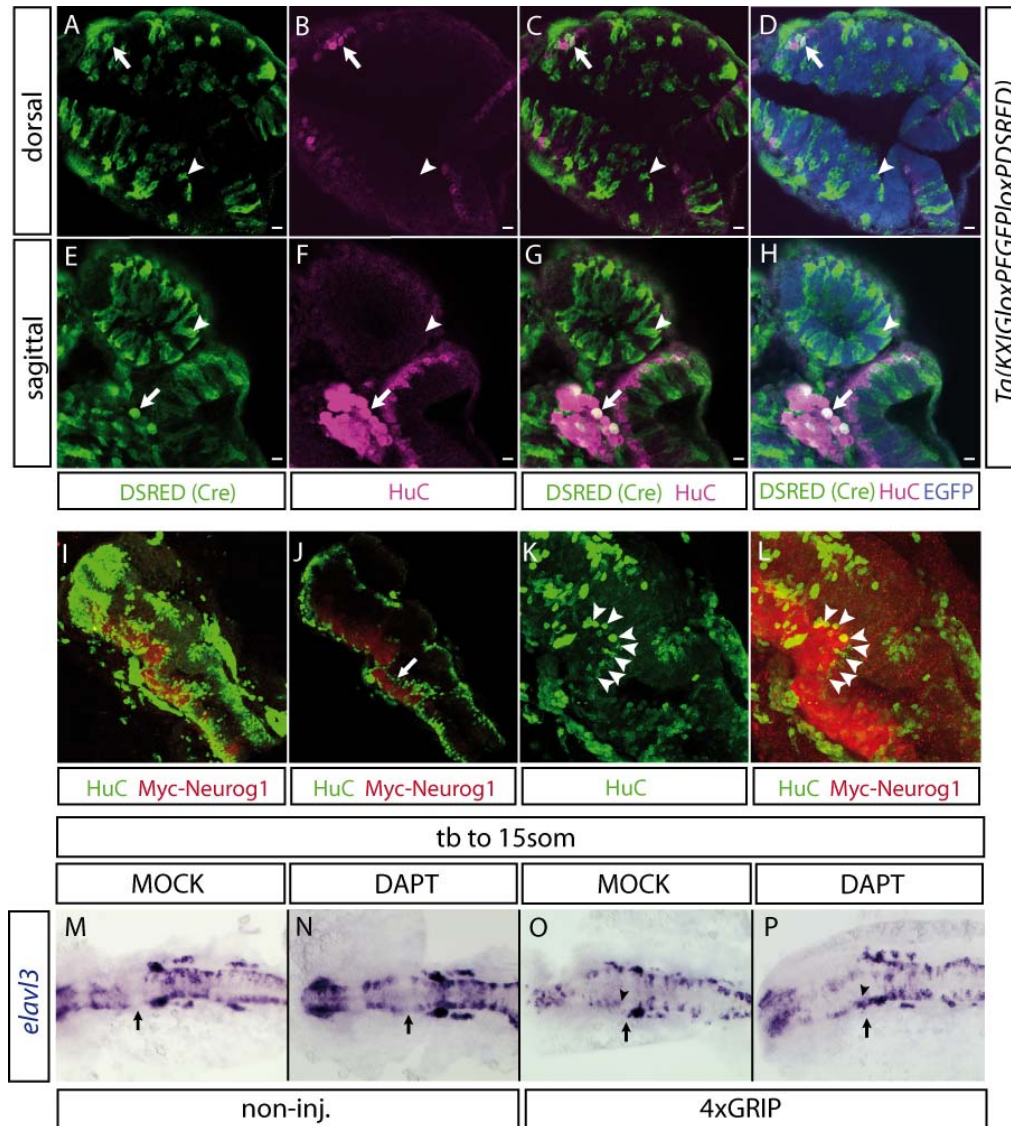


Figure 52: Neither overexpression of *her5VP16* nor overexpression of *neurog1* nor concomitant blockage of non canonical E(Spl) activity and Notch signalling leads to a broad and persistent induction of neurogenesis. (A-H) Clonal overexpression was conducted by co-injection of *her5VP16* (5ng/ μ l) and *cre* capped-mRNA (50ng/ μ l) into 1 of 16 cells at the 16-cell stage into the transgenic line *Tg(KXIGloxPEGFPloxPDSRED)* (Christoph Leucht, unpublished). Cre mediated recombination leads to stable DSRED expression (color-coded in green) in this line and therefore allows tracing of injected cells. Differentiating neurons are revealed by anti-HuC [411] immunohistochemistry (magenta). Ubiquitous EGFP expression outlines morphological landmarks (D, H; color-coded in blue). Images are optical sections obtained by confocal laser-scanning microscopy (anterior is in the upper left corner, posterior in the lower right corner of panels; A-D dorsal views; E-H are para-sagittal views; scale bar 10 μ m). Note that Her5VP16-overexpressing cells (DSRED-positive) are only HuC-positive in regions of endogenous HuC expression (examples indicated by white arrow) while overexpressing cells are not HuC-positive in the remaining neural tissue (examples highlighted by white arrowheads). (I-L) Clonal overexpression of Myc-tagged *neurog1* (revealed by anti-Myc immunohistochemistry; color-coded in red) leads to ectopic HuC induction (color-coded in green) at boundary zones of overexpressing clones (highlighted by arrow in J and arrowheads in K and L). Images are obtained by confocal laser scanning microscopy (I optical maximum intensity projection of z-stack; J-L optical single slices). (M-P) Dorsal views of flat mount preparations of RNA in-situ hybridizations with *elav3* riboprobe marking terminally differentiating neurons (anterior is to the left). The Notch signalling inhibitor DAPT [221] was applied between the tailbud-stage and the time of fixation at the 15-somite stage. The position of the MHB progenitor pool is indicated by a black arrow. 'MOCK' are control treatments with same concentration of carrier (DMSO) than in DAPT treatment. Note that ectopic neurogenesis induced by injection of 4xGRIP is not enhanced by blocking Notch signalling (O versus P).

Blockage of cell cycle progression does not induce ectopic neurogenesis

As the downregulation of non-canonical E(Spl) factors by 4xGRIP injection did not lead to the expected premature neurogenesis that would be needed to assess timing changes in the MH-neuronal identity map, I attempted to induce premature neurogenesis by acting on the cell cycle. In the mouse, lengthening of the cell cycle mediated by the cell cycle inhibitor Olomoucine leads to premature neurogenesis [371]. Therefore I applied the cell cycle inhibitors Olomoucine [371,412], Mimosine [412] and Aphidicolin [170,412] onto embryos and assessed the effect on neurogenesis by *neurog1* RNA in-situ hybridization. With no cell cycle inhibitor could I observe ectopic *neurog1*-positive cells, although these treatments reduced the number of pH3-positive cells (for Aphidicolin see Figure 53). This is in line with previous findings in our lab using aphidicolin [170]. An interesting way to go would be to overexpress $p27^{Xic1}$ in a conditional manner as $p27^{Xic1}$ has been shown to induce ectopic neuronal differentiation in *Xenopus* [247].

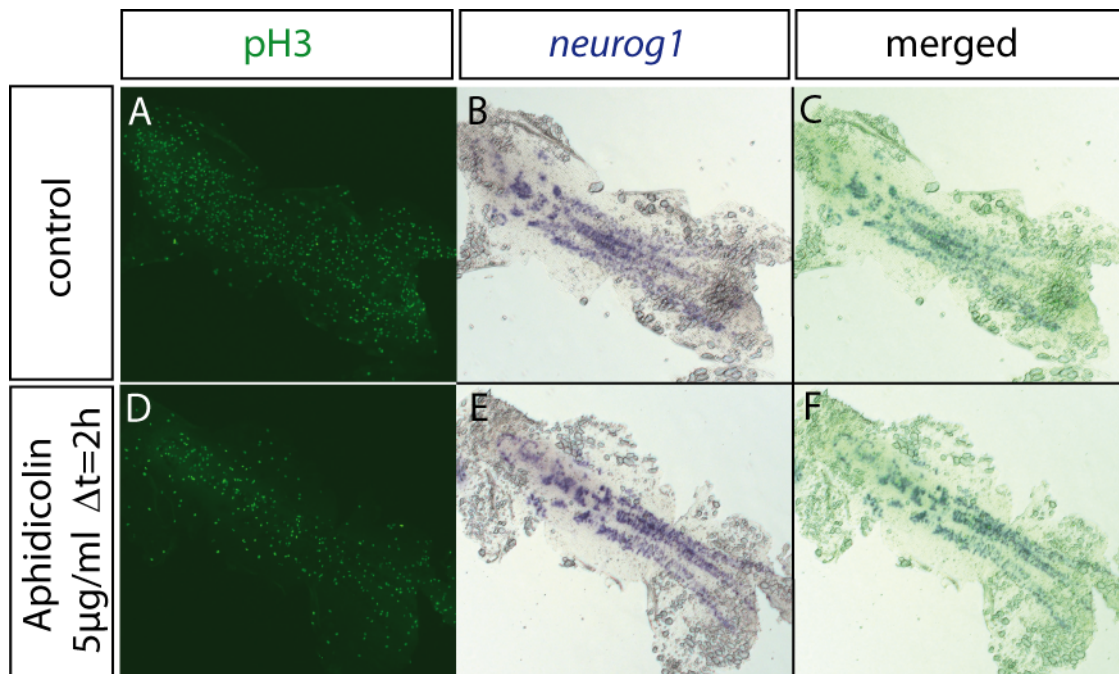


Figure 53: Blockade of the cell cycle does not induce ectopic neurogenesis. Dorsal views of flat mount preparations (anterior is at the upper left, posterior to the lower right). The treatment of dechorionated embryos with 5µg/ml Aphidicolin (D-F) for a 2h-interval up to the 5 somite-stage leads to a reduction in the number of proliferating cells to approximately half of normal levels (A versus D). Note that this does not result in ectopic neurogenesis (B versus E).

Blocking Notch-signalling by the γ -Secretase inhibitor DAPT induces neurogenesis in proliferating precursors but not in the MHB progenitor pool

As neither the downregulation of non-canonical E(Spl) factors (4xGRIP) nor blocking the cell cycle induced a neurogenic phenotype sufficient to test if a timer mechanism defines neuronal identities in the MH domain, I decided to induce premature neurogenesis in the Notch-dependent proliferating precursor population. This can be achieved by the γ -secretase inhibitor DAPT [221] (see Figure 54A and B). As an effect of DAPT treatment on boundary formation and *fgf8* expression has been reported for somatic tissue, I first tested if DAPT treatment affected MHB

maintenance [221], which would complicate my timing analysis. However, an analysis of MHB markers revealed that DAPT treatment has no obvious effect on IsO formation and maintenance (see Figure 54C and D), nor on the maintenance of the MHB progenitor pool as revealed by *elav/3* RNA in-situ hybridization at 27hpf (see Figure 54E and F). Hence, DAPT treatment appears as a good approach to selectively induce premature neurogenesis within proneural clusters in the proliferating neural precursors population. Because these progenitors arise from the MHB progenitor pool in a spatio-temporally ordered fashion (see 3.1.5) [70], applying DAPT at different time points can be used to target different populations of progenitors. As a first approach towards assessing the effect of DAPT on neuronal identity, I tested the influence of long term DAPT treatment on the MH neuronal identity marker *sax2*. Remarkably, DAPT treatment leads to a robust up-regulation of *sax2* expression (see Figure 54G and H). This finding prompted me to further analyse the effect of DAPT treatments on MH neuronal identities in time course experiments.

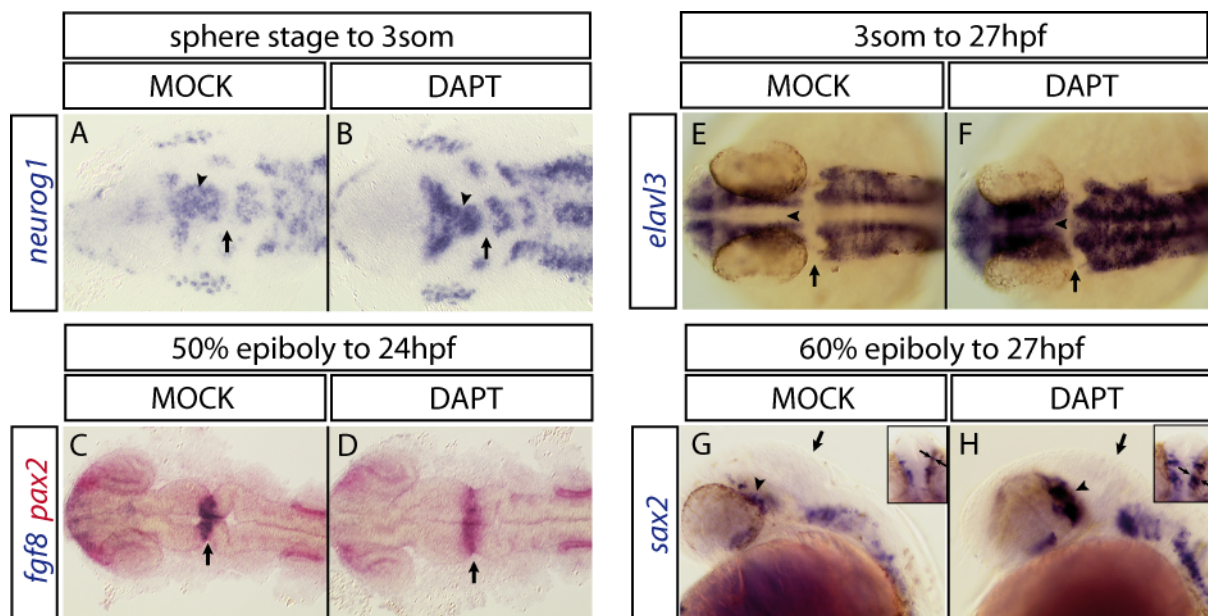


Figure 54: Blocking Notch-signalling by DAPT treatment induces neurogenesis in proliferating precursors but not in progenitors at the proliferation pool. Embryos were treated with the Notch signalling inhibitor DAPT at a concentration of 100 μ M [221] or with the same concentration of carrier (DMSO) than in DAPT treatment (MOCK) in time intervals as specified above the panels (riboprobes are indicated on the left of panels; anterior is left). The position of the MHB is indicated by a black arrow. (A-D) Dorsal views on flat-mounted preparations after RNA whole-mount in-situ hybridization. (A-B) DAPT treatment leads to more *neurog1*-expressing cells within proneural clusters but not to ectopic *neurog1*-positive cells outside proneural clusters. (C-D) MHB markers *fgf8* and *pax2* are maintained even after prolonged DAPT treatment spanning from 50% epiboly to 24hpf. (E-F) The MHB stays free of differentiating *elav/3*-positive neurons after DAPT treatment. Note that the ventricular proliferation zones at the midline are *elav/3*-positive after DAPT treatment (indicated by black arrowheads). (G-H) DAPT treatment leads to an expansion of the midbrain expression domain of *sax2* (indicated by arrowheads). Small insets show frontal views. Note the medio-lateral expansion of the *sax2* expression (indicated by black arrows).

In order to determine the critical time-point of DAPT effect for the different neuronal identities, I treated embryos with DAPT in a series of different time intervals. The expansion of the *sax2* midbrain domain was only clearly visible in the longest treatment interval (70% epiboly to 27 hpf) (see Figure 55A to B'). In later onset treatments (i.e. beginning at 5 somites or 16 somites) the *sax2* midbrain domain was only moderately affected, if at all (see Figure 55C to F'), suggesting that the relevant time-window for DAPT action in the emergence of the *sax2*-positive identity is situated between 70% epiboly and 5 somites. The hypothesis of a timing mechanism implies that the extra *sax2*-positive neurons formed upon DAPT treatment should develop at the expense of another neuronal identity normally arising later from the same progenitor pool. Alternatively, if the neuronal populations that I selected arise from different sets of proliferating precursors, I should be able to affect these sets at different time points with DAPT. However, although neurons of each type would of course need to be precisely counted, I observed that the DAPT treatments described above did not induce obvious changes to the expression of *phox2b* (see Figure 55G to L') or other MH neuronal identity markers (not shown). It is possible that other identities would need to be considered. With the tools and markers I have at hands, however, I can at present only conclude that *sax2* identity is encoded in progenitors that enter neurogenesis between 70% epiboly and 5 somites, but this is insufficient to postulate on a mechanism. In particular, it might reflect a lateral fate induction/binary choice mechanism as described recently for the spinal cord [413], rather than a timing mechanism.

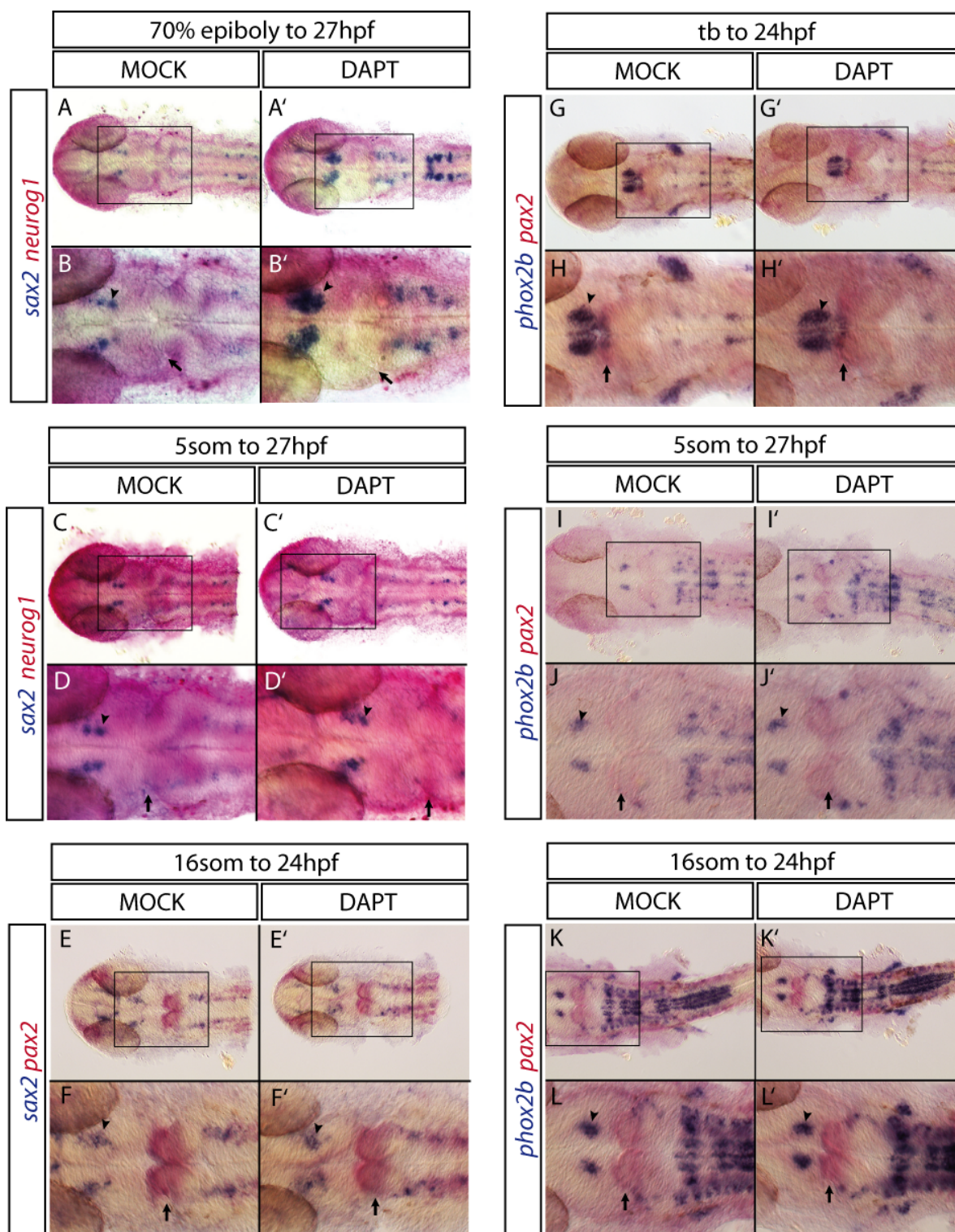


Figure 55: Effect of DAPT treatment on MH neuronal identities in time series experiments. Dorsal views on flat mounted preparations after RNA whole-mount double in-situ hybridization (RNA probes are color-coded on the left). Embryos were treated with the Notch signalling inhibitor DAPT at a concentration of 100 μ M [221] or with the same concentration of carrier (DMSO) than in DAPT treatment (MOCK) during the time intervals indicated above the panels (RNA probes are indicated on the left of panels; anterior is left). The position of the MHB is indicated by a black arrow and black arrowheads point to the position of the midbrain domain of the neuronal identity marker. The areas of higher magnification are boxed in black in the lower magnification panels above. (A-F') Note that the expansion of the *sax2* midbrain domain is prominent only in the longest treatment interval (A' and B'). (G-L') The midbrain domain of *phox2b* seems unchanged comparing DAPT treated to MOCK control embryos.

Conditional blockade of neurogenesis does not change the overall pattern of MH neuronal identities

The approaches described above, attempting to induce premature neurogenesis to test for the implication of timing in neuronal fate definition, were unsuccessful. As an alternative, I decided to take a reverse approach and hinder progenitors to differentiate into neurons. To this aim, I made use of the transgenic line *Tg(hsp:her5 Δ 3')* [170]. This line overexpresses a stabilized form of *her5* upon heatshock and therefore blocks neurogenesis. To assess if neuronal identities at the MH can be impaired at all by *her5* overexpression I conducted serial heatshock experiments. These lead to a strong downregulation or even abolishment of *sax2* and *phox2b* neuronal identities (see Figure 56A to D). Having shown that heatshocking *Tg(hsp:her5 Δ 3')* can affect neuronal identities I proceeded to a more refined analysis with less heatshock pulses. Application of only a single heatshock pulse with a 15 minute duration starting at 60% epiboly did not alter neuronal identities in the MH domain. After two consecutive heatshocks started at 60% epiboly (see Figure 56J) *sax2* and *phox2b* MH domains showed a slight reduction in intensity (see Figure 56F to I). Even after 3, 4 or 5 consecutive heatshocks I could not observe more severe aberrations in the neuronal identity profile. Most importantly, I never observed that time-limited heat-shocks that decrease the size of a given neuronal population increase the size of another.

Together, these results do not speak in favour of a timer mechanism, as the overall pattern of neuronal identities is either not impaired or is equally affected for most neuronal identities upon changes in neuronal differentiation timing. Rather, the findings could be better explained by a spatial mechanism. As the tissue growth is not crucially impaired during periods with elevated levels of Her5 activity [170] (see Figure 56G and I), cells can read out their positional information like in the normal situation as soon as the neurogenesis repression is relieved, and can normally resume differentiation. This scenario leads to neuronal identity pattern resembling the normal situation although the overall timing of appearance of the differentiated cells might be shifted forwards.

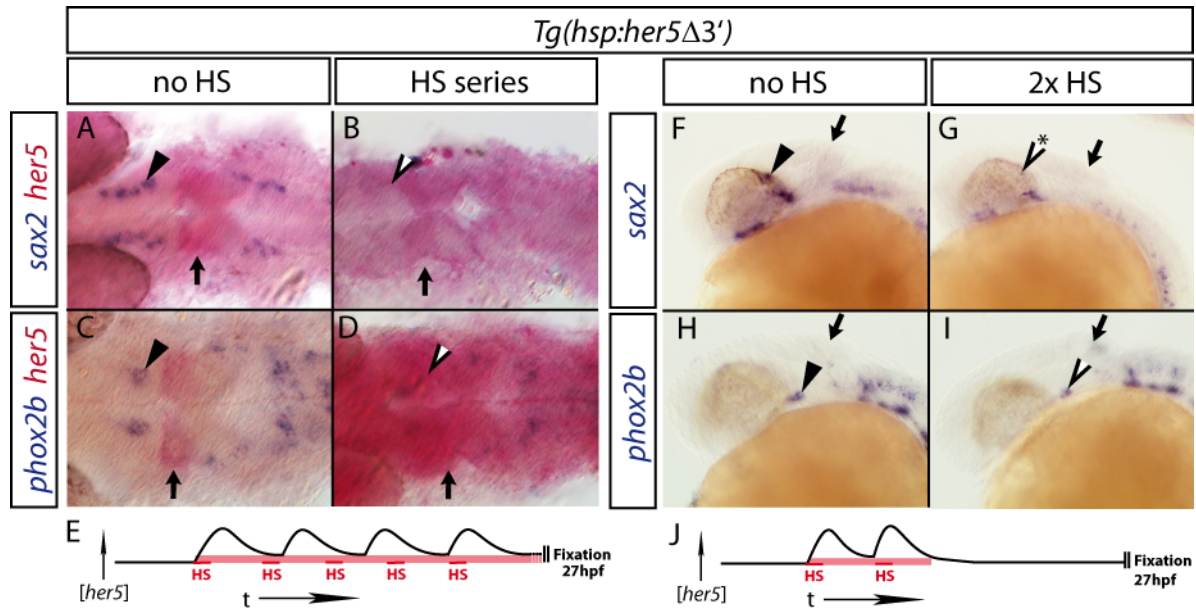


Figure 56: Overexpression of *her5* leads to a reduction of early identities but not to a gain in late identities or an overall change in the neuronal identity pattern. The MHB is indicated by black arrows and midbrain neuronal identity marker domains by arrowheads. (A-D) Dorsal views on flat-mounted preparations after RNA whole-mount double in-situ hybridization (RNA probes are color-coded on the left; anterior is left). The heat-shock protocol is schematized below in E. Heat-shock pulses (HS) of 15min are followed by 1h and 45min cooling to normal incubation temperature. Note that *her5* RNA concentration [*her5*] stays continuously elevated [170] as indicated by the light red horizontal bar. Continuous high levels of *her5* from 60% epiboly to 27hpf leads to a strong down regulation (D) or loss (B) of midbrain neuronal identity marker expression (see open arrowheads). (F-I) Sagittal views of whole-mount embryos (RNA probes are color-coded on the left; anterior is left) show that two heat-shock pulses lead only to down regulation but not a complete loss of ventral midbrain neuronal identity marker expression (G, I) while the dorsal domain of *sax2* seems to be strongly downregulated (indicated by asterisk). The heat-shock protocol is schematized below in J. Two heat-shock pulses (HS) of 15min duration are each followed by 45min cooling to 28°C in between pulses.

Conclusion

To conclude, my data do not strongly support the hypothesis that a timer mechanism has a central role in neuronal identity definition at the MH domain. Nevertheless, up to now, I also cannot formally exclude that a timer plays a role in neuronal identity definition in the MH domain, since most of my results used indirect approaches, such as acting on proliferating precursors (with DAPT) rather than on the progenitor pool itself, or on blocking neurogenesis rather than inducing it prematurely (with *hsp:her5*). A clear answer in the 4xGRIP experiments was mostly hindered by the fact that the ectopically induced neurogenesis was quickly and robustly down-regulated at the MHB after 4xGRIP injections, and I also did not succeed in elucidating the mechanism responsible for this neurogenesis blockade. Nevertheless, these experiments have revealed several interesting facts about the MHB progenitor pool. Firstly, I established a neuronal identity map of many post-mitotic markers of the basal MH domain. Secondly, I could identify two new factors involved in the formation of the MHB progenitor pool (Her3 and Her9) and show that the down-regulation of non-canonical E(Spl) activity results in a similar phenotype in fish as the one described in mouse. Thirdly, I could show that the thereby induced neurogenesis phenotype is mostly transient, pointing to additional neurogenesis blockade mechanisms that will be interesting to focus upon in future studies.

4. Discussion and perspectives

My thesis project sheds light on several different aspects of progenitor pools, ranging from the specification and maintenance to the mechanisms of fate determination. I focused on the specification of the eye field progenitor pool by *rx3*, the roles and interaction partners of non-canonical *her* genes at the MHB, the implication of miR-9 in the late maintenance of MHB and the function of the MHB progenitor pool in MH neuronal fate specification. Furthermore, I looked onto the role of non-canonical *her* genes and Fgf signalling in the adult brain. In the following I want to discuss the data I obtained and give perspectives on future directions in the analysis of these different aspects of progenitor pools.

Role of Rx3 in anterior forebrain patterning and the eye field progenitor pool

Looking for the mechanisms that lead to the loss of the eye field progenitor pool, I observed a transformation of eye field to telencephalic identities in *rx3* deficient zebrafish. This type of transformation is highly reminiscent of classical homeotic transformations as originally described and analyzed in *Drosophila* [414] where Homeobox containing genes were found to convey A/P segmental identity [415]. Similarly, homeobox containing genes in vertebrates (*hox*) convey A/P segmental identity within the mesoderm [416]. This is also the case for brain patterning where Hox genes assign segmental identity in posterior parts of the CNS, namely in the hindbrain and the spinal cord. The Hox gene mediated specification happens in a rostro-caudally nested manner resulting in a so called 'Hox code' of brain segment identity [417-419]. Interestingly, these Hox genes are not only expressed in a collinear and nested manner, but are also genetically closely linked in so called 'Hox clusters' whereby their genomic 3' to 5' position mirrors their A/P expression domains, both in *Drosophila* and vertebrates [418]. A comparable Hox code and genetically linked clusters could not be identified for anterior vertebrate brain structures. Nevertheless, many different homeobox containing genes confer segment identity within anterior brain structures in a segment-like manner, whereby the corresponding segments have been named neuromeres or prosomeres [420-423]. This opens up the perspective that an ancestral homeobox gene code for anterior brain structures has been broken up early on during evolution into single unclustered genes spread throughout the genome. Retinal homeobox genes are part of these non-clustered Homeobox containing genes that have a distinct role in anterior brain patterning. It would be interesting to dissect their evolutionary relationships and origins and to test if they are part of an ancestral cluster of 'anterior brain Hox' genes. State of the art phylogenetic algorithms and the availability of an increasing number of sequenced genomes [424] could be extremely helpful for such an approach. But still, experimental assays that test the functionality, exchangeability and competence for anterior brain Homeobox genes in model organisms (and increasingly also in non-model organisms) may shed light on these questions in the near future. One important experiment in this respect would be to test if the zebrafish *rx3* paralogs *rx1* and *rx2*, which are expressed significantly later in development than *rx3*, can take over the early role of *rx3* in forebrain patterning. Rescue experiments with *rx1* and/or *rx2* in *rx3* null mutants would be one predictive way to test this. Furthermore, cross-species rescue experiments would be a promising way to test the evolutionary and functional relationships of *rx* orthologs and their paralogs. Interestingly, it has been

already shown in overexpression studies with *rx1* and *rx2* that these genes can promote retinal versus telencephalic identity [425]. It is important to note that in these experiments *rx1* and *rx2* mediated the telencephalic to retinal fate change at significantly later stages than *rx3* functions in initial eye field specification. In addition, no alterations in early telencephalic markers such as *foxg1* and *emx3* were observed in these experiments [425]. This speaks already for a specific functional role of *rx3* rather than only an earlier expression onset compared to the other paralogs. In this respect, it would be promising to analyze the differences in the protein sequence between Rx1, Rx2 and Rx3 in detail as it has been shown that a 8-10 amino acid domain directly downstream of the homeodomain is necessary and sufficient to mediate the specific differences in protein activity of the two closely related homeobox containing factors XOt2 and XOt5b in the retina of *Xenopus* [426]. Furthermore, the initial expression of *rx* genes during early forebrain patterning is highly conserved within vertebrates [60,68,427]. This argues for a primary ancestral role of Rx in the specification of early anterior progenitors. Recently, it has been shown that Rx factors also have a highly conserved role in forebrain cells with neurosecretory function. In zebrafish this is represented by a population of cells in the basal hypothalamus and the neighboring pituitary [428]. Loss of function of *rx3* leads to defects in the corticotrope axis, namely in the arcuate nucleus and the anterior pituitary, which result in deficiencies in *proopiomelanocortin a (pomca)* expression and circadian rhythm control [428]. Interestingly, homozygous *chk* mutants also completely lose *vasotocin neurophysin (vsnp)* expression which was corroborated in our *chk^{ne2611}* allele [429]. Moreover, this specific expression of *rx3* in *vasotocin neurophysin* neurosecretory cells is highly conserved as even the annelid *Platynereis dumerilii* has an *rx* homolog that is expressed in a homologous forebrain neurosecretory structure that controls *vasotocin neurophysin* secretion. Control of anterior vasotocinergic progenitors by *rx* genes might therefore be an ancestral feature of the whole bilaterian clade [429]. Notably, these forebrain neurosecretory cell populations are also photoreceptive, opening up the perspective that Rx has a more general role in specifying forebrain photoreceptive progenitors [429]. A further crucial open question that has not been addressed yet is the consequence of potentially altered Wnt signalling in *rx3* mutants. Several observations indicate an implication of *rx3* gene function in Wnt mediated forebrain patterning. Firstly, the sFRP family member and secreted Wnt inhibitor Tlc shows a largely broader expression in *rx3* mutants at post gastrulation stages compared to wildtype due to ectopic maintenance (see Figure 7). Secondly, data from Medaka indicates that another sFRP family member and secreted Wnt modulator, *olSfrp1*, is involved in eye field patterning [430-432]. Thirdly, *rx3* overexpression induces head truncations which is reminiscent of phenotypes induced by exaggerated Wnt signalling [55]. Therefore it would be highly interesting to directly address the implications of *rx3* loss and gain of function on Wnt signalling in the anterior neural plate.

The role of Gli1 in generating medial to lateral differences in neurogenesis propensity in progenitor pools

As we identified Gli1 to be central for generating medial to lateral difference in neurogenesis propensity within the MHB progenitor pool, it would be interesting to address if other progenitor pools show a similar regulation by midline Gli1 activity. A good candidate for that would be the eye field progenitor pool as it has a high rate of midline *gli1* expression before the end of gastrulation. Intriguingly, similar to the situation at the MH domain, neurogenesis starts ventrally and then spreads dorsally

in the eye [339,433]. But in contrast to the situation at the IZ, the retinal differentiation seems to be directly coupled to Shh signalling [339]. In this context, a neurogenesis promoting role for Gli1 has been reported in the zebrafish retina, where blocking of Gli1/2 function leads to a blockade of the progression of the Ath5 mediated neurogenesis wave. It has been shown in *Xenopus* that Hedgehog signalling works pro-neurogenic in the retina by bringing progenitors from a slow cycling stem cell state to a fast cycling progenitor state [434].

Functions of miR-9 in vertebrate brain development

As progenitor pools serve several different functions during brain development, a crucial question is how these different characteristics are orchestrated. Our analysis of miR-9 identified one such unifying mechanism. This microRNA controls by itself at least two characteristics of the MHB progenitor pool: it restricts its organizer activity by repressing Fgf signalling, and it restricts its anti-neurogenic activity by downregulating Her activity. It would now be highly interesting to test if miR-9 plays yet further roles within the MH. One obvious process to test would be the control of neuronal identities. MicroRNAs have been considered as good candidates for neuronal identity control in the context of the vertebrate retinal timer [344]. Similarly, miR-9 could play a role in neuronal identity choices in the MH domain.

A very interesting observation is the potential coregulation of *En2* and *Canopy1* by miR-9, as they are closely genetically linked in mouse [85]. Similarly, in zebrafish *eng2b* and *cnpy1* are closely linked^a. A shared locus is suggestive of a close coregulation as it has been shown for *her5* and *her11* [186], for example. Because of its role in Fgf signalling one would expect a similar sharp expression at the MHB for *cnpy1* as for *fgf8* and other synexpression group members. In sharp contrast to that, later in development, *cnpy1* is broadly expressed in the MH domain similar to *eng2*. The wide coexpression of *cnpy1* with miR-9 (see chapter 3.1.4 and Appendix 4) is suggestive of a role of miR-9 in down-regulating the broad transcription of *cnpy1* to a refined translation at the MHB. This hypothesis could be easily tested by comparing antibody staining detecting actual Cnpy1 protein and RNA in-situ hybridization with a *cnpy1* specific probe.

Furthermore, it would be highly relevant to test if there are more in-vivo targets of miR-9 than the ones we tested. Interestingly, in the list of predicted targets, there are several more Fgf signalling pathway members than the ones we experimentally validated. For example, miRBase^b predicts *fgf18* and *fgf18l* as additional targets of miR-9. In addition, refined prediction algorithms that take into account the experimental data of the in-vivo validated targets that we have at hand now would help to identify new bona fide targets that could subsequently be tested experimentally similar to the approaches that were used to test the Fgf and Her targets, i.e. using sensor and target protection assays.

Moreover, the expression of miR-9 in other regions of the CNS than the MH domain is suggestive of a more widespread role in progenitor pool regulation. In that respect it would be crucial to test the early role of miR-9 in the telencephalon where miR-9 expression appears first. In addition, miR-9 expression has been described in maturing cells in the ciliary marginal zone, the progenitor pool of the retina during later embryonic up to adult stages [272].

Furthermore, it will be interesting to see in how far miR-9 has similar bipartite, or multipartite, roles in progenitor pool control in other vertebrates. First suggestive hints

^a Data available at the Ensembl webpage: www.ensembl.org

^b miRBASE webpage: <http://microrna.sanger.ac.uk/>

come from expression analysis in other vertebrate model species. miR-9 is expressed in patterns similar to the one in zebrafish during early nervous system development in chicken [435], *Xenopus tropicalis* [436] and mouse [437].

Finally, it would be key experiments to test the role miR-9 in adult neurogenesis and Fgf signalling control. In general it is expressed in periventricular zones and differentiated cells in the adult brain which fits largely its expression at embryonic stages [272]. There are only minor deviations such as additional expression in the adult habenular and lateral torus cells of the hypothalamus where no expression has been described at embryonic stages [272].

Canonical and non-canonical *E(Spl)* genes in zebrafish versus mouse embryonic brains

Several cellular characteristics that potentially differ between midbrain proliferating neural precursors that express canonical *her* genes such as *her4*, and cells at the MHB progenitor pools that express non-canonical *her* genes such as *her3/5/9/11*, have been dissected in my thesis project. I could observe a clear difference in cell division characteristics between these two populations. In contrast, early MHB progenitors and midbrain proliferating precursors cannot be distinguished by GFAP expression or proliferation rate. Differences in proliferation rate are only apparent at later stages. Another glia marker, 'fatty acid binding protein 7, brain, a' (*Fabp7a*), also known as 'Brain lipid-binding protein' (BLBP), might need to be further analyzed in this respect as its expression pattern at 19 to 30hpf (available at the Zebrafish Model Organism Database ZFIN^a) shows overall strong expression in the MH domain with a clear gap at the MHB. To date, however, the results suggest that we cannot draw a direct parallel between the two types of early zebrafish progenitors and the early progenitors of the mouse (neuroepithelial cells versus radial glia progenitors). Asymmetrical divisions, which characterize mouse radial glia progenitors as opposed to neuroepithelial progenitors, were so far only observed in MHB pool cells. However, symmetrical proliferative divisions, which in the mouse characterize neuroepithelial progenitors, are also found in zebrafish within the MHB pool. It is possible that the mouse-like types of progenitors can be observed at a later stage in zebrafish, and it would be important to conduct tracings after 27hpf, when MHB progenitor pool cells have acquired a slow division mode.

Furthermore, in the light of the recently published data from mouse that showed that *Hes1* expression is periodically cycling in compartment progenitors [238], it would be highly revealing to test in how far zebrafish *her* genes show a similar periodic expression in neural progenitors. This might be feasible in zebrafish with a similar approach than the one which was used in mouse, i.e. the highly time sensitive luciferase reporter system [238]. In concordance with data from the mouse model one would expect canonical *her* genes, such as *her4*, to be expressed periodically while non-canonical *her* genes such as *her3/5/9/11* to be expressed constantly at high levels.

Non-canonical *her* genes in the adult brain

I could show that the non-canonical *her* genes *her3* and *her9* are also expressed in a progenitor pool in the adult zebrafish brain, the IPZ. My analysis is relying on gene expression patterns of these *her* genes and co-expression analysis with proliferation markers which provide reliable positional information on the location of proliferation

^a www.zfin.org

zones. Yet a more detailed marker analysis similar to the one that has been undertaken for *her5* at the IPZ [13] would be very fruitful for the detailed understanding of the roles of non-canonical *her* genes at the IPZ and their relation to each other. First, it would be crucial to analyze the cellular characteristics of *her3*- and/or *her9*-positive cells by testing for co-expression with radial glia markers such as GFAP and BLBP^a. Furthermore, co-labelling with stem cells markers such as *sox2* would shed light on the stemness character of *her3*- and/or *her9*-expressing cells. Moreover, a test if *her3*- and/or *her9*-positive cells are self-renewing and multipotent would clarify if these cells are bona fide adult neural stem cells. This could be accomplished by BrdU pulse labelling and long term tracing of these cells combined with PCNA labelling. Cells that are both positive for BrdU and PCNA after several months are self-renewing cells. Multipotency could be tested by immunolabelling for the neuronal differentiation marker HuC, the oligodendrocyte precursor markers O4^b, Quaking (Qki) and the astrocyte markers S100 β and GFAP, for example [13,14]. Furthermore, analysis of their cellular morphology, their migration pathways, final destination and projection pattern could give further insight into their potentialities. Moreover, I observed that *her3* and *her9* are also expressed at other progenitor pools in the adult brain, in addition to the IPZ. In contrast to that, *her11* expression in the CNS gets downregulated early in development at around 36hpf despite of the fact that *her5* and *her11* share 3,3kb of their upstream regulatory sequences [186]. *her9* is broadly expressed in the periventricular zone of the hypothalamus, the telencephalic ventricular zone, the valvula cerebelli and the cerebellum, amongst several other zones with weaker *her9* expression. In contrast to that, additional *her3* expression zones are restricted to small paired regions in the midbrain. A more detailed expression and co-labelling analysis of these additional zones would shed light on whether all adult neural progenitor pools are covered by expression of *her3/5/9* [13,14]. Co-labelling with canonical *her* genes, such as *her4*, would provide information on the relation of progenitor pools to proliferative neural precursors. Yet the difference and characteristics of these two different populations remain to be established in more detail.

Fgf-signalling in the adult brain – breaking up of the Fgf synexpression group

During the expression analysis of Fgf signalling components in the adult brain, we observed a significant difference in the expression domains compared to embryonic stages. While the expression of some genes, such as *fgf8a*, is much more restricted in the adult brain compared to the embryonic, the expression of others, such as *fgf4* and *fgf17b*, is more widespread or in some cases nearly ubiquitous in adult brains. Furthermore, in the adult, several of the downstream components of Fgf signalling are often non-overlapping with the broadly expressed *fgfs*. Similarly, *fgfr4* shows a strong divergence in expression between embryonic stages, where it is rather restricted [161,406], and adult stages, where it is very broadly expressed. This implicates that the Fgf synexpression group [119,158] is broken up in the adult brain. Similar differences between embryonic and adult brain expressions have been already documented for several genes, such as *neurog1*, *pax6b* and *ascl1a* [14] and the microRNAs miR-34, miR-218a and miR-219 [272]. Interestingly, also enhancer trap lines that faithfully recapitulate many of embryonic expression domains of trapped genes show clearly different regulation in adult stages. This discrepancy between embryonic versus adult expression patterns is not yet understood at the

^a Brain Lipid Binding Protein

^b Oligodendrocyte antigen (numbered 1 to 4) [438]

functional level. Most likely it is due to larger changes in the cis-regulatory control mediated by epigenetic changes such as DNA methylation and chromatin modifications.

Neuronal identity determination in the MH domain by a timer mechanism

In order to test whether a timing component is implicated in neuronal fate specification and determination in the MH domain, it would be important to test further ways to conditionally induce ectopic neurogenesis or ectopically repress neurogenesis in this domain. One possible way to go would be to try to induce ectopic neurogenesis by applying the cell cycle inhibitor *Xgadd-45* conditionally [344]. This technical approach has proven to be useful in the *Xenopus* retina and should therefore in principle also work for the zebrafish embryonic nervous system [344]. Conditional expression could be conferred by using a heat shock promoter construct, for example.

In order to assess whether an intrinsic differentiation timer exists in MH progenitors, it would be highly revealing, though technically demanding, to apply explant approaches and transfer cells out of the MH into cell culture at different time points of development and assess their fates [439]. Recent progress in zebrafish embryonic cell culture using trout stromal cells as feeder layer would make this assay feasible. This feeder layer is crucial to the success of such an experiment as it provides the not yet commercially available fish specific growth factors which are necessary for the survival of the explanted cells [440]. Extreme caution has to be used with such an approach as it can be that the feeder cells also provide cell fate determinants which might obscure the assessment of the explant culture experiment. Furthermore, heterochronic transplantations in vivo, similar to the ones that have been done to analyse the vertebrate cortex timer [321,324,325], would be a meaningful way to assess the contribution of intrinsic timer programs to fate specification in the zebrafish MH domain.

Recently, a progenitor pool with a differentiation timer has been described in the cerebellar rhombic lip of the chicken using an in ovo heterochronic grafting experiments [351]. In the normal situation at embryonic day 4 (E4), rhombic lip progenitors give rise to extracerebellar neurons. Two days later, at E6, the same progenitor pool gives rise to granule cell precursors. With these in ovo heterochronic grafting experiments it has been shown that this process is temporally controlled by intrinsic programmes but that extrinsic cues are required additionally for the correct temporal transitions. A similar process has been described for the zebrafish rhombic lip [198,441]. Therefore it would be revealing to apply an explant approach, as described above, also to the rhombic lip progenitor pool cells in order to characterize the potential differentiation timer in zebrafish.

Conclusion

Taken together, my work contributed to a better understanding of the specification, maintenance and fate determination of progenitor pools in the zebrafish central nervous system. I have used zebrafish as neurogenetic model organism and applied a wide range of experimental approaches, ranging from classical mutant analysis, molecular genetics, transplantation approaches, fate tracing with fluorescent dyes to in vivo imaging approaches. With my work I can also provide new resources for the research community. For the *rx3* gene I could establish a new mutant line that is already successfully used by other labs [429] and similarly an enhancer trap line [134,357]. Furthermore, several mutants that I recovered during screening have been deposited to the Zebrafish Information Network webpage^a and are publicly available to the community.

^a http://zfin.org/SearchApp/category_search.jsp?query=zf-models+serotonergic

5. Bibliography

1. Pelvig DP, Pakkenberg H, Stark AK, Pakkenberg B. Neocortical glial cell numbers in human brains. *Neurobiol Aging*, (2007).
2. Tang Y, Nyengaard JR, De Groot DM, Gundersen HJ. Total regional and global number of synapses in the human brain neocortex. *Synapse*, 41(3), 258-273 (2001).
3. Driever W, Solnica-Krezel L, Schier AF *et al.* A genetic screen for mutations affecting embryogenesis in zebrafish. *Development*, 123, 37-46 (1996).
4. Streisinger G, Walker C, Dower N, Knauber D, Singer F. Production of clones of homozygous diploid zebra fish (*Brachydanio rerio*). *Nature*, 291(5813), 293-296 (1981).
5. Haffter P, Granato M, Brand M *et al.* The identification of genes with unique and essential functions in the development of the zebrafish, *Danio rerio*. *Development*, 123, 1-36 (1996).
6. Amsterdam A, Nissen RM, Sun Z, Swindell EC, Farrington S, Hopkins N. Identification of 315 genes essential for early zebrafish development. *Proc Natl Acad Sci U S A*, 101(35), 12792-12797 (2004).
7. Geisler R, Rauch GJ, Geiger-Rudolph S *et al.* Large-scale mapping of mutations affecting zebrafish development. *BMC Genomics*, 8, 11 (2007).
8. Kawakami K. Tol2: a versatile gene transfer vector in vertebrates. *Genome Biol*, 8 Suppl 1, S7 (2007).
9. Laplante M, Kikuta H, Konig M, Becker TS. Enhancer detection in the zebrafish using pseudotyped murine retroviruses. *Methods*, 39(3), 189-198 (2006).
10. Asakawa K, Suster ML, Mizusawa K *et al.* Genetic dissection of neural circuits by Tol2 transposon-mediated Gal4 gene and enhancer trapping in zebrafish. *Proc Natl Acad Sci U S A*, 105(4), 1255-1260 (2008).
11. Koster RW, Fraser SE. Tracing transgene expression in living zebrafish embryos. *Dev Biol*, 233(2), 329-346 (2001).
12. Chapouton P, Jagasia R, Bally-Cuif L. Adult neurogenesis in non-mammalian vertebrates. *Bioessays*, 29(8), 745-757 (2007).
13. Chapouton P, Adolf B, Leucht C *et al.* *her5* expression reveals a pool of neural stem cells in the adult zebrafish midbrain. *Development*, 133(21), 4293-4303 (2006).
14. Adolf B, Chapouton P, Lam CS *et al.* Conserved and acquired features of adult neurogenesis in the zebrafish telencephalon. *Dev Biol*, 295(1), 278-293 (2006).
15. Campos-Ortega JA. Mechanisms of early neurogenesis in *Drosophila melanogaster*. *J Neurobiol*, 24(10), 1305-1327 (1993).
16. Bertrand N, Castro DS, Guillemot F. Proneural genes and the specification of neural cell types. *Nat Rev Neurosci*, 3(7), 517-530 (2002).
17. Kimmel CB, Warga RM. Indeterminate cell lineage of the zebrafish embryo. *Dev Biol*, 124(1), 269-280 (1987).
18. Kimmel CB, Ballard WW, Kimmel SR, Ullmann B, Schilling TF. Stages of embryonic development of the zebrafish. *Dev Dyn*, 203(3), 253-310 (1995).
19. Kozlowski DJ, Murakami T, Ho RK, Weinberg ES. Regional cell movement and tissue patterning in the zebrafish embryo revealed by fate mapping with caged fluorescein. *Biochem Cell Biol*, 75(5), 551-562 (1997).
20. Helde KA, Wilson ET, Cretekos CJ, Grunwald DJ. Contribution of early cells to the fate map of the zebrafish gastrula. *Science*, 265(5171), 517-520 (1994).
21. Woo K, Fraser SE. Order and coherence in the fate map of the zebrafish nervous system. *Development*, 121(8), 2595-2609 (1995).
22. Solnica-Krezel L, Cooper MS. Cellular and genetic mechanisms of convergence and extension. *Results Probl Cell Differ*, 40, 136-165 (2002).
23. Varga ZM, Wegner J, Westerfield M. Anterior movement of ventral diencephalic precursors separates the primordial eye field in the neural plate and requires *cyclops*. *Development*, 126(24), 5533-5546 (1999).
24. Langeland JA, Kimmel CB. *Fishes* (eds. Gilbert, SF, Raunio, AM) (Sinauer Associates, Sunderland, 1997).

25. Schmitz B, Papan C, Campos-Ortega JA. Neurulation in the anterior trunk region of the zebrafish *Brachydanio rerio*. *Development Genes and Evolution*, 202(5), 250-259 (1993).
26. Chapouton P, Bally-Cuif L. Neurogenesis. *Methods Cell Biol*, 76, 163-206 (2004).
27. Papan C, Campos-Ortega JA. On the formation of the neural keel and neural tube in the zebrafish *Danio (Brachydanio) rerio*. *Development Genes and Evolution*, 203(4), 178-186 (1994).
28. Tawk M, Araya C, Lyons DA *et al*. A mirror-symmetric cell division that orchestrates neuroepithelial morphogenesis. *Nature*, 446(7137), 797-800 (2007).
29. Wilson SW, Houart C. Early steps in the development of the forebrain. *Dev Cell*, 6(2), 167-181 (2004).
30. Appel B, Chitnis A. Neurogenesis and specification of neuronal identity. *Results Probl Cell Differ*, 40, 237-251 (2002).
31. Stern CD. Neural induction: old problem, new findings, yet more questions. *Development*, 132(9), 2007-2021 (2005).
32. Hemmati-Brivanlou A, Melton D. Vertebrate embryonic cells will become nerve cells unless told otherwise. *Cell*, 88(1), 13-17 (1997).
33. Wilson SI, Edlund T. Neural induction: toward a unifying mechanism. *Nat Neurosci*, 4 Suppl, 1161-1168 (2001).
34. Hammerschmidt M, Serbedzija GN, McMahon AP. Genetic analysis of dorsoventral pattern formation in the zebrafish: requirement of a BMP-like ventralizing activity and its dorsal repressor. *Genes Dev*, 10(19), 2452-2461 (1996).
35. Fekany-Lee K, Gonzalez E, Miller-Bertoglio V, Solnica-Krezel L. The homeobox gene *bozozok* promotes anterior neuroectoderm formation in zebrafish through negative regulation of BMP2/4 and Wnt pathways. *Development*, 127(11), 2333-2345 (2000).
36. Nguyen VH, Schmid B, Trout J, Connors SA, Ekker M, Mullins MC. Ventral and lateral regions of the zebrafish gastrula, including the neural crest progenitors, are established by a *bmp2b/swirl* pathway of genes. *Dev Biol*, 199(1), 93-110 (1998).
37. Dick A, Hild M, Bauer H *et al*. Essential role of *Bmp7* (*snailhouse*) and its prodomain in dorsoventral patterning of the zebrafish embryo. *Development*, 127(2), 343-354 (2000).
38. Hild M, Dick A, Rauch GJ *et al*. The *smad5* mutation *somitabun* blocks *Bmp2b* signaling during early dorsoventral patterning of the zebrafish embryo. *Development*, 126(10), 2149-2159 (1999).
39. Bally-Cuif L, Hammerschmidt M. Induction and patterning of neuronal development, and its connection to cell cycle control. *Curr Opin Neurobiol*, 13(1), 16-25 (2003).
40. Wilson SI, Graziano E, Harland R, Jessell TM, Edlund T. An early requirement for FGF signalling in the acquisition of neural cell fate in the chick embryo. *Curr Biol*, 10(8), 421-429 (2000).
41. Streit A, Berliner AJ, Papanayotou C, Sirulnik A, Stern CD. Initiation of neural induction by FGF signalling before gastrulation. *Nature*, 406(6791), 74-78 (2000).
42. Linker C, Stern CD. Neural induction requires BMP inhibition only as a late step, and involves signals other than FGF and Wnt antagonists. *Development*, 131(22), 5671-5681 (2004).
43. Kudoh T, Concha ML, Houart C, Dawid IB, Wilson SW. Combinatorial *Fgf* and *Bmp* signalling patterns the gastrula ectoderm into prospective neural and epidermal domains. *Development*, 131(15), 3581-3592 (2004).
44. Delaune E, Lemaire P, Kodjabachian L. Neural induction in *Xenopus* requires early FGF signalling in addition to BMP inhibition. *Development*, 132(2), 299-310 (2005).
45. Pera EM, Wessely O, Li SY, De Robertis EM. Neural and head induction by insulin-like growth factor signals. *Dev Cell*, 1(5), 655-665 (2001).
46. Eivers E, McCarthy K, Glynn C, Nolan CM, Byrnes L. Insulin-like growth factor (IGF) signalling is required for early dorso-anterior development of the zebrafish embryo. *Int J Dev Biol*, 48(10), 1131-1140 (2004).
47. Kretzschmar M, Doody J, Massague J. Opposing BMP and EGF signalling pathways converge on the TGF-beta family mediator *Smad1*. *Nature*, 389(6651), 618-622 (1997).
48. Pera EM, Ikeda A, Eivers E, De Robertis EM. Integration of IGF, FGF, and anti-BMP signals via *Smad1* phosphorylation in neural induction. *Genes Dev*, 17(24), 3023-3028 (2003).
49. Furthauer M, Thisse C, Thisse B. A role for FGF-8 in the dorsoventral patterning of the zebrafish gastrula. *Development*, 124(21), 4253-4264 (1997).

50. Furthauer M, Van Celst J, Thisse C, Thisse B. Fgf signalling controls the dorsoventral patterning of the zebrafish embryo. *Development*, 131(12), 2853-2864 (2004).
51. Rentzsch F, Bakkers J, Kramer C, Hammerschmidt M. Fgf signaling induces posterior neuroectoderm independently of Bmp signaling inhibition. *Dev Dyn*, 231(4), 750-757 (2004).
52. Heisenberg CP, Houart C, Take-Uchi M *et al.* A mutation in the Gsk3-binding domain of zebrafish Masterblind/Axin1 leads to a fate transformation of telencephalon and eyes to diencephalon. *Genes Dev*, 15(11), 1427-1434 (2001).
53. van de Water S, van de Wetering M, Joore J *et al.* Ectopic Wnt signal determines the eyeless phenotype of zebrafish masterblind mutant. *Development*, 128(20), 3877-3888 (2001).
54. Kelly GM, Greenstein P, Erezyilmaz DF, Moon RT. Zebrafish wnt8 and wnt8b share a common activity but are involved in distinct developmental pathways. *Development*, 121(6), 1787-1799 (1995).
55. Kim CH, Oda T, Itoh M *et al.* Repressor activity of Headless/Tcf3 is essential for vertebrate head formation. *Nature*, 407(6806), 913-916 (2000).
56. Dorsky RI, Itoh M, Moon RT, Chitnis A. Two tcf3 genes cooperate to pattern the zebrafish brain. *Development*, 130(9), 1937-1947 (2003).
57. Lagutin OV, Zhu CC, Kobayashi D *et al.* Six3 repression of Wnt signaling in the anterior neuroectoderm is essential for vertebrate forebrain development. *Genes Dev*, 17(3), 368-379 (2003).
58. Houart C, Westerfield M, Wilson SW. A small population of anterior cells patterns the forebrain during zebrafish gastrulation. *Nature*, 391(6669), 788-792 (1998).
59. Houart C, Caneparo L, Heisenberg C, Barth K, Take-Uchi M, Wilson S. Establishment of the telencephalon during gastrulation by local antagonism of Wnt signaling. *Neuron*, 35(2), 255-265 (2002).
60. Mathers PH, Grinberg A, Mahon KA, Jamrich M. The Rx homeobox gene is essential for vertebrate eye development. *Nature*, 387(6633), 603-607 (1997).
61. Chuang JC, Mathers PH, Raymond PA. Expression of three Rx homeobox genes in embryonic and adult zebrafish. *Mech Dev*, 84(1-2), 195-198 (1999).
62. Winkler S, Loosli F, Henrich T, Wakamatsu Y, Wittbrodt J. The conditional medaka mutation eyeless uncouples patterning and morphogenesis of the eye. *Development*, 127(9), 1911-1919 (2000).
63. Loosli F, Staub W, Finger-Baier KC *et al.* Loss of eyes in zebrafish caused by mutation of chokh/rx3. *EMBO Rep*, 4(9), 894-899 (2003).
64. Rembold M, Loosli F, Adams RJ, Wittbrodt J. Individual cell migration serves as the driving force for optic vesicle evagination. *Science*, 313(5790), 1130-1134 (2006).
65. Casarosa S, Andreazzoli M, Simeone A, Barsacchi G. Xrx1, a novel Xenopus homeobox gene expressed during eye and pineal gland development. *Mech Dev*, 61(1-2), 187-198 (1997).
66. Furukawa T, Kozak CA, Cepko CL. rax, a novel paired-type homeobox gene, shows expression in the anterior neural fold and developing retina. *Proc Natl Acad Sci U S A*, 94(7), 3088-3093 (1997).
67. Deschet K, Bourrat F, Ristoratore F, Chourrout D, Joly JS. Expression of the medaka (*Oryzias latipes*) OI-Rx3 paired-like gene in two diencephalic derivatives, the eye and the hypothalamus. *Mech Dev*, 83(1-2), 179-182 (1999).
68. Bailey TJ, El-Hodiri H, Zhang L, Shah R, Mathers PH, Jamrich M. Regulation of vertebrate eye development by Rx genes. *Int J Dev Biol*, 48(8-9), 761-770 (2004).
69. Wurst W, Bally-Cuif L. Neural plate patterning: upstream and downstream of the isthmic organizer. *Nat Rev Neurosci*, 2(2), 99-108 (2001).
70. Tallafuss A, Bally-Cuif L. Tracing of her5 progeny in zebrafish transgenics reveals the dynamics of midbrain-hindbrain neurogenesis and maintenance. *Development*, 130(18), 4307-4323 (2003).
71. Marin F, Puelles L. Patterning of the embryonic avian midbrain after experimental inversions: a polarizing activity from the isthmus. *Dev Biol*, 163(1), 19-37 (1994).
72. Zervas M, Millet S, Ahn S, Joyner AL. Cell behaviors and genetic lineages of the mesencephalon and rhombomere 1. *Neuron*, 43(3), 345-357 (2004).
73. Partanen J. FGF signalling pathways in development of the midbrain and anterior hindbrain. *J Neurochem*, 101(5), 1185-1193 (2007).
74. Nakamura H, Takagi S, Tsuji T, Matsui KA, Fujisawa H. The Prosencephalon Has the Capacity to Differentiate into the Optic Tectum: Analysis by Chick-Specific Monoclonal Antibodies in Quail-Chick-Chimeric Brains. (Quail-chick-chimera/monoclonal antibody/chick specific/prosencephalon/optic tectum). *Development, Growth & Differentiation*, 30(6), 717-725 (1988).

75. Alvarado-Mallart RM, Martinez S, Lance-Jones CC. Pluripotentiality of the 2-day-old avian germinative neuroepithelium. *Dev Biol*, 139(1), 75-88 (1990).
76. Martinez S, Wassef M, Alvarado-Mallart RM. Induction of a mesencephalic phenotype in the 2-day-old chick prosencephalon is preceded by the early expression of the homeobox gene *en*. *Neuron*, 6(6), 971-981 (1991).
77. Gardner CA, Barald KF. The cellular environment controls the expression of engrailed-like protein in the cranial neuroepithelium of quail-chick chimeric embryos. *Development*, 113(3), 1037-1048 (1991).
78. Bally-Cuif L, Wassef M. Ectopic induction and reorganization of Wnt-1 expression in quail/chick chimeras. *Development*, 120(12), 3379-3394 (1994).
79. Nakamura H, Nakano KE, Igawa HH, Takagi S, Fujisawa H. Plasticity and rigidity of differentiation of brain vesicles studied in quail-chick chimeras. *Cell Differ*, 19(3), 187-193 (1986).
80. Cowan WM, Finger TE. *Regeneration and Regulation in the Developing Central Nervous System* (ed. Spitzer, NC) (Plenum Press, New York, 1982).
81. Joyner AL, Liu A, Millet S. Otx2, Gbx2 and Fgf8 interact to position and maintain a mid-hindbrain organizer. *Curr Opin Cell Biol*, 12(6), 736-741 (2000).
82. Liu A, Joyner AL. Early anterior/posterior patterning of the midbrain and cerebellum. *Annu Rev Neurosci*, 24, 869-896 (2001).
83. Raible F, Brand M. Divide et Impera--the midbrain-hindbrain boundary and its organizer. *Trends Neurosci*, 27(12), 727-734 (2004).
84. Reifers F, Bohli H, Walsh EC, Crossley PH, Stainier DY, Brand M. Fgf8 is mutated in zebrafish acerebellar (*ace*) mutants and is required for maintenance of midbrain-hindbrain boundary development and somitogenesis. *Development*, 125(13), 2381-2395 (1998).
85. Jukkola T, Lahti L, Naserke T, Wurst W, Partanen J. FGF regulated gene-expression and neuronal differentiation in the developing midbrain-hindbrain region. *Dev Biol*, 297(1), 141-157 (2006).
86. Simeone A, Acampora D, Gulisano M, Stornaiuolo A, Boncinelli E. Nested expression domains of four homeobox genes in developing rostral brain. *Nature*, 358(6388), 687-690 (1992).
87. Bouillet P, Chazaud C, Oulad-Abdelghani M, Dolle P, Chambon P. Sequence and expression pattern of the *Stra7* (*Gbx-2*) homeobox-containing gene induced by retinoic acid in P19 embryonal carcinoma cells. *Dev Dyn*, 204(4), 372-382 (1995).
88. Wassarman KM, Lewandoski M, Campbell K *et al*. Specification of the anterior hindbrain and establishment of a normal mid/hindbrain organizer is dependent on *Gbx2* gene function. *Development*, 124(15), 2923-2934 (1997).
89. Hidalgo-Sanchez M, Millet S, Simeone A, Alvarado-Mallart RM. Comparative analysis of *Otx2*, *Gbx2*, *Pax2*, *Fgf8* and *Wnt1* gene expressions during the formation of the chick midbrain/hindbrain domain. *Mech Dev*, 81(1-2), 175-178 (1999).
90. Tour E, Pillemer G, Gruenbaum Y, Fainsod A. *Gbx2* interacts with *Otx2* and patterns the anterior-posterior axis during gastrulation in *Xenopus*. *Mech Dev*, 112(1-2), 141-151 (2002).
91. Rhinn M, Lun K, Amores A, Yan YL, Postlethwait JH, Brand M. Cloning, expression and relationship of zebrafish *gbx1* and *gbx2* genes to Fgf signaling. *Mech Dev*, 120(8), 919-936 (2003).
92. Prakash N, Wurst W. Specification of midbrain territory. *Cell Tissue Res*, 318(1), 5-14 (2004).
93. Meinhardt H. Cell determination boundaries as organizing regions for secondary embryonic fields. *Dev Biol*, 96(2), 375-385 (1983).
94. Simeone A. Positioning the isthmus organizer where *Otx2* and *Gbx2* meet. *Trends Genet*, 16(6), 237-240 (2000).
95. Li JY, Joyner AL. *Otx2* and *Gbx2* are required for refinement and not induction of mid-hindbrain gene expression. *Development*, 128(24), 4979-4991 (2001).
96. Rowitch DH, McMahon AP. *Pax-2* expression in the murine neural plate precedes and encompasses the expression domains of *Wnt-1* and *En-1*. *Mech Dev*, 52(1), 3-8 (1995).
97. Puschel AW, Westerfield M, Dressler GR. Comparative analysis of *Pax-2* protein distributions during neurulation in mice and zebrafish. *Mech Dev*, 38(3), 197-208 (1992).
98. Davis CA, Joyner AL. Expression patterns of the homeobox-containing genes *En-1* and *En-2* and the proto-oncogene *int-1* diverge during mouse development. *Genes Dev*, 2(12B), 1736-1744 (1988).
99. Wilkinson DG, Bailes JA, McMahon AP. Expression of the proto-oncogene *int-1* is restricted to specific neural cells in the developing mouse embryo. *Cell*, 50(1), 79-88 (1987).

100. Wurst W, Auerbach AB, Joyner AL. Multiple developmental defects in Engrailed-1 mutant mice: an early mid-hindbrain deletion and patterning defects in forelimbs and sternum. *Development*, 120(7), 2065-2075 (1994).
101. Krauss S, Johansen T, Korzh V, Fjose A. Expression pattern of zebrafish pax genes suggests a role in early brain regionalization. *Nature*, 353(6341), 267-270 (1991).
102. Krauss S, Johansen T, Korzh V, Fjose A. Expression of the zebrafish paired box gene pax[zf-b] during early neurogenesis. *Development*, 113(4), 1193-1206 (1991).
103. Krauss S, Maden M, Holder N, Wilson SW. Zebrafish pax[b] is involved in the formation of the midbrain-hindbrain boundary. *Nature*, 360(6399), 87-89 (1992).
104. Lekven AC, Buckles GR, Kostakis N, Moon RT. Wnt1 and wnt10b function redundantly at the zebrafish midbrain-hindbrain boundary. *Dev Biol*, 254(2), 172-187 (2003).
105. Lun K, Brand M. A series of no isthmus (noi) alleles of the zebrafish pax2.1 gene reveals multiple signaling events in development of the midbrain-hindbrain boundary. *Development*, 125(16), 3049-3062 (1998).
106. Pfeffer PL, Gerster T, Lun K, Brand M, Busslinger M. Characterization of three novel members of the zebrafish Pax2/5/8 family: dependency of Pax5 and Pax8 expression on the Pax2.1 (noi) function. *Development*, 125(16), 3063-3074 (1998).
107. Asano M, Gruss P. Pax-5 is expressed at the midbrain-hindbrain boundary during mouse development. *Mech Dev*, 39(1-2), 29-39 (1992).
108. Fjose A, Njolstad PR, Nornes S, Molven A, Krauss S. Structure and early embryonic expression of the zebrafish engrailed-2 gene. *Mech Dev*, 39(1-2), 51-62 (1992).
109. Ingham PW. Segment polarity genes and cell patterning within the Drosophila body segment. *Curr Opin Genet Dev*, 1(2), 261-267 (1991).
110. Schier AF, Neuhauss SC, Harvey M *et al.* Mutations affecting the development of the embryonic zebrafish brain. *Development*, 123, 165-178 (1996).
111. Belting HG, Hauptmann G, Meyer D *et al.* spiel ohne grenzen/pou2 is required during establishment of the zebrafish midbrain-hindbrain boundary organizer. *Development*, 128(21), 4165-4176 (2001).
112. Reim G, Brand M. Spiel-ohne-grenzen/pou2 mediates regional competence to respond to Fgf8 during zebrafish early neural development. *Development*, 129(4), 917-933 (2002).
113. Burgess S, Reim G, Chen W, Hopkins N, Brand M. The zebrafish spiel-ohne-grenzen (spg) gene encodes the POU domain protein Pou2 related to mammalian Oct4 and is essential for formation of the midbrain and hindbrain, and for pre-gastrula morphogenesis. *Development*, 129(4), 905-916 (2002).
114. Tallafuss A, Wilm TP, Crozatier M, Pfeffer P, Wassef M, Bally-Cuif L. The zebrafish buttonhead-like factor Bts1 is an early regulator of pax2.1 expression during mid-hindbrain development. *Development*, 128(20), 4021-4034 (2001).
115. Shamim H, Mahmood R, Logan C, Doherty P, Lumsden A, Mason I. Sequential roles for Fgf4, En1 and Fgf8 in specification and regionalisation of the midbrain. *Development*, 126(5), 945-959 (1999).
116. Tsang M, Friesel R, Kudoh T, Dawid IB. Identification of Sef, a novel modulator of FGF signalling. *Nat Cell Biol*, 4(2), 165-169 (2002).
117. Furthauer M, Lin W, Ang SL, Thisse B, Thisse C. Sef is a feedback-induced antagonist of Ras/MAPK-mediated FGF signalling. *Nat Cell Biol*, 4(2), 170-174 (2002).
118. Niehrs C, Meinhardt H. Modular feedback. *Nature*, 417(6884), 35-36 (2002).
119. Niehrs C, Pollet N. Synexpression groups in eukaryotes. *Nature*, 402(6761), 483-487 (1999).
120. Crossley PH, Martin GR. The mouse Fgf8 gene encodes a family of polypeptides and is expressed in regions that direct outgrowth and patterning in the developing embryo. *Development*, 121(2), 439-451 (1995).
121. Chi CL, Martinez S, Wurst W, Martin GR. The isthmus organizer signal FGF8 is required for cell survival in the prospective midbrain and cerebellum. *Development*, 130(12), 2633-2644 (2003).
122. Liu A, Li JY, Bromleigh C, Lao Z, Niswander LA, Joyner AL. FGF17b and FGF18 have different midbrain regulatory properties from FGF8b or activated FGF receptors. *Development*, 130(25), 6175-6185 (2003).
123. Reifers F, Adams J, Mason IJ, Schulte-Merker S, Brand M. Overlapping and distinct functions provided by fgf17, a new zebrafish member of the Fgf8/17/18 subgroup of Fgfs. *Mech Dev*, 99(1-2), 39-49 (2000).
124. Olsen SK, Li JY, Bromleigh C *et al.* Structural basis by which alternative splicing modulates the organizer activity of FGF8 in the brain. *Genes Dev*, 20(2), 185-198 (2006).

125. Mason I. Initiation to end point: the multiple roles of fibroblast growth factors in neural development. *Nat Rev Neurosci*, 8(8), 583-596 (2007).
126. Maruoka Y, Ohbayashi N, Hoshikawa M, Itoh N, Hogan BL, Furuta Y. Comparison of the expression of three highly related genes, Fgf8, Fgf17 and Fgf18, in the mouse embryo. *Mech Dev*, 74(1-2), 175-177 (1998).
127. Xu J, Liu Z, Ornitz DM. Temporal and spatial gradients of Fgf8 and Fgf17 regulate proliferation and differentiation of midline cerebellar structures. *Development*, 127(9), 1833-1843 (2000).
128. Crossley PH, Martinez S, Martin GR. Midbrain development induced by FGF8 in the chick embryo. *Nature*, 380(6569), 66-68 (1996).
129. Martinez S, Crossley PH, Cobos I, Rubenstein JL, Martin GR. FGF8 induces formation of an ectopic isthmic organizer and isthmicocerebellar development via a repressive effect on Otx2 expression. *Development*, 126(6), 1189-1200 (1999).
130. Irving C, Mason I. Signalling by FGF8 from the isthmus patterns anterior hindbrain and establishes the anterior limit of Hox gene expression. *Development*, 127(1), 177-186 (2000).
131. Lee SM, Danielian PS, Fritsch B, McMahon AP. Evidence that FGF8 signalling from the midbrain-hindbrain junction regulates growth and polarity in the developing midbrain. *Development*, 124(5), 959-969 (1997).
132. Meyers EN, Lewandoski M, Martin GR. An Fgf8 mutant allelic series generated by Cre- and Flp-mediated recombination. *Nat Genet*, 18(2), 136-141 (1998).
133. Sato T, Araki I, Nakamura H. Inductive signal and tissue responsiveness defining the tectum and the cerebellum. *Development*, 128(13), 2461-2469 (2001).
134. Kikuta H, Laplante M, Navratilova P *et al*. Genomic regulatory blocks encompass multiple neighboring genes and maintain conserved synteny in vertebrates. *Genome Res*, 17(5), 545-555 (2007).
135. Jovelin R, He X, Amores A *et al*. Duplication and divergence of fgf8 functions in teleost development and evolution. *J Exp Zool B Mol Dev Evol*, 308(6), 730-743 (2007).
136. Itoh N, Konishi M. The zebrafish fgf family. *Zebrafish*, 4(3), 179-186 (2007).
137. Walshe J, Mason I. Expression of FGFR1, FGFR2 and FGFR3 during early neural development in the chick embryo. *Mech Dev*, 90(1), 103-110 (2000).
138. Scholpp S, Groth C, Lohs C, Lardelli M, Brand M. Zebrafish fgfr1 is a member of the fgf8 synexpression group and is required for fgf8 signalling at the midbrain-hindbrain boundary. *Dev Genes Evol*, 214(6), 285-295 (2004).
139. Blak AA, Naserke T, Weisenhorn DM, Prakash N, Partanen J, Wurst W. Expression of Fgf receptors 1, 2, and 3 in the developing mid- and hindbrain of the mouse. *Dev Dyn*, 233(3), 1023-1030 (2005).
140. Trokovic R, Jukkola T, Saarimaki J *et al*. Fgfr1-dependent boundary cells between developing mid- and hindbrain. *Dev Biol*, 278(2), 428-439 (2005).
141. Saarimaki-Vire J, Peltopuro P, Lahti L *et al*. Fibroblast growth factor receptors cooperate to regulate neural progenitor properties in the developing midbrain and hindbrain. *J Neurosci*, 27(32), 8581-8592 (2007).
142. Blak AA, Naserke T, Saarimaki-Vire J *et al*. Fgfr2 and Fgfr3 are not required for patterning and maintenance of the midbrain and anterior hindbrain. *Dev Biol*, 303(1), 231-243 (2007).
143. Ornitz DM. FGFs, heparan sulfate and FGFRs: complex interactions essential for development. *Bioessays*, 22(2), 108-112 (2000).
144. Lin X, Buff EM, Perrimon N, Michelson AM. Heparan sulfate proteoglycans are essential for FGF receptor signaling during Drosophila embryonic development. *Development*, 126(17), 3715-3723 (1999).
145. Inatani M, Irie F, Plump AS, Tessier-Lavigne M, Yamaguchi Y. Mammalian brain morphogenesis and midline axon guidance require heparan sulfate. *Science*, 302(5647), 1044-1046 (2003).
146. Norton WH, Ledin J, Grandel H, Neumann CJ. HSPG synthesis by zebrafish Ext2 and Extl3 is required for Fgf10 signalling during limb development. *Development*, 132(22), 4963-4973 (2005).
147. Bottcher RT, Niehrs C. Fibroblast growth factor signaling during early vertebrate development. *Endocr Rev*, 26(1), 63-77 (2005).
148. Schenck A, Goto-Silva L, Collinet C *et al*. The Endosomal Protein Appl1 Mediates Akt Substrate Specificity and Cell Survival in Vertebrate Development. *Cell*, 133(3), 486-497 (2008).
149. Munchberg SR, Ober EA, Steinbeisser H. Expression of the Ets transcription factors erm and pea3 in early zebrafish development. *Mech Dev*, 88(2), 233-236 (1999).

150. Raible F, Brand M. Tight transcriptional control of the ETS domain factors Erm and Pea3 by Fgf signaling during early zebrafish development. *Mech Dev*, 107(1-2), 105-117 (2001).
151. Roehl H, Nusslein-Volhard C. Zebrafish pea3 and erm are general targets of FGF8 signaling. *Curr Biol*, 11(7), 503-507 (2001).
152. Hacohen N, Kramer S, Sutherland D, Hiromi Y, Krasnow MA. sprouty encodes a novel antagonist of FGF signaling that patterns apical branching of the Drosophila airways. *Cell*, 92(2), 253-263 (1998).
153. Furthauer M, Reifers F, Brand M, Thisse B, Thisse C. sprouty4 acts in vivo as a feedback-induced antagonist of FGF signaling in zebrafish. *Development*, 128(12), 2175-2186 (2001).
154. Guy GR, Wong ES, Yusoff P *et al.* Sprouty: how does the branch manager work? *J Cell Sci*, 116(Pt 15), 3061-3068 (2003).
155. Minowada G, Jarvis LA, Chi CL *et al.* Vertebrate Sprouty genes are induced by FGF signaling and can cause chondrodysplasia when overexpressed. *Development*, 126(20), 4465-4475 (1999).
156. Hanafusa H, Torii S, Yasunaga T, Nishida E. Sprouty1 and Sprouty2 provide a control mechanism for the Ras/MAPK signalling pathway. *Nat Cell Biol*, 4(11), 850-858 (2002).
157. Sasaki A, Taketomi T, Kato R *et al.* Mammalian Sprouty4 suppresses Ras-independent ERK activation by binding to Raf1. *Nat Cell Biol*, 5(5), 427-432 (2003).
158. Thisse B, Thisse C. Functions and regulations of fibroblast growth factor signaling during embryonic development. *Dev Biol*, 287(2), 390-402 (2005).
159. Kovalenko D, Yang X, Nadeau RJ, Harkins LK, Friesel R. Sef inhibits fibroblast growth factor signaling by inhibiting FGFR1 tyrosine phosphorylation and subsequent ERK activation. *J Biol Chem*, 278(16), 14087-14091 (2003).
160. Tsang M, Maegawa S, Kiang A, Habas R, Weinberg E, Dawid IB. A role for MKP3 in axial patterning of the zebrafish embryo. *Development*, 131(12), 2769-2779 (2004).
161. Hirate Y, Okamoto H. Canopy1, a novel regulator of FGF signaling around the midbrain-hindbrain boundary in zebrafish. *Curr Biol*, 16(4), 421-427 (2006).
162. Erickson T, Scholpp S, Brand M, Moens CB, Waskiewicz AJ. Pbx proteins cooperate with Engrailed to pattern the midbrain-hindbrain and diencephalic-mesencephalic boundaries. *Dev Biol*, 301(2), 504-517 (2007).
163. O'Hara FP, Beck E, Barr LK, Wong LL, Kessler DS, Riddle RD. Zebrafish Lmx1b.1 and Lmx1b.2 are required for maintenance of the isthmus organizer. *Development*, 132(14), 3163-3173 (2005).
164. Langenberg T, Brand M. Lineage restriction maintains a stable organizer cell population at the zebrafish midbrain-hindbrain boundary. *Development*, 132(14), 3209-3216 (2005).
165. McMahon AP, Joyner AL, Bradley A, McMahon JA. The midbrain-hindbrain phenotype of Wnt-1/Wnt-1-mice results from stepwise deletion of engrailed-expressing cells by 9.5 days postcoitum. *Cell*, 69(4), 581-595 (1992).
166. Thomas KR, Musci TS, Neumann PE, Capecchi MR. Swaying is a mutant allele of the proto-oncogene Wnt-1. *Cell*, 67(5), 969-976 (1991).
167. Bally-Cuif L, Cholley B, Wassef M. Involvement of Wnt-1 in the formation of the mes/metencephalic boundary. *Mech Dev*, 53(1), 23-34 (1995).
168. Kimmel CB. Patterning the brain of the zebrafish embryo. *Annu Rev Neurosci*, 16, 707-732 (1993).
169. Hollyday M. Neurogenesis in the vertebrate neural tube. *Int J Dev Neurosci*, 19(2), 161-173 (2001).
170. Geling A, Itoh M, Tallafuss A *et al.* bHLH transcription factor Her5 links patterning to regional inhibition of neurogenesis at the midbrain-hindbrain boundary. *Development*, 130(8), 1591-1604 (2003).
171. Easter SS, Jr., Burrill J, Marcus RC, Ross LS, Taylor JS, Wilson SW. Initial tract formation in the vertebrate brain. *Prog Brain Res*, 102, 79-93 (1994).
172. Grunwald DJ, Kimmel CB, Westerfield M, Walker C, Streisinger G. A neural degeneration mutation that spares primary neurons in the zebrafish. *Dev Biol*, 126(1), 115-128 (1988).
173. Mueller T, Wullmann MF. Expression domains of neuroD (nrd) in the early postembryonic zebrafish brain. *Brain Res Bull*, 57(3-4), 377-379 (2002).
174. Mueller T, Wullmann MF. BrdU-, neuroD (nrd)- and Hu-studies reveal unusual non-ventricular neurogenesis in the postembryonic zebrafish forebrain. *Mech Dev*, 117(1-2), 123-135 (2002).
175. Wullmann MF, Knipp S. Proliferation pattern changes in the zebrafish brain from embryonic through early postembryonic stages. *Anat Embryol (Berl)*, 202(5), 385-400 (2000).

176. Stigloher C, Chapouton P, Adolf B, Bally-Cuif L. Identification of neural progenitor pools by E(Spl) factors in the embryonic and adult brain. *Brain Res Bull*, 75(2-4), 266-273 (2008).
177. Ross LS, Parrett T, Easter SS, Jr. Axonogenesis and morphogenesis in the embryonic zebrafish brain. *J Neurosci*, 12(2), 467-482 (1992).
178. Lecaudey V, Anselme I, Dildrop R, Ruther U, Schneider-Maunoury S. Expression of the zebrafish Iroquois genes during early nervous system formation and patterning. *J Comp Neurol*, 492(3), 289-302 (2005).
179. Gomez-Skarmeta JL, Glavic A, de la Calle-Mustienes E, Modolell J, Mayor R. Xiro, a Xenopus homolog of the Drosophila Iroquois complex genes, controls development at the neural plate. *Embo J*, 17(1), 181-190 (1998).
180. Bellefroid EJ, Kobbe A, Gruss P, Pieler T, Gurdon JB, Papalopulu N. Xiro3 encodes a Xenopus homolog of the Drosophila Iroquois genes and functions in neural specification. *Embo J*, 17(1), 191-203 (1998).
181. Itoh M, Kudoh T, Dedekian M, Kim CH, Chitnis AB. A role for iro1 and iro7 in the establishment of an anteroposterior compartment of the ectoderm adjacent to the midbrain-hindbrain boundary. *Development*, 129(10), 2317-2327 (2002).
182. Fisher A, Caudy M. The function of hairy-related bHLH repressor proteins in cell fate decisions. *Bioessays*, 20(4), 298-306 (1998).
183. Hans S, Scheer N, Riedl I, v Weizsacker E, Blader P, Campos-Ortega JA. her3, a zebrafish member of the hairy-E(spl) family, is repressed by Notch signalling. *Development*, 131(12), 2957-2969 (2004).
184. Geling A, Plessy C, Rastegar S, Strahle U, Bally-Cuif L. Her5 acts as a prepattern factor that blocks neurogenin1 and coe2 expression upstream of Notch to inhibit neurogenesis at the midbrain-hindbrain boundary. *Development*, 131(9), 1993-2006 (2004).
185. Bae YK, Shimizu T, Hibi M. Patterning of proneuronal and inter-proneuronal domains by hairy- and enhancer of split-related genes in zebrafish neuroectoderm. *Development*, 132(6), 1375-1385 (2005).
186. Ninkovic J, Tallafuss A, Leucht C *et al.* Inhibition of neurogenesis at the zebrafish midbrain-hindbrain boundary by the combined and dose-dependent activity of a new hairy/E(spl) gene pair. *Development*, 132(1), 75-88 (2005).
187. Davis RL, Turner DL. Vertebrate hairy and Enhancer of split related proteins: transcriptional repressors regulating cellular differentiation and embryonic patterning. *Oncogene*, 20(58), 8342-8357 (2001).
188. Paroush Z, Finley RL, Jr., Kidd T *et al.* Groucho is required for Drosophila neurogenesis, segmentation, and sex determination and interacts directly with hairy-related bHLH proteins. *Cell*, 79(5), 805-815 (1994).
189. Bray S, Furriols M. Notch pathway: making sense of suppressor of hairless. *Curr Biol*, 11(6), R217-221 (2001).
190. Villares R, Cabrera CV. The achaete-scute gene complex of *D. melanogaster*: conserved domains in a subset of genes required for neurogenesis and their homology to myc. *Cell*, 50(3), 415-424 (1987).
191. Murre C, McCaw PS, Baltimore D. A new DNA binding and dimerization motif in immunoglobulin enhancer binding, daughterless, MyoD, and myc proteins. *Cell*, 56(5), 777-783 (1989).
192. Ferre-D'Amare AR, Prendergast GC, Ziff EB, Burley SK. Recognition by Max of its cognate DNA through a dimeric b/HLH/Z domain. *Nature*, 363(6424), 38-45 (1993).
193. Kele J, Simplicio N, Ferri AL *et al.* Neurogenin 2 is required for the development of ventral midbrain dopaminergic neurons. *Development*, 133(3), 495-505 (2006).
194. Blader P, Fischer N, Gradwohl G, Guillemot F, Strahle U. The activity of neurogenin1 is controlled by local cues in the zebrafish embryo. *Development*, 124(22), 4557-4569 (1997).
195. Kim CH, Bae YK, Yamanaka Y *et al.* Overexpression of neurogenin induces ectopic expression of HuC in zebrafish. *Neurosci Lett*, 239(2-3), 113-116 (1997).
196. Wang X, Chu LT, He J, Emelyanov A, Korzh V, Gong Z. A novel zebrafish bHLH gene, neurogenin3, is expressed in the hypothalamus. *Gene*, 275(1), 47-55 (2001).
197. Allende ML, Weinberg ES. The expression pattern of two zebrafish achaete-scute homolog (ash) genes is altered in the embryonic brain of the cyclops mutant. *Dev Biol*, 166(2), 509-530 (1994).
198. Koster RW, Fraser SE. Direct imaging of in vivo neuronal migration in the developing cerebellum. *Curr Biol*, 11(23), 1858-1863 (2001).
199. Adolf B, Bellipanni G, Huber V, Bally-Cuif L. atoh1.2 and beta3.1 are two new bHLH-encoding genes expressed in selective precursor cells of the zebrafish anterior hindbrain. *Gene Expr Patterns*, 5(1), 35-41 (2004).

200. Wang X, Emelyanov A, Korzh V, Gong Z. Zebrafish atonal homologue *zath3* is expressed during neurogenesis in embryonic development. *Dev Dyn*, 227(4), 587-592 (2003).
201. Bally-Cuif L, Dubois L, Vincent A. Molecular cloning of *Zco2*, the zebrafish homolog of *Xenopus Xco2* and mouse *EBF-2*, and its expression during primary neurogenesis. *Mech Dev*, 77(1), 85-90 (1998).
202. Fischer A, Gessler M. Delta-Notch--and then? Protein interactions and proposed modes of repression by *Hes* and *Hey* bHLH factors. *Nucleic Acids Res*, 35(14), 4583-4596 (2007).
203. Kageyama R, Ohtsuka T, Kobayashi T. Roles of *Hes* genes in neural development. *Development, Growth & Differentiation*, 50(s1), 87-103 (2008).
204. Bray SJ. Notch signalling: a simple pathway becomes complex. *Nat Rev Mol Cell Biol*, 7(9), 678-689 (2006).
205. Romain P, Khechumian K, Seugnet L, Arbogast N, Ackermann C, Heitzler P. Novel Notch alleles reveal a *Deltex*-dependent pathway repressing neural fate. *Curr Biol*, 11(22), 1729-1738 (2001).
206. Okabe M, Imai T, Kurusu M, Hiromi Y, Okano H. Translational repression determines a neuronal potential in *Drosophila* asymmetric cell division. *Nature*, 411(6833), 94-98 (2001).
207. Brennan K, Gardner P. Notching up another pathway. *Bioessays*, 24(5), 405-410 (2002).
208. Lai EC. Notch signaling: control of cell communication and cell fate. *Development*, 131(5), 965-973 (2004).
209. Guo M, Bier E, Jan LY, Jan YN. *tramtrack* acts downstream of *numb* to specify distinct daughter cell fates during asymmetric cell divisions in the *Drosophila* PNS. *Neuron*, 14(5), 913-925 (1995).
210. Appel B, Fritz A, Westerfield M, Grunwald DJ, Eisen JS, Riley BB. Delta-mediated specification of midline cell fates in zebrafish embryos. *Curr Biol*, 9(5), 247-256 (1999).
211. Holley SA, Geisler R, Nusslein-Volhard C. Control of *her1* expression during zebrafish somitogenesis by a delta-dependent oscillator and an independent wave-front activity. *Genes Dev*, 14(13), 1678-1690 (2000).
212. Gray M, Moens CB, Amacher SL, Eisen JS, Beattie CE. Zebrafish *deadly seven* functions in neurogenesis. *Dev Biol*, 237(2), 306-323 (2001).
213. Itoh M, Kim CH, Palardy G *et al.* *Mind bomb* is a ubiquitin ligase that is essential for efficient activation of Notch signaling by *Delta*. *Dev Cell*, 4(1), 67-82 (2003).
214. Golling G, Amsterdam A, Sun Z *et al.* Insertional mutagenesis in zebrafish rapidly identifies genes essential for early vertebrate development. *Nat Genet*, 31(2), 135-140 (2002).
215. Cau E, Wilson SW. *Ash1a* and *Neurogenin1* function downstream of *Floating head* to regulate epiphyseal neurogenesis. *Development*, 130(11), 2455-2466 (2003).
216. Dornseifer P, Takke C, Campos-Ortega JA. Overexpression of a zebrafish homologue of the *Drosophila* neurogenic gene *Delta* perturbs differentiation of primary neurons and somite development. *Mech Dev*, 63(2), 159-171 (1997).
217. Appel B, Eisen JS. Regulation of neuronal specification in the zebrafish spinal cord by *Delta* function. *Development*, 125(3), 371-380 (1998).
218. Haddon C, Smithers L, Schneider-Maunoury S, Coche T, Henrique D, Lewis J. Multiple *delta* genes and lateral inhibition in zebrafish primary neurogenesis. *Development*, 125(3), 359-370 (1998).
219. Appel B, Givan LA, Eisen JS. *Delta*-Notch signaling and lateral inhibition in zebrafish spinal cord development. *BMC Dev Biol*, 1, 13 (2001).
220. Dovey HF, John V, Anderson JP *et al.* Functional gamma-secretase inhibitors reduce beta-amyloid peptide levels in brain. *J Neurochem*, 76(1), 173-181 (2001).
221. Geling A, Steiner H, Willem M, Bally-Cuif L, Haass C. A gamma-secretase inhibitor blocks Notch signaling in vivo and causes a severe neurogenic phenotype in zebrafish. *EMBO Rep*, 3(7), 688-694 (2002).
222. Takke C, Dornseifer P, v Weizsacker E, Campos-Ortega JA. *her4*, a zebrafish homologue of the *Drosophila* neurogenic gene *E(spl)*, is a target of NOTCH signalling. *Development*, 126(9), 1811-1821 (1999).
223. Leve C, Gajewski M, Rohr KB, Tautz D. Homologues of *c-hairy1* (*her9*) and *lunatic fringe* in zebrafish are expressed in the developing central nervous system, but not in the presomitic mesoderm. *Dev Genes Evol*, 211(10), 493-500 (2001).
224. Müller M, von Weizsäcker E, Campos-Ortega JA. Transcription of a zebrafish gene of the hairy-Enhancer of split family delineates the midbrain anlage in the neural plate. *Development Genes and Evolution*, 206(2), 153-160 (1996).

225. Hatakeyama J, Bessho Y, Katoh K *et al.* Hes genes regulate size, shape and histogenesis of the nervous system by control of the timing of neural stem cell differentiation. *Development*, 131(22), 5539-5550 (2004).
226. Akazawa C, Sasai Y, Nakanishi S, Kageyama R. Molecular characterization of a rat negative regulator with a basic helix-loop-helix structure predominantly expressed in the developing nervous system. *J Biol Chem*, 267(30), 21879-21885 (1992).
227. Sasai Y, Kageyama R, Tagawa Y, Shigemoto R, Nakanishi S. Two mammalian helix-loop-helix factors structurally related to *Drosophila* hairy and Enhancer of split. *Genes Dev*, 6(12B), 2620-2634 (1992).
228. Ishibashi M, Ang SL, Shiota K, Nakanishi S, Kageyama R, Guillemot F. Targeted disruption of mammalian hairy and Enhancer of split homolog-1 (HES-1) leads to up-regulation of neural helix-loop-helix factors, premature neurogenesis, and severe neural tube defects. *Genes Dev*, 9(24), 3136-3148 (1995).
229. Ohtsuka T, Ishibashi M, Gradwohl G, Nakanishi S, Guillemot F, Kageyama R. Hes1 and Hes5 as notch effectors in mammalian neuronal differentiation. *Embo J*, 18(8), 2196-2207 (1999).
230. Hirata H, Tomita K, Bessho Y, Kageyama R. Hes1 and Hes3 regulate maintenance of the isthmic organizer and development of the mid/hindbrain. *Embo J*, 20(16), 4454-4466 (2001).
231. Ishibashi M, Moriyoshi K, Sasai Y, Shiota K, Nakanishi S, Kageyama R. Persistent expression of helix-loop-helix factor HES-1 prevents mammalian neural differentiation in the central nervous system. *Embo J*, 13(8), 1799-1805 (1994).
232. Ohtsuka T, Sakamoto M, Guillemot F, Kageyama R. Roles of the basic helix-loop-helix genes Hes1 and Hes5 in expansion of neural stem cells of the developing brain. *J Biol Chem*, 276(32), 30467-30474 (2001).
233. Baek JH, Hatakeyama J, Sakamoto S, Ohtsuka T, Kageyama R. Persistent and high levels of Hes1 expression regulate boundary formation in the developing central nervous system. *Development*, 133(13), 2467-2476 (2006).
234. Takebayashi K, Sasai Y, Sakai Y, Watanabe T, Nakanishi S, Kageyama R. Structure, chromosomal locus, and promoter analysis of the gene encoding the mouse helix-loop-helix factor HES-1. Negative autoregulation through the multiple N box elements. *J Biol Chem*, 269(7), 5150-5156 (1994).
235. Hirata H, Yoshiura S, Ohtsuka T *et al.* Oscillatory expression of the bHLH factor Hes1 regulated by a negative feedback loop. *Science*, 298(5594), 840-843 (2002).
236. Jouve C, Palmeirim I, Henrique D *et al.* Notch signalling is required for cyclic expression of the hairy-like gene HES1 in the presomitic mesoderm. *Development*, 127(7), 1421-1429 (2000).
237. Masamizu Y, Ohtsuka T, Takashima Y *et al.* Real-time imaging of the somite segmentation clock: revelation of unstable oscillators in the individual presomitic mesoderm cells. *Proc Natl Acad Sci U S A*, 103(5), 1313-1318 (2006).
238. Shimojo H, Ohtsuka T, Kageyama R. Oscillations in notch signaling regulate maintenance of neural progenitors. *Neuron*, 58(1), 52-64 (2008).
239. Curry CL, Reed LL, Nickoloff BJ, Miele L, Foreman KE. Notch-independent regulation of Hes-1 expression by c-Jun N-terminal kinase signaling in human endothelial cells. *Lab Invest*, 86(8), 842-852 (2006).
240. Nolo R, Abbott LA, Bellen HJ. Senseless, a Zn finger transcription factor, is necessary and sufficient for sensory organ development in *Drosophila*. *Cell*, 102(3), 349-362 (2000).
241. Dubois L, Bally-Cuif L, Crozatier M, Moreau J, Paquereau L, Vincent A. X_{Coe2}, a transcription factor of the Col/Olf-1/EBF family involved in the specification of primary neurons in *Xenopus*. *Curr Biol*, 8(4), 199-209 (1998).
242. Bae S, Bessho Y, Hojo M, Kageyama R. The bHLH gene Hes6, an inhibitor of Hes1, promotes neuronal differentiation. *Development*, 127(13), 2933-2943 (2000).
243. Lee JE, Hollenberg SM, Snider L, Turner DL, Lipnick N, Weintraub H. Conversion of *Xenopus* ectoderm into neurons by NeuroD, a basic helix-loop-helix protein. *Science*, 268(5212), 836-844 (1995).
244. Perron M, Opdecamp K, Butler K, Harris WA, Bellefroid EJ. X_{ngnr-1} and X_{ath3} promote ectopic expression of sensory neuron markers in the neurula ectoderm and have distinct inducing properties in the retina. *Proc Natl Acad Sci U S A*, 96(26), 14996-15001 (1999).
245. Fode C, Gradwohl G, Morin X *et al.* The bHLH protein NEUROGENIN 2 is a determination factor for epibranchial placode-derived sensory neurons. *Neuron*, 20(3), 483-494 (1998).
246. Cau E, Casarosa S, Guillemot F. Mash1 and Ngn1 control distinct steps of determination and differentiation in the olfactory sensory neuron lineage. *Development*, 129(8), 1871-1880 (2002).

247. Vernon AE, Devine C, Philpott A. The cdk inhibitor p27Xic1 is required for differentiation of primary neurones in *Xenopus*. *Development*, 130(1), 85-92 (2003).
248. Mutoh H, Naya FJ, Tsai MJ, Leiter AB. The basic helix-loop-helix protein BETA2 interacts with p300 to coordinate differentiation of secretin-expressing enteroendocrine cells. *Genes Dev*, 12(6), 820-830 (1998).
249. Park HC, Boyce J, Shin J, Appel B. Oligodendrocyte specification in zebrafish requires notch-regulated cyclin-dependent kinase inhibitor function. *J Neurosci*, 25(29), 6836-6844 (2005).
250. Lee RC, Feinbaum RL, Ambros V. The *C. elegans* heterochronic gene *lin-4* encodes small RNAs with antisense complementarity to *lin-14*. *Cell*, 75(5), 843-854 (1993).
251. Wightman B, Ha I, Ruvkun G. Posttranscriptional regulation of the heterochronic gene *lin-14* by *lin-4* mediates temporal pattern formation in *C. elegans*. *Cell*, 75(5), 855-862 (1993).
252. Stefani G, Slack FJ. Small non-coding RNAs in animal development. *Nat Rev Mol Cell Biol*, 9(3), 219-230 (2008).
253. Bushati N, Cohen SM. microRNA functions. *Annu Rev Cell Dev Biol*, 23, 175-205 (2007).
254. Bartel DP. MicroRNAs: genomics, biogenesis, mechanism, and function. *Cell*, 116(2), 281-297 (2004).
255. Ruvkun G. Molecular biology. Glimpses of a tiny RNA world. *Science*, 294(5543), 797-799 (2001).
256. Miska EA, Alvarez-Saavedra E, Abbott AL *et al*. Most *Caenorhabditis elegans* microRNAs Are Individually Not Essential for Development or Viability. *PLoS Genet*, 3(12), e215 (2007).
257. Borchert GM, Lanier W, Davidson BL. RNA polymerase III transcribes human microRNAs. *Nat Struct Mol Biol*, 13(12), 1097-1101 (2006).
258. Cai X, Hagedorn CH, Cullen BR. Human microRNAs are processed from capped, polyadenylated transcripts that can also function as mRNAs. *Rna*, 10(12), 1957-1966 (2004).
259. Denli AM, Tops BB, Plasterk RH, Ketting RF, Hannon GJ. Processing of primary microRNAs by the Microprocessor complex. *Nature*, 432(7014), 231-235 (2004).
260. Han J, Lee Y, Yeom KH *et al*. Molecular basis for the recognition of primary microRNAs by the Drosha-DGCR8 complex. *Cell*, 125(5), 887-901 (2006).
261. Bohnsack MT, Czaplinski K, Gorlich D. Exportin 5 is a RanGTP-dependent dsRNA-binding protein that mediates nuclear export of pre-miRNAs. *Rna*, 10(2), 185-191 (2004).
262. Hutvagner G, McLachlan J, Pasquinelli AE, Balint E, Tuschl T, Zamore PD. A cellular function for the RNA-interference enzyme Dicer in the maturation of the *let-7* small temporal RNA. *Science*, 293(5531), 834-838 (2001).
263. Schwarz DS, Hutvagner G, Du T, Xu Z, Aronin N, Zamore PD. Asymmetry in the assembly of the RNAi enzyme complex. *Cell*, 115(2), 199-208 (2003).
264. Ruby JG, Jan C, Player C *et al*. Large-scale sequencing reveals 21U-RNAs and additional microRNAs and endogenous siRNAs in *C. elegans*. *Cell*, 127(6), 1193-1207 (2006).
265. Hutvagner G, Zamore PD. A microRNA in a multiple-turnover RNAi enzyme complex. *Science*, 297(5589), 2056-2060 (2002).
266. Lewis BP, Burge CB, Bartel DP. Conserved seed pairing, often flanked by adenosines, indicates that thousands of human genes are microRNA targets. *Cell*, 120(1), 15-20 (2005).
267. Kosik KS, Krichevsky AM. The Elegance of the MicroRNAs: A Neuronal Perspective. *Neuron*, 47(6), 779-782 (2005).
268. Lim LP, Lau NC, Garrett-Engle P *et al*. Microarray analysis shows that some microRNAs downregulate large numbers of target mRNAs. *Nature*, 433(7027), 769-773 (2005).
269. Joglekar MV, Parekh VS, Hardikar AA. New pancreas from old: microregulators of pancreas regeneration. *Trends Endocrinol Metab*, 18(10), 393-400 (2007).
270. Cao X, Yeo G, Muotri AR, Kuwabara T, Gage FH. Noncoding RNAs in the mammalian central nervous system. *Annu Rev Neurosci*, 29, 77-103 (2006).
271. Miska EA, Alvarez-Saavedra E, Townsend M *et al*. Microarray analysis of microRNA expression in the developing mammalian brain. *Genome Biol*, 5(9), R68 (2004).
272. Kapsimali M, Kloosterman WP, de Bruijn E, Rosa F, Plasterk RH, Wilson SW. MicroRNAs show a wide diversity of expression profiles in the developing and mature central nervous system. *Genome Biol*, 8(8), R173 (2007).

273. Makeyev EV, Zhang J, Carrasco MA, Maniatis T. The MicroRNA miR-124 promotes neuronal differentiation by triggering brain-specific alternative pre-mRNA splicing. *Mol Cell*, 27(3), 435-448 (2007).
274. Visvanathan J, Lee S, Lee B, Lee JW, Lee SK. The microRNA miR-124 antagonizes the anti-neural REST/SCP1 pathway during embryonic CNS development. *Genes Dev*, 21(7), 744-749 (2007).
275. Choi PS, Zakhary L, Choi WY *et al.* Members of the miRNA-200 family regulate olfactory neurogenesis. *Neuron*, 57(1), 41-55 (2008).
276. Wienholds E, Kloosterman WP, Miska E *et al.* MicroRNA expression in zebrafish embryonic development. *Science*, 309(5732), 310-311 (2005).
277. Lagos-Quintana M, Rauhut R, Yalcin A, Meyer J, Lendeckel W, Tuschl T. Identification of tissue-specific microRNAs from mouse. *Curr Biol*, 12(9), 735-739 (2002).
278. Sempere LF, Freemantle S, Pitha-Rowe I, Moss E, Dmitrovsky E, Ambros V. Expression profiling of mammalian microRNAs uncovers a subset of brain-expressed microRNAs with possible roles in murine and human neuronal differentiation. *Genome Biol*, 5(3), R13 (2004).
279. Conaco C, Otto S, Han JJ, Mandel G. Reciprocal actions of REST and a microRNA promote neuronal identity. *Proc Natl Acad Sci U S A*, 103(7), 2422-2427 (2006).
280. Wu J, Xie X. Comparative sequence analysis reveals an intricate network among REST, CREB and miRNA in mediating neuronal gene expression. *Genome Biol*, 7(9), R85 (2006).
281. Stark A, Brennecke J, Bushati N, Russell RB, Cohen SM. Animal MicroRNAs confer robustness to gene expression and have a significant impact on 3'UTR evolution. *Cell*, 123(6), 1133-1146 (2005).
282. Li Y, Wang F, Lee JA, Gao FB. MicroRNA-9a ensures the precise specification of sensory organ precursors in *Drosophila*. *Genes Dev*, 20(20), 2793-2805 (2006).
283. Leucht C, Stigloher C, Wizenmann A, Klafke R, Folchert A, Bally-Cuif L. MicroRNA-9 directs late organizer activity of the midbrain-hindbrain boundary. *Nat Neurosci*, advanced online publication (2008).
284. Abrous DN, Koehl M, Le Moal M. Adult neurogenesis: from precursors to network and physiology. *Physiol Rev*, 85(2), 523-569 (2005).
285. Ming GL, Song H. Adult neurogenesis in the mammalian central nervous system. *Annu Rev Neurosci*, 28, 223-250 (2005).
286. Berninger B, Hack MA, Gotz M. Neural stem cells: on where they hide, in which disguise, and how we may lure them out. *Handb Exp Pharmacol*, (174), 319-360 (2006).
287. Jagasia R, Song H, Gage FH, Lie DC. New regulators in adult neurogenesis and their potential role for repair. *Trends Mol Med*, 12(9), 400-405 (2006).
288. Zupanc GK, Hinsch K, Gage FH. Proliferation, migration, neuronal differentiation, and long-term survival of new cells in the adult zebrafish brain. *J Comp Neurol*, 488(3), 290-319 (2005).
289. Grandel H, Kaslin J, Ganz J, Wenzel I, Brand M. Neural stem cells and neurogenesis in the adult zebrafish brain: origin, proliferation dynamics, migration and cell fate. *Dev Biol*, 295(1), 263-277 (2006).
290. Pellegrini E, Mouriec K, Anglade I *et al.* Identification of aromatase-positive radial glial cells as progenitor cells in the ventricular layer of the forebrain in zebrafish. *J Comp Neurol*, 501(1), 150-167 (2007).
291. Stump G, Durrer A, Klein A-L, Lütolf S, Suter U, Taylor V. Notch1 and its ligands Delta-like and Jagged are expressed and active in distinct cell populations in the postnatal mouse brain. *Mechanisms of Development*, 114(1-2), 153-159 (2002).
292. Ohtsuka T, Imayoshi I, Shimojo H, Nishi E, Kageyama R, McConnell SK. Visualization of embryonic neural stem cells using Hes promoters in transgenic mice. *Mol Cell Neurosci*, 31(1), 109-122 (2006).
293. Lindsey BW, Tropepe V. A comparative framework for understanding the biological principles of adult neurogenesis. *Prog Neurobiol*, 80(6), 281-307 (2006).
294. Kessar N, Pringle N, Richardson WD. Ventral neurogenesis and the neuron-glia switch. *Neuron*, 31(5), 677-680 (2001).
295. Pearson BJ, Doe CQ. Specification of temporal identity in the developing nervous system. *Annu Rev Cell Dev Biol*, 20, 619-647 (2004).
296. Wolpert L. One hundred years of positional information. *Trends Genet*, 12(9), 359-364 (1996).
297. Tabata T, Takei Y. Morphogens, their identification and regulation. *Development*, 131(4), 703-712 (2004).
298. Ashe HL, Briscoe J. The interpretation of morphogen gradients. *Development*, 133(3), 385-394 (2006).

299. Price SR, Briscoe J. The generation and diversification of spinal motor neurons: signals and responses. *Mech Dev*, 121(9), 1103-1115 (2004).
300. Roelink H, Augsburger A, Heemskerk J *et al*. Floor plate and motor neuron induction by vhh-1, a vertebrate homolog of hedgehog expressed by the notochord. *Cell*, 76(4), 761-775 (1994).
301. Roelink H, Porter JA, Chiang C *et al*. Floor plate and motor neuron induction by different concentrations of the amino-terminal cleavage product of sonic hedgehog autoproteolysis. *Cell*, 81(3), 445-455 (1995).
302. Marti E, Bumcrot DA, Takada R, McMahon AP. Requirement of 19K form of Sonic hedgehog for induction of distinct ventral cell types in CNS explants. *Nature*, 375(6529), 322-325 (1995).
303. Chiang C, Litingtung Y, Lee E *et al*. Cyclopia and defective axial patterning in mice lacking Sonic hedgehog gene function. *Nature*, 383(6599), 407-413 (1996).
304. Ericson J, Rashbass P, Schedl A *et al*. Pax6 controls progenitor cell identity and neuronal fate in response to graded Shh signaling. *Cell*, 90(1), 169-180 (1997).
305. Briscoe J, Chen Y, Jessell TM, Struhl G. A hedgehog-insensitive form of patched provides evidence for direct long-range morphogen activity of sonic hedgehog in the neural tube. *Mol Cell*, 7(6), 1279-1291 (2001).
306. Bingham S, Nasevicius A, Ekker SC, Chandrasekhar A. Sonic hedgehog and tiggy-winkle hedgehog cooperatively induce zebrafish branchiomotor neurons. *Genesis*, 30(3), 170-174 (2001).
307. Chandrasekhar A, Warren JT, Jr., Takahashi K *et al*. Role of sonic hedgehog in branchiomotor neuron induction in zebrafish. *Mech Dev*, 76(1-2), 101-115 (1998).
308. Chandrasekhar A, Schauerte HE, Haffter P, Kuwada JY. The zebrafish detour gene is essential for cranial but not spinal motor neuron induction. *Development*, 126(12), 2727-2737 (1999).
309. Liem KF, Jr., Tremml G, Roelink H, Jessell TM. Dorsal differentiation of neural plate cells induced by BMP-mediated signals from epidermal ectoderm. *Cell*, 82(6), 969-979 (1995).
310. Stathopoulos A, Levine M. Dorsal gradient networks in the Drosophila embryo. *Dev Biol*, 246(1), 57-67 (2002).
311. Pierani A, Brenner-Morton S, Chiang C, Jessell TM. A sonic hedgehog-independent, retinoid-activated pathway of neurogenesis in the ventral spinal cord. *Cell*, 97(7), 903-915 (1999).
312. Jacob J, Briscoe J. Gli proteins and the control of spinal-cord patterning. *EMBO Rep*, 4(8), 761-765 (2003).
313. Hynes M, Ye W, Wang K *et al*. The seven-transmembrane receptor smoothed cell-autonomously induces multiple ventral cell types. *Nat Neurosci*, 3(1), 41-46 (2000).
314. Wijgerde M, McMahon JA, Rule M, McMahon AP. A direct requirement for Hedgehog signaling for normal specification of all ventral progenitor domains in the presumptive mammalian spinal cord. *Genes Dev*, 16(22), 2849-2864 (2002).
315. Briscoe J, Ericson J. Specification of neuronal fates in the ventral neural tube. *Curr Opin Neurobiol*, 11(1), 43-49 (2001).
316. Giles RH, van Es JH, Clevers H. Caught up in a Wnt storm: Wnt signaling in cancer. *Biochim Biophys Acta*, 1653(1), 1-24 (2003).
317. Raff M. The mystery of intracellular developmental programmes and timers. *Biochem Soc Trans*, 34(Pt 5), 663-670 (2006).
318. Broadus J, Doe CQ. Extrinsic cues, intrinsic cues and microfilaments regulate asymmetric protein localization in Drosophila neuroblasts. *Curr Biol*, 7(11), 827-835 (1997).
319. Isshiki T, Pearson B, Holbrook S, Doe CQ. Drosophila neuroblasts sequentially express transcription factors which specify the temporal identity of their neuronal progeny. *Cell*, 106(4), 511-521 (2001).
320. Berry M, Rogers AW, Eayrs JT. Pattern of Cell Migration During Cortical Histogenesis. *Nature*, 203, 591-593 (1964).
321. McConnell SK. Fates of visual cortical neurons in the ferret after isochronic and heterochronic transplantation. *J Neurosci*, 8(3), 945-974 (1988).
322. Luskin MB, Shatz CJ. Studies of the earliest generated cells of the cat's visual cortex: cogeneration of subplate and marginal zones. *J Neurosci*, 5(4), 1062-1075 (1985).
323. Luskin MB, Shatz CJ. Neurogenesis of the cat's primary visual cortex. *J Comp Neurol*, 242(4), 611-631 (1985).
324. Mizutani K, Gaiano N. Chalk one up for 'nature' during neocortical neurogenesis. *Nat Neurosci*, 9(6), 717-718 (2006).

325. Frantz GD, McConnell SK. Restriction of late cerebral cortical progenitors to an upper-layer fate. *Neuron*, 17(1), 55-61 (1996).
326. Hanashima C, Li SC, Shen L, Lai E, Fishell G. Foxg1 suppresses early cortical cell fate. *Science*, 303(5654), 56-59 (2004).
327. Young RW. Cell differentiation in the retina of the mouse. *Anat Rec*, 212(2), 199-205 (1985).
328. Cepko CL, Austin CP, Yang X, Alexiades M, Ezzeddine D. Cell fate determination in the vertebrate retina. *Proc Natl Acad Sci U S A*, 93(2), 589-595 (1996).
329. Chang WS, Harris WA. Sequential genesis and determination of cone and rod photoreceptors in *Xenopus*. *J Neurobiol*, 35(3), 227-244 (1998).
330. Hu M, Easter SS. Retinal neurogenesis: the formation of the initial central patch of postmitotic cells. *Dev Biol*, 207(2), 309-321 (1999).
331. Turner DL, Cepko CL. A common progenitor for neurons and glia persists in rat retina late in development. *Nature*, 328(6126), 131-136 (1987).
332. Holt CE, Bertsch TW, Ellis HM, Harris WA. Cellular determination in the *Xenopus* retina is independent of lineage and birth date. *Neuron*, 1(1), 15-26 (1988).
333. Turner DL, Snyder EY, Cepko CL. Lineage-independent determination of cell type in the embryonic mouse retina. *Neuron*, 4(6), 833-845 (1990).
334. Fekete DM, Perez-Miguelsanz J, Ryder EF, Cepko CL. Clonal analysis in the chicken retina reveals tangential dispersion of clonally related cells. *Dev Biol*, 166(2), 666-682 (1994).
335. Moody SA, Chow I, Huang S. Intrinsic bias and lineage restriction in the phenotype determination of dopamine and neuropeptide Y amacrine cells. *J Neurosci*, 20(9), 3244-3253 (2000).
336. Belliveau MJ, Cepko CL. Extrinsic and intrinsic factors control the genesis of amacrine and cone cells in the rat retina. *Development*, 126(3), 555-566 (1999).
337. Belliveau MJ, Young TL, Cepko CL. Late retinal progenitor cells show intrinsic limitations in the production of cell types and the kinetics of opsin synthesis. *J Neurosci*, 20(6), 2247-2254 (2000).
338. Neophytou C, Vernallis AB, Smith A, Raff MC. Muller-cell-derived leukaemia inhibitory factor arrests rod photoreceptor differentiation at a postmitotic pre-rod stage of development. *Development*, 124(12), 2345-2354 (1997).
339. Neumann CJ, Nusslein-Volhard C. Patterning of the zebrafish retina by a wave of sonic hedgehog activity. *Science*, 289(5487), 2137-2139 (2000).
340. Shkumatava A, Neumann CJ. Shh directs cell-cycle exit by activating p57Kip2 in the zebrafish retina. *EMBO Rep*, 6(6), 563-569 (2005).
341. Shkumatava A, Fischer S, Muller F, Strahle U, Neumann CJ. Sonic hedgehog, secreted by amacrine cells, acts as a short-range signal to direct differentiation and lamination in the zebrafish retina. *Development*, 131(16), 3849-3858 (2004).
342. Zhang XM, Yang XJ. Regulation of retinal ganglion cell production by Sonic hedgehog. *Development*, 128(6), 943-957 (2001).
343. Levine EM, Roelink H, Turner J, Reh TA. Sonic hedgehog promotes rod photoreceptor differentiation in mammalian retinal cells in vitro. *J Neurosci*, 17(16), 6277-6288 (1997).
344. Decembrini S, Andreazzoli M, Vignali R, Barsacchi G, Cremisi F. Timing the generation of distinct retinal cells by homeobox proteins. *PLoS Biol*, 4(9), e272 (2006).
345. Sanes DH, Reh TA, Harris WA. *Development of the Nervous System* (Academic Press, Burlington, USA, 2006).
346. Puelles E. Genetic control of basal midbrain development. *J Neurosci Res*, 85(16), 3530-3534 (2007).
347. Ye W, Shimamura K, Rubenstein JL, Hynes MA, Rosenthal A. FGF and Shh signals control dopaminergic and serotonergic cell fate in the anterior neural plate. *Cell*, 93(5), 755-766 (1998).
348. Agarwala S, Sanders TA, Ragsdale CW. Sonic hedgehog control of size and shape in midbrain pattern formation. *Science*, 291(5511), 2147-2150 (2001).
349. Prakash N, Brodski C, Naserke T *et al*. A Wnt1-regulated genetic network controls the identity and fate of midbrain-dopaminergic progenitors in vivo. *Development*, 133(1), 89-98 (2006).
350. Pattyn A, Vallstedt A, Dias JM *et al*. Coordinated temporal and spatial control of motor neuron and serotonergic neuron generation from a common pool of CNS progenitors. *Genes Dev*, 17(6), 729-737 (2003).

351. Wilson LJ, Wingate RJ. Temporal identity transition in the avian cerebellar rhombic lip. *Dev Biol*, 297(2), 508-521 (2006).
352. Xuan S, Baptista CA, Balas G, Tao W, Soares VC, Lai E. Winged helix transcription factor BF-1 is essential for the development of the cerebral hemispheres. *Neuron*, 14(6), 1141-1152 (1995).
353. Kita A, Imayoshi I, Hojo M *et al.* Hes1 and Hes5 control the progenitor pool, intermediate lobe specification, and posterior lobe formation in the pituitary development. *Mol Endocrinol*, 21(6), 1458-1466 (2007).
354. Pinto L, Gotz M. Radial glial cell heterogeneity--the source of diverse progeny in the CNS. *Prog Neurobiol*, 83(1), 2-23 (2007).
355. Hatakeyama J, Kageyama R. Notch1 expression is spatiotemporally correlated with neurogenesis and negatively regulated by Notch1-independent Hes genes in the developing nervous system. *Cereb Cortex*, 16 Suppl 1, i132-137 (2006).
356. Lutolf S, Radtke F, Aguet M, Suter U, Taylor V. Notch1 is required for neuronal and glial differentiation in the cerebellum. *Development*, 129(2), 373-385 (2002).
357. Stigloher C, Ninkovic J, Laplante M *et al.* Segregation of telencephalic and eye-field identities inside the zebrafish forebrain territory is controlled by Rx3. *Development*, 133(15), 2925-2935 (2006).
358. Stigloher C. Molecular and phenotypical characterization of new zebrafish mutants affected in embryonic development of the central nervous system. Diplomarbeit. *Fakultät für Biologie*. (Bayrische Julius-Maximilians Universität Würzburg, Würzburg, 2004)
359. Ohsawa R, Kageyama R. Regulation of retinal cell fate specification by multiple transcription factors. *Brain Res*, (2007).
360. Kennedy BN, Stearns GW, Smyth VA *et al.* Zebrafish rx3 and mab21l2 are required during eye morphogenesis. *Dev Biol*, 270(2), 336-349 (2004).
361. Rojas-Munoz A, Dahm R, Nusslein-Volhard C. chokh/rx3 specifies the retinal pigment epithelium fate independently of eye morphogenesis. *Dev Biol*, 288(2), 348-362 (2005).
362. Ellingsen S, Laplante MA, König M *et al.* Large-scale enhancer detection in the zebrafish genome. *Development*, 132(17), 3799-3811 (2005).
363. Hedgepeth CM, Conrad LJ, Zhang J, Huang HC, Lee VM, Klein PS. Activation of the Wnt signaling pathway: a molecular mechanism for lithium action. *Dev Biol*, 185(1), 82-91 (1997).
364. Klein PS, Melton DA. A molecular mechanism for the effect of lithium on development. *Proc Natl Acad Sci U S A*, 93(16), 8455-8459 (1996).
365. Lewis JL, Bonner J, Modrell M *et al.* Reiterated Wnt signaling during zebrafish neural crest development. *Development*, 131(6), 1299-1308 (2004).
366. Jia J, Amanai K, Wang G, Tang J, Wang B, Jiang J. Shaggy/GSK3 antagonizes Hedgehog signalling by regulating Cubitus interruptus. *Nature*, 416(6880), 548-552 (2002).
367. Price MA, Kalderon D. Proteolysis of the Hedgehog signaling effector Cubitus interruptus requires phosphorylation by Glycogen Synthase Kinase 3 and Casein Kinase 1. *Cell*, 108(6), 823-835 (2002).
368. Zhang W, Zhao Y, Tong C *et al.* Hedgehog-regulated Costal2-kinase complexes control phosphorylation and proteolytic processing of Cubitus interruptus. *Dev Cell*, 8(2), 267-278 (2005).
369. Hammerschmidt M, Bitgood MJ, McMahon AP. Protein kinase A is a common negative regulator of Hedgehog signaling in the vertebrate embryo. *Genes Dev*, 10(6), 647-658 (1996).
370. Strahle U, Fischer N, Blader P. Expression and regulation of a netrin homologue in the zebrafish embryo. *Mech Dev*, 62(2), 147-160 (1997).
371. Calegari F, Huttner WB. An inhibition of cyclin-dependent kinases that lengthens, but does not arrest, neuroepithelial cell cycle induces premature neurogenesis. *J Cell Sci*, 116(Pt 24), 4947-4955 (2003).
372. Karlstrom RO, Tyurina OV, Kawakami A *et al.* Genetic analysis of zebrafish gli1 and gli2 reveals divergent requirements for gli genes in vertebrate development. *Development*, 130(8), 1549-1564 (2003).
373. Huangfu D, Anderson KV. Signaling from Smo to Ci/Gli: conservation and divergence of Hedgehog pathways from Drosophila to vertebrates. *Development*, 133(1), 3-14 (2006).
374. Sheng T, Chi S, Zhang X, Xie J. Regulation of Gli1 localization by the cAMP/protein kinase A signaling axis through a site near the nuclear localization signal. *J Biol Chem*, 281(1), 9-12 (2006).
375. Riobo NA, Manning DR. Pathways of signal transduction employed by vertebrate Hedgehogs. *Biochem J*, 403(3), 369-379 (2007).

376. Blader P, Plessy C, Strahle U. Multiple regulatory elements with spatially and temporally distinct activities control neurogenin1 expression in primary neurons of the zebrafish embryo. *Mech Dev*, 120(2), 211-218 (2003).
377. Marcus RC, Easter SS, Jr. Expression of glial fibrillary acidic protein and its relation to tract formation in embryonic zebrafish (*Danio rerio*). *J Comp Neurol*, 359(3), 365-381 (1995).
378. Tomizawa K, Inoue Y, Nakayasu H. A monoclonal antibody stains radial glia in the adult zebrafish (*Danio rerio*) CNS. *J Neurocytol*, 29(2), 119-128 (2000).
379. Nielsen AL, Jorgensen AL. Structural and functional characterization of the zebrafish gene for glial fibrillary acidic protein, GFAP. *Gene*, 310, 123-132 (2003).
380. Bernardos RL, Raymond PA. GFAP transgenic zebrafish. *Gene Expr Patterns*, 6(8), 1007-1013 (2006).
381. Raymond PA, Barthel LK, Bernardos RL, Perkowski JJ. Molecular characterization of retinal stem cells and their niches in adult zebrafish. *BMC Dev Biol*, 6, 36 (2006).
382. Gotz M, Huttner WB. The cell biology of neurogenesis. *Nat Rev Mol Cell Biol*, 6(10), 777-788 (2005).
383. Castella P, Sawai S, Nakao K, Wagner JA, Caudy M. HES-1 repression of differentiation and proliferation in PC12 cells: role for the helix 3-helix 4 domain in transcription repression. *Mol Cell Biol*, 20(16), 6170-6183 (2000).
384. Takahashi T, Nowakowski RS, Caviness VS, Jr. The cell cycle of the pseudostratified ventricular epithelium of the embryonic murine cerebral wall. *J Neurosci*, 15(9), 6046-6057 (1995).
385. Hendzel MJ, Wei Y, Mancini MA *et al*. Mitosis-specific phosphorylation of histone H3 initiates primarily within pericentromeric heterochromatin during G2 and spreads in an ordered fashion coincident with mitotic chromosome condensation. *Chromosoma*, 106(6), 348-360 (1997).
386. Ryu S, Holzschuh J, Erhardt S, Ettl AK, Driever W. Depletion of minichromosome maintenance protein 5 in the zebrafish retina causes cell-cycle defect and apoptosis. *Proc Natl Acad Sci U S A*, 102(51), 18467-18472 (2005).
387. Megason SG, Fraser SE. Digitizing life at the level of the cell: high-performance laser-scanning microscopy and image analysis for in toto imaging of development. *Mech Dev*, 120(11), 1407-1420 (2003).
388. Koster RW, Fraser SE. Time-lapse microscopy of brain development. *Methods Cell Biol*, 76, 207-235 (2004).
389. Lille Saar C, Tannhauser B, Stigloher C, Kremmer E, Bally-Cuif L. The serotonergic phenotype is acquired by converging genetic mechanisms within the zebrafish central nervous system. *Dev Dyn*, 236(4), 1072-1084 (2007).
390. Bellipanni G, Rink E, Bally-Cuif L. Cloning of two tryptophan hydroxylase genes expressed in the diencephalon of the developing zebrafish brain. *Mech Dev*, 119 Suppl 1, S215-220 (2002).
391. Teraoka H, Russell C, Regan J *et al*. Hedgehog and Fgf signaling pathways regulate the development of tphR-expressing serotonergic raphe neurons in zebrafish embryos. *J Neurobiol*, 60(3), 275-288 (2004).
392. Hendricks T, Francis N, Fyodorov D, Deneris ES. The ETS domain factor Pet-1 is an early and precise marker of central serotonin neurons and interacts with a conserved element in serotonergic genes. *J Neurosci*, 19(23), 10348-10356 (1999).
393. Pfaar H, von Holst A, Vogt Weisenhorn DM, Brodski C, Guimera J, Wurst W. mPet-1, a mouse ETS-domain transcription factor, is expressed in central serotonergic neurons. *Dev Genes Evol*, 212(1), 43-46 (2002).
394. Iyo AH, Porter B, Deneris ES, Austin MC. Regional distribution and cellular localization of the ETS-domain transcription factor, FEV, mRNA in the human postmortem brain. *Synapse*, 57(4), 223-228 (2005).
395. Tallafuss A, Adolf B, Bally-Cuif L. Selective control of neuronal cluster size at the forebrain/midbrain boundary by signaling from the prechordal plate. *Dev Dyn*, 227(4), 524-535 (2003).
396. Schubert FR, Lumsden A. Transcriptional control of early tract formation in the embryonic chick midbrain. *Development*, 132(8), 1785-1793 (2005).
397. Bae YK, Shimizu T, Muraoka O *et al*. Expression of sax1/nkx1.2 and sax2/nkx1.1 in zebrafish. *Gene Expr Patterns*, 4(4), 481-486 (2004).
398. McClintock JM, Carlson R, Mann DM, Prince VE. Consequences of Hox gene duplication in the vertebrates: an investigation of the zebrafish Hox paralogue group 1 genes. *Development*, 128(13), 2471-2484 (2001).

399. McClintock JM, Jozefowicz C, Assimacopoulos S, Grove EA, Louvi A, Prince VE. Conserved expression of Hoxa1 in neurons at the ventral forebrain/midbrain boundary of vertebrates. *Dev Genes Evol*, 213(8), 399-406 (2003).
400. Agarwala S, Ragsdale CW. A role for midbrain arcs in nucleogenesis. *Development*, 129(24), 5779-5788 (2002).
401. Becker T, Lieberoth BC, Becker CG, Schachner M. Differences in the regenerative response of neuronal cell populations and indications for plasticity in intraspinal neurons after spinal cord transection in adult zebrafish. *Mol Cell Neurosci*, 30(2), 265-278 (2005).
402. Guo S, Brush J, Teraoka H *et al*. Development of noradrenergic neurons in the zebrafish hindbrain requires BMP, FGF8, and the homeodomain protein soulless/Phox2a. *Neuron*, 24(3), 555-566 (1999).
403. Pattyn A, Morin X, Cremer H, Goridis C, Brunet JF. Expression and interactions of the two closely related homeobox genes Phox2a and Phox2b during neurogenesis. *Development*, 124(20), 4065-4075 (1997).
404. McGaughey DM, Vinton RM, Huynh J, Al-Saif A, Beer MA, McCallion AS. Metrics of sequence constraint overlook regulatory sequences in an exhaustive analysis at phox2b. *Genome Res*, 18(2), 252-260 (2008).
405. Cheng CW, Yan CH, Choy SW, Hui MN, Hui CC, Cheng SH. Zebrafish homologue irx1a is required for the differentiation of serotonergic neurons. *Dev Dyn*, 236(9), 2661-2667 (2007).
406. Sleptsova-Friedrich I, Li Y, Emelyanov A, Ekker M, Korzh V, Ge R. fgfr3 and regionalization of anterior neural tube in zebrafish. *Mech Dev*, 102(1-2), 213-217 (2001).
407. Williams JA, Holder N. Cell turnover in neuromasts of zebrafish larvae. *Hear Res*, 143(1-2), 171-181 (2000).
408. Ma Q, Kintner C, Anderson DJ. Identification of neurogenin, a vertebrate neuronal determination gene. *Cell*, 87(1), 43-52 (1996).
409. Vernon AE, Movassagh M, Horan I, Wise H, Ohnuma S, Philpott A. Notch targets the Cdk inhibitor Xic1 to regulate differentiation but not the cell cycle in neurons. *EMBO Rep*, 7(6), 643-648 (2006).
410. Bally-Cuif L, Goutel C, Wassef M, Wurst W, Rosa F. Coregulation of anterior and posterior mesendodermal development by a hairy-related transcriptional repressor. *Genes Dev*, 14(13), 1664-1677 (2000).
411. Park HC, Hong SK, Kim HS *et al*. Structural comparison of zebrafish Elav/Hu and their differential expressions during neurogenesis. *Neurosci Lett*, 279(2), 81-84 (2000).
412. Murphey RD, Stern HM, Straub CT, Zon LI. A chemical genetic screen for cell cycle inhibitors in zebrafish embryos. *Chem Biol Drug Des*, 68(4), 213-219 (2006).
413. Shin J, Poling J, Park HC, Appel B. Notch signaling regulates neural precursor allocation and binary neuronal fate decisions in zebrafish. *Development*, 134(10), 1911-1920 (2007).
414. Lewis EB. A gene complex controlling segmentation in Drosophila. *Nature*, 276(5688), 565-570 (1978).
415. Gehring WJ, Affolter M, Burglin T. Homeodomain proteins. *Annu Rev Biochem*, 63, 487-526 (1994).
416. Amores A, Force A, Yan YL *et al*. Zebrafish hox clusters and vertebrate genome evolution. *Science*, 282(5394), 1711-1714 (1998).
417. Gavalas A, Ruhrberg C, Livet J, Henderson CE, Krumlauf R. Neuronal defects in the hindbrain of Hoxa1, Hoxb1 and Hoxb2 mutants reflect regulatory interactions among these Hox genes. *Development*, 130(23), 5663-5679 (2003).
418. McGinnis W, Krumlauf R. Homeobox genes and axial patterning. *Cell*, 68(2), 283-302 (1992).
419. Shimizu T, Bae YK, Hibi M. Cdx-Hox code controls competence for responding to Fgfs and retinoic acid in zebrafish neural tissue. *Development*, 133(23), 4709-4719 (2006).
420. Puelles L, Rubenstein JL. Expression patterns of homeobox and other putative regulatory genes in the embryonic mouse forebrain suggest a neuromeric organization. *Trends Neurosci*, 16(11), 472-479 (1993).
421. Puelles L, Rubenstein JL. Forebrain gene expression domains and the evolving prosomeric model. *Trends Neurosci*, 26(9), 469-476 (2003).
422. Hauptmann G, Soll I, Gerster T. The early embryonic zebrafish forebrain is subdivided into molecularly distinct transverse and longitudinal domains. *Brain Res Bull*, 57(3-4), 371-375 (2002).
423. Hauptmann G, Gerster T. Regulatory gene expression patterns reveal transverse and longitudinal subdivisions of the embryonic zebrafish forebrain. *Mech Dev*, 91(1-2), 105-118 (2000).

424. Brown S. Top billing for platypus at end of evolution tree. *Nature*, 453(7192), 138-139 (2008).
425. Chuang JC, Raymond PA. Zebrafish genes rx1 and rx2 help define the region of forebrain that gives rise to retina. *Dev Biol*, 231(1), 13-30 (2001).
426. Onorati M, Cremisi F, Liu Y, He RQ, Barsacchi G, Vignali R. A specific box switches the cell fate determining activity of XOTX2 and XOTX5b in the *Xenopus* retina. *Neural Develop*, 2, 12 (2007).
427. Andreazzoli M, Gestri G, Angeloni D, Menna E, Barsacchi G. Role of Xrx1 in *Xenopus* eye and anterior brain development. *Development*, 126(11), 2451-2460 (1999).
428. Dickmeis T, Lahiri K, Nica G *et al.* Glucocorticoids play a key role in circadian cell cycle rhythms. *PLoS Biol*, 5(4), e78 (2007).
429. Tessmar-Raible K, Raible F, Christodoulou F *et al.* Conserved sensory-neurosecretory cell types in annelid and fish forebrain: insights into hypothalamus evolution. *Cell*, 129(7), 1389-1400 (2007).
430. Bovolenta P, Esteve P, Ruiz JM, Cisneros E, Lopez-Rios J. Beyond Wnt inhibition: new functions of secreted Frizzled-related proteins in development and disease. *J Cell Sci*, 121(Pt 6), 737-746 (2008).
431. Esteve P, Lopez-Rios J, Bovolenta P. SFRP1 is required for the proper establishment of the eye field in the medaka fish. *Mech Dev*, 121(7-8), 687-701 (2004).
432. Esteve P, Bovolenta P. Secreted inducers in vertebrate eye development: more functions for old morphogens. *Curr Opin Neurobiol*, 16(1), 13-19 (2006).
433. Masai I, Yamaguchi M, Tonou-Fujimori N, Komori A, Okamoto H. The hedgehog-PKA pathway regulates two distinct steps of the differentiation of retinal ganglion cells: the cell-cycle exit of retinoblasts and their neuronal maturation. *Development*, 132(7), 1539-1553 (2005).
434. Locker M, Agathocleous M, Amato MA, Parain K, Harris WA, Perron M. Hedgehog signaling and the retina: insights into the mechanisms controlling the proliferative properties of neural precursors. *Genes Dev*, 20(21), 3036-3048 (2006).
435. Darnell DK, Kaur S, Stanislaw S, Konieczka JH, Yatskievych TA, Antin PB. MicroRNA expression during chick embryo development. *Dev Dyn*, 235(11), 3156-3165 (2006).
436. Walker JC, Harland RM. Expression of microRNAs during embryonic development of *Xenopus tropicalis*. *Gene Expression Patterns*, In Press, Corrected Proof).
437. Kloosterman WP, Wienholds E, de Bruijn E, Kauppinen S, Plasterk RH. In situ detection of miRNAs in animal embryos using LNA-modified oligonucleotide probes. *Nat Methods*, 3(1), 27-29 (2006).
438. Schachner M, Kim SK, Zehle R. Developmental expression in central and peripheral nervous system of oligodendrocyte cell surface antigens (O antigens) recognized by monoclonal antibodies. *Dev Biol*, 83(2), 328-338 (1981).
439. Watanabe T, Raff MC. Rod photoreceptor development in vitro: intrinsic properties of proliferating neuroepithelial cells change as development proceeds in the rat retina. *Neuron*, 4(3), 461-467 (1990).
440. Xing JG, Lee LE, Fan L, Collodi P, Holt SE, Bols NC. Initiation of a zebrafish blastula cell line on rainbow trout stromal cells and subsequent development under feeder-free conditions into a cell line, ZEB2J. *Zebrafish*, 5(1), 49-63 (2008).
441. Volkmann K, Rieger S, Babaryka A, Koster RW. The zebrafish cerebellar rhombic lip is spatially patterned in producing granule cell populations of different functional compartments. *Dev Biol*, 313(1), 167-180 (2008).

6. Abbreviations

A	Adenine
AC	Anterior Commissure
ace	acerebellar [mutant; locus: fgf8a]
ADAM	A Disintegrin And Metalloproteinase
aei	after eight [mutant; locus: dld]
Alu	Arthrobacter luteus restriction endonuclease
ANB	Anterior Neural Border / Anterior Border of the Neural plate
ANR	Anterior Neural Ridge
A/P	anterior/posterior
arx	aristaless related homeobox
AS-C	achaete-scute complex [Drosophila]
ascl	achaete-scute complex-like
ash	achaete-scute homolog
ath	atonal homolog
ato	atonal [Drosophila]
atoh	atonal homolog
BAC	Bacterial Artificial Chromosome
bHLH	basic Helix-loop-Helix
bHLH-O	basic Helix-loop-Helix-Orange
bhlhb	basic helix-loop-helix domain containing, class b
BLBP	Brain Lipid Binding Protein
BMP	Bone Morphogenetic Protein
bts	buttonhead [Drosophila] Sp-related
btd	buttonhead [Drosophila]
BrdU	5-Bromo-2'-deoxyuridine
C	Cytosine
C	Chicken [used in front of some gene/protein names of Gallus gallus]
cAMP	cyclic Adenosine Mono-Phosphate
Cas	Castor [Drosophila]
Cdk	Cyclin-dependent kinase
cdkn	cyclin-dependent kinase inhibitor
chk	chokh [mutant; locus: rx3]
CLGY	pCL [vector from Murine Leukemia Virus] GATA2 YFP
Cnpy	Canopy
CNS	Central Nervous System
CNTF	Ciliary Neurotrophic Factor
Coe	[derived from:] Collier/Olf-1/EBF
Cy	Cyanine
Da	Daughterless [Drosophila]
DAPT	N-[N-(3,5-difluorophenacetyl)-l-alanyl]-S-phenylglycine t-butyl ester
des	deadly seven [mutant; locus: notch1a]
det	detour [mutant; locus: gli1]
dla	deltaA
dlb	deltaB
Dll1	Delta-like 1
dlx	distal-less homeobox
DMSO	Dimethyl sulfoxide
DNA	Deoxyribonucleic acid

dnReg dominant negative form of the Regulatory subunit of PKA
 drc dorso-rostral cluster
 DSRed Discosoma species Red
 Dusp6 Dual specificity phosphatase 6
 D/V dorso/ventral
 DVDT Dorso-Ventral Diencephalic Tract
 E Embryonic day [Mus musculus and Gallus gallus; staging]
 E E-proteins
 ec epiphyseal cluster
 EGFP Enhanced Green Fluorescent Protein
 elav embryonic lethal, abnormal vision
 emx empy spiracles homeobox
 En Engrailed [Mus musculus; name origin: Drosophila]
 eng engrailed
 ENU N-ethyl-N-nitrosourea
 ep epiboly [staging]
 ER Endoplasmic reticulum
 ERK Extracellular-signal Regulated Kinase
 Erm ETS related molecule
 E(Spl) Enhancer of Split
 esr Enhancer of Split related
 ETS Erythroblast Transformation Specific
 Exd Extradenticle [Drosophila]
 Fev Fifth ewing sarcoma variant
 Fgf Fibroblast growth factor
 Fgfr Fgf receptor
 Fox Forkhead box
 G Guanine
 G1 Gap 1 [phase in cell cycle]
 G2 Gap 2 [phase in cell cycle]
 gadd growth arrest and DN-A-damage-inducible
 GATA GATA [nucleotide sequence] binding protein
 GCL Ganglion Cell Layer
 gbx gastrulation brain homeobox
 GFAP Glial Fibrillary Acidic Protein
 GFP Green Fluorescent Protein
 Gli Glioma associated oncogene homolog
 GMC Ganglion Mother Cell
 Grg Groucho related gene [Mus musculus]
 gripNA grip Nucleid Acids [antisense oligonucleotide with modified backbone]
 GSK3 β Glycogen Synthase Kinase 3 beta
 Hb Hunchback [Drosophila]
 her hairy (and E(Spl)-related
 Hes Hairy and E(Spl)
 hesx homeo box expressed in ES cells
 HH Hamburger-Hamilton stage [Gallus gallus; staging]
 him her5 image
 HLH Helix-loop-Helix
 hox homeo box
 hpf hours post fertilization
 hsp heat shock promoter/protein

HSPG	Heparan Sulphate Proteoglycans
HuC	Hu-syndrome [antigen]
IGF	Insulin-like Growth Factors
INC	Interstitial Nucleus of Cajal
INL	Inner Nuclear Layer
IPZ	Isthmic Proliferation Zone
iro	iroquois [Drosophila]
irx	iroquois homeobox
isl-1	islet-1
IsO	Isthmic Organizer
kb	kilo base
kDA	kilo Dalton
Kr	Krüppel [Drosophila]
IZ	Intervening Zone
JAK	Janus Kinase
l	like [used with gene abbreviations]
Lck	Lymphocyte-specific protein tyrosine kinase
lhx	LIM homeobox
LIF	Leukemia Inhibitory Factor
LIM... [domain name derived from:]	LIN-11 [C. elegans], Isl-1, MEC-3 [C. elegans]
lin	abnormal cell lineage [C. elegans]
LIZ	Lateral Intervening Zone
Imx	LIM homeobox transcription factor
LRL	Lower Rhombic Lip
M	Mouse [used in front of some gene/protein names of Mus musculus]
M	Mitosis [phase in cell cycle]
MAML	Mastermind-like
MAPK	Mitogen-Activated Protein Kinase
MB	Midbrain
mab	male abnormal [C. elegans]
mab2112	mab 21 like 2
mb1	masterblind [mutant; locus: axin1]
mcm	minichromosome maintenance deficient
mec	mechanosensory abnormality [C. elegans]
MFB	Midbrain-Forebrain Border
MHB	Midbrain-Hindbrain Boundary
MH	Midbrain-Hindbrain
mib	mind bomb [mutant; locus: mib]
miR	microRNA
miRNA	microRNA
MIZ	Medial Intervening Zone
MKP	MAPK Phosphatase
mRNA	messenger RNA
Myc	Myelocytomatosis viral oncogene homolog
N	Nucleotide
ne	Neuherberg [mutant identification code with origin of line]
neurod	neurogenic differentiation
neurog	neurogenin
NICD	Notch Intracellular Domain
nkx	NK1 transcription factor (homeobox)
MLF	Medial Longitudinal Fascicle

nMLF	nucleus of the <u>M</u> edial <u>L</u> ongitudinal <u>F</u> ascicle
noi	<u>n</u> o <u>i</u> sthmus [mutant; locus: pax2a]
otx	orthodenticle homolog (homeobox)
O	<u>O</u> ligodendrocyte antigen [numbered 1 to 4]
Oct	<u>O</u> ctamer-binding factor
ol	<u>O</u> ryzia [latipes [used in front of gene/protein names]
ONL	<u>O</u> uter <u>N</u> uclear <u>L</u> ayer
OTDZT	2,4-Dibenzyl-5-oxo <thiadia< th="">zolidine-3-thione</thiadia<>
PAC	<u>P</u> 1 [phage derived] <u>A</u> rtificial <u>C</u> hromosome
Pasha	<u>P</u> artner of <u>D</u> rosha
pax	<u>p</u> aired box
pbx	<u>p</u> re- <u>B</u> -cell leukemia homeobox transcription factor
PC	<u>P</u> osterior <u>C</u> ommissure
PCNA	<u>P</u> roliferating <u>C</u> ell <u>N</u> uclear <u>A</u> ntigen
Pdm	<u>P</u> OU <u>d</u> omain protein [Drosophila]
Pea	<u>P</u> olyomavirus <u>e</u> nhancer <u>a</u> ctivator
Pet	<u>P</u> heochromocytoma 12 <u>E</u> TS (E26 transformation-specific)
pH3	phosphorylated histone <u>H</u> 3
phox	<u>p</u> aired-like <u>h</u> omeobox
PI-3-K	<u>P</u> hosphatidyl- <u>I</u> nositol-3- <u>K</u> inase
Pit-1	<u>P</u> ituitary-1 [Mus musculus]
PKA	<u>P</u> rotein <u>K</u> inase <u>A</u>
PKA*	constitutively active form of PKA
PLC γ	phospholipase C-gamma
PNS	<u>P</u> eripheral <u>N</u> ervous <u>S</u> ystem
POC	<u>P</u> ost- <u>O</u> ptic <u>C</u> ommissure
polB	DNA <u>p</u> olymerase <u>b</u> eta
POU	[protein domain name derived from:] <u>P</u> it-1, <u>O</u> ct-1 and <u>u</u> nc-85
Pol II	RNA <u>P</u> olymerase <u>I</u> l
pomc	<u>p</u> roopiomelanocortin
pre-miRNA	<u>p</u> recursor <u>m</u> icro <u>R</u> NA
pri-miRNA	<u>p</u> rimary <u>m</u> icro <u>R</u> NA
PSM	<u>P</u> re- <u>S</u> omitic <u>M</u> esoderm
Ptc	<u>P</u> atched
Qki	<u>Q</u> uaking
RA	<u>R</u> etinoic <u>A</u> cid
Raf	<u>R</u> apidly growing fibrosarcoma
Ras	<u>R</u> at <u>s</u> arcoma
RBPJ κ	<u>R</u> ecombination signal <u>B</u> inding <u>P</u> rotein for immunoglobulin kappa <u>J</u> region
RE	<u>R</u> epressor <u>E</u> lement
REST	<u>R</u> epressor <u>E</u> lement 1 <u>S</u> ilencing <u>T</u> ranscription Factor
RFP	<u>R</u> ed <u>F</u> luorescent <u>P</u> rotein
RISC	<u>R</u> NA- <u>I</u> nduced <u>S</u> ilencing <u>C</u> omplex
RMS	<u>R</u> ostral <u>M</u> igratory <u>S</u> ream
RNA	<u>R</u> ibonucleic acid
RNase	<u>R</u> ibonuclease
r	rhombomere
robo	<u>r</u> oundabout [Drosophila]
rx	<u>r</u> etinal homeobox
S	DNA- <u>S</u> ynthesis [phase in cell cycle]
sFRP	<u>s</u> ecreted <u>F</u> rizzled <u>R</u> elated <u>P</u> roteins

SGZ	Subgranular Zone
shh	sonic hedgehog
Sef	Similar expression to Egf genes
SEZ	Subependymal Zone
six	sine oculis homeobox homolog
SMAD	Small Mothers Against Decapentaplegic
som	somites [number of somites is used for staging]
SOT	Supraoptic Tract
sox	SRY-box containing gene
spg	spiel ohne grenzen [mutant; locus: pou5f1]
spry	sprouty
SRY	Sex determining Region of the Y gene
STAT	Signal Transducer and Activators of Transcription
Su(H)	Suppressor of Hairless [Drosophila]
sw	swaying [Mus musculus mutant; locus: Wnt1]
syu	sonic you [mutant; locus: shha]
tcf	transcription factor
T	Thymine
TACE	Tumor necrosis factor-Alpha-Converting Enzyme
TGF- β	Transforming Growth Factor beta
THC	Tract of the Habenular Commissure
TK	Tyrosine Kinase
TLE	Transducin-like Enhancer of Split homolog
TPC	Tract of the Posterior Commissure
TPOC	Tract of the Postoptic Commissure
tb	tailbud [stage]
tbr	T-box, brain
Tg	Transgene
tph2	tryptophan hydroxylase 2 [= tphR]
twhh	tiggy-winkle hedgehog
UAS	Upstream Activating Sequence
unc	uncoordinated [C. elegans]
URL	Upper Rhombic Lip
UTR	Untranslated Region
vcc	ventro-caudal cluster
vrc	ventro-rostral cluster
vsnp	vasotocin neurophysin
vsx	visual system homeobox homolog
VTA	Ventral Tegmental Area
Wnt	Wingless int-1
WRPW	Tryptophan Arginine Proline Tryptophan [4 amino acid motif]
X	Xenopus [used in front of gene/protein names]
YFP	Yellow Fluorescent Protein
4xGRIP	gripNA combination [targeting her3, her5, her9 and her11]
ngnr	neurogenin related
Zic	Zinc family protein of the cerebellum
ZFIN	Zebrafish Information Network [www.zfin.org]
ZLI	Zona Limitans Intrathalamica

Remark on nomenclature usage in the text: In general, the nomenclature is used according to the Zebrafish Information Network (ZFIN; www.zfin.org). Only when referring to other organism the corresponding nomenclature is used.

7. Index of definitions

Term	Chapter
Basic helix-loop-helix transcription factors	1.3.2
Boundary (mouse neural development)	1.3.5.2
Compartment (mouse neural development)	1.3.5.2
Differentiation timer	1.4.2
Enhancer of Split factors	1.3.1
Eye field progenitor pool	1.1
Hairy and Enhancer of Split factors	1.3.3
Intervening Zone	3.1.3
Istmic Organizer	1.2.2
Isthmic Proliferation Zone	1.3.8
Lateral inhibition	1.3.4
Lateral Intervening Zone	3.1.3
Medial Intervening Zone	3.1.3
MicroRNA	1.3.7
Midbrain-Hindbrain Boundary	1.2.2.2
Morphogen gradient	1.4.1
Neural induction	1.2.1
Neurogenesis	1.2
Neuronal identity	1.4
Non-canonical <i>her</i> genes	1.3.5.1
Prepatterning	1.3
Progenitor pool	1.3
Proliferating neural precursors	3.1.1
Proneural cluster	1.3
Proneural gene	1.3.2
Synexpression group	1.2.2.2

8. Appendices

Appendix 1

Review in ***Brain Research Bulletin***

Identification of neural progenitor pools by E(Spl) factors in the embryonic and adult brain

Christian Stigloher, Prisca Chapouton, Birgit Adolf and Laure Bally-Cuif

Brain Research Bulletin 75, 266–273 (2008)

Contribution:

For this review I collected data from published articles and my own experiments for all three figures. Furthermore, I designed all the figures. Previously unpublished data from my experiments on *her* gene function at embryonic stages is presented in chapter 2 of this article (Figure 1 and text). The corresponding data is presented in chapters 3.1.5 and 3.2.3 of this thesis. Further unpublished data from my experiments on *her* gene expression at adult stages is mentioned in chapter 3 of this article (chapter 3.1.6 of this thesis). I discussed data and literature with my co-authors, and the review was written in common by all co-authors.

Review

Identification of neural progenitor pools by E(Spl) factors in the embryonic and adult brain

Christian Stigloher, Prisca Chapouton, Birgit Adolf, Laure Bally-Cuif*

GSF-National Research Center for Environment and Health, Department Zebrafish Neurogenetics, Institute of Developmental Genetics, Ingolstaedter Landstrasse 1, D-85764 Neuherberg, Germany

Received 13 August 2007; accepted 17 October 2007

Available online 20 November 2007

Abstract

The maintenance of progenitor cells is a crucial aspect of central nervous system development and maturation, and bHLH transcription factors of the E(Spl) subfamily are involved in this process in all vertebrates studied to date. In the zebrafish embryonic neural plate, a large number of *E(Spl)* genes (*her* genes) are at play. We review recent data on this point, and propose a model where distinct subsets of these genes define different progenitor subtypes. Analysis of *her* genes expression in the adult zebrafish brain suggests that part of the embryonic *her* cascade might also be reused to define progenitors during adulthood. Further, available evidence on orthologous genes in the mouse (*Hes* genes) point to different modes of *Hes* regulation depending on cell location within the embryonic neural tube, perhaps associated with distinct progenitor types in this species as well. Out of these comparisons emerges a simple model of neural stem cell maintenance applicable from embryonic development until adulthood as well as across species. This working model suggests the directions for future experiments.

© 2007 Elsevier Inc. All rights reserved.

Keywords: Neurogenesis; Neural stem cell; Neural progenitor; E(Spl); *her*; *Hes*

Contents

1. Introduction	266
2. Atypical E(Spl) factors define progenitor pools in the zebrafish embryonic neural plate	267
3. Do mechanisms driving neurogenesis in the adult zebrafish brain also rely on E(Spl) factors?	267
4. Involvement of E(Spl) factors in the control of long-lasting progenitors in the mouse	269
5. Questions to be addressed	269
5.1. Progressive restriction of zebrafish progenitor pools to cells at boundaries	269
5.2. Boundary cells as neuronal progenitor pools	270
5.3. Different properties and fate of progenitor pools versus proliferating neural precursors	270
5.4. Lineage relationship between embryonic progenitors located at neural tube boundaries and adult neural stem cells	271
5.5. Association of long-lasting progenitors with signaling centers	271
6. Conclusion	271
Acknowledgements	271
References	271

1. Introduction

Neurogenesis and gliogenesis in the central nervous system (CNS) are genetically controlled in time and space to permit the differentiation of the appropriate cell types at the right locations and in correct numbers. In addition, sets of progenitors must be maintained that can be recruited for later events of CNS growth,

* Corresponding author.

E-mail address: bally@gsf.de (L. Bally-Cuif).

adaptation or repair. In spite of their crucial function, the molecular mechanisms regulating progenitor fate within the vertebrate CNS are only beginning to be appreciated. Recent findings point to the involvement of basic helix-loop-helix (bHLH) transcription factors of the Enhancer-of-Split (E(Spl)) subfamily in maintaining the undifferentiated state of neural progenitors, in a manner that varies between progenitor type but might be conserved across species. We review these findings below, taking as starting point the zebrafish embryonic neural plate, to draw a working model that we next challenge against the zebrafish adult CNS and progenitor maintenance control in amniotes.

2. Atypical E(Spl) factors define progenitor pools in the zebrafish embryonic neural plate

The onset of neurogenesis in the zebrafish neural plate becomes apparent at late gastrulation by the expression of a set of genes called “proneural”, which drive cellular commitment towards neurogenesis [7,19]. The first proneural genes expressed encode transcription factors such as the bHLH proteins Neurogenin1 (Neurog1) [16,42] and Achaete-scute1 (Ash1a) [4] or the non-basic HLH transcription factor Coe2 [13]. Transcription of these genes is not ubiquitous but restricted to cell clusters (“proneural clusters”), from which the nuclei of the primary neuronal network will arise [63]. As initially worked out in the *Drosophila* neuroepithelium, not all cells of a proneural cluster are equal and differentiate immediately. Rather, within each cluster, cells expressing higher levels of proneural genes are selected as “neuroblasts” for further commitment and differentiation, while concomitantly maintaining their neighbors as proliferating neural precursors available for a later round of neuroblast selection [22]. This process of “lateral inhibition” relies on Notch signaling, via its upregulation of expression of bHLH transcription factors of the E(Spl) family [8,9,34]. E(Spl) factors expressed in proneural clusters include Her4 [9,34,59], Hes5 (Her15) [11], Her2 and Her12 [11]. Her4 function has been experimentally studied, and, like *Drosophila* E(Spl), it inhibits expression of the proneural genes [59]. Hence, Her4-like factors regulate the progenitor state undergoing lateral inhibition.

At the neural plate stage in zebrafish, large domains that do not express proneural genes separate the proneural clusters (for reviews: [14,55]). These domains exhibit delayed differentiation, and, when available, cell tracing indicates that they will be only progressively recruited in early neurogenesis, and/or will participate in later neurogenesis events. For instance, the progenitor pool “IZ” (intervening zone) intervenes the ventro-caudal cluster (vcc) and presumptive neurons of rhombomere 2. At the onset of neurogenesis, the IZ contains progenitors that will give rise to differentiated cells within the entire midbrain–hindbrain domain [60]. At later stages, the IZ is restricted to cells at the midbrain–hindbrain boundary (MHB). Progenitor pools are characterized by expression of a specific set of transcription factors, including Zic, BF, Anf and Rx proteins that, at least in other vertebrates, have been involved in inhibiting neurogenesis [14]. Interestingly, recent publications (as well as C.S., unpublished observations) also demonstrate expression of a distinct set of E(Spl) genes in progenitor pools. These four genes are

her3, *her5*, *her9* and *her11/him*, expressed in various combinations in most domains of progenitor pools [11,30,31,35,51] (Fig. 1A). When ectopically expressed as capped RNA into wild-type zebrafish embryos, each of these factors is capable of broadly inhibiting *neurog1* expression. Loss-of-function experiments, based on injection of antisense oligonucleotides or mutant analyses, demonstrate that these factors are required to prevent *neurog1* transcription in all or part of their expression domains. Blockage of several of these factors in combination further shows that they exhibit partially redundant functions in the domains where they are co-expressed. Hence, a crucial mechanism that defines progenitor pools within the embryonic neural plate is an active process of inhibition of neurogenesis, mediated by the factors Her3/5/9/11. These factors block expression of several proneural genes (*neurog1*, *ash1a*, *coe2*) and of cyclin-dependent kinase inhibitors, but their direct transcriptional targets remain unknown.

The results above suggest that the early zebrafish neural plate consists of (at least) two types of neural progenitors: the “proliferating neural precursors”, that express *her4* and are set aside within proneural clusters by the lateral inhibition process, and the “progenitor pools”, expressing a combination of *her3/5/9/11* (Fig. 1B). An important remaining question is to understand whether and how these two populations differ in their properties, e.g. their division mode, differentiation and/or fate.

A meaningful hint comes from analyzing their specifically expressed *her* genes. Indeed, recent evidence demonstrate that, within the *her* family (comprising at least 15 members in zebrafish) [28], *her3/5/9/11* show a strikingly atypical regulation by Notch: while other *her* genes’ expression is activated by Notch signaling (and mediates Notch function, in particular during lateral inhibition), genetic and chemical blockage of Notch signaling indicate that *her3/5/9/11* do not require Notch for their expression in vivo. Moreover, the latter genes are down regulated when Notch signaling is experimentally activated, for instance by overexpression of the Notch intracellular fragment NICD into wild-type embryos [11,31,35]. Hence, it seems that instead of being triggered by Notch, like proliferating neural precursors, progenitor pools must be protected from Notch.

3. Do mechanisms driving neurogenesis in the adult zebrafish brain also rely on E(Spl) factors?

An interesting question is which of the above-discussed processes are maintained or reused to potentially define different types of progenitors in the adult zebrafish. The adult brain of teleost fish is characterized by numerous zones of proliferation located in virtually all brain subdivisions [41,45], in fitting with the continuous growth of the fish, including its brain, throughout life. Recent studies in zebrafish analyzed the nature and fate of proliferating cells. Short pulses of the thymidine analog BrdU followed by cell tracing showed that fast proliferating cell populations give rise to neurons in all brain areas [2,18,32,53,66]. Most proliferating zones are almost completely overlapping with domains expressing proneural/neurogenic genes (such as *delta* genes and *ash1a*) or the Notch target *her4*, suggesting that they undergo neurogenesis events reminiscent of those occurring in

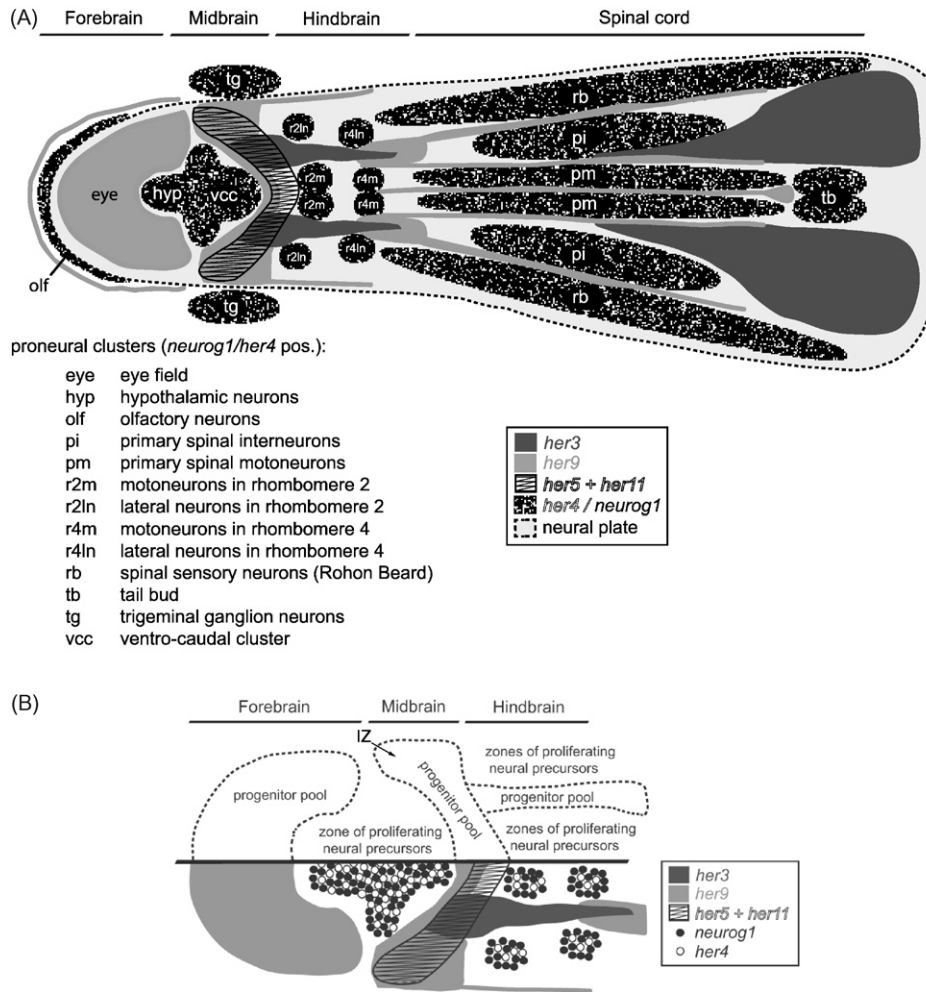


Fig. 1. (A) Schematic representation of the spatial distribution of proneural clusters (black) and intervening progenitor pools (gray or hatched) in the zebrafish embryonic neural plate at the 3-somite stage (dorsal views, anterior left). (B) Enlargement of the anterior neural plate area, showing that proneural clusters contain a salt-and-pepper distribution of proliferating neural precursors (e.g. *neurog1*+), while progenitor pools are entirely composed of cells that are refractory to neurogenesis and express various combination of the *her* genes *her3*, *5*, *9* and *11* (grey scale) (from [11,30,35,59]) (only *her* genes with experimentally demonstrated function in progenitor cells are represented, but see text for details). One example of a progenitor pool is the intervening zone (IZ).

embryonic proneural clusters [18]. Cumulative BrdU incorporation experiments, followed by long-term tracing and staining for the proliferation marker PCNA, demonstrated that proliferation zones also contain slow-dividing precursors, which do not dilute the BrdU label and remain in cycle over long time periods. These long-lasting progenitors are interpreted as adult neural stem cells. Their molecular components remain mostly unknown, although we noted that they are contained within areas expressing the transcription factors Sox2 and Pax6b ([2,18] and B.A., unpublished).

One such population is located at the alar/basal junction between the midbrain and hindbrain, the so-called “isthmus proliferation zone” (IPZ) [18] (Fig. 2). Cells in this location are very slow cycling, a hallmark of adult neural stem cells, and are at the origin of newborn local neurons and glia. Our laboratory recently demonstrated that, in contrast to neighboring fast cycling populations, IPZ cells are characterized by expression of *her5* [18]. Strikingly, using a transgenic line expressing a stable form of GFP under control of the entire set of *her5* regulatory

elements and permitting visualizing even low expression levels of *her5*, we further noted expression of Her5-GFP in some periventricular cells of the hypothalamus, an area where we also detected neural stem cells [18]. More recently, we could document expression of related *her* genes in these and other adult neural stem cell zones (C.S., J. Ninkovic, unpublished). Hence, domains containing adult neural stem cells display expression of genes of the *her3/5/9/11* subclass, and, at least at the IPZ, expression of these genes is selectively associated with the slow proliferating and stem cell state.

The function and mode of regulation of Her3/5/9/11 in adult cells, as well as the exact characterization of adult progenitors, remain crucial questions to answer before a strict parallel can be drawn with the embryonic situation. Nevertheless, our current results strongly suggest that part of the embryonic neurogenetic cascade involved in encoding progenitor pools is maintained, or re-used, to regulate the stem cell state during adulthood, while that defining proliferating neural precursors could characterize faster proliferating zones.

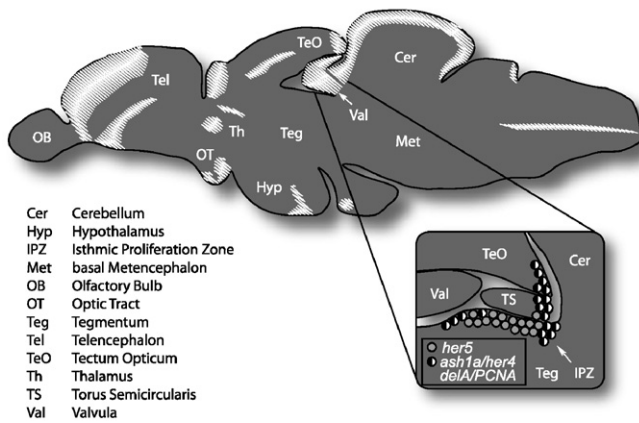


Fig. 2. Schematic representation of proliferation and neurogenesis zones (shaded areas) on a slightly parasagittal section of the adult zebrafish brain (from [2,32,45,53,66], section adapted from [64]). In the telencephalon, most of the ventricular zone is located at the midline, hence the broad staining in this plane of section. Inset: magnification of the isthmic proliferation zone (IPZ) showing the juxtaposition of slowly proliferating *her5*-positive neural stem cells with fast proliferating domains expressing *ash1a*, *her4*, *delA* and PCNA (from [18]).

4. Involvement of E(Spl) factors in the control of long-lasting progenitors in the mouse

The first neurons and related axonal scaffold established in the early neural tube display striking similarities between vertebrate embryos, including the amniotes. In all species, prominent neuronal clusters in the forebrain are the nucleus of the medial longitudinal fascicle (*vcc* in zebrafish, interstitial nucleus of Cajal in mouse and chicken) or the nucleus of the tract of the postoptic commissure; in the hindbrain, rhombomeres 2 and 4 differentiate earlier than others [20,26,49]. Hence, at least at early neural tube stages, a basic spatial alternation of actively neurogenic zones and zones where differentiation is delayed seems evolutionarily conserved. Subpopulations of progenitors with restricted fates, arguing for the existence of distinct progenitor subtypes, have also been identified within the early mouse neural tube ([47], Zalc, personal communication).

It is interesting, therefore, to ask whether the molecular mechanisms that distinguish progenitor cells within these domains are also conserved across species. Seven *E(Spl)*-like genes, called *Hes*, have been isolated in the mouse, among which *Hes1*, 3 and 5 are expressed at high levels in the developing neural tube. Knock-out experiments demonstrate that these genes are required, in a partially redundant manner, to prevent premature neuronal differentiation [36,38,39]. At the MHB, abrogation of *Hes1* and *Hes3* function further leads to the non-maintenance of MHB organizer genes' expression and loss of MHB activity [38]. This situation is reminiscent of the function of zebrafish *her* genes. However, expression of *Hes1/3/5* is clearly broader than the MHB alone, and expression of *Hes1/3/5* is generally activated by Notch [40]. Hence, the extent of functional similarity between *her* and *Hes* genes is unclear.

Recently, detailed analyses pointed to differences in *Hes1* expression between neurogenic zones and boundaries/signaling zones such as the MHB, the zona limitans intrathalamica (ZLI), interrhombomeric boundaries, and the roof and floor plates of

the spinal cord [12]. In neurogenic zones, *Hes1* is expressed at low levels and in a salt-and-pepper manner, alternating with cells expressing high levels of the proneural gene *Mash1*, and it responds to lateral inhibition. In contrast, at boundaries, *Hes1* is expressed at high levels in all cells. It would be most interesting to study the mode of regulation of *Hes1* expression in boundary progenitors, where, at least at the MHB, it might play a role equivalent to the zebrafish *her3/5/9/11* set of *her* genes. The early onset of expression of *Hes1* (and *Hes3*) in the mouse neural plate, which precedes *Notch* expression [37], and the maintenance of *Hes1* and *Hes3* expression in mouse mutants lacking *Notch* in the midbrain–hindbrain [46], indeed strongly suggests that these genes can be activated independently of Notch signaling in some contexts. Hence, in contexts where zebrafish would have devoted a selective set of *her* genes, the mouse could deploy a specific regulation of otherwise widely used *Hes* genes (Fig. 3). To date, speculations on a *Hes*-dependent Notch-independent mode of progenitor cells maintenance has been mostly related to time: during neural tube development, progenitors would switch from a *Hes*-dependent Notch-independent to a *Hes*-dependent Notch-dependent control as they transit from the neuroepithelial to the radial glial state [36,37]. The observations above suggest that both modes might also coexist over time but be associated with distinct types of progenitors, and it is crucial to test this hypothesis directly.

Hes genes are also recruited at sites of adult neuro- and gliogenesis in the mouse. For instance, *Hes1* expression highlights GFAP-positive cells in the dentate gyrus of the hippocampus, the sub-ependymal zone (SEZ) of the lateral ventricle, and Müller glia in the retina, and *Hes5* is expressed in the ciliary marginal zone of the retina [52], all domains that have been shown to contain neural stem cells and produce neurons during adulthood (reviewed in [1,15,54]). The role of *Hes* genes in these locations, as well as their mode of regulation, remains to be tested, but it is likely that they are involved in controlling the progenitor state. Two such states have been defined in the adult mouse brain, the slow-proliferating neural stem and the fast proliferating transient amplifying progenitors deriving from the stem cells [25,56]. Again, by analogy with the situation in zebrafish, it will be crucial to find out whether (and which) *Hes* genes are primarily active in stem cells and/or in transient amplifying progenitors.

5. Questions to be addressed

The observations above are suggestive of striking parallels between mouse and zebrafish in the usage and regulation of *E(Spl)* genes and their regulation of different progenitor types. Several points however still need to be addressed, in one species or the other, for the comparison to be substantiated. These points are briefly discussed below.

5.1. Progressive restriction of zebrafish progenitor pools to cells at boundaries

Cells expressing high levels of *Hes1* in the mouse appear located along boundaries within the embryonic neural tube, one of which, the MHB, also abuts cells expressing *her3/5/9/11*

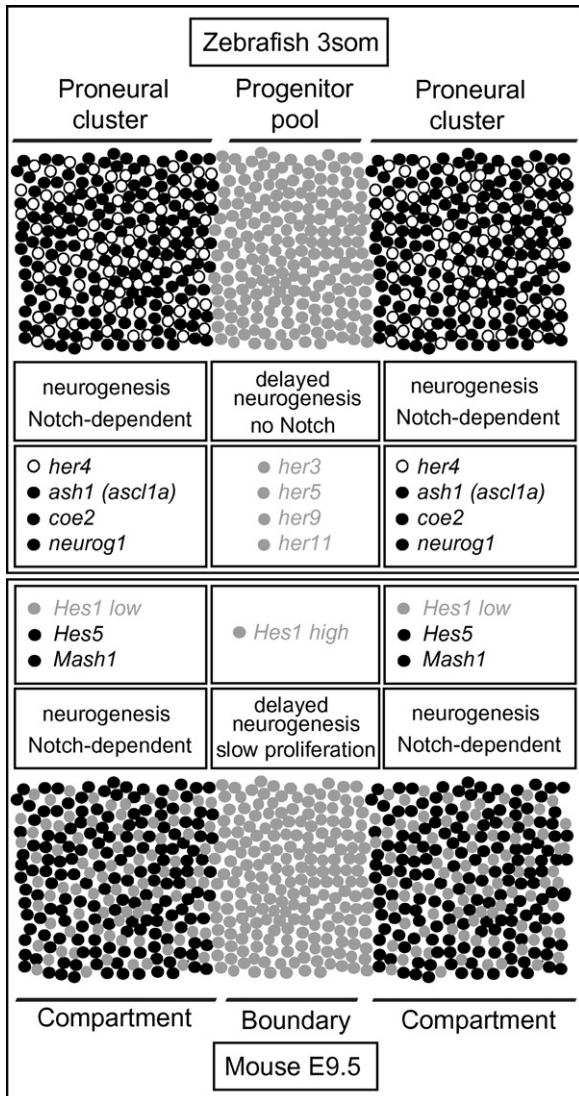


Fig. 3. Working model on the correspondence between progenitor types within the embryonic midbrain–hindbrain domain of zebrafish (3-somite stage) and mouse (E9.5). In zebrafish, a progenitor pool exhibiting delayed neurogenesis and expressing *her3/5/9/11* is present at the midbrain–hindbrain boundary (MHB). These genes do not require Notch for their activation. On either side, proneural clusters containing *her4*-positive proliferating neural precursors undergo neurogenesis in a Notch-dependent manner (only *her* genes with experimentally demonstrated function are shown, but see text for details). Hence, distinct sets of *her* genes are used at the MHB versus adjacent areas. In the mouse, the MHB is characterized by delayed neurogenesis, slow proliferation and high expression of *Hes1* in all cells. This contrasts with salt-and-pepper and weaker expression of *Hes1* in adjacent neurogenic domains (“compartments”) (from [12]). Hence, mouse might use a different regulation of expression of the same *Hes* genes to distinguish progenitors of boundary and compartments.

in zebrafish. Whether progenitor pools other than MHB cells in zebrafish also line boundaries is unclear, as they have been mostly studied at the neural plate stage, before the morphological appearance and unambiguous localization of boundaries. Hence, the situation is not directly comparable to studies in mouse and chick. It would now be important to trace zebrafish progenitor pools over time to monitor their progressive restriction and final location, as performed for the MHB.

5.2. Boundary cells as neuronal progenitor pools

Our model is primarily based on the MHB, and in fact few boundary cells have been specifically and precisely traced in the embryo. As described above, the early MHB pool was traced in zebrafish by means of GFP stability in *her5:gfp* transgenics, and shown to produce midbrain and anterior hindbrain neurons [44,60]. In the mouse, *Wnt1*-positive cells, which overlap the area of slow proliferation around the MHB at E9.5 [61], also contribute at that stage neurons to the midbrain [65]. Transplantation experiments in chick demonstrated that the ZLI area gives rise to some thalamic nuclei [29]; in the mouse, ZLI cells generate radial glia (Martinez, Zalc, personal communication), the fate of which has not yet been analyzed. Cells at rhombomere boundaries in zebrafish can serve as progenitors at late embryonic stages (discussed in [5]) but this property is not ascertained in chicken or mouse. Likewise, fate map analyses of the roof and floor plates have not been performed in zebrafish, and remain ambiguous in the mouse and chick. The mouse roof plate primarily gives rise to the choroid plexus [10,23], and, based on *Gdf7* expression, to a subset of cortical marginal zone neurons [50]. However, at early stages *Gdf7* expression in the dorsal neural tube might be broader than the presumptive roof plate. Similarly, the *Shh*-expressing ventral midline gives rise to neurons in the midbrain and hypothalamus [6,48], but whether *Shh* strictly identifies the floor plate in these regions is unknown. Hence, we are far from an understanding of the long-term fate of neural tube boundary regions, and a precise comparison of the different model systems is also needed, to determine how general a model is where boundaries serve as progenitor pools.

5.3. Different properties and fate of progenitor pools versus proliferating neural precursors

Our discussion above highlights that progenitor pools and proliferating neural precursors, in the embryonic neural tube, differ in their sensitivity to Notch and the subclass of *her* genes (or the mode of regulation of *Hes* genes) that they express. One may now wonder how relevant these differences are during CNS construction, and important questions remain in particular to determine whether these two types of progenitors are endowed with different cellular properties. In mouse, boundaries also display a slow division mode [12,61], and high levels of *Hes1* expression push cells towards quiescence in several systems [12,17,24]. It would be important to determine whether slow cell division is a general characteristic of progenitor pools in zebrafish as well. Both progenitor types might also differ in their cell division properties (e.g. asymmetric versus symmetric, neurogenic versus non-neurogenic), and tracing single cells in vivo would be needed to assess this point. Finally, it remains to be studied in detail whether (and where) these two progenitor types are related in lineage (with for instance progenitor pools contributing to proneural clusters and giving rise to some proliferating neural precursors) and/or whether they acquire at least partially different fates. In the adult zebrafish, it remains to be tested whether long-lasting, slow-proliferating progenitors also give rise to fast-dividing progenitors (like the

stem cells and transient amplifying progenitors of the adult mouse).

5.4. Lineage relationship between embryonic progenitors located at neural tube boundaries and adult neural stem cells

A series of indirect arguments point to this direction: (i) long-lasting progenitors in the adult brain are characterized by their slow proliferation mode, and embryonic progenitor pools at boundaries generally rapidly acquire a slow proliferation mode during embryogenesis (this has been demonstrated at least for the mouse MHB [12,61], the mouse ZLI and spinal cord roof and floor plates [12], the zebrafish, chicken and mouse rhombomere boundaries [5,12,21,33]); (ii) the perdurance of a progenitor pool along the MHB in the zebrafish embryo and adult, as well as its expression of *her5* at all stages, are suggestive of a lineage relationship, (iii) the progenitor zones in the adult teleost brain are associated with boundaries between brain subdivisions (and periventricular areas) [27]; (iv) in the mouse, the adult neural stem cells in the sub-ependymal zone are located at the boundary between ventral and dorsal telencephalon, an area which contains the progeny of embryonic telencephalic neural stem cells present at least from the E15.5 stage onwards [3]. These adult SEZ cells share molecular markers with cells located at the boundary between pallium and the dorsal aspect of the lateral ganglionic eminence (subpallium) in the embryo [57,58,62]. Here again, systematic genetic tracing of boundary cells of the embryonic neural tube, both in zebrafish and mouse, would be important. A possible way would be conditional activation of CreERT under control of boundary promoters at a stage when boundaries are clearly demarcated, e.g. E9.5 or later in the mouse or 15–20 somites in zebrafish. At least in zebrafish, regulatory elements of *her3/5/9/11* would likely be appropriate tools.

5.5. Association of long-lasting progenitors with signaling centers

The association of long-lasting progenitors with the MHB in zebrafish throughout life, and in the mouse and chick at least through embryogenesis, is striking. Most interestingly, the MHB hosts the isthmus organizer, involved in maintaining and patterning the midbrain and anterior hindbrain via Fgf8 and Wnt1 signaling. *her5* and *her11* expression, for instance, directly or indirectly depend on signaling by these two molecules [51]. Importantly, the converse is also true, and an undifferentiated state at the MHB area is absolutely necessary for the maintenance of the signaling activities of cells at the MHB. For instance, when neuronal differentiation is experimentally forced in this location, e.g. via injection of capped mRNA encoding Neurog1, expression of MHB organizer genes is lost [30]. Hence, at least in this location of the early neural plate, there is an intricate interdependence between signaling activities and the neurogenesis inhibition events leading to progenitor pool maintenance. Along these lines, the simultaneous loss of *Hes1*, *Hes3* and *Hes5* expression lead to reduced signaling activities of the ZLI and roof plate, as revealed by expression of *Shh* and

Wnt1 [12]. Our preliminary observations also suggest that Fgf signaling is active near the adult IPZ (Topp, unpublished), and mouse adult neural stem cells receive Wnt and Hh signaling [3,43]. It remains an important question now to determine how general the relationship between long-lasting progenitors and signaling centers is during embryogenesis and adulthood, both in zebrafish and mouse, and to which extent it is inherited from embryo to adult.

6. Conclusion

Analysis of *E(Spl)* genes subclasses and their expression suggests a model where they would identify distinct progenitor types. This pattern is recognizable within the embryonic and adult CNS in zebrafish, and at least in the mouse embryo. Specific analyses of lineage, cellular properties and comparative neuroanatomy are however still required to consolidate this interpretation. Next, studies on the regulation of expression of these different *E(Spl)* genes and their molecular cascades might provide an entry point into dissecting the dynamics of stem cell maintenance and neurogenesis, in space, time and across species, to approach, for instance, the mechanisms that might account for the non-maintenance of widespread adult neurogenesis in the mammalian brain. As discussed, functional similarity within this family of homologous genes is not obvious, but, among the mouse *Hes* genes studied to date, *Hes1* seems functionally the closest relation to *her3/5/9/11*. Indeed, it can be expressed independently of Notch, it shows a different mode of expression at boundaries, and it is maintained in adult neural stem cells. Hence it would be important to define the function of *Hes1* in the adult mouse brain, and to analyze the regulatory events leading to the restriction of expression of this gene to the forebrain stem cell zones along life. Along these lines, it will also be relevant to assess the extent of Notch signaling and signaling centers in the adult brain, in both zebrafish and mouse.

Acknowledgements

We are grateful to past and present members of the LBC lab for providing experimental data discussed in this review, to Drs. S. Martinez and B. Zalc for communicating results prior to publication, and to Dr. M. Wassef for her insightful ideas and critical reading of the manuscript. Work in the LBC laboratory is funded by a junior group grant from the Volkswagen Association, the EU 6th framework integrated project ZF-Models (contract no. LSHC-CT-2003-503466), the Life Science Association (no. GSF 2005/01), and a special research grant from the Institut du Cerveau et de la Moelle épinière (ICM, Paris). P.C. is recipient of a long-term EMBO fellowship and B.A. of a grant from the Deutsche Forschungsgemeinschaft (Munich Center for Integrated Protein Science, CIPSM).

References

- [1] D.N. Abrons, M. Koehl, M. Le Moal, Adult neurogenesis: from precursors to network and physiology, *Physiol. Rev.* 85 (2005) 523–569.

- [2] B. Adolf, P. Chapouton, C.S. Lam, S. Topp, B. Tannhäuser, U. Strähle, M. Götz, L. Bally-Cuif, Conserved and acquired features of adult neurogenesis in the zebrafish telencephalon, *Dev. Biol.* 295 (2006) 278–293.
- [3] S. Ahn, A.L. Joyner, In vivo analysis of quiescent adult neural stem cells responding to Sonic hedgehog, *Nature* 437 (2005) 894–897.
- [4] M.L. Allende, E.S. Weinberg, The expression pattern of two zebrafish achaete-scute homolog (ash) genes is altered in the embryonic brain of the cyclops mutant, *Dev. Biol.* 166 (1994) 509–530.
- [5] M. Amoyel, Y.C. Cheng, Y.J. Jiang, D.G. Wilkinson, Wnt1 regulates neurogenesis and mediates lateral inhibition of boundary cell specification in the zebrafish hindbrain, *Development* 132 (2005) 775–785.
- [6] E. Andersson, U. Tryggvason, Q. Deng, S. Friling, Z. Alekseenko, B. Robert, T. Perlmann, J. Ericson, Identification of intrinsic determinants of midbrain dopamine neurons, *Cell* 124 (2006) 393–405.
- [7] B. Appel, A.B. Chitnis, Neurogenesis and specification of neuronal identity, *Results Probl. Cell Differ.* 40 (2002) 237–251.
- [8] B. Appel, J.S. Eisen, Regulation of neuronal specification in the zebrafish spinal cord by Delta function, *Development* 125 (1998) 371–380.
- [9] B. Appel, L.A. Givan, J.S. Eisen, Delta-Notch signaling and lateral inhibition in zebrafish spinal cord development, *BMC Dev. Biol.* 1 (2001) 13.
- [10] R. Awatramani, P. Soriano, C. Rodriguez, J.J. Mai, S.M. Dymecki, Cryptic boundaries in roof plate and choroid plexus identified by intersectional gene activation, *Nat. Genet.* 35 (2003) 70–75.
- [11] Y.K. Bae, T. Shimizu, M. Hibi, Patterning of proneuronal and interproneuronal domains by hairy- and enhancer of split-related genes in zebrafish neuroectoderm, *Development* 132 (2005) 1375–1385.
- [12] J.H. Baek, J. Hatakeyama, S. Sakamoto, T. Ohtsuka, R. Kageyama, Persistent and high levels of Hes1 expression regulate boundary formation in the developing central nervous system, *Development* 133 (2006) 2467–2476.
- [13] L. Bally-Cuif, L. Dubois, A. Vincent, Molecular cloning of Zcoe2, the zebrafish homolog of Xenopus Xcoe2 and mouse EBF-2, and its expression during primary neurogenesis, *Mech. Dev.* 77 (1998) 85–90.
- [14] L. Bally-Cuif, M. Hammerschmidt, Induction and patterning of neuronal development, and its connection to cell cycle control, *Curr. Opin. Neurobiol.* 13 (2003) 16–25.
- [15] B. Berninger, M.A. Hack, M. Götz, Neural stem cells: on where they hide, in which disguise, and how we may lure them out, *Handb. Exp. Pharmacol.* (2006) 319–360.
- [16] P. Blader, N. Fischer, G. Gradwohl, F. Guillemont, U. Strähle, The activity of neurogenin1 is controlled by local cues in the zebrafish embryo, *Development* 124 (1997) 4557–4569.
- [17] P. Castella, S. Sawai, K. Nakao, J.A. Wagner, M. Caudy, HES-1 repression of differentiation and proliferation in PC12 cells: role for the helix 3-helix 4 domain in transcription repression, *Mol. Cell Biol.* 20 (2000) 6170–6183.
- [18] P. Chapouton, B. Adolf, C. Leucht, B. Tannhäuser, S. Ryu, W. Driever, L. Bally-Cuif, her5 expression reveals a pool of neural stem cells in the adult zebrafish midbrain, *Development* 133 (2006) 4293–4303.
- [19] P. Chapouton, L. Bally-Cuif, Neurogenesis, in: H.W. Detrich, M. Westerfield, L.I. Zon (Eds.), *Methods in Cell Biology: the Zebrafish*, vol. 76, Academic Press London, 2004, pp. 163–206.
- [20] A. Chédotal, O. Pourquié, C. Sotelo, Initial tract formation in the brain of the chick embryo: selective expression of the BEN/SC1/DM-GRASP cell adhesion molecule, *Eur. J. Neurosci.* 7 (1995) 198–212.
- [21] Y.C. Cheng, M. Amoyel, X. Qiu, Y.J. Jiang, Q. Xu, D.G. Wilkinson, Notch activation regulates the segregation and differentiation of rhombomere boundary cells in the zebrafish hindbrain, *Dev. Cell* 6 (2004) 539–550.
- [22] A.B. Chitnis, Control of neurogenesis—lessons from frogs, fish and flies, *Curr. Opin. Neurobiol.* 9 (1999) 18–25.
- [23] D.S. Currie, X. Cheng, C.M. Hsu, E.S. Monuki, Direct and indirect roles of CNS dorsal midline cells in choroid plexus epithelia formation, *Development* 132 (2005) 3549–3559.
- [24] C.L. Curry, L.L. Reed, B.J. Nickoloff, L. Miele, K.E. Foreman, Notch-independent regulation of Hes-1 expression by c-Jun N-terminal kinase signaling in human endothelial cells, *Lab. Invest.* 86 (2006) 842–852.
- [25] F. Doetsch, J.M. Garcia-Verdugo, A. Alvarez-Buylla, Cellular composition and three-dimensional organization of the subventricular germinal zone in the adult mammalian brain, *J. Neurosci.* 17 (1997) 5046–5061.
- [26] S.S. Easter Jr., J. Burrill, R.C. Marcus, L. Ross, J.S.H. Taylor, S.W. Wilson, Initial tract formation in the vertebrate brain, *Prog. Brain Res.* 102 (1994) 79–93.
- [27] P. Ekstrom, C.M. Johnsson, L.M. Ohlin, Ventricular proliferation zones in the brain of an adult teleost fish and their relation to neuromeres and migration (secondary matrix) zones, *J. Comp. Neurol.* 436 (2001) 92–110.
- [28] M. Gajewski, H. Elmasri, M. Girschick, D. Sieger, C. Winkler, Comparative analysis of her genes during fish somitogenesis suggests a mouse/chick-like mode of oscillation in medaka, *Dev. Genes Evol.* 216 (2006) 315–332.
- [29] R. Garcia-Lopez, C. Vieira, D. Echevarria, S. Martinez, Fate map of the diencephalon and the zona limitans at the 10-somites stage in chick embryos, *Dev. Biol.* 268 (2004) 514–530.
- [30] A. Geling, M. Itoh, A. Tallafuss, P. Chapouton, B. Tannhäuser, J.Y. Kuwada, A.B. Chitnis, L. Bally-Cuif, bHLH transcription factor Her5 links patterning to regional inhibition of neurogenesis at the midbrain–hindbrain boundary, *Development* 130 (2003) 1591–1604.
- [31] A. Geling, C. Plessy, S. Rastegar, U. Strähle, L. Bally-Cuif, Her5 acts as a prepattern factor that blocks neurogenin1 and coe2 expression upstream of Notch to inhibit neurogenesis at the midbrain–hindbrain boundary, *Development* 131 (2004) 1993–2006.
- [32] H. Grandel, J. Kaslin, J. Ganz, I. Wenzel, M. Brand, Neural stem cells and neurogenesis in the adult zebrafish brain: origin, proliferation dynamics, migration and cell fate, *Dev. Biol.* 295 (2006) 263–277.
- [33] S. Guthrie, M. Butcher, A. Lumsden, Patterns of cell division and interkinetic nuclear migration in the chick embryo hindbrain, *J. Neurobiol.* 22 (1991) 742–754.
- [34] C. Haddon, L. Smithers, S. Schneider-Maunoury, T. Coche, D. Henrique, J. Lewis, Multiple delta genes and lateral inhibition in zebrafish primary neurogenesis, *Development* 125 (1998) 359–370.
- [35] S. Hans, N. Scheer, I. Riedl, E. v. Weizsäcker, P. Blader, J.A. Campos-Ortega, her3, a zebrafish member of the hairy-E(spl) family, is repressed by Notch signalling, *Development* 131 (2004) 2957–2969.
- [36] J. Hatakeyama, Y. Bessho, K. Katoh, S. Ookawara, M. Fujioka, F. Guillemot, R. Kageyama, Hes genes regulate size, shape and histogenesis of the nervous system by control of the timing of neural stem cell differentiation, *Development* 131 (2004) 5539–5550.
- [37] J. Hatakeyama, R. Kageyama, Notch1 expression is spatiotemporally correlated with neurogenesis and negatively regulated by Notch1-independent Hes genes in the developing nervous system, *Cereb. Cortex* 16 (Suppl. 1) (2006) i132–i137.
- [38] H. Hirata, K. Tomita, Y. Bessho, R. Kageyama, Hes1 and Hes3 regulate maintenance of the isthmus organizer and development of the mid/hindbrain, *EMBO J.* 20 (2001) 4454–4466.
- [39] M. Ishibashi, K. Moriyoshi, Y. Sasai, K. Shiota, S. Nakanishi, R. Kageyama, Persistent expression of helix-loop-helix factor HES-1 prevents mammalian neural differentiation in the central nervous system, *EMBO J.* 13 (1994) 1799–1805.
- [40] R. Kageyama, T. Ohtsuka, J. Hatakeyama, R. Ohsawa, Roles of bHLH genes in neural stem cell differentiation, *Exp. Cell Res.* 306 (2005) 343–348.
- [41] J. Kaslin, J. Ganz, M. Brand, Proliferation, neurogenesis and regeneration in the non-mammalian vertebrate brain, *Philos. Trans. R. Soc. Lond. B Biol. Sci.* (2007).
- [42] V. Korzh, U. Strähle, Proneural, prosensory, antiglial: the many faces of neurogenins, *Trends Neurosci.* 25 (2002) 603–605.
- [43] D.C. Lie, S.A. Colamarino, H.J. Song, L. Desire, H. Mira, A. Consiglio, E.S. Lein, S. Jessberger, H. Lansford, A.R. Dearie, F.H. Gage, Wnt signalling regulates adult hippocampal neurogenesis, *Nature* 437 (2005) 1370–1375.
- [44] C. Lillesaar, B. Tannhäuser, C. Stigloher, E. Kremmer, L. Bally-Cuif, The serotonergic phenotype is acquired by converging genetic mechanisms within the zebrafish central nervous system, *Dev. Dyn.* 236 (2007) 1072–1084.
- [45] B.W. Lindsey, V. Tropepe, A comparative framework for understanding the biological principles of adult neurogenesis, *Prog. Neurobiol.* 80 (2006) 281–307.

- [46] S. Lutolf, F. Radtke, M. Aguet, U. Suter, V. Taylor, Notch1 is required for neuronal and glial differentiation in the cerebellum, *Development* 129 (2002) 373–385.
- [47] R. Machold, G. Fishell, Math1 is expressed in temporally discrete pools of cerebellar rhombic-lip neural progenitors, *Neuron* 48 (2005) 17–24.
- [48] L. Manning, K. Ohyama, B. Saeger, O. Hatano, S.A. Wilson, M. Logan, M. Placzek, Regional morphogenesis in the hypothalamus: a BMP-Tbx2 pathway coordinates fate and proliferation through Shh downregulation, *Dev. Cell* 11 (2006) 873–885.
- [49] G.S. Mastick, S.S. Easter Jr., Initial organization of neurons and tracts in the embryonic mouse fore- and midbrain, *Dev. Biol.* 173 (1996) 79–94.
- [50] E.S. Monuki, F.D. Porter, C.A. Walsh, Patterning of the dorsal telencephalon and cerebral cortex by a roof plate-Lhx2 pathway, *Neuron* 32 (2001) 591–604.
- [51] J. Ninkovic, A. Tallafuss, C. Leucht, J. Topczewski, B. Tannhäuser, L. Solnica-Krezel, L. Bally-Cuif, Inhibition of neurogenesis at the zebrafish midbrain–hindbrain boundary by the combined and dose-dependent activity of a new hairy/E(spl) gene pair, *Development* 132 (2005) 75–88.
- [52] T. Ohtsuka, I. Imayoshi, H. Shimojo, E. Nishi, R. Kageyama, S.K. McConnell, Visualization of embryonic neural stem cells using Hes promoters in transgenic mice, *Mol. Cell Neurosci.* 31 (2006) 109–122.
- [53] E. Pellegrini, K. Mouriec, I. Anglade, A. Menuet, Y. Le Page, M.M. Gueguen, M.H. Marmignon, F. Brion, F. Pakdel, O. Kah, Identification of aromatase-positive radial glial cells as progenitor cells in the ventricular layer of the forebrain in zebrafish, *J. Comp. Neurol.* 501 (2007) 150–167.
- [54] M. Perron, W.A. Harris, Retinal stem cells in vertebrates, *Bioessays* 22 (2000) 685–688.
- [55] Y. Sasai, Identifying the missing links: genes that connect neural induction and primary neurogenesis in vertebrate embryos, *Neuron* 21 (1998) 455–458.
- [56] B. Seri, J.M. Garcia-Verdugo, B.S. McEwen, A. Alvarez-Buylla, Astrocytes give rise to new neurons in the adult mammalian hippocampus, *J. Neurosci.* 21 (2001) 7153–7160.
- [57] J. Stenman, H. Toresson, K. Campbell, Identification of two distinct progenitor populations in the lateral ganglionic eminence: implications for striatal and olfactory bulb neurogenesis, *J. Neurosci.* 23 (2003) 167–174.
- [58] J. Stenman, R.T. Yu, R.M. Evans, K. Campbell, Tlx and Pax6 co-operate genetically to establish the pallio-subpallial boundary in the embryonic mouse telencephalon, *Development* 130 (2003) 1113–1122.
- [59] C. Takke, P. Dornseifer, E. v. Weizsäcker, J.A. Campos-Ortega, her4, a zebrafish homologue of the Drosophila neurogenic gene E(spl), is a target of NOTCH signalling, *Development* 126 (1999) 1811–1821.
- [60] A. Tallafuss, L. Bally-Cuif, Tracing of her5 progeny in zebrafish transgenics reveals the dynamics of midbrain–hindbrain neurogenesis and maintenance, *Development* 130 (2003) 4307–4323.
- [61] R. Trokovic, T. Jukkola, J. Saarimäki, P. Peltopuro, T. Naserke, D.M. Weisenhorn, N. Trokovic, W. Wurst, J. Partanen, Fgfr1-dependent boundary cells between developing mid- and hindbrain, *Dev. Biol.* 278 (2005) 428–439.
- [62] R.R. Waclaw, B. Wang, K. Campbell, The homeobox gene Gsh2 is required for retinoid production in the embryonic mouse telencephalon, *Development* 131 (2004) 4013–4020.
- [63] S. Wilson, L.S. Ross, T. Parrett, S.S. Easter Jr., The development of a simple scaffold of axon tracts in the brain of the embryonic zebrafish, *Brachydanio rerio*, *Development* 108 (1990) 121–145.
- [64] M. Wullmann, B. Rupp, H. Reichert, in: M.F. Wullmann (Ed.), *Neuroanatomy of the Zebrafish Brain: A Topological Atlas*, Birkhäuser Verlag, Basel, 1996, pp. 1–144.
- [65] M. Zervas, S. Millet, S. Ahn, A.L. Joyner, Cell behaviors and genetic lineages of the mesencephalon and rhombomere 1, *Neuron* 43 (2004) 345–357.
- [66] G.K. Zupanc, K. Hinsch, F.H. Gage, Proliferation, migration, neuronal differentiation, and long-term survival of new cells in the adult zebrafish brain, *J. Comp. Neurol.* 488 (2005) 290–319.

Appendix 2

Article in *Development*

Segregation of telencephalic and eye-field identities inside the zebrafish forebrain territory is controlled by Rx3

Christian Stigloher, Jovica Ninkovic, Mary Laplante, Andrea Geling, Birgit Tannhäuser, Stefanie Topp, Hiroshi Kikuta, Thomas Becker, Corinne Houart and Laure Bally-Cuif

Development 133, 2925-2935 (2006)

Contribution:

For this article I conducted most of the experiments (all Figures except Figures 7A,B). The mutant *chk*^{ne2611} was originally found by Jovica Ninkovic. The enhancer trap line *CLGY469* that I used for transplantation experiments was found by Andrea Geling and subsequently raised and molecularly described by Mary Laplante, Hiroshi Kikuta and Thomas Becker. Corinne Houart provided probes and conducted the transplantation experiments shown in Figure 7A and B. Stefanie Topp and Birgit Tannhäuser provided experimental support. Furthermore, we discussed data with Corinne Houart and Thomas Becker. I conducted the statistical analysis with the help of Jovica Ninkovic. I wrote the first version of the manuscript.

Segregation of telencephalic and eye-field identities inside the zebrafish forebrain territory is controlled by Rx3

Christian Stigloher¹, Jovica Ninkovic^{1,*}, Mary Laplante², Andrea Geling^{1,†}, Birgit Tannhäuser¹, Stefanie Topp¹, Hiroshi Kikuta², Thomas S. Becker², Corinne Houart³ and Laure Bally-Cuif^{1,‡}

Anteroposterior patterning of the vertebrate forebrain during gastrulation involves graded Wnt signaling, which segregates anterior fields (telencephalon and eye) from the diencephalon. How the telencephalic and retinal primordia are subsequently subdivided remains largely unknown. We demonstrate that at late gastrulation the Paired-like homeodomain transcription factor Rx3 biases cell specification choices towards the retinal fate within a population of bipotential precursors of the anterior forebrain: direct cell tracing demonstrates that retinal precursors acquire a telencephalic fate in embryos homozygous for the *rx3*-null allele *ckh^{ne2671}*, characterized by an enlarged telencephalon and a lack of eyes. Chimera analyses further indicate that this function of Rx3 is cell autonomous. Transfating of the eye field in the absence of Rx3 function correlates with a substantial posterior expansion of expression of the Wnt antagonist Tlc and the winged-helix transcription factor Foxg1. These results suggest that the process segregating the telencephalic and eye fields is isolated from diencephalic patterning, and is mediated by Rx3.

KEY WORDS: Zebrafish, Telencephalon, Eye field, Forebrain, Rx3

INTRODUCTION

The vertebrate forebrain is prefigured at embryonic stages by the anteriorly located telencephalon and retinae, the ventral hypothalamus and the caudal diencephalon. How their domains are initially established is incompletely understood.

Following the specification of forebrain identity during gastrulation, local organizers refine and maintain forebrain patterning (Foley and Stern, 2001; Wilson and Houart, 2004). One organizer, located at the anterior margin of the neural plate (ANB or ANR), controls development of anterior forebrain identities (Houart et al., 2002; Houart et al., 1998; Shimamura and Rubenstein, 1997). The ANB expresses the secreted factors Fgf3 and Fgf8 (Eagleson and Dempewolf, 2002), as well as potent Wnt antagonists (Houart et al., 2002). In zebrafish, one of these antagonists is the secreted Frizzled Related Protein (sFRP) Tlc. Ectopic expression of Tlc mimics ectopic ANB activity in telencephalic induction, and abrogation of Tlc function impairs the formation of telencephalon and eyes (Houart et al., 2002). Conversely, increased canonical Wnt activity, for instance by overexpression of Wnt8b normally produced in the posterior diencephalon (Kelly et al., 1995), or by the loss of function of Axin1, leads to an enlargement of the diencephalon at the expense of the telencephalon and eyes (Heisenberg et al., 2001; Houart et al., 2002; van de Water et al., 2001), and the lack of

telencephalon can be corrected by increased levels of Tlc. Similarly, abrogation of the Wnt inhibitors Tcf3 or Six3 abolishes anterior forebrain development at the benefit of more posterior identities in zebrafish and mouse (Dorsky et al., 2003; Kim et al., 2000; Lagutin et al., 2003). These results suggest a model where the level of canonical Wnt activity, determined by the antagonism between a posterior local source and anterior local inhibitors, patterns forebrain development during gastrulation (Wilson and Houart, 2004).

Manipulations of Wnt or its antagonists at an early stage affect simultaneously the presumptive telencephalon and eye field, suggesting that these two domains are initially defined as one in their early response to Wnt activity. The factors controlling the later separation of the telencephalon and the eye field within the anterior forebrain are unknown. One candidate might be olSfrp1, a sFRP expressed in the anteriormost region of the neural plate in Medaka: abrogation of olSfrp1 function using morpholino antisense oligonucleotides produces embryos with reduced eyes and a complementarily enlarged telencephalon, without modifying diencephalic size (Esteve et al., 2004). How olSfrp1 acts at the cellular and molecular levels, and whether it indeed controls cell specification choices, however, remains unknown.

The specification of the eye field is correlated with sustained expression of Pax6, Six3 and Rx1–Rx3, shown to be crucial for eye development (Bailey et al., 2004; Graw, 2003; Hanson, 2003; Mathers and Jamrich, 2000). *Rx* genes encode paired-like homeodomain proteins. At late gastrulation, expression of the mouse *Rx* gene is intense in the eye field and is non-overlapping with the adjacent telencephalic field (Bailey et al., 2004; Chuang et al., 1999). A similar pattern is observed for zebrafish *rx3*, the earliest and only *rx* gene expressed at the open neural plate stage (Chuang et al., 1999). Knock-out of the single mouse *Rx* gene, and inhibition of *Xenopus* *Xrx1* function, abolishes the formation of eye structures (Casarosa et al., 2003; Mathers et al., 1997). Conversely, ectopic expression of *rx1* and *rx2* by mRNA injection in zebrafish triggers an expansion of retinal tissue (Chuang and Raymond, 2001). These observations suggest that the *Rx* genes are involved in the specification or maintenance of retinal progenitors (Bailey et al., 2004), in contrast with the proposed later function of zebrafish and Medaka *rx3* in retinal evagination; in null

¹Zebrafish Neurogenetics Junior Research Group, Institute of Virology, Technical University-Munich, Trogerstrasse 4b, D-81675, Munich, Germany and GSF-National Research Center for Environment and Health, Department Zebrafish Neurogenetics, Institute of Developmental Genetics, Ingolstaedter Landstrasse 1, D-85764 Neuherberg, Germany. ²Sars Centre for Marine Molecular Biology, University of Bergen, Thormoehlsensgt.55, N-5008 Bergen, Norway. ³MRC Centre for Developmental Neurobiology, New Hunt's House, King's College London, SE1 9RT London, UK.

*Present address: GSF-National Research Center for Environment and Health, Institute of Stem Cell Research, Ingolstaedter Landstrasse 1, D-85764 Neuherberg, Germany

†Present address: Mischterlich and Partners, Postfach 330609, 80066 Munich, Germany

‡Author for correspondence (e-mail: bally@gsf.de)

mutants for Rx3 [*chokh* (*ckh*) and *eyeless* (*el*), respectively], early anterior genes such as *six3* or *pax6* are expressed, but the optic vesicle fails to evaginate (Kennedy et al., 2004; Loosli et al., 2003; Loosli et al., 2001; Winkler et al., 2000). Because forebrain patterning defects had not been noted, Rx3 was proposed to be an unusual member of the Rx family controlling retinal morphogenesis.

We describe here a zebrafish mutant, *ne2611*, with an expanded telencephalon and a lack of eyes. We report that *ne2611* is a null allele of *rx3*, and that retinal precursors in *ne2611* ectopically express *tlc* at late gastrulation and acquire a telencephalic fate. We reanalyzed the published allele *ckh*³⁹⁹ and demonstrate that *tlc* and telencephalic expansion are also apparent in this mutant. These results identify Rx3 as a key determinant controlling specification choices between eye field and telencephalon during anterior forebrain patterning.

MATERIALS AND METHODS

Fish strains

Embryos of AB wild-type or ENU-treated fish were raised and staged according to Kimmel et al. (Kimmel et al., 1995). *chokh* (*ckh*³⁹⁹) (Loosli et al., 2003) mutants were obtained by pairwise mating of heterozygous adult carriers. *ckh*^{ne2611} fish were recovered in a small scale screen focusing on CNS defects. The screen setup followed that of Haffter et al. (Haffter et al., 1996), except that an incross was conducted in the F1 generation. The specific locus rate was 1/670 against the *golden* locus and 442 genomes were screened to recover *ne2611*.

Molecular identification of *ne2611*

The *rx3* locus of *ckh*^{ne2611} mutants was analyzed for putative mutations by direct sequencing of PCR products (Sequiseive) of each of the three exons comparing homozygous wild-type with homozygous mutant embryos. Primers were designed to bind intronic sequences flanking the exons to include putative splice site mutations. An exception was exon 1, where the forward primer was designed containing the ATG-start site.

*rx3*_exon1_forward, 5'-GCACGAGGTTCAATGAGGC-3';
*rx3*_exon1_reverse, 5'-AAGTTAGAAGTTAGGATAAAGTTGTCAA-3';
*rx3*_exon2_forward, 5'-TGCACTTTCTCACATATTTCTCACTG-3';
*rx3*_exon2_reverse, 5'-TATTATGCTGTATTAGTTTGAACAGAA-3';
*rx3*_exon3_forward, 5'-ATAAGCTCCTCAACTACATCTTTAACTT-3';
 and
*rx3*_exon3_reverse, 5'-AGACCACTGATTTTGAAGATACAAA-3'.

The only significant alteration was found at nucleotide position 382 of the coding sequence. This T to C transition leads to the introduction of a new *SatI* endonuclease restriction site.

RNA and BAC injections

chk/rx3 cDNA (IMAGp998G108961Q) was obtained from RZPD (Deutsches Ressourcenzentrum für Genomforschung GmbH, www.rzpd.de) and subsequently subcloned into the pCS2+ Vector. *chk*^{ne2611}/*rx3* was cloned by PCR from reverse-transcribed RNA from homozygous *ne2611* mutant embryos, followed by direct cloning using the TOPO cloning kit (Invitrogen) and subcloning into pCS2+:

*rx3*_cDNA_forward, 5'-AAATCGTTCAATGAGGCTTGT-3'; and
*rx3*_cDNA_reverse, 5'-TCTCATCTACCACGCTTCCCTATA-3'

chk/rx3 and *chk*^{ne2611}/*rx3* capped RNA was synthesized using the Ambion mMessage mMachine Kit, following the recommended procedure. Capped RNA was injected at the concentration of 50 or 100 ng/μl into the embryos at the one-cell stage.

The BAC CHORB736A01233Q containing the *rx3* locus was obtained from RZPD, amplified and purified with the Large-Construct Kit (QIAGEN) and injected at a concentration of 35 ng/μl into embryos at the one-cell stage.

Bioinformatic analysis

The JPRED algorithm (Cuff et al., 1998) was used to find a nearly related secondary structure that has been analyzed in detail (<http://www.compbio.dundee.ac.uk/~www-jpred/>). The input was the

protein sequence of Rx3 (ENSDARP0000022866) from the Sanger Centre zebrafish assembly version 4 (Zv4) using the ENSEMBL server. The primary output of the algorithm (1FJL.pdb) was used for further sequence and structure analysis using the MAGE software package version 6.36 (<http://kinemage.biochem.duke.edu/software/mage.php>).

Cell transplantations between *ne2611* and wild type

Wild-type donor embryos were injected with biotin-dextran (Molecular Probes) at the one-cell stage. Thirty to 40 cells were transplanted isotopically and isochronically onto the animal pole of shield-stage wild-type or *ne2611* embryos. Recipient embryos were processed at 30 hpf for immunochemical detection of the biotin tracer.

CLGY469 transgenic donor embryos were injected with 1.5% lysine-fixable (fluoro-ruby) Tetramethylrhodamine Dextran (10,000 *M_r*, Molecular Probes) in water (Ambion) at the one-cell stage. Cell transplantations were as previously described (Ho and Kane, 1990), with recipient and donor embryos maintained in the dark at all stages. Transplantation of around 10 cells was conducted in a homotypic manner at the animal pole at dome stage. The appropriate localization of transplanted cells was checked under fluorescent light, and donor and recipient embryos were documented and subsequently fixed at around 30 hpf.

Uncaging experiments

A solution of DMNB-Caged Fluorescein dextran and biotin, lysine fixable (5 mg/ml; Molecular Probes), was injected into one-cell embryos, which were allowed to develop further in the dark. At the early tailbud stage, the dye was activated in a few cells using a UV-beam (DAPI-channel) focused with a pinhole. Irradiated embryos were imaged at the 24 hpf stage, using the FITC-channel on a Zeiss Axioplan2 Microscope with a Zeiss Axiocam Hrm Camera and the Axiovision Software Package (Zeiss), and subsequently fixed overnight in 4% paraformaldehyde at 4°C and processed for anti-fluorescein immunocytochemistry.

In situ hybridization and immunohistochemistry

Probe synthesis, in situ hybridization and immunohistochemistry were carried out according to standard protocols (Hammerschmidt et al., 1996). The anti-Phospho-Histone H3 antibody (Upstate Biotechnology) was used in a final dilution of 1/200. Purified rabbit anti-GFP antibody (ams biotechnology) was used in a 1/500 to 1/1000 dilution. They were revealed using FITC-conjugated goat anti-rabbit secondary antibody (Jackson ImmunoResearch Laboratories) or Cy3-conjugated goat anti-mouse secondary antibody (Jackson ImmunoResearch Laboratories) (1/200). Embryos were scored and photographed under a Zeiss SV 11 stereomicroscope or a Zeiss Axioplan photomicroscope.

Isolation and mapping of the *CLGY469* insertion

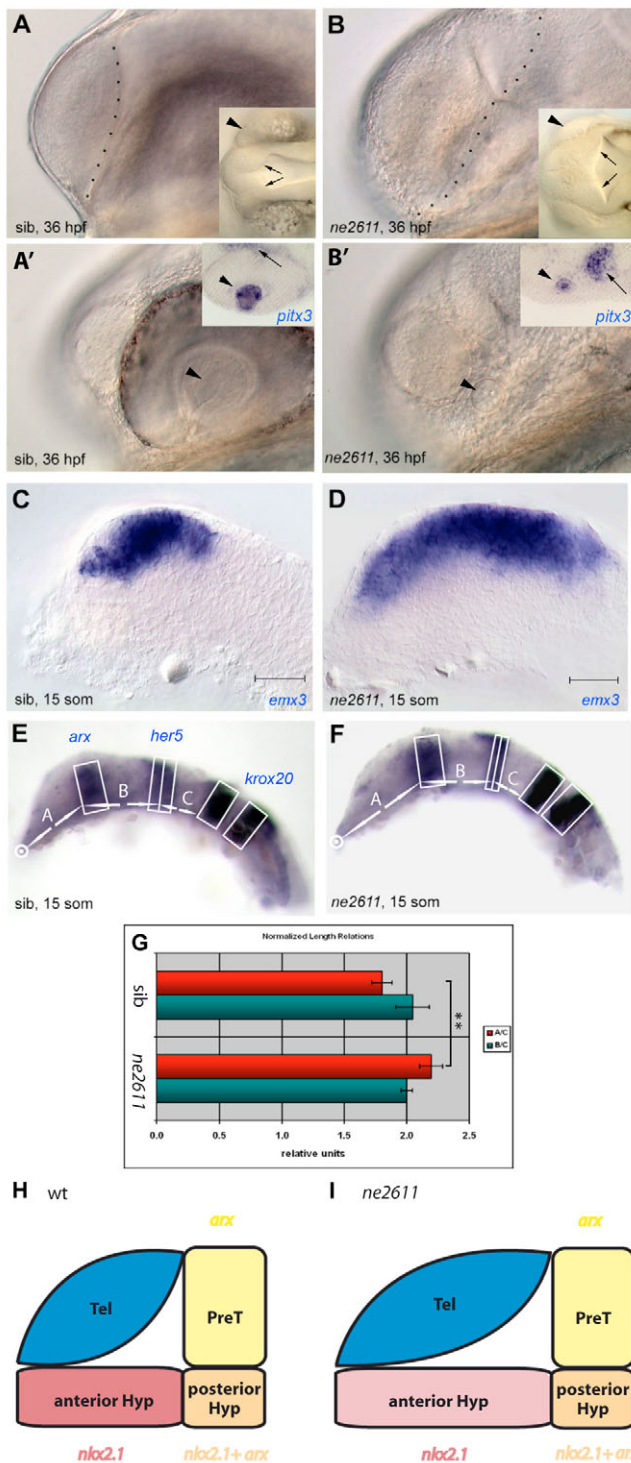
CLGY469 was recovered in a retrovirus-mediated large-scale enhancer detection screen for its expression in the retina. The 3' sequence flanking the insertion was identified by linker-mediated PCR as described previously (Ellingsen et al., 2005). This sequence (TAAAAAAAAAATTTGGGGT-CAATATTACAAG) maps to chromosome 10, 37,390 base pairs upstream of the *rx3* locus (Sanger Centre zv5 release).

RESULTS

Selective enlargement of the anteriormost forebrain domain in *ne2611* mutant embryos

In *ne2611* homozygous embryos at 36 hours post-fertilization (hpf), the constriction separating the telencephalon from the diencephalon lies far posterior compared with wild type (wt) and the diencephalic ventricle is wide open (Fig. 1A,B) (*n*>100, 100% of cases); of the eye, only a small lens is visible (Fig. 1A',B', arrowheads). By contrast, the size of the nasal placodes and epiphysis were not affected.

Telencephalic expansion in *ne2611* was confirmed at the 15-somites stage with molecular markers (*emx3* – previously *emx1*-, *emx2*, *pax6.1*) (Fig. 1C,D; data not shown), and occurs along the anteroposterior (AP) and mediolateral axes. To determine whether this phenotype reflected broader AP patterning defects, we compared the relative sizes of the different forebrain and midbrain



domains (telencephalon, hypothalamus, prethalamus, thalamus, preteum and midbrain). We used *lhx5* and *arx* as markers of the prethalamus and posterior hypothalamus at 15 somites, and *nkx2.1b* to reveal the anterior and posterior hypothalamus (Fig. 1E,F; data not shown; see also scheme in Fig. 1H,I). *her5* expression identified the midbrain-hindbrain boundary, and the size of the anterior hindbrain, limited by *krox20*, served as a reference to correct for variations in embryo length. We confirmed that *ne2611* embryos suffer from substantially elongated neural tissue anterior to the prethalamus (Fig. 1G, red bars, $P < 0.01$, $n = 10$ embryos measured for

Fig. 1. Enlarged telencephalon and lack of retina in *ne2611*. All views are lateral, anterior left. (A-B') Compared morphology of *ne2611* (B,B') and wild-type siblings (sib; A,A') at 36 hpf; views with parasagittal and lateral focus, respectively. (A,B) Note the enlarged telencephalon, delimited by a dashed line, in *ne2611*. Insets are dorsal views of the same embryos showing absence of the retina (arrowheads) and an expanded diencephalic ventricle (arrows) in *ne2611*. (A',B') Note the maintenance of a lens (arrowhead) in *ne2611*, albeit smaller than in wild-type siblings. Insets show expression of *pitx3*, molecularly identifying the lens (arrowheads) in both genotypes. The adjacent domain of *pitx3* expression (small arrows) is hypothalamic, it is displaced towards the lens in *ne2611* due to the absence of eyes. (C,D) Compared expression of the telencephalic marker *emx3* at the 15-somite stage in *ne2611* (D) and wild-type siblings (C); scale bar: 0.02 mm. The mutants display a massive anteroposterior enlargement of the *emx3* domain. (E-G) Relative anteroposterior sizes of the anteriormost forebrain (domain A) versus prethalamus, thalamus, preteum and midbrain (domain B) at 15 somites in *ne2611* (E) compared with wild-type siblings (F). (G) Measurements are normalized to the size of the anterior hindbrain (domain C), and the domains are defined with the genes indicated in E. Bars indicate s.e.m. The difference in A/C length between wild type and *ne2611* is statistically significant (two-sample independent Student's *t*-test, P values are given in the text). (H,I) Schematic representation of the size of the different anterior forebrain territories in wild type versus *ne2611* siblings at 15 somites. The genes used as landmarks are color coded (yellow: *arx* only, prethalamus; red: *nkx2.1* only, anterior hypothalamus; orange: *arx+nkx2.1*, posterior hypothalamus). Prethalamus and posterior hypothalamus are unchanged in the mutants. The anterior hypothalamus appears elongated, but might be simply stretched (hence the lighter red color) by the anteroposterior enlargement of the telencephalon. Later, the anterior hypothalamus appears reduced or missing (see also Fig. S11,J in the supplementary material).

each genotype), and found that this phenotype is local, as the prethalamus itself, as well as structures located posterior to the *lhx5/arx* domain, is unchanged compared with wild-type siblings (Fig. 1G, blue bars, $P = 0.75$, i.e. no significant change, $n = 10$ embryos measured for each genotype) (size of the *arx* domain between wild type and *ne2611*: $P = 0.15$, i.e. no significant change, $n = 10$ embryos measured for each genotype) (schematized in Fig. 1H,I).

We next analyzed *ne2611* embryos for potential patterning phenotypes in telencephalic organization, as well as for the presence of cells having maintained molecular eye identity. We found that the telencephalon maintains a grossly normal dorsoventral polarity [see the dorsal and ventral telencephalic markers *emx3* (Fig. 3D-F) and *dlx2a* (see Fig. S1A,B in the supplementary material), respectively, and a normal mediolateral patterning (see Fig. S1C,D in the supplementary material)]. We noted, however, a perturbed expression of several regional markers, such as *flh* (telencephalic domain absent in *ne2611*) or *emx2* (scattered in *ne2611*) (see Fig. S1E-H in the supplementary material). This prompted us to analyze whether cells with retinal identity were present in the telencephalic domain of mutant embryos. We found that the enlarged telencephalon of *ne2611* never expressed retinal markers at post-somitogenesis stages (see *otx2* in Fig. 2A,B, and *atoh7* – previously *ath5* – and *vax2*, not shown).

The absence of expression of eye markers could result from the non-specification or the non-maintenance of eye precursors, and, to resolve this issue, we probed *ne2611* mutants for the expression of

the earliest eye-field markers. In order of appearance, we selected *rx3* (at 70% epiboly), followed by *rx1* and *rx2* (at the 3-somite stage) (Chuang et al., 1999; Chuang and Raymond, 2001). We found that *rx3* and *rx1* expression followed a normal spatiotemporal pattern in *ne2611* mutants compared with their wild-type siblings (Fig. 2C-H), but that their expression was lost during somitogenesis (not shown). By contrast, *rx2* was never expressed (Fig. 2I-K). Thus, an incomplete eye-field identity (*rx3*⁺, *rx1*⁺ but *rx2*⁻) is specified in *ne2611*, but this transient phase is followed by the loss of expression of all retinal markers.

ne2611 is a null allele of *rx3/chokh*

Reduced or absent eyes characterize the zebrafish mutants *headless* (*hdl*; *tcf711a*) (Kim et al., 2000), *masterblind* (*mbl*; *axin1*) (Heisenberg et al., 2001; van de Water et al., 2001) and *chokh* (*ckh*; *rx3*) (Kennedy et al., 2004; Loosli et al., 2003; Rojas-Munoz et al., 2005). In addition, *hdl* and *mbl* embryos display various degrees of brain posteriorization leading to forebrain truncations, while the existing *ckh* alleles *ckh*^{s399}, *ckh*^{w29} and *ckh*^{hu499} were described as not affecting telencephalic development (Kennedy et al., 2004; Loosli et al., 2003). We found, however, that *ne2611* is allelic to *ckh* (23 embryos lacking eyes in 78

embryos from a *ne2611/+* × *ckh*^{s399/+} intercross in two independent experiments). Sequencing of the *rx3* cDNA from *ne2611* embryos revealed a T to C transition within exon 2 in nucleotide position 382 (Fig. 3A), leading to a Serine to Proline substitution at amino acid position 128 of the Rx3 protein (T382N, Fig. 3B,C). Comparison using the JPRED algorithm with the structure of the *Drosophila* Paired homeodomain predicts this substitution to a coiled domain separating helix 1 and 2 of the Rx3 homeodomain.

We were puzzled that no telencephalic defects had been reported in the studies of existing *ckh* alleles (Kennedy et al., 2004; Loosli et al., 2003; Rojas-Munoz et al., 2005). The above T382N mutation segregated with the *ne2611* telencephalon and eye phenotypes in DNA sequenced from eight independent embryos. The mutation creates a *Sat1* restriction site that also segregated with loss of eyes and expanded telencephalon in more than 50 embryos tested by PCR and *Sat1* digestion (not shown). In addition, we found that all eyeless embryos from a *ne2611/+* × *ckh*^{s399/+} intercross, but no embryos with normal eyes from such crosses, had an enlarged telencephalon (not shown). We also could rescue both the retinal and telencephalic defects of *ne2611* embryos following injection of BAC CHORB736A01233Q, which contains the *rx3* locus (Sanger centre and RZPD; 79% of the mutant embryos were at least partially rescued, *n*=64; Fig. 3G-K). Finally, a re-analysis of *ckh*^{s399} revealed that mutant embryos display an enlarged telencephalon identical to *ne2611* (100% of cases, *n*=23; Fig. 3D-F, see also Fig. 4D). We conclude that *ne2611* is an allele of *ckh*, henceforth referred to as *ckh*^{ne2611}, and reveals a previously undiscovered role of Rx3 in telencephalic development.

As mentioned above, structural considerations predict that the Rx3^{ne2611} protein is dysfunctional, and we found the telencephalic and eye phenotype caused by the *ne2611* mutation to be as severe as those of *ckh*^{s399}, which truncates the Rx3 homeodomain (Loosli et al., 2003). This suggests that *ne2611* might represent a null allele of *rx3*. To support this interpretation, we overexpressed *rx3*^{ne2611} RNA in wild-type embryos. Ectopic expression of wild-type *rx3* mRNA produced embryos with head truncations at 24 hpf in a dose-dependent manner (10% of cases, *n*=56, Fig. 3L,N). By contrast, no morphological defects were noted following injection of *rx3*^{ne2611} mRNA (Fig. 3M,N). These results suggest that *ne2611* is a null allele of *rx3*.

Rx3 controls patterning of the telencephalon and eye field at gastrulation

Zebrafish *rx3* expression is initiated at late gastrulation and is first restricted to the presumptive eye field and hypothalamus (Chuang et al., 1999), which abut the telencephalic primordium (Wilson and Houart, 2004). To determine whether the telencephalic phenotype of *ckh* reflects an early role of Rx3 in anterior neural plate development, we examined expression of telencephalic markers during these stages in both *ckh*^{ne2611} and *ckh*^{s399}.

tlc is one of the earliest markers of the presumptive anterior forebrain at late gastrulation, and is excluded from the hypothalamus and eye field (Houart et al., 2002) to become adjacent to the *rx3* domain at tail-bud stage (Fig. 4E,F). The earliest phenotype in both *ckh*^{ne2611} and *ckh*^{s399} mutants was the posterior expansion of *tlc* staining at the tail-bud stage (100% of *ckh*^{ne2611} mutant embryos, confirmed by genotyping, have expanded *tlc* expression, *n*>50; 24% of embryos from a cross between *ckh*^{s399} heterozygotes have a similar phenotype, *n*=82; Fig. 4A-D). Ectopic *tlc* expression was prominent from bud stage onwards (Fig. 4E-G). *emx3* and *foxl1* (*bfl*) also label the presumptive telencephalon, and we compared their expression with that of *tlc* expression in a time-course analysis. *foxl1* expression appeared identical in wild type and *ckh*^{ne2611}

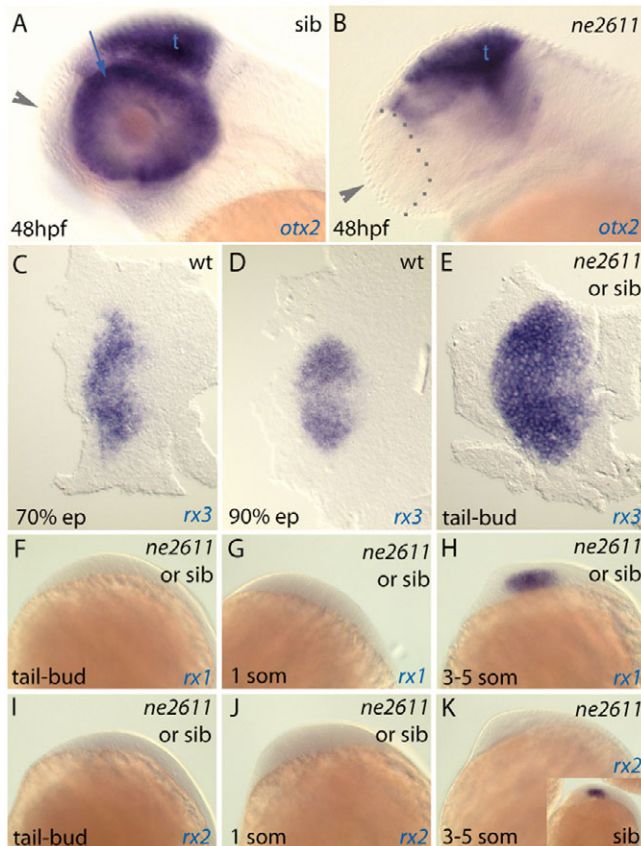


Fig. 2. The eye field is partially specified but is not maintained in *ne2611* mutants. All views, anterior left. (A,B) Expression of *otx2*, labeling the wild-type retina (A, blue arrow) but not the telencephalon, is absent in the enlarged telencephalon of *ne2611* sibling embryos (B). Lateral views; t, optic tectum; telencephalon (arrowhead) delimited by gray dots in B. (C-H) Expression of the earliest eye-field marker *rx3* (C-E; dorsal views of flat-mounted embryos), and of *rx1* (F-H; lateral views of whole embryos), is initiated normally in *ne2611*. (I-K) Expression of *rx2*, normally detected at 3-somites in wild type (K, inset), is never initiated in *ne2611* (K). Lateral views of whole embryos.

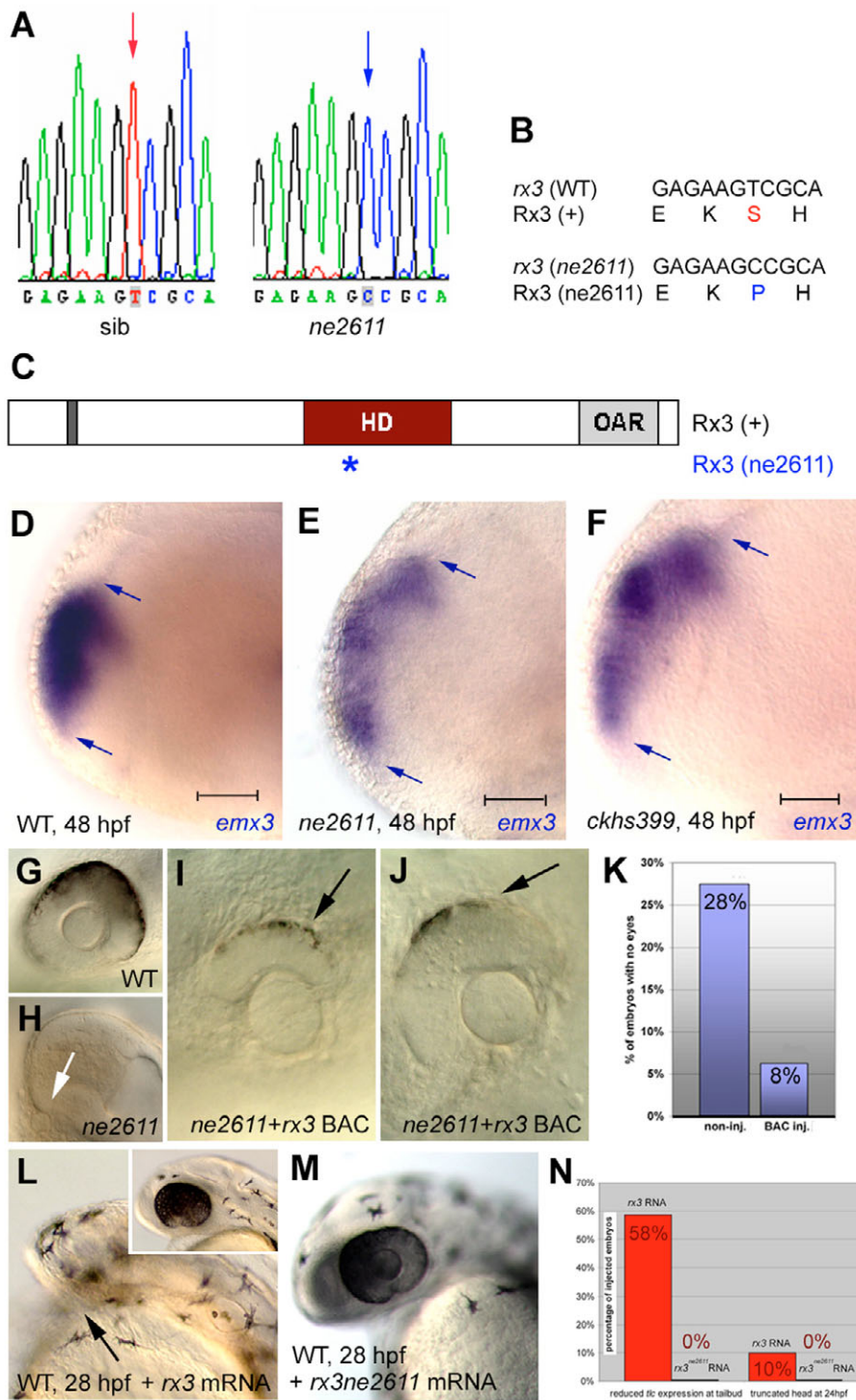


Fig. 3. *ne2611* is a new null allele of *rx3*. (A) Sequencing trace data of *rx3* cDNA from a *ne2611* mutant (right) and a wild-type sibling (left) reveals a T to C transition (arrows). (B,C) Rx3 protein sequences (B) and structures (C) in wild type (+) and *ne2611* mutants. The *ne2611* mutation leads to a Serine to Proline exchange within the Rx3 homeodomain (asterisk in C). Dark gray box, octapeptide; red box, homeodomain; light gray box, otp-ristaless-rx domain. (D-F) Expression of the telencephalic marker *emx3* in wild-type (D), *ne2611* (E) and *ckh^{s399}* (F) embryos at 48 hpf (lateral views, anterior left; scale bar: 0.02 mm). *ckh^{s399}* embryos display a telencephalic expansion similar to that of *ne2611* mutants. (G-K) Embryos from a *ne2611*/+ × *ne2611*/+ cross were injected at the one-cell stage with BAC CHORB736A01233Q containing the *rx3* locus and are observed at 24 hpf. (L,J) Representative injected *ne2611* mutants; note the restoration of the retina compared with uninjected wild type (G) or *ne2611* (H; small lens in H indicated by the white arrow). (K) Percentage of embryos lacking eyes after BAC injection compared with non-injected embryos. BAC injection restored retinal development in 79% of mutant embryos. (L,M) Phenotypes triggered by ectopic expression of wild-type *rx3* versus *rx3^{ne2611}* mRNA. Wild-type embryos were injected at the one-cell stage and observed at 24 hpf (lateral views, anterior left). Ectopic expression of *rx3* causes head truncations (L, arrow; compare with wild type, inset) whereas *rx3^{ne2611}* has no effect (M). (N) Percentage of embryos showing reduction of *tlc* expression (left two bars) (see Fig. S2 in the supplementary material) or head truncation (right two bars) following injection of *rx3* or *rx3^{ne2611}* mRNA (as indicated).

mutants at bud stage (Fig. 4H), but was expanded posteriorly from the one-somite stage onwards; *emx3* expression was unaffected in *ckh^{ne2611}* embryos until the 3-somite stage (Fig. 4K-M), only becoming visibly ectopic a few hours afterwards (not shown). Double stainings further demonstrated that *tlc* and *foxf1* expression largely overlaps *rx3* expression at the stages when they become ectopic in *ckh* (Fig. 4G,J), suggesting that these posterior expansions result from a failure to be repressed within the *rx3* domain. Accordingly, overexpression of *rx3*, but not *rx3^{ne2611}*, by mRNA injections into wild-type embryos, reduced expression of early

telencephalic markers such as *tlc* and *hex1* (*anf*) at the tail-bud stage (58% of cases, *n*=18; see Fig. S2 in the supplementary material; data not shown).

Given that *rx3* expression starts at late gastrulation, we conclude that telencephalic expansion in *ckh* reflects a role of Rx3 at its onset of expression in limiting telencephalic extent in the anterior neural plate. This function is normally manifested by the early downregulation of *tlc* expression within the *rx3*-positive domain, followed by the downregulation of *foxf1* and *emx3*.

Rx3 function accounts for the higher proliferation of eye-field cells when compared with telencephalic precursors

We next addressed the processes underlying this early function of Rx3. Several non-exclusive mechanisms affecting early telencephalic precursors might account for telencephalic expansion in *ckh*: their reduced cell death, their increased proliferation, or an ectopic specification of such precursors within the anterior neural plate. We analyzed cell death profiles in *ckh^{ne2611}* embryos between

90% epiboly and 3 somites using acridine orange and immunostaining of cleaved caspase 3. We did not detect any significant difference between mutant and wild-type siblings at these stages ($n=19$), although we did observe apoptosis in the telencephalon of *ckh^{ne2611}* mutants at 28 hpf (not shown).

We next monitored proliferation in the presumptive telencephalon and eye field using anti-phosphohistone H3 (PH3) immunocytochemistry. In wild-type embryos at tail-bud stage, the telencephalic anlage was identified by its expression of *tlc* (domain 3 in Fig. 5) and the eye field by *rx3* (domain 1 in Fig. 5). Corresponding domains in *ckh^{ne2611}* mutants were defined as *tlc* positive, *rx3* negative (domain 4 in Fig. 5), versus *rx3* positive (domain 2 in Fig. 5). Counts of PH3-positive cells within each domain revealed significantly decreased numbers of cells in M phase within the *rx3*-positive domain in *ckh^{ne2611}* when compared with wild-type siblings ($P<0.02$; compare domains 1 and 2), whereas proliferation within the more anterior *rx3*-negative domain is not affected (compare domains 3 and 4; $P=0.86$; Fig. 5A,B,E-G). This observation suggests either that Rx3 promotes proliferation inside the eye field during gastrulation, and/or that the acquisition of presumptive telencephalic identity imposes a low proliferation

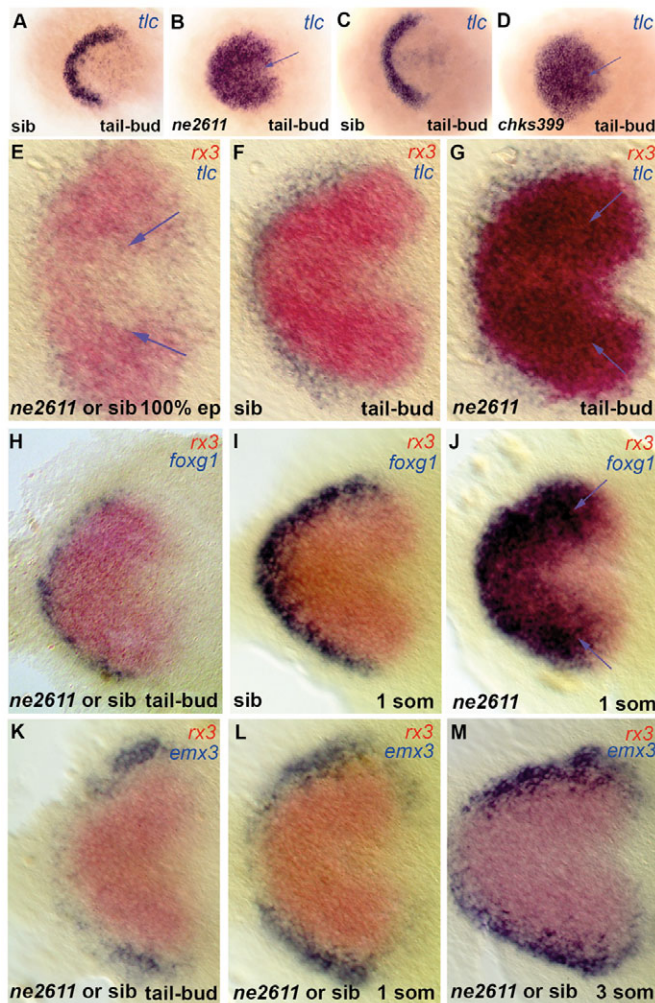
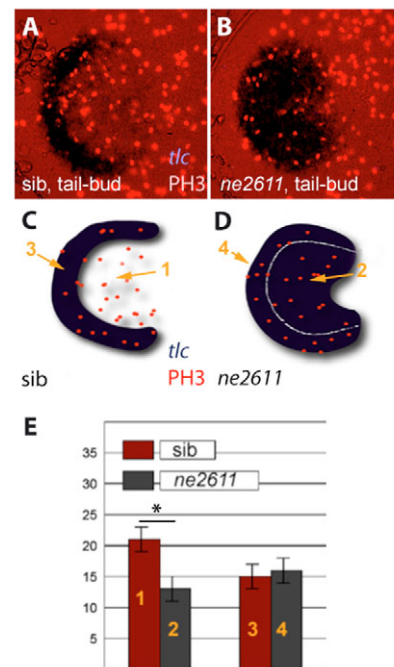


Fig. 4. Rx3 controls early patterning of the presumptive anterior forebrain. Expression of the markers indicated (color coded) in *ckh^{ne2611}* (B,G,I), *ckh^{s399}* (D) or their wild-type siblings (A,C,F,I); E,H,K-M are non-genotyped embryos from crosses between *ckh^{ne2611}/+* heterozygotes. All views are dorsal anterior left in whole embryos (A-D) or flat mounts (E-M). (A-D) *tlc* expression identifies the presumptive telencephalon at tail-bud stage and is massively expanded in both *ckh^{ne2611}* (B) and *ckh^{s399}* (D) mutants compared with their wild-type siblings (A,C). (E-G) No difference in *tlc* expression is observed between wild-type and mutant embryos at 100% epiboly, when *tlc* expression is downregulated from the presumptive eye and hypothalamus fields, labeled by *rx3* (see the few remaining *tlc*-positive cells in the *rx3*-positive domain at 100% epiboly; arrows in E, absent in F). At tail-bud stage the ectopic *tlc* expression overlaps the *rx3* domain (G, blue arrows). (H-J) Expansion of *foxg1* across the eye field is absent at tail-bud stage (H) but is visible at the one-somite stage (J, blue arrows). (K-M) The relative expression of *emx3* and *rx3* are not noticeably affected in mutants before the 3-somite stage.



Rx3 accounts for the higher proliferation of eye field versus telencephalic precursors.

(A,B) Immunodetection of the M-phase marker Phosphohistone-H3 (red nuclei) in the anterior neural plate of *ckh^{ne2611}* mutants (right panel) and their wild-type siblings (left panel) at tail-bud stage (dorsal views, anterior left). *tlc* expression (ISH, blue) serves as a marker of the presumptive telencephalon in wild-type embryos and of the telencephalon+eye field in *ckh^{ne2611}*.

(C,D) Schematic representation of the embryos in A,B to localize the presumptive telencephalic and eye fields in wild-type embryos (domains 3 and 1, respectively) and the corresponding territories in *ckh^{ne2611}* siblings (domains 4 and 2, respectively) at tail-bud stage. (E) Number of PH3-positive cells in domains 1-4 (see C,D) in wild-type (red) versus *ckh^{ne2611}* (gray) embryos. Bars indicate standard errors. Proliferation is significantly decreased in the presumptive eye field, but is unaltered in the presumptive telencephalon, in *ckh^{ne2611}* compared with wild-type embryos at tail-bud stage (two-sample independent Student's *t*-test, *P* values are given in the text).

rate. A role for Rx3 in controlling positively proliferation of retinal precursors had been suspected at the stage of optic vesicle evagination (Loosli et al., 2003). We show that Rx3 may exert this role already within the anterior neural plate.

Rx3 attributes eye versus telencephalic identity to anterior forebrain precursors

Decreased proliferation of retinal precursors might partially account for the lack of eyes of *ckh* mutants, but cannot be the direct cause of telencephalic expansion. By contrast, the co-expression of *tlc* or *foxg1* and mutant *rx3* RNAs in the presumptive eye-field territory of early *ckh^{ne2611}* embryos (Fig. 4G,J) suggests that telencephalic specification extends posteriorly at the expense of eye identity in the mutants.

To test this hypothesis, we traced the fate of eye-field precursors in *ckh^{ne2611}* mutants. Caged fluorescein was injected into one-cell stage embryos, and was activated in a small number (~10) of eye-field precursor cells at the early tail-bud stage (Fig. 6A,B); the location of the progeny of these labeled cells was then determined at 24 hpf by morphological inspection under fluorescence and

Nomarski optics (Fig. 6C-I). At the early tail-bud stage, the eye and telencephalic fields are intermingled (Woo and Fraser, 1995); however, we found that uncaging at the position indicated in Fig. 6A mostly revealed retinal precursors in wild-type embryos (Table 1); pure retinal clones were recovered in 45% of cases (Fig. 6C), and clones contributing to the retina and other forebrain derivatives except the telencephalon in 45+21=66% of cases (Fig. 6D). This compared with 34% of cases contributing to the telencephalon (Fig. 6E; $n=29$). By contrast, all labeled clones contributed to the telencephalon in *ckh^{ne2611}* embryos (100% of cases, $n=10$; Table 1, Fig. 6F-I). Because extensive labeled clones were recovered in all activated *ckh^{ne2611}* mutants (Table 1), we conclude that retinal precursors lacking Rx3 tend to join the telencephalon. We never detected expression of retinal markers in the expanded telencephalon of *ckh^{ne2611}* (see *otx2* on Fig. 2B, or *atox7* and *vax2*, not shown), supporting the interpretation that presumptive eye-field cells may acquire a telencephalic fate in the absence of Rx3 function.

The role of Rx3 in controlling retinal versus telencephalic identity is cell autonomous

Using transplantation experiments, Winkler et al. (Winkler et al., 2000) proposed that Medaka Eyeless, the ortholog of zebrafish Rx3, is responsible for retinal evagination in a cell-autonomous manner. The same is true for zebrafish Rx3: when large numbers of wild-type cells (25-40) are homotopically transplanted to the animal pole of a shield-stage *ckh^{ne2611}* embryo, they often give rise to a normally evaginated retina (36% of cases, $n=11$), which is always composed exclusively of wild-type cells (Fig. 7A). By contrast, *ckh^{ne2611}* cells transplanted into a wild-type host never contribute to the retina (not shown).

Our results support an earlier role of Rx3 in specification choices of eye field versus telencephalic identity. To determine whether this earlier function of Rx3 was also cell autonomous, we uncoupled it from morphogenesis control by transplanting a small number of cells (4-5). Indeed, we observed that when a low number of wild-type cells are transplanted into the presumptive eye field of a *ckh^{ne2611}* host, these integrate into the anterior forebrain and no evagination takes place (0% of cases, $n=14$; Fig. 7B). This finding suggests either that the wild-type cells are topologically misplaced in a mutant environment but keep their eye-field identity, or that when in a minority inside a Rx3-depleted environment, the wild-type cells are subjected to a non-autonomous cell fate change and adopt telencephalic identity.

To discriminate between these two possibilities and to assess the identity of the progeny of these transplanted cells, we made use of a sensitive transgenic retinal marker. In an enhancer detection screen following the technology described by Ellingsen et al. (Ellingsen et al., 2005), we recovered a transgenic line, *CLGY469*, which expresses YFP in the retina but not in the telencephalon (Fig. 7D). As mapping indicates, this line is likely to detect an *rx3* enhancer (see Materials and methods). YFP expression is observed in *CLGY469* transgenic embryos from the tail-bud stage onwards (see Fig. 7C for a 5-somite embryo), and thus precedes retinal evagination and is an early marker of retinal specification. We therefore used *CLGY469* expression as a selective and sensitive marker for retinal specification in our transplantation experiments with a low number of cells. When a few wild-type cells taken from the animal pole of a *CLGY469* transgenic donor were homotopically and isochronically transplanted into a *ckh^{ne2611}* non-transgenic host at the sphere stage, we repeatedly observed that some of these cells turn on expression of the transgene (80% of cases, $n=5$; Fig. 7F), in

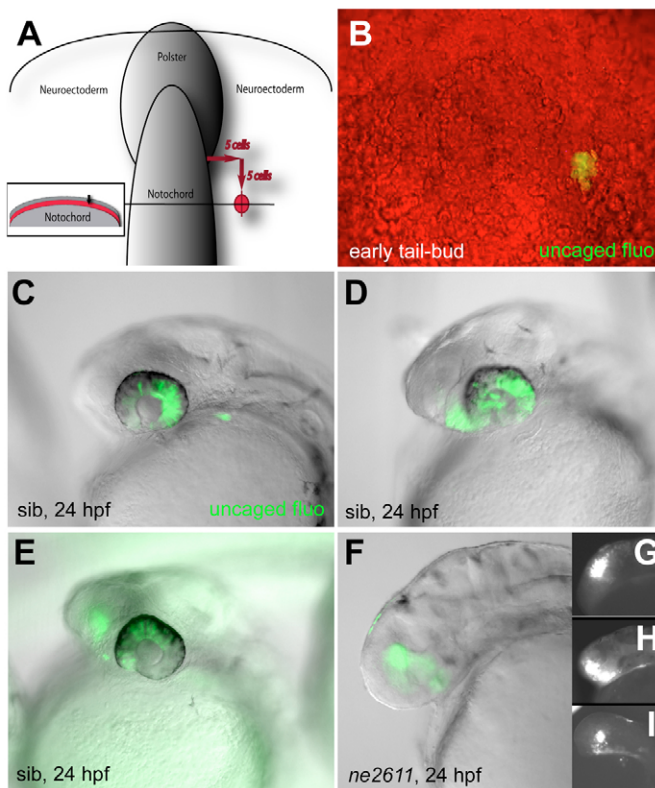


Fig. 6. Cells of the presumptive eye field acquire a telencephalic identity in the absence of Rx3. (A,B) Location of uncaged cells compared with the notochord, polster and enveloping layer (inset in A) at the early tail-bud stage, and photomicrograph of the fluorescent clone immediately following uncaging (B) (dorsal views, anterior up). (C-E) Fate of the uncaged progeny in wild-type embryos at 24 hpf (overlay of fluorescence and Nomarski optics views, anterior left). (C) Retina only (45% of cases); (D) retina and anterior hypothalamus (21% of cases); (E) retina and telencephalon (31% of cases) (see also Table 1). (F-I) Fate of the uncaged progeny in *ckh^{ne2611}* embryos at the 24 hpf stage (overlay of fluorescence and Nomarski optics views in F, fluorescence only in G-I, anterior left). All clones contribute to the telencephalon (100% of cases, see Table 1).

Table 1. Fate of cell clones uncaged, as indicated in Fig. 6A, at the early tail-bud stage in wild-type and *ckh^{ne2611}* mutant siblings

Experiment	Wild type					<i>ckh^{ne2611}</i>		
	n	Ret w/o Tel		Tel±others		n	Tel±others	
		Retina only	Ret+ventral CNS*	Ret+Tel	Tel		Tel	Tel+Tec
1	3	1	1	1	0	1	1	0
2	12	4	3	4	1	2	2	0
3	5	3	2	0	0	3	2	1
4	7	4	0	3	0	2	2	0
5	2	1	0	1	0	2	2	0
Sum	29	13	6	9	1	10	9	1
%	100	45	21	31	3	100	90	10
Total %			66		34			100

*Ventral structures of the rostral CNS (optic nerve and hypothalamus).

Five independent experiments were conducted. Labeled clones were recovered in all embryos. The values listed are the number (or percentage) of uncaged embryos where labeled clones contribute to the structures indicated.

Ret, retina; Hyp, hypothalamus; Tel, telencephalon; Tec, tectum.

conditions where no morphological retina is visible. We can rule out that the transplanted cells, although YFP-negative at the time of transplantation, were already determined to express the transgene: similar grafts into non-transgenic wild-type hosts usually gave rise to YFP expression in cells that populated the retina, but not in cells that contributed to other structures (usually the telencephalon; Fig. 7G; 86% of cases, $n=7$). We conclude that the maintenance of eye-field identity, and repression of telencephalon fate, is cell-autonomously encoded by Rx3 expression.

DISCUSSION

Our results demonstrate that, at late gastrulation, zebrafish Rx3 is the determinant biasing cells of the eye field towards a retinal fate at the expense of a telencephalic fate. This function is performed in a

cell-autonomous manner, and is accompanied by the repression of *tlc* and *foxf1* expression by Rx3. These findings, which identify a molecular component of the anterior forebrain-patterning cascade, shed light on the processes segregating the telencephalon and eye field during anterior forebrain patterning. Given the previously demonstrated roles of Rx3 in controlling retinal evagination (Kennedy et al., 2004; Loosli et al., 2003; Loosli et al., 2001; Winkler et al., 2000) and formation of the pigmented retinal epithelium (Rojas-Munoz et al., 2005), they also suggest that the link between several crucial steps of retinal development, namely the maintenance of retinal precursors, the morphogenetic shaping of the retina into an optic cup and the specification of the pigmented retinal epithelium, are accomplished at least in part by the use of the same molecule, Rx3.

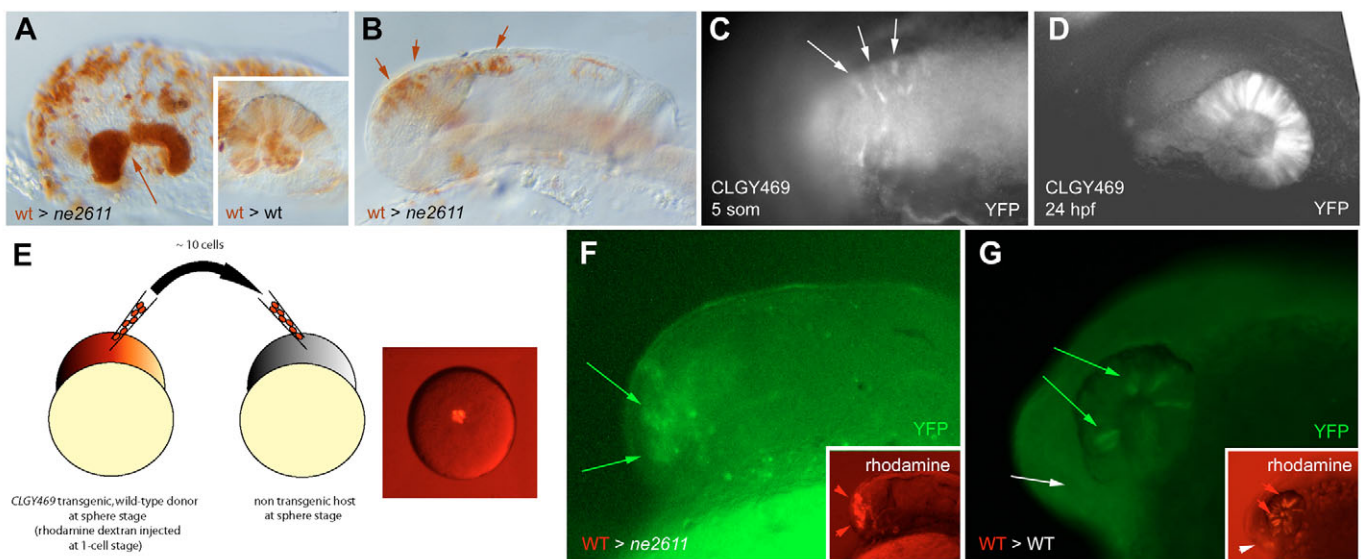


Fig. 7. Rx3 controls eye field versus telencephalic fate in a cell-autonomous manner. (A,B) Transplantation of wild-type cells (brown) into the anterior forebrain of a *ckh^{ne2611}* or wild-type (inset) host. (A) When a large number of cells are transplanted, retinal structures are rescued and evaginate (arrow). They are entirely composed of wild-type cells, whereas transplanted cells distribute randomly in a wild-type host (inset). (B) When a low number of cells is transplanted, retinal evagination does not occur. (C,D) Expression of YFP (revealed by anti-GFP immunocytochemistry) in transgenic CLGY469 embryos before (C; dorsal view) and after (D; lateral view) retinal evagination. YFP expression is restricted to eye-field cells and their descendants. It is absent in *ckh^{ne2611}* mutants (see text). (E-G) Transplantation of a few wild-type cells transgenic for CLGY469 into the animal pole of a *ckh^{ne2611}* (F) or wild-type (G) host. In a mutant host (F), retinal evagination does not occur (as in B), but expression of the transgene (green) is rescued in some transplanted cells (red, inset), indicating rescue of the eye-field fate. In a wild-type host, transplanted cells contribute to the retina (red arrowheads) and telencephalon (white arrowhead; G, inset), but only retinal cells express the transgene (G, green arrows, as opposed to white arrow).

The complete *ne2611* phenotype results from the loss of Rx3 function

Previous analyses of *ckh* mutant alleles did not report telencephalic defects (Kennedy et al., 2004; Loosli et al., 2003; Rojas-Munoz et al., 2005), making it crucial to ascertain that the *ne2611* phenotype results solely from the loss of Rx3 function. Our observations that telencephalic and eye phenotypes in *ckh^{ne2611}* always co-segregate and are concomitantly rescued by injection of an *rx3*-containing BAC support the interpretation that Rx3, directly or indirectly, controls the early development of both telencephalon and eyes. A further decisive argument towards this interpretation is provided by our re-analysis of *ckh^{s399}*, and the finding that *ckh^{s399}* mutants display expanded *tlc* and *emx3* expression from the tail-bud and somite stages onwards, respectively, in a manner indistinguishable from *ckh^{ne2611}* (Fig. 3F, Fig. 4D). These observations lead us to propose an early role for Rx3 in limiting extension of the telencephalic field at late gastrulation. This finding is in keeping with the onset of zebrafish *rx3* expression during gastrulation, earlier than *rx1* and *rx2*, and in a domain adjacent to but non-overlapping with the presumptive telencephalon (Chuang et al., 1999). The phenotype of *Rx* mutant mice is complex and includes both lack of eyes and anterior forebrain truncations (Mathers et al., 1997). Given that the mouse harbors a single *Rx* gene, successive functions for Rx might be difficult to appreciate experimentally; however, the precocious downregulation of retinal markers in these mutants is compatible with an early role of Rx in controlling retinal specification. Medaka, where loss of Rx3/el seems to be only associated with morphogenesis defects, is a more puzzling case (Loosli et al., 2001; Winkler et al., 2000). Unlike zebrafish Rx3 (Chuang and Raymond, 2001) (this paper), overexpression of Rx3/el in Medaka does not cause head truncations (Loosli et al., 2001). Rx3/el can, however, rescue the *ckh* phenotype (Loosli et al., 2003). Thus, zebrafish Rx3 and Medaka Rx3/el might have similar regulatory capacities, but not all can be revealed in the Medaka context. This observation might relate to the recent demonstration of a genetic background-dependent effect of Rx3 in zebrafish (Rojas-Munoz et al., 2005). However, the evolutionary conservation of an early expression of Rx genes during brain development in vertebrates and invertebrates (Bailey et al., 2004) lends support to a primary ancestral role of Rx in the specification of early anterior progenitors.

Rx3 function maintains retinal versus telencephalic identity

The expanded telencephalon and lack of eyes of *ckh* mutants might have been subsequent but unrelated phenomena reflecting two independent roles of Rx3. Contrary to this hypothesis, we found that retinal precursors, although at least partially specified (e.g. expressing *rx3* and *rx1* RNAs, Fig. 2C-D,H), are affected already at late gastrulation in *ckh^{ne2611}* mutants. This is noticeable in two ways: first, their proliferation is reduced (Fig. 5B,E); and second, their identity is altered, as revealed by the co-expression of *tlc* or *foxx1* and *rx3* within the eye field in *ckh^{ne2611}* at the tail-bud or one-somite stage (Fig. 4G,J), combinations never observed in wild-type embryos. Direct tracing of eye-field cells from the tail-bud stage further demonstrates that these cells, in mutants, populate the telencephalon instead of the retina and probably acquire a telencephalic fate (Fig. 6). Together, these results are best interpreted by postulating an early role of Rx3 in permitting the maintenance of retinal versus telencephalic specification during gastrulation.

Based on overexpression studies, zebrafish Rx1 and Rx2 were postulated to promote retinal versus telencephalic identity (Chuang and Raymond, 2001). Notably however, the telencephalic to retinal fate switch imposed by injection of *rx1* or *rx2* mRNA was only observed at a late stage (neural keel), while no alteration in *emx3* or *foxx1* expression could be detected at the neural plate stage. It will be important to support these data by loss-of-function analyses to determine whether the distinction between the eye and telencephalic identities is a general property of Rx factors, and, if so, whether these factors act in a timely regulated cascade.

An additional phenotype of *ckh^{ne2611}* mutants is the decreased proliferation of eye-field precursors at the tail-bud stage (Fig. 5), suggesting that Rx3, in addition to imparting cell identity, also promotes proliferation of its expressing cells at late gastrulation. This finding is in line with previous analyses of *Xenopus* Xrx1, which has been shown to increase the clonal proliferation of retinal progenitors in ectopic expression experiments (Casarosa et al., 2003). Whether the impaired proliferation of the eye field in *ckh^{ne2611}* mutants is a consequence of the altered identity of these cells or reflects an independent role of Rx3 in proliferation control remains to be resolved. Similarly, Xrx1 promotes both proliferation and retinal identity.

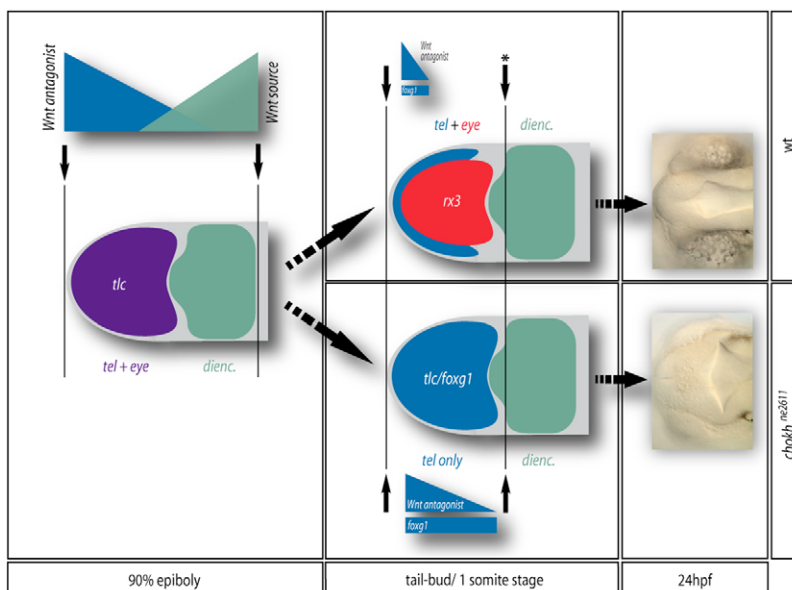


Fig. 8. Model for the segregation of the telencephalic and eye anlage during zebrafish forebrain patterning.

Patterning boundaries are indicated by black arrows. During gastrulation (left panel), a prevalent view is that the forebrain is patterned as a whole by the opposite activities of a posterior Wnt source located at the level of the posterior diencephalon (green gradient) and Wnt antagonists (purple gradient) located at the ANB (Wilson and Houart, 2004). 'High Wnt' defines the presumptive diencephalon (green), whereas 'low Wnt' defines an anterior domain (purple) including the presumptive telencephalon and eyes. At the tail-bud stage (middle panel), a posterior patterning boundary (black arrow with star) is set-up in front of the diencephalon, isolating the anterior forebrain. Within the latter domain, Rx3 activity (red) represses *tlc* expression (blue gradient) and *foxx1* (blue bar) and attributes retinal fate to its expressing cells at the expense of a telencephalic fate, thereby segregating retinal and telencephalic identities (top panel). In the absence of Rx3, retinal precursors acquire a telencephalic fate (bottom panel), leading at 24 hpf to the absence of eyes and an enlarged telencephalon (right panel).

Molecular cascade of Rx3 function in the development of the presumptive eye field versus telencephalon

The initiation of *rx3* expression does not depend on Pax6 or Six3 (Carl et al., 2002), and identifying the upstream regulators of the Rx3-mediated retinal specification cascade will be an important step in our understanding of anterior forebrain patterning. Known targets of Rx3 include *rx2* and *mab21l2*, which are absent or downregulated in *ckh* (Kennedy et al., 2004). *six3* or *pax6.1* expression appeared unaffected in *ckh^{ne2611}* at the 3-somite stage (not shown); however, both genes also label the telencephalic primordium at that stage, preventing a straightforward interpretation of these results. We identify here, however, two new and possibly important targets of Rx3: *tlc* and *foxd1*. Their expression is modified in *ckh^{ne2611}* prior to the normal timing of optic vesicle evagination, strongly suggesting that these genes respond to the early function of Rx3. Whether Rx factors display transcriptional repressor or activator functions is unresolved (Chuang and Raymond, 2001), and our results do not permit us to determine whether the regulation of expression of *tlc* and *foxd1* by Rx3 is direct.

Finally, we observed that *ckh^{ne2611}* cells transplanted into the animal pole of a wild-type host preferentially populate the telencephalon (not shown). Thus, in addition to attributing an eye-field identity to its expressing cells, Rx3 may also endow these cells with specific cell surface recognition properties that distinguish them from telencephalic precursors. This phenomenon might be an integral part of the Rx3-encoded specification maintenance process.

A model for the subdivision of the anterior forebrain into telencephalon and eye field

A major finding of our study is that, at late gastrulation, Rx3 controls cell identity choices between the presumptive telencephalic and retinal fields but spares most other diencephalic domains, with the possible exception of the anterior hypothalamus (see Fig. 1E-I). These results permit for the first time the proposal of a model for the segregation of the telencephalon and eye field (Fig. 8). Following global AP forebrain patterning during gastrulation, a boundary of the patterning field is established between the diencephalon and eye field (Fig. 8, asterisk), demarcating the posterior limit of a patterning process specific to the anterior forebrain and segregating eye versus telencephalic identities. Without Rx3 function, retinal precursors adopt a telencephalic fate, demonstrating that Rx3 biases cell fate choices in bipotential precursors. Whether telencephalic precursors at that stage would also be capable of acquiring a retinal fate remains to be demonstrated. It is also unknown whether these precursors are defined by default by the absence of Rx3 expression, or whether they also necessitate instructive information.

Whether the specific Rx3-mediated anterior forebrain patterning process involves graded positional information, in a manner reminiscent of global forebrain patterning at an earlier stage (Wilson and Houart, 2004), remains unknown. Several findings suggest a possible involvement of Wnt signaling in this early Rx3-dependent process. First, the earliest alteration in gene expression in *ckh^{ne2611}* is the ectopic maintenance of *tlc* expression (Fig. 4A-G; Fig. 8, blue gradient). Second, overexpression of *rx3* by mRNA injection leads to head truncations (Fig. 3), and a similar phenotype is caused by exaggerated Wnt signaling (Kim et al., 2000). Thus, the Rx3 overexpression phenotype might result from a (premature) positive interaction of Rx3 with Wnt activity. Finally, *olSfrp1*, which was recently proposed to also participate in anterior forebrain patterning, belongs, like *Tlc*, to the sFRP family of Wnt-binding factors (Esteve

et al., 2004). Thus, whether *Tlc* activity is instrumental in the anterior forebrain cell-specification defects of *ckh^{ne2611}*, and whether an appropriate source of Wnt is positioned at the eye field/diencephalon border at late gastrulation, remain important issues to address. Another, non-exclusive, interesting candidate that might account for the *ckh^{ne2611}* phenotype is *Foxg1* (Fig. 8, blue bars). However, the early expression domain of *foxd1*, in wild type, is not completely restricted to the telencephalic primordium but also includes a small portion of the ventral retinal field (Lisa Winstanley and C.H., unpublished). Thus, *Foxg1* involvement in telencephalic versus eye specification would be complex and is likely to imply context-dependent activities, which might be related to the presence or absence of Rx3.

We are grateful to K. Imai, R. Koester and other lab members for critical advice during this work, to H. Baier and J. Wittbrodt for the *ckh^{s399}* line, to F. Rosa for help with ENU mutagenesis, and to numerous colleagues for the gift of probes. C.S. and L.B.-C. are supported by a VW Stiftung junior group grant, and C.S., L.B.-C. and T.S.B. by EU 6th Framework contract number LSHC-CT-2003-503466. Work in T.S.B.'s laboratory is further supported by a Sars Centre core grant, by the National Programme in Functional Genomics in Norway (FUGE) in the Research Council of Norway, and by additional funding from the University of Bergen.

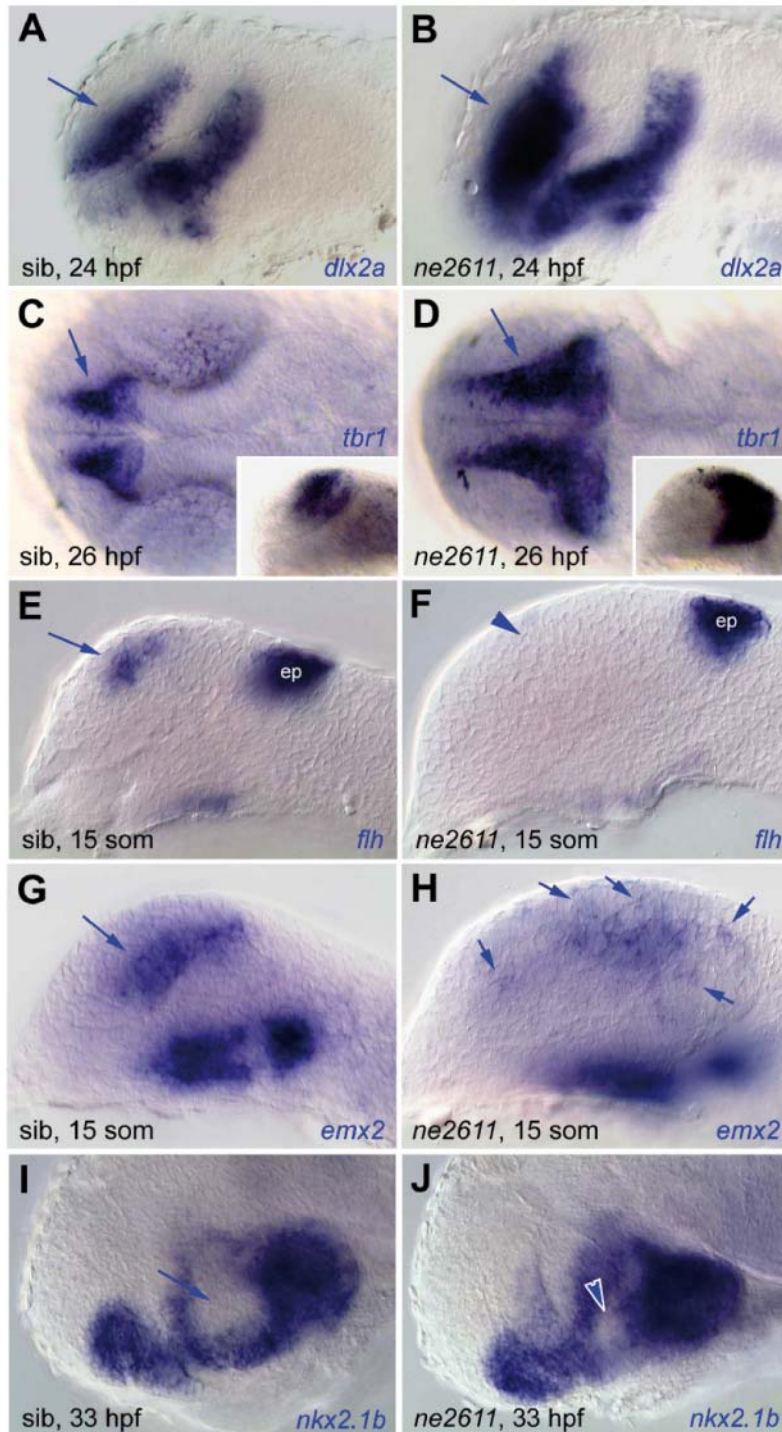
Supplementary material

Supplementary material for this article is available at <http://dev.biologists.org/cgi/content/full/133/15/2925/DC1>

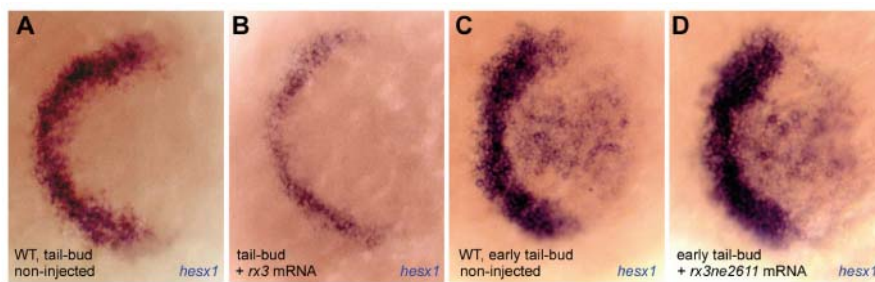
References

- Bailey, T. J., El-Hodiri, H., Zhang, L., Shah, R., Mathers, E. H. and Jamrich, M. (2004). Regulation of vertebrate eye development by Rx genes. *Int. J. Dev. Biol.* **48**, 761-770.
- Carl, M., Loosli, F. and Wittbrodt, J. (2002). Six3 inactivation reveals its essential role for the formation and patterning of the vertebrate eye. *Development* **129**, 4057-4063.
- Casasosa, S., Amato, M. A., Andreazzoli, M., Gestri, G., Barsacchi, G. and Cremisi, F. (2003). *Xrx1* controls proliferation and multipotency of retinal progenitors. *Mol. Cell. Neurosci.* **22**, 25-36.
- Chuang, J. C. and Raymond, P. A. (2001). Zebrafish genes *rx1* and *rx2* help define the region of forebrain that gives rise to retina. *Dev. Biol.* **231**, 13-30.
- Chuang, J., Mathers, P. and Raymond, P. (1999). Expression of three Rx homeobox genes in embryonic and adult zebrafish. *Mech. Dev.* **84**, 195-198.
- Cuff, J. A., Clamp, M. E., Siddiqui, A. S., Finlay, M. and Barton, G. J. (1998). JPred: a consensus secondary structure prediction server. *Bioinformatics* **14**, 892-893.
- Dorsky, R. I., Itoh, M., Moon, R. T. and Chitnis, A. (2003). Two *tcf3* genes cooperate to pattern the zebrafish brain. *Development* **130**, 1937-1947.
- Eagleson, G. W. and Dempewolf, R. D. (2002). The role of the anterior neural ridge and Fgf-8 in early forebrain patterning and regionalization in *Xenopus laevis*. *Comp. Biochem. Physiol. B Biochem. Mol. Biol.* **132**, 179-189.
- Ellingsen, S., Laplante, M. A., König, M., Kikuta, H., Furmanek, T., Hoivik, E. A. and Becker, T. S. (2005). Large-scale enhancer detection in the zebrafish genome. *Development* **132**, 3799-3811.
- Esteve, P., Lopez-Rios, J. and Bovolenta, P. (2004). SFRP1 is required for the proper establishment of the eye field in the medaka fish. *Mech. Dev.* **121**, 687-701.
- Foley, A. C. and Stern, C. D. (2001). Evolution of vertebrate forebrain development: how many different mechanisms? *J. Anat.* **199**, 35-52.
- Graw, J. (2003). The genetic and molecular basis of congenital eye defects. *Nat. Rev. Genet.* **4**, 876-888.
- Haffter, P., Granato, M., Brand, M., Mullins, M. C., Hammerschmidt, M., Kane, D. A., Odenthal, J., van Eeden, F. J., Jiang, Y. J., Heisenberg, C. P. et al. (1996). The identification of genes with unique and essential functions in the development of the zebrafish, *Danio rerio*. *Development* **123**, 1-36.
- Hammerschmidt, M., Pelegri, F., Mullins, M. C., Kane, D. A., van Eeden, F. J., Granato, M., Brand, M., Furutani-Seiki, M., Haffter, P., Heisenberg, C. P. et al. (1996). *dino* and *mercedes*, two genes regulating dorsal development in the zebrafish embryo. *Development* **123**, 95-102.
- Hanson, I. M. (2003). PAX6 and congenital eye malformations. *Pediatr. Res.* **54**, 791-796.
- Heisenberg, C. P., Houart, C., Take-Uchi, M., Rauch, G. J., Young, N., Coutinho, P., Masai, I., Caneparo, L., Concha, M. L., Geisler, R. et al. (2001). A mutation in the Gsk3-binding domain of zebrafish *Masterblind/Axin1* leads to a fate transformation of telencephalon and eyes to diencephalon. *Genes Dev.* **15**, 1427-1434.

- Ho, R. K. and Kane, D. A. (1990). Cell-autonomous action of zebrafish spt-1 mutation in specific mesodermal precursors. *Nature* **348**, 728-730.
- Houart, C., Westerfield, M. and Wilson, S. W. (1998). A small population of anterior cells patterns the forebrain during zebrafish gastrulation. *Nature* **391**, 788-792.
- Houart, C., Caneparo, L., Heisenberg, C., Barth, K., Take-Uchi, M. and Wilson, S. (2002). Establishment of the telencephalon during gastrulation by local antagonism of Wnt signaling. *Neuron* **35**, 255-265.
- Kelly, G. M., Greenstein, P., Erezilmaz, D. F. and Moon, R. T. (1995). Zebrafish wnt8 and wnt8b share a common activity but are involved in distinct developmental pathways. *Development* **121**, 1787-1799.
- Kennedy, B. N., Stearns, G. W., Smyth, V. A., Ramamurthy, V., Van Eeden, F., Ankoudinova, I., Raible, D., Hurley, J. B. and Brockerhoff, S. E. (2004). Zebrafish rx3 and mab2112 are required during eye morphogenesis. *Dev. Biol.* **270**, 336-349.
- Kim, C. H., Oda, T., Itoh, M., Jiang, D., Artinger, K. B., Chandrasekharappa, S. C., Driever, W. and Chitnis, A. B. (2000). Repressor activity of Headless/Tcf3 is essential for vertebrate head formation. *Nature* **407**, 913-916.
- Kimmel, C. B., Ballard, W. W., Kimmel, S. R., Ullmann, B. and Schilling, T. F. (1995). Stages of embryonic development of the zebrafish. *Dev. Dyn.* **203**, 253-310.
- Lagutin, O. V., Zhu, C. C., Kobayashi, D., Topczewski, J., Shimamura, K., Puelles, L., Russell, H. R., McKinnon, P. J., Solnica-Krezel, L. and Oliver, G. (2003). Six3 repression of Wnt signaling in the anterior neuroectoderm is essential for vertebrate forebrain development. *Genes Dev.* **17**, 368-379.
- Loosli, F., Winkler, S., Burgtorf, C., Wurmbach, E., Ansoerge, W., Henrich, T., Grabher, C., Arendt, D., Carl, M., Krone, A. et al. (2001). Medaka eyeless is the key factor linking retinal determination and eye growth. *Development* **128**, 4035-4044.
- Loosli, F., Staub, W., Finger-Baier, K. C., Ober, E. A., Verkade, H., Wittbrodt, J. and Baier, H. (2003). Loss of eyes in zebrafish caused by mutation of chokh/rx3. *EMBO Rep.* **4**, 894-899.
- Mathers, P. H. and Jamrich, M. (2000). Regulation of eye formation by the Rx and pax6 homeobox genes. *Cell. Mol. Life Sci.* **57**, 186-194.
- Mathers, P. H., Grinberg, A., Mahon, K. A. and Jamrich, M. (1997). The Rx homeobox gene is essential for vertebrate eye development. *Nature* **387**, 603-607.
- Rojas-Munoz, A., Dahm, R. and Nusslein-Volhard, C. (2005). chokh/rx3 specifies the retinal pigment epithelium fate independently of eye morphogenesis. *Dev. Biol.* **288**, 348-362.
- Shimamura, K. and Rubenstein, J. L. (1997). Inductive interactions direct early regionalization of the mouse forebrain. *Development* **124**, 2709-2718.
- van de Water, S., van de Wetering, M., Joore, J., Esseling, J., Bink, R., Clevers, H. and Zivkovic, D. (2001). Ectopic Wnt signal determines the eyeless phenotype of zebrafish masterblind mutant. *Development* **128**, 3877-3888.
- Wilson, S. W. and Houart, C. (2004). Early steps in the development of the forebrain. *Dev Cell* **6**, 167-181.
- Winkler, S., Loosli, F., Henrich, T., Wakamatsu, Y. and Wittbrodt, J. (2000). The conditional medaka mutation eyeless uncouples patterning and morphogenesis of the eye. *Development* **127**, 1911-1919.
- Woo, K. and Fraser, S. E. (1995). Order and coherence in the fate map of the zebrafish nervous system. *Development* **121**, 2595-2609.



Supplemental Figure 1 - Fig. S1. Local patterning defects in the telencephalon and hypothalamus, in *ne2611* mutants compared with their wild-type siblings. (A,C,E,G,I) Wild-type siblings; (B,D,F,H,J) *ne2611* mutants. All views are lateral (except for C,D: dorsal views), anterior left, at the stages indicated. In *ne2611* mutants, the expression domains of the ventral and proximal telencephalic markers *dlx2a* (A,B) and *tbr1* (C,D, insets are lateral views of the same embryos) are enlarged but normally organized, the telencephalic but not epiphyseal (ep) expression of *flh* is absent (E,F, arrowhead) and that of *emx2* is disorganized (G,H, arrows). The anterior hypothalamus, revealed by *nkx2.1b* (arrows in I) is reduced (arrowheads in J).



Supplemental Figure 2 - Fig. S2. Expression of the early telencephalic marker *hesx1*. (A-D) Expression of the early telencephalic marker *hesx1* in wild-type embryos (A,C) compared with embryos injected with *rx3* (B) or *rx3^{ne2611}* (D) mRNA at the stages indicated. All views are dorsal, anterior left. Note that *rx3*, but not *rx3^{ne2611}*, reduces *hesx1* expression. An identical result is obtained when probing for *tlc* expression (not shown).

Appendix 3

Article in revision in *Development*

GSK3 β /PKA and Gli1 interact with E(Spl) factors activity in the maintenance of neural progenitors at the midbrain-hindbrain boundary

Jovica Ninkovic*, Christian Stigloher* and Laure Bally-Cuif

* shared first authorship

Contribution:

This project was initiated and mainly conducted by Jovica Ninkovic. I contributed with the fate tracing analysis shown in Figure 5A and B and described in chapter “MIZ and LIZ cells differ intrinsically in a cell cycle-independent process” in the manuscript. Furthermore, I tested several putative upstream regulators of Gli1 such as Nodal signalling and Fgf-signalling. This data is not shown in the manuscript. I wrote the methods part referring to my contributions. In addition, I am now involved in most experimental and re-writing aspects needed for the revision of this paper.

GSK3 β /PKA and Gli1 interact with E(Spl) factors activity in the maintenance of neural progenitors at the midbrain-hindbrain boundary

Jovica Ninkovic^{§,#}, Christian Stigloher[§] and Laure Bally-Cuif*

HelmholtzZentrum muenchen, German Research Center for Environmental health,
Department Zebrafish Neurogenetics, Institute of Developmental Genetics,
Ingolstaedter Landstrasse 1, D-85764 Neuherberg, Germany

*Corresponding author at bally@helmholtz-muenchen.de

[§]Shared first authorship

[#]Present address: HelmholtzZentrum muenchen, German Research Center for Environmental Health, Institute of Stem Cell Research, Ingolstaedter Landstrasse 1, D-85764 Neuherberg, Germany

Keywords: E(Spl), Her5, Her11, zebrafish, midbrain-hindbrain boundary, neural progenitor, GSK3 β , PKA, Gli1

Running title: molecular control of midbrain-hindbrain boundary progenitors

Word count: 8.200

Figures: 8

Abstract

Neuronal production in the midbrain-hindbrain domain (MH) of the vertebrate embryonic neural tube is dependent on a progenitor pool called “intervening zone” (IZ), located at the midbrain-hindbrain boundary. The progressive recruitment of IZ progenitors along the mediolateral (future dorsoventral) axis prefigures the earlier maturation of the MH basal plate. It also correlates with a lowered sensitivity of medial versus lateral IZ progenitors to the neurogenesis inhibition process maintaining the IZ pool. This process is exerted in zebrafish by the E(Spl) factors Her5 and Her11, but the molecular cascades involving Her5/11, and those accounting for their lowered effect in the medial IZ, remain unknown. We demonstrate here that the kinases GSK3 β and PKA are novel determinants of IZ formation and cooperate with E(Spl) activity in a dose-dependent manner. Like for E(Spl), we show that the activity of GSK3 β /PKA is sensed differently by medial versus lateral IZ progenitors. We further identify the transcription factor Gli1, expressed in medial IZ cells, as an antagonist of E(Spl) and GSK3 β /PKA, and demonstrate that the neurogenesis-promoting activity of Gli1 accounts for the lowered sensitivity of medial IZ progenitors to neurogenesis inhibitors and their increased propensity to differentiate. Surprisingly, we also show that the expression and activity of Gli1 in this process are independent of Hedgehog signaling. Together, our results suggest a model where the modulation of E(Spl) and GSK3 β /PKA activities by Gli1 underlies the dynamic properties of IZ maintenance and recruitment.

Introduction

Neurogenesis in the embryonic vertebrate neural tube is strictly controlled in time and space to coordinate neuronal production and the maintenance of progenitor cells. Neural progenitors are crucial to produce neurons and glia for later events of brain maturation, but the mechanisms underlying their

maintenance, recruitment and fate are only partially understood (Bally-Cuif and Hammerschmidt, 2003; Kageyama et al., 2005; Panchision and McKay, 2002). To approach these mechanisms, we are focusing on an evolutionarily conserved progenitor pool, the “intervening zone” (IZ), which adjoins the midbrain-hindbrain boundary (MHB) in the neural tube of all vertebrate embryos (Bally-Cuif et al., 1993; Geling et al., 2003; Stigloher et al., 2007; Vaage, 1969) (Fig.1A-C). Lineage tracing of the IZ pool in the zebrafish embryo demonstrates that it lasts at least throughout embryogenesis and progressively contributes neurons to the entire midbrain-hindbrain domain (MH) (Tallafuss and Bally-Cuif, 2003), a territory involved in a number of physiological and integrative functions including sensory processing, motor control and social behavior.

The multiple functional outputs of the MH necessitate a diversity of neuronal subtypes in a precise neuroanatomical pattern, and two properties of the IZ speak for its importance in organizing MH maturation. Along the anteroposterior (AP) axis, the temporal order with which cells leave the IZ to populate the differentiating MH correlates with the future spatial organization and subtype of the neurons that they generate ((Tallafuss and Bally-Cuif, 2003) (and C.S., unpublished). Hence the mechanisms controlling maintenance of the IZ along AP likely influence the generation of MH neuronal subtypes. Along the dorsoventral axis (DV, initially mediolateral), IZ cells exhibit clear differences in their propensity to undergo neurogenesis, which correlate with the earlier maturation of the basal plate compared to the alar plate (Easter et al., 1994). Indeed, at early neurogenesis stages, medial (future ventral) IZ cells (MIZ) are more prone to undergo neurogenesis than lateral (future dorsal) IZ cells (LIZ) (Ninkovic et al., 2005).

The maintenance of IZ progenitors is under control of bHLH transcription factors of the E(Spl) family, such as mouse Hes1 and Hes3 or zebrafish Her5 and Her11/Him (below referred to as Her11) which inhibit expression of proneural genes such as *neurogenin1* (*neurog1*) (Hatakeyama et al., 2004;

Kageyama et al., 2005; Stigloher et al., 2007). Mouse Hes1 and 3 are expressed across the MH domain, concentrating at the MHB over time, and their compound genetic ablation leads to the premature differentiation of the IZ, MH collapse and loss of MH neuronal identities (Hatakeyama et al., 2004; Hirata et al., 2001). Expression of *her5* and *her11* is identical and delineates the IZ at all stages (Ninkovic et al., 2005). Loss-of-function experiments by means of antisense oligonucleotide injected into zebrafish embryos demonstrate that Her5 and Her11 play redundant roles in IZ maintenance, which is sensitive to a global level of Her5 + Her11 with differences along the mediolateral axis. Specifically, three copies of *her5* and/or *her11* are sufficient to maintain the IZ, two copies are enough to maintain the LIZ but not the MIZ (which transforms into a *neurog1*-positive zone) (Fig.1B), and a lower amount leads to the ectopic expression of *neurog1* across the LIZ as well (Ninkovic et al., 2005) (Fig.1C). Hence, E(Spl) activity controls IZ maintenance and is sensed differently by MIZ and LIZ cells.

her5 and *her11*, as well as other family members such as *her3* and *her9* involved in the formation of other progenitor pools of the zebrafish embryonic neural plate, are not activated by Notch signaling (Bae et al., 2005; Geling et al., 2004; Hans et al., 2004), and this mechanism likely applies to mouse early progenitor pools as well (Hatakeyama and Kageyama, 2006; Stigloher et al., 2007). To date, the molecular cascades involving E(Spl) activity during IZ formation remain unknown. Similarly, the mechanisms rendering MIZ cells less sensitive to E(Spl) activity than LIZ cells need to be discovered. To reveal these mechanisms, we used sensitized conditions where the total level of E(Spl) activity is lowered, thereby bringing IZ cells closer to choosing between the progenitor and neurogenesis states, and we tested the influence of several signaling cascades and signal transduction pathways active in the anterior neural plate. We show here that the kinases GSK3 β and PKA are novel determinants of IZ formation, and demonstrate that GSK3 β /PKA cooperate with E(Spl) activity in a dose-dependent manner throughout the IZ. Like for E(Spl) factors, we report that GSK3 β /PKA activity is sensed

differentially along the mediolateral axis. We further identify the transcription factor Gli1, expressed within the MIZ, as an antagonist of E(Spl) and GSK3 β /PKA, and demonstrate that the neurogenic activity of Gli1 accounts for differential response of MIZ and LIZ to neurogenesis inhibitors. Surprisingly, we also show that this activity of Gli1 is independent of Hh signaling. Together, our results provide a molecular framework to understand IZ maintenance and its properties along the AP and DV axes.

Materials and Methods

Zebrafish strains and transgenic lines

Embryos obtained from natural spawning of AB wild-type or transgenic fish, *hsp70:tcf3-GFP^{w26}* (Lewis et al., 2004) and *tg(her5PAC:EGFP)^{ne1939}* (Tallafuss and Bally-Cuif, 2003) were raised and staged according to Kimmel et al. (Kimmel et al., 1995). *smoothened (smu^{b641})* (Varga et al., 2001) and *D^{w5/w5}* (Lekven et al., 2003) mutants were obtained by pairwise mating of heterozygous adult carriers.

In situ hybridization

In situ hybridization experiments were carried out as previously described (Hammerschmidt et al., 1996b; Ninkovic et al., 2005). The following probes were used: *her5* (Müller et al., 1996), *neurog1* (Korz et al., 1998), *pax2.1* (Lun and Brand, 1998), *gli1* (Karlstrom et al., 2003), *gli2* (Karlstrom et al., 2003); *gli3* (Tyurina et al., 2005), *wnt1* (Molven et al., 1991), *myoD* (Weinberg et al., 1996), *shh* (Krauss et al., 1993) and *egfp* (clontech). Primary antibodies used for immunohistochemistry were rabbit anti-GFP (ams biotechnology Europe, TP401) used at a final dilution of 1/500, mouse antihuman neural protein HuC/HuD (MoBiTec A-21271) (1/300), rat anti BrdU (abcam) 1/200 and rabbit anti-phospho-histone H3 (Upstate Biotechnology) 1/200. They were revealed using FITC-conjugated goat anti-rabbit secondary antibody (Jackson ImmunoResearch Laboratories, 111-095-003), Cy3-conjugated goat anti-rat secondary antibody (Jackson ImmunoResearch Laboratories, 112-165-003)

(1/200) or Cy3-conjugated goat anti-mouse secondary antibody (Jackson ImmunoResearch Laboratories, 115-165-044) (1/200), as appropriate. Embryos were pretreated for BrdU immunohistochemistry with 3.3 N HCl for 30 min at room temperature followed with the 2 15 min washings in sodium tetraborate buffer (0.1 M, pH 8.5). Embryos were scored and photographed under a Zeiss SV 11 stereomicroscope or a Zeiss Axioplan photomicroscope.

RNA, morpholino and gripNA injections

Capped RNAs were synthesized using the Ambion mMessage mMachine kit following the supplier's instructions. Capped RNAs was injected at the one-cell stage at the following concentrations: constitutively active form of protein kinase A *PKA** (Hammerschmidt et al., 1996a) 20 ng/μl; dominant negative Reg *dnReg* (Strahle et al., 1997) 50 ng/μl. Morpholino antisense oligonucleotides (*gli1MO*) (Gene-Tools, Inc. (Oregon, USA)) and GripNA antisense oligonucleotides (*her11GripNA* and *her5GripNA*) (Active Motif (Belgium)) were dissolved to a stock concentration of 5 and 2 mM, respectively, in H₂O and injected into one-cell stage embryos at 0.5 mM. Sequences of antisense oligonucleotides were as follows: *her5GripNA*: 5'-GGTTCGCTCATTTTGTG-3'; *her11GripNA*^{ATG}: 5'-ATTCGGTGTGCTCTTCAT-3' (Ninkovic et al., 2005) and *gli1MO*: 5'-CCGACACACCCGCTACACCCACAGT-3' (Karlstrom et al., 2003). All injection experiments were repeated at least three times.

Pharmacological treatments

Glycogen synthase kinase-3beta (GSK3β) inhibition was achieved by applying either LiCl or GSK3β inhibitor III (2,4-Dibenzyl-5-oxothiadiazolidine-3-thione, OTDZT)(Calbiochem, Germany). Lithium (0.3 M LiCl) treatments were carried out at 28 °C in embryo medium at 80% epiboly stage embryos for 10 minutes, unless stated differently. Treated embryos were subsequently washed 3 times in embryo medium and fixed at desired stage of development. OTDZT was diluted in embryo medium to concentration 1mM from a stock of 100mM dissolved in DMSO. WT embryos were soaked in OTDZT solution at

28 °C at 80% epiboly stage for 10 min and subsequently washed 3 times in embryo medium. Embryos treated with 1 % DMSO dissolved in embryo medium (the concentration of DMSO in the OTDZT solution) were indistinguishable from the untreated WT embryos.

Cyclopamine (BIOMOL, Germany) was diluted in embryo medium to 100 µM from a stock of 20 mM in DMF. Embryos were manually dechorionated and soaked in cyclopamine-containing medium in the 1% agarose-coated dish from the 8 cells stage until they were processed for ISH. Embryos soaked in 0.5 % DMF were undistinguishable from the untreated embryos.

Uncaging experiments

Caged fluorescein – dextran, biotin, lysine fixable (Molecular Probes Inc., Eugene, USA) was injected at a concentration of 5mg/ml into one-cell stage embryos of the transgenic line *Tg(her5PAC:EGFP)^{ne1939}* (Tallafuss and Bally-Cuif, 2003). The photo-convertible dye was activated in a small population of approximately 5 cells at 50 to 60% epiboly following general procedures as described in (Stigloher et al., 2006). The tip of the notochord was used as orientation landmark. Activated embryos developed further in the dark and were fixed at the late tailbud-stage in 4% paraformaldehyde. After immunohistochemistry (chicken anti-GFP (Aves Labs, Tigard, USA); mouse anti-fluorescein (Roche Diagnostics, Mannheim, Germany); Alexa Fluor 555 goat anti-mouse and Alexa Fluor 488 goat anti-chicken antibodies (Invitrogen, Carlsbad, USA)) embryos were flat-mounted and imaged with a Zeiss Axioplan2 and a Zeiss LSM510 Confocal Laser Scanning Microscope.

BrdU labeling

WT embryos were manually dechorionated and soaked in BrdU solution containing 10 mM BrdU and 15 % DMSO in embryo medium for 10 min on ice at specified stage of development. Subsequently, embryos were washed 3 times for 10 min with the washing buffer containing 15 % DMSO in embryo medium on ice, fixed immediately afterwards and processed for BrdU immunohistochemistry as described above.

Results

LiCl, but not canonical Wnt signaling, modulate IZ neurogenesis

We hypothesized that signaling pathways expressed along the IZ at the onset of neurogenesis might influence the neurogenic potential of MIZ and LIZ cells. At late gastrulation, expression of *wnt1*, *wnt3a* and *wnt10b* are confined within the IZ area, at high levels within the LIZ and low or undetectable levels medially ((Buckles et al., 2004; Lekven et al., 2003) and our unpublished observations). Because Wnt signaling has been implicated in controlling neurogenesis in other instances (e.g. (Megason and McMahon, 2002; Panhuysen et al., 2004; Zechner et al., 2003)), in particular by supporting the proliferating state, we tested whether it might influence the behavior of MIZ and LIZ cells. We expected that Wnt would favor the progenitor state and that higher Wnt signaling laterally would account for the decreased tendency of LIZ cells to differentiate, and/or for their higher sensitivity to the inhibition provided by Her5/Her11.

To address this issue, we first looked whether the Wnt signaling activator LiCl (Hedgepeth et al., 1997; Klein and Melton, 1996) could affect IZ formation. Wild-type embryos were incubated in 0.3 M LiCl during a 15-minute pulse at late gastrulation, then washed and let develop until the 3-somite stage, at which point they were analyzed for *neurog1* expression. When LiCl was applied at 60% epiboly, the anterior neural plate was posteriorized, mimicking the situation in mutants with early hyperactivated Wnt (Dorsky et al., 2003; Heisenberg et al., 2001; Kim et al., 2000; van de Water et al., 2001) (Fig.2A). In these animals, the IZ was enlarged along AP, but neurogenesis inhibition was not affected (90% of cases, n=50) (Fig.2A). In striking contrast, when LiCl was applied at 80% epiboly, prominent expression of *neurog1* was observed ectopically instead of the MIZ in most embryos analyzed (83% of cases,

n=60) (Fig.2B,E,E', arrows, compare to 2D,F,F'), with only a moderate effect on AP patterning. This neurogenic phenotype was crucially dependent on the moment of LiCl application, since incubations at later time points did not affect IZ formation (88% of cases, n=56) (Fig.2C). Thus, LiCl applied at 80% epiboly induces the premature commitment of MIZ progenitors towards differentiation.

Because LIZ cells are less prone to undergo neurogenesis than MIZ cells, it is possible that LiCl modulates neurogenesis throughout the IZ, but that its effects are only visible medially in the wild-type embryo. To test this possibility, we further applied LiCl onto embryos where Her5 activity was decreased by injection of an antisense oligonucleotide blocking the translation of *her5* mRNA (*her5* gripNA). In these conditions, *neurog1* expression was induced by LiCl throughout the IZ (86.5% of cases, n=52) (not shown, but see below Fig.2L), a phenotype never obtained in *her5* knock-down embryos alone (Fig.1B and (Ninkovic et al., 2005)). We conclude that, in the presence of LiCl, IZ cells are globally rendered more susceptible to undergo neurogenesis. *her5* or *her11* expression were not modified in LiCl-treated embryos (96% of cases, n=30) (not shown). LiCl might rather modulate Her5/Her11 activity, or act downstream or in parallel to these factors.

Importantly however, the observed effect of LiCl is opposite to that expected if endogenous Wnt signaling controlled the behavior of MIZ and LIZ cells: as mentioned, the expression of Wnt ligands in the LIZ would predict that activated Wnt decreases cells' tendency to differentiation. This observation suggests that the neurogenic effects of LiCl might not be linked to Wnt signaling activation. To directly test this interpretation, we assessed the effects of LiCl upon blockage of the canonical Wnt pathway downstream of LiCl activity. We used for this analysis embryos carrying the transgene *hsp70l:tcf3-GFP^{w26}*, which express upon heat-shock a N-terminally truncated form of Tcf3a that acts as a dominant repressor of canonical Wnt signaling (Lewis et al., 2004). We submitted transgenic embryos to a heat-shock pulse at 50% epiboly, followed two hours later by LiCl treatment (i.e. at 80% epiboly

as described previously), and analyzed *neurog1* expression at the 3-somite stage. A delay of two hours after the heat-shock pulse is sufficient to significantly antagonize Wnt activity at gastrulation (Lewis et al., 2004), thus we expect that GSK3 β inhibition by LiCl occurred while downstream components of canonical Wnt signaling were blocked. In these embryos however, *neurog1* expression was still strongly induced by LiCl in place of the MIZ (83% of cases, n=42) (Fig.2G, compare to 2H). We conclude that LiCl is unlikely to influence IZ neurogenesis via activation of Tcf-mediated Wnt signaling.

Further arguments do not support a role for endogenous Wnt signaling in attributing mediolateral differences towards neurogenesis within the IZ. First, in transgenic reporter embryos *Tg(TOP:GFP)^{w25}*, where GFP expression is under control of multimerized Tcf binding sites (Dorsky et al., 2002), we were unable to reveal active canonical Wnt signaling in this area of the neural plate at the onset of neurogenesis (98% of cases, n>=100), while *gfp* expression was obvious in active Wnt signaling domains such as the embryonic margin (not shown). Second, lowering Wnt signaling (e.g. in *hsp70l:tcf3-GFP^{w26}* transgenic embryos heat-shocked at the 50% epiboly stage) did not change the profile of *neurog1* induction, neither by itself nor upon blocking Her5 activity (not shown). In the latter case, in particular, it did not lead to ectopic expression of *neurog1* within the LIZ. Together, we conclude that endogenous canonical Wnt signaling is not involved in modulating the propensity of IZ cells to undergo neurogenesis, and that LiCl affects neurogenesis control at the IZ independently of this signaling pathway.

LiCl effect on neurogenesis control is mimicked by inhibiting GSK3 β

LiCl effects are broad-ranged, but primarily inhibit the activity of GSK3 β (Berridge et al., 1989; Hedgepeth et al., 1997; Klein and Melton, 1996). To confirm that LiCl-induced neurogenesis across the IZ was mediated by the blockage of GSK3 β , we tested the effects of the selective GSK3 β inhibitor

OTDZT (Martinez et al., 2002) on *neurog1* expression. Like for LiCl treatment, wild-type embryos were incubated in 1 mM OTDZT at 80% epiboly for 15 minutes, and processed for *neurog1* in situ hybridization at the 3-somite stage. Strikingly, OTDZT induced ectopic *neurog1* expression in place of the MIZ, mimicking the effect of LiCl (87% of cases, n=38) (Fig.2I-J'). Further, like for LiCl, lowering Her5/Her11 dosage revealed that GSK3 β is active throughout the IZ (85% of cases, n=40) (Fig.2K,L). Thus, the neurogenic effect of LiCl is faithfully mimicked by inhibiting GSK3 β , identifying GSK3 β activity as a crucial element modulating neurogenesis at the IZ and required in vivo for the formation and early maintenance of the MIZ.

Activated PKA compensates for GSK3 β inhibition or lowered E(Spl) activity

In addition to targeting canonical Wnt, GSK3 β is involved in a number of signaling pathways, where it triggers the enhanced phosphorylation of target proteins after these have been primed by phosphorylation by cAMP-dependent protein kinase A (PKA) (Jia et al., 2002; Price and Kalderon, 2002; Zhang et al., 2005). To assess whether such a process was at play during IZ formation, we tested whether PKA activation could affect the neurogenic effect of inhibiting GSK3 β . In agreement with previous findings, only few embryos (approximately 50% in our case) injected with capped mRNA encoding a constitutively active catalytic subunit of PKA (PKA*) (Hammerschmidt et al., 1996a) developed a normal neural plate (Blader et al., 1997). Among these, all formed a normal IZ (Fig.3A,F compare with D,H, respectively). Strikingly however, in these cases, PKA* inhibited the neurogenic effect of LiCl, restoring the MIZ when LiCl was applied at 80% epiboly onto PKA*-injected embryos (88% of cases, n=61) (Fig.3C, compare with B). Thus, general activation of PKA does not in itself expand the IZ but it can compensate for the loss of GSK3 β function to maintain neurogenesis inhibition in this location.

We next addressed whether PKA activation could also compensate for a downregulation of E(Spl)-mediated neurogenesis inhibition at the MHB. For this, we tested the effects of co-injecting *her5* gripNA and *PKA** capped RNA into wild-type embryos. While blocking Her5 function with gripNAs lead to loosing the MIZ in the vast majority of cases (92% of cases, n=26) (Fig.3E), the co-expression of *PKA** efficiently rescued this phenotype and restored MIZ formation (66% of cases, n=50) (Fig.3G, compare to H). Thus, general activation of PKA also promotes neurogenesis inhibition within the IZ downstream or in parallel to Her5 function.

Activated PKA and GSK3 β act in concert with E(Spl) factors to permit IZ formation

To determine whether PKA was in itself required for IZ formation, we blocked its activity by injection of capped RNA encoding a dominant negative form of the regulatory subunit of PKA, dnReg (Strahle et al., 1997). dnReg robustly prevents the transcription of downstream targets of the Hh pathway, such as *spalt*, which require PKA for their expression (88% of cases, n=72) (not shown). In embryos expressing dnReg, the MIZ was replaced by ectopic *neurog1* expression (84% of cases, n=50) (Fig. 4B,F compare to D,H). When Her5 activity was also inhibited by the co-injection of *her5* gripNA, *neurog1* expression was also induced within the LIZ (86% of cases, n=35)(Fig.4C,L arrows, compare to A,I and B,F,J, white arrowheads). Thus, blocking PKA activity increases the propensity of all IZ cells to undergo neurogenesis, and PKA is crucially required *in vivo* to inhibit neurogenesis in the medial aspect of the IZ and permit MIZ formation.

Because blocking PKA or GSK3 β triggers identical phenotypes, we wondered whether these two factors act cooperatively. Hence, we inhibited concomitantly both activities by treating *dnReg*-injected embryos with OTDZT. As described above, when PKA and GSK3 β are manipulated separately, *neurog1* expression is induced in place of the MIZ but the LIZ is unaffected

(Fig.2K, 4B,J;E,K). In contrast, the co-inhibition of PKA and GSK3 β induced ectopic *neurog1*-positive cells within the LIZ (75% of cases, n=62) (Fig.4G,M). These results suggest a dose-dependent process co-regulated by PKA and GSK3 β .

Together, the results above place neurogenesis inhibition by GSK3 β /PKA downstream or in parallel to the activity of E(Spl) factors. To resolve this issue, we tested whether increased E(Spl) activity would be able to compensate for decreased GSK3 β /PKA. To this aim, we blocked PKA in *Tg(her5PAC:EGFP)^{ne1939}* transgenic fish (Tallafuss and Bally-Cuif, 2003), which carry one additional copy of the *her11* gene under control of its own regulatory elements, and thereby express 3 doses of Her5/Her11 activity in a correct spatio-temporal manner (Ninkovic et al., 2005). This transgenic background is sufficient to permit normal MIZ formation in the absence of Her5 (Ninkovic et al., 2005). However, it proved insufficient to block ectopic *neurog1* activation and rescue the MIZ upon expression of dnReg (79% of cases, n=56) (Fig.4N, compare to O), while dnReg had no obvious effect on the level of expression of *her5* and *her11* and we failed to detect putative PKA or GSK3 β phosphorylation sites on Her5 and Her11 (not shown). Although we cannot exclude that even higher doses of Her5/Her11 could be effective, these results are best compatible with GSK3 β /PKA acting functionally downstream of E(Spl) factors.

MIZ and LIZ cells differ intrinsically in a cell cycle-independent process

The results above identify the GSK3 β /PKA pathway as a novel component of neurogenesis inhibition throughout the IZ that, like Her5/Her11, is sensed differently by MIZ and LIZ cells. Hence, we next searched for a mechanism rendering the MIZ and LIZ different in their response to the GSK3 β /PKA and/or Her5/Her11 pathways.

Either cell-intrinsic components or local signaling cues could account for this difference. To test for the possible relevance of cell-intrinsic mechanisms, we

first assessed whether the MIZ and LIZ differ in lineage. Extensive cell exchanges across the midline of the neural tube in the zebrafish embryo have been documented, as well as dorsoventral dispersion, after the 2-somite stage (Papan and Campos-Ortega, 1997), but not before (Woo and Fraser, 1995). However, the specific case of IZ precursors has not been studied. To address this issue, we injected embryos with caged-fluorescein at the one cell-stage, activated this label in a small group of cells overlapping with the presumptive MIZ at 50-60% epiboly using a UV light focused by a pinhole (Fig.5A), and monitored the position of activated cells along the mediolateral axis at the end of gastrulation (late tailbud stage). To facilitate identification of the IZ, we performed these experiments in *Tg(her5PAC:EGFP)^{ne1939}* transgenic embryos, where *her5*-expressing cells are also positive for GFP (Tallafuss and Bally-Cuif, 2003). Double staining of activated embryos for GFP and uncaged-fluorescein revealed that cells located in the presumptive medial IZ at 50-60% epiboly remained in this location until the tailbud stage, without contribution to the LIZ (100% of cases, n=3) (Fig.5B). Thus, starting at least at 50-60% epiboly, MIZ and LIZ cells remain spatially segregated, making it possible that they inherit different determinants.

Such cell-intrinsic components might act on cell proliferation, on the degree of cellular commitment towards differentiation, or both. In particular, cell cycle kinetics has a crucial influence on a cell's capacity to enter the neurogenesis process in the CNS (Calegari and Huttner, 2003). To address this issue, we tested whether MIZ and LIZ cells differed intrinsically in their proliferation characteristics at the onset of neurogenesis. Markers for the S phase (BrdU incorporation) and M phase (PH3, and mitotic figures) were analyzed together with the IZ marker *her5* RNA in triple labeled preparations at 75% epiboly, 90% epiboly and tailbud. At these stages, there is still a tendency for cells to divide synchronously (Kimmel et al., 1994), thus the co-analysis of S and M phase markers on single specimen was important to distinguish between differences in cell cycle length versus cell division timing. At all these stages, we observed that cell cycle kinetics did not significantly differ between the MIZ and LIZ in more than 50 embryos analyzed (Fig.5C and data not shown). We

also found no difference in the expression of other known proliferation-controlling factors (e.g. p27^{Xic}) between the MIZ and LIZ (not shown). Together, these observations suggest that the cell division characteristics of the MIZ and LIZ are comparable, and that these populations differ in their commitment in a manner independent of cell cycle control.

Gli1 counteracts the neurogenesis inhibition process that creates the IZ and accounts for the differential sensitivity of MIZ and LIZ cells to neurogenesis inhibitors

Among commitment factors expressed within the early neural plate, transcription factors of the Gli family have been implicated in neurogenesis control in many systems (see (Agathocleous et al., 2007; Ruiz et al., 2002) for reviews). Further, these have been identified as intracellular targets for the PKA/GSK3 β pair (Huangfu and Anderson, 2006; Riobo and Manning, 2007). Finally, *gli1* appeared expressed differentially between the MIZ and LIZ: in agreement with published data (Karlstrom et al., 2003), we confirmed that *gli1* is transcribed within the anterior neural plate following a clear mediolateral gradient starting at 80% epiboly, with high expression levels medially (including the MIZ) contrasting with undetectable levels laterally (including the LIZ) (Fig.5D-F). Three other *gli* genes have been identified to date in zebrafish (Karlstrom et al., 2003; Ke et al., 2005; Tyurina et al., 2005), but *gli2b* was not expressed at detectable levels within the IZ area at late gastrulation / early somitogenesis, while *gli2a* and *gli3* expression was ubiquitous (not shown).

To address the function of Gli1 during IZ formation, we blocked *gli1* translation by injection of a *gli1* morpholino (MO) (Karlstrom et al., 2003) into wild-type embryos. This manipulation did not alter the IZ area (82% of cases, n=71) (Fig.5H,L, compare to J,N; Fig.6C, compare to A), although it was efficient at blocking expression of the Hh target *nkx2.1* along the ventral midline of the anterior neural tube (96% of cases, n=30) (not shown). Strikingly however, blocking Gli1 totally abolished the neurogenic effect of LiCl: when *gli1* MO-

injected embryos were subjected to LiCl treatment at 80% epiboly, the MIZ formed normally (82% of cases, n=52) (Fig.5I, compare to G). Thus blocking Gli1 function can increase neurogenesis inhibition and rescue IZ formation in the absence of GSK3 β activity. Using a similar approach, we tested whether blocking Gli1 could compensate for the lack of PKA activity, by co-injecting *gli1* MO and *dnReg* capped RNA into wild-type embryos. We observed that the co-inhibition of Gli1 and PKA abolished the neurogenic effect of blocking PKA alone and rescued MIZ formation (84% of cases, n=61) (Fig.5M, compare to K). Together, these results demonstrate that Gli1 exerts a neurogenesis-promoting activity that opposes the activity of GSK3 β /PKA. Under normal conditions, the activity of Gli1 is sub-threshold, such that neurogenesis inhibition is obtained. It becomes visible in the absence of GSK3 β or PKA activity, where the repression of Gli1 alone suffices to restore neurogenesis inhibition.

The co-regulation of IZ formation by GSK3 β /PKA and E(Spl) factors described above suggests that Gli1 function should also influence E(spl) function. To verify this point, we lowered E(Spl)-mediated neurogenesis inhibition by injection of *her5* gRNA into wild-type embryos, and we simultaneously blocked Gli1 by the co-injection of *gli1* MO. We observed that the ectopic neurogenesis triggered by Her5 blockage was abolished by the loss of Gli1 function, restoring the IZ (89% of cases, n=72) (Fig.6D, compare to B). Thus, Gli1 expression also acts antagonistically to E(Spl) activity by increasing the tendency of IZ cells towards neurogenesis, an effect that becomes apparent when E(Spl) dosage is lowered.

This neurogenesis-promoting function of Gli1, as well as its MIZ-specific expression, makes Gli1 a good candidate to render the MIZ more prone than the LIZ to undergo neurogenesis. As described, blocking Gli1 activity increases the sensitivity of MIZ cells to two copies (or less) of Her5/Her11 (Fig.6D). In addition, in the absence of Gli1, we observed that both the MIZ and LIZ concomitantly lost their responsiveness to a further down-regulation of Her5/Her11 and that they upregulated *neurog1* in an identical manner (90%

of cases, n=56) (Fig.6E,E'). These results identify Gli1 as a crucial element rendering MIZ and LIZ cells differentially sensitive to E(Spl) factors.

IZ formation and Gli1 activity are not under control of Hh signaling

We next searched for mechanisms controlling Gli1 expression or activity within the MIZ. *Shh* is expressed in the presumptive axial mesoderm from 50% epiboly onwards (Ertzer et al., 2007; Krauss et al., 1993), and Gli factors are among the main targets of Hh signaling. Further, Gli1 traditionally behaves as a positive activator of Hh targets, and the results above would be compatible with a model where Hh signaling at the midline activates Gli1 expression, enhancing cell capacity for neurogenesis. To test this interpretation, we studied whether IZ formation and Gli1 expression in this area were sensitive to Hh signaling. To this aim, we blocked Hh signaling upstream of PKA / GSK3 β action by incubating wild-type embryos into the alkaloid cyclopamine. Cyclopamine blocks the function of the transmembrane protein Smoothed (Chen et al., 2002), which normally initiates intracellular Hh signaling events and in particular the inhibition of GSK3 β and PKA (Huangfu and Anderson, 2006; Riobo and Manning, 2007). As expected, such treatment performed at 50% epiboly efficiently inhibited expression of *myoD* in adaxial cells (97% of cases, n=40) (Fig.7B, compare to A), a characteristic of Hh signaling deficiencies (Barresi et al., 2000; Chen et al., 2001) and *spalt* expression in the anterior neural plate (not shown). Surprisingly however, we observed that cyclopamine treatment did not affect the expression of *gli1* in the IZ area (96% of cases, n=52) (not shown). It also did not affect IZ formation (Fig.7D, compare to F). Because Hh signaling might promote Gli1 activity rather than trigger its expression, we further assessed whether cyclopamine could downregulate Gli1 function. For this, we first lowered the amount of E(spl) activity at the IZ by injecting wild-type embryos with the *her5* gripNA, and applied cyclopamine at 50% epiboly onto these injected embryos. While inhibiting Gli1 function in such cases led to a rescue of the MIZ (Fig.6D), we observed that cyclopamine was without effect and incapable of

counteracting ectopic *neurog1* induction (89% of cases, n=75) (Fig.7E, compare to C). We conclude that cyclopamine treatment affects neither the expression nor the function of Gli1 at the IZ. Similar results were obtained in *smu^{b641}* mutants deficient in Smoothed function (Varga et al., 2001) (not shown). These observations strongly suggest that the neurogenic activity of Gli1 at the IZ is independent of Hh signaling.

Discussion

The IZ acts as an evolutionarily conserved long-lasting progenitor pool, giving rise over time and in spatio-temporal order along the anteroposterior axis to the large majority of midbrain-hindbrain neurons (Tallafuss and Bally-Cuif, 2003). We previously demonstrated that the activity of the two E(spl) factors Her5 and Her11 (“E(spl) activity”) is a crucial mechanism inhibiting neurogenesis to permit IZ formation (Geling et al., 2003; Geling et al., 2004; Ninkovic et al., 2005). We identify here a collaborative mechanism, relying on the activity of the two protein kinases PKA and GSK3 β . The E(Spl) and GSK3 β /PKA pathways act in a dose-dependent manner, and one of their activities is to oppose the neurogenic effect of the transcription factor Gli1. While the E(Spl) and GSK3 β /PKA pathways are expressed and act throughout the IZ, their effect is sensed differently by MIZ and LIZ cells. We further show that Gli1 is mediating this difference by rendering MIZ cells more prone to undergo neurogenesis. This mechanism might account for the earlier differentiation of basal versus alar plate neurons during midbrain-hindbrain development. Together, these results help refine a molecular model for the sequential differentiation of midbrain-hindbrain neurons along the anteroposterior and mediolateral (dorsoventral) axes (Fig.8).

Co-regulation of IZ formation by the GSK3 β /PKA and E(Spl) pathways

An important finding of our work is the identification of GSK3 β and PKA as new mediators of IZ formation. Both enzymes often act sequentially on the

same targets in vivo, phosphorylation by PKA priming target proteins for a subsequent phosphorylation by GSK3 β (Price and Kalderon, 2002), but alternative models are emerging where PKA and GSK3 β independently phosphorylate the same target (Taurin et al., 2006). At the IZ, the enhanced effect of lowering both GSK3 β and PKA, and the fact that constitutive PKA activation can compensate for lowered GSK3 β activity, suggest the involvement of an unconventional dose-dependent process incorporating the level of activity of both enzymes. PKA and GSK3 β might be rate limiting for the full phosphorylation necessary to functionally modify the same target, or would act on distinct targets cooperating during IZ formation.

We further show that E(Spl) and GSK3 β /PKA act in an additive manner, and our observations are in favor of parallel activities of E(Spl) and GSK3 β /PKA on a dose-dependent process measuring a global level of both pathways. GSK3 β /PKA and E(spl) inhibition may converge onto common targets promoting neurogenesis inhibition, or have parallel targets collaborating in the neurogenesis inhibition process. The direct targets of E(Spl) activity during IZ formation (as in most E(Spl)-dependent processes) remain unknown, but this activity down-regulates expression of the proneural genes *neurog1* and *coe2* and the cyclin-dependent kinase inhibitor p57 (Geling et al., 2004). A number of targets inhibited by GSK3 β /PKA phosphorylation have been identified including factors involved in the control of cell cycle (e.g. N-myc1) (Kenney et al., 2004; Mill et al., 2005), cell differentiation (e.g. XNeuroD, Xash1 and Mash1) (Moore et al., 2002) or both (e.g. β catenin or Gli proteins) (reviewed in (Frame and Cohen, 2001; Huangfu and Anderson, 2006; Riobo and Manning, 2007)). None of our observations suggest a major role for cell proliferation control in IZ formation, corroborating previous findings where neurogenesis does not systematically follow cell cycle exit at the early neural plate stage (Geling et al., 2003; Hardcastle and Papalopulu, 2000; Harris and Hartenstein, 1991). Rather, in this system, entry into the *neurog1*-positive state follows information unlinked to cell cycle characteristics and we favor commitment factors as main targets for the GSK3 β /PKA pathway.

There are target sites for GSK3 β on zebrafish NeuroD (Moore et al., 2002) but not on Neurog1 (our observations) and, in the IZ, GSK3 β /PKA indirectly affects *neurog1* transcription rather than its activity. We failed to identify GSK3 β or PKA target sites on Her5 and Her11 (not shown), but an indirect role of GSK3 β /PKA on the activity of these factors cannot be excluded, and would be in agreement with our observation that increased levels of Her11 expression cannot compensate for lowered PKA activity. Gli1, expressed through the MIZ and antagonizing the non-neurogenic activity of GSK3 β /PKA, appears as an obvious candidate target. Indeed, GSK3 β /PKA classically regulate the nuclear translocation (Gli1) or processing (Gli2, Gli3) of Gli factors in a manner antagonized by Hh signaling (reviewed in (Huangfu and Anderson, 2006; Riobo and Manning, 2007)). However, GSK3 β /PKA are also active at blocking neurogenesis in the LIZ, where *gli1* is not expressed. Hence, other direct targets of GSK3 β /PKA remain to be identified that permit IZ formation.

Finally, like for E(Spl) factors, the upstream pathways involving GSK3 β /PKA at the IZ are currently unknown. Classically, Wnt and Hh inhibit GSK3 β and/or PKA to permit signal transduction (reviewed in (Hooper and Scott, 2005; Huangfu and Anderson, 2006; Logan and Nusse, 2004; Riobo and Manning, 2007)). At the IZ, it is the ectopic inhibition of GSK3 β /PKA that poses a developmental problem suggesting a mechanism where the IZ is shaped through the non-activity of GSK3 β /PKA inhibitory pathways. However, Wnt reporters remained silent in the anterior neural plate at the stage of interest (not shown), and we show that blocking Wnt or Hh activities or ubiquitously enhancing PKA activity did not expand the IZ. Hence, IZ formation might be achieved through a constitutive activation of GSK3 β /PKA in concert with local cofactors, and/or through other signaling pathways than Wnt and Hh involved in shaping GSK3 β /PKA action. A number of upstream regulators have been identified for these kinases, in particular classical mitogenic pathways driven by PI3 kinase and Akt (Dudek et al., 1997; Kenney et al., 2004), and it will be important to test their implication during IZ formation.

Gli1 activity at the midline renders MIZ cells less sensitive to E(Spl)- and GSK3 β /PKA-mediated neurogenesis inhibition

Searching for factors that might account for the differential sensitivity of MIZ versus LIZ cells to neurogenesis inhibition, we observed that *gli1* expression is concentrated medially in the MIZ, and has a neurogenesis-promoting effect, albeit at sub-threshold levels. Significantly, we showed that blocking Gli1 activity abolishes the difference between MIZ and LIZ towards E(Spl)-mediated neurogenesis inhibition. These results identify Gli1 as a crucial element rendering MIZ cells less sensitive than LIZ to neurogenesis inhibition. Although multiple additional blocks might still exist between *neurog1* expression and the completion of the neuronal differentiation program, the mechanism uncovered here likely facilitates the transition of MIZ cells towards neuronal production and might be relevant to the earlier maturation of the midbrain basal plate observed in all vertebrates during development (Easter et al., 1994; Puelles et al., 1987; Ross et al., 1992; Wilson et al., 1990).

Positive and negative effects were reported for Gli1 on neurogenesis depending on the cell type or cell state considered. Supporting a neurogenesis-promoting role, *neurog1* induction or the progression of *ath5* expression fail when Gli1 function is blocked in the *Xenopus* neural plate or zebrafish retina, respectively (Masai et al., 2005; Nguyen et al., 2005). In contrast, a similar down-regulation of Gli1 prevents reentry into S phase in the chicken ventral neural tube, suggesting a cell division-promoting effect (Cayuso et al., 2006). Divergent outcomes also follow manipulations of Hh activity (Cayuso et al., 2006; Masai et al., 2005; Shkumatava and Neumann, 2005; Takamiya and Campos-Ortega, 2006; Ungos et al., 2003; Wechsler-Reya and Scott, 1999) of which a direct output is Gli1 expression. Like recently proposed for Hh signaling (Agathocleous et al., 2007), a unifying hypothesis might be that Gli1 brings cells closer to differentiation, hence pushing early progenitors to amplify and later progenitor to a final cell cycle.

At the IZ, however, where an amplifying population has been observed neither within the IZ nor at the transition with the neurogenic zones, an effect on the cell cycle is improbable and we propose that Gli1 targets are rather cell cycle-independent commitment genes or genes that prime progenitors towards responding to commitment factors. Further supporting arguments to this hypothesis stem from previous analyses of the zebrafish *gli1/detour* mutants (Karlstrom et al., 1999). These mutants lack cranial motorneurons, including nerve III (Chandrasekhar et al., 1999) (which likely originates from the MIZ, (Tallafuss and Bally-Cuif, 2003), and C. Webb and C.S., unpublished), but display no defects in neurogenesis at 18 hours, pointing to a differentiation rather than an induction defect (Chandrasekhar et al., 1999). It remains unclear, however, whether the lack of nerve III results from failure of the early function of Gli1 that we uncovered or from a later role in neuronal differentiation. In more posterior hindbrain areas, the critical period for motorneuron induction is 9 hpf or earlier (Vanderlaan et al., 2005), a time frame compatible with our observations at the IZ. However, the lack of cranial motorneurons of *gli1/detour* mutants can be mimicked by loss of Smoothed function or by cyclopamine treatment (Vanderlaan et al., 2005), hence might be a result of impaired Hh signaling, which contrasts with our interpretation of Gli1 regulation at the MIZ. In any case, however, both analyses point to a role for Gli1 in promoting differentiation in a manner independent of cell cycle control.

Hh-independent regulation of Gli1

Given the importance of Gli1 function in neurogenesis progression or timing, a crucial question remains to uncover the pathway(s) controlling Gli1 expression in the MIZ. Gli1 is a known down-regulated target of GSK3 β /PKA (Huangfu and Anderson, 2006; Riobo and Manning, 2007), which, as described in this paper, is active across the IZ. This pathway might down-regulate Gli1 during IZ formation, as suggested by the fact that loss of Gli1 function rescues the lack of GSK3 β or PKA activities. Predictably, this effect likely occurs at the

post-transcriptional level, as *gli1* transcript levels did not appear modified (not shown). However, this down-regulation of Gli1 by GSK3 β /PKA is only partial, given that blocking Gli1 activity has further phenotypical consequences. A most surprising aspect of our study is that Gli1 expression and activity at the IZ are not under control of Hh signaling alone. Indeed, blocking Hh with cyclopamine or in *smu* mutants affected neither *gli1* expression nor IZ formation. Although surprising, these findings are in fitting with previous observations by Karlstrom et al. who reported maintenance of *gli1* expression in the anterior neural plate of *smu* mutants or cyclopamine-treated embryos (Karlstrom et al., 2003). Recently, a discrepancy between the effects of *smu* mutations or cyclopamine, which block Hh signaling upstream of PKA, and the effects of forskolin, which activates PKA, were also noted during retinal neurogenesis in zebrafish: while forskolin strongly impaired neurogenesis progression, *smu* or cyclopamine-treated embryos exhibited only mild defects (Masai et al., 2005). Our results here are very comparable with these observations and, we believe, lead to questioning a role of Hh at all in Gli1 regulation across the IZ. In a few instances, activation of Gli1 (or Gli2) has been reported to follow activation of the ERK pathway by Fgf signaling (Brewster et al., 2000; Riobo et al., 2006a; Riobo et al., 2006b) or of the PI3K and Akt pathway by mitogens (Riobo et al., 2006b). It is possible that such an atypical, Hh-independent mechanism is involved at the midline of the anterior neural plate. Unraveling this process will be an important future direction in our understanding of neurogenesis control and the cross-regulatory activities of Hh signaling pathway components.

Acknowledgements

We are grateful to Dr. Kenji Imai and to members of the Bally-Cuif laboratory for support and discussions, and to Silvia Krutsch for technical support. We also wish to thank Drs. Rolf Karlstrom, Uwe Strähle and Masanari Takamiya for sharing knowledge and reagents on the Hedgehog pathway and neurogenesis. Work in LBC laboratory is funded by a junior group grant from the Volkswagen Association, the EU 6th framework integrated project ZF-

Models (contract No. LSHC-CT-2003-503466), the Life Science Association (No. GSF 2005/01), and a special research grant from the Institut du Cerveau et de la Moelle épinière (ICM, Paris).

References

- Agathocleous, M., Locker, M., Harris, W. A. and Perron, M.** (2007). A general role of hedgehog in the regulation of proliferation. *Cell Cycle* **6**, 156-9.
- Bae, Y. K., Shimizu, T. and Hibi, M.** (2005). Patterning of proneuronal and inter-proneuronal domains by hairy- and enhancer of split-related genes in zebrafish neuroectoderm. *Development* **132**, 1375-85.
- Bally-Cuif, L., Golidis, C. and Santoni, M. J.** (1993). The mouse NCAM gene displays a biphasic expression pattern during neural tube development. *Development* **117**, 543-52.
- Bally-Cuif, L. and Hammerschmidt, M.** (2003). Induction and patterning of neuronal development, and its connection to cell cycle control. *Curr Opin Neurobiol* **13**, 16-25.
- Barresi, M. J., Stickney, H. L. and Devoto, S. H.** (2000). The zebrafish slow-muscle-omitted gene product is required for Hedgehog signal transduction and the development of slow muscle identity. *Development* **127**, 2189-99.
- Berridge, M. J., Downes, C. P. and Hanley, M. R.** (1989). Neural and developmental actions of lithium: a unifying hypothesis. *Cell* **59**, 411-9.
- Blader, P., Fischer, N., Gradwohl, G., Guillemont, F. and Strähle, U.** (1997). The activity of neurogenin1 is controlled by local cues in the zebrafish embryo. *Development* **124**, 4557-69.
- Brewster, R., Mullor, J. L. and Ruiz i Altaba, A.** (2000). Gli2 functions in FGF signaling during antero-posterior patterning. *Development* **127**, 4395-405.
- Buckles, G. R., Thorpe, C. J., Ramel, M. C. and Lekven, A. C.** (2004). Combinatorial Wnt control of zebrafish midbrain-hindbrain boundary formation. *Mech Dev* **121**, 437-47.
- Calegari, F. and Huttner, W. B.** (2003). An inhibition of cyclin-dependent kinases that lengthens, but does not arrest, neuroepithelial cell cycle induces premature neurogenesis. *J Cell Sci* **116**, 4947-55.
- Cayuso, J., Ulloa, F., Cox, B., Briscoe, J. and Marti, E.** (2006). The Sonic hedgehog pathway independently controls the patterning, proliferation and survival of neuroepithelial cells by regulating Gli activity. *Development* **133**, 517-28.
- Chandrasekhar, A., Schauerte, H. E., Haffter, P. and Kuwada, J. Y.** (1999). The zebrafish *detour* gene is essential for cranial but not spinal motor neuron induction. *Development* **126**, 2727-37.
- Chen, J. K., Taipale, J., Cooper, M. K. and Beachy, P. A.** (2002). Inhibition of Hedgehog signaling by direct binding of cyclopamine to Smoothened. *Genes Dev* **16**, 2743-8.
- Chen, W., Burgess, S. and Hopkins, N.** (2001). Analysis of the zebrafish *smoothened* mutant reveals conserved and divergent functions of hedgehog activity. *Development* **128**, 2385-96.
- Dorsky, R. I., Itoh, M., Moon, R. T. and Chitnis, A.** (2003). Two *tcf3* genes cooperate to pattern the zebrafish brain. *Development* **130**, 1937-47.
- Dorsky, R. I., Sheldahl, L. C. and Moon, R. T.** (2002). A transgenic *Lef1*/beta-catenin-independent reporter is expressed in spatially restricted domains throughout zebrafish development. *Dev Biol* **241**, 229-37.
- Dudek, H., Datta, S. R., Franke, T. F., Birnbaum, M. J., Yao, R., Cooper, G. M., Segal, R. A., Kaplan, D. R. and Greenberg, M. E.** (1997). Regulation of neuronal survival by the serine-threonine protein kinase Akt. *Science* **275**, 661-5.
- Easter, S. S., Jr., Burrill, J., Marcus, R. C., Ross, L., Taylor, J. S. H. and Wilson, S. W.** (1994). Initial tract formation in the vertebrate brain. *Progress in Brain Research* **102**, 79-93.
- Ertzer, R., Muller, F., Hadzhiev, Y., Rathnam, S., Fischer, N., Rastegar, S. and Strähle, U.** (2007). Cooperation of sonic hedgehog enhancers in midline expression. *Dev Biol* **301**, 578-89.
- Frame, S. and Cohen, P.** (2001). GSK3 takes centre stage more than 20 years after its discovery. *Biochem J* **359**, 1-16.

- Geling, A., Itoh, M., Tallafuss, A., Chapouton, P., Tannhäuser, B., Kuwada, J. Y., Chitnis, A. B. and Bally-Cuif, L.** (2003). bHLH transcription factor Her5 links patterning to regional inhibition of neurogenesis at the midbrain-hindbrain boundary. *Development* **130**, 1591-1604.
- Geling, A., Plessy, C., Rastegar, S., Strähle, U. and Bally-Cuif, L.** (2004). Her5 acts as a prepattern factor that blocks neurogenin1 and coe2 expression upstream of Notch to inhibit neurogenesis at the midbrain-hindbrain boundary. *Development* **131**, 1993-2006.
- Hammerschmidt, M., Bitgood, M. J. and McMahon, A. P.** (1996a). Protein kinase A is a common negative regulator of Hedgehog signaling in the vertebrate embryo. *Genes Dev* **10**, 647-58.
- Hammerschmidt, M., Pelegri, F., Mullins, M. C., Kane, D. A., van Eeden, F. J., Granato, M., Brand, M., Furutani-Seiki, M., Haffter, P., Heisenberg, C. P. et al.** (1996b). dino and mercedes, two genes regulating dorsal development in the zebrafish embryo. *Development* **123**, 95-102.
- Hans, S., Scheer, N., Riedl, I., v Weizsacker, E., Blader, P. and Campos-Ortega, J. A.** (2004). her3, a zebrafish member of the hairy-E(spl) family, is repressed by Notch signalling. *Development* **131**, 2957-69.
- Hardcastle, Z. and Papalopulu, N.** (2000). Distinct effects of XBF-1 in regulating the cell cycle inhibitor p27(XIC1) and imparting a neural fate. *Development* **127**, 1303-14.
- Harris, W. A. and Hartenstein, V.** (1991). Neuronal determination without cell division in *Xenopus* embryos. *Neuron* **6**, 499-515.
- Hatakeyama, J., Bessho, Y., Katoh, K., Ookawara, S., Fujioka, M., Guillemot, F. and Kageyama, R.** (2004). Hes genes regulate size, shape and histogenesis of the nervous system by control of the timing of neural stem cell differentiation. *Development* **131**, 5539-50.
- Hatakeyama, J. and Kageyama, R.** (2006). Notch1 expression is spatiotemporally correlated with neurogenesis and negatively regulated by Notch1-independent Hes genes in the developing nervous system. *Cereb Cortex* **16** Suppl 1, i132-7.
- Hedgepeth, C. M., Conrad, L. J., Zhang, J., Huang, H. C., Lee, V. M. and Klein, P. S.** (1997). Activation of the Wnt signaling pathway: a molecular mechanism for lithium action. *Dev Biol* **185**, 82-91.
- Heisenberg, C. P., Houart, C., Take-Uchi, M., Rauch, G. J., Young, N., Coutinho, P., Masai, I., Caneparo, L., Concha, M. L., Geisler, R. et al.** (2001). A mutation in the Gsk3-binding domain of zebrafish Masterblind/Axin1 leads to a fate transformation of telencephalon and eyes to diencephalon. *Genes Dev* **15**, 1427-34.
- Hirata, H., Tomita, K., Bessho, Y. and Kageyama, R.** (2001). Hes1 and Hes3 regulate maintenance of the isthmic organizer and development of the mid/hindbrain. *Embo J* **20**, 4454-66.
- Hooper, J. E. and Scott, M. P.** (2005). Communicating with Hedgehogs. *Nat Rev Mol Cell Biol* **6**, 306-17.
- Huangfu, D. and Anderson, K. V.** (2006). Signaling from Smo to Ci/Gli: conservation and divergence of Hedgehog pathways from *Drosophila* to vertebrates. *Development* **133**, 3-14.
- Jia, J., Amanai, K., Wang, G., Tang, J., Wang, B. and Jiang, J.** (2002). Shaggy/GSK3 antagonizes Hedgehog signalling by regulating Cubitus interruptus. *Nature* **416**, 548-52.
- Kageyama, R., Ohtsuka, T., Hatakeyama, J. and Ohsawa, R.** (2005). Roles of bHLH genes in neural stem cell differentiation. *Exp Cell Res* **306**, 343-8.
- Karlstrom, R. O., Talbot, W. S. and Schier, A. F.** (1999). Comparative synteny cloning of zebrafish you-too: mutations in the Hedgehog target gli2 affect ventral forebrain patterning. *Genes Dev* **13**, 388-93.
- Karlstrom, R. O., Tyurina, O. V., Kawakami, A., Nishioka, N., Talbot, W. S., Sasaki, H. and Schier, A. F.** (2003). Genetic analysis of zebrafish gli1 and gli2 reveals divergent requirements for gli genes in vertebrate development. *Development* **130**, 1549-64.
- Ke, Z., Emelyanov, A., Lim, S. E., Korzh, V. and Gong, Z.** (2005). Expression of a novel zebrafish zinc finger gene, gli2b, is affected in Hedgehog and Notch signaling related mutants during embryonic development. *Dev Dyn* **232**, 479-86.
- Kenney, A. M., Widlund, H. R. and Rowitch, D. H.** (2004). Hedgehog and PI-3 kinase signaling converge on Nmyc1 to promote cell cycle progression in cerebellar neuronal precursors. *Development* **131**, 217-28.

- Kim, C. H., Oda, T., Itoh, M., Jiang, D., Artinger, K. B., Chandrasekharappa, S. C., Driever, W. and Chitnis, A. B.** (2000). Repressor activity of Headless/Tcf3 is essential for vertebrate head formation. *Nature* **407**, 913-6.
- Kimmel, C. B., Ballard, W. W., Kimmel, S. R., Ullmann, B. and Schilling, T. F.** (1995). Stages of embryonic development of the zebrafish. *Dev Dyn* **203**, 253-310.
- Kimmel, C. B., Warga, R. M. and Kane, D. A.** (1994). Cell cycles and clonal strings during formation of the zebrafish central nervous system. *Development* **120**, 265-76.
- Klein, P. S. and Melton, D. A.** (1996). A molecular mechanism for the effect of lithium on development. *Proc Natl Acad Sci U S A* **93**, 8455-9.
- Korzh, V., Sleptsova, I., Liao, J., He, J. and Gong, Z.** (1998). Expression of zebrafish bHLH genes *ngn1* and *nrd* defines distinct stages of Neural differentiation. *Dev. Dynam.* **213**, 92-104.
- Krauss, S., Concordet, J. P. and Ingham, P. W.** (1993). A functionally conserved homolog of the *Drosophila* segment polarity gene *hh* is expressed in tissues with polarizing activity in zebrafish embryos. *Cell* **75**, 1431-44.
- Lekven, A. C., Buckles, G. R., Kostakis, N. and Moon, R. T.** (2003). Wnt1 and *wnt10b* function redundantly at the zebrafish midbrain-hindbrain boundary. *Dev Biol* **254**, 172-87.
- Lewis, J. L., Bonner, J., Modrell, M., Ragland, J. W., Moon, R. T., Dorsky, R. I. and Raible, D. W.** (2004). Reiterated Wnt signaling during zebrafish neural crest development. *Development* **131**, 1299-308.
- Logan, C. Y. and Nusse, R.** (2004). The Wnt signaling pathway in development and disease. *Annu Rev Cell Dev Biol* **20**, 781-810.
- Lun, K. and Brand, M.** (1998). A series of no isthmus (*noi*) alleles of the zebrafish *pax2.1* gene reveals multiple signaling events in development of the midbrain-hindbrain boundary. *Development* **125**, 3049-62.
- Martinez, A., Alonso, M., Castro, A., Perez, C. and Moreno, F. J.** (2002). First non-ATP competitive glycogen synthase kinase 3 beta (GSK-3beta) inhibitors: thiadiazolidinones (TDZD) as potential drugs for the treatment of Alzheimer's disease. *J Med Chem* **45**, 1292-9.
- Masai, I., Yamaguchi, M., Tonou-Fujimori, N., Komori, A. and Okamoto, H.** (2005). The hedgehog-PKA pathway regulates two distinct steps of the differentiation of retinal ganglion cells: the cell-cycle exit of retinoblasts and their neuronal maturation. *Development* **132**, 1539-53.
- Megason, S. G. and McMahon, A. P.** (2002). A mitogen gradient of dorsal midline Wnts organizes growth in the CNS. *Development* **129**, 2087-98.
- Mill, P., Mo, R., Hu, M. C., Dagnino, L., Rosenblum, N. D. and Hui, C. C.** (2005). Shh controls epithelial proliferation via independent pathways that converge on N-Myc. *Dev Cell* **9**, 293-303.
- Molven, A., Njolstad, P. R. and Fjose, A.** (1991). Genomic structure and restricted neural expression of the zebrafish *wnt-1* (*int-1*) gene. *Embo J* **10**, 799-807.
- Moore, K., Schneider, M. and Vetter, M.** (2002). Posttranslational mechanisms control the timing of bHLH function and regulate retinal cell fate. *Neuron* **34**, 183-195.
- Müller, M., v. Weizsäcker, E. and Campos-Ortega, J. A.** (1996). Transcription of a zebrafish gene of the hairy-Enhancer of split family delineates the midbrain anlage in the neural plate. *Dev. Genes Evol.* **206**, 153-160.
- Nguyen, V., Chokas, A. L., Stecca, B. and Altaba, A. R.** (2005). Cooperative requirement of the Gli proteins in neurogenesis. *Development* **132**, 3267-79.
- Ninkovic, J., Tallafuss, A., Leucht, C., Topczewski, J., Tannhauser, B., Solnica-Krezel, L. and Bally-Cuif, L.** (2005). Inhibition of neurogenesis at the zebrafish midbrain-hindbrain boundary by the combined and dose-dependent activity of a new hairy/E(spl) gene pair. *Development* **132**, 75-88.
- Panchision, D. M. and McKay, R. D.** (2002). The control of neural stem cells by morphogenic signals. *Curr Opin Genet Dev* **12**, 478-87.
- Panhuisen, M., Vogt-Weisenhorn, D., Blanquet, V., Brodski, C., Heinzmann, U., Beister, W. and Wurst, W.** (2004). Effects of Wnt signaling on proliferation in the developing mid-hindbrain region. *Mol. Cell. Neurosc.* **26**, 101-111.
- Papan, C. and Campos-Ortega, J. A.** (1997). A clonal analysis of spinal cord development in the zebrafish. *Dev. Genes Evol.* **207**, 71-81.

- Price, M. A. and Kalderon, D.** (2002). Proteolysis of the Hedgehog signaling effector Cubitus interruptus requires phosphorylation by Glycogen Synthase Kinase 3 and Casein Kinase 1. *Cell* **108**, 823-35.
- Puelles, L., Amat, J. A. and Martinez-de-la-Torre, M.** (1987). Segment-related, mosaic neurogenetic pattern in the forebrain and mesencephalon of early chick embryos: I. Topography of AChE-positive neuroblasts up to stage HH18. *J Comp Neurol* **266**, 247-68.
- Riobo, N. A., Haines, G. M. and Emerson, C. P., Jr.** (2006a). Protein kinase C-delta and mitogen-activated protein/extracellular signal-regulated kinase-1 control GLI activation in hedgehog signaling. *Cancer Res* **66**, 839-45.
- Riobo, N. A., Lu, K. and Emerson, C. P., Jr.** (2006b). Hedgehog signal transduction: signal integration and cross talk in development and cancer. *Cell Cycle* **5**, 1612-5.
- Riobo, N. A. and Manning, D. R.** (2007). Pathways of signal transduction employed by vertebrate Hedgehogs. *Biochem J* **403**, 369-79.
- Ross, L., Parrett, T. and Easter, S. J.** (1992). Axonogenesis and morphogenesis in the embryonic zebrafish brain. *J. Neurosci.* **12**, 467-482.
- Ruiz, I. A. A., Palma, V. and Dahmane, N.** (2002). Hedgehog-Gli signalling and the growth of the brain. *Nat Rev Neurosci* **3**, 24-33.
- Shkumatava, A. and Neumann, C. J.** (2005). Shh directs cell-cycle exit by activating p57Kip2 in the zebrafish retina. *EMBO Rep* **6**, 563-9.
- Stigloher, C., Chapouton, P., Adolf, B. and Bally-Cuif, L.** (2007). Identification of neural progenitor pools by E(Spl) factors in the embryonic and adult brain. *Brain Res. Bull.* in press.
- Stigloher, C., Ninkovic, J., Laplante, M., Geling, A., Tannhauser, B., Topp, S., Kikuta, H., Becker, T. S., Houart, C. and Bally-Cuif, L.** (2006). Segregation of telencephalic and eye-field identities inside the zebrafish forebrain territory is controlled by Rx3. *Development* **133**, 2925-35.
- Strahle, U., Fischer, N. and Blader, P.** (1997). Expression and regulation of a netrin homologue in the zebrafish embryo. *Mech Dev* **62**, 147-60.
- Takamiya, M. and Campos-Ortega, J. A.** (2006). Hedgehog signalling controls zebrafish neural keel morphogenesis via its level-dependent effects on neurogenesis. *Dev Dyn* **235**, 978-97.
- Tallafuss, A. and Bally-Cuif, L.** (2003). Tracing of her5 progeny in zebrafish transgenics reveals the dynamics of midbrain-hindbrain neurogenesis and maintenance. *Development* **130**, 4307-4323.
- Taurin, S., Sandbo, N., Qin, Y., Browning, D. and Dulin, N. O.** (2006). Phosphorylation of beta-catenin by cyclic AMP-dependent protein kinase. *J Biol Chem* **281**, 9971-6.
- Tyurina, O. V., Guner, B., Popova, E., Feng, J., Schier, A. F., Kohtz, J. D. and Karlstrom, R. O.** (2005). Zebrafish Gli3 functions as both an activator and a repressor in Hedgehog signaling. *Dev Biol* **277**, 537-56.
- Ungos, J. M., Karlstrom, R. O. and Raible, D. W.** (2003). Hedgehog signaling is directly required for the development of zebrafish dorsal root ganglia neurons. *Development* **130**, 5351-62.
- Vaage, S.** (1969). Segmentation of the primitive neural tube in chick embryos. *Ergebn. Anat. Entwickl.-Gesch.* **41**, 1-88.
- van de Water, S., van de Wetering, M., Joore, J., Esseling, J., Bink, R., Clevers, H. and Zivkovic, D.** (2001). Ectopic Wnt signal determines the eyeless phenotype of zebrafish masterblind mutant. *Development* **128**, 3877-88.
- Vanderlaan, G., Tyurina, O. V., Karlstrom, R. O. and Chandrasekhar, A.** (2005). Gli function is essential for motor neuron induction in zebrafish. *Dev Biol* **282**, 550-70.
- Varga, Z. M., Amores, A., Lewis, K. E., Yan, Y. L., Postlethwait, J. H., Eisen, J. S. and Westerfield, M.** (2001). Zebrafish smoothed functions in ventral neural tube specification and axon tract formation. *Development* **128**, 3497-509.
- Wechsler-Reya, R. J. and Scott, M. P.** (1999). Control of neuronal precursor proliferation in the cerebellum by Sonic Hedgehog. *Neuron* **22**, 103-14.
- Weinberg, E. S., Allende, M. L., Kelly, C. S., Abdelhamid, A., Murakami, T., Andermann, P., Doerre, O. G., Grunwald, D. J. and Riggleman, B.** (1996). Developmental regulation of zebrafish MyoD in wild-type, no tail and spadetail embryos. *Development* **122**, 271-80.

- Wilson, S., Ross, L., Parrett, T. and Easter, S.** (1990). The development of a simple scaffold of axon tracts in the brain of the embryonic zebrafish *Brachydanio rerio*. *Development* **108**, 121-145.
- Woo, K. and Fraser, S. E.** (1995). Order and coherence in the fate map of the zebrafish nervous system. *Development* **121**, 2595-2609.
- Zechner, D., Fujita, Y., Hulsken, J., Muller, T., Walther, I., Taketo, M., Crenshaw, E. r., Birchmeier, W. and Birchmeier, C.** (2003). beta-catenin signals regulate cell growth and the balance between progenitor cell expansion and differentiation in the nervous system. *Dev. Biol.* **258**, 406-418.
- Zhang, W., Zhao, Y., Tong, C., Wang, G., Wang, B., Jia, J. and Jiang, J.** (2005). Hedgehog-regulated Costal2-kinase complexes control phosphorylation and proteolytic processing of *Cubitus interruptus*. *Dev Cell* **8**, 267-78.

Legends for figures

Figure 1. Summary of the location and properties of the “Intervening Zone” (IZ) pool of neural progenitors. A: Scheme of the zebrafish anterior neural plate at 3-somites, dorsal view anterior up. The IZ area (identical to the expression domain of *her5* and *her11*) is surrounded in red and is composed of medial and lateral cell populations (MIZ and LIZ, respectively). The IZ separates early *neurog1*-positive proneural clusters (r2l: presumptive lateral neurons of rhombomere 2, r2MN: presumptive motorneurons of rhombomere 2; vcc: ventro-caudal cluster). **B:** Phenotype observed at 3 somites (orientation as in A) when two doses of “Her5 + Her11” are lost (e.g. injection of anti-*her5* or anti-*her11* antisense oligonucleotides): the MIZ is lost and replaced by a *neurog1*-positive proneural cluster (arrows), while the LIZ is intact. **C:** Phenotype when four doses of “Her5 + Her11” are lost (e.g. injection of anti-*her5* and anti-*her11* antisense oligonucleotides): *neurog1* expression also becomes induced within the LIZ (arrows). After (Ninkovic et al., 2005; Tallafuss and Bally-Cuif, 2003).

Figure 2. LiCl enhances neurogenesis in place of the IZ independently of canonical Wnt signaling and its effects are mimicked by GSK3 β inhibition. All embryos are analyzed at the 3-somite stage by in situ hybridization (probes indicated, *neurog1* +/- *pax2.1*, color-coded) and flat-mounted anterior up; in A-D, the brackets indicate the MIZ. **A-F’:** Treatment with LiCl at 80% epiboly (B,E,E’), compared to untreated embryos (D,F,F’) induces ectopic *neurog1* expression in place of the MIZ (blue arrows in B, E’), while it rather posteriorizes the anterior neural plate when applied earlier (A), and is without effect when applied later (C). **G,H:** Effect of LiCl applied at 80% epiboly (G) in transgenic *hsp70l:tcf3-GFP^{w3}* embryos expressing a dominant-negative Tcf3 upon heat-shock. Note that expression of this transgene alone, which blocks canonical Wnt signaling, does not perturb IZ formation (H). **I-L:** GSK3 β activity is required for IZ formation. The selective GSK3 β inhibitor OTDZT triggers ectopic *neurog1* expression in place of the MIZ (I,I’, compare

to J,J'), as well as within the LIZ when Her5 activity is lowered by *her5* gripNA injection (L, compare to K). These effects are identical to those triggered by LiCl.

Figure 3. Activated PKA can compensate for lowered GSK3 β or E(Spl) activity to promote IZ formation. All embryos are analyzed at the 4-somite stage for expression of *neurog1* and *pax2.1* (color-coded) and flat-mounted anterior up; brackets to the MIZ, arrows to ectopic *neurog1* expression. **A-D:** Activated PKA (PKA*, injected as capped RNA at the one-cell stage) does not affect IZ formation (compare A and D, see also F) and blocks *neurog1* normally triggered by LiCl in place of the MIZ (compare B and C). **E-H:** Coinjection of PKA* RNA and *her5*GripNA (G) blocks the neurogenic effect induced by *her5*GripNA alone (E) and restores the MIZ.

Figure 4. Activated PKA is required for IZ formation in cooperation with GSK3 β and E(Spl) activity. All embryos are analyzed at the 3-somite stage for expression of *neurog1* and *pax2.1* (color-coded) and flat-mounted anterior up; blue arrows to ectopic *neurog1* expression, white arrowheads to *neurog1*-free LIZ. **A-D,I,J,L:** PKA is required for IZ formation and cooperates with E(Spl). Expression of a dominant-negative form of PKA (dnReg) induces *neurog1* expression in place of the MIZ (B), like down-regulating E(Spl) activity (A). Concomitant down-regulation of both pathways further leads to ectopic *neurog1* expression within the LIZ (C,L, compare to I,J). **E-H,K,M:** GSK3 β and PKA cooperate to permit IZ formation. Inhibiting each activity in isolation leads to loss of the MIZ (E,F, see also B and Fig. 2K,K'), while co-inhibition also induces ectopic *neurog1* expression within the LIZ (G,M, compare to K). **N,O:** Increase in E(Spl) activity does not suffice to compensate for down-regulation of PKA to permit IZ formation. Transgenic *Tg(her5PAC:EGFP)* embryos express one additional copy of the *her11* gene. The effect of blocking PKA remains however unchanged in this background (O, compare to B,F).

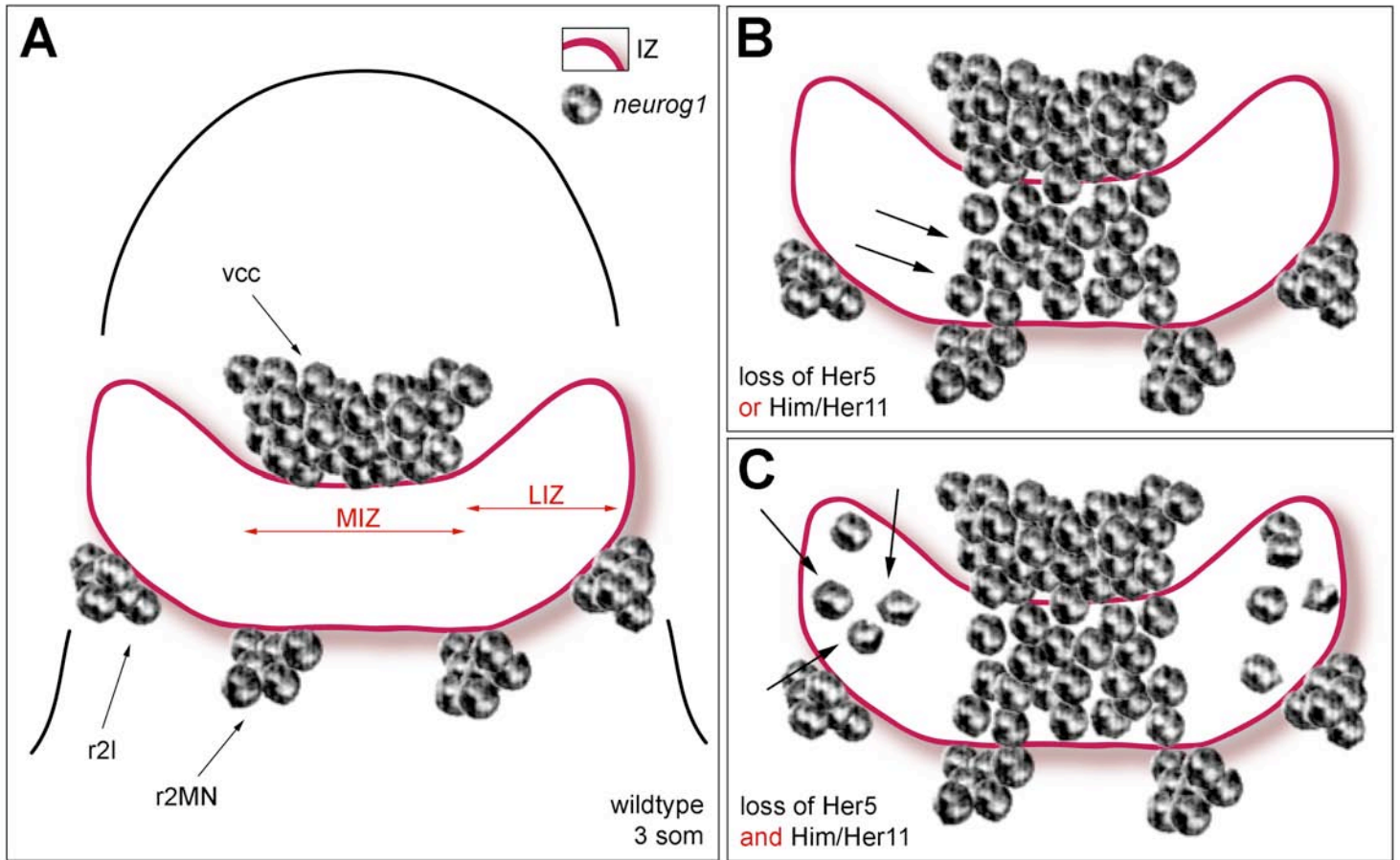
Figure 5. MIZ and LIZ cells differ in lineage and in their expression of Gli1, whose activity pushes cells towards neurogenesis and is a down-regulated target of GSK3 β /PKA during IZ formation. **A,B:** Activation of caged fluorescein at 50-60% epiboly as schematically indicated (A, dorsal view with the shield schematized as dark grey cells and the uncaged point as red cells) labels MIZ precursors (identified at tailbud by their co-expression of uncaged fluorescein -red- and GFP -green- in the transgenic *her5PAC:EGFP* background) (B, insets show single 2 μ m confocal planes in single and merged channels) and shows that these never give rise to cells located within the LIZ. **C:** Compared cell cycle characteristics of MIZ and LIZ cells during the time of IZ formation. The percentage of cells incorporating BrdU among all MIZ or LIZ cells (dapi) is identical at all stages. **D-F:** Expression of *gli1* (blue) and *pax2.1* (red) (flat-mounted embryos, anterior up, stages indicated) shows that *gli1* is transcribed at higher levels within the MIZ (arrows) than LIZ. **G-N:** Embryos analyzed at the 3-somite stage for expression of *neurog1* and *pax2.1* (color-coded) and flat-mounted anterior up; bracket to the MIZ, blue arrows to ectopic *neurog1* expression. **G-J:** Gli1 activity is a required mediator of the neurogenic effect of LiCl. Blocking Gli1 activity does not affect IZ formation (H, compare to J) but prevents the induction of *neurog1* expression across the MIZ normally triggered by LiCl treatment (I, compare to G). **K-N:** Gli1 is a down-regulated target of PKA for IZ formation. Blocking Gli1 activity is sufficient to rescue the MIZ normally lost upon PKA down-regulation (M, compare to K).

Figure 6. Gli1 accounts for the differential sensitivity of the MIZ and LIZ to E(Spl) neurogenesis inhibitors. Embryos analyzed at the 3-somite stage for expression of *neurog1* and *pax2.1* (color-coded) and flat-mounted anterior up; brackets to the MIZ, blue arrows to ectopic *neurog1* expression. In the absence of Gli1, cells of the MIZ are unaffected by the loss of Her5 i.e. respond to a lower dose of neurogenesis inhibition than normal (D, compare to B). Rather, cells of the LIZ and MIZ become concomitantly affected by a further down-regulation of E(Spl) activity (loss of both Her5 and Her11), when

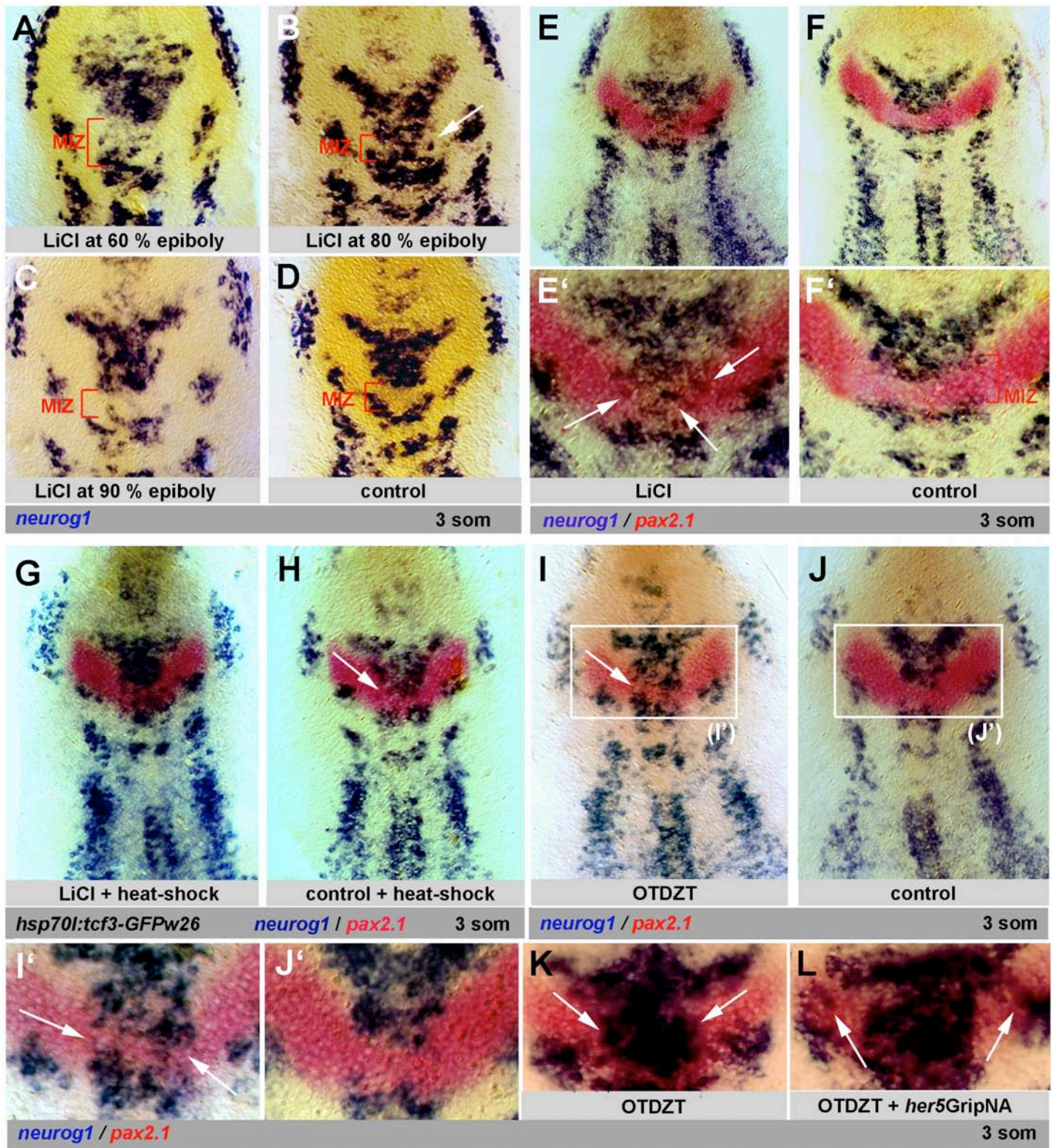
they upregulate *neurog1* in an indistinguishable manner (E, E'). Hence, in the absence of Gli1, MIZ cells behave like LIZ cells.

Figure 7. Gli1 expression is not under control of Hh signaling during IZ formation. **A,B:** Expression of *myoD* (blue) and *pax2.1* (red) on flat-mounted 3-somite old embryos (dorsal views, anterior left) upon cyclopamine treatment (B) compared to mock treatment (A). Cyclopamine leads to a strong down-regulation of *myoD* expression in adaxial cells (white arrowhead in B, compare to blue arrow in A). **C-F:** Expression of *neurog1* (blue) and *pax2.1* (red) at 3 somites, flat-mounted embryos anterior up; blue arrows to ectopic *neurog1* expression. Cyclopamine treatment does not affect IZ formation (D, compare to F) and does not rescue the effects of *her5*GripNA injections (E, compare to C), unlike blocking Gli1 activity (Fig.6D).

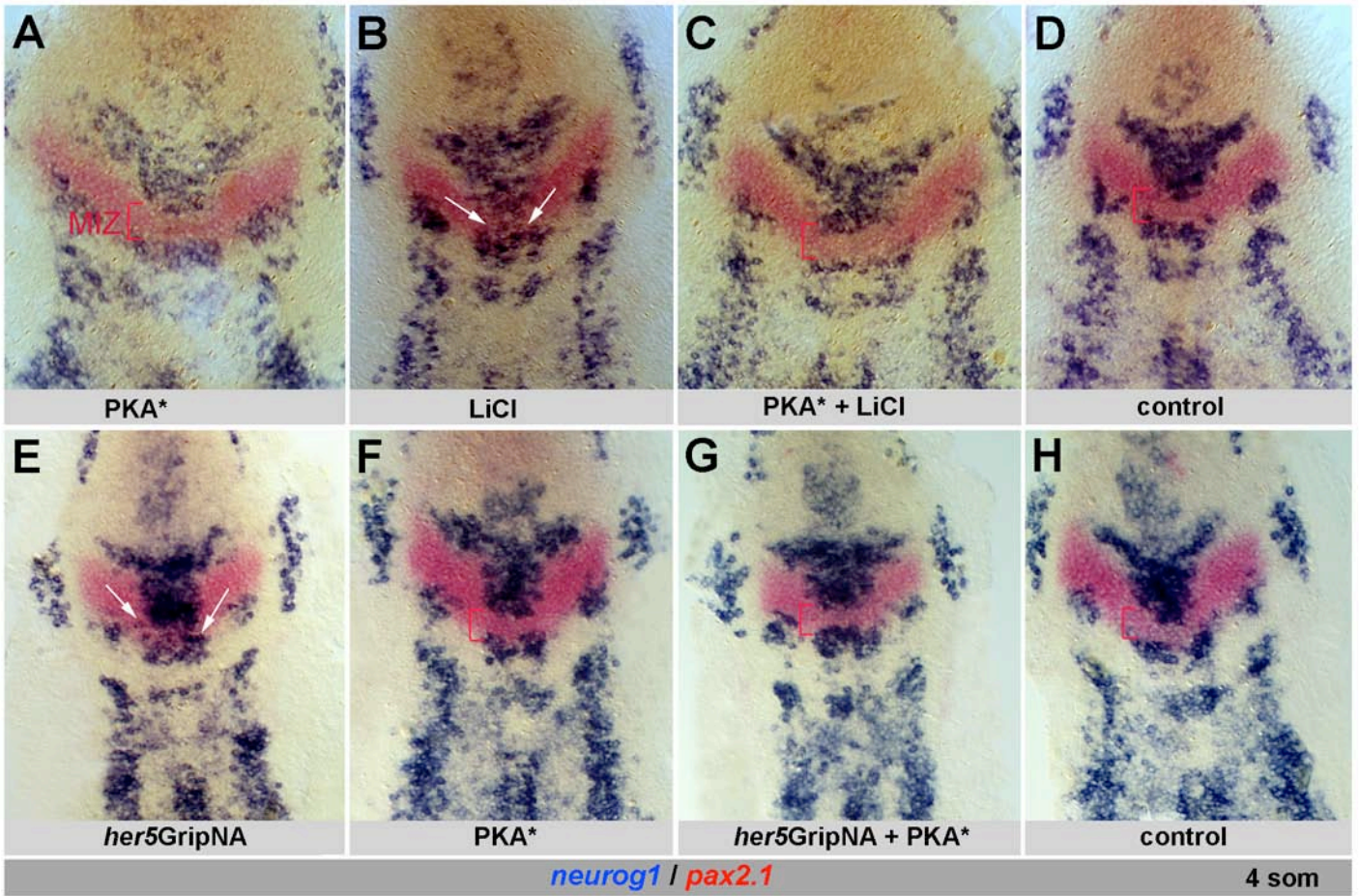
Figure 8. Model for IZ formation. One side of the neural plate is schematically represented (gray bar to the axial midline, red: MIZ and *gli1* expression domain, back: LIZ). The E(Spl) (Her5/Her11) and GSK3 β /PKA pathways inhibit neurogenesis throughout the IZ, in a dose-dependent and cooperative manner. Gli1, expressed in the MIZ in a manner independent of Hh alone, acts antagonistically, favoring cell commitment to neurogenesis. Gli1 activity might be partially down-regulated by GSK3 β /PKA. Responding to the sum of these activities, MIZ cells are more prone to commit towards neurogenesis than LIZ cells.



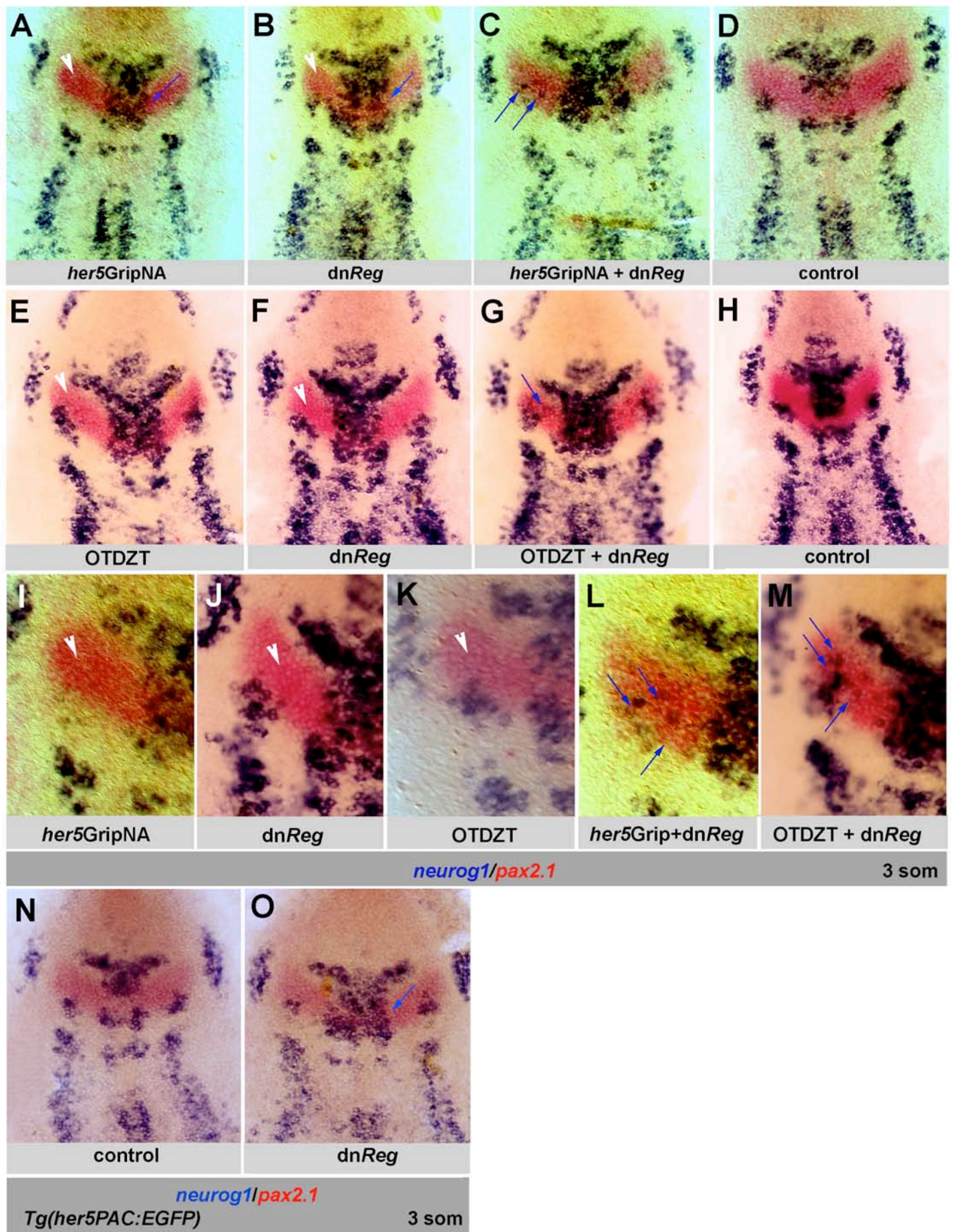
Ninkovic et al., Figure 1



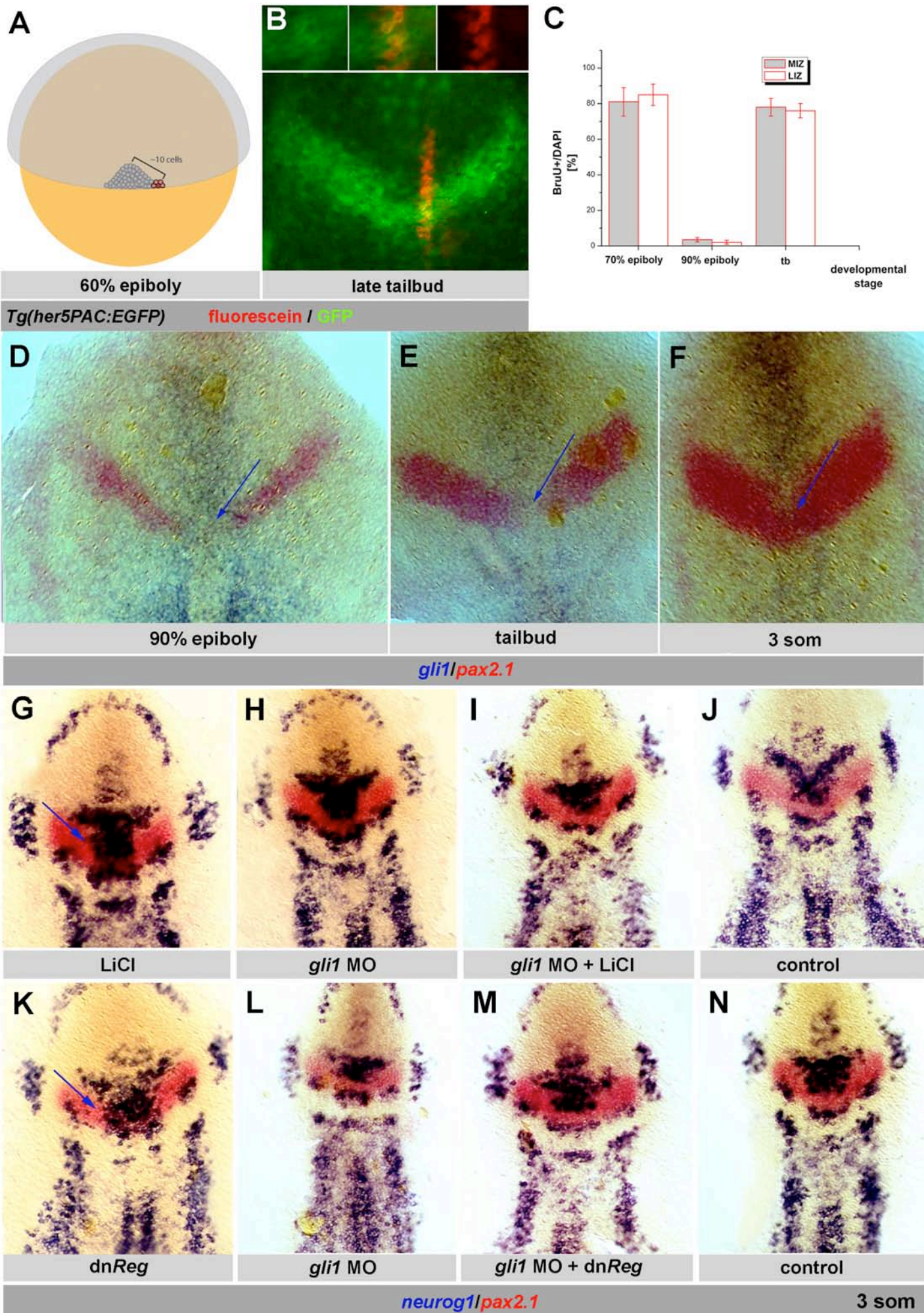
Ninkovic et al., Fig.2

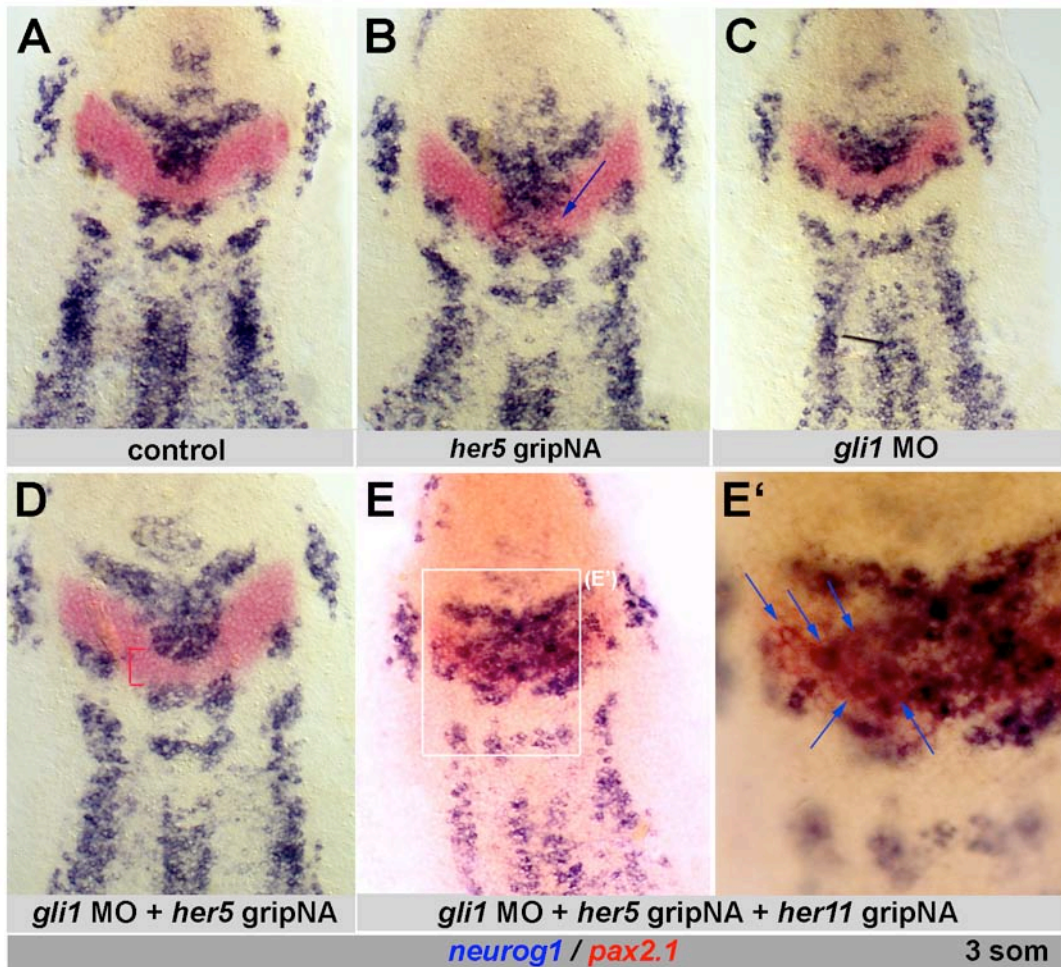


Ninkovic et al., Figure 3

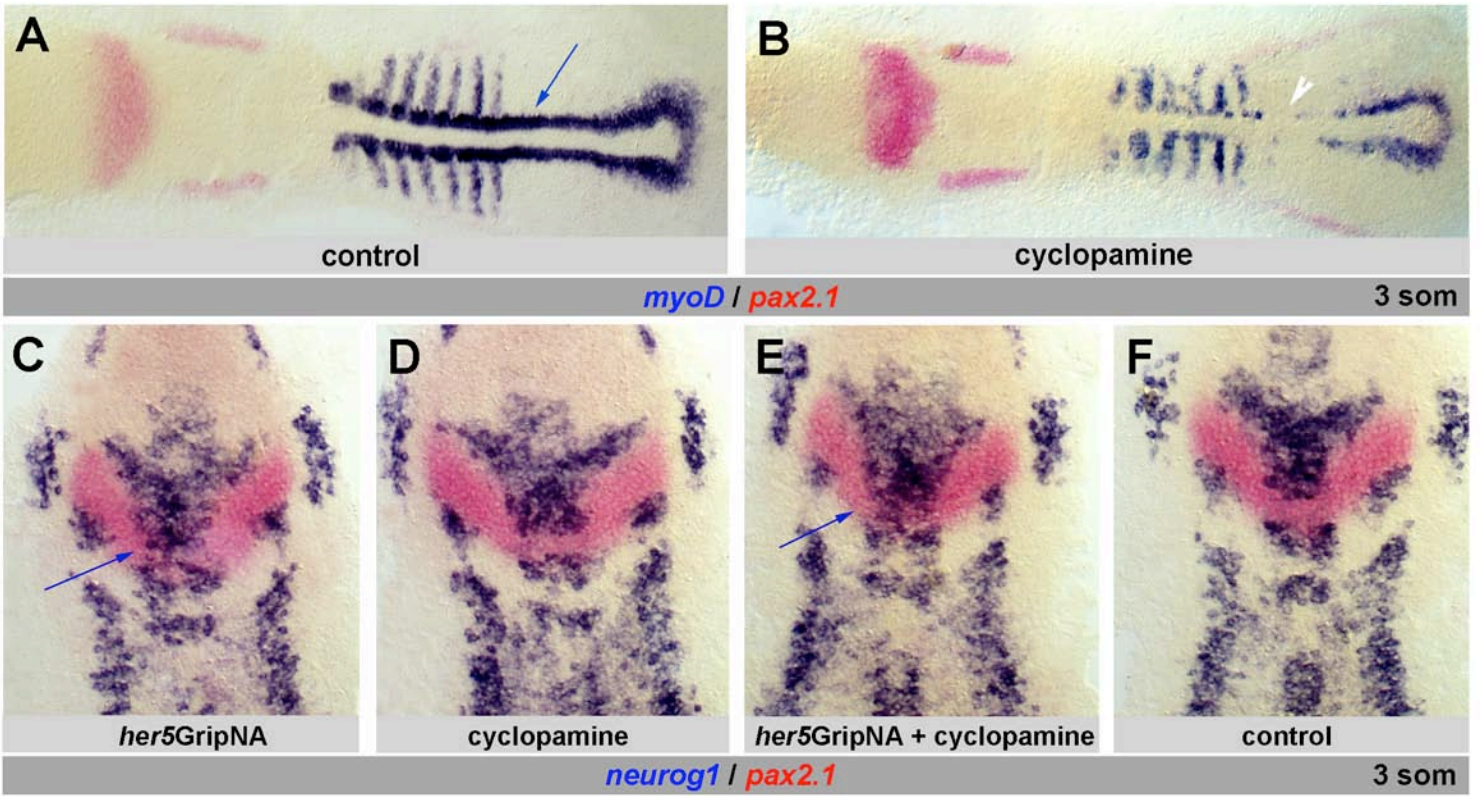


Ninkovic et al., Figure 4

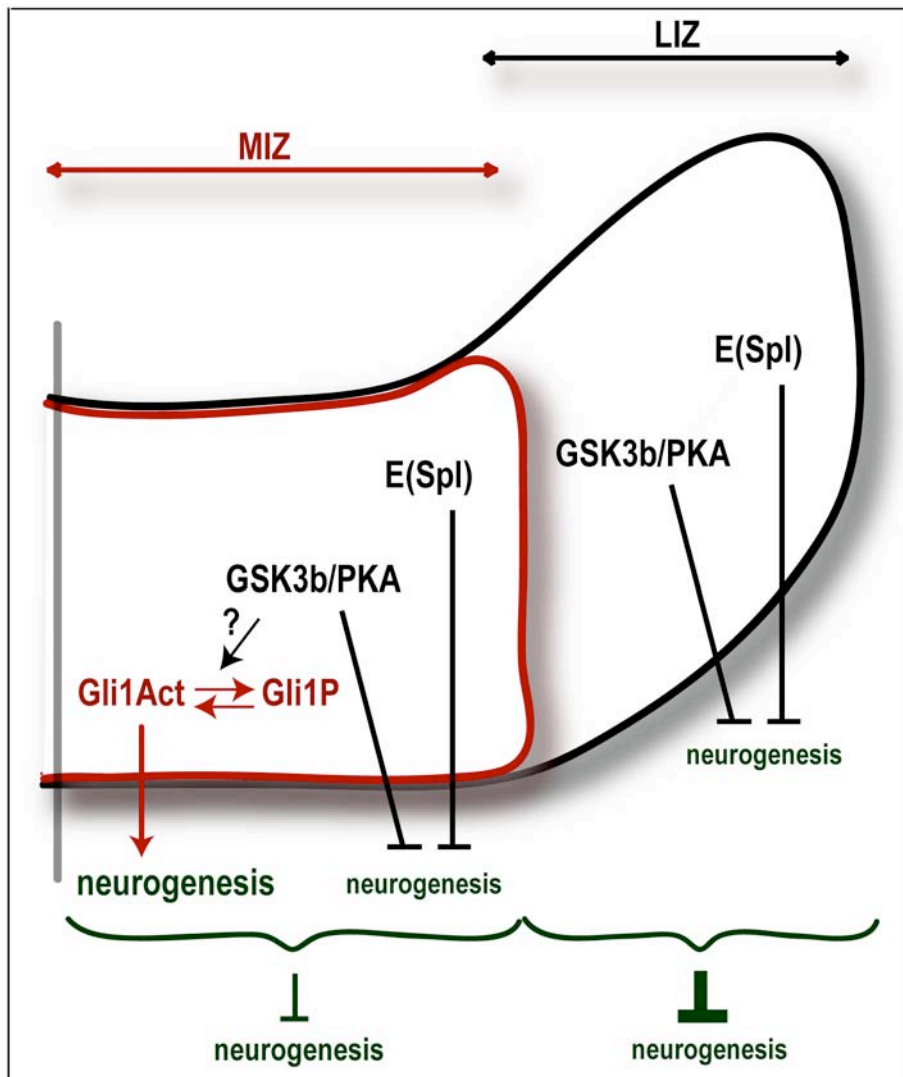




Ninkovic et al., Figure 6



Ninkovic et al., Figure 7



Ninkovic et al., Figure 8

Appendix 4

Article in press (online available) in ***Nature Neuroscience***

MicroRNA-9 directs late organizer activity of the midbrain-hindbrain boundary

Christoph Leucht*, Christian Stigloher*, Andrea Wizenmann,
Ruth Klafke, Anja Folchert and Laure Bally-Cuif

* shared first authorship

Contribution:

Christoph Leucht and I jointly conducted the experiments. I did gain-of-function and loss-of-function experiments (see Figures 1, 6, S2 and S3 in the article). Furthermore, I performed the sensor assay experiments with mutated binding sites (see Figure 2 in the article). In addition, I conducted the 'Binding Site Morpholino' (BSMO) experiments (see Figures 3, 4 and Supplementary Table 1) and gripNA experiments (Figures 4 and 7). Anja Folchert provided technical support. Andrea Wizenmann and Ruth Klafke performed parallel experiments in the chicken model in order to support our data (not shown in article). Finally, I contributed to the expression pattern analysis shown in Figure 5. Laure Bally-Cuif supervised the project. Christoph Leucht and Laure Bally-Cuif jointly wrote the manuscript.

MicroRNA-9 directs late organizer activity of the midbrain-hindbrain boundary

Christoph Leucht^{1,5}, Christian Stigloher^{1,5}, Andrea Wizenmann^{2,4}, Ruth Klafke³, Anja Folchert¹ & Laure Bally-Cuif¹

The midbrain-hindbrain boundary (MHB) is a long-lasting organizing center in the vertebrate neural tube that is both necessary and sufficient for the ordered development of midbrain and anterior hindbrain (midbrain-hindbrain domain, MH). The MHB also coincides with a pool of progenitor cells that contributes neurons to the entire MH. Here we show that the organizing activity and progenitor state of the MHB are co-regulated by a single microRNA, miR-9, during late embryonic development in zebrafish. Endogenous miR-9 expression, initiated at late stages, selectively spares the MHB. Gain- and loss-of-function studies, *in silico* predictions and sensor assays *in vivo* demonstrate that miR-9 targets several components of the Fgf signaling pathway, thereby delimiting the organizing activity of the MHB. In addition, miR-9 promotes progression of neurogenesis in the MH, defining the MHB progenitor pool. Together, these findings highlight a previously unknown mechanism by which a single microRNA fine-tunes late MHB coherence via its co-regulation of patterning activities and neurogenesis.

The architecture of the vertebrate CNS, first subdivided into prosencephalon, mesencephalon, hindbrain and spinal cord, is progressively refined by local organizing centers, of which the best characterized is the MHB¹. Organizers are not only involved in providing graded patterning cues to neighboring areas, but also act as long-lasting coordinators of many cellular events, such as cell fate, survival, proliferation, differentiation and migration. At early developmental stages, strong signaling from organizers, reinforced by positive regulatory loops and facilitated by the relatively short distances in the neural tube, ensures the spatial coherence of these cellular events. For instance, a crucial event in MHB maintenance and activity is signaling by the diffusible protein Fgf8 (ref. 1), which mainly exerts its function via its receptor Fgfr1 (ref. 2). However, a major question remains as to how this coordination can be maintained at later stages; organizer activity tends to decrease over time, and the distances that signals have to travel in the embryo and the diversity of cellular states around the organizer increase. The mechanisms active at these late stages remain unknown. Notably, organizers are often found in spatial overlap with areas of delayed cellular differentiation (reviewed in ref. 3). As an example, MHB activity in all vertebrates also coincides with a zone of long-lasting progenitors that separate midbrain from anterior hindbrain neuronal clusters^{4–6}. In zebrafish, the bHLH Hairy/E(spl) transcription factors Her3, 5, 9 and 11 inhibit neurogenesis in this location^{7–9} (C.S., unpublished data), and experimentally induced neurogenesis across the MHB ultimately causes late MHB loss⁶. In the mouse, a lack of Hes1 and Hes3 also leads to premature differentiation at the MHB and to the failure to maintain (but not to initiate) MHB activity¹⁰. Therefore, it

appears to be crucial for proper MHB maintenance to ensure the spatial coincidence of the Fgf and neurogenesis inhibition pathways. Looking for a mechanism involved in this process, we searched for microRNAs that could simultaneously target the Fgf signaling and neurogenesis inhibition pathways.

We found that miR-9 is expressed in the late embryonic zebrafish CNS in a profile that selectively avoids the MHB. Using loss- and gain-of-function experiments, as well as sensor and target protection assays, we identified *her5*, *her9* and several components of the Fgf signaling pathway (*fgf8*, *fgfr1* and *canopy1*) as *in vivo* targets of miR-9. We demonstrate that some of these targets mediate the simultaneous interference of miR-9 with both Fgf signaling and the maintenance of the neural progenitor state *in vivo*, and that these activities converge to negatively delimit the MHB, where miR-9 is not expressed. These results provide a mechanism for maintaining a coherent MHB where organizer activity and neurogenesis inhibition are in spatial register and suggest a new role for microRNAs as major components of the cascades fine-tuning late organizers in the neural tube.

RESULTS

Overexpression of miR-9 RNA causes MHB loss

We found that the 3' UTRs of zebrafish MHB genes share putative miR-9 binding sites. This is, in particular, true for important effectors of MHB activity, such as *fgf8* (two sites), *fgfr1* (two sites) and *canopy1* (one site)^{2,11,12}, and genes encoding MHB neurogenesis inhibitors, such as *her5* (one site) and *her9* (one site)⁶ (C.S., unpublished data) (**Supplementary Fig. 1** online). To test whether these sites might be functionally

¹Department of Zebrafish Neurogenetics, Institute of Developmental Genetics, ²Institute of Stem Cell Research, ³Institute of Developmental Genetics, Helmholtz-Zentrum München, German Research Center for Environmental Health, Ingolstädter Landstrasse 1, D-85764 Neuherberg, Germany. ⁴Present address: Institute of Anatomy, University of Tübingen, Österbergstrasse 3, D-72074 Tübingen, Germany. ⁵These authors contributed equally to the work. Correspondence should be addressed to C.L. (leucht@topforscher.de) or L.B.-C. (bally@helmholtz-muenchen.de).

Received 27 February; accepted 24 March; published online 4 May 2008; doi:10.1038/nn.2115



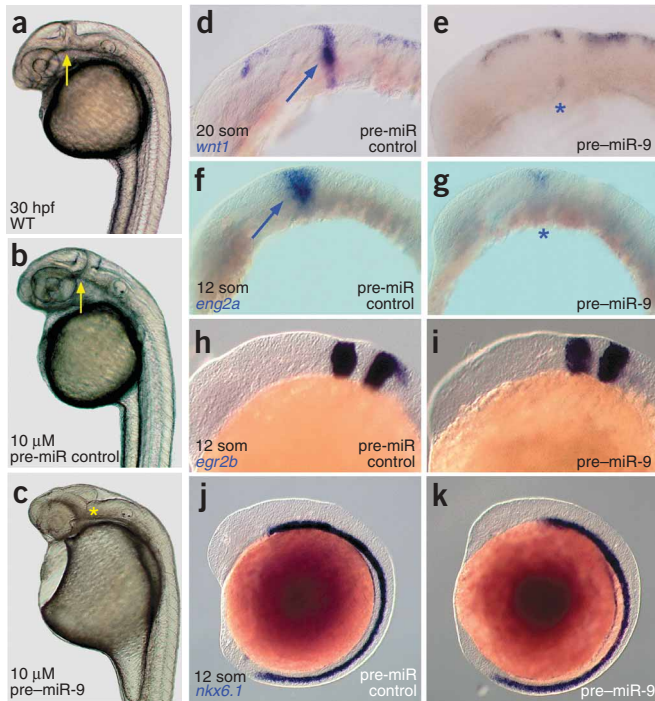


Figure 1 Gain of miR-9 function causes MHB loss. (**a–k**) Embryos were injected at the one-cell stage with pre-miR-9-1 (**c, e, g, i, k**) or the same concentration of a pre-miR control (**b, d, f, h, j**), with no predicted binding sites on *her5*, *her9*, *canopy1*, *fgf8* and *fgfr1*; **a** shows an uninjected embryo (wild type, WT). Arrows indicate the location of the MHB; asterisks indicate a missing MHB. Morphology of injected embryos at 30 hpf (lateral views, anterior left; **a–c**). The MHB is missing on overexpression of pre-miR-9 (**c**). Expression of neural tube regionalization markers in pre-miR-9-overexpressing embryos (sagittal views, anterior left; embryos in **d–g** are deyolled and flat-mounted). MHB markers were downregulated (**d–g**), but other regional markers were not (**h–k**) (see also **Supplementary Fig. 3**). Som, somites.

quantified via western blot (**Fig. 2b,c**). We found a strong interaction of miR-9 with the 3' UTR elements of *her5*, *her9*, *canopy1*, *fgf8* and *fgfr1*, as shown by a downregulation of d2EGFP. For the latter two genes, the putative binding sites *fgf8-1* and *fgfr-1*, but not *fgf8-2* and *fgfr1-2*, mediated this downregulation (**Fig. 2b**, see **Supplementary Fig. 1** for sequences of the binding sites).

We next focused on one example gene for each regulatory pathway considered (*fgfr1* for Fgf signaling and *her5* for neurogenesis inhibition) and further confirmed these findings using 3' UTR reporter constructs carrying engineered point mutations in their predicted miR-9 binding sites (site *fgfr1-1* for *fgfr1*), which abolished downregulation by miR-9 (constructs *her5mt* and *fgfr1mt*; **Fig. 2b,c**). We conclude that *her5*, *her9*, *canopy1*, *fgf8* and *fgfr1* are probably *in vivo* targets of miR-9 and, in the case of the latter two genes, probably interact with miR-9 via the predicted binding sites *fgf8-1* and *fgfr1-1*.

relevant *in vivo*, we monitored the effect of miR-9 RNA overexpression at an early stage in zebrafish. Given the known function of the above-mentioned genes in early MHB development, we expected a detectable MHB phenotype if one or more of these genes were ectopically targeted by miR-9 *in vivo* in these experimental conditions.

We injected 10 μ M miR-9, either as a duplex or as a precursor hairpin molecule (pre-miR-9-1, sequences in **Supplementary Fig. 1**), into fertilized oocytes and analyzed the resulting embryos by morphology at 30 h postfertilization (hpf). All embryos ($n > 100$) had a prominent and marked phenotype that was characterized by a strong reduction of the MHB and the cerebellum (**Fig. 1a–c**). Additionally, somitic boundaries appeared to be blurred and the otic vesicles were reduced, an effect that was previously reported for *fgf8* mutants and *fgfr1* knockdown embryos^{2,13} (**Supplementary Fig. 2** online). This phenotype was not observed on injection of several other CNS-expressed miRNAs (**Supplementary Fig. 2** and data not shown) and was not accompanied by typical nonspecific effects (reviewed in ref. 14) such as enlarged hearts or truncated tails (**Supplementary Fig. 2**), which only occurred at exaggerated doses (20 μ M or more) (**Supplementary Fig. 2**). The selectivity of the miR-9-induced MHB phenotype was further substantiated by the expression analysis of MHB markers, which were lost on miR-9 injection (**Fig. 1d–g** and **Supplementary Fig. 3** online), whereas other neural tube patterning markers were unaffected (**Fig. 1h–k** and **Supplementary Fig. 3**).

In vivo confirmation of predicted miR-9 binding sites

To test whether overexpressed miR-9 was capable of directly interacting with its predicted binding sites (**Supplementary Fig. 1**) and silencing the expression of its candidate genes *in vivo*, we conducted sensor assays for *fgf8*, *fgfr1*, *cnpy1* (*canopy1*), *her5* and *her9* (**Fig. 2**). We engineered fusions of the *d2egfp* cDNA to the full 3' UTR or to the putative miR-9 binding sites of each gene (**Fig. 2a**) and injected capped mRNA generated from these constructs, together with miR-9 duplex or a control microRNA with a shuffled miR-9 sequence, into one-celled embryos. The amount of d2EGFP protein expressed after 7 h was

miR-9 overexpression downregulates Fgf signaling

The phenotype triggered by miR-9 overexpression (**Fig. 1** and **Supplementary Figs. 2** and **3**) is very reminiscent of that of the zebrafish *fgf8* mutant *ace*, which also lacks the cerebellum, MHB and expression of MHB marker genes¹³, and of *fgfr1* morphants that show many aspects of the *ace* phenotype². We therefore addressed whether miR-9 overexpression blocks Fgf signaling. Consistent with this hypothesis, we found that the expression of Fgf target genes such as *dusp6* (ref. 15) and *pea3* (ref. 16) was strongly downregulated throughout the embryo after miR-9 injections (**Fig. 3a–d**), although the 3' UTR of *dusp6* does not interact with miR-9 (ref. 17) and we could not predict a miR-9-binding site in the 3' UTR of *pea3* (data not shown). Another hallmark of Fgf loss of function at the MHB, unraveled in *ace* mutants, is that MH cells express abnormal identities¹⁸; posterior MH cells, normally free of expression of the midbrain marker *otx2* (**Fig. 3e**), aberrantly expressed *otx2* in *ace*. Therefore, we also assessed the effects of miR-9 injections on MH cell fate using the transgenic line Tg(*her5PAC:egfp*)^{ne1939} (later referred to as *her5PAC:egfp*)¹⁸. In this line, GFP traces all MH cells until approximately 24 hpf. *her5PAC:egfp* embryos injected with miR-9 were stained for *otx2* expression, and we quantified the territory coexpressing GFP and *otx2* (indicative of midbrain identity) relative to the entire MH (GFP-positive cells) (**Fig. 3f**). This ratio was significantly higher in *ace* and miR-9-injected embryos than in wild type, indicating that both backgrounds similarly promote the transformation of posterior MH to midbrain identity (wild type and *ace*, $P < 0.01$; wild type and miR-9, $P < 0.05$; *ace* and miR-9, $P < 0.05$). Together, these observations strongly suggest an interaction of miR-9 with components of the Fgf signaling pathway.

To formally prove that the targeting of Fgf signaling by miR-9 was instrumental in causing the MHB deletion of miR-9-overexpressing embryos, we protected the miR-9 binding sites of endogenous *fgfr1* transcripts concomitantly to miR-9 overexpression. To achieve this, we injected the miR-9 duplex into one-celled embryos together with a 'target protector'¹⁹ morpholino antisense oligonucleotide specific to

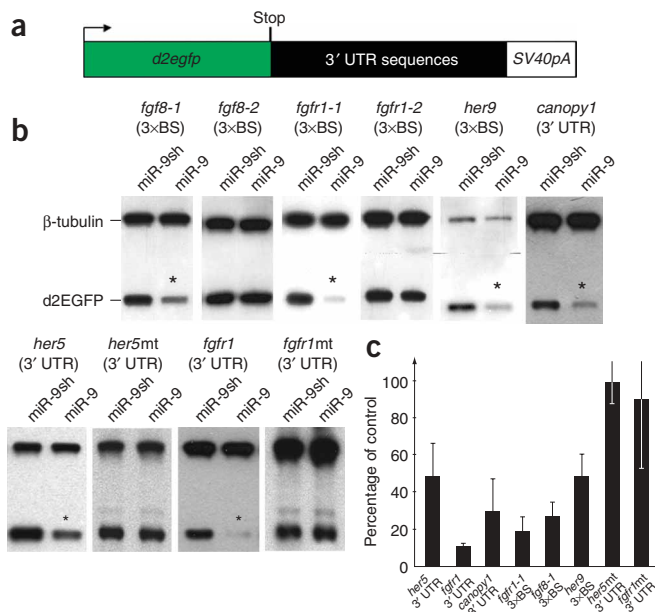


Figure 2 Sensor assay to reveal direct interaction of miR-9 with predicted binding sites. **(a)** Scheme of the sensor mRNA that was co-injected with the miR-9 duplex or a control miR duplex (a shuffled miR-9 sequence, miR-9sh). **(b)** We subjected embryos to western blot analysis 7 h after injection. β-tubulin was used as an internal loading control. Asterisks indicate cases where d2EGFP expression was downregulated in a statistically significant manner by miR-9 compared with miR-9sh. 3×BS, three copies of the predicted binding site were fused to *d2egfp*; 3' UTR, the full 3' UTR was fused to *d2egfp*; mt, full 3' UTR carrying engineered point mutations in predicted miR-9 binding sites (see **Supplementary Fig. 1**). **(c)** Densitometric analysis showed a downregulation of d2EGFP by miR-9 via the *fgfr1*, *canopy1* and *her9* 3' UTRs, and the *fgf8-1*, *fgf8-2* and *her9* binding sites. We found no downregulation of d2EGFP via the predicted miR-9 binding sites *fgfr1-2* and *fgf8-2*. Point mutations engineered in the 3' UTR of *her9* and *fgfr1* (site *fgfr1-1*) abolished the downregulation by miR-9. Data are means ± s.d., $P < 0.05$ (t test, unpaired). All lanes were normalized to the β-tubulin signal.

miR-9 promotes neurogenesis *in vivo*

In addition, two sets of observations suggest that an interaction of miR-9 with pathways other than Fgf contributes to the MHB phenotype of miR-9-injected embryos. First, downregulation of Fgf signaling, as shown by *pea3* and *dusp6* expression (**Fig. 3a–d**), was initiated at a later stage on miR-9 injection (10–12 somites) than in *ace* mutants (5 somites), and chemical blockade of Fgf signaling in wild-type embryos at this later stage was not sufficient to consistently produce MHB loss (data not shown). Second, and paradoxically, the loss of expression of MHB markers in miR-9-injected embryos (**Fig. 1d–g** and **Supplementary Fig. 3**) was more complete and occurred earlier than in *ace* mutants; before 18 somites, *ace* embryos only show ventrally reduced expression of, for example, *eng2a* and *wnt1* at the MHB¹³, whereas these were already almost completely downregulated at 12 somites on miR-9 injection (**Fig. 1d–g**). We conclude that miR-9 targets more than the Fgf pathway when affecting MHB maintenance on overexpression.

Abrogation of Hes1 and Hes3 function in the mouse induces premature neurogenesis at the MHB and thereby triggers MHB loss¹⁰. Thus, one process contributing to MHB failure on miR-9 injection might be the promotion of neurogenesis in the MHB

the predicted miR-9 binding site *fgfr1-1*. We observed that protecting *fgfr1-1* was sufficient to rescue the MHB and expression of MHB markers in a substantial proportion of miR-9-overexpressing embryos (**Fig. 3g–j** and **Supplementary Table 1** online). We conclude that overexpression of miR-9 impairs Fgf signaling at the MHB, at least in part by targeting *fgfr1* transcripts, and that this effect is instrumental in causing MHB loss. The interaction of microRNAs with their target genes does not necessarily result in reduced mRNA levels, but rather inhibits protein translation (for a review, see ref. 20). Together with the fact that we could not detect miR-9 binding sites on, for example, *wnt1* (data not shown), the effect of miR-9 on Fgf signaling suggests that the loss of MHB marker genes reported above (**Fig. 1**, **Supplementary Fig. 3**) is not a direct effect, but, as in *ace* mutants, is instead a result of interference in the MHB regulatory loop.

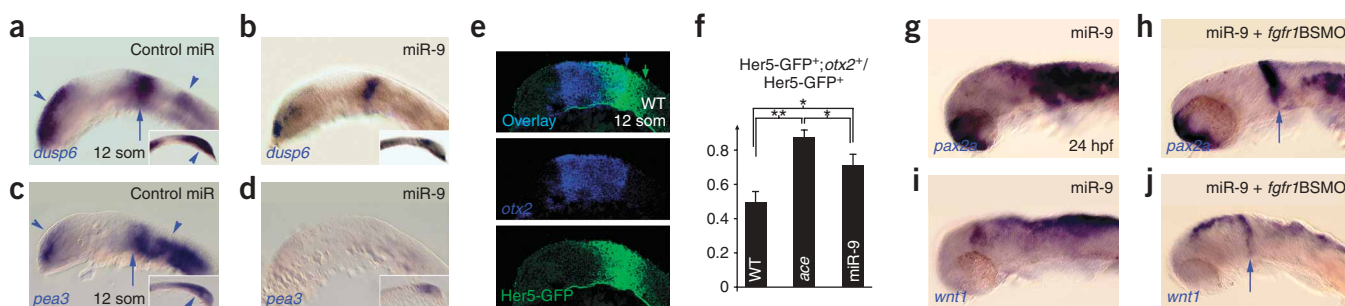


Figure 3 miR-9 overexpression downregulates Fgf signaling. **(a–d)** Expression of Fgf target genes (*dusp6* and *pea3*, as indicated) at the 12-somite stage in embryos injected with 10 μM miR-9 duplex (**b,d**) or the same amount of the control miR-9 shuffled duplex (**a,c**) (lateral views of the head of flat-mounted embryos, anterior left; insets show the posterior trunk and tail of each embryo; arrows to the MHB and arrowheads to other expression domains in the telencephalon, hindbrain and tail). miR-9 downregulated expression of *dusp6* and *pea3* at all sites. **(e,f)** Assessment of posterior MH fate on miR-9 overexpression. Comparing the expression of Her5-GFP (GFP immunocytochemistry, green) and *otx2* (ISH, blue) allowed the identification of the midbrain (Her5-GFP⁺; *otx2*⁺) and the posterior MH (rhombomere 1, Her5-GFP⁺; *otx2*⁻) in *her5:egfp* transgenic wild-type embryos (posterior limits of *otx2* and Her5-GFP expression indicated by color-coded arrowheads) (confocal views of sagittal cryosections, focus on the head, anterior left; **e**). Quantification of the relative extent of midbrain identity in the MH of wild-type embryos, *ace* mutants and miR-9-overexpressing embryos (**f**). There was a significant increase in midbrain extent in the two latter backgrounds, indicative of a fate transformation of posterior MH into midbrain ($n = 3$ embryos, means ± s.d., $*P < 0.05$, $**P < 0.01$; t -test, unpaired). **(g–j)** Targeting of *fgfr1* mRNA by overexpressed miR-9 was instrumental in causing MHB loss. Expression of the MHB markers *pax2a* and *wnt1* (as indicated) in embryos injected with 10 μM miR-9 duplex alone (**g,i**) or in combination with a morpholino (*fgfr1*BSMO) protecting the miR-9 binding site *fgfr1-1* on endogenous *fgfr1* transcripts (**h,j**) (sagittal views of flat-mounted embryos, anterior left). Arrows point to rescued expression domains at the MHB (see **Supplementary Table 1** for values and statistics).

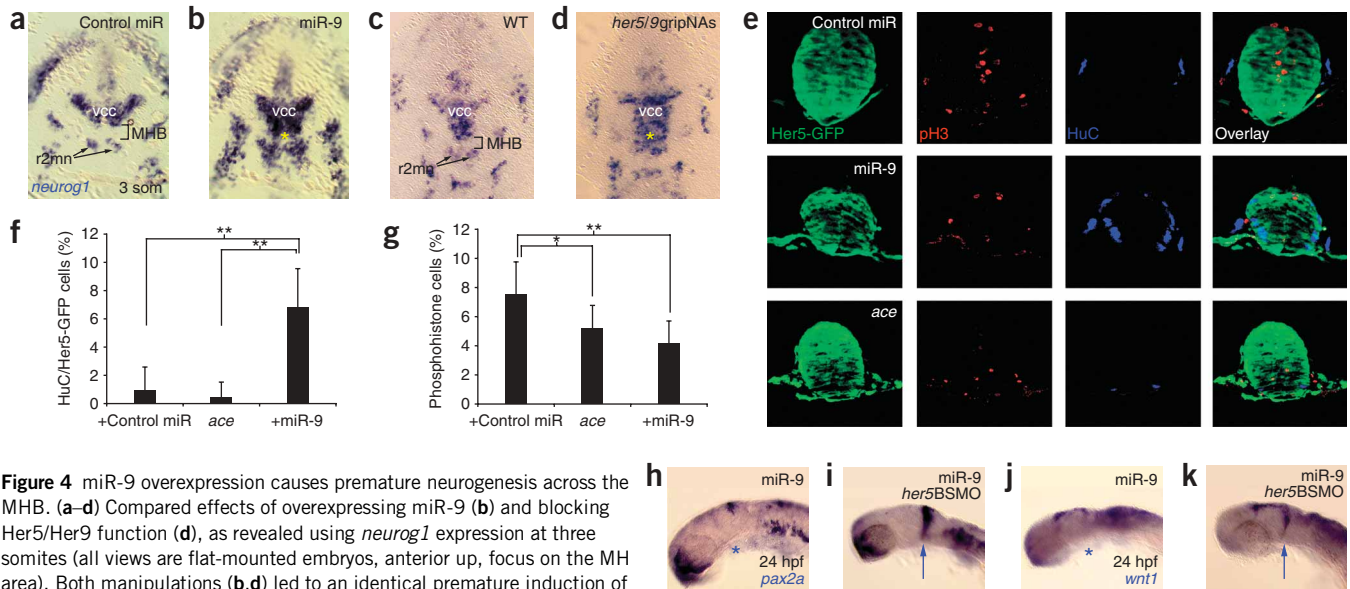


Figure 4 miR-9 overexpression causes premature neurogenesis across the MHB. (**a–d**) Compared effects of overexpressing miR-9 (**b**) and blocking Her5/Her9 function (**d**), as revealed using *neurog1* expression at three somites (all views are flat-mounted embryos, anterior up, focus on the MH area). Both manipulations (**b,d**) led to an identical premature induction of *neurog1* expression across the MHB (asterisks). In control embryos, the MHB at this stage is the *neurog1*-free zone (brackets in **a** and **c**) separating the proneural clusters vcc (ventro-caudal cluster) and r2mn (presumptive motorneurons of rhombomere 2). (**e–g**) Quantification of the miR-9-induced neurogenesis phenotype at 18 somites, using immunohistochemistry for the early pan-neuronal marker HuC (blue) and the proliferative marker pH3 (red) in the *her5PAC:gfp* background (GFP, green; MH) (all panels in **e** are cross sections of embryos at the MH level). (**f,g**) Statistical analysis of the percentage of HuC-positive cells (**d**) and pH3-positive cells (**e**) in the MH. Embryos overexpressing miR-9, but not *ace* mutants, showed an increased number of postmitotic neurons at MH levels (**f**). In contrast, miR-9-injected and *ace* embryos showed a comparable decrease in proliferation (**g**). Means \pm s.d.; * $P < 0.05$, ** $P < 0.01$ (*t* test, unpaired). (**h–k**) Expression of the MHB markers *pax2a* and *wnt1* in embryos co-injected with miR-9 duplex and a *her5* target protector (*her5BSMO*) (**i,k**) compared with embryos overexpressing miR-9 duplex alone (**h,j**). Blockade of miR-9 binding to *her5* by the target protector rescued the loss of MHB markers (see **Supplementary Table 1** for values and statistics).

progenitor pool, possibly by targeting the second set of predicted miR-9 targets, antineurogenic genes such as *her5* or *her9* (Fig. 2). To assess this issue, we first tested whether miR9 overexpression induces a neurogenic phenotype and whether this phenotype is comparable to that of abrogating Her5 and Her9 function. Simultaneous blockade of *her5* and *her9* by injection of antisense oligonucleotides triggered the activation of *neurogenin1* (*neurog1*) expression across the medial aspect of the MHB at three somites (Fig. 4 and ref. 6), a zone that was normally free of neurogenesis (Fig. 4c,d). miR-9 overexpression resulted in an identical phenotype (Fig. 4a,b), strengthening the hypothesis that *her5/her9* are direct targets of miR-9, as suggested by the predictions (Supplementary Fig. 1) and sensors assays (Fig. 2). To further test for an influence of miR-9 on neurogenesis and to make sure that this effect was independent of the regulation of Fgf signaling by miR-9, we analyzed cell proliferation and differentiation in the MH of miR-9-injected embryos in comparison with *ace* and control embryos at 18 somites (Fig. 4e–g). We again made use of the *her5PAC:egfp* background, where GFP identifies the MH at this stage¹⁸, combined with immunostaining for the M phase marker phosphorylated histone H3 (pH3) or the neuronal differentiation marker HuC (Fig. 4e). In the MH, we observed significantly less mitotic cells in miR-9-injected embryos compared with control embryos ($P < 0.01$; Fig. 4g). Because this is also the case in *ace* mutants (Fig. 4g), we attribute this effect to the impairment of Fgf signaling as a result of miR-9 overexpression. Notably, however, we found a marked increase in the number of HuC-positive cells in the MH of miR-9-injected embryos compared with both *ace* and control embryos (Fig. 4f), demonstrating that miR-9 strongly promotes MH neurogenesis *in vivo*, independently of its action on Fgf signaling.

Finally, to prove that targeting of the Her5/9 pathway was contributing to the MHB-loss phenotype that follows miR-9 overexpression, we

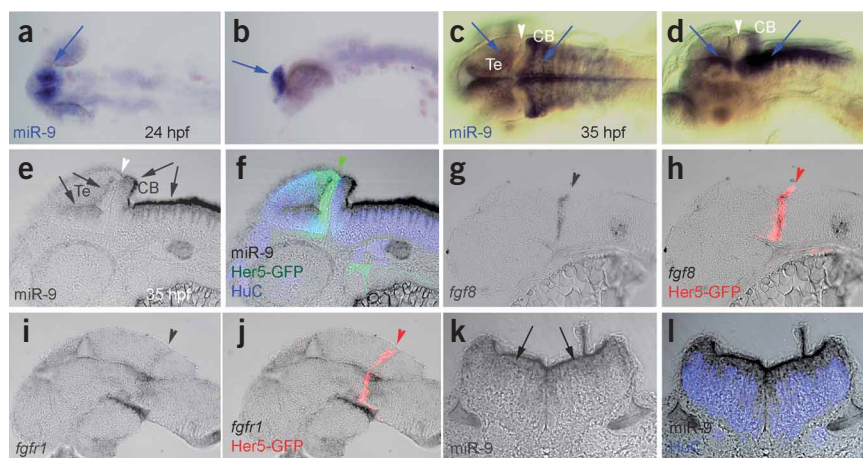
injected embryos with both miR-9 and a target protector¹⁹ against the predicted miR-9-binding site in the *her5* 3' UTR. This manipulation should reactivate Her5 function and leave other miR-9 targets unaffected. We observed that reactivation of Her5 rescued MHB markers (Fig. 4h–k and Supplementary Table 1). Together with the above results on Fgf signaling, these observations show that blockade of both the Her and Fgf pathways by miR-9, at least via binding *her5* and *fgfr1*, contributes to the complete MHB-loss phenotype induced by miR-9 overexpression.

miR-9 expression spares the MHB at late embryonic stages

Expression of miR-9 started at 20–24 hpf (approximately 30 somites) in the telencephalon (Fig. 5a,b) and later spread (starting at approximately 30 hpf) throughout the CNS (Fig. 5c,d). At 30 hpf and later stages, *in situ* hybridization (ISH) in the *her5PAC:egfp* background (GFP selectively labeling the MHB at that stage¹⁸) revealed that miR-9 expression consistently spared the MHB (Fig. 5e,f, see also Fig. 5c,d), but was found in immediately adjacent territories, such as the cerebellar plate and the ventricular zone of the tectum (Fig. 5c–f). The Her5-GFP-positive MHB domain avoided by miR-9 expression also precisely coincided with the territory expressing *fgf8* and *fgfr1* (Fig. 5g–j). This profile, together with the gain-of-function effects reported above, is compatible with miR-9 having a role in the anteroposterior restriction of Her and Fgf activities, hence of the MHB and its properties, at these stages.

In addition, along the mediolateral axis, miR-9 expression mostly highlighted the ventricular zone, directly adjacent to the HuC-positive domain, with few cells expressing both factors (Fig. 5f,k,l). This suggests that miR-9 expression stops when cells differentiate and is consistent with miR-9 driving the commitment of progenitors toward neurogenesis.

Figure 5 Endogenous miR-9 expression in the MH area avoids the MHB and postmitotic domains. (a–d) ISH for miR-9 (whole-mount embryos with focus on the brain area, anterior left, dorsal views in a and c, sagittal views in b and d). Expression was first detectable at 24 hpf in the telencephalon (a and b, arrows) and then extended to the rest of the neural tube. At 35 hpf in the MH, miR-9 stained the midbrain and hindbrain (c and d, arrows) but avoided the MHB (white arrowheads). (e–j) ISH for miR-9, *fgf8* or *fgfr1*, as indicated (black staining), in the *her5PAC:egfp* transgenic background at 35 hpf (GFP, green or red, highlights the MHB) (all views are sagittal sections observed under confocal microscopy with focus on the head, anterior left; e and f, g and h, and i and j are pairs of identical sections viewed under bright field alone or with superimposed fluorescence, respectively; f is a triple staining to detect the postmitotic neuronal marker HuC, blue). miR-9 was expressed in the mid- and hindbrain (e, arrows; CB, cerebellar plate; Te, tectum), but avoided the Her5-GFP-positive area (MHB, arrowheads). *fgf8* and *fgfr1* expression overlapped with Her5-GFP (g–j, arrowheads). (k, l) Expression of miR-9 (black) compared with HuC (blue on l, same section as k visualized under bright field and fluorescence) at hindbrain levels. miR-9 expression was largely confined to the ventricular zone (see also f).



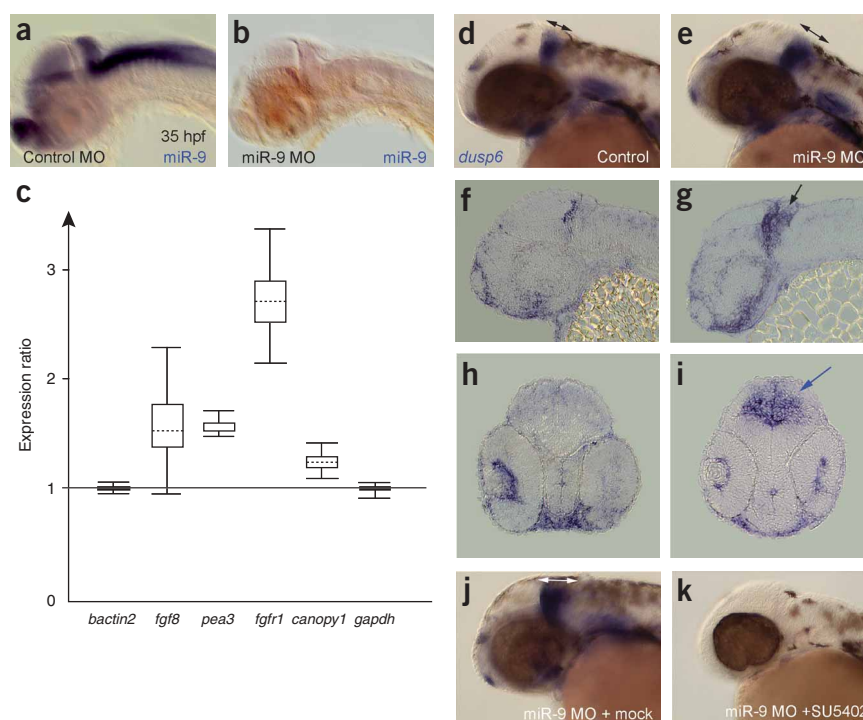
miR-9 activity delimits Fgf signaling and the MHB

We used a morpholino oligonucleotide specific to miR-9 (miR-9MO) to inactivate miR-9 function *in vivo*. Injection of miR-9MO resulted in a complete blockade of miR-9, as shown by miR-9 ISH after injection (Fig. 6a,b). We first analyzed the effects of miR-9 blockade on the expression of Fgf targets at the MHB. Obvious changes in the spatial extent of expression of most MHB markers were difficult to assess by ISH, but we did find significant differences in the relative transcripts levels of these genes at 35 hpf using qPCR; the expression of *fgf8*, *pea3*, *fgfr1* and *canopy1* were significantly upregulated on miR-9MO injection ($P < 0.05$; Fig. 6c). Again, because microRNAs generally do not modify expression of their target mRNAs²⁰ and because we did not

predict miR-9 binding to *pea3*, this general upregulation probably reflects increased Fgf signaling amplifying the expression of MHB markers via the MHB regulatory loop. In addition, we observed an obvious enlargement of the most sensitive Fgf read-out, *dusp6* expression, at 35 hpf at the MHB using ISH. *dusp6* expression expanded into the cerebellum (Fig. 6d–g), a region where miR-9 is normally expressed (Fig. 5c–f), as well as along the mediolateral axis at levels immediately posterior to the MHB (Fig. 6h,i).

To further support the hypothesis that the upregulation of *dusp6* in the absence of miR-9 activity resulted from increased Fgf signaling, we treated miR-9MO-injected embryos with the Fgf signaling inhibitor SU5402. In all such embryos, *dusp6* expression was abolished, including

Figure 6 Morpholino knockdown of miR-9 affects Fgf signaling in a manner opposite to miR-9 gain of function. (a,b) miR-9MO-injected embryos and embryos injected with the control miR-9MO were analyzed for miR-9 expression using a digoxigenin-labeled probe against miR-9 at 35 hpf (sagittal views of whole-mount embryos, anterior left). Injection of miR-9MO at 2 mM completely blocked detectable miR-9 expression in all cases (b, compare with a). (c) A whisker-box plot showing the results of the quantitative PCR on several components of the Fgf signaling pathway in miR-9MO-injected versus uninjected samples. Expression of *fgf8*, *pea3*, *fgfr1* and *canopy1* were increased. $P < 0.05$ for all genes. (d–k) Effect of blocking miR-9 activity on *dusp6* expression revealed by ISH (blue) (d,e,j,k, sagittal views of whole-mount embryos, anterior left; f,g, sagittal sections, anterior left; h,i, cross sections at the level of the anterior hindbrain, dorsal up; double arrow to MH expansion in j). *dusp6* expression expanded along the anteroposterior (e, double arrow; g, arrow) and mediolateral (i, arrow) axes in embryos injected with the miR-9MO (e,g,i), but not with the control MO (d,f,h) (d is an uninjected embryo). *dusp6* expression and expansion was blocked when miR-9MO-injected embryos were treated with the Fgf signaling inhibitor SU5402 (k; compared with mock-treated embryos, j; double arrow to MH expansion in j).



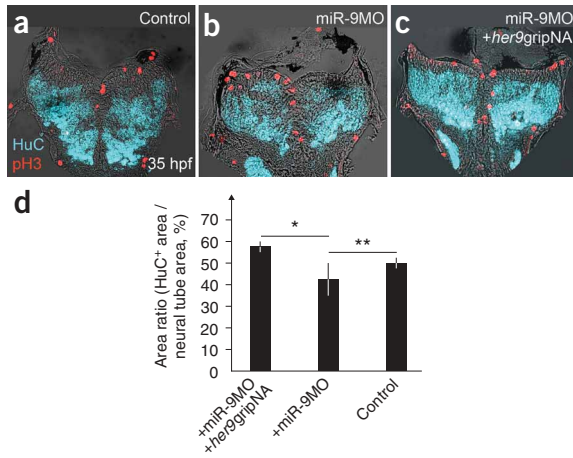


Figure 7 Morpholino knockdown of miR-9 affects neurogenesis in a manner opposite to miR-9 gain of function. (a–c) Control embryos (a), miR-9MO–injected embryos (b), or embryos injected with both miR-9MO and *her9gripNA* (c) were analyzed for the expression of the proliferation marker pH3 (red) and the neuronal differentiation marker HuC (blue) (cross-sections at anterior hindbrain levels). (d) The relative extent of the HuC-positive area was quantified. miR-9MO–injected embryos showed reduced neuronal differentiation, and this defect was rescued by the co-inhibition of Her9 activity. Data are means \pm s.d.; two-sample *t*-test. * $P = 6.37 \times 10^{-6}$, ** $P < 0.02$.

on the cerebellar plate (Fig. 6j,k). Consistent with our gain-of-function experiments, these results demonstrate that the absence of miR-9 function increases activity of the Fgf signaling pathway at the MHB, in turn amplifying expression of MHB markers and MHB extent.

miR-9 activity controls MH neurogenesis progression

We next analyzed the requirement for miR-9 in neurogenesis progression, focusing on regions that show high levels of miR-9 expression, such as the anterior hindbrain. Immunostaining for HuC on cross sections at hindbrain levels revealed a statistically significant reduction of the relative HuC-positive area at 35 hpf on miR-9 blockade ($P = 0.01161$; Fig. 7a,b), demonstrating an impairment of neuronal differentiation in the absence of miR-9. The proportion of mitotic cells (pH3 positive) in the ventricular zone was not substantially affected (data not shown). Hence, endogenous miR-9 is required for neurogenesis progression in this neural tube domain. This effect was not accompanied by increased expression of the predicted miR-9 targets involved in neurogenesis inhibition, that is, *her5* and *her9*, as revealed by qPCR (data not shown). Again, however, miR-9 activity probably does not directly modify expression of its targets, and we used epistasis experiments to address the implication of *her* genes downstream of miR-9 in neurogenesis control *in vivo*.

We focused on *her9* because its expression extends into the anterior hindbrain²¹. Blocking Her9 activity by the injection of an antisense *her9gripNA* oligonucleotide into one-celled embryos led to ectopic *neurog1* expression in inter-proneural domains of the presumptive spinal cord at three somites, as reported using a *her9* morpholino oligonucleotide (*her9MO*)²¹ (data not shown). Notably, we observed that abrogating Her9 activity antagonized the phenotype of decreased neurogenesis induced by miR-9 blockade, bringing neurogenesis back to higher levels in embryos co-injected with *her9gripNA* and miR-9MO (Fig. 7c,d). Again, this effect did not involve substantial alterations in cell proliferation, which supports a direct rescue of the miR-9–induced phenotype. These results demonstrate that miR-9 is necessary to control neuronal differentiation in the MH *in vivo* and strongly suggest that this occurs, at least in part, via its regulation of *her* genes.

DISCUSSION

Our data demonstrate that miR-9 has at least two roles in the vertebrate CNS: it globally regulates Fgf signaling by inhibition of *fgf8*, *fgfr1* and *canopy1*, and it exerts a proneurogenesis effect, notably by inhibiting expression of antineurogenic bHLH transcription factor–encoding genes such as *her5* and *her9*. It is probable that the targeting of Fgf

pathway genes is even more extensive than we report here, as we could also predict miR-9–binding sites in the 3' UTRs of *fgf3*, *fgf17a* and *fgf18l* (C.L., unpublished data). miR-9 thus appears to be a major regulator of the Fgf pathway during CNS development, an activity that is probably conserved across species, as we could also predict miR-9–binding sites on the 3' UTRs of human *FGFR1* and multiple *Fgf* genes in human and mouse (C.L., unpublished data).

The expression of miR-9 in neural progenitors through most of the CNS of zebrafish, chicken and mouse^{22–25} and the effects of its gain- and loss-of-function on neuronal differentiation that we observed here suggest a role in vertebrate neurogenesis control that is not limited to the MH. Specifically, the effect of miR-9 blockade via Her factors is compatible with a role for miR-9 in pushing commitment toward the differentiation state without having direct control over the proliferation of early progenitors. The promotion of neurogenesis progression by miR-9 might a priori seem surprising given its expression in the ventricular zone of the neural tube, where progenitors reside. At the stages analyzed, however, this is also the domain of expression of proneural genes like *neurog1* (ref. 26), hence the zone where commitment toward neurogenesis takes place.

An involvement of miR-9 in neurogenesis was previously suggested on the basis of *in silico* predictions and expression analysis of miR-9a in *Drosophila*²⁷. However, experimental assignment of miR-9a function in *Drosophila* led to results that diverge from ours^{28,29}; a previous study illustrated an antineuronal role of miR-9a in the *Drosophila* PNS²⁹, where it maintains cells in the non-neuronal (epidermal) state by repressing the proneural gene *senseless*. The expression of *Drosophila* miR-9a highlights epidermal, as opposed to neuronal, precursors, a situation that parallels the expression of vertebrate miR-9 in neural progenitors, as opposed to differentiated neurons. miR-9 activity therefore results in two markedly different outcomes between species. This functional divergence might be a result of different types of genes being targeted *in vivo* by miR-9 depending on the species, for example, proneural genes in *Drosophila* versus neurogenesis inhibitors in zebrafish. miR-9 was also predicted to target human, mouse and chicken *Hes1* (data not shown), which maintains progenitor pools³⁰. The effect of miR-9 on neurogenesis might also be aided, possibly in a variable manner between species, by interaction with the transcriptional repressor REST^{31,32}, although *in vivo* evidence for this interaction remains to be provided.

The endogenous expression of miR-9 in the MH started after 30 hpf and was consistently found immediately adjacent to, but nonoverlapping with, the MHB. The targets of miR-9 identified in this study (*fgf8*, *fgfr1*, *canopy1*, *her5* and *her9*) are all expressed at the MHB at late developmental stages, similar to the predicted targets *fgf3*, *fgf17a* and *fgf18l*. These findings are consistent with the target/antitarget theory, which argues that microRNAs and their targets are expressed in a largely nonoverlapping manner²⁷. In the present case, this expression pattern, together with the dual effects of miR-9 on Fgf signaling and *her* genes, imposes a special status on the MHB as a domain where miR-9 effects are concurrently released. Our results therefore support a model

whereby miR-9 expression and functions converge to contribute to the late coherence of the MHB *in vivo*; through its absence at the MHB, miR-9 regulates MHB correct positioning, spatial restriction and the coincidence of MHB patterning and neurogenesis inhibition activities (Supplementary Fig. 4 online). One implication of our model is that microRNAs not only control isolated events during development or cell specification, but probably provide a metabolically cheap method for the organism to regulate complex processes, such as the maintenance of progenitor pools or organizing centers, by targeting several converging components of these processes. In addition, our results identify, to the best of our knowledge, the first known mechanism involved in assisting the spatial coherence of late neural tube organizers and suggest that such coordinating activity of the multiple functional inputs and outputs of organizing centers might constitute a previously unknown function of microRNAs.

METHODS

Fish strains. Embryos were obtained from natural spawning of AB wild-type or transgenic fish, *ace*^{ti282a} or *her5PAC:egfp* [Tg(*her5PAC:EGFP*)^{ne1939}]^{18,33}. Embryos were staged according to a previous study³⁴. All experiments were performed in accordance with the regulations of the Regierung von Oberbayern.

Computational analysis of miR-9-binding sites. Binding sites were analyzed using the programs MIRANDA³⁵, MicroInspector³⁶, RNA22 (ref. 37) and RNAHybrid³⁸. Sequences of predicted sites are provided in Supplementary Figure 1.

miR-9 duplexes, and pre-miR-9 and miR-9 morpholino injections. Doses injected were always two- to fivefold lower than those reported to trigger general nonspecific effects (Supplementary Fig. 2 and see ref. 14 for a review). miR-9, miR-124 and miR-138 RNA duplexes and a duplex containing a shuffled miR-9 sequence were obtained as siRNAs (miR-9: sense 5'-UCU UUG GUU AUC UAG CAG AAU G_{RNA}, antisense 5'-AUA CAG CUA GAU AAC CAA AGA_{RNA} TT_{DNA}; miR-124: sense 5'-UCA CAG UGA ACC GGU CUC UUU U_{RNA}, antisense 5'-AAG AGA CCG GUU CAC UGU G_{RNA} TT_{DNA}; miR-138: sense 5'-AGC UGG UGU UGU GAA UCA GGC C_{RNA}, antisense 5'-CCU GAU UCA CAA CAC CAG CU_{RNA} TT_{DNA}; shuffled miR-9: sense 5'-UAU CAC UUC UAU AUG GUU UGG U_{RNA}, antisense 5'-CCA AAC CAU AUA GAA GUG AU_{RNA} TT_{DNA}) and injected into one-celled fertilized embryos at a concentration of 10 μ M. Pre-miR-9-1 RNA (sequence in Supplementary Fig. 1) and a pre-miR negative control (Ambion pre-miR control #1) were obtained from Ambion and used at 10 μ M. All morpholinos were obtained from Gene Tools and used as follows: miR-9MO (5'-TCA TAC AGC TAG ATA ACC AAA GA-3') was injected at 2 mM, the control morpholino oligonucleotide (a shuffled sequence of miR9MO: 5'-CAC CAA ACC ATA TAG AAG TGA TA-3') was injected at 2 mM, *her5* target protector (*her5*BSMO, 5'-ATC TTT GGC ATC TAC TGT ACA AAA T-3') was injected at 0.1 mM or 0.5 mM, and *fgfr1-1* target protector (*fgfr1*BSMO, 5'-CTT TGG CGG TTT TGT GTG CAG CTG T-3') was injected at 0.1 mM or 0.5 mM. *her9*gripNA was obtained from Active Motifs (Carlsbad) (5'-TGA TTT TTA CCT TTC TAT-3') and was based on the published *her9*MO²¹. It was favored over *her9*MO for its absence of toxicity (data not shown).

Quantitative real-time PCR. Total RNA was extracted from sample and control group embryos (a pool of 30–35-hpf-old embryos) using the RNeasy kit (Qiagen). We used 1 μ g of total RNA to generate cDNA using the Transcriptor First Strand cDNA Synthesis Kit (Roche). Quantitative real-time PCR was carried out on a LightCycler 1.2 system (Roche) using probes from the Universal Probe Library (Roche) and the TaqMan Master Mix (Roche) (for sequences of primers and the respective Universal Probe Library probes, see Supplementary Table 2 online). For each transcript, eight replications were performed and the results were normalized using *bactin2* and *gapdh*. The relative expression software tool REST³⁹ was used to analyze and normalize the data. It uses a hypothesis test to determine significant differences between control and sample groups that performs 50,000 random reallocations of samples and controls

between the groups and counts the number of times the relative expression of the randomly assigned group is greater than that of the sample data.

SU5402 treatments. Dechorionated embryos were incubated from the 24-hpf stage into 10 μ M SU5402 in Hank's embryo medium (0.137 M NaCl, 5.4 mM KCl, 0.25 mM Na₂HPO₄, 0.44 mM KH₂PO₄, 1.3 mM CaCl₂, 1.0 mM Mg SO, 4.2 mM NaHCO₃), 0.1% DMSO. Mock-treated embryos were incubated for the same duration in Hank's medium containing only 0.1% DMSO. Treated and control embryos were fixed for ISH at 35 hpf.

ISH and immunohistochemistry. Probe synthesis, ISH and immunohistochemistry were carried out as described⁸. The following *in situ* antisense RNA probes were used: *her5* (ref. 40), *fgf8* (ref. 13), *fgfr1* (ref. 41), *pax2a*⁴², *wnt1* (ref. 43), *eng2a*⁴⁴, *pea3* (ref. 16), *dusp6* (ref. 15), *shh*⁴⁵, *nkx6.1* (ref. 46), *foxa2* (ref. 47) and *egr2b*⁴⁸. For ISH of miR-9, a digoxigenin tail was added to the miRCURY detection probe (LNA) hsa-miR-9 (Exiqon) using the DIG tailing Kit (Roche). The miR-9 LNA probe was hybridized at 45 °C, and all other steps were carried out as described⁸. For sagittal or cross sections, embryos were cryostat-sectioned. We used chicken antibody to GFP (1:500, Aves Labs), rabbit antibody to GFP (TP401, 1:500, AMS), mouse antibody to human neural protein HuC/HuD (A-21271, 1:300, MoBiTec) and human antibody to Hu (kindly provided by B. Zalc (INSERM U711, Hôpital de la Salpêtrière), 1:600) as primary antibodies for immunohistochemistry, and goat antibody to rabbit Cy2, goat antibody to rabbit Cy3, goat antibody to human Cy5, goat antibody to mouse Cy5, goat antibody to mouse Cy3 (all Jackson Laboratories) goat antibody to chicken Alexa488, goat antibody to rabbit Alexa555 and goat antibody to mouse Alexa647 (Invitrogen) as secondary antibodies. Embryos and flat mounts were photographed under a Zeiss Axioplan photomicroscope, and sections were photographed and analyzed under a Zeiss confocal microscope (LSM 510 Meta). For the statistical analysis in Figure 4f,g, we used three embryos per background, and counted 1,505 cells for control, 2,040 for miR-9-injected and 1,853 for *ace* embryos to calculate the percentage of HuC-positive cells in the MH and the percentage of pH3-positive cells. In Figure 7d, the size of the HuC-positive area was calculated as a percentage of the size of the neural tube ($n = 3$ embryos per assay; 3 cross-sections per embryo were analyzed).

Sensor assay. *d2egfp* was cloned into *pCS2+* using EcoRI and XhoI. Three copies of putative miR-9-binding sites of *fgf8* (*fgf8-1* and *fgf8-2*), *fgfr1* (*fgfr1-1* and *fgfr1-2*), *canopy1*, *her5* and *her9* were fused to the 3' end of *d2egfp* using XhoI and XbaI, as described previously⁴⁹. The oligonucleotides in Supplementary Table 3 online were phosphorylated, annealed and ligated in *pCS2+d2egfp* (at XhoI/Xba1) for each binding site. The 3' UTRs of *fgfr1*, *her5* and *canopy1* were amplified using the primers in Supplementary Table 3 and fused to the 3' end of *d2egfp*. For *fgfr1*, we found the 3' UTR to be at least 226 bp longer than the published sequence (NM_152962), as we could amplify the 3' UTR from embryonic cDNA using the primers in Supplementary Table 3 that extend further in the 3' direction than in the published sequence. Full 3'-UTR sequences carrying point mutations in the predicted miR-9-binding sites of *her5* and *fgfr1* (binding site *fgfr1-1*) were engineered by Sloning, PCR amplified and fused to *d2egfp*, as described above. For all constructs, capped mRNA was generated using the mMMESSAGE mMACHINE Kit (Ambion). The mRNA was injected with either miR-9 duplex or the control miR duplex containing a shuffled miR-9 sequence. Embryos were pooled and prepared for western blot analysis at 7 hpf.

Western blot. Embryos were pooled (ten embryos each) and SDS sample buffer was added, followed by a denaturation at 95 °C for 5 min, vortexing and a second incubation at 95 °C. The protein solution was centrifuged for 2 min in a table-top centrifuge. The samples were directly loaded onto a NuPage 10% Bis-Tris gel (Invitrogen) with MOPS running buffer. The gels were blotted onto a PVDF Hybond-P membrane (GE Healthcare) and blocked with 4% nonfat dry milk (wt/vol) in phosphate-buffered saline (with 1% Tween-20, wt/vol). Immunodetection was carried out using rabbit antibody to GFP (TP401, 1:10,000 to 1:2,000, Torrey Pines Biolabs) and β -tubulin (ab6046, 1:15,000, Abcam) as primary antibodies, and antibody to rabbit HRP (1:10,000, Jackson Laboratories) as the secondary antibody. Detection was carried out using the Western Lightning chemiluminescence reagent (Perkin Elmer). From pools of 10 embryos, the equivalent of one embryo was loaded per lane; for statistical

analysis, three injected batches were each analyzed by densitometry ($n = 30$ embryos for each binding site). The blots were scanned and the bands were quantified using ImageJ (US National Institutes of Health). The intensities of all bands were normalized with respect to the β -tubulin signal to circumvent loading inaccuracies.

Note: Supplementary information is available on the Nature Neuroscience website.

ACKNOWLEDGMENTS

We are grateful to members of the L.B.-C. laboratory for discussions and to M. Götz, W. Norton and M. Wassef for their insightful ideas and critical reading of the manuscript. This work was funded by a junior group grant from the Volkswagen Association, the EU 6th framework integrated project ZF-Models (contract No. LSHC-CT-2003-503466), the Life Science Association (No. GSF 2005/01), a special research grant from the Institut du Cerveau et de la Moelle épinière, the Excellence Center for Protein Science, Munich, and the Helmholtz 'Impuls und Vernetzungsfond'.

AUTHORS CONTRIBUTIONS

C.L. and C.S. jointly conducted the experiments. A.W. and R.K. conducted parallel analyses in chicken to support the findings described here. A.F. provided technical assistance and L.B.-C. supervised the project. C.L. and L.B.-C. wrote the manuscript.

Published online at <http://www.nature.com/natureneuroscience>

Reprints and permissions information is available online at <http://npg.nature.com/reprintsandpermissions>

- Wurst, W. & Bally-Cuif, L. Neural plate patterning: upstream and downstream of the isthmus organizer. *Nat. Rev. Neurosci.* **2**, 99–108 (2001).
- Schollp, S., Groth, C., Lohs, C., Lardelli, M. & Brand, M. Zebrafish *fgfr1* is a member of the *fgf8* synexpression group and is required for *fgf8* signalling at the midbrain-hindbrain boundary. *Dev. Genes Evol.* **214**, 285–295 (2004).
- Stigloher, C., Chapouton, P., Adolf, B. & Bally-Cuif, L. Identification of neural progenitor pools by E(Spl) factors in the embryonic and adult brain. *Brain Res. Bull.* **75**, 266–273 (2008).
- Bally-Cuif, L., Goridis, C. & Santoni, M.J. The mouse NCAM gene displays a biphasic expression pattern during neural tube development. *Development* **117**, 543–552 (1993).
- Vaage, S. The segmentation of the primitive neural tube in chick embryos (*Gallus domesticus*). A morphological, histochemical and autoradiographical investigation. *Ergeb. Anat. Entwicklungsgesch.* **41**, 3–87 (1969).
- Geling, A. *et al.* bHLH transcription factor Her5 links patterning to regional inhibition of neurogenesis at the midbrain-hindbrain boundary. *Development* **130**, 1591–1604 (2003).
- Geling, A., Plessy, C., Rastegar, S., Strähle, U. & Bally-Cuif, L. Her5 acts as a prepattern factor that blocks neurogenin1 and *coe2* expression upstream of Notch to inhibit neurogenesis at the midbrain-hindbrain boundary. *Development* **131**, 1993–2006 (2004).
- Ninkovic, J. *et al.* Inhibition of neurogenesis at the zebrafish midbrain-hindbrain boundary by the combined and dose-dependent activity of a new hairy/E(spl) gene pair. *Development* **132**, 75–88 (2005).
- Hans, S. *et al.* *her3*, a zebrafish member of the hairy-E(spl) family, is repressed by Notch signalling. *Development* **131**, 2957–2969 (2004).
- Hirata, H., Tomita, K., Bessho, Y. & Kageyama, R. Hes1 and Hes3 regulate maintenance of the isthmus organizer and development of the mid/hindbrain. *EMBO J.* **20**, 4454–4466 (2001).
- Hirate, Y. & Okamoto, H. Canopy1, a novel regulator of FGF signaling around the midbrain-hindbrain boundary in zebrafish. *Curr. Biol.* **16**, 421–427 (2006).
- Lun, K. & Brand, M. A series of no isthmus (*noi*) alleles of the zebrafish *pax2.1* gene reveals multiple signaling events in development of the midbrain-hindbrain boundary. *Development* **125**, 3049–3062 (1998).
- Reifers, F. *et al.* *Fgf8* is mutated in zebrafish acerebellar (*ace*) mutants and is required for maintenance of midbrain-hindbrain boundary development and somitogenesis. *Development* **125**, 2381–2395 (1998).
- Fjose, A. & Drivenes, O. RNAi and microRNAs: from animal models to disease therapy. *Birth Defects Res. C. Embryo Today* **78**, 150–171 (2006).
- Kawakami, Y. *et al.* MKP3 mediates the cellular response to FGF8 signaling in the vertebrate limb. *Nat. Cell Biol.* **5**, 513–519 (2003).
- Munchberg, S.R., Ober, E.A. & Steinbeisser, H. Expression of the Ets transcription factors *erm* and *pea3* in early zebrafish development. *Mech. Dev.* **88**, 233–236 (1999).
- Yan, X. *et al.* Improving the prediction of human microRNA target genes by using ensemble algorithm. *FEBS Lett.* **581**, 1587–1593 (2007).
- Tallafuss, A. & Bally-Cuif, L. Tracing of *her5* progeny in zebrafish transgenics reveals the dynamics of midbrain-hindbrain neurogenesis and maintenance. *Development* **130**, 4307–4323 (2003).
- Choi, W.Y., Giraldez, A.J. & Schier, A.F. Target protectors reveal dampening and balancing of Nodal agonist and antagonist by miR-430. *Science* **318**, 271–274 (2007).
- Valencia-Sanchez, M.A., Liu, J., Hannon, G.J. & Parker, R. Control of translation and mRNA degradation by miRNAs and siRNAs. *Genes Dev.* **20**, 515–524 (2006).
- Bae, Y.K., Shimizu, T. & Hibi, M. Patterning of proneuronal and inter-proneuronal domains by hairy- and enhancer of split-related genes in zebrafish neuroectoderm. *Development* **132**, 1375–1385 (2005).
- Wienholds, E. *et al.* MicroRNA expression in zebrafish embryonic development. *Science* **309**, 310–311 (2005).
- Darnell, D.K. *et al.* MicroRNA expression during chick embryo development. *Dev. Dyn.* **235**, 3156–3165 (2006).
- Kapsimali, M. *et al.* MicroRNAs show a wide diversity of expression profiles in the developing and mature central nervous system. *Genome Biol.* **8**, R173 (2007).
- Kloosterman, W.P., Wienholds, E., de Bruijn, E., Kauppinen, S. & Plasterk, R.H. *In situ* detection of miRNAs in animal embryos using LNA-modified oligonucleotide probes. *Nat. Methods* **3**, 27–29 (2006).
- Mueller, T. & Wullmann, M.F. Anatomy of neurogenesis in the early zebrafish brain. *Brain Res. Dev. Brain Res.* **140**, 137–155 (2003).
- Stark, A., Brennecke, J., Bushati, N., Russell, R.B. & Cohen, S.M. Animal MicroRNAs confer robustness to gene expression and have a significant impact on 3' UTR evolution. *Cell* **123**, 1133–1146 (2005).
- Leaman, D. *et al.* Antisense-mediated depletion reveals essential and specific functions of microRNAs in *Drosophila* development. *Cell* **121**, 1097–1108 (2005).
- Li, Y., Wang, F., Lee, J.A. & Gao, F.B. MicroRNA-9a ensures the precise specification of sensory organ precursors in *Drosophila*. *Genes Dev.* **20**, 2793–2805 (2006).
- Nakamura, Y. *et al.* The bHLH gene *hes1* as a repressor of the neuronal commitment of CNS stem cells. *J. Neurosci.* **20**, 283–293 (2000).
- Wu, J. & Xie, X. Comparative sequence analysis reveals an intricate network among REST, CREB and miRNA in mediating neuronal gene expression. *Genome Biol.* **7**, R85 (2006).
- Conaco, C., Otto, S., Han, J.J. & Mandel, G. Reciprocal actions of REST and a microRNA promote neuronal identity. *Proc. Natl. Acad. Sci. USA* **103**, 2422–2427 (2006).
- Brand, M. *et al.* Mutations in zebrafish genes affecting the formation of the boundary between midbrain and hindbrain. *Development* **123**, 179–190 (1996).
- Kimmel, C.B., Ballard, W.W., Kimmel, S.R., Ullmann, B. & Schilling, T.F. Stages of embryonic development of the zebrafish. *Dev. Dyn.* **203**, 253–310 (1995).
- Enright, A.J. *et al.* MicroRNA targets in *Drosophila*. *Genome Biol.* **5**, R1 (2003).
- Rusinov, V., Baev, V., Minkov, I.N. & Tabler, M. MicroInspector: a web tool for detection of miRNA binding sites in an RNA sequence. *Nucleic Acids Res.* **33**, W696–700 (2005).
- Miranda, K.C. *et al.* A pattern-based method for the identification of MicroRNA binding sites and their corresponding heteroduplexes. *Cell* **126**, 1203–1217 (2006).
- Rehmsmeier, M., Steffen, P., Hochsmann, M. & Giegerich, R. Fast and effective prediction of microRNA/target duplexes. *RNA* **10**, 1507–1517 (2004).
- Pfaffl, M.W., Horgan, G.W. & Dempfle, L. Relative expression software tool (REST) for group-wise comparison and statistical analysis of relative expression results in real-time PCR. *Nucleic Acids Res.* **30**, e36 (2002).
- Müller, M., von Weizsäcker, E. & Campos-Ortega, J.A. Transcription of a zebrafish gene of the hairy-Enhancer of split family delineates the midbrain anlage in the neural plate. *Dev. Genes Evol.* **206**, 153–160 (1996).
- Tonou-Fujimori, N. *et al.* Expression of the FGF receptor 2 gene (*fgfr2*) during embryogenesis in the zebrafish *Danio rerio*. *Mech. Dev.* **119** Suppl 1: S173–S178 (2002).
- Krauss, S. *et al.* Zebrafish *pax(zf-a)*: a paired box-containing gene expressed in the neural tube. *EMBO J.* **10**, 3609–3619 (1991).
- Molven, A., Njolstad, P.R. & Fjose, A. Genomic structure and restricted neural expression of the zebrafish *wnt-1 (int-1)* gene. *EMBO J.* **10**, 799–807 (1991).
- Ekker, M., Wegner, J., Akimenko, M.A. & Westerfield, M. Coordinate embryonic expression of three zebrafish *engrailed* genes. *Development* **116**, 1001–1010 (1992).
- Hammerschmidt, M., Bitgood, M.J. & McMahon, A.P. Protein kinase A is a common negative regulator of Hedgehog signaling in the vertebrate embryo. *Genes Dev.* **10**, 647–658 (1996).
- Cheesman, S.E., Layden, M.J., Von Ohlen, T., Doe, C.Q. & Eisen, J.S. Zebrafish and fly Nkx6 proteins have similar CNS expression patterns and regulate motoneuron formation. *Development* **131**, 5221–5232 (2004).
- Strahle, U., Blader, P., Henrique, D. & Ingham, P.W. Axial, a zebrafish gene expressed along the developing body axis, shows altered expression in cyclops mutant embryos. *Genes Dev.* **7**, 1436–1446 (1993).
- Oxtoby, E. & Jowett, T. Cloning of the zebrafish *krox-20* gene (*krx-20*) and its expression during hindbrain development. *Nucleic Acids Res.* **21**, 1087–1095 (1993).
- Giraldez, A.J. *et al.* MicroRNAs regulate brain morphogenesis in zebrafish. *Science* **308**, 833–838 (2005).

SUPPLEMENTARY MATERIAL

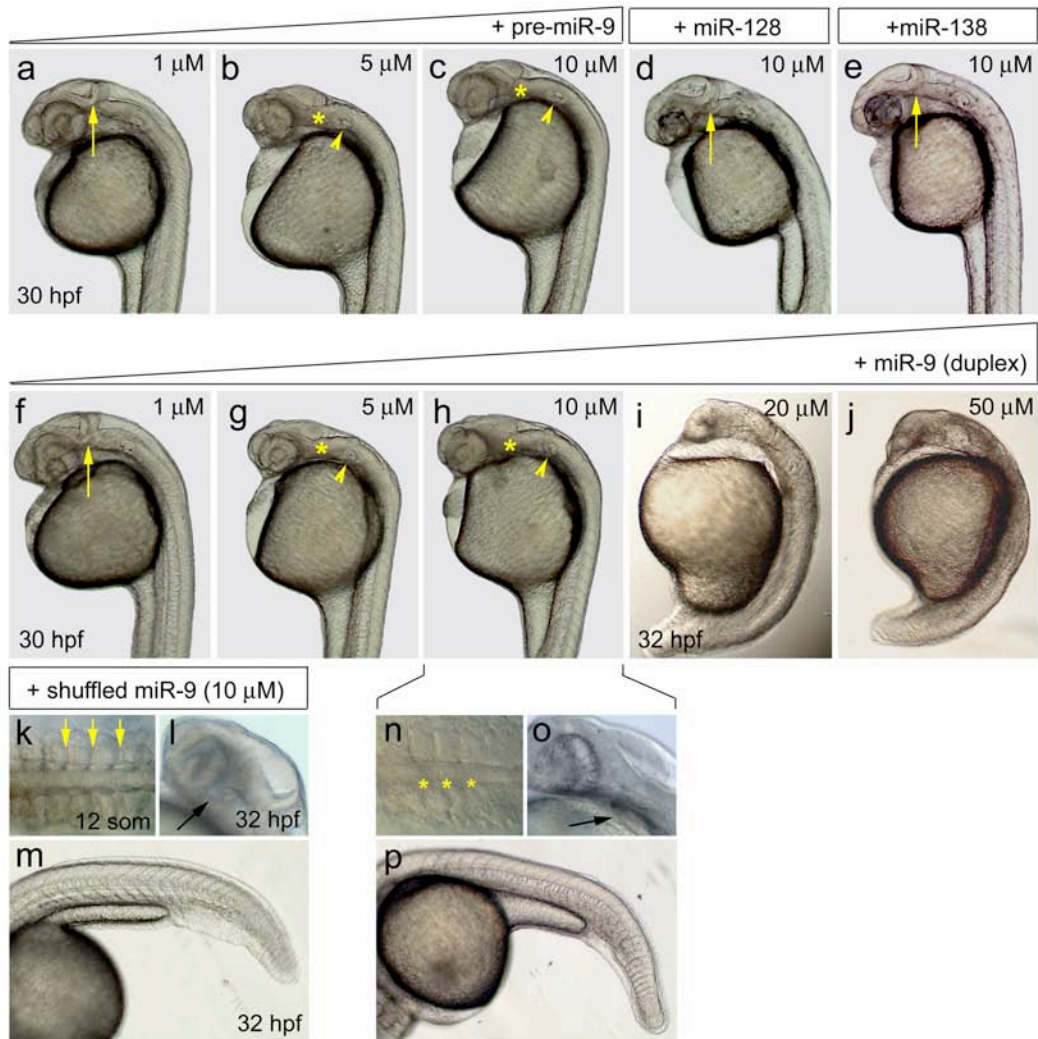
MicroRNA-9 directs late organizer activity of the midbrain-hindbrain boundary

C. Leucht, C. Stigloher, A. Wizenmann, R. Klafke, A. Folchert, L. Bally-Cuif



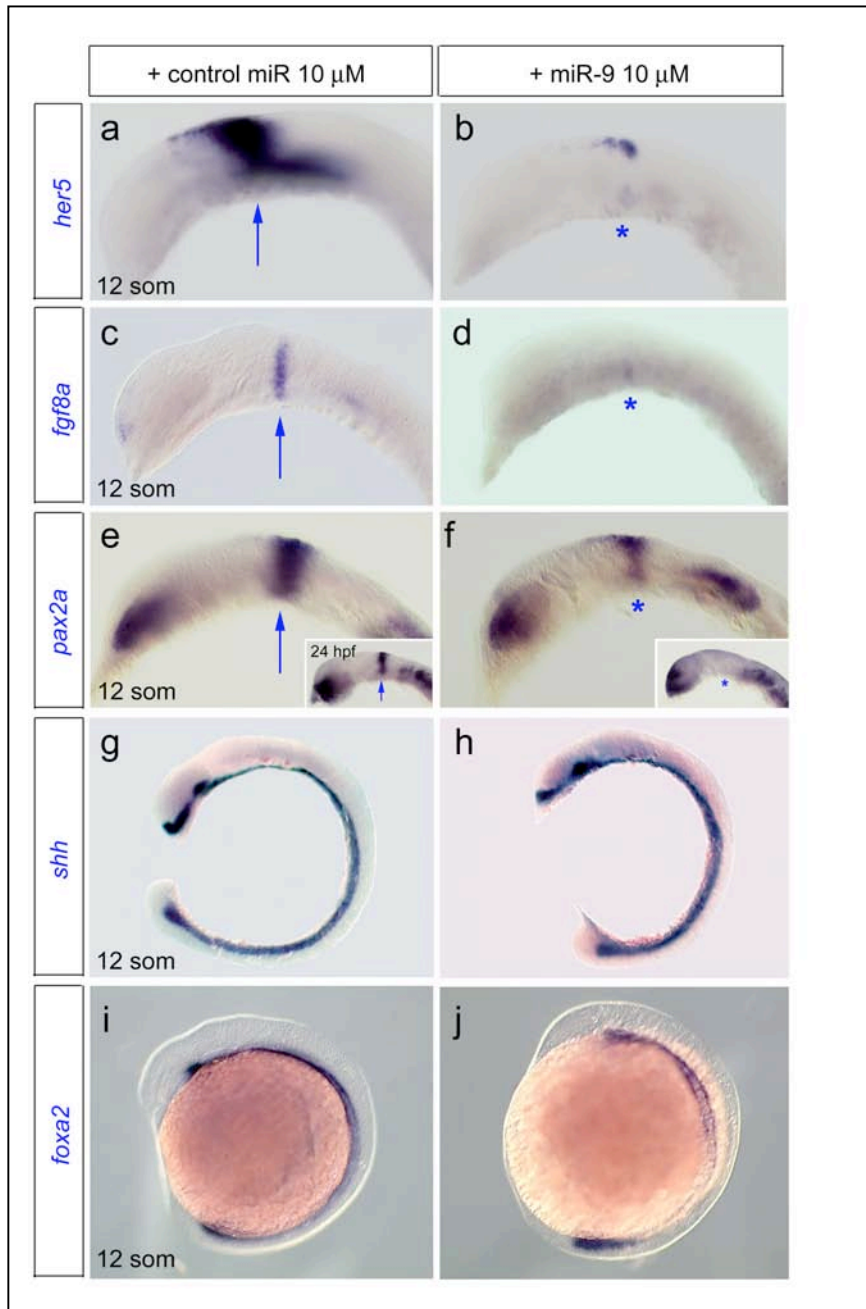
Leucht et al., Supp. 1

Supplementary Figure 1. (a) Sequences of pre-miR-9 RNAs, of the miR-9 duplex and miR-9MO. There are 7 miR-9 genes identified in the zebrafish genome (*zv7*), all with the same mature miR-9 sequence (boxed in yellow). The miR-9 probe, miR-9MO and miR-9 duplex used in this study are based on the mature miR-9 sequence hence detect, block or mimic activity of all miR-9 genes. **(b)** Predicted duplex formation of miR-9 with binding sites on the 3'UTRs of *fgf8*, *fgfr1*, *canopy1*, *her5* and *her9*. Base pairing is indicated by a I, wobble base pairing by a colon. *fgfr1-2* might sit outside the 3'UTR of *fgfr1* and shows no interaction with miR-9 in the sensor assay (Fig. 2c). *fgf8-2* similarly shows no interaction with miR-9 in the sensor assay (Fig. 2c). For *fgfr1-1* and *her5*, the mutated binding sites engineered in the full 3'UTR sensor constructs (see Fig. 2) are also given (*fgfr1-1mt* and *her5mt*, respectively, mutated nucleotides boxed in grey).

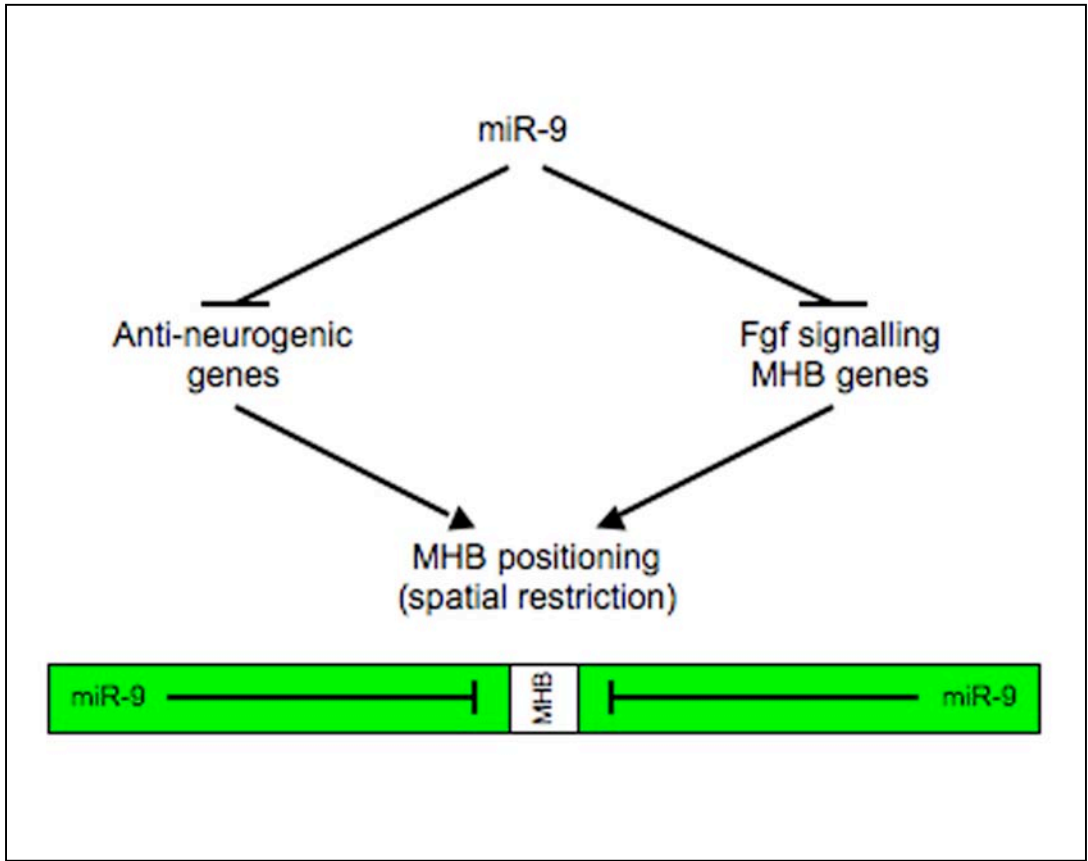


Leucht et al., Supp. 2

Supplementary Figure 2. Dose-dependent morphological alterations caused by overexpression of miR-9 compared to other miRs (a-j, l, m, o, p are sagittal views, anterior left; k, n are dorsal views, anterior left). Embryos were injected with miR-9 duplex, miR-128 duplex, miR-138 duplex, pre-miR-9-1 or a duplex containing a shuffled miR-9 sequence (see Materials and Methods and **Supplementary Fig. 3** for sequences), as indicated above the panels. Panels **n-q** refer to the injection of 10 μM miR-9 duplex. Increasing doses of pre-miR-9 (**a-c**) or miR-9 duplex (**f-h**) up to 10 μM lead to disappearance of the MHB (asterisks in **b, c, g, h**, compare to **a, f**, arrows), reduced otic vesicle size (arrowheads) and blurred somatic boundaries (asterisks in **n**, compare to arrows in **k**). These defects are not observed upon overexpression of miR-128 or miR-138 at the same dose (**d, e**) and are not accompanied by decreased heart size (arrow in **l, o**) or by tail shortening (**m, p**). Overexpression of miR-9 or another miR (not shown) at higher doses leads to non-specific general alterations of embryo morphology (**i, j**), as reported¹⁴.



Supplementary Figure 3. Expression of neural tube regionalization markers in miR-9-overexpressing embryos. Embryos were injected at the one-cell stage with miR-9 or a control miR (miR-124 or miR-138) and analyzed by in situ hybridization at 12 somites, 20 somites and 24 hours-post-fertilization (hpf) (all panels are sagittal views, anterior left, embryos in a-h are deyolled and flat-mounted). Arrows and asterisks indicate staining (or no staining, respectively) at the MHB. Expression of MHB markers (**a-f**), but not of other neural tube patterning markers (**g-j**), is strongly down-regulated upon miR-9 overexpression.



Supplementary Figure 4: Model for the converging effects of miR-9 on MHB maintenance. miR-9 expression (green) in the late embryonic neural tube selectively spares the MHB. It independently down-regulates Fgf signaling and the neurogenesis inhibition cascades, contributing to the maintenance of these two pathways in spatial register at the MHB and the stabilization of a coherent MHB.

MHB marker gene	Injection mix	n	Nb of embryos w/ wt pattern	%	p-value
<i>pax2a</i>	control miR	21	21	100%	
	miR-9	18	0	0%	
	miR-9 + <i>fgfr1</i> BSMO 0.1mM	23	16	70%	2.56E-06
	miR-9 + <i>her5</i> BSMO 0.1mM	29	4	14%	0.283
	miR-9 + <i>her5</i> BSMO 0.5mM	26	18	69%	1.57E-06
<i>wnt1</i>	control miR	25	25	100%	
	miR-9	20	0	0%	
	miR-9 + <i>fgfr1</i> BSMO 0.1mM	31	11	35%	0.003542
	miR-9 + <i>fgfr1</i> BSMO 0.5mM	5	5	100%	1.88E-05
	miR-9 + <i>her5</i> BSMO 0.1mM	37	14	38%	0.0009746
	miR-9 + <i>her5</i> BSMO 0.5mM	7	4	57%	0.001994

Supplementary Table 1. Target protection experiments and MHB rescue. One-celled embryos were injected with miR-9 alone or together with MOs directed against the miR-9 binding sites of endogenous *fgfr1* or *her5* transcripts (*fgfr1*-BSMO and *her5*BSMO, respectively) (*fgfr1*-BSMO protect the binding site *fgfr1*-1). Values indicate the percentage of embryos showing normal *pax2a* or *wnt1* staining at 24 hpf at the MHB among all injected embryos (n). Significance was tested using Fischer's exact test, p-values refer in each case to the difference between embryos injected with miR-9 + BSMO and embryos injected with miR-9 alone.

Transcript	Forward/reverse primer	Probe No. (UPL)
<i>fgf8</i>	GAAGATGGCGACGTTTGTG/ CCCTCCTGTTTCATACAGATGTAAA	17
<i>fgfr1</i>	CTCTCAGGGGTCTCCGAATA/ GAGGTTTCCCGAGAACCAG	43
<i>canopy1</i>	CCTCTTGTTTTACGTAACGTCT/ GCCACAAGAACAAGGCAAAT	54
<i>pea3</i>	CCAGCAAGTGCCTTATACTTTAGC/ TGCGTCCATGTATTTCTTTT	147
<i>her5</i>	GGAGCAAAAAGACATGAGAAGG/ TCTCAAGGTTTCTAGGCTTTGATT	63
<i>her9</i>	GAGCGAGAATCAACGAGAGC/ TCCAATTTAGAGTGTCTGGAGCTA	44
<i>bactin2</i>	AAGGCCAACAGGGAAAAGAT/ GTGGTACGACCAGAGGCATAC	56
<i>gapdh</i>	AACTTTGGTATTGAGGAGGCTCT/ TCTTCTGTGTGGCGGTGTAG	114

Supplementary Table 2. Primers and probes for qPCR.

Supplementary Table 3: Oligonucleotides used for cloning of sensor constructs	
a. <i>fgf8-1</i>	a 5'-tcgagaatctagattacacaggcagcagccggggctagta-3' b 5'-ttacacaggcagcagccggggctagtattacacaggcagcagccggggcg-3' c 5'-ctagcgcgcccggtgctgctgtgtaatactagccccggctgc-3' d 5'-tgctgtgtaatactagccccggctgctgctgtgtaatctagattc-3'
b. <i>fgf8-2</i>	a 5'-tcgagaatctagactgacctgtgaagattataggaagcgaagctagta-3' b 5'-ctgacctgtgaagattataggaagcgaagctagactgacctgtgaagattataggaagcgaagcg-3' c 5'-ctagcgcttcgcttacctataatcttacacaggcagctagcttcgcttacctata-3' d 5'-atcttacacaggcagctagcttcgcttacctataatcttacacaggcagctagctagattc-3'
c. <i>fgfr1-1</i>	a 5'-tcgagaatctagAACATACAGCTGCACACAAAACCGCCAAAGCTAGTA-3' b 5'-acatacagctgcacacaaaaccgccaagctagAACATACAGCTGCACACAAAACCGCCAAAGCG-3' c 5'-ctagcgctttggcggtttgtgtgcagctgtatgttactagctttggcggtttg-3' d 5'-tgtgcagctgtatgttactagctttggcggtttgtgtgcagctgtatgttctagattc-3'
d. <i>fgfr1-2</i>	a 5'-tcgagaatctagatcatcgacgcagctagtggtcAAAAATAGTA-3' b 5'-tcatcgacgcagctagtggtcAAAAATAGTATCATCGACGCAGCTAGTGGTCAAAAAG-3' c 5'-ctagcttttgagccactagctgcgctgatgatactattttgagccacta-3' d 5'-gctgcgctgatgatactattttgagccactagctgcgctgatgatactagattc-3'
e. <i>canopy1</i>	a 5'-tcgagaatctagatcaaaaacctggaccaaagtagta-3' b 5'-tcaaaaacctggaccaaagtagatcaaaaacctggaccaaagtg-3' c 5'-ctagcactttggccagggttttgataactaactttggctc-3' d 5'-agggttttgataactaactttggccagggttttgatctagattc-3'
f. <i>her5</i>	a 5'-tcgagaatctagattgtacagtagatgccaagatagat-3' b 5'-ttgtacagtagatgccaagatagattgtacagtagatgccaagag-3' c 5'-ctagctctttggcatctactgtacaatactatctttggcat-3' d 5'-ctactgtacaatactatctttggcatctactgtacaatctagattc-3'
g. <i>her9</i>	a 5'-tcgagaatctagatataaagtactttttaaatcaagatagta-3' b 5'-tataaagtactttttaaatcaagatagatataaagtactttttaaatcaagag-3' c 5'-ctagctctttgatttaaaaagtactttatatactatctttgattaaa-3' d 5'-aaagtactttatatactatctttgatttaaaaagtactttatatactagattc-3'
h. <i>her5</i> 3'UTR	forward 5'-ccgctcgagaagatcatggcctaagtccctgtg-3' reverse 5'-gctctagaagaatatacctcagagagggttaattcctt-3'
i. <i>fgfr1</i> 3'UTR	forward 5'-ccgctcgagtatctagaggactcatttactcagtggtgtgtg-3' reverse 5'-gactagtaccatttcggtggatctcagtttg-3'
j. <i>canopy1</i> 3'UTR	forward 5'-ccgctcgagtatctagacttcaccgctgatctgctggag-3' reverse 5'-gactagtcacagagtgaacagtcacaattgacac-3'

Appendix 5

Article accepted in ***Journal of Comparative Neurology***

Fgf signaling in the zebrafish adult brain: association of Fgf activity with ventricular zones but not cell proliferation

Stefanie Topp, Christian Stigloher, Anna Komisarczuk,
Birgit Adolf, Thomas Becker and Laure Bally-Cuif

Contribution:

This project was mainly conducted by Stefanie Topp. I participated in the design of the molecular analysis and cloning of probes (see Figures 1, 3, 5), interpretation of expression patterns and initial analysis of enhancer trap lines (data not shown).

Fgf signaling in the zebrafish adult brain: association of Fgf activity with ventricular zones but not cell proliferation

Stefanie Topp¹, Christian Stigloher¹, Anna Z. Komisarczuk², Birgit Adolf¹, Thomas S. Becker², Laure Bally-Cuif^{1,§}

¹HelmholtzZentrum muenchen, German Research Center for Environmental Health, Department Zebrafish Neurogenetics, Institute of Developmental Genetics, Ingolstaedter Landstrasse 1, D-85764 Neuherberg, Germany; ²Sars Center for Marine Molecular Biology, University of Bergen, N-5008 Bergen, Norway; §corresponding author at bally@helmholtz-muenchen.de

Running head: Fgf signaling in the adult zebrafish brain

Associate Editor: Dr. John L.R. Rubenstein

Key words: Fgf, P-ERK, *sprouty*, zebrafish, neural progenitor, adult brain

Corresponding author:

Laure Bally-Cuif
HelmholtzZentrum muenchen
German Research Center for Environmental Health
Department Zebrafish Neurogenetics
Institute of Developmental Genetics, Ingolstaedter Landstrasse 1
D-85764 Neuherberg, Germany
Phone: +49.89.3187.3562
Fax: +49.89.3187.3099
Email: bally@helmholtz-muenchen.de

Support and grant information: This work was supported by a VWStiftung Junior Group grant (to LBC), the Life Science Stiftung (contract GSF 2005/01) (to LBC), the Center for Protein Science-Munich (CIPSM) (to LBC), the EU Integrated Project ZF-MODELS (contract n°LSHC-CT-2003-503466) (to LBC and TSB), the Institut du Cerveau et de la Moelle Epinière (ICM, Paris, France) (to LBC and TSB), and a core grant from the Sars Centre (to TSB).

Abstract

The zebrafish adult brain contains numerous neural progenitors and is a good model to approach the general mechanisms of adult neural stem cell maintenance and neurogenesis. Here we use this model to test for a correlation between Fgf signaling and cell proliferation in adult progenitor zones. We report expression of Fgf signals (*fgf3, 4, 8a, 8b, 17b*), receptors (*fgfr1-4*) and targets (*erm, pea3, dusp6, spry1, 2, 4* and P-ERK) and document that genes of the embryonic *fgf8* synexpression group acquire strikingly divergent patterns in the adult brain. We further document the specific expression of *fgf3, fgfr1-3, dusp6* and P-ERK in ventricular zones, which contain neural progenitors. In these locations however, a comparison at the single-cell level of *fgfr*/P-ERK expression with BrdU incorporation and the proliferation marker MCM5 indicates that Fgf signaling is not specifically associated with proliferating progenitors. Rather, it correlates with the ventricular radial glia state, some of which only are progenitors. Together these results stress the importance of Fgf signaling in the adult brain and establish the basis to study its function in zebrafish, in particular in relation to adult neurogenesis.

Introduction

Understanding the molecular mechanisms of adult neural stem cell maintenance and recruitment is an important issue with direct relevance to neurodegeneration and ageing. As a novel approach towards this aim, we recently initiated a molecular study of adult neural progenitors and their environment in the telost zebrafish, *Danio rerio*. BrdU incorporation and tracing analyses demonstrated the existence of multiple neurogenic niches in the zebrafish adult brain (Adolf et al., 2006; Grandel et al., 2006; Pellegrini et al., 2007; Zupanc et al., 2005), and the presence of label-retaining progenitors in all these locations (Adolf et al., 2006; Chapouton et al., 2007; Grandel et al., 2006). Hence, this model permits the comparison of neural progenitors from different brain subdivisions, an approach that should help distinguish regional from core stem cell characters. We further showed that progenitors located along the ventricle of the adult zebrafish telencephalic subpallium and the midline of the pallium generate neuroblasts that are for a large part fated to form TH-positive and GABA-ergic neurons in the olfactory bulb (Adolf et al., 2006). This is identical to the fate of mammalian neural stem cells from the subependymal zone (SEZ) (Alvarez-Buylla and Garcia-Verdugo, 2002; Betarbet et al., 1996), and the zebrafish and mouse progenitors further share expression of several transcription factors (Adolf et al., 2006). Thus, knowledge generated from zebrafish adult neural stem cells can likely be extended to mammals.

With this in mind, we first focused on Fgf signaling as a pleiotropic pathway that, among numerous other activities, influences cell proliferation and differentiation within the developing and mature central nervous system (Dono, 2003; Reuss and von Bohlen und Halbach, 2003; Thisse and Thisse, 2005a). To date, four Fgf receptors (FgFR1-4) and 22 Fgf signals have been identified in rodents (Itoh and Ornitz, 2004) (28 Fgfs in zebrafish), of which several are expressed in the adult brain (reviewed in (Dono, 2003)). In spite of extensive studies at embryonic stages, however, functional analyses in the adult brain largely focused on basic Fgf (Fgf2). Fgf2 expression is broad and includes neurogenic zones (Ernfors et al., 1990; Gomez-Pinilla et al., 1992), it stimulates the proliferation of progenitor cells when applied to cultures derived from the adult hippocampus (Gage et al., 1995; Palmer et al., 1995; Vescovi et al., 1993), and increases neurogenesis in the dentate gyrus and subependymal zone upon infusion into the brain (Jin et al., 2003; Kuhn et al., 1997; Tao et al., 1997; Wagner et al., 1999). During adulthood in the mouse, knock-out of

Fgf2 massively decreases the number of dividing neural progenitors (potential neural stem cells and their amplifying progeny) in the SEZ under normal conditions and upon injury (Yoshimura et al., 2001; Zheng et al., 2004), as well as the number of newborn neurons in the olfactory bulb (Zheng et al., 2004). Besides *Fgf2*, one study reports a proliferation- and differentiation-promoting effect of *Fgf4* on neural progenitors in adult neurospheres (Kosaka et al., 2006). Except for *FgfR4*, *FgfRs* are broadly expressed in the adult brain and also encompass progenitor zones (reviewed in (Dono, 2003; Reuss and von Bohlen und Halbach, 2003). However, functional analyses during adulthood upon targeting *FgfRs* in the mouse has been impaired by the early embryonic lethality of *Fgfr1*^{-/-} (Deng et al., 1994; Yamaguchi et al., 1994) and *Fgfr2*^{-/-} (Arman et al., 1998) knock-out animals, while to date *Fgfr3*- and *Fgfr4*-depleted mice (Deng et al., 1996; Weinstein et al., 1998) have not been analyzed during adulthood for neurological phenotypes. Recently however, a conditional knock-out of *Fgfr1* in *Nestin:Cre* mice was used to target *Fgfr1* loss to neural progenitor cells. This resulted in decreased BrdU incorporation and the formation of a lowered number of newborn neurons in the adult dentate gyrus (Zhao et al., 2007), adding strong support to a prominent role of endogenous *Fgf* signaling in adult neural stem cell maintenance and fate. Alterations of this signaling pathway might also be relevant to neurogenesis-associated mood disorders, such as depression, bipolar disorder and schizophrenia, where higher expression of *Fgfr1* and lower expression of *Fgf2* have been noted in the hippocampus (Gaughran et al., 2006), as well as alterations in the *Fgf* signaling regulator NPAS3 (Pieper et al., 2005).

To gain further insight into the cell types, signals and receptors possibly mediating *Fgf* activity in the adult brain, as well as into the general use of these pathways in adult neurogenesis, we report here an expression analysis of *Fgf* signals, receptors and targets in relation to proliferation zones of the adult zebrafish brain. We focused on three neurogenic domains of the adult zebrafish brain that have been well characterized: the telencephalic ventricle, the periventricular zone of the hypothalamus, and the midbrain-hindbrain boundary area (containing proliferating areas such as the isthmus proliferation zone, the tectal proliferation zone and the valvula cerebelli) (Adolf et al., 2006; Chapouton et al., 2006; Grandel et al., 2006; Pellegrini et al., 2007). To better complement studies performed in rodents, we chose to focus on *Fgf* signals expressed in association with neural progenitor pools during embryogenesis, such as *Fgf3*, 4, 8a, 8b (previously 17a) and 17b (Cao et al., 2004; Kiefer et al., 1996; Kikuta et al., 2007; Phillips et al., 2001; Reifers et al., 2000; Reifers et al., 1998; Thisse and Thisse, 2005b). We placed particular emphasis on cells receiving and processing *Fgf* signals by studying in detail the expression of all four receptors (*Fgfr1-4*) and of phosphorylated ERK (P-ERK) as a read-out of tyrosine kinase receptor activity, a major output of the *Fgf* pathway (reviewed in (Eswarakumar et al., 2005; Thisse and Thisse, 2005a)). Finally, we also studied expression of other genes identified as *Fgf* pathway targets in the embryonic neural tube such as *erm*, *pea3*, *dusp6* and *sprouty* genes (*spry1*, 2 and 4) (Furthauer et al., 2002; Kawakami et al., 2003; Komisacszuk, in prep; Raible and Brand, 2001; Roehl and Nusslein-Volhard, 2001) (reviewed in (Thisse and Thisse, 2005a)). Our results show that the expression of genes of the *fgf8* synexpression group widely diverge in the adult brain. There, *dusp6* and P-ERK best reflect *fgfr1-3* expression, and expression of these genes (as well as of *fgf3*) is in particular associated with radial glia cells present along ventricular zones. Although these are sites of adult neurogenesis (Adolf et al., 2006; Grandel et al., 2006; Pellegrini et al., 2007), P-ERK and *fgfr1-3* expression generally do not correlate with proliferating cells, suggesting roles other than the stimulation of neural progenitor proliferation.

Materials and methods

Fish

Adult zebrafish from the wild-type AB strain or the transgenic line *Tg(gfap:GFP)^{mi2001}* (Bernardos and Raymond, 2006) of both sexes aged 3-9 months were used. All experiments were carried out in accordance with the regulations of the Regierung von Oberbayern on animal welfare.

BrdU injections

The animals were briefly anesthetized and injected intraperitoneally with 50mg/g body weight bromo-deoxy-uridine (BrdU) in solution in 110 mM NaCl pH7.0. Two injections were performed with a 2-hour interval, and the animals were killed 2 hours after the second injection.

Cloning of zebrafish *spry1*

spry1 was cloned by PCR from genomic DNA using the following primer set: 5`-GCACATCATCATCATCTTCACC-3` and 5`-CACCATCAGTTTGTGCCTCAGGAT-3`. The reaction was carried out at 94°C for 5 min., then 35 cycles at 94°C for 30s, 53°C for 30s, 72°C for 90s and a final extension at 72°C for 5 min. The PCR product was directly processed for a nested PCR using the following primers: 5`-GCATAGGTGTTGGAATTGACATC-3` and 5`-CAGTTTGTGCCTCAGGATGGTTTCC-3`, under similar conditions as described above. The PCR product was subcloned into pCR II-Topo Vector (Invitrogen). The sequence of zebrafish *spry1* has been submitted to Genbank (accession N. bankit1053103 EU379656).

In situ hybridization and immunocytochemistry

Animals were sacrificed following anesthesia and the brains were dissected out after a brief fixation in 4% paraformaldehyde (PFA). Dissected brains were then post-fixed in 4% PFA overnight at 4°C. Following rinsing in PBT, the brains were embedded in albumin-gelatine:sucrose denatured with glutaraldehyde and cut serially into 100 μ m thick slices using a vibratome. The sections were dehydrated in methanol series and either stored at -20°C or processed for in situ hybridization or immunocytochemistry using published protocols (Lillesaar et al., 2007). For each probe and each section plane, a minimum of two brains was analyzed; we did not detect variations in expression patterns between samples. For single in situ hybridization, staining was revealed using NBT/BCIP. We used the following probes: *fgf3* (nt 1-1810) (Kiefer et al., 1996), *fgf4* (probe en142, 634 nt) (Thisse and Thisse, 2005b), *fgf8a* (previously *fgf8*) (nt 1-630) (Reifers et al., 1998), *fgf8b* (previously *fgf17a*) (nt 1-2351) (Kikuta et al., 2007; Reifers et al., 2000), *fgf17b* (nt 1-2052) (Cao et al., 2004), *erm* (nt 1-2779) (Raible and Brand, 2001), *pea3* (nt 1-1813) (Raible and Brand, 2001), *duosp6* (Norton et al., 2005), *spry1* (912 nt, see above), *spry2* (nt 1-1509) (Furthauer et al., 2002), *spry4* (nt 1-2890) (Furthauer et al., 2001), *fgfr1* (nt 1-2532) (Scholpp et al., 2004), *fgfr2* (nt 1-4778) (Tonou-Fujimori et al., 2002), *fgfr3* (nt 1-3002) (Sleptsova-Friedrich et al., 2002), *fgfr4* (nt 1-4705) (Sleptsova-Friedrich et al., 2002). For double in situ hybridization / immunocytochemistry staining, in situ hybridization was performed first and revealed either with fast red (Sigma) in 0.4M NaCl, Tris 0.1M, pH 8.2 buffer, or using tyramide amplification (TSATM Plus Cyanine 3 System, Perkin Elmer) (for Fig.2G) according to the manufacturer's instruction, with sequential incubation in anti-digoxigenin-HRP (1/1000) antibody and revealed with tyramide Cy3 working solution (1/50). The sections were then rinsed in PBT and directly processed for immunocytochemistry, which was revealed using a secondary antibody coupled to Alexa Fluor[®] 488.

The following primary antibodies were used: rabbit anti-MCM5 (1/1000; (Ryu et al., 2005)), monoclonal anti-MAP Kinase, activated anti-DPERK (1/3500;Sigma ref.M8159), monoclonal rat anti-BrdU (1/200;Abcam ref.ab6326), polyclonal rabbit anti-GFP (1/1000;Torrey Pines Biolabs), monoclonal mouse anti-Human neuronal

protein (HuC/D) (1/500;Molecular Probes ref.16A11), polyclonal rabbit anti-BLBP (1/1500;Chemicon ref.AB9558). The following secondary antibodies were used: Alexa Fluor® 555 goat anti-rabbit IgG (1/500; Invitrogen), Alexa Fluor® 488 goat anti-mouse IgG (1/500;Invitrogen), Alexa Fluor® 488 goat anti-rat IgG (1/500;Invitrogen).

Specificity of the primary antibodies: (i) rabbit anti-MCM5: this antibody was raised against the N-terminal 241 amino acids of zebrafish MCM5, and its specificity was verified on Western blot using extracts from zebrafish embryos compared to embryos injected with a *mcm5* morpholino antisense oligonucleotide. In the latter extracts, the anti-MCM5 band disappears at 4 days-post-fertilization, following the turn-over of maternal MCM5 protein (Ryu et al., 2005); (ii) monoclonal anti-MAP Kinase, activated anti-DPERK: this antibody was raised against a 11 amino acid-peptide (HTGFLpTEpYVAT) corresponding to the phosphorylated form of the mouse ERK-activation loop. It has been used to reveal ERK activation in zebrafish during development (Shinya et al., 2001). Its specificity is attested by the fact that its staining pattern mimics that of Fgf expression in the early neural tube, and by the verification that this signal is abolished upon incubation of zebrafish embryos in inhibitors of Fgf signaling, both on whole-mount specimen and on Western blot (Shinya et al., 2001); (iii) monoclonal rat anti-BrdU: this antibody has been used in several studies of proliferation in the zebrafish brain (Adolf et al., 2006; Chapouton et al., 2006; Grandel et al., 2006; Pellegrini et al., 2007). This antibody does not detect any cells in animals that have not been subject to BrdU administration. Stained cells after a short BrdU pulse are only found within domains positive for other proliferation markers such as PCNA or MCM5, and their number increases upon cumulative BrdU administration. (iv) Monoclonal mouse anti-Human neuronal protein (HuC/D): this antibody was raised against the human HuD peptide QAQRFRLDNLN. It binds to human Elav family members HuD, HuDpro (alternatively spliced form of HuD) and HuC. In addition, the peptide used is found in the sequences of HuCSL (alternatively spliced form of HuC) and Hel-N1 (Marusich et al., 1994). It specifically cross-reacts with zebrafish HuC protein, as it produced an identical staining to GFP in the adult brain of *HuC:gfp* transgenic zebrafish (Park et al., 2000) (S. Simonovic, S. T. and L. B-C., unpublished). (v) BLBP: this antibody was raised against recombinant whole mouse BLBP protein, and its specificity was assessed on Western blot (Feng et al., 1994). It cross-reacts with zebrafish BLBP_a (*Fabp7a*) and produces an identical staining pattern as the *fabp7a* probe and as GFAP in zebrafish adult brain tissue ((Adolf et al., 2006) and P. Chapouton, unpublished).

Imaging

Single in situ hybridizations were photographed on a Zeiss Axioplan photomicroscope mounted with a 3CCD color video camera and processed with Axiovision 4.5 (Zeiss). All double stainings were documented on a Zeiss LSM510Meta confocal microscope and processed using the LSM software (Zeiss). We illustrate either 50 micron projections of recorded stacks or, to assess the double labeling of single cells, 2 micron sections (Figs.2M1-3,N1-3;4I1-3,J1-3;6E1-2,F1). The pictures were mounted using the Adobe Photoshop 7.0 software with, when necessary for fluorescent pictures, adjustment of brightness and contrast to optimize visualization of the stainings in the different channels.

Results

All anatomical terms below originate from (Wullimann et al., 1996). Expression of *fgf4* and *fgfr4* proved generally ubiquitous (not shown) and will not be detailed.

Fgf signaling in the adult telencephalon and olfactory bulb

Fgf signals

Telencephalon

fgf8b appeared expressed rather broadly and at moderate levels, with increased levels at the telencephalon–olfactory bulb (OB) junction (Fig.1C, blue arrow). In contrast, *fgf3* and *8a* were expressed at high levels in very discrete telencephalic domains. Both genes highlight the ventricular domain located at the junction between subpallium (dorsal nucleus) and OB (Fig.1A,B, blue arrows), a domain identified as a major proliferation and neurogenic zone (see below) (Adolf et al., 2006). In addition, strong expression of *fgf3* could be seen in ventricular cells of the parvocellular preoptic nucleus (Fig.1A, arrowhead), another proliferation domain in the adult brain. *fgf17b* was strongly expressed in most telencephalic domains (not shown).

Olfactory bulb

fgf8a and *8b* were also expressed in discrete postmitotic cells of the OB granular layer (no proliferation has been reported in this domain) (Fig.1B,C, white arrows), and *fgf17b* was strong and widespread in all OB layers (not shown).

Fgf pathway targets

spry1, *2* and *4* were generally weakly expressed and in much broader domains than merely at or around the sites of strong *fgf3* and *8a* expression. In the telencephalon and OB, *spry1* transcripts concentrated in fiber-like structures reminiscent of described GFAP-positive radial glial fibers that, in the telencephalon proper, extend from the ventricle to the lateral subpallium or posterior pallium (Fig.1E,E') (Adolf et al., 2006). *spry2* expression was most intense medially (Fig.1F) and virtually absent from lateral telencephalic areas (Fig.1F'), and *spry4* was expressed in a low number of cells of the central, dorsal and lateral domains of the pallium (Fig.1G,G'). Expression of *erm* was found along the telencephalic ventricular zone (Fig.1D) as well as in more lateral, non-proliferating areas (Fig.1D' and not shown). Expression of *dusp6* and P-ERK were more discrete and concentrated in the ventricular zone (Figs.1H-I',2I-N) (see also below). In addition, P-ERK was detected in the OB (Fig.1I, arrow).

Fgf receptors

Expression of *fgfrs* identifies the cells susceptible to receive and process Fgf signaling, hence their expression was analyzed in more detail. *fgfr1*, *-2* and *-3*, were expressed almost exclusively in the telencephalic ventricular zone (Fig.1K,K',L,M,M',O,O'). They varied however in their fine distribution and intensity of expression. *fgfr1* expression was strongest in the subpallium and midline of the pallium (Fig.1K,K', arrows), undetectable in the dorsal pallium, and weak more laterally, *fgfr2* expression covered the entire ventricular zone, encompassing all pallial domains (i.e. including the dorsal –albeit at weaker levels-, lateral and medial pallium) (Fig.1L-M', arrows and arrowheads), and *fgfr3* was limited to the subpallium and midline of the pallium in the anterior telencephalon (Fig.1O, arrow) but extended to the medial and lateral pallium more caudally (Fig.1N,O', arrowheads). In addition, *fgfr1* expression extended into non-ventricular domains in the dorsal nucleus of the subpallium, the medial and posterior pallium (Fig.1K,K', asterisks), and both *fgfr1* and *2* were expressed in the OB (Fig.1J,L,L').

To gain insight into which cell types process the Fgf signal, in particular in the telencephalic progenitor zone, we next used double-labeling procedures to directly compare expression of *fgfr1-3* with BrdU incorporation (proliferating cells in S phase) and the Hu protein (a marker of post-mitotic neurons) (Mueller and Wullmann, 2002). Most cells expressing *fgfr1* and *2* in the OB corresponded to Hu-positive post-mitotic neurons (not shown). In contrast, the location of cells expressing all three receptors at the telencephalic midline coincided with the BrdU incorporation zone (Fig.2A-D). *fgfr1* and to a minor extent *fgfr3* (but not *fgfr2*) expression further encompassed Hu-

positive cells located immediately adjacent to the midline (Fig.2E-H, arrows) and in parenchymal domains immediately lining the edge of the lateral and medial pallium, where newborn neurons have been described (Adolf et al., 2006; Grandel et al., 2006; Pellegrini et al., 2007; Zupanc et al., 2005).

While most *fgfr1-3*-positive, Hu-positive cells appeared negative for P-ERK (both in the OB and in the telencephalon proper) (Fig.2I and not shown), expression of *fgfr1-3* precisely coincided with P-ERK staining at the ventricular zone (Fig.2I,J and not shown), suggesting that P-ERK can be used as a read-out of Fgf signaling in this location. We hence used this marker to refine our analysis of Fgf signaling and proliferation at the single cell level. P-ERK specifically highlighted ventricular cells of radial morphology along the entire subpallial and pallial ventricles (Fig.2I-O), in a manner reminiscent of radial glia markers such as GFAP and BLBP (Adolf et al., 2006) and our unpublished observations). Double-labeling of telencephalic cross-sections for P-ERK and GFP in transgenic *gfap:GFP* fish (Bernardos and Raymond, 2006) or for P-ERK and BLBP (not shown) indeed revealed a large extent of co-expression in most ventricular domains, in particular obvious in the dorsal subpallium (Fig.2K,L) where P-ERK expression is strongest. The radial GFAP- and BLBP-positive population comprises cells identified as neural progenitors in the zebrafish adult telencephalon (Adolf et al., 2006; Grandel et al., 2006; Pellegrini et al., 2007). However, comparison of P-ERK expression with expression of the proliferation marker MCM5, which labels all cell cycle phases (Ryu et al., 2005), demonstrated that only a very minor fraction of P-ERK-positive cells were actually proliferating (Fig.2K-N). Overall, ventricular sub-domains rich in proliferating cells (such as the subpallial proliferation stripe, (Adolf et al., 2006), see Fig.2P) appeared largely P-ERK-negative, while ventricular sub-domains containing fewer proliferating cells were strongly stained for P-ERK (Fig.2O). Hence, the telencephalic ventricular zone is composed of a mixture of radial glia cells, which are either in cycle or expressing P-ERK, with a minor overlap.

In summary, a striking feature of *fgfr1-3* in the adult telencephalon is their common expression in ventricular zone cells. Strong Fgf signaling in these cells is further substantiated by their high expression of P-ERK. The ventricular zone primarily consists of radial glia cells, some of which proliferate and serve as neural progenitors, while others are post-mitotic or quiescent. P-ERK expression is largely associated with the latter population.

In detail, *fgfr1-3* differ in the extent of their expression domain along the telencephalic ventricle, defining a domain of *fgfr1-3* expression (subpallium and midline of the pallium), a domain expressing *fgfr2* only (anterior aspects of the dorsal and lateral pallium) and a domain expressing *fgfr2* and *3* (caudal aspect of the dorsal, lateral and posterior pallium). P-ERK is expressed along the entire extent of the ventricular zone.

Finally, expression of *fgfr1* and *2* can also be found in postmitotic neurons (*fgfr1* in the OB and telencephalon proper, *fgfr2* in the OB only) but these cells are not positive for P-ERK.

A schematic cross-section highlights some of these findings (Fig.1P).

Fgf signaling in the adult hypothalamus

Fgf signals

Strong expression of *fgf17b* was detected virtually ubiquitously (Fig.3D). In contrast, *fgf3*, *8a* and *8b* were discretely expressed in the periventricular hypothalamus (Fig.3A-C, arrows).

Fgf pathway targets

The expression of all genes and factors tested (*erm*, *dusp6*, *spry1,2,4* and P-ERK) was also restricted to the periventricular hypothalamus (Fig.3E-I, arrows, and Fig.4G-J), pointing to strong Fgf signaling in this location.

Fgf receptors

fgfr1-3 were discretely expressed and restricted to the periventricular area along the entire anteroposterior extent of the hypothalamus, including both the lateral and posterior recess (Fig.3J-O).

The most ventricular cell row(s) of the adult hypothalamus is an identified proliferation and neurogenesis zone (Adolf et al., 2006; Grandel et al., 2006; Pellegrini et al., 2007), and we therefore used double staining to determine the proliferation/differentiation status of the cells susceptible to receive Fgf signals. A short BrdU pulse indicated that most *fgfr1-3*-expressing cells are in the BrdU incorporation zone (Fig.4A-C). At the ventricle however, detailed inspection suggested that only some *fgfr1-3*-positive cells incorporated BrdU (e.g. Fig.4B1, and not shown). In addition, *fgfr1* expression, but not that of *fgfr2-3*, extends to neighboring Hu-positive domains (Fig.4D-F).

Comparison with P-ERK expression showed that, like in the telencephalon, ventricular *fgfr1-3*-positive cells, but not *fgfr1*-positive cells of the subventricular zone, expressed P-ERK (Fig.4G,H and not shown). The coincidence of P-ERK staining with expression of all three *fgfrs* at the ventricle strongly supports use of P-ERK as a read-out of Fgf signaling in this location, permitting a study of proliferation at the single cell level. We compared P-ERK and MCM5 expression using confocal microscopy and found that most P-ERK-positive cells were MCM5-negative, with a few exceptions. Along the hypothalamic midline, P-ERK and MCM5-positive cells were mixed, with a few isolated double-positive cells (Fig.4I). Along the ventricles of the lateral recess, P-ERK-positive cells were mostly covering the dorso-lateral domains, while proliferating cells were ventro-medial (Fig.4J). Isolated double-positive cells were found in all these domains.

In summary, in the adult zebrafish hypothalamus, Fgf signaling was most intense in the proliferating periventricular domain, and might be processed in this location through all *fgfrs*. In addition, *fgfr1* was expressed in neurons immediately surrounding this domain. Ventricular cells expressing *fgfr1-3* (but not subventricular cells expressing *fgfr1* only) were positive for P-ERK, but, although they were located in the hypothalamic proliferation zone, were mostly negative for proliferation markers. Expression of *fgfrs* and *fgf* signals is summarized on a schematic cross-section in Fig.3P.

Fgf signaling in the adult midbrain-hindbrain

Fgf signals

Here again, expression profiles for the different *fgf* genes varied markedly. As mentioned above, *fgf4* expression was virtually ubiquitous, and *fgf17b* broadly distributed at extremely strong levels, with most intense staining in the granular zones of the optic tectum (TeO) and cerebellum (including those of the valvula cerebelli (val), corpus cerebellaris (Ce) and crista cerebellaris (CC)) (not shown). *fgf8a* expression highlighted the torus longitudinalis (TL) of the TeO and the granular zones of the val, Ce and CC (Fig.5B,B'). Both *fgf3* and *8b* were exclusively expressed along the ventricular zone of the midbrain, however in discrete domains: *fgf8b* expression highlighted the ventricular layer of the posterior aspect of the valvula cerebelli and most of the tegmentum (Tg) (Fig.5C,C'), while *fgf3* expression was restricted to the most posterior tegmentum (Fig.5A').

Fgf pathway targets

erm was expressed in a manner very similar to *fgf8a*, with prominent signal in the TL and the granular zones of the cerebellum (Fig.5D,D'). In addition, strong expression was detected in the periventricular grey zone (PGZ) of the TeO (Fig.5D'). Expression of *spry1,2,4* was weak but globally more in keeping with the profiles displayed by *fgf3* and *-8b*: expression of all three genes was most prominent along the ventricular zone of the mid- and/or hindbrain (with *spry1* restricted to the most anterior midbrain) (Fig.5F-H'). In addition, *spry2* was expressed in scattered cells of the molecular and Purkinje/eurydendroid cell layers of the cerebellum (Fig.5F, arrowheads), and *spry4* in the PGZ of the TeO (Fig.5G', arrowheads). Expression of *dusp6* was very similar to that of *spry4* and also highlighted ventricular domains and the periventricular grey zone (Fig.5H,H'). In the midbrain, expression of P-ERK was prominent in the ventricular zone (Fig.5I,I', arrows). In addition, the molecular layer of the Ce and medial val displayed intense staining of both cell bodies and fibers (Fig.5I,I', arrowheads), while weaker expression was also detectable in the granular zones of these domains. Finally, we observed strongly positive cells in the nucleus lateralis valvulae (Fig.5I', asterisk).

Fgf receptors

fgfr4 expression was observed in all structures and cell layers with the exception of the TeO and TL (not shown). *fgfr1-3* were expressed in ventricular zones of the mid- and hindbrain (Fig.5J-O, arrows) albeit with noticeable differences: *fgfr2* expression was of high intensity and encompassed the entire ventricular zone, while *fgfr1* tended to be stronger laterally than medially and *fgfr3* was only detectable in the most anterior midbrain domains. In addition to these ventricular domains, intense expression of *fgfr1* was observed in the nucleus isthmi (Fig.5J',K, arrow), *fgfr3* labeled scattered cells of the cerebellar molecular layer, and *fgfr2* was expressed at high levels in numerous cells of the molecular and granular layers of the cerebellum as well as in isolated cells the rhombencephalon. Expression of Fgf signals and receptors is schematically summarized in 3-dimension on Fig.6A, and in cross-section on Fig.6B.

The midbrain-hindbrain displays a complex organization of several proliferating populations, located along the tegmental ventricle, at the edge of the TeO (tectal proliferation zone) or in the granular zones of the val and Ce, as well as an identified population of slow-proliferating neural stem cells (Chapouton et al., 2006). To determine the proliferation/differentiation status of *fgfr1-3*-expressing cells, we first compared *fgfr1-3* expression with BrdU-incorporation zones and Hu-positive cells. In the granular zones of the Ce and val, *fgfr2-3*-expressing cells were BrdU-negative after a short incorporation pulse, and co-stained for Hu (Fig.7B,C,J,K). Hence, these cells largely correspond to neurons, as do most other non-ventricular cells labeled by the different receptors (Fig.7G,H,J,K, arrows), with the possible exception of some *fgfr2*-positive cells in the Ce molecular layer. Among non-ventricular cells, only those located in the granular layers of the Ce or val were in P-ERK-positive areas (although exact co-expression was difficult to assess since the P-ERK staining did not delimit cell contours in this domain), but other domains (e.g. nucleus isthmi, hindbrain) were P-ERK-negative (not shown).

In contrast, along the ventricle, BrdU-incorporation zones coincided with ventricular domains expressing *fgfr1-2* (Fig.7A-C, and data not shown). Expression of *fgfr1-2* along the ventricular zone however expanded further than the proliferation zones: the latter was prominent along the val, but was limited at the edge of the TeO and TS, while *fgfr1-2* were strongly expressed in these locations (Fig.7A,B).

Ventricular *fgfr1*- and *2*-positive cells also expressed P-ERK (see Fig.5I', and not shown) and, here again, we used this marker in comparison with MCM5 to determine the proliferation status of single cells processing the Fgf signal. We found globally complementary distributions of P-ERK- versus MCM5-positive cells along the

ventricular surface of the val (Fig.7D,E) and the tegmental ventricle (Fig.7F), with a minor proportion of double-positive cells, while the ventricular edge of the TeO and TS expressed P-ERK only (Fig.7D,E).

In summary, a common feature is that all three receptors are expressed in various combinations in ventricular cells, and that these cells are also positive for P-ERK. Although ventricular cells encompass progenitor populations (Adolf et al., 2006; Chapouton et al., 2006), most ventricular P-ERK-positive cells appeared negative for the proliferation marker MCM5.

Discussion

Expression profiles spatially differ between embryonic stages and adulthood

A first observation that can be drawn from our results is the striking difference, observed virtually for all genes of the Fgf pathway tested here, between their embryonic and adult expression profile, both in their spatial organization and in the nature of positive cells. To cite a few examples, *fgf8* expression highlights neural progenitors in multiple organizing centers of the embryonic neural tube (anterior neural ridge, dorsal diencephalon, MHB) (Reifers et al., 1998) and becomes restricted to a narrow string of cells separating OB and subpallium and the granular zone of the cerebellum in the adult brain, although embryonic *fgf8*-positive domains give rise to other adult territories where neural progenitors are maintained (e.g. (Chapouton et al., 2006)). Another extreme is *fgf4* expression, restricted to neural progenitors at the MHB in embryos (Thisse and Thisse, 2005b) and becoming quasi-ubiquitous in the adult brain, both in space and cell type. This temporal evolution leads to the complete splitting of the *fgf8* synexpression group (reviewed in (Thisse and Thisse, 2005a)) (schematized in Fig.8). The mechanisms underlying these changes are unclear, but they may be mediated by a switch in the regulatory elements used in the adult brain compared to the embryonic neural tube, as we already observed for several genes. These include *neurog1* (Adolf et al., 2006) and enhancer trap lines reporting expression of *spry1* and *2*, which faithfully highlight the expression domains of these genes in the embryonic but not the adult CNS (A.Z.K., in prep, S.T. unpublished observations). Whatever the case, these changes also clearly mean that “classical” read-outs of Fgf signaling activity used during embryogenesis, such as *pea3*, *erm* and *sprouty* genes, have to be considered with caution during adulthood, and for instance should be carefully compared with the expression of FgfRs. Doing so, *dusp6* and P-ERK seem reliable tracers of Fgf activity in the adult zebrafish brain, at least in the telencephalic and hypothalamic ventricular zones.

Species-specific variations in the expression of FgfRs in the adult brain

Understanding the distribution and cell type-specific expression of FgfRs can give important insight into the action of Fgf signaling on adult brain physiology. Expression of FgfRs has been reported with some precision in the adult mouse and rat brain. While *FgfR4* expression appears essentially restricted to the lateral habenular nucleus (Fuhrmann et al., 1999; Itoh et al., 1994), *FgfR1-3* expression is widely distributed and found in the forebrain (lateral ventricle, hippocampus, amygdala, basal ganglia, septum, hypothalamus), the midbrain (tegmental nuclei and tectum) and virtually all nuclei of the pons and medulla (Asai et al., 1993; Belluardo et al., 1997; Weickert et al., 2005; Yazaki et al., 1994). In detail however, cells expressing *FgfR1-3* differ, with FgfR2 primarily expressed by astrocytes (Asai et al., 1993; Chadashvili and Peterson, 2006) while *FgfR3* might stain other glial cells

(Miyake et al., 1996; Yazaki et al., 1994) and *Fgfr1* large weakly stained cells excluded from the white matter, perhaps mostly neurons in the rat adult brain (Belluardo et al., 1997). This spatial and cell type-specific distribution strikingly differs from what we observed for the orthologous zebrafish genes. Zebrafish *fgfr4* is expressed broadly while *fgfr1* and *3* exhibit highly restricted expression domains. Although *fgfr2*, like mammalian *Fgfr2*, was also expressed in most brain subdivisions, we could clearly document its expression in neurons, at least in the cerebellum and brainstem. Finally, *fgfr1-3* display a large degree of co-expression. It remains to be seen whether the species-specific use of one receptor or the other leads to meaningful changes in signal transduction. The maintenance of different expression profiles of the four receptors within one species speaks for a differential trophic role of these different receptors; although very similar in sequence, they have been proposed to differ in the strength of signaling that they transduce (reviewed in (Reuss and von Bohlen und Halbach, 2003)). An additional level of complexity includes the existence of different isoforms for each receptor, between which our probes do not allow us to distinguish.

Fgf signaling and adult neural progenitors

A most interesting feature of *fgfr1-3* is their common expression in ventricular cells. Although documented here only for the telencephalic, the hypothalamic and the midbrain ventricular zones, this observation was general throughout the brain. Strong P-ERK and *dusp6* staining is found in the same domains (at cellular resolution for P-ERK in this study), in strong support of a prominent transduction of Fgf signals in ventricular cells. The glial nature of ventricular cells and the neurogenic potential of ventricular zones in the zebrafish adult brain ((Adolf et al., 2006; Grandel et al., 2006; Pellegrini et al., 2007) and S. Simonovic, unpublished), suggest a parallel between our observations and the reported expression of *Fgfr1* and *2* in progenitor cells of the subgranular zone of the dentate gyrus of the hippocampus, the subependymal zone of the lateral ventricle, and the rostral migratory stream in adult mouse and rat (Belluardo et al., 1997; Chadashvili and Peterson, 2006; Gonzalez et al., 1995; Matsuo et al., 1994; Ohkubo et al., 2004; Zheng et al., 2004). Studies conducted in rodents strongly focused on Fgf signaling and the proliferation and neurogenic potential of these progenitor zones (Gage et al., 1995; Palmer et al., 1995; Vescovi et al., 1993; Yoshimura et al., 2001; Zhao et al., 2007; Zheng et al., 2004). However, in the ventricular zone of the zebrafish subpallium and midline of the pallium, comparable to the above-listed progenitor zones in rodents (Adolf et al., 2006), our analysis at the single cell level clearly shows that P-ERK and *fgfr* expression are not directly associated with the proliferating status. Indeed, all ventricular cells express P-ERK or *fgfr1-3*, while the ventricular cell population comprises a mixture of slow- and fast-dividing progenitors (positive for proliferation markers such as PCNA or MCM5) and quiescent or differentiated cells (negative for these markers). Rather, P-ERK and *fgfr1-3* expression correlates with the radial glia nature of ventricular cells (positive for BLBP) (Adolf et al., 2006), and this finding can be generalized to the other ventricular zones studied here. These observations of course do not preclude a role of Fgf signaling on neural progenitor proliferation but suggest that the situation is more complex, perhaps in rodents as well, and that the zebrafish adult brain will be an interesting model to approach this issue. Along these lines, it is also interesting to note the tendency for post-mitotic neurons (Hu-positive) expressing *fgfr1*, *2* or *3* to be negative for P-ERK, both around progenitor zones (where *fgfr1* expression is always slightly broader than *fgfr2-3* and encompasses Hu-positive neurons) and in the brainstem. This observation might suggest alternative Fgf signal transduction pathways for neuronal cells than for progenitors and/or glia. A further important question will be to determine which Fgf signal is relevant in the different brain areas or cell types. We observed a striking alternation of broad (e.g.

fgf4, *fgf17b*) and very restricted (e.g. *fgf3*, *fgf8*) transcripts distributions, which here again may suggest different functions. Among the Fgf signals tested in this study, it is interesting to note that *fgf3* expression is almost exclusively restricted to progenitor zones and might therefore be an important player in adult neurogenesis; it would be interesting to contrast these findings with *Fgf3* expression in adult rodents.

Together, our results constitute the first step towards an analysis of Fgf signaling in the adult brain using the zebrafish model. The widespread distribution of Fgf pathway members reinforces the notion that Fgf signaling plays crucial roles in adult brain physiology, also via Fgf signals other than Fgf2. The coexpression of *fgfr1-3*, P-ERK and *dusp6* in ventricular zones further points to a prominent activation during all or most adult neurogenesis events.

Acknowledgements

We are grateful to all lab members for support and in particular to Dr. Prisca Chapouton for her insightful suggestions and help with interpretation of the data. We thank P. Chapouton, C. Lillesaar and W. Norton for their comments on the manuscript, and P. Raymond for providing *Tg(gfap:GFP)* fish. Thanks also to M. Götz for her long-standing support and collaboration on zebrafish adult neural stem cells projects, to R. Köster for maintaining the imaging set-up, and to the zebrafish facility crew.

References

- Adolf B, Chapouton P, Lam CS, Topp S, Tannhauser B, Strähle U, Götz M, Bally-Cuif L. 2006. Conserved and acquired features of adult neurogenesis in the zebrafish telencephalon. *Dev Biol* 295(1):278-293.
- Alvarez-Buylla A, Garcia-Verdugo M. 2002. Neurogenesis in adult subventricular zone. *J Neurosci* 22:629-634.
- Arman E, Haffner-Krausz R, Chen Y, Heath JK, Lonai P. 1998. Targeted disruption of fibroblast growth factor (FGF) receptor 2 suggests a role for FGF signaling in pregastrulation mammalian development. *Proc Natl Acad Sci U S A* 95(9):5082-5087.
- Asai T, Wanaka A, Kato H, Masana Y, Seo M, Tohyama M. 1993. Differential expression of two members of FGF receptor gene family, FGFR-1 and FGFR-2 mRNA, in the adult rat central nervous system. *Brain Res Mol Brain Res* 17(1-2):174-178.
- Belluardo N, Wu G, Mudo G, Hansson AC, Pettersson R, Fuxe K. 1997. Comparative localization of fibroblast growth factor receptor-1, -2, and -3 mRNAs in the rat brain: in situ hybridization analysis. *J Comp Neurol* 379(2):226-246.
- Bernardos RL, Raymond PA. 2006. GFAP transgenic zebrafish. *Gene Expr Patterns* 6(8):1007-1013.
- Betarbet R, Zigova T, Bakay RA, Luskin MB. 1996. Dopaminergic and GABAergic interneurons of the olfactory bulb are derived from the neonatal subventricular zone. *Int J Dev Neurosci* 14(7-8):921-930.
- Cao Y, Zhao J, Sun Z, Zhao Z, Postlethwait J, Meng A. 2004. *fgf17b*, a novel member of Fgf family, helps patterning zebrafish embryos. *Dev Biol* 271(1):130-143.
- Chadashvili T, Peterson DA. 2006. Cytoarchitecture of fibroblast growth factor receptor 2 (FGFR-2) immunoreactivity in astrocytes of neurogenic and non-neurogenic regions of the young adult and aged rat brain. *J Comp Neurol* 498(1):1-15.
- Chapouton P, Adolf B, Leucht C, Ryu S, Driever W, Bally-Cuif L. 2006. *her5* expression reveals a pool of neural stem cells in the adult zebrafish midbrain. *Development* 133:4293-4303.
- Chapouton P, Jagasia R, Bally-Cuif L. 2007. Adult neurogenesis in non-mammalian vertebrates. *Bioessays* 29(8):745-757.

- Deng C, Wynshaw-Boris A, Zhou F, Kuo A, Leder P. 1996. Fibroblast growth factor receptor 3 is a negative regulator of bone growth. *Cell* 84(6):911-921.
- Deng CX, Wynshaw-Boris A, Shen MM, Daugherty C, Ornitz DM, Leder P. 1994. Murine FGFR-1 is required for early postimplantation growth and axial organization. *Genes Dev* 8(24):3045-3057.
- Dono R. 2003. Fibroblast growth factors as regulators of central nervous system development and function. *Am J Physiol Regulatory Integrative comp Physiol* 284:867-881.
- Ernfors P, Lonnerberg P, Ayer-LeLievre C, Persson H. 1990. Developmental and regional expression of basic fibroblast growth factor mRNA in the rat central nervous system. *J Neurosci Res* 27(1):10-15.
- Eswarakumar VP, Lax I, Schlessinger J. 2005. Cellular signaling by fibroblast growth factor receptors. *Cytokine Growth Factor Rev* 16(2):139-149.
- Feng L, Hatten ME, Heintz N. 1994. Brain lipid-binding protein (BLBP): a novel signaling system in the developing mammalian CNS. *Neuron* 12(4):895-908.
- Fuhrmann V, Kinkl N, Leveillard T, Sahel J, Hicks D. 1999. Fibroblast growth factor receptor 4 (FGFR4) is expressed in adult rat and human retinal photoreceptors and neurons. *J Mol Neurosci* 13(1-2):187-197.
- Furthauer M, Lin W, Ang SL, Thisse B, Thisse C. 2002. Sef is a feedback-induced antagonist of Ras/MAPK-mediated FGF signalling. *Nat Cell Biol* 4(2):170-174.
- Furthauer M, Reifers F, Brand M, Thisse B, Thisse C. 2001. sprouty4 acts in vivo as a feedback-induced antagonist of FGF signaling in zebrafish. *Development* 128(12):2175-2186.
- Gage FH, Coates P, Palmer T, Kuhn H, Fisher L, Suhonen J, Peterson D, Sufr S, Ray J. 1995. Survival and differentiation of adult neuronal progenitor cells transplanted to the adult brain. *Proc Natl Acad Sci USA* 92:11879-11883.
- Gaughran F, Payne J, Sedgwick PM, Cotter D, Berry M. 2006. Hippocampal FGF-2 and FGFR1 mRNA expression in major depression, schizophrenia and bipolar disorder. *Brain Res Bull* 70(3):221-227.
- Gomez-Pinilla F, Lee JW, Cotman CW. 1992. Basic FGF in adult rat brain: cellular distribution and response to entorhinal lesion and fimbria-fornix transection. *J Neurosci* 12(1):345-355.
- Gonzalez AM, Berry M, Maher PA, Logan A, Baird A. 1995. A comprehensive analysis of the distribution of FGF-2 and FGFR1 in the rat brain. *Brain Res* 701(1-2):201-226.
- Grandel H, Kaslin J, Ganz J, Wenzel I, Brand M. 2006. Neural stem cells and neurogenesis in the adult zebrafish brain: origin, proliferation dynamics, migration and cell fate. *Dev Biol* 295(1):263-277.
- Itoh N, Ornitz DM. 2004. Evolution of the Fgf and Fgfr gene families. *Trends Genet* 20(11):563-569.
- Itoh N, Yazaki N, Tagashira S, Miyake A, Ozaki K, Minami M, Satoh M, Ohta M, Kawasaki T. 1994. Rat FGF receptor-4 mRNA in the brain is expressed preferentially in the medial habenular nucleus. *Brain Res Mol Brain Res* 21(3-4):344-348.
- Jin K, Sun Y, Xie L, Batteur S, Mao X, Smelick C, Logvinova A, Greenberg D. 2003. Neurogenesis and aging: FGF-2 and HB-EGF restore neurogenesis in hippocampus and subventricular zone of aged mice. *Aging Cell* 2:175-183.
- Kawakami Y, Rodriguez-Leon J, Koth CM, Buscher D, Itoh T, Raya A, Ng JK, Esteban CR, Takahashi S, Henrique D, Schwarz MF, Asahara H, Izpisua Belmonte JC. 2003. MKP3 mediates the cellular response to FGF8 signalling in the vertebrate limb. *Nat Cell Biol* 5(6):513-519.
- Kiefer P, Strahle U, Dickson C. 1996. The zebrafish Fgf-3 gene: cDNA sequence, transcript structure and genomic organization. *Gene* 168(2):211-215.
- Kikuta H, Laplante M, Navratilova P, Komisarczuk AZ, Engstrom PG, Fredman D, Akalin A, Caccamo M, Sealy I, Howe K, Ghislain J, Pezeron G, Mourrain P, Ellingsen S, Oates AC, Thisse C, Thisse B, Foucher I, Adolf B, Geling A, Lenhard B, Becker TS. 2007. Genomic regulatory blocks encompass multiple neighboring genes and maintain conserved synteny in vertebrates. *Genome Res* 17(5):545-555.
- Komisarsczuk A. in prep.
- Kosaka N, Kodama M, Sasaki H, Yamamoto Y, Takeshita F, Takaham Y, Sakamoto H, Kato T, Terada M, Ochiya T. 2006. FGF-4 regulates neural progenitor cell proliferation and neuronal differentiation. *FASEB J* 20:1484-1485.

- Kuhn H, Winkler J, Kempermann G, Thal L, Gage FH. 1997. Epidermal growth factor and fibroblast growth factor-2 have different effects on neural progenitors in the adult brain. *J Neurosci* 17:5820-5829.
- Lillesaar C, Tannhauser B, Stigloher C, Kremmer E, Bally-Cuif L. 2007. The serotonergic phenotype is acquired by converging genetic mechanisms within the zebrafish central nervous system. *Dev Dyn* 236(4):1072-1084.
- Marusich M, Furneaux H, Henion P, Weston J. 1994. Hu neuronal proteins are expressed in proliferating neurogenic cells. *J Neurobiol* 25:143-155.
- Matsuo A, Tooyama I, Isobe S, Oomura Y, Akiguchi I, Hanai K, Kimura J, Kimura H. 1994. Immunohistochemical localization in the rat brain of an epitope corresponding to the fibroblast growth factor receptor-1. *Neuroscience* 60(1):49-66.
- Miyake A, Hattori Y, Ohta M, Itoh N. 1996. Rat oligodendrocytes and astrocytes preferentially express fibroblast growth factor receptor-2 and -3 mRNAs. *J Neurosci Res* 45(5):534-541.
- Mueller T, Wullmann MF. 2002. BrdU-, neuroD (nrd)- and Hu-studies reveal unusual non-ventricular neurogenesis in the postembryonic zebrafish forebrain. *Mech Dev* 117(1-2):123-135.
- Norton WH, Ledin J, Grandel H, Neumann CJ. 2005. HSPG synthesis by zebrafish Ext2 and Ext3 is required for Fgf10 signalling during limb development. *Development* 132(22):4963-4973.
- Ohkubo Y, Uchida AO, Shin D, Partanen J, Vaccarino FM. 2004. Fibroblast growth factor receptor 1 is required for the proliferation of hippocampal progenitor cells and for hippocampal growth in mouse. *J Neurosci* 24(27):6057-6069.
- Palmer T, Ray J, Gage FH. 1995. FGF-2-responsive neuronal progenitors reside in proliferative and quiescent regions of the adult rodent brain. *Mol Cell Neurosci* 6:474-486.
- Park HC, Kim CH, Bae YK, Yeo SY, Kim SH, Hong SK, Shin J, Yoo KW, Hibi M, Hirano T, Miki N, Chitnis AB, Huh TL. 2000. Analysis of upstream elements in the HuC promoter leads to the establishment of transgenic zebrafish with fluorescent neurons. *Dev Biol* 227(2):279-293.
- Pellegrini E, Mouriec K, Anglade I, Menuet A, Le Page Y, Gueguen MM, Marmignon MH, Brion F, Pakdel F, Kah O. 2007. Identification of aromatase-positive radial glial cells as progenitor cells in the ventricular layer of the forebrain in zebrafish. *J Comp Neurol* 501(1):150-167.
- Phillips BT, Bolding K, Riley BB. 2001. Zebrafish fgf3 and fgf8 encode redundant functions required for otic placode induction. *Dev Biol* 235(2):351-365.
- Pieper AA, Wu X, Han TW, Estill SJ, Dang Q, Wu LC, Reece-Fincannon S, Dudley CA, Richardson JA, Brat DJ, McKnight SL. 2005. The neuronal PAS domain protein 3 transcription factor controls FGF-mediated adult hippocampal neurogenesis in mice. *Proc Natl Acad Sci U S A* 102(39):14052-14057.
- Raible F, Brand M. 2001. Tight transcriptional control of the ETS domain factors Erm and Pea3 by Fgf signaling during early zebrafish development. *Mech Dev* 107(1-2):105-117.
- Reifers F, Adams J, Mason IJ, Schulte-Merker S, Brand M. 2000. Overlapping and distinct functions provided by fgf17, a new zebrafish member of the Fgf8/17/18 subgroup of Fgfs. *Mech Dev* 99(1-2):39-49.
- Reifers F, Bohli H, Walsh EC, Crossley PH, Stainier DY, Brand M. 1998. Fgf8 is mutated in zebrafish acerebellar (ace) mutants and is required for maintenance of midbrain-hindbrain boundary development and somitogenesis. *Development* 125(13):2381-2395.
- Reuss B, von Bohlen und Halbach O. 2003. Fibroblast growth factors and their receptors in the central nervous system. *Cell Tissue Res* 313:139-157.
- Roehl H, Nusslein-Volhard C. 2001. Zebrafish pea3 and erm are general targets of FGF8 signaling. *Curr Biol* 11(7):503-507.
- Ryu S, Holzschuh J, Erhardt S, Ettl AK, Driever W. 2005. Depletion of minichromosome maintenance protein 5 in the zebrafish retina causes cell-cycle defect and apoptosis. *Proc Natl Acad Sci U S A* 102(51):18467-18472.
- Scholpp S, Groth C, Lohs C, Lardelli M, Brand M. 2004. Zebrafish fgfr1 is a member of the fgf8 synexpression group and is required for fgf8 signalling at the midbrain-hindbrain boundary. *Dev Genes Evol* 214(6):285-295.

- Shinya M, Koshida S, Sawada A, Kuroiwa A, Takeda H. 2001. Fgf signalling through MAPK cascade is required for development of the subpallial telencephalon in zebrafish embryos. *Development* 128(21):4153-4164.
- Sleptsova-Friedrich I, Li Y, Emelyanov A, Ekker M, Korzh V, Ge R. 2002. fgfr3 and regionalization of anterior neural tube in zebrafish. *Mech Dev* 102:213-217.
- Tao Y, Black I, DiCicco-Bloom E. 1997. In vivo neurogenesis is inhibited by neutralizing antibodies to basic fibroblast growth factor. *J Neurobiol*(33):289-296.
- Thisse B, Thisse C. 2005a. Functions and regulations of fibroblast growth factor signaling during embryonic development. *Dev Biol* 287:390-402.
- Thisse B, Thisse C. 2005b. High throughput expression analysis of ZF-Models consortium clones. ZFIN direct data submission.
- Tonou-Fujimori N, Takahashi M, Onodera H, Kikuta H, Koshida S, Takeda H, Yamasu K. 2002. Expression of the FGF receptor 2 gene (fgfr2) during embryogenesis in the zebrafish *Danio rerio*. *Mech Dev* 119 Suppl 1:S173-178.
- Vescovi A, Reynolds B, Fraser D, Weiss S. 1993. bFGF regulates the proliferative fate of unipotent (neuronal) and bipotent (neuronal/astroglial) EGF-generated CNS progenitor cells. *Neuron* 11:951-966.
- Wagner JP, Black IB, DiCicco-Bloom E. 1999. Stimulation of neonatal and adult brain neurogenesis by subcutaneous injection of basic fibroblast growth factor. *J Neurosci* 19(14):6006-6016.
- Weickert CS, Kittell DA, Saunders RC, Herman MM, Horlick RA, Kleinman JE, Hyde TM. 2005. Basic fibroblast growth factor and fibroblast growth factor receptor-1 in the human hippocampal formation. *Neuroscience* 131(1):219-233.
- Weinstein M, Xu X, Ohyama K, Deng CX. 1998. FGFR-3 and FGFR-4 function cooperatively to direct alveogenesis in the murine lung. *Development* 125(18):3615-3623.
- Wullmann M, Rupp B, Reichert H. 1996. Neuroanatomy of the zebrafish brain: a topological atlas. Birkhäuser Verlag, Basel, Wullmann MF, Ed:1-144.
- Yamaguchi TP, Harpal K, Henkemeyer M, Rossant J. 1994. fgfr-1 is required for embryonic growth and mesodermal patterning during mouse gastrulation. *Genes Dev* 8(24):3032-3044.
- Yazaki N, Hosoi Y, Kawabata K, Miyake A, Minami M, Satoh M, Ohta M, Kawasaki T, Itoh N. 1994. Differential expression patterns of mRNAs for members of the fibroblast growth factor receptor family, FGFR-1-FGFR-4, in rat brain. *J Neurosci Res* 37(4):445-452.
- Yoshimura S, Takagi Y, Harada J, Teramoto T, Thomas S, Waeber C, Bakowska J, Breakefield X, Moskowitz M. 2001. FGF-2 regulation of neurogenesis in adult hippocampus after brain injury. *Proc natl Acad Sci USA* 98:5874-5879.
- Zhao M, Li D, Shimazu K, Zhou Y-X, Lu B, Deng C-X. 2007. Fibroblast growth factor receptor-1 is required for long-term potentiation, memory consolidation, and neurogenesis. *Biol Psychiatry* 62:381-390.
- Zheng W, Nowakowski R, Vaccarino F. 2004. Fibroblast growth factor 2 is required for maintaining the neural stem cell pool in the mouse brain subventricular zone. *Dev Neurosci* 26:181-196.
- Zupanc GK, Hinsch K, Gage FH. 2005. Proliferation, migration, neuronal differentiation, and long-term survival of new cells in the adult zebrafish brain. *J Comp Neurol* 488(3):290-319.

Figure legends

Figure 1. Expression of Fgf pathway members in the zebrafish adult telencephalon and olfactory bulb. The genes tested are indicated on the left of each panel series, and the plane of section is indicated on the schematic dorsal views of the brain. All expression are revealed by in situ hybridization (blue staining) except for P-ERK (immunocytochemistry). Note expression of *fgf3*, *8a* and *8b* at the telencephalon /OB junction (arrows in A-C), and the expression of *fgfr1-3* along the telencephalic ventricle (the section in L is almost perfectly midsagittal). In J-O', arrows to gene expression along the ventricle of the subpallium and midline of the pallium, arrowheads to expression along the ventricle of the lateral and posterior pallium. Expression of *fgfr1* in post-mitotic neurons is indicated by asterisks (see also Fig.2E,F). Expression of *fgfrs* and *fgf* signals is summarized in the cross-section in P (color coded, one brain hemisphere, midline to the right). **Abbreviations:** D: dorsal telencephalon, Dp: posterior zone of D, Vd: dorsal zone of the ventral diencephalon, Vv: ventral zone of the ventral diencephalon. Scale bars for A-E' and J-O': 100 μ m.

Figure 2. Expression of *fgfr1-3* and P-ERK in relation with proliferation domains, radial glia and post-mitotic neurons in the telencephalon. All section planes and insets are indicated on the schemes (top left) or in the low magnification panels (C,O,P), and gene/protein expression are color-coded. All pictures are viewed under confocal microscopy, panels K, L, O1-3 and P1-3 are 2 microm sections, all other panels are 50 microm projections. **A-D:** comparison of *fgfr1-3*-positive domains (in situ hybridization) with BrdU incorporating cells (short pulse) (immunocytochemistry). *fgfr1-3* are highly expressed along the ventricular zone but only some cells are BrdU-positive (arrows color-coded, yellow for double-positive cells). **E-H:** comparison of *fgfr1-3* expression (in situ hybridization) with Hu-positive post-mitotic neurons (immunocytochemistry). *fgfr2* and *3* expression at the ventricle do not encompass the Hu-positive domain (G,H), while *fgfr1* expression does (E,F, yellow arrows). **I,J:** compared expression of *fgfr1-2* (in situ hybridization) and P-ERK (immunocytochemistry) along the subpallial midline. Note the coexpression at the ventricle (yellow arrows), while only *fgfr1* extends to the subventricular zone (I, red arrow). **K,L:** compared expression of P-ERK and the radial glia marker GFAP-GFP (double immunocytochemistry, K and L are from two different brains from transgenic *gfap:GFP* fish) in the ventricular zone of the dorsal nucleus of the ventral telencephalon (Vd). Note the overlap in expression (yellow arrows), while cells singly positive for P-ERK are found away from the midline (red arrows). **M-P:** compared expression of P-ERK and the proliferation marker MCM5 (double immunocytochemistry) in ventricular zones of the dorsal pallium (M), lateral pallium (N), midline of the pallium (O) and subpallium (P). Note the quasi-complementary expression of these factors, with a minor proportion of double-positive cells (yellow arrows). Scale bars: A-D: 100 μ m, E-P: 8 μ m.

Figure 3. Expression of Fgf pathway members in the zebrafish adult hypothalamus. The genes tested are indicated on the left of each panel, and the plane of section is indicated on the schematic dorsal view of the brain (top left) or in specific panels (J,L,N). All expression are revealed by in situ hybridization (blue staining). Note expression of most signals, receptors and targets in the hypothalamic periventricular area (arrows), except for *spry* genes, weak overall. Expression of *fgfrs* and *fgf* signals is summarized in the cross-section in P (color coded, one brain hemisphere, midline to the right). **Abbreviations:** DIL: diffuse nucleus of the inferior lobe, DiV: diencephalic ventricle, Hc: central zone of periventricular hypothalamus, LR: lateral recess of the hypothalamic ventricle, TLA: torus lateralis. Scale bars for A-I and J-O: 100 μ m.

Figure 4. Expression of *fgfr1-3* and P-ERK in relation with proliferation domains and post-mitotic neurons in the hypothalamus. All section planes and insets are indicated on the schemes (top left) or in the low magnification panels (B,I,J), and gene/protein expression are color-coded. All pictures are viewed under confocal microscopy, panels I1-3 and J1-3 are 2 microm sections, all other panels are 50 microm projections. **A-C:** comparison of *fgfr1-3*-positive domains (in situ hybridization) with BrdU incorporating cells (short pulse) (immunocytochemistry). *fgfr1-3* are expressed in the BrdU incorporation zone (periventricular area) but only some cells are double labeled. **D-F:** comparison of *fgfr1-3* expression (in situ hybridization) with Hu-positive post-mitotic neurons (immunocytochemistry). *fgfr1* expression, but not that of *fgfr2-3*, extends to subventricular Hu-positive cells. **G-H:** compared expression of *fgfr1-2* (in situ hybridization) and P-ERK (immunocytochemistry). Ventricular *fgfr*-expressing cells (yellow arrows), but not subventricular *fgfr1*-expressing cells (G, red arrow), are P-ERK-positive. **I,J:** compared expression of P-ERK and the proliferation marker MCM5 (double immunocytochemistry) in the hypothalamic periventricular zone. Only a minor proportion of P-ERK-expressing cells are also MCM5-positive (yellow arrows). Scale bars: A-C: 100 μm , D-H: 10 μm , I,J: 20 μm .

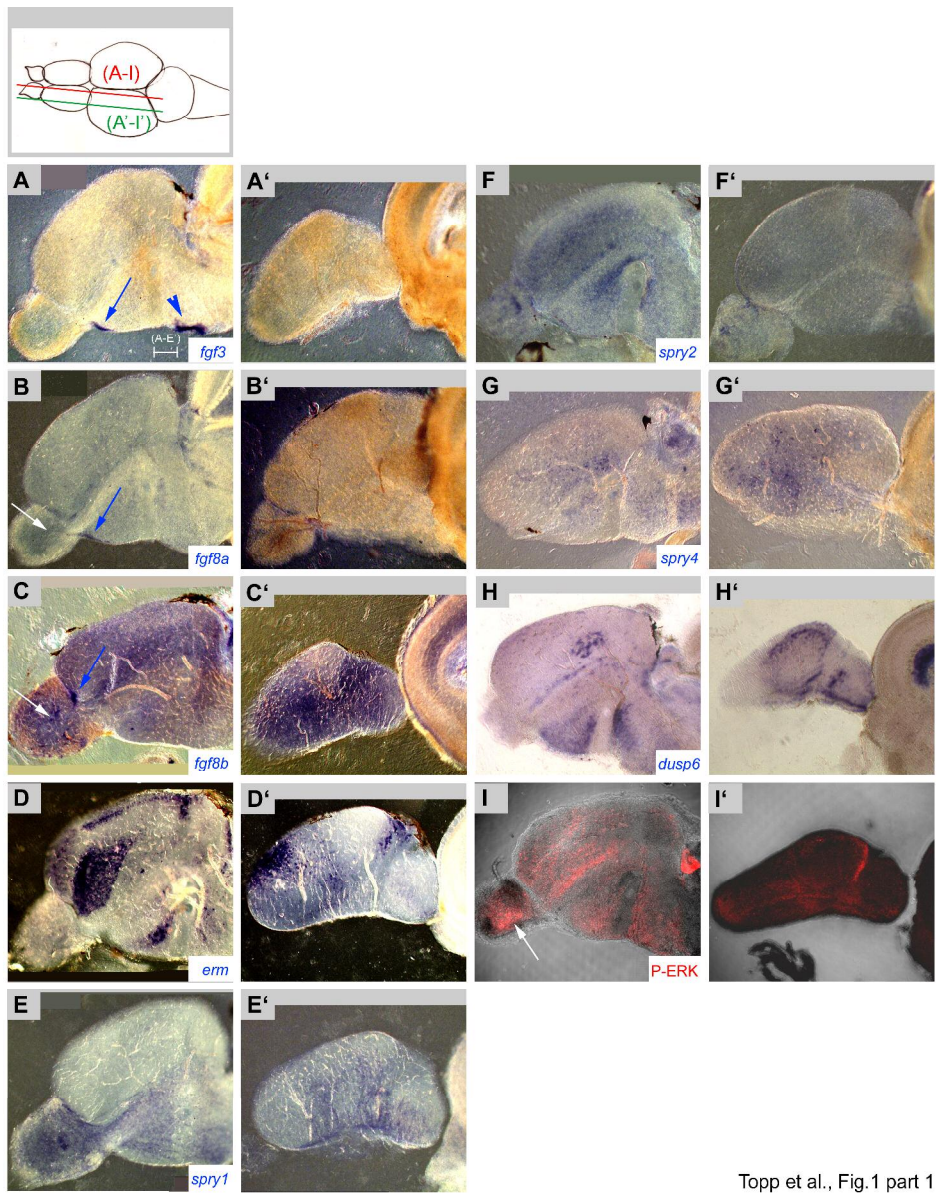
Figure 5. Expression of Fgf pathway members in the zebrafish adult midbrain-hindbrain. The genes tested are indicated on the left of each panel series, and the plane of section (midsagittal, parasagittal or frontal) is indicated on the schematic dorsal views. All expression are revealed by in situ hybridization (blue staining) except for P-ERK (I,I') (immunocytochemistry). In E-O, arrows point to ventricular expression, arrowheads to expression in the periventricular gray zone. In J',K, asterisk to *fgfr1* expression is the isthmus nucleus. Abbreviations: Ce: corpus cerebellaris; Tg: tegmentum; TL: torus longitudinalis; TSc: torus semicircularis; val: valvula cerebelli. Scale bars for A-I' and J-O: 100 μm .

Figure 6. Summarized expression domains of *fgf3,8a,8b* and *fgfr1-3* on (A) a schematic 3D view of the midbrain-hindbrain area (one hemisphere drawn seen from the midline) and (B) a schematic cross-section (level indicated in A). Expression domains are color-coded. **Abbreviations:** Gr: granular layer of the cerebellum; Mol: molecular layer of the cerebellum; NLV: nucleus lateralis valvulae; PGZ: periventricular gray zone; P/E: Purkinje/Eudendroyd cell layer of the cerebellum; Tg: tegmentum; TeO: tectum opticum; TL: torus longitudinalis; Tsc: torus semicircularis; Val: valvula cerebelli lateralis; Vam: valvula cerebelli, medial part.

Figure 7. Expression of *fgfr1-3* and P-ERK in relation with proliferation domains and post-mitotic neurons in the midbrain-hindbrain domain. All section planes and insets are indicated on the schemes (top left) or in the low magnification panels (B,D-F), and gene/protein expression are color-coded. All pictures are viewed under confocal microscopy, panels E1, E2 and F1 are 2 microm sections, all other panels are 50 microm projections. **A-C:** comparison of *fgfr1-3*-positive domains (in situ hybridization) with BrdU incorporating cells (short pulse) (immunocytochemistry). Note the quasi-absence of double labeled cells in the valvula cerebelli, a major proliferation domain (arrows in B1). **D-F:** compared expression of P-ERK and the proliferation marker MCM5 (double immunocytochemistry). While P-ERK expression can be found along the ventricular zone bordering the optic tectum, the torus semicircularis, the valvula and the tegmentum, MCM5-positive cells are restricted to the ventricular zone of the valvula and tegmentum. In these locations, a minor proportion of MCM5-positive cells also express P-ERK (see E1-2, F1). **G-K:** compared expression of *fgfr1-3* (in situ hybridization) and the neuronal marker Hu (immunocytochemistry). Note that *fgfr1-3* is generally expressed in neurons in non-

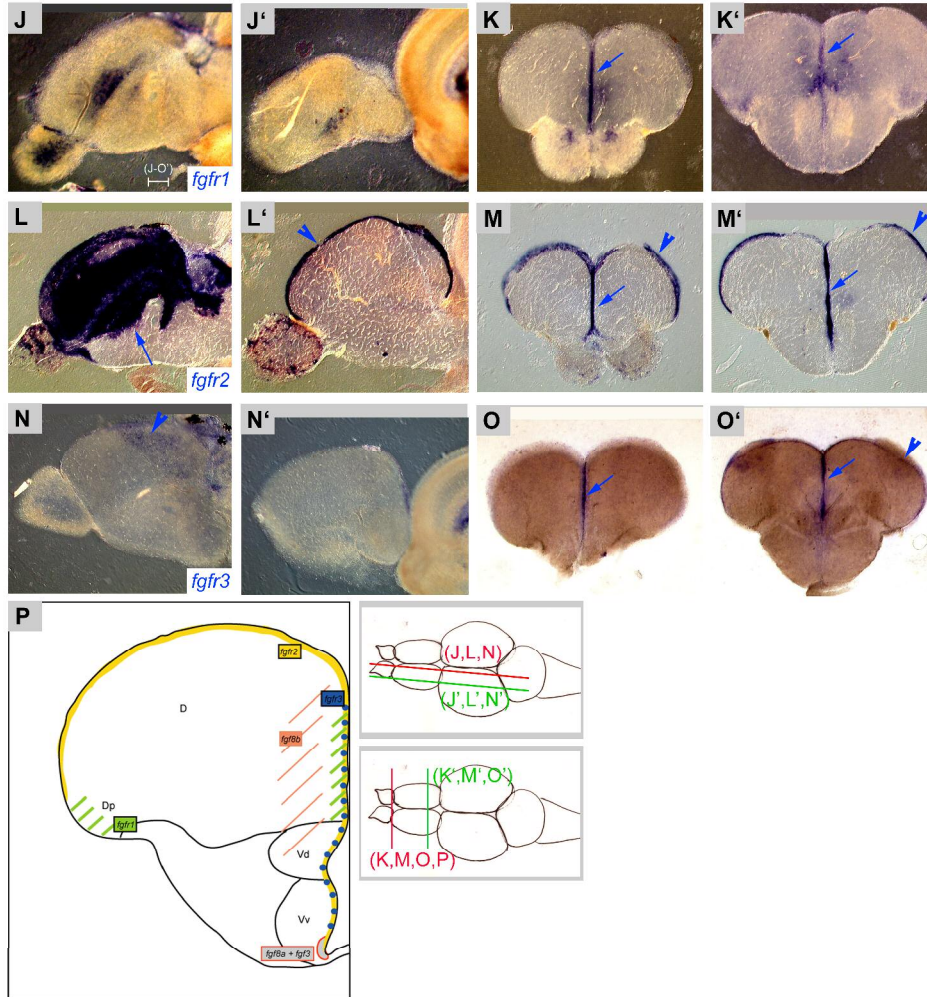
ventricular areas (G: isthmic nucleus; H: myelencephalon; I: tegmentum; J-K: Purkinje/eudendrocyte cell layer of the cerebellum). Abbreviations: Ce: corpus cerebellaris; Tg: tegmentum; TeO: tectum opticum; TSc: torus semicircularis; val: valvula cerebelli. Scale bars: A-D: 100 μm , F: 20 μm , G-K: 10 μm .

Figure 8. Schematic representation of the expression domains of *fgf8* synexpression group genes in the embryonic and adult brain (lateral views of approximately midsagittal sections, anterior left; the embryonic brain is that of a 20-25 somite-old embryo). Expression domains are color-coded and the genes involved are indicated on the schemes or in the legend box; only the genes relevant to this study are documented. Note that, while these genes share expression domains during embryogenesis, these widely diverge in the adult brain. Abbreviations: Ce: corpus cerebellaris; ddi: dorsal diencephalon; hyp: hypothalamus; MHB: midbrain-hindbrain boundary; OB: olfactory bulb; os: optic stalk; rh4: rhombomere 4; tel: telencephalon; Tg: tegmentum; TeO: tectum opticum; val: valvula cerebelli.



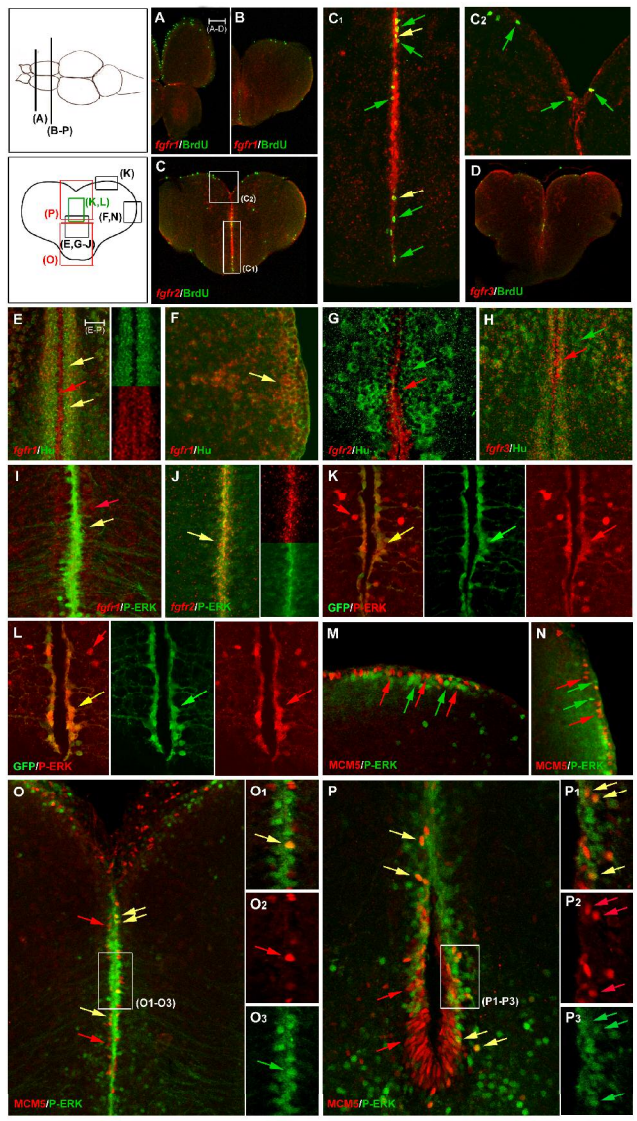
Topp et al., Fig.1 part 1

1058x1320mm (72 x 72 DPI)



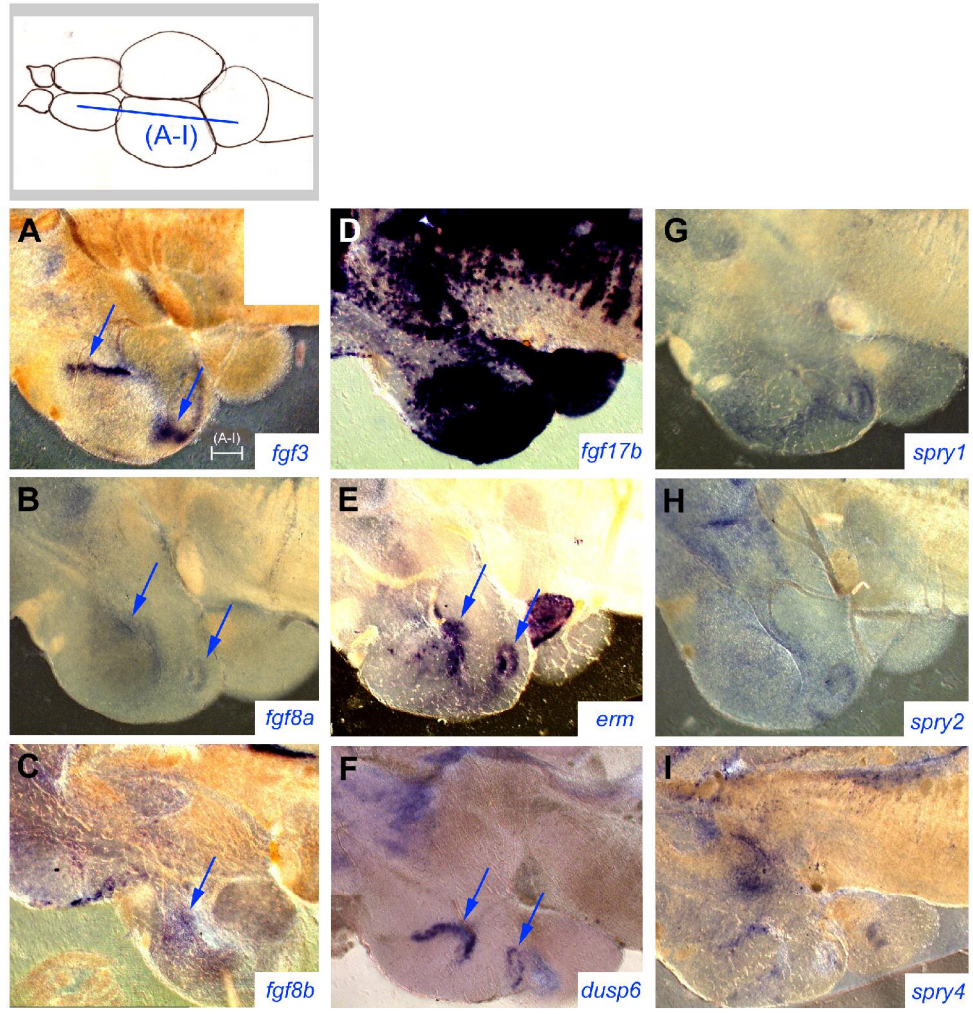
Topp et al., Fig.1 part 2

1094x1197mm (72 x 72 DPI)



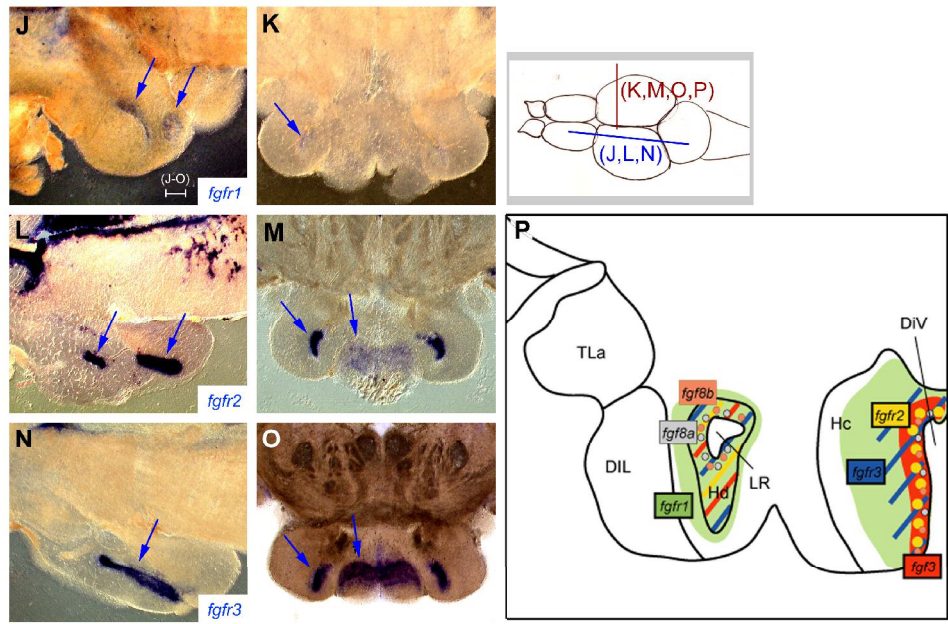
Topp et al., Fig-2

482x705mm (150 x 150 DPI)



Topp et al., Fig.3 part 1

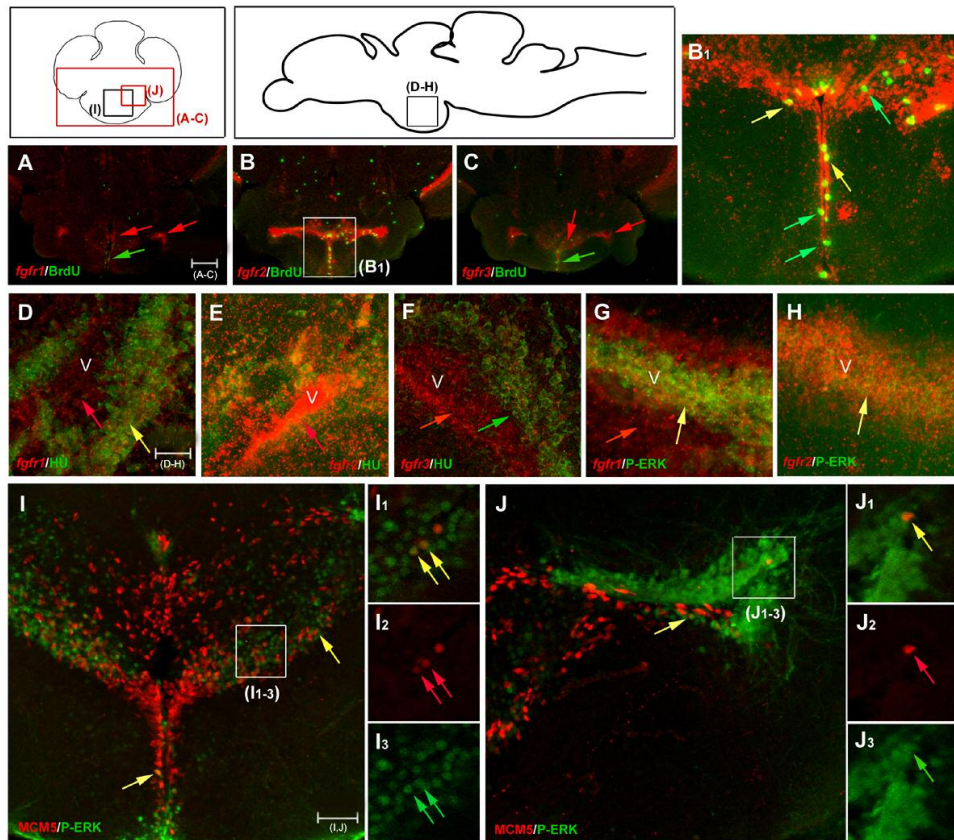
768x853mm (72 x 72 DPI)



Topp et al., Fig.3 part 2

997x739mm (72 x 72 DPI)

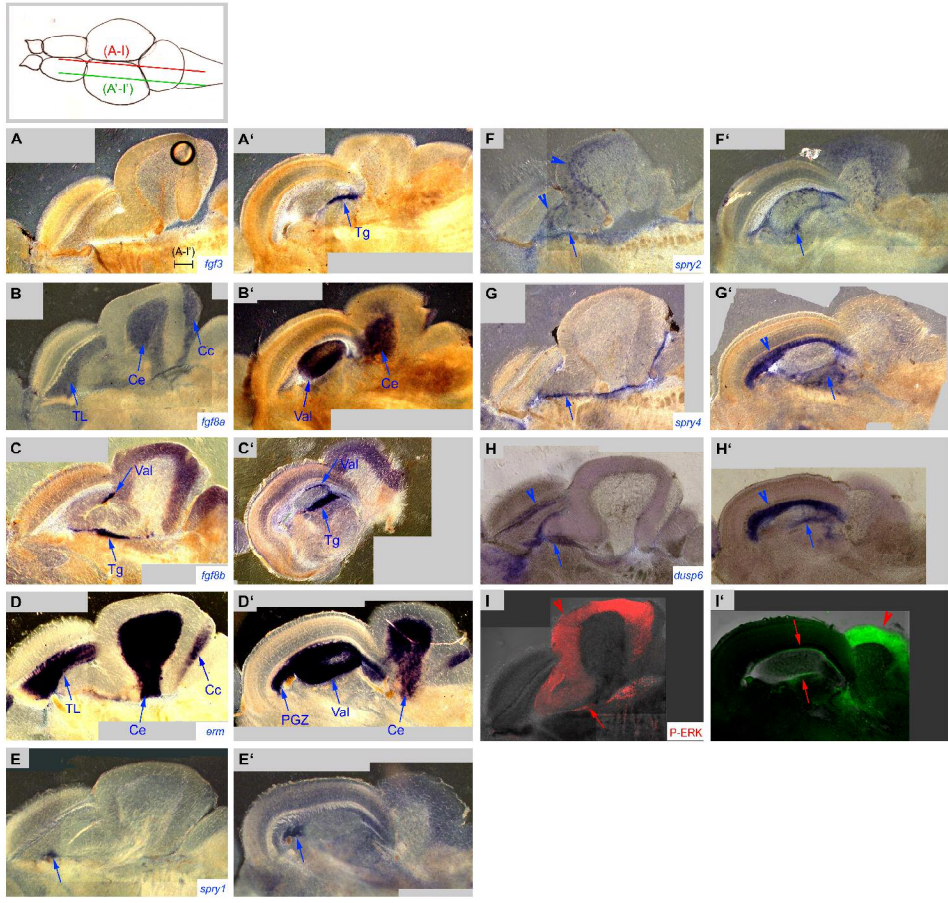
review



Topp et al., Fig.4

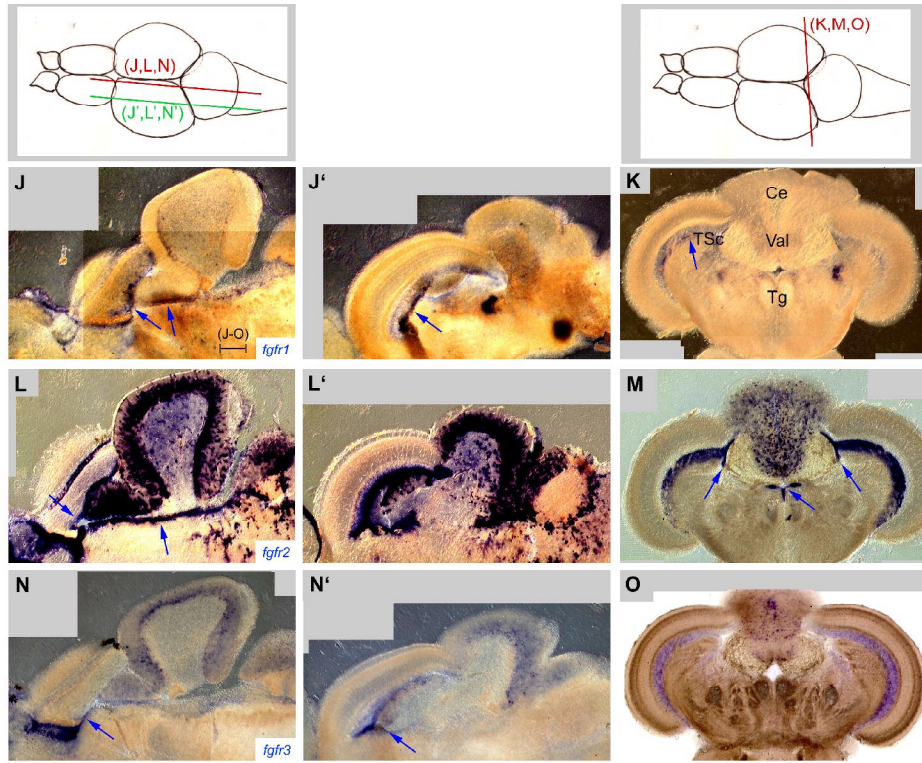
209x189mm (150 x 150 DPI)





Topp et al., Fig.5 part 1

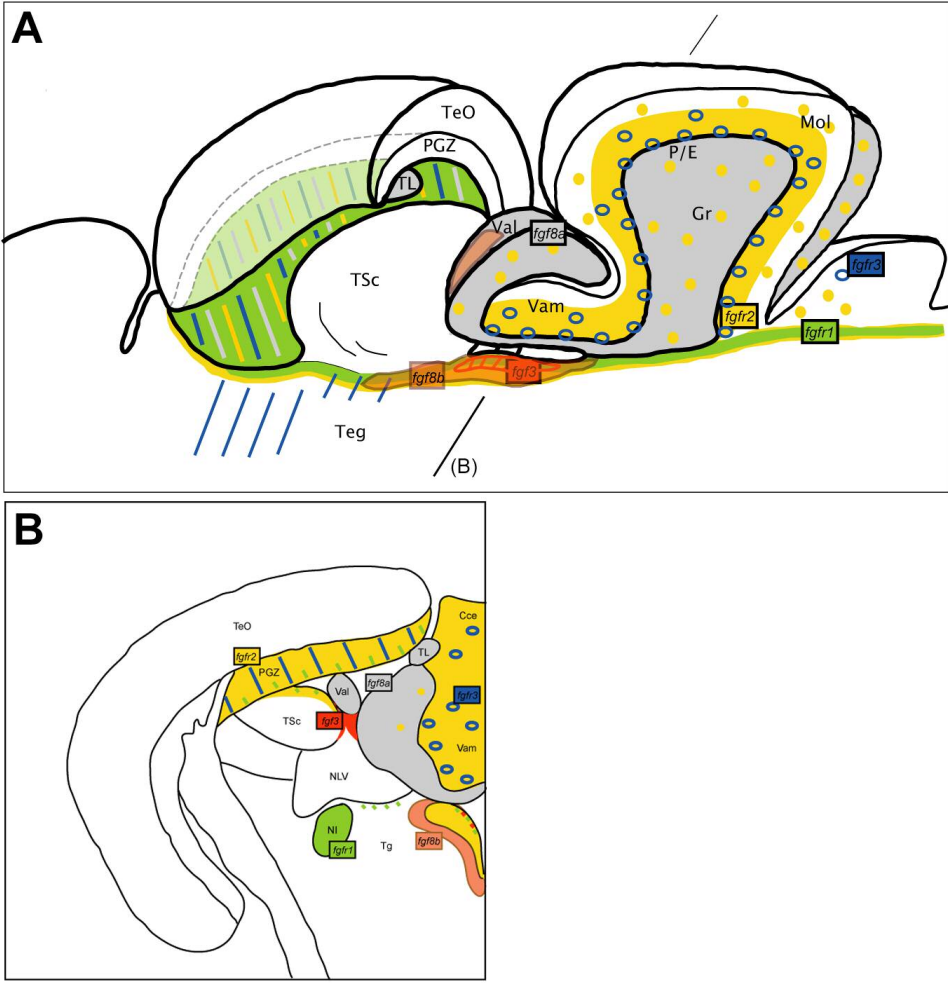
1583x1553mm (72 x 72 DPI)



Topp et al., Fig.5 part 2

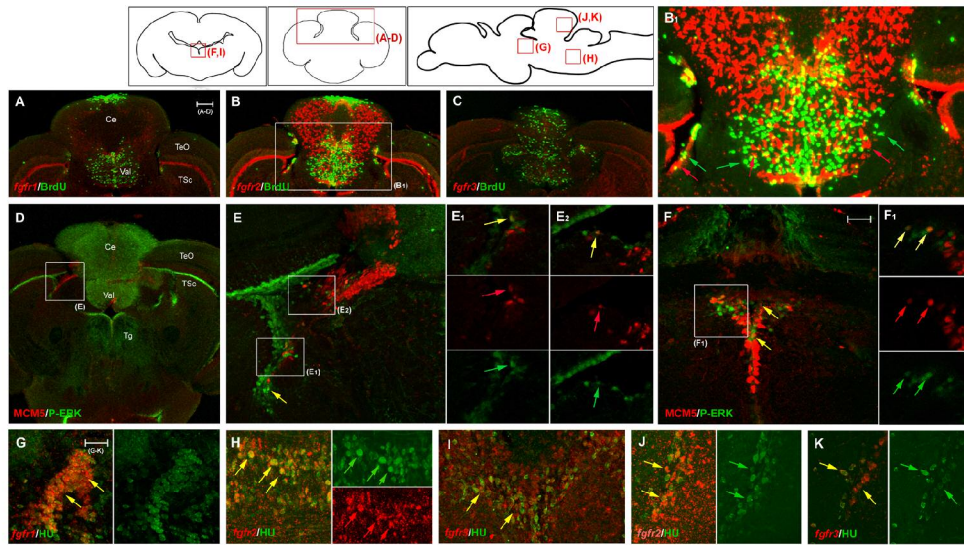
1226x1120mm (72 x 72 DPI)





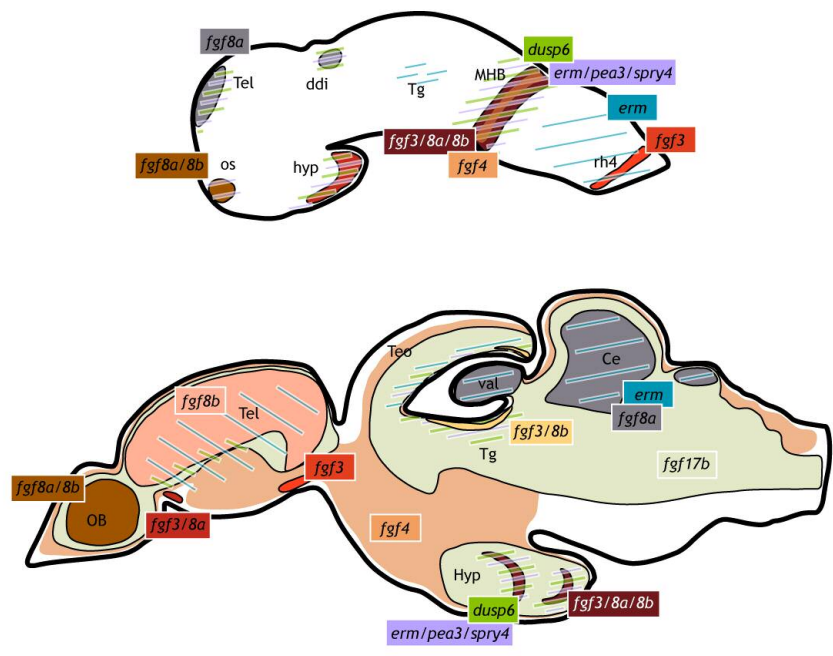
Topp et al., Fig.6

241x259mm (150 x 150 DPI)



Topp et al., Fig.7

280x164mm (150 x 150 DPI)



219x180mm (150 x 150 DPI)

view

Appendix 6

Article in *Developmental Dynamics*

The serotonergic phenotype is acquired by converging genetic mechanisms within the zebrafish central nervous system

Christina Lillesaar, Birgit Tannhäuser, Christian Stigloher,
Elisabeth Kremmer and Laure Bally-Cuif

Developmental Dynamics 236, 1072-1084 (2007)

Contribution:

The project that is published in the following article was mainly conducted by Christina Lillesaar. I contributed to this project with molecular and phylogenetic analysis (see Figure 1).

The Serotonergic Phenotype Is Acquired by Converging Genetic Mechanisms Within the Zebrafish Central Nervous System

Christina Lillesaar,¹ Birgit Tannhäuser,¹ Christian Stigloher,¹ Elisabeth Kremmer,² and Laure Bally-Cuif^{1*}

To gain knowledge about the developmental origin of serotonergic precursors and the regulatory cascades of serotonergic differentiation in vertebrates, we determined the spatiotemporal expression profile of the Ets-domain transcription factor-encoding gene *pet1* in developing and adult zebrafish. We show that it is an early, specific marker of raphe serotonergic neurons, but not of other serotonergic populations. We then use *pet1* expression together with tracing techniques to demonstrate that serotonergic neurons of rhombomeres (r) 1–2 largely originate from a progenitor pool at the midbrain–hindbrain boundary. Furthermore, by combining expression analyses of *pet1* and the raphe tryptophan hydroxylase (Tph2) with rhombomere identity markers, we show that anterior and posterior hindbrain clusters of serotonergic precursors are separated by r3, rather than r4 as in other vertebrates. Our findings establish the origin of r1–2 serotonergic precursors, and strengthen the evidence for molecular, ontogenic and phylogenetic heterogeneities among the vertebrate brain serotonergic cell populations. *Developmental Dynamics* 236: 1072–1084, 2007. © 2007 Wiley-Liss, Inc.

Key words: *pet1*; *tph2*; serotonin; zebrafish; raphe

Accepted 16 January 2007

INTRODUCTION

Serotonin (5HT) is a monoamine neurotransmitter involved in a wide range of behaviors and physiological processes. Accordingly, dysfunction of the serotonergic neurons in the anterior raphe, the main source of 5HT in the mammalian brain, has been implicated in several psychiatric diseases, including affective disorders, schizophrenia, abnormal anxiety, and addiction to psychostimulant drugs (re-

viewed in Lieberman et al., 1998; Lucki, 1998). Several observations suggest that 5HT might also have developmental functions by controlling embryonic growth, neuronal differentiation, neurite growth, synaptogenesis, and the migration of cells (Bailey et al., 1992; reviewed in Vitalis and Parnavelas, 2003; Fricker et al., 2005; Côté et al., 2007) as well as growth cone navigation (Zhou and Cohan, 2001; reviewed in Gaspar et al., 2003).

In addition, recent studies in mammals have highlighted a role of the serotonergic system in neurogenesis (Brezun and Daszuta, 1999; Santarelli et al., 2003; reviewed in Djavanian, 2004).

In mammals, serotonergic innervation of the central nervous system (CNS) originates from two main clusters: the anterior and the posterior raphe. These clusters can be further subdivided into nine nuclei, B1 to B9,

¹Zebrafish Neurogenetics Junior Research Group, Institute of Virology, Technical University-Munich, Munich, Germany and GSF-National Research Center for Environment and Health, Department of Zebrafish Neurogenetics, Institute of Developmental Genetics, Neuherberg, Germany

²GSF-Research Center for Environment and Health, Institute of Molecular Immunology, Munich, Germany

Grant sponsor: Alexander von Humboldt Foundation; Grant sponsor: Swedish Research Council; Grant sponsor: Volkswagen Association; Grant sponsor: Integrated Project ZF-Models of the EU 6th Framework; Grant number: LSHC-CT-2003-503466; Grant sponsor: Institut du Cerveau et de la Moelle Epinière.

*Correspondence to: Laure Bally-Cuif, Zebrafish Neurogenetics, Institute of Developmental Genetics, Ingolstaedter Landstrasse 1, D-85764 Neuherberg, Germany. E-mail: bally@gsf.de

DOI 10.1002/dvdy.21095

Published online 15 February 2007 in Wiley InterScience (www.interscience.wiley.com).

where B4–B9 project to more anterior brain areas and correspond to the anterior raphe complex (dorsal, median, and pontis raphe), while B1–B3 form the posterior raphe and project to the spinal cord (reviewed in Cordes, 2005). Ontogenetically, based on the expression of either 5HT, the 5HT-synthesizing enzyme tryptophan hydroxylase (Tph) or the 5HT transporter (Sert), it has been observed that the earliest serotonergic neurons are born in anterior rhombomeres, and it was suggested that they give rise to the anterior raphe (Lidov and Molliver, 1982; Aitken and Törk, 1988; Hansson et al., 1998). Among these, neurons forming the most dorsal cluster (B9, dorsal raphe) are interpreted to originate from rhombomere 1 (r1; Cordes, 2005). In contrast, the posterior raphe is believed to derive from posterior rhombomeres at a slightly later stage. A similar organization of the mature and developing raphe serotonergic system has been described in lower vertebrates such as teleosts, although fewer subnuclei are recognized at the adult stage (B6–B9 for the anterior raphe, B1–B2 for the posterior raphe; Kah and Chambolle, 1983; Ekström and Van Veen, 1984; Ekström et al., 1985; Kaslin and Panula, 2001). At early postembryonic stages in zebrafish, all caudal projections can be traced back to the caudal hindbrain cluster, suggesting that it is the origin of the posterior raphe (McLean and Fetcho, 2004a,b). The exact hindbrain localization and developmental origin of the presumptive anterior raphe neurons in zebrafish, as well as the regulatory steps leading to the development of the raphe serotonergic phenotype, have not been determined and are the subjects of the present study.

To address these issues, we first aimed to characterize an early and specific marker of presumptive raphe neurons in zebrafish. Despite the fundamental role of central serotonergic neurons, our knowledge about their developmental specification remains fragmentary, and few selective markers or processes have been found. In mammals and chicken, the generation of rostral hindbrain 5HT neurons depends on both the midline signal Sonic hedgehog (Shh), the isthmic organizer signal fibroblast growth factor 8

(Fgf8), and possibly also Fgf2 and/or Fgf4 from the primitive streak at early stages (Ye et al., 1998; Cordes, 2005). Recent results indicate that similar mechanisms control the induction of serotonergic raphe neurons in the zebrafish embryo (Teraoka et al., 2004). Studies in mammals and chicken identified several distinct transcription factors involved in induction or maturation of 5HT raphe neurons. These factors include intracellular targets for Shh signaling (Nkx2.2, 2.9, 6.1, and Gli2), GATA factors 2 and 3, the LIM domain factor Lmx1b, and the Ets-domain transcription factor Pet-1 (van Doorninck et al., 1999; Cheng et al., 2003; Ding et al., 2003; Craven et al., 2004). Pet-1 is exclusively expressed in postmitotic 5HT neurons and controls their final differentiation, i.e., the expression of the 5HT transmitter phenotype encoded by Tph, aromatic L-amino acid decarboxylase and Sert (Hendricks et al., 1999). Thus, in chicken misexpression of *pet-1*, *lmx1b*, and *nkx2.2* is necessary and sufficient to generate ectopic 5HT neurons in the dorsal spinal cord (Craven et al., 2004). Furthermore, in *Pet-1*-null mice the majority of the 5HT expression is lost (Hendricks et al., 2003). A small population of raphe neurons still produces 5HT, but shows reduced levels of Tph, Sert, and vesicular monoamine transporter 2. These observations suggest that Pet-1 is necessary for the final steps in the specification of the serotonergic phenotype, and can be used as a selective marker for raphe serotonergic neurons detectable earlier than Tph.

To identify the origin of anterior raphe 5HT neurons in zebrafish, and to start analyzing the 5HT regulatory cascade in this species, we cloned the zebrafish homologue of mouse *Pet-1* (Pfaar et al., 2002). We analyzed its temporal and spatial expression pattern during development and adulthood, thereby also verifying *pet1* as a specific marker for anterior raphe serotonergic neurons in zebrafish. Three Tph enzymes with largely nonoverlapping expression domains share 5HT synthesis in this species (Bellipanni et al., 2002; Teraoka et al., 2004), and *pet1* transcription precedes expression of the *tph* ortholog specific for the raphe, *tph2*. However, other *tph2*-positive 5HT clusters, for example, in the

pretectum, appear not to rely on Pet1 expression for their development. Surprisingly, we found that anterior and posterior clusters of 5HT neuronal precursors in the zebrafish hindbrain are separate at the level of r3, unlike the situation in mouse or chicken where the gap is in r4. We then used *pet1* in combination with the *her5PAC:egfp* transgene (Tallafuss and Bally-Cuif, 2003) to trace the origin of anterior raphe serotonergic precursors. Our results demonstrate that the majority of the serotonergic precursors located in r1–2, but not those located further posteriorly (r4 and beyond), originate from a progenitor cell pool located at the midbrain–hindbrain boundary (MHB). Our findings highlight heterogeneity in the developmental origin of raphe 5HT neurons and in the regulatory cascades leading to *tph* (and 5HT) expression.

RESULTS

Cloning of Zebrafish *pet1*

To identify and clone zebrafish orthologs of mouse *Pet-1*, the mouse protein sequence (AAL 13055) was blasted against the zebrafish peptide database using Ensembl (www.ensembl.org, zv6). One single candidate was identified located on chromosome 9 at position 10.196.186–10.197.882 (ENSDARG00000009242). Genscan predicted in that location a 235 amino acid (aa) protein (GENSCAN00000022621) showing 60% overall identity to mouse Pet-1 and 89% identity within the Ets-domain (Fig. 1C), and clustering with Pet-1/FEV from other species, but not with Fli-1 or ERG (Fig. 1D). Hence, we refer to this protein as zebrafish Pet1 (GenBank Accession EF370169). We verified the sequence for this predicted protein and the intron/exon boundaries by combining direct reverse transcriptase-polymerase chain reaction (RT-PCR)-mediated cloning, 5'-rapid amplification of cDNA ends (RACE) and sequencing of a partial RZPD expressed sequence tag (EST) clone (IMAGp998C2214692Q). We found that zebrafish *pet1* consists of three exons as in other species (Fig. 1A,B). However, in contrast to mouse *Pet-1* and human *FEV*, our PCR analysis demonstrates that zebrafish *pet1* mRNA encompasses an upstream ATG (numbered 1 in Fig. 1A,B) likely at the

origin of 13 additional N-terminal aa not found in any other species by in silico search.

Sequencing of the RZPD clone showed that it spans exons 2 and 3, and links exon 2 with an in frame 27 base

pair 5' fragment distinct from exon 1 (GenBank Accession EF370170). This sequence matches to a genomic stretch located 870 bp upstream of ATG 1, and might, therefore, belong to an alternative 5'-exon (exon E1_{up}, Fig. 1A–C). We could verify the coexistence of transcripts E1_{up} and E1 by RT-PCR at 1, 2, and 4 days postfertilization (dpf) using forward primers in exon E1_{up} or exon E1 and reverse primers in exon E3 (not shown), but could not recover the E1_{up} transcript in 5'-RACE experiments, suggesting that it might correspond to a minor proportion of *pet1* transcripts. Our expression studies below use a probe spanning exons 2–3, which will not distinguish between these two alternative splice variants of the *pet1* transcript.

***pet1* Expression Highlights Raphe Neurons and Precedes *tph2* Transcription in the Developing and Adult Zebrafish Brain**

To determine whether *pet1* could be used as a specific marker for raphe serotonergic neurons, and to establish its relationship with *tph2*, we per-

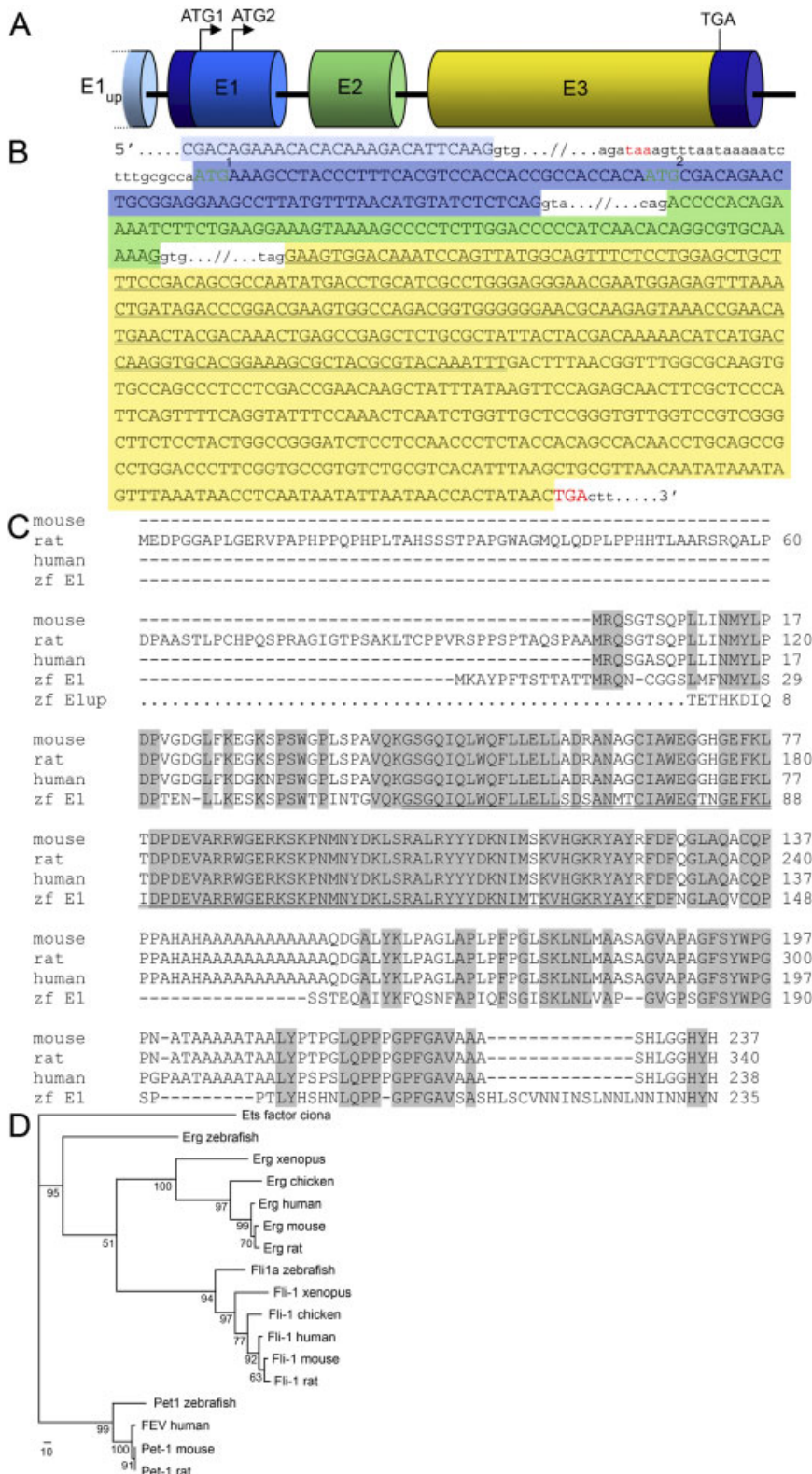


Fig. 1.

formed a temporal analysis of its expression spanning development from 20 somites to 6 dpf (Fig. 2). In addition, we analyzed the presence and location of *pet1* transcripts in the adult brain (Figs. 3, 4).

At 20 somites, *pet1* expression was detected in cells located bilaterally along the midline and more posteriorly in the tail region (Fig. 2A). These cells might correspond to adrenal gland cells (Fig. 2Aa' and see Bb' for 25 hpf; Zhao et al., 2006) and blood precursors (Fig. 2Aa"; Detrich et al., 1995), respectively. Indeed, *Pet-1* has been detected in the mammalian adrenal medulla during embryonic development (Fyodorov et al., 1998). Expression of zebrafish *pet1* in presumptive adrenal gland cells and blood precursors was transient. In the anterior rhombencephalon, the first *pet1*-positive cells were detected at approximately 25 hours postfertilization (hpf; Fig. 2Bb', and C,D, arrowheads). This time precedes the expression of *tph2* by approximately 5 hr (Fig. 2M–P, arrowheads). At 36 hpf, cells located in the posterior rhombencephalon also express *pet1* (Fig. 2E,F arrows), and at 48 hpf, both *pet1* and *tph2* expression domains are clearly organized in an anterior and a posterior cluster, separated by a gap, which is negative for expression. Both clusters consist of two bilaterally symmetrical adaxial columns lining the floor plate (Fig. 2G,H,S,T). In addition, *pet1* is transiently expressed in a cell cluster located just dorsal to the hindbrain population strongly positive for both *pet1* and *tph2* (Fig. 2H, stars in h', compare with 2Tt'). The identity of these cells remains to be elucidated. Conversely, *tph2* (but not *pet1*) is also detectable in the epiphysis and at later stages in a pretecal area in the diencephalon (Fig. 2O–Y). At later stages (60 hpf and 6 dpf), expression of *pet1* and *tph2* in the hindbrain strongly resembles each other and have adopted an adult-like pattern (see below).

In the adult zebrafish brain, *pet1* transcripts are present in the anterior raphe (Fig. 3Aa', 4A,B) as well as in scattered cells likely belonging to the posterior raphe (Fig. 3Aa"; Kaslin and Panula, 2001). *tph2* has a similar expression pattern (Figs. 3Bb", b"', 4D,E), but transcripts are also de-

tected in the pretecal area (Figs. 3Bb', 4C) and in the epiphysis (not shown). This finding is in contrast to *tph1*, expressed exclusively in the hypothalamus (Fig. 3C). To verify that *pet1* and *tph2* are coexpressed in the raphe, we raised an antibody against Tph2. The specificity of this antibody was demonstrated by double immunocytochemistry and in situ hybridization stainings, where it selectively labels neurons expressing *tph2* transcripts (Figs. 3B, all insets, and 4C–E). We observed that all cells expressing *pet1* were also positive for Tph2 (Figs. 3A, all insets, and 4A,B), proving the specificity of *pet1* expression for raphe serotonergic neurons. However, we could find in the raphe some cells with strong Tph2 immunoreactivity that displayed no or only a weak *pet1* in situ staining (not shown).

Mapping of the Border Between Anterior and Posterior Raphe Precursors Within the Developing Hindbrain

According to previous studies in the chicken and mouse, the precursor neurons for the anterior and the posterior raphe are segregated at early stages by a gap in r4, where no 5HT neurons are generated, but, instead visceral motor neurons of the facial nerve innervating the branchial arch derivatives (Lumsden and Keynes, 1989; Marshall et al., 1992; Carpenter et al., 1993; Pattyn et al., 2003a). To map the gap separating the anterior and the posterior hindbrain *pet1*-positive clusters in zebrafish, we performed Tph2 immunohistochemistry on brains from *isl1:gfp* transgenic larvae, expressing green fluorescent protein (GFP) in cranial motor neurons of the hindbrain (Higashijima et al., 2000). Using this line at 6 dpf, we could readily identify the trigeminal central neurons (Va, Vp) located in r2 and r3, respectively (Fig. 5B; Chandrasekhar et al., 1997; Higashijima et al., 2000), as well as a third cluster immediately posterior (Fig. 5B, star). We mapped this third cluster to r4 by comparison with the position of retrogradely traced Mauthner neurons (Fig. 5A,C; Kimmel et al., 1981; O'Malley et al., 1996). Thus, *isl1:gfp*

transgenic larvae allow precise positioning of r2, 3, and 4, and we subsequently labeled Tph2-positive neurons in this line (Fig. 5D–F). We found that the gap separating anterior and posterior serotonergic clusters (Fig. 5D, inset) overlaps with the position of Vp, in r3, and not with the third *isl1:gfp*-positive cluster in r4 (Fig. 5F). Hence, we conclude that, in contrast to earlier findings in other species, the gap separating the anterior from the posterior clusters of raphe precursors in zebrafish is located in r3.

pet1-Positive Cells Located in r1–2 Originate From the Midbrain–Hindbrain Boundary Progenitor Pool

Previous observations suggest that the different clusters of serotonergic neurons in the raphe complex might have different embryological origins (Craven et al., 2004; Cordes, 2005), but these neurons have not been directly traced. We, therefore, addressed whether the serotonergic precursors of the r1–2 group originate from common or distinct locations.

By combining *pet1* in situ hybridization with the detection of *rfng* transcripts to identify rhombomeric borders (Qiu et al., 2004), we observed that the first *pet1*-positive cells were located in r1, close to the MHB (data not shown). Because previous results from our laboratory also suggested that the MHB progenitor pool contributed neurons to the ventral anterior hindbrain (Tallafuss and Bally-Cuif, 2003), we specifically tested for the contribution of this pool to r1–2 serotonergic precursors. We used *her5PAC:egfp* transgenic embryos, which allow us to locate the early MHB pool by GFP expression at late gastrulation. The stability of GFP in these embryos is too short to permit direct tracing of MHB progeny cells until the appearance of the first *pet1*-positive cells. Thus, we injected caged-fluorescein at the one-cell stage and uncaged this compound between the 90% epiboly to tail bud stage in a few cells located either within the GFP-expressing domain, or immediately posterior to it (Fig. 6A). Cross-sections of 34–36 hpf embryos uncaged within the GFP-positive area (Fig. 6Ai) showed cells double labeled for un-

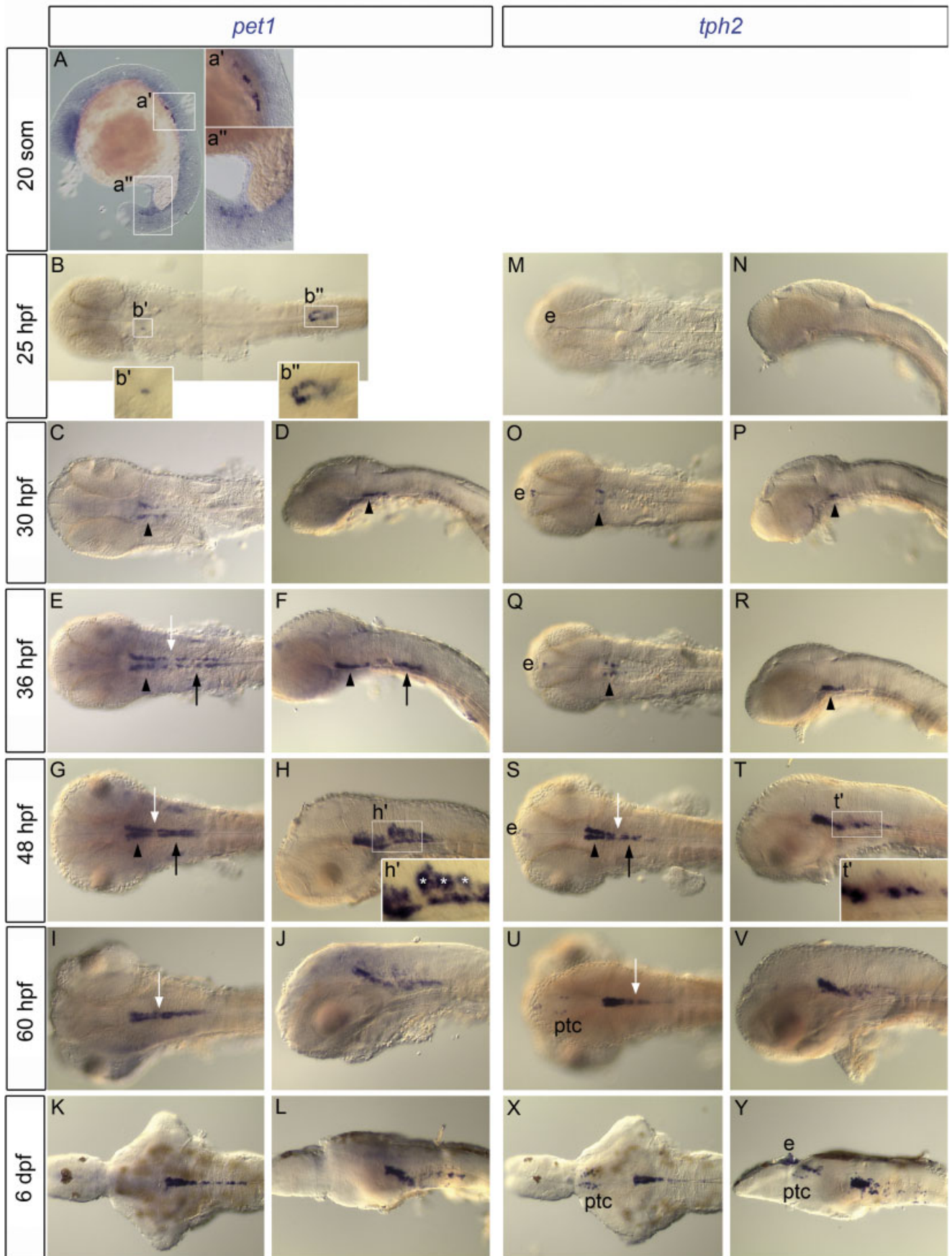


Fig. 2.

caged fluorescein and *pet1* in the anterior rhombencephalon (r1–2; Fig. 6B), but not more posteriorly (r4–7; not shown). This finding is in contrast to embryos where the uncaging was done posterior to the GFP-positive area (Fig. 6Aii). There, fluorescein-positive cells populated the floor plate in the anterior hindbrain region as well as a large domain roughly spanning the whole dorsoventral extent of the neural tube at the level of r3, where *pet1* is not expressed (not shown), while *pet1*-positive cells of r1 and r2 were unlabeled (Fig. 6C). Thus, *pet1*-positive serotonergic precursors of r1–2, but not those located more posteriorly, originate from the MHB progenitor pool.

DISCUSSION

In the present study, we cloned and analyzed the spatial and temporal expression pattern of the zebrafish Ets-domain transcription factor-encoding gene *pet1*. We showed that *pet1* is expressed in the subpopulation of *tph2*-positive cells located in the raphe, but not in other *tph*-positive clusters. We next used this marker in combination with tracing techniques to locate the origin of anterior hindbrain serotonergic precursors. Our results demonstrate that the serotonergic neurons of r1 and r2 largely originate from a progenitor cell pool located at the MHB.

This finding is in contrast to serotonergic neurons located more posterior in the hindbrain, which, according to previous findings, might originate from ventral neuroepithelial progenitors close to the floor plate at their respective anteroposterior level (reviewed in Goridis and Rohrer, 2002). Furthermore, by combining identification of the raphe serotonergic neurons using their specific expression of *pet1* and *Tph2* with rhombomere identity markers we show that, in contrast to many other vertebrates, the gap separating the anterior from the posterior hindbrain clusters of serotonergic precursors is located in r3 in zebrafish and not in r4. Our findings strengthen the evidence for heterogeneity among the serotonergic cell populations of the vertebrate brain, both in the transcription factors presiding to their differentiation and in their developmental origin, with possible further differences between species.

Organization of the Zebrafish *pet1* Gene

Pet-1 belongs to the family of Ets transcription factors, which are characterized by a highly conserved DNA-binding Ets-domain (Peter et al., 1997; reviewed in Laudet et al., 1999; Oikawa and Yamada, 2003). The Ets family contains some 30 different members, of which Erg and Fli-1 are most closely related to Pet-1. In the present study, we have identified one zebrafish homologue of Pet-1 showing 89% identity to mouse Pet-1 within the Ets domain (Pfaar et al., 2002). As reported for mammals (Peter et al., 1997; Fyodorov et al., 1998; Pfaar et al., 2002), the main form of zebrafish Pet1 is encoded by three exons. However, we identified for this transcript 39 additional base pairs in the fish genome, giving rise to 13 additional N-terminal aa, which we could not find in other species by *in silico* search. The existence of this extra sequence was confirmed by RT-PCR. Furthermore, we demonstrated the existence of an alternative 5'-exon that is at least partially coding. The two alternative transcripts co-exist *in vivo*. Whether they are differentially expressed, however, remains to be determined, because our *in situ* probe does not distinguish between the two. A differential promoter usage in *Pet-1*

has not been reported in other species to date.

pet1 Is a Selective Marker for Raphe Serotonergic Neurons in Zebrafish

Previous studies of chicken, mouse, rat, and human have identified *Pet-1/FEV* as a specific marker for postmitotic raphe serotonergic neurons preceding the expression of serotonergic neuron-specific proteins such as Tph and Sert (Hendricks et al., 1999; Pfaar et al., 2002; Craven et al., 2004; Maurer et al., 2004). Our findings that *pet1* has a similar expression pattern as *tph2* in the hindbrain during embryonic, larval, and adult stages, suggests that *pet1* is also a valid marker for this specific cell population in zebrafish. This assumption was verified by showing that *pet1* transcripts are colocalized with Tph2 protein in the adult brain. We further demonstrate that *pet1* transcripts can be detected approximately 5 hr earlier than *tph2* transcripts in the anterior rhombencephalon (r1), demonstrating that it is also a comparatively early marker in zebrafish. Finally, like in other vertebrates, zebrafish *pet1* is expressed in serotonergic precursors only at the postmitotic stage (C. Stigloher, unpublished observations).

Location of the Border Between Anterior and Posterior Raphe Precursors

Our finding that the gap separating the anterior from the posterior clusters of serotonergic precursors is located in r3 in zebrafish was unexpected considering observations from other species, where it has been found in r4 (Lumsden and Keynes, 1989; Marshall et al., 1992; Carpenter et al., 1993; Pattyn et al., 2003a). In agreement with our finding, Teraoka et al. (2004) described expression of *tph2* in the anterior cluster located just posterior to the trochlear nucleus (nIV) and anterior to the trigeminal motor nucleus (nV). We do not as yet have a mechanistic interpretation for this surprising interspecies difference. It is possible that the location of the border between anterior and posterior raphe precursors depends on the extent

Fig. 2. A–Y: Expression of *pet1* (A–L) and *tph2* (M–Y) revealed by *in situ* hybridization on whole-mount embryos/larvae (A–J and M–V) or brains (K–L and X–Y). Insets show higher magnifications of the boxed areas. The earliest *pet1*-positive cells are likely adrenal gland (Aa' and Bb'') and blood (Aa'') precursors. B: The first *pet1*-expressing cells in the rhombencephalon are detected at 25 hours postfertilization (hpf). O: Expression of *tph2* in this location is not detected until a few hours later. Afterward, *pet1* and *tph2* expression highlights two parallel stripes of precursors lining the hindbrain floor plate. E, G, I, S, U: These are organized in an anterior (arrowhead) and posterior (arrow) cluster separated by a gap (white arrow). H: An additional column of *pet1*-positive cells runs along this domain in a slightly more dorsal location (stars in h'). Starting from 60 hpf *tph2* expression can also be seen in an additional cluster of cells corresponding to the pretectal complex (Kaslin and Panula, 2001). In addition, *tph2* was detected in the epiphysis at all stages examined. e, epiphysis; ptc, pretectal and thalamic complex.

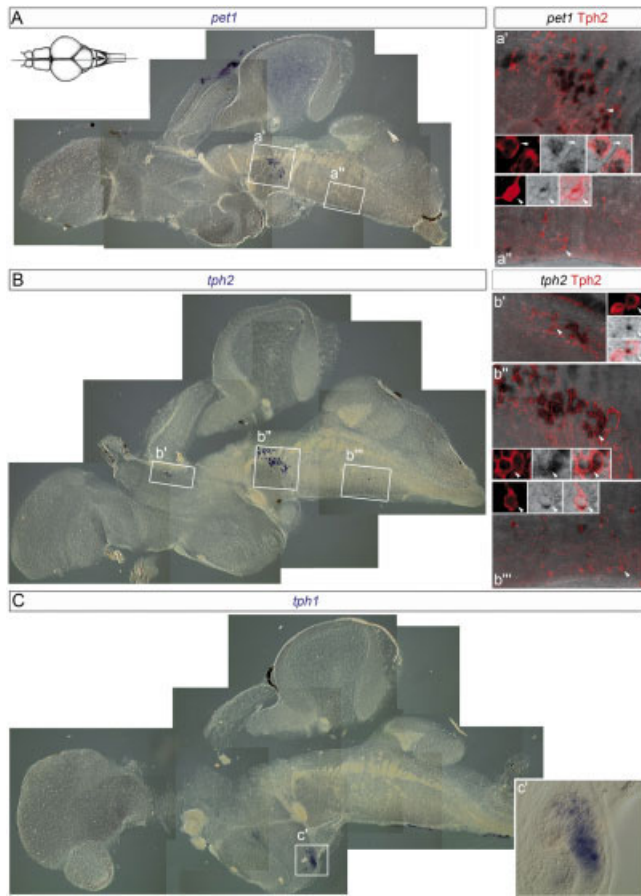


Fig. 3.

of the posteriorward migration of MHB-derived cells, on local specification cues, or both. In the mouse, a specific mechanism relying on r4-expressed genes (e.g., *Hoxb1* and *Phox2b*) accounts for the lack of serotonergic specification in this location (Pattyn et al., 2003a), and orthologous genes are also expressed in r4 in zebrafish (Guo et al., 1999; McClintock et al., 2002). However, we note that zebrafish-specific features have been observed in several specification or migration mechanisms in the hind-brain. For instance, a migration of the facial cranial nerve from r4 to r6 is observed in zebrafish but not in chicken (Chandrasekhar et al., 1997), and zebrafish r4 (but not mouse r4) expresses *fgf8* (Maves et al., 2002; Walshe et al., 2002). Thus, it remains possible, in particular, that the regulatory events involving *Hoxb1* function differ between zebrafish and other vertebrates. Another important question will be to determine whether, in all species, the gap between ante-

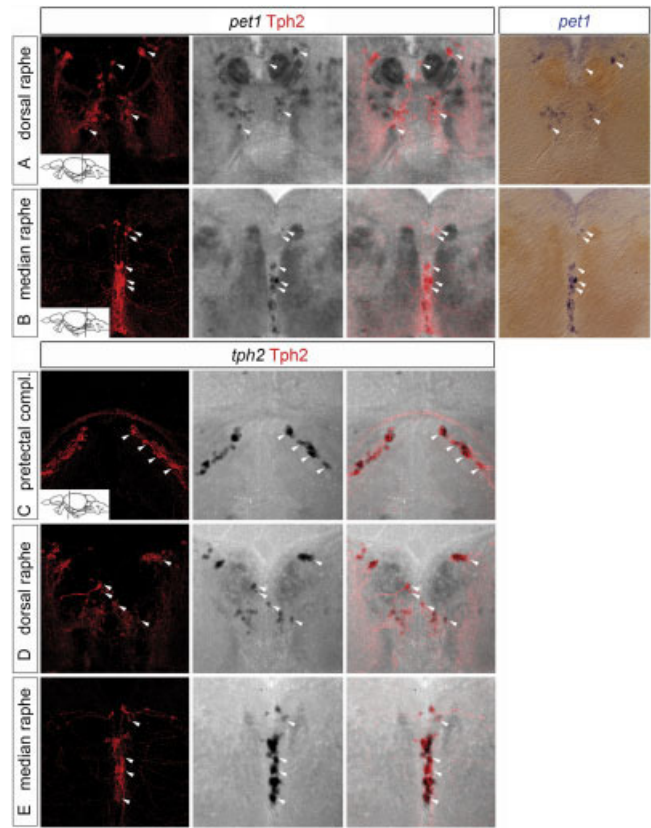


Fig. 4.

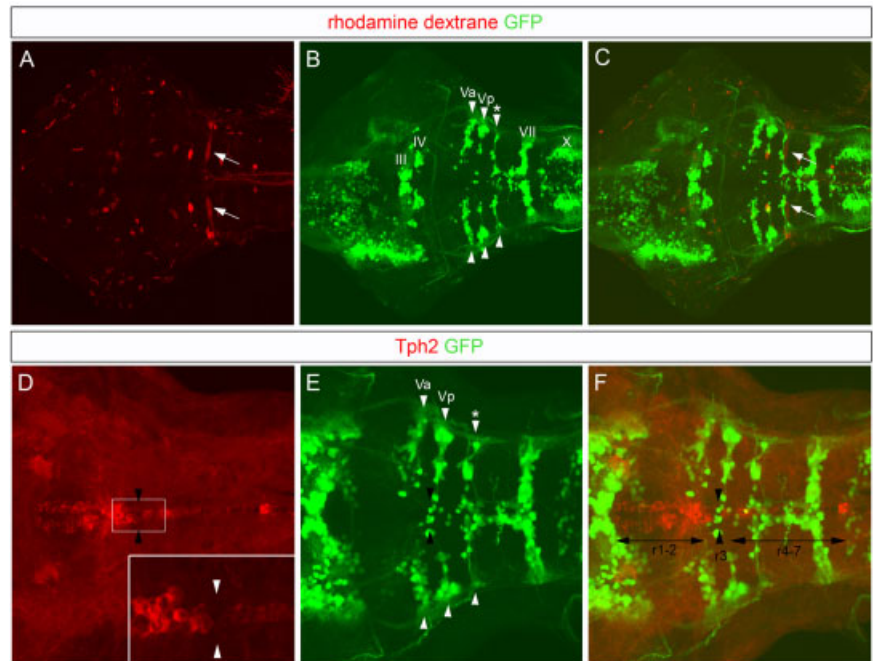


Fig. 5.

rior and posterior hindbrain clusters corresponds to the distinction between the precursors fated to form the anterior versus the posterior raphe, a conclusion currently mostly inferred from analyzing the spatiotemporal evolution of serotonergic markers during development (Lidov and Molliver, 1982; Aitken and Törk, 1988) and from back-filling caudal serotonergic projections in zebrafish (McLean and Fetcho, 2004a,b).

***pet1*-Positive Cells Located in r1–2 Originate From the MHB Progenitor Pool**

According to the present literature, 5HT neurons arise from the ventral neuroepithelial progenitors located close to the floor plate (pMNv area) that, in r2 and beyond, also produce branchiomotor and visceromotor neuronal precursors (Goridis and Rohrer, 2002; Pattyn et al., 2003a; but see Craven et al., 2004; Cordes, 2005). The origin of r1 progenitors was unresolved, as no branchio- and visceromotor neurons arise from r1. Making use of the amenability of zebrafish embryos to direct lineage tracing, we demonstrate here that most, if not all, *pet1*-positive cells of r1 and r2 originate from the pool of progenitor cells located at the MHB at the end of gastrulation. Whether a single MHB progenitor gives rise to both r1 and r2

neurons cannot be concluded at this point. These results add to our previous observation that the early MHB progenitor pool generates cells populating r1 and r2 (and possibly also, to a low extent, r3 and r4; Tallafuss and Bally-Cuif, 2003). They also extend fate mapping data for *Wnt1*-positive cells in the embryonic day (E) 7.5 mouse embryo that gave rise to a few 5HT neurons of the anterior raphe (Zervas et al., 2004). In fish, the MHB pool partially overlaps with *wnt1* expression (Tallafuss et al., 2001).

Interestingly, the contribution of the MHB pool to serotonergic precursors appears to be precisely limited to the anterior hindbrain cluster. Thus, the anterior and posterior clusters are distinct not only in position, molecular specification, and fate (van Doorninck et al., 1999), but also in the developmental process that originally sets them aside within the neural tube.

Differential Regulation of the Serotonergic Phenotype in Zebrafish

In the zebrafish CNS, serotonergic neurons are found in several distinct clusters: in the epiphysis, the hypothalamus, a pretecal area of diencephalon, and the anterior and posterior raphe nuclei (Kaslin and Panula, 2001). The synthesis of 5HT in these different cell populations is controlled

by at least three different Tph enzymes, all with a unique temporal and spatial expression pattern (Fig. 7). *tph1* is present in 5HT-containing cells of the embryonic and adult hypothalamus and transiently in cells along the floor plate of the spinal cord (Bellipanni et al., 2002). The expression of *tph1-like* is restricted to a preoptic cell cluster during late embryonic stages (Bellipanni et al., 2002). *tph2* is expressed by cells in the anterior and posterior raphe in embryonic until adult stages (Teraoka et al., 2004; present data). In addition, we detected *tph2* transcripts in a cluster of 5HT-positive cells in the pretecal area of the diencephalon from 3 dpf and onward (this study).

As opposed to *tph*, we could only identify one *pet1* gene in zebrafish, with expression limited to the anterior and posterior raphe. Furthermore, although *tph2* is expressed both in the diencephalon and in the hindbrain serotonergic neurons, *pet1* was only expressed at detectable levels in the hindbrain population. These findings demonstrate heterogeneity not only among 5HT nuclei but also within the Tph2-expressing population itself, with respect to the transcription factors required for activating serotonergic identity. In the mouse, the specification of 5HT progenitors further differs in r1 and r2, as r1 is not under control of *Nkx2.2* and *Phox2b* functions (Briscoe et al., 1999; Ding et al., 2003;

Fig. 3. Comparison of the localization of *pet1*, *tph2*, and *tph1* transcripts (in situ hybridization, blue/black) and of Tph2 protein (immunohistochemistry, red) on adult brain sagittal sections. **A:** In situ staining for *pet1* in anterior (a') and posterior (a'') raphe nuclei. a' and a'' (optical projections) show higher magnification of boxed areas in A together with Tph2 immunostaining in red. Note the double-labeled cells, some of which (arrowheads) are further magnified in the small insets (optical sections). **B:** In situ staining for *tph2* in anterior (b') and posterior (b'') raphe nuclei and in the pretecal complex (b'). b', b'', and b''' (optical projections) show higher magnification of boxed areas in B together with Tph2 immunostaining. Double labeling was observed in all three regions for all cells, some of which (arrowheads) are further magnified in the small insets (optical sections). **C:** In situ staining for *tph1* in the hypothalamus. c' shows higher magnification of boxed area in C. Schematic picture was modified from Wullimann et al. (1996).

Fig. 4. Compared localization of *pet1* and *tph2* transcripts (in situ hybridization, black/blue) and of Tph2 protein (immunohistochemistry, red) on adult brain coronal sections. Arrowheads indicate examples of double-labeled cells. **A,B:** *pet1* transcripts and Tph2 protein shown in optical projections of sections through the dorsal and the medial raphe, respectively, at the level indicated in the schematic pictures. Color brightfield pictures were included (right panels) to clarify the distinction between cross-cut fiber bundles (that appear dark on black–white images, but are negative for *pet1* transcripts) and blue in situ staining. The dorsal raphe (corresponding to cluster B6–B7) is located more dorsally and laterally than the medial raphe (B8–B9; Kaslin and Panula, 2001). **C–E:** The location of *tph2* transcripts and Tph2 protein in the pretecal complex (level of section indicated in schematic picture) is illustrated (C) in addition to the dorsal (D) and median (E) raphe in optical projections. Schematic picture was modified from Wullimann et al. (1996).

Fig. 5. Location of the gap separating the anterior and posterior *pet1*-positive raphe precursors in relation to green fluorescent protein (GFP)-positive cell clusters in the *isl1:gfp* transgenic line. Photomicrographs are confocal optical projections of dorsal views at hindbrain levels, anterior left. **A:** Mauthner neurons (arrows), located in rhombomere (r) 4, were labeled by retrograde tracing in 6 days postfertilization (dpf) *isl1:gfp* transgenic larvae using rhodamine dextran. **B,C:** Thereby, the spatial distribution of GFP-expressing cells (B, arrowheads) in relation to rhombomeres was determined (C, overlay of A and B). C: Note that the Mauthner neurons overlap with a cluster of GFP-positive cells (*) just posterior to the trigeminal nuclei (Va and Vp, arrows). **D:** The anterior and posterior clusters of serotonergic precursors were identified using an antibody against tryptophan hydroxylase (Tph) 2. The inset shows a higher magnification of the boxed area, and white arrowheads in the inset indicate the gap between the anterior and posterior Tph-positive clusters (optical section). **E,F:** Note, in F (overlay of D and E) that this gap overlaps with Vp, in r3 (black arrowheads), rather than with Mauthner neurons, in r4. Thus, the anterior Tph cluster spans r1–2, and the posterior cluster spans r4 and beyond.

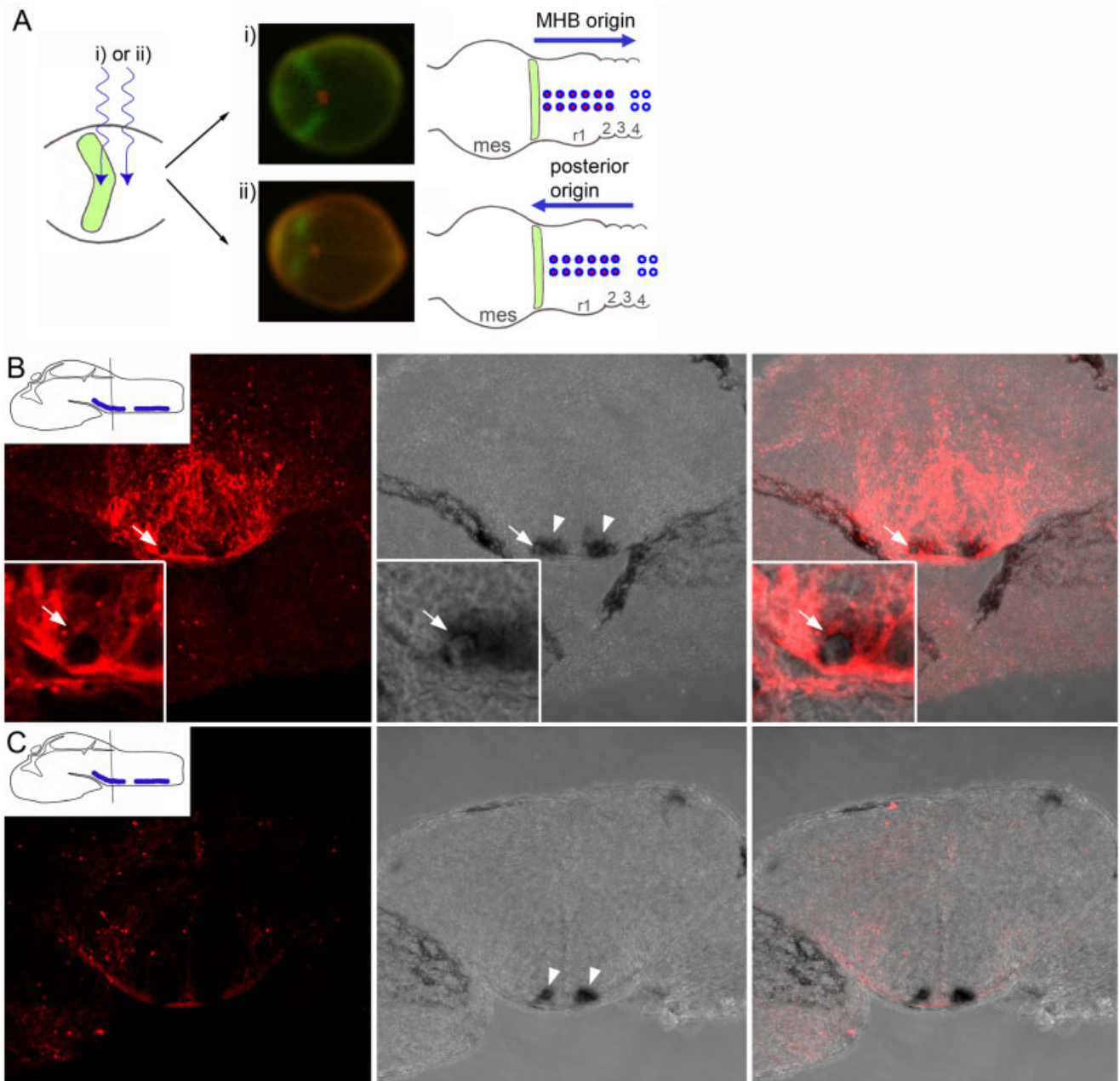


Fig. 6.

Pattyn et al., 2003b). If a similar phenomenon occurs in zebrafish, the common origin of r1 and r2 precursors suggests that their acquisition of distinct genetic cascades to realize the serotonergic phenotype is an event that likely follows their exit from the MHB.

Together, these observations strongly support a model where the serotonergic phenotype is differentially regulated at multiple steps among the serotonergic populations within the zebrafish CNS, and would be mostly acquired by the progressive convergence of different

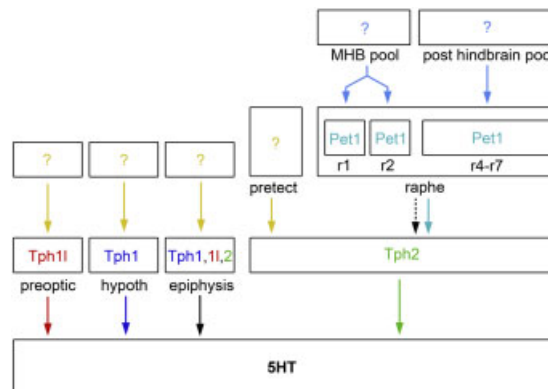


Fig. 7.

combinations of developmental factors toward expression of the 5HT neurotransmitter. The mechanisms that sustain the setting-up of these distinct genetic pathways and their convergence toward a common outcome remain an interesting future issue.

EXPERIMENTAL PROCEDURES

Cloning of Zebrafish *pet1*

A predicted zebrafish *pet1* ortholog (ENSDARG0000009242) was cloned and verified using a 5'-RACE protocol modified for GC-rich domains, according to the manufacturers' recommendations (Invitrogen). Briefly, total RNA was extracted from 56 hpf embryos using Trizol (Invitrogen). Total RNA was then treated with DNase I and reverse transcribed into cDNA using gene specific primer (GSP) 1 (5'caggttggtgctgtgtaga3'), purified on SNAP-columns and dA-tailed. Subsequently, the dA-tailed first-strand cDNA was reverse transcribed in a second-strand cDNA synthesis using a 3'-RACE adapter primer (5'ggc-cacgctcgactagtagac(t)₁₇3'), and SNAP-column purified a second time. The 5'-RACE was followed by a nested

PCR using an abridged universal amplification primer (AUAP; 5'ggc-cacgctcgactagtagac3') and GSP 2 (5'gctgtgtagagggttgga3') and 3 (5'ct-gaatgggagcgaagtgtg3'), generating a major amplification product corresponding to transcript E1 starting at ATG2 (Fig. 1B). To determine whether ATG1 was generally included in transcript E1, additional nested RT-PCR reactions were performed on cDNA reverse-transcribed from 56 hpf embryos with random hexamers. The forward PCR primers were located upstream, downstream, or spanning either of the two ATGs as follows: upstream of ATG1: primer 1, 5'atttat-tccagatcacagttttgag3'; primer 2, 5'-aaagttaataaaaaatctttgagc3'; spanning ATG1: primer 3, 5'aaaatctttgagc-caatg3'; primer 4, 5'gttaataaaaaatctt-gcgcgaatg3'; downstream of ATG1: primer 5, 5'aagcctacccttcacgctc3'; primer 6, 5'ttccagctcaccaccg3'; spanning ATG2: primer 7, 5'atgcgaca-gaactgagg3'; downstream of ATG2: primer 8, 5'agaactgagggaagcc3'. GSP 2 and 3 were used as reverse primers. Specific amplification products were obtained using primers 4–8, demonstrating that ATG1 is contained within transcript E1.

Sequencing of an EST clone

(IMAGp998C2214692Q, RZPD Deutsches Ressourcenzentrum für Genomforschung GmbH, www.rzpd.de; used for subsequent in situ hybridizations) showed that it spans exons 2 and 3, and links exon 2 with a 27-base pair 5'-fragment from the same genomic locus but distinct from exon 1 (see below; Fig. 1A,B). The existence of such a transcript ("E1_{up}") was verified by PCR reactions performed on cDNA reverse transcribed from 1, 2, and 4 dpf embryos with random hexamers using a forward primer in exon E1_{up} (5'cga-cagaacacacaaagacattca3') and a reverse primer in exon 3 (5'cttcgtc-cgggtctatcagtttaa3').

Molecular Phylogenetic Analysis

Multiple alignment of amino acid sequences for Pet-1/FEV, Erg, and Fli-1 were obtained by using Clustal Method in MegAlign software (version Power Macintosh 3.01, DNA Star, Inc.). A parsimony tree based on full-length sequences for the three different vertebrate Ets-domain transcription factors belonging to the Erg subfamily and a *Ciona* Ets-domain factor (BAE06415) as outgroup was constructed using PAUP* software (version 4.0b10, David L. Swofford, Florida State University, Sinauer Associates, Inc., Publishers). Probabilities were calculated using bootstrap with 1,000 replicates. The following protein sequences were used: Erg chicken (CAA54404), human (NP_004440), mouse (BAB69948), rat (AAH72519), *Xenopus* (CAB46567), zebrafish (AAH86811), Fli-1 human (AAH01670), mouse (NP_032052), rat (AAX83256), chicken (NP_001026079), *Xenopus* (CAA47389), Fli1a zebrafish (AAH66571), FEV human (NP_059991), Pet-1 rat (NP_653354), and mouse (AAL13055). Trees were printed using the program TreeviewPPC (version 1.6.6; <http://taxonomy.zoology.gla.ac.uk/rod/treeview.html>).

Generation of Monoclonal Antibodies (mAbs) Against Tph2

An internal peptide of Tph2 (₁₁₁CT-KKEFNELVQHLKDHVNIV₁₃₀) was synthesized and coupled to KLH or ovalbumin (PSL, Heidelberg). Rats were immunized with 50 µg of pep-

Fig. 6. Origin of rhombomere (r) 1–2 serotonergic precursors. **A:** Strategy for tracing the origin of r1–2 serotonergic precursors in *her5PAC:egfp* transgenic embryos injected with caged-fluorescein at one-cell stage (dorsal views, anterior left). An ultraviolet-light beam was focused along the midline (i) within or (ii) posterior to the green fluorescent protein (GFP)-expressing area at 90% epiboly/tail bud (left drawing; green GFP-positive midbrain–hindbrain boundary [MHB] progenitor pool). Photomicrographs: control embryos fixed directly after uncaging and processed for GFP (green) and fluorescein (red) immunostaining. Schematic pictures: two possible outcomes at 36 hours postfertilization (hpf). Top: uncaging within the GFP-positive area and *pet1*-positive cells of r1–2 fluorescein-labeled (red); origin within the MHB pool; Bottom: uncaging posterior to the GFP-positive area and *pet1*-positive cells of r1–2 fluorescein-labeled; origin posterior to the MHB pool. **B:** A 16-µm optical projection of a coronal cryosection through r1–2 of embryos uncaged within the GFP-expressing domain. Insets: High magnifications of 1-µm optical section of double-labeled cell indicated with an arrow. Arrowheads: *pet1*-positive cells on each side of the floor plate within r1–2. Note anti-fluorescein labeling of these *pet1*-positive cells. **C:** Same analysis in an embryo uncaged posterior to the GFP-expressing domain. mes, mesencephalon. Schematic picture modified from Mueller and Wullimann (2005).

Fig. 7. The serotonergic phenotype in the zebrafish central nervous system (CNS) is acquired by converging mechanisms. Schematic model of the genetic cascades encoding serotonin (5HT) neurotransmitter identity in the zebrafish CNS; the genes involved are color-coded, and their territories of expression are represented by boxes. The factors accounting for Tph1, 1l, and 2 expression in the pretectal, preoptic, hypothalamic, and epiphyseal clusters are unknown and, although depicted with a single color, might differ between these domains and/or the tryptophan hydroxylase (Tph) target gene. In addition to *tph1* expression in the preoptic cluster a temporally nonoverlapping expression of *tph1* has been found in cells located in the preoptic area. Whether these cells are different from the *tph1*-expressing cells or if there is a shift from *tph1* to *tph1* is not known (Bellipanni et al., 2002). The differential regulation of *pet1* expression in r1 and r2 is inferred from studies in the mouse (Briscoe et al., 1999; Ding et al., 2003; Pattyn et al., 2003a). The dotted arrow leading to *tph2* expression in the raphe refers to the persistence of 5HT neurons in *Pet1*^{-/-} mice (Hendricks et al., 2003), suggesting a partially redundant mechanism.

tide-KLH using CPG 2006 (Tib Molbiol, Berlin) and IFA as adjuvant. After a 6-week interval, a final boost without adjuvant was given 3 days before fusion of the rat spleen cells with the murine myeloma cell line P3X63-Ag8.653. Hybridoma supernatants were tested in a differential enzyme-linked immunosorbent assay with the specific peptide or an irrelevant peptide coupled to ovalbumin. Positive-reacting hybridomas (IgG2a) were further analyzed by immunohistochemistry, and mAb 2E5 was found to specifically recognize Tph2.

In Situ Hybridization and Immunohistochemistry

Whole-mount in situ hybridization was performed on AB/AB embryos staged according to Kimmel et al. (1995) or on AB/AB adult brains as described elsewhere (Thisse et al., 1993; Adolf et al., 2006). The following probes were used: *tph2* (previously *tphR*; Teraoka et al., 2004), *tph1* (previously *tphD1*; Bellipanni et al., 2002), and *radical fringe* (*rfrng*; Qiu et al., 2004). The RZPD EST clone IMAGp998C2214692Q was used to detect *pet1* transcripts. Immunocytochemical stainings were performed with the following antibodies: monoclonal rat α -Tph2 (1:8; see above), rabbit α -GFP (1:1,000; Torrey Pines Biolabs), or mouse α -fluorescein (1:200; Roche) and secondary antibodies coupled to Cy2 or Cy3 (Jackson ImmunoResearch). Flat-mounted preparations or cryostat sections of embryos, as well as Vibratome sections of adult brains, were photographed using a Zeiss Axioplan microscope equipped with a 3CCD color video camera (Sony) and processed with AxioVision 4.5 software (Zeiss), or a laser scanning confocal microscope (LSM510Meta, Zeiss). Subsequent image processing was done using LSM software (version 3.2 SP1.1, Zeiss) and Photoshop (version 9.0, Adobe Systems).

Mapping of the Gap Separating the Presumptive Anterior and Posterior Serotonergic Precursors in the Hindbrain

To locate the border between anterior and posterior raphe, larvae at 6 dpf

from an *isl1:gfp* transgenic line (Higashijima et al., 2000) were processed for Tph2 immunohistochemistry (see above). For comparison and identification of r4, Mauthner neurons were retrogradely traced with fixable rhodamine dextran (10 kDa; Molecular Probes) by cutting the tail of *isl1:gfp* transgenic larvae with a scalpel soaked in dye. The larvae were fixed in 4% paraformaldehyde after 6 hr, and the brains were subsequently dissected, mounted, and imaged using a Zeiss Confocal microscope.

Tracing of *pet1*-Expressing Cells

The origin of the *pet1*-expressing cells located in r1–2 after 24 hpf was traced using uncaging of DMNB-caged fluorescein (10 kDa; 5 mg/ml; Molecular Probes) injected into one-cell stage embryos from a *her5PAC:egfp* transgenic line (Tallafuss and Bally-Cuif, 2003). Injected GFP-positive embryos were uncaged at 90% epiboly to tail bud stage, when a distinct GFP expression could be seen identifying the MHB progenitor pool (Fig. 6A). The uncaging was done using the ultraviolet (UV) excitation beam of a Zeiss Axioplan microscope, focused through a 0.1-mm pinhole and with a $\times 63$ water immersion objective, leading to labeling of an area approximately five cell bodies in diameter. The UV beam was aimed at medial cells located either within the GFP-expressing domain or immediately posterior to it. To verify the location of the labeling, a set of embryos ($n = 5$ within the GFP-expressing domain, $n = 6$ posterior to the GFP-expressing domain) was fixed immediately after uncaging and processed for double immunocytochemistry against GFP and fluorescein (Fig. 6A i and ii). On average the posterior uncaging was done 2–3 cell rows behind the GFP-expressing area. The rest of the embryos were fixed at 33–35 hpf, a stage when *pet1* expression is clearly detectable in both anterior and posterior rhombomeric clusters, and processed for *pet1* in situ hybridization followed by immunodetection of uncaged fluorescein (see above). To visualize double-labeled cells, stained embryos were cryosectioned coronally at 25 μ m.

ACKNOWLEDGMENTS

We thank other members of the L. Bally-Cuif laboratory for constant support and critical input, the Dr. R. Köster team for discussions, and the GSF fish facility staff for expert fish care. The *rfrng* probe was a kind gift of Dr. Y.-J. Jiang. We also thank Drs. W. Norton and P. Vernier for their critical reading of the manuscript. C. Lille-saar was funded by the Alexander von Humboldt Foundation and the Swedish Research Council and a Junior group grant from the Volkswagen Association, the Integrated Project ZF-Models of the EU 6th Framework, and a special grant of the Institut du Cerveau et de la Moelle Epinière (ICM, Paris) to L. Bally-Cuif.

REFERENCES

- Adolf B, Chapouton P, Lam CS, Topp S, Tannhäuser B, Strähle U, Götz M, Bally-Cuif L. 2006. Conserved and acquired features of adult neurogenesis in the zebrafish telencephalon. *Dev Biol* 295:278–293.
- Aitken AR, Törk I. 1988. Early development of serotonin-containing neurons and pathways as seen in whole-mount preparations of the fetal rat brain. *J Comp Neurol* 274:32–47.
- Bailey CH, Chen M, Keller F, Kandel ER. 1992. Serotonin-mediated endocytosis of apCAM: an early step of learning-related synaptic growth in *Aplysia*. *Science* 256:645–649.
- Bellipanni G, Rink E, Bally-Cuif L. 2002. Cloning of two tryptophan hydroxylase genes expressed in the diencephalon of the developing zebrafish brain. *Mech Dev* 119(Suppl 1):S215–S220.
- Brezun JM, Daszuta A. 1999. Depletion in serotonin decreases neurogenesis in the dentate gyrus and the subventricular zone of adult rats. *Neuroscience* 89:999–1002.
- Briscoe J, Sussel L, Serup P, Hartigan-O'Connor D, Jessell TM, Rubenstein JL, Ericson J. 1999. Homeobox gene *Nkx2.2* and specification of neuronal identity by graded Sonic hedgehog signalling. *Nature* 398:622–627.
- Carpenter EM, Goddard JM, Chisaka O, Manley NR, Capecchi MR. 1993. Loss of *Hox-A1* (*Hox-1.6*) function results in the reorganization of the murine hindbrain. *Development* 118:1063–1075.
- Chandrasekhar A, Moens CB, Warren JT Jr, Kimmel CB, Kuwada JY. 1997. Development of branchiomotor neurons in zebrafish. *Development* 124:2633–2644.
- Cheng L, Chen CL, Luo P, Tan M, Qiu M, Johnson R, Ma Q. 2003. *Lmx1b*, *Pet-1*, and *Nkx2.2* coordinately specify serotonergic neurotransmitter phenotype. *J Neurosci* 23:9961–9967.

- Cordes SP. 2005. Molecular genetics of the early development of hindbrain serotonergic neurons. *Clin Genet* 68:487–494.
- Côté F, Fligny C, Bayard E, Launay J-M, Gershon MD, Mallet J, Vodjdani G. 2007. Maternal serotonin is crucial for murine embryonic development. *Proc Natl Acad Sci U S A* 104:329–334.
- Craven SE, Lim KC, Ye W, Engel JD, de Sauvage F, Rosenthal A. 2004. Gata2 specifies serotonergic neurons downstream of sonic hedgehog. *Development* 131:1165–1173.
- Detrich HW III, Kieran MW, Chan FY, Barone LM, Yee K, Rundstadler JA, Pratt S, Ransom D, Zon LI. 1995. Intraembryonic hematopoietic cell migration during vertebrate development. *Proc Natl Acad Sci U S A* 92:10713–10717.
- Ding YQ, Marklund U, Yuan W, Yin J, Wegman L, Ericson J, Deneris E, Johnson RL, Chen ZF. 2003. Lmx1b is essential for the development of serotonergic neurons. *Nat Neurosci* 6:933–938.
- Djavadian RL. 2004. Serotonin and neurogenesis in the hippocampal dentate gyrus of adult mammals. *Acta Neurobiol Exp (Wars)* 64:189–200.
- Ekström P, Van Veen T. 1984. Distribution of 5-hydroxytryptamine (serotonin) in the brain of the teleost *Gasterosteus aculeatus* L. *J Comp Neurol* 226:307–320.
- Ekström P, Nyberg L, van Veen T. 1985. Ontogenetic development of serotonergic neurons in the brain of a teleost, the three-spined stickleback. An immunohistochemical analysis. *Brain Res* 349:209–224.
- Fricker AD, Rios C, Devi LA, Gomes I. 2005. Serotonin receptor activation leads to neurite outgrowth and neuronal survival. *Brain Res Mol Brain Res* 138:228–235.
- Fyodorov D, Nelson T, Deneris E. 1998. Pet-1, a novel ETS domain factor that can activate neuronal nAChR gene transcription. *J Neurobiol* 34:151–163.
- Gaspar P, Cases O, Maroteaux L. 2003. The developmental role of serotonin: news from mouse molecular genetics. *Nat Rev Neurosci* 4:1002–1012.
- Goridis C, Rohrer H. 2002. Specification of catecholaminergic and serotonergic neurons. *Nat Rev Neurosci* 3:531–541.
- Guo S, Brush J, Teraoka H, Goddard A, Wilson SW, Mullins MC, Rosenthal A. 1999. Development of noradrenergic neurons in the zebrafish hindbrain requires BMP, FGF8, and the homeodomain protein *soulless/Phox2a*. *Neuron* 24:555–566.
- Hansson SR, Mezey E, Hoffman BJ. 1998. Serotonin transporter messenger RNA in the developing rat brain: early expression in serotonergic neurons and transient expression in non-serotonergic neurons. *Neuroscience* 83:1185–1201.
- Hendricks T, Francis N, Fyodorov D, Deneris ES. 1999. The ETS domain factor Pet-1 is an early and precise marker of central serotonin neurons and interacts with a conserved element in serotonergic genes. *J Neurosci* 19:10348–10356.
- Hendricks TJ, Fyodorov DV, Wegman LJ, Lelutiu NB, Pehek EA, Yamamoto B, Silver J, Weeber EJ, Sweatt JD, Deneris ES. 2003. Pet-1 ETS gene plays a critical role in 5-HT neuron development and is required for normal anxiety-like and aggressive behavior. *Neuron* 37:233–247.
- Higashijima S, Hotta Y, Okamoto H. 2000. Visualization of cranial motor neurons in live transgenic zebrafish expressing green fluorescent protein under the control of the islet-1 promoter/enhancer. *J Neurosci* 20:206–218.
- Kah O, Chambolle P. 1983. Serotonin in the brain of the goldfish, *Carassius auratus*. An immunocytochemical study. *Cell Tissue Res* 234:319–333.
- Kaslin J, Panula P. 2001. Comparative anatomy of the histaminergic and other aminergic systems in zebrafish (*Danio rerio*). *J Comp Neurol* 440:342–377.
- Kimmel CB, Sessions SK, Kimmel RJ. 1981. Morphogenesis and synaptogenesis of the zebrafish Mauthner neuron. *J Comp Neurol* 198:101–120.
- Kimmel CB, Ballard WW, Kimmel SR, Ullmann B, Schilling TF. 1995. Stages of embryonic development of the zebrafish. *Dev Dyn* 203:253–310.
- Laudet V, Hanni C, Stehelin D, Duterque-Coquillaud M. 1999. Molecular phylogeny of the ETS gene family. *Oncogene* 18:1351–1359.
- Lidov HG, Molliver ME. 1982. Immunohistochemical study of the development of serotonergic neurons in the rat CNS. *Brain Res Bull* 9:559–604.
- Lieberman JA, Mailman RB, Duncan G, Sikich L, Chakos M, Nichols DE, Kraus JE. 1998. Serotonergic basis of antipsychotic drug effects in schizophrenia. *Biol Psychiatry* 44:1099–1117.
- Lucki I. 1998. The spectrum of behaviors influenced by serotonin. *Biol Psychiatry* 44:151–162.
- Lumsden A, Keynes R. 1989. Segmental patterns of neuronal development in the chick hindbrain. *Nature* 337:424–428.
- Marshall H, Nonchev S, Sham MH, Muchamore I, Lumsden A, Krumlauf R. 1992. Retinoic acid alters hindbrain Hox code and induces transformation of rhombomeres 2/3 into a 4/5 identity. *Nature* 360:737–741.
- Maurer P, Rorive S, de Kerchove d'Exaerde A, Schiffmann SN, Salmon I, de Launoit Y. 2004. The Ets transcription factor *Fev* is specifically expressed in the human central serotonergic neurons. *Neurosci Lett* 357:215–218.
- Maves L, Jackman W, Kimmel CB. 2002. FGF3 and FGF8 mediate a rhombomere 4 signaling activity in the zebrafish hindbrain. *Development* 129:3825–3837.
- McClintock JM, Kheirbek MA, Prince VE. 2002. Knockdown of duplicated zebrafish *hoxb1* genes reveals distinct roles in hindbrain patterning and a novel mechanism of duplicate gene retention. *Development* 129:2339–2354.
- McLean DL, Fetcho JR. 2004a. Ontogeny and innervation patterns of dopaminergic, noradrenergic, and serotonergic neurons in larval zebrafish. *J Comp Neurol* 480:38–56.
- McLean DL, Fetcho JR. 2004b. Relationship of tyrosine hydroxylase and serotonin immunoreactivity to sensorimotor circuitry in larval zebrafish. *J Comp Neurol* 480:57–71.
- Mueller T, Wullimann MF. 2005. Atlas of early zebrafish brain development. A tool for molecular neurogenetics. Amsterdam: Elsevier. 183 p.
- Oikawa T, Yamada T. 2003. Molecular biology of the Ets family of transcription factors. *Gene* 303:11–34.
- O'Malley DM, Kao YH, Fetcho JR. 1996. Imaging the functional organization of zebrafish hindbrain segments during escape behaviors. *Neuron* 17:1145–1155.
- Pattyn A, Vallstedt A, Dias JM, Samad OA, Krumlauf R, Rijli FM, Brunet JF, Ericson J. 2003a. Coordinated temporal and spatial control of motor neuron and serotonergic neuron generation from a common pool of CNS progenitors. *Genes Dev* 17:729–737.
- Pattyn A, Vallstedt A, Dias JM, Sander M, Ericson J. 2003b. Complementary roles for Nkx6 and Nkx2 class proteins in the establishment of motoneuron identity in the hindbrain. *Development* 130:4149–4159.
- Peter M, Couturier J, Pacquement H, Michon J, Thomas G, Magdelenat H, Delatre O. 1997. A new member of the ETS family fused to EWS in Ewing tumors. *Oncogene* 14:1159–1164.
- Pfaar H, von Holst A, Vogt Weisenhorn DM, Brodski C, Guimera J, Wurst W. 2002. mPet-1, a mouse ETS-domain transcription factor, is expressed in central serotonergic neurons. *Dev Genes Evol* 212:43–46.
- Qiu X, Xu H, Haddon C, Lewis J, Jiang YJ. 2004. Sequence and embryonic expression of three zebrafish fringe genes: lunate fringe, radical fringe, and manic fringe. *Dev Dyn* 231:621–630.
- Santarelli L, Saxe M, Gross C, Surget A, Battaglia F, Dulawa S, Weisstaub N, Lee J, Duman R, Arancio O, Belzung C, Hen R. 2003. Requirement of hippocampal neurogenesis for the behavioral effects of antidepressants. *Science* 301:805–809.
- Tallafuss A, Bally-Cuif L. 2003. Tracing of her5 progeny in zebrafish transgenics reveals the dynamics of midbrain-hindbrain neurogenesis and maintenance. *Development* 130:4307–4323.
- Tallafuss A, Wilm TP, Crozatier M, Pfeffer P, Wassef M, Bally-Cuif L. 2001. The zebrafish buttonhead-like factor *Bts1* is an early regulator of pax2.1 expression during mid-hindbrain development. *Development* 128:4021–4034.
- Teraoka H, Russell C, Regan J, Chandrasekhar A, Concha ML, Yokoyama R, Higashi K, Take-Uchi M, Dong W, Hiraga T, Holder N, Wilson SW. 2004. Hedgehog and Fgf signaling pathways regulate the development of tphR-expressing serotonergic raphe neurons in zebrafish embryos. *J Neurobiol* 60:275–288.

- Thisse C, Thisse B, Schilling TF, Postlethwait JH. 1993. Structure of the zebrafish *snail1* gene and its expression in wild-type, *spadetail* and *no tail* mutant embryos. *Development* 119:1203–1215.
- Walshe J, Maroon H, McGonnell IM, Dickson C, Mason I. 2002. Establishment of hindbrain segmental identity requires signaling by FGF3 and FGF8. *Curr Biol* 12:1117–1123.
- van Doorninck JH, van Der Wees J, Karis A, Goedknecht E, Engel JD, Coesmans M, Rutteman M, Grosveld F, De Zeeuw CI. 1999. GATA-3 is involved in the development of serotonergic neurons in the caudal raphe nuclei. *J Neurosci* 19:RC12.
- Vitalis T, Parnavelas JG. 2003. The role of serotonin in early cortical development. *Dev Neurosci* 25:245–256.
- Wullmann MF, Rupp B, Reichert H. 1996. *Neuroanatomy of the zebrafish brain*. Basel: Birkhauser. 144 p.
- Ye W, Shimamura K, Rubenstein JL, Hynes MA, Rosenthal A. 1998. FGF and Shh signals control dopaminergic and serotonergic cell fate in the anterior neural plate. *Cell* 93:755–766.
- Zervas M, Millet S, Ahn S, Joyner AL. 2004. Cell behaviors and genetic lineages of the mesencephalon and rhombomere 1. *Neuron* 43:345–357.
- Zhao Y, Yang Z, Phelan JK, Wheeler DA, Lin S, McCabe ER. 2006. Zebrafish *dax1* Is Required for Development of the Interrenal Organ, the Adrenal Cortex Equivalent. *Mol Endocrinol* 20:2630–2640.
- Zhou FQ, Cohan CS. 2001. Growth cone collapse through coincident loss of actin bundles and leading edge actin without actin depolymerization. *J Cell Biol* 153:1071–1084.

Appendix 7

Serotonergic Screen Assay

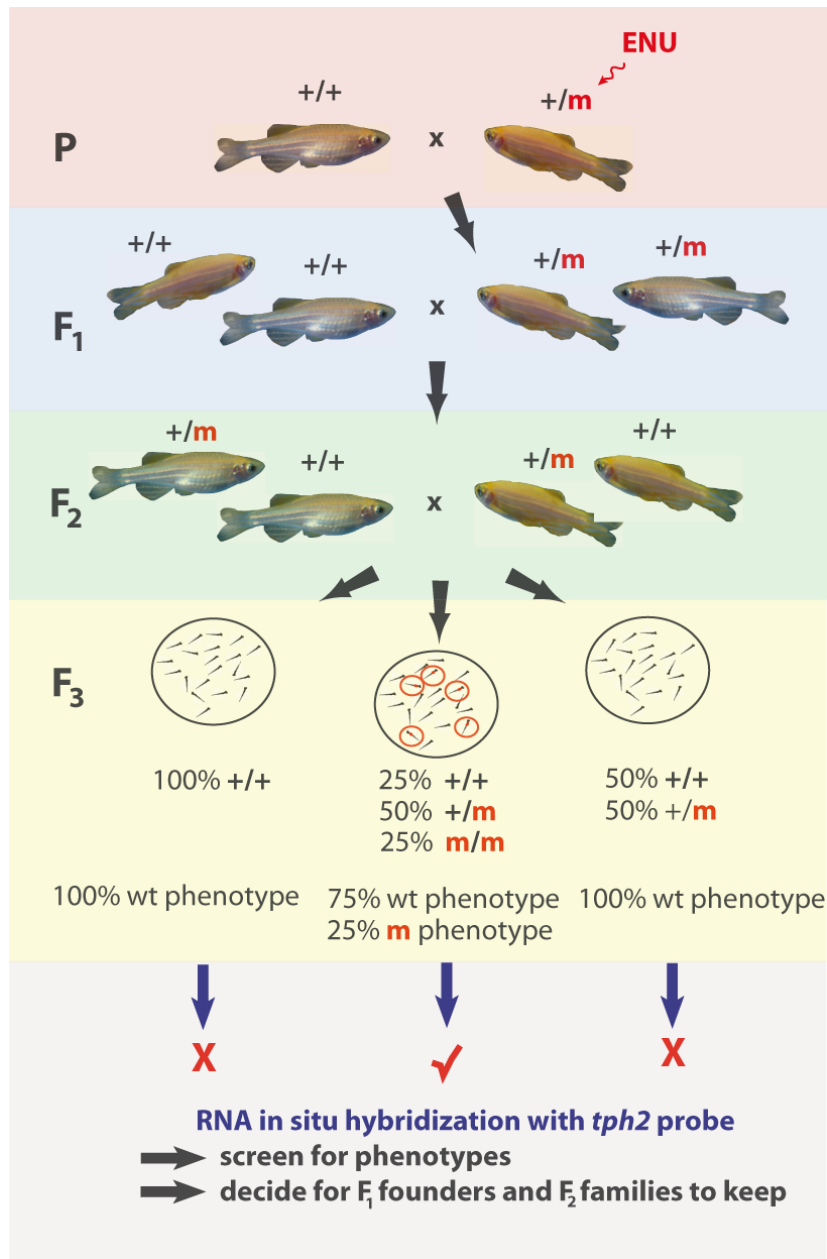


Figure 1: Scheme of recessive ENU mutagenesis screen in zebrafish. Scheme is explained from top to bottom. Males of the F₀ generation are treated with the mutagen ENU (induced mutation is indicated by red 'm') and subsequently outcrossed with wildtype females. The thereby raised F₁ generation is outcrossed again with wildtypes. The F₂ generation is increased. F₃ batches (indicated by fish larvae in black ellipse) where approximately 25% of the larvae show phenotype of interest in the morphological assay are noted and corresponding F₂ families are used for further experiments and raising of the line. Note that this is also the step of morphological pre-screening for RNA in situ screen. Note further, that at this step the *rx3* mutant *chk^{ne2611}* was identified. For the RNA in situ hybridization F₃ batches are processed for RNA in situ hybridization and afterwards assessed for batches with approximately 25% of larvae with phenotype of interest. Corresponding F₂ families are used for further experiments and raising of the line.

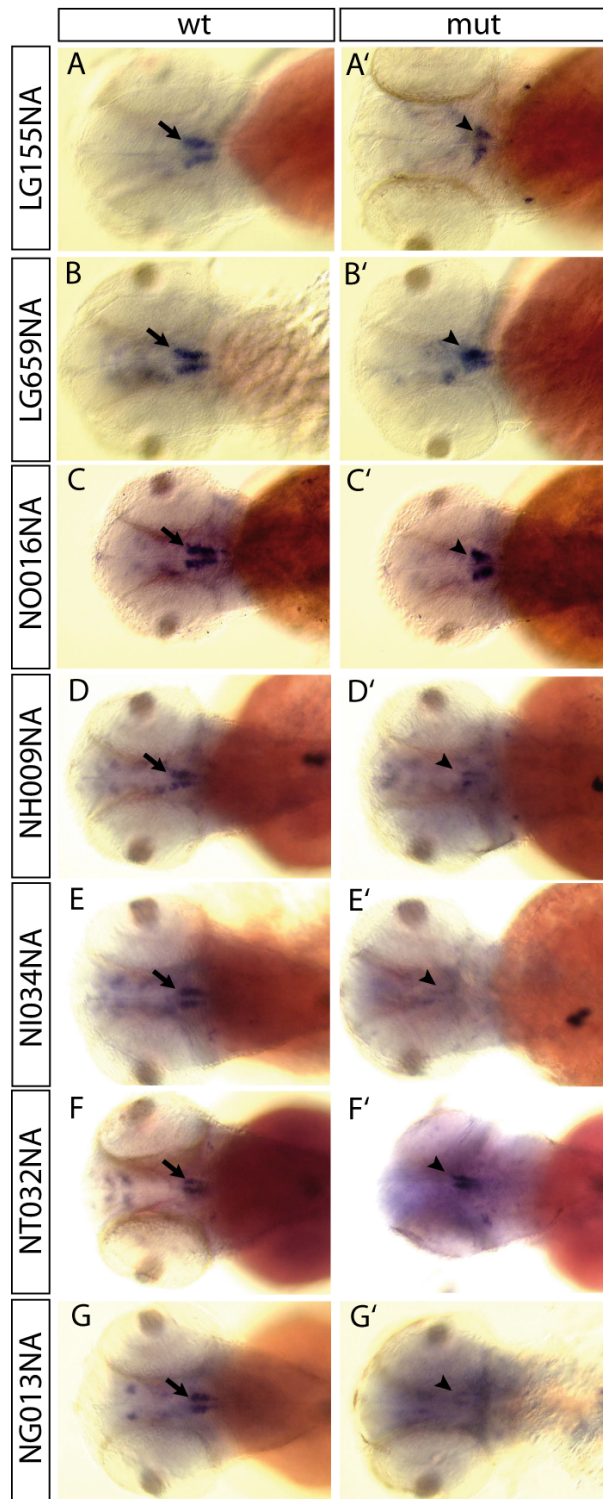


Figure 2: Overview of mutants recovered from Tübingen ZF-models raphe serotonergic screen. *tph2* expression domain in wt (left) is indicated by arrow. Mutant *tph2* raphe serotonergic patterns (right) are indicated by arrowhead. Mutant line identification code is given on the left. Dorsal views and anterior is left. (A') *tph2* domains are condensed in A/P but broadened in the lateral extent. (B') *tph2* domains is merged at the midline. (C') *tph2* domain is slightly condensed in A/P but also slightly broadened in the lateral extent. (D') *tph2* expression is clearly weaker. (E') *tph2* expression is nearly lost. (F') *tph2* domains is merged at the midline. (G') *tph2* domains is is clearly weaker. Note that this screening assay contains also probes of our screening partner (more anterior expression domains).

Acknowledgements

First of all, I want to thank Dr. Laure Bally-Cuif for her great support and outstanding supervision during all the years that I have been working in her group. I deeply appreciate that she always had time for me for small and big burning questions and discussions. I also want to thank Laure for great aid for my applications for courses, scholarships and my future position. Furthermore, she gave me many answers to my 'burning curiosity' and I could always develop my own ideas and experimental approaches.

Next, I want to thank Prof. Dr. Wolfgang Wurst for his support, supervision and the opportunity to conduct my PhD project in an encouraging atmosphere at the Institute of Developmental Genetics at the Helmholtz Center Munich. I want to thank him also for the great support for my applications.

Of course I want to say many, many and very BIG "Thanks!" to all my colleagues in the laboratory!

... and in particular:

Very deeply I want to thank Stina! For her help with her great anatomical and experimental expertise, for all the collaborations and the challenge to brake the all-time coffee records and ... for everything else! Tack så mycket!

I thank Steffi T. for super expert support with experiments and our collaborations... and, not to forget, for her even greater help with super gluing all my lab equipment – so that it was even stable in the strongest lab storms!

Anja I want to thank, in particular, for the perfect collaboration over the years and in particular during the "miR"-times. Thanks also for many nice discussions about live out of the lab and providing good movies and music.

I am grateful to Birgit T. for her super experimental support and introducing me into the sometimes magic art of in situ hybridizations at the very beginning.

Thanks to Prisca I got a lot of new ideas on the neuronal identity project but also on adult neurogenesis. Thanks for being a great bench neighbor – and recently also desk neighbor!

Will and Katherine I want to thank for improving my English (language as well as music appreciation) and for many discussions!

Susie for being a good bench neighbor – even if only for a short time – before I disappeared with writing (and in this respect, thanks for the peaceful desk!).

Furthermore, I want to thank Steffi S. for the progenitor project collaboration and being a good bench neighbor.

I want to thank also Marion, Karin and Paulina for collaborations and discussions!

To our secretaries Regina, Eva and also the IDG secretaries I am very grateful for helping me through the jungle of bureaucracy and the many many orderings.

Deeply, I also want to thank my former lab colleagues:

- Christoph for excellent collaborations, especially on the miR project and construction of the transgenic *her9* line and being a perfect FM4-DJ!
- Andrea for helping me getting started with the neuronal identity project and for finding the *CLGY469* line during dark polar nights in Bergen.
- Jovica, for giving me always good hints and advices with experiments!

- Birgit A. for helping me to understand the world of adult neurogenesis and for the collaborations!

...and also Silvia, Gianfranco and Alex!

Birgit T., Anja and Jovica I want to thank again to help me survive the hard mid-winter screen times in Tübingen! Furthermore, I want to thank Gabi Nica for being a great screen collaborator and the whole ZF-MODELS screen crew and people at the MPI (and the workshop)!

I want to say many thanks to the 'Fish facility crew' for keeping my fish happy - and me as well with some 'Bavarian' talking which I else might have nearly forgotten! Merci! And I want to thank Richie in particular for great music and discussions!

Furthermore, I want to thank the scientific environment at the IDG and neighboring institutes: In particular Chichung (also for the great support with applications) and his lab, in particular Ravi for helping me to make my first steps in the *C. elegans* world, Andrea and her lab, Magdalena and her lab, Torben and Prof. Dr. Jochen Graw for the *eya* collaboration, Reinhard and his lab for great assistance with live-imaging and all the other people at the IDG, present and past, with whom I have been collaborating and discussing. I am grateful to Ruth Klafke and Andrea Wizenman not only for the great collaboration on the miR project but also to keep the Würzburg memories alive!

I also want to thank the Marine Biology Laboratory in Woods Hole for giving me the great chance to take part in the outstandingly interesting and encouraging 'Embryology Course' in 2006. In particular I want to thank the course directors Prof. Dr. Richard Harland and Prof. Dr. Joel Rothman, as well as, Prof. Dr. Mark Martindale and Dr. Paola Oliveri for great discussions, new insights and good advice! Moreover, I want to thank all the instructors, assistants and people who provided funding! But I also want to thank all my course colleagues – it was really a great experience!

In the same line I want to thank EMBO, the Boehringer Ingelheim Fonds and in particular Dr. Thomas Becker, the instructors, course assistants and colleagues for a great EMBO course in 2005 in Bergen!

Prof. Dr. Georg Krohne supports me since the start of my studies at the Biocenter in Würzburg in a very friendly and encouraging way - I am very grateful for that!

I want to thank also my first 'students' Steffi Hirn and Anne Tessier for being so interested, enthusiastic and very hard working on the projects.

Of course, I want to thank also our close collaborators: Prof. Dr. Uwe Strähle, Dr. Corinne Houart and Dr. Thomas Becker for discussions and new input on our common projects.

I am very grateful to the DFG and members of the Graduiertenkolleg 1048 'Molecular basis of organ development in vertebrates' and in particular Dr. Christoph Winkler, Prof. Dr. Manfred Scharl and Prof. Dr. Christoph Englert for giving me the opportunity to be an external member at the Kolleg! I want to also thank also my colleagues, in particular Toni, Daniel, Marieke, Gabi and last but not least Basti Linder, my former study colleague, for so many encouraging discussions and for his and Tina's great hospitality during my stays in Würzburg!

Am Ende möchte ich noch ganz besonders meinen Eltern, meiner Schwester, Romy, Stefan und meinen Großeltern danken! Sie haben mich stets tatkräftig unterstützt und mir immer wieder Mut gemacht. Vielen, vielen Dank!

Curriculum Vitae

Christian Stigloher

Address:

Department Zebrafish Neurogenetics - ZEN
Institute of Developmental Genetics - IDG
Helmholtz Center Munich
German Research Center for Environmental Health
Ingolstädter Landstraße 1
D-85764 München-Neuherberg
Germany

Email: christian.stigloher@helmholtz-muenchen.de
Tel.: +49 (0)89 3187 3686; +49 (0)89 3187 2944
Fax: +49 (0)89 3187 3099

Birthdate: 1978, November 14th
Nationality: German
Age: 29
Sex: male

Education and Professional Training

- 1985-1998 **Primary Education and Secondary Education** in Rosenheim, Germany
Abitur at the Finsterwalder-Gymnasium Rosenheim
Final Grade: 1.3 (scale 1 to 6 where 1 is best)
Award granted by the Georg-Dax-Foundation for the Abitur
- 1998-1999 **Zivildienst** (alternative service in lieu of military service)
- 1999-2001 **University Studies**
Basic Studies in Biology (major subject),
Chemistry and Physics (minor subjects)
at the Biocenter of the University of Würzburg, Germany
Vordiplom: October 2001
Grades: Biology: very good
 Chemistry: good
 Physics: very good
- ✦ Member of the German National Academic Foundation
(Studienstiftung des deutschen Volkes) since Summer 2001
- 2001-2003 **Main Studies** in Biology
Major subject: Cell and Developmental Biology
Minor subjects: Biochemistry, Genetics, Bioinformatics
Additional subject: Neurobiology

August 2002 until May 2003:

Exchange Program at Duke University, Durham, North Carolina, USA
DAAD-Scholarship (German Academic Exchange Service)
(Integrated Studies Abroad Program)

Final Exams (Diplom theoretical exams) Winter 2003 in Würzburg:

Major subject: Cell and Developmental Biology (Grade:1.0)

Minor subjects: Biochemistry (1.0), Genetics (1.0), Bioinformatics (1.0)
(1.0 equals ,excellent')

2004

Diplom Thesis in Dr. Laure Bally-Cuif's Laboratory
,Zebrafish Neurogenetics' at the Technical University of Munich
and the GSF-National Research Center for Environment and Health
(since 2008: Helmholtz Center Munich)
Institute of Developmental Genetics
Supervisors: Dr. Laure Bally-Cuif; Prof. Dr. Wolfgang Wurst

Project title:

'Molecular and phenotypical characterization of new zebrafish mutants affected in embryonic development of the central nervous system'

November 2004:

Grade of the Diplom Thesis: 1.0 (equals 'excellent')

Final Grade of Diplom: 'with honors'

2005-2008

PhD-Thesis project in Dr. Laure Bally-Cuif's Laboratory
,Zebrafish Neurogenetics' at the Technical University of Munich
and the GSF - National Research Center for Environment and Health
(since 2008: Helmholtz Center Munich)
Department Zebrafish Neurogenetics
Institute of Developmental Genetics
Supervisors: Dr. Laure Bally-Cuif; Prof. Dr. Wolfgang Wurst

Project title:

'Specification, maintenance and fate determination of neural progenitor pools in the zebrafish central nervous system'

✦ Associated member of the DFG (German Research Foundation) funded Graduate College 1041 'Molecular Basis of Organ Development' situated at the Biocenter of the University of Würzburg, Germany

✦ Participation in the first round of the ZF-MODELS ENU mutagenesis screen organized by the Max Planck Institute for Developmental Biology (Dept. Genetics, Nüsslein-Volhard laboratory) January 2005 – April 2005 in Tübingen, Germany

✦ Participation in the EMBO Practical Course 'Enhancer Detection, Gene Trapping, and TILLING in Zebrafish',
August 1st - 11th 2005

Sars International Centre for Marine Molecular Biology, Bergen, Norway
Scholarships from EMBO (European Molecular Biology Organization)
and 'Boehringer Ingelheim Fonds'

✦ Participation in the 2006 six weeks MBL Summer Course 'Embryology'
June 10th - 23rd July 2006

Marine Biological Laboratory, Woods Hole, MA
Scholarships from 'S.O. Mast Founders' Scholarship', 'Caswell Grave Scholarship Fund' and 'Boehringer Ingelheim Fonds'

Publications:

Published:

Stigloher C, Ninkovic J, Laplante M, Geling A, Tannhäuser B, Topp S, Kikuta H, Becker TS, Houart C, Bally-Cuif L

Segregation of telencephalic and eye-field identities inside the zebrafish forebrain territory is controlled by Rx3

Development

August 2006

133(15):2925-35

Lillesaar C, Tannhäuser B, Stigloher C, Kremmer E, Bally-Cuif L

The serotonergic phenotype is acquired by converging genetic mechanisms within the zebrafish central nervous system.

Developmental Dynamics

April 2007

236(4):1072-84.

Stigloher C, Chapouton P, Adolf B, Bally-Cuif L

Identification of neural progenitor pools by E(Spl) factors in the embryonic and adult brain

Brain Research Bulletin

March 2008

75(2-4):266-73

In press:

Leucht C*, Stigloher C*, Wizenmann A, Klafke R, Folchert A, Bally-Cuif L

MicroRNA-9 directs late organizer activity of the midbrain-hindbrain boundary

Nature Neuroscience

published online: May 2008

* shared first authorship

Accepted:

Topp S, Stigloher C, Komisarczuk AZ, Adolf B, Becker TS, Bally-Cuif L

Fgf signaling in the zebrafish adult brain: association of Fgf activity with ventricular zones but not cell proliferation

Journal of Comparative Neurology

In Revision:

Ninkovic J*, Stigloher C*, Bally-Cuif L

GSK3 β /PKA and Gli1 interact with E(Spl) factors activity in the maintenance of neural progenitors at the midbrain-hindbrain boundary

Development

* shared first authorship

Söker T, Stigloher C, Topp S, Floss T, Wurst W, Bally-Cuif L, Graw J

Functional differences for Eya3 among vertebrates

Developmental Dynamics

Lillesaar C, Stigloher C, Tannhäuser B, Wullimann M, Bally-Cuif L

Establishment and distribution of axonal projections originating from raphe serotonergic neurons in the developing and adult zebrafish, Danio rerio

Journal of Comparative Neurology

Komisarczuk AZ, Topp S, Stigloher C, Kapsimali M, Bally-Cuif L, Becker TS

Enhancer detection and developmental expression of zebrafish sprouty1, a member of the fgf8 synexpression group

Developmental Dynamics